PO Box 2345, Beijing 100023, China
Fax: +86-10-85381893
E-mail: wjg@wjgnet.com www.wjgnet.com

World J Gastroenterol 2004;10(17):2465-2467
World Journal of Gastroenterology
Copyright © 2004 by The WJG Press ISSN 1007-9327

• REVIEW •

Toward a definition of colonic inertia

Gabrio Bassotti, Giuseppe de Roberto, Luca Sediari, Antonio Morelli

Gabrio Bassotti, Giuseppe de Roberto, Luca Sediari, Antonio Morelli, Gastroenterology and Hepatology Section, Department of Clinical and Experimental Medicine, University of Perugia Medical School, Perugia 06131, Italy
Correspondence to: Dr Gabrio Bassotti, Strada del Cimitero, 2/a, 06131 San Marco Perugia, Italy. gabassot@tin.it
Fax: +39-75-584-7570
Received: 2004-02-02 **Accepted:** 2004-02-24

Abstract

Chronic constipation is a relatively frequent symptom; among its subtypes, the so called-colonic inertia represents a disease condition that is often considered for surgery. However, to date, there has been no agreement on definition of colonic inertia, and a literature review showed that this definition was given to numerous entities that differ from each other. In this paper these concepts are reviewed and a more stringent definition of colonic inertia is proposed.

Bassotti G, de Roberto G, Sediari L, Morelli A. Toward a definition of colonic inertia. *World J Gastroenterol* 2004; 10 (17): 2465-2467
http://www.wjgnet.com/1007-9327/10/2465.asp

INTRODUCTION

Starting from the (interrupted) building of the Babylon Tower, human beings have been plagued by a difficulty in understanding each other, even for that concerns trivial concepts. This is especially true in the medical field, and the concept of functional gastrointestinal disorders appears to be a particularly fertile one. In fact, apparently simple complaints such as dyspepsia, diarrhea and constipation bear no single label and are still variously defined. A few years ago, a process was started that aimed at having at least a common discussion ground in defining functional gastrointestinal disorders. This process, through the work of several working teams, produced a series of documents to define the various functional gastrointestinal entities by means of the so-called Rome Criteria, now in their second version (Rome II Criteria)[1].

Defining and diagnosing constipation

Chronic constipation is one of the most common gastrointestinal complaints[2], and is usually defined by symptoms such as infrequent bowel movements, the presence of hard stools, an excessive time necessary to evacuate, straining, and the sense of incomplete evacuation of the bowel[3].

The Rome II Criteria for constipation[4] are shown in Table 1. Although these criteria represent a common ground to define constipation for research purposes, they do not take into consideration the various types of constipation, which may further be classified in to three main subgroups: normal transit constipation, disorders of defecatory or rectal evacuation (outlet obstruction), and slow transit constipation (STC)[5].

Recent guidelines on constipation[6] thoroughly summarize the current diagnostic approach to this symptom, obviously taking into account the fact that the suggested diagnostic tests still do not have their sensitivities established and the details of their performances have not been well specified[7]. Colonic transit studies with radiopaque markers are simple and reproducible tests[8] that can be recommended for any patient undergoing evaluation for constipation. Other tests mainly focus on the anorectal and pelvic function: the balloon expulsion test (simple, inexpensive)[9] is a useful screening one for major evacuatory dysfunctions; defecography (simple, minimal radiation exposure) can quantify defecatory function[10]; anorectal manometry (variable methodologies, data from different centers not standardized) is useful to exclude Hirschsprung's disease and provide supportive data for a diagnosis of pelvic floor dysfunction[11]. These tests are commonly employed in the diagnostic work-up of constipated patients, with further specific tests (rectal perception or distention or electrical stimuli, electromyography of the external sphincter or puborectalis, pudendal nerve terminal motor latency, pancolonic electromyography or manometry) usually being carried out only in clinical research or not generally applicable in common daily practice[12].

Colonic inertia: a "smoky" entity

Among the above reported subtypes of constipation, the STC one (characterized by an abnormally delayed colonic transit time) represents approximately 15-30% of constipated patients[13] and usually includes those with intractable constipation[14]. The latter are usually those "refractory" to medical management, often labeled as "colonic inertia" patients, and frequently referred to the surgeon for a more drastic approach[15]. However, it appears to be some semantic confusion concerning the term colonic inertia, which is often inappropriately used to define various types of constipation (see below).

How is colonic inertia perceived?

An internet-based search strategy of the Medline and Science Citation Index was performed using the keywords colon, colonic, inertia in various combinations with the Boolean operators AND, OR and NOT. Only articles related to human studies were used, and manual cross-referencing was also performed. Articles published in English between January 1965 and October 2003 were selected; however, a search in non-English languages and in older than 1965 journals was also performed in our library. Letters and case reports were excluded, and abstracts quoted only when the full papers were unavailable.

Table 2 summarizes the various definitions of colonic inertia found in literature, according to the method employed for diagnosis; however, although grouped together for practical purposes, it must be noted that even these subgroups have some internal differences which increase the simple definition of this entity to a number of twelve, and make difficult the interpretation of results.

According to the most frequently performed diagnostic study, radiopaque markers transit, colonic inertia patients have been classified as: (1) having a delayed transit with markers scattered throughout the viscus[16-20], with exclusion of obstructed defecation on manometry or defecography[21,22]; (2) synonymous of STC (without specification of markers' distribution)[23-34]; (3) presenting markers' delay in the ascending[35] or the right colon[36]; (4) showing a delayed transit only in the left colon, or in both the left and right colon[37]; or (5) displaying a delayed right and left colonic transit, but with normal transit in the sigmoid colon and rectum[38].

Table 1 Rome II Criteria for constipation[4]

Two or more of the following for at least 12 wk (not necessarily consecutive) in the preceding 12 mo:
- Straining during >25% of bowel movements;
- Lumpy or hard stools for >25% of bowel movements;
- Sensation of incomplete evacuation for >25% of bowel movements;
- Sensation of anorectal blockage for >25% of bowel movements;
- Manual maneuvers (digital evacuation, support of the pelvic floor) to facilitate >25% of bowel movements;
- Less than 3 bowel movements per week;
Loose stools are not present, and there are insufficient criteria for irritable bowel syndrome

Table 2 The various definitions of colonic inertia in literature

According to radiopaque transit studies:
- Delayed colonic transit with markers distributed throughout the colon;
- Colonic inertia equates to slow transit constipation;
- Delayed transit in the right colon;
- Delayed transit in the left colon, or both in the left and right colon;
- Delayed transit in the right and left colon, with normal transit in the sigmoid and rectum
According to scintigraphic transit studies:
- Scintigraphic delay in the transverse and splenic flexure;
- Scintigraphic delay in the cecum, ascending colon, hepatic flexure, and transverse colon;
- Scintigraphic delay in the whole colon
According to manometric and/or electromyographic findings:
- Almost complete or complete absence of colonic motility
Miscellaneous:
- Decreased colonic motility;
- Severe constipation and abdominal pain, abnormal transit study, normal anorectal manometry;
- Refractory constipation and motility abnormalities only of the lower gastrointestinal tract

Analysis of these reports shows that, whereas patients in group 1 could indeed somewhat represent a homogeneous group, those in groups 2-5 are highly heterogeneous, and probably include subjects with specific abnormalities (particularly outlet obstruction).

As regards colonic inertia patients defined by scintigraphic transit, they have been classified as: (1) with delay limited to the transverse colon and the splenic flexure[39]; (2) with delay limited to the cecum, ascending colon, hepatic flexure, and transverse colon[40]; and (3) with delay in the whole colon[41]. Once again, it may be noted that colonic inertia is differently defined by different authors, and the patients under investigation do not represent a homogeneous entity.

Things are not better when colonic inertia patients are classified on the basis of instrumental evaluations, which include: (1) a generic "decrease" of colonic motility[42]; (2) disturbance of colonic motility, defined by severe constipation and abdominal pain, abnormal transit study, and normal anorectal manometry[43]; (3) refractory constipation and motility abnormalities only of the lower gastrointestinal tract[44]; and (4) complete or almost complete absence of colonic motility, documented by manometry or electromyography[45-48]. Again, the great variability of definitions makes likely confusion between entities, as some of the patients in groups 1-3 could easily fit criteria for the irritable bowel syndrome.

The above considerations, far from the simple semantic misunderstanding, are important in that many of the reports described in these series came from surgical groups, and were pertinent to patients in whom a surgical operation was performed, or to patients evaluated for surgery. It is therefore intuitive that such a confusion in defining an entity with potential surgical implications also generates confusion on which patients should be referred for surgery, objective evidence indicates that severely constipated patients judged to be "intractable" might actually respond to colonic pharmacologic stimulation[49,50], suggesting that they might be responsive to more aggressive forms of medical treatment.

Toward a definition of colonic inertia

On the above grounds, colonic inertia should be better defined, and it should not be synonymous of STC or other well-categorized subtypes of constipation. The Rome Criteria have already given us a common definition of functional constipation and pelvic floor dyssynergia[51], and STC is well recognized by the delayed colonic transit with radiopaque markers scattered within the colon, there might be the possibility of an intermediate form combining the two entities.

Colonic inertia could be characterized as a distinct form: in fact, the term *inert* literally means "(1) *inactivity* or (2) *activity or motion modest or absent*"[52]. Under these terms, this (actually rare) form might be defined by: (1) severe functional constipation (according to Rome Criteria); (2) absence of outlet obstruction; (3) delayed transit with markers distributed throughout the colon; (4) manometric and/or electromyographic documentation of absent or almost absent colonic motor activity (including responses to meals); and (5) no response to pharmacologic stimulation (bisacodyl, others) during colonic motility recording.

It remains to be shown, however, whether this definition could predict the success of surgery more accurately, help select more accurately those patients actually needing surgery, as their colon is beyond each possible therapeutic rescue, and better understand the basic mechanisms of constipation through selection of more homogeneous cohorts of patients.

REFERENCES

1 **Drossman DA**, Corazziari E, Talley NJ, Thompson WG, Whitehead WE. Rome II: The functional gastrointestinal disorders. *Degnon Associates McLean (Va)* 2000

2 **Stewart WF**, Liberman JN, Sandler RS, Woods MS, Stemhagen A, Chee E, Lipton RB, Farup CE. Epidemiology of constipation (EPOC) study in the United States: relation of clinical subtypes to sociodemographic features. *Am J Gastroenterol* 1999; **94**: 3530-3540

3 **Koch A**, Voderholzer WA, Klauser AG, Muller-Lissner S. Symp-

toms in chronic constipation. *Dis Colon Rectum* 1997; **40**: 902-906
4 **Thompson WG**, Longstreth GF, Drossman DA, Heaton KW, Irvine EJ, Muller-Lissner SA. Functional bowel disorders and functional abdominal pain. *Gut* 1999; **45**(Suppl II): II43-II47
5 **Lembo A**, Camilleri M. Chronic constipation. *N Engl J Med* 2003; **349**: 1360-1368
6 **Locke GR**, Pemberton JH, Phillips SF. American Gastroenterological Association medical position statement: guidelines on constipation. *Gastroenterology* 2000; **119**: 1761-1766
7 **Locke GR**, Pemberton JH, Phillips SF. AGA technical review on constipation. *Gastroenterology* 2000; **119**: 1766-1778
8 **Degen LP**, Phillips SF. Variability of gastrointestinal transit in healthy women and men. *Gut* 1996; **39**: 299-305
9 **Preston DM**, Lennard-Jones JE. Anismus in chronic constipation. *Dig Dis Sci* 1985; **30:** 413-418
10 **Shorvon PJ**, McHugh S, Diamant NE, Somers S, Stevenson GW. Defecography in normal volunteers: results and implications. *Gut* 1989; **30**: 1737-1749
11 **Diamant NE**, Kamm MA, Wald A, Whitehead WE. AGA technical review on anorectal testing techniques. *Gastroenterology* 1999; **116**: 735-754
12 **Wald A**. Anorectum. In Schuster MM. Atlas of Gastrointestinal Motility in Health and Disease. Baltimore: *Williams Wilkins* 1993: 229-249
13 **Knowles CH**, Martin JE. Slow transit constipation: a model of human gut dysmotility. Review of possible aetiologies. *Neurogastroenterol Mot* 2000; **12**: 181-196
14 **Camilleri M**, Thompson WG, Fleshman JW, Pemberton JH. Clinical management of intractable constipation. *Ann Intern Med* 1994; **121**: 520-528
15 **Schiller LR**. Review article: the therapy of constipation. *Aliment Pharmacol Ther* 2001; **15:** 749-763
16 **Schang JC**, Devroede G, Duguay C, Hémond M, Hébert M. Constipation par inertie colique et obstruction distale: étude électromyographique. *Gastroenterol Clin Biol* 1985; **9**: 480-485
17 **Wald A**. Colonic transit and anorectal manometry in chronic idiopathic constipation. *Arch Intern Med* 1986; **146**: 1713-1716
18 **Berman IR**, Manning DH, Harris MS. Streamlining the management of defecation disorders. *Dis Colon Rectum* 1990; **33**: 778-785
19 **Bergin AJ**, Read NW. The effect of preliminary bowel preparation on a simple test of colonic transit in constipated subjects. *Int J Colorect Dis* 1993; **8**: 75-77
20 **Herman R**, Gregorczyk A, Walega P, Kawiorski W. Radiologic methods of evaluating colonic transit time in functional disorders of the large intestine. *Przegl Lek* 1994; **51**: 343-346
21 **Wexner SD**, Daniel N, Jagelman DG. Colectomy for constipation: physiologic investigation is the key to success. *Dis Colon Rectum* 1991; **34**: 851-856
22 **Costalat G**, Garrigues JM, Didelot JM, Yousfi A, Boccasanta P. Subtotal colectomy with ceco-rectal anastomosis (Deloyers) for severe idiopathic constipation: an alternative to total colectomy reducing risks of digestive sequelae. *Ann Chir* 1997; **51**: 248-255
23 **Willocx R**. Colonic inertia and rectal obstruction (Arbuthnot Lane disease). *Ann Gastroenterol Hepatol* 1986; **22**: 347-352
24 **Wehrli H**, Akovbiantz A. Surgical therapy of severe idiopathic constipation. *Schweitz Med Wochenschr* 1990; **120**: 496-498
25 **Meyer-Wyss B**. Motility of the large intestine: from irritable colon to obstipation. *Ther Umsch* 1991; **48**: 488-493
26 **Fleshman JW**, Dreznik Z, Cohen E, Fry RD, Kodner IJ. Balloon expulsion facilitates diagnosis of pelvic floor outlet obstruction due to nonrelaxing puborectalis muscle. *Dis Colon Rectum* 1992; **35**: 1019-1025
27 **Mollen RM**, Claassen AT, Kuijpers JH. The evaluation and treatment of functional constipation. *Scand J Gastroenterol* 1997; **223**(Suppl): 8-17
28 **Bernini A**, Madoff RD, Lowry AC, Spencer MP, Gemlo BT, Jensen LL, Wang WD. Should patients with combined colonic inertia and nonrelaxing pelvic floor undergo subtotal colectomy? *Dis Colon Rectum* 1998; **41**: 1363-1366
29 **Thiede A**, Kraemer M, Sailer M, Fuchs KH. Open surgical therapy of constipation. *Zentralbl Chir* 1999; **124**: 812-817
30 **Fan CW**, Wang JY. Subtotal colectomy for colonic inertia. *Int Surg* 2000; **85**: 309-312
31 **Santos SL**, Barcelos IK, Mesquita MA. Total and segmental colonic transit time in constipated patients with Chagas' disease without megaesophagus or megacolon. *Braz J Med Biol Res* 2000; **33**: 43-49
32 **Thompson WG**. Constipation: a physiological approach. *Can J Gastroenterol* 2000; **14**(Suppl D): 155D-162D
33 **Sarli L**, Costi R, Sarli D, Roncoroni L. Pilot study of subtotal colectomy with antiperistaltic cecoproctostomy for the treatment of chronic slow-transit constipation. *Dis Colon Rectum* 2001; **44**: 1514-1520
34 **Zhao RH**, Baig MK, Thaler KJ, Mack J, Abramson S, Woodhouse S, Tamir H, Wexner SD. Reduced expression of serotonin receptor(s) in the left colon of patients with colonic inertia. *Dis Colon Rectum* 2003; **46**: 81-86
35 **Watier A**, Devroede G, Duranceau A, Abdel-Rahman M, Duguay C, Forand MD, Tetreault L, Arhan P, Lamarche J, Elhiali M. Constipation with colonic inertia. A manifestation of systemic disease? *Dig Dis Sci* 1983; **28**: 1025-1033
36 **Husni-Hag-Ali R**, Gomez Rodriguez BJ, Mendoza Olivares FJ, Garcia Montes JM, Sachez-Gey Venegas S, Herrerias Gutierrez JM. Measuring coloic transit time in chronic idiopathic constipation. *Rev Esp Enferm Dig* 2003; **95**: 186-190
37 **Verne GN**, Hocking MP, Davis RH, Howard RJ, Sabetai MM, Mathias JR, Schuffler MD, Sninsky CA. Long-term response to subtotal colectomy in colonic inertia. *J Gastrointest Surg* 2002; **6**: 738-744
38 **You YT**, Wang JY, Changchien CR, Chen JS, Hsu KC, Tang R, Chiang JM, Chen HH. Segmental colectomy in the management of colonic inertia. *Am Surg* 1998; **64**: 775-777
39 **Roberts JP**, Newell MS, Deeks JJ, Waldron DW, Garvie NW, Williams NS. Oral [^{111}In]DTPA scintigraphic assessment of colonic transit in constipated subjects. *Dig Dis Sci* 1993; **38**: 1032-1039
40 **Krevsky B**, Maurer AH, Fisher RS. Patterns of colonic transit in chronic idiopathic constipation. *Gastroenterology* 1989; **84**: 127-132
41 **Stivland T**, Camilleri M, Vassallo M, Proano M, Rath D, Brown M, Thomforde G, Pemberton J, Phillips S. Scintigraphic measurement of regional gut transit in idiopathic constipation. *Gastroenterology* 1991; **101**: 107-115
42 **Smout AJ**, Brummer RJ. Gastrointestinal surgery and gastroenterology. IX. Obstipation: etiology and diagnosis. *Ned Tijdsch Geneeskd* 2000; **144**: 878-884
43 **Webster C**, Dayton M. Results after colectomy for colonic inertia: a sixteen-year experience. *Am J Surg* 2001; **182**: 639-644
44 **Redmond JM**, Smith GW, Barofsky I, Ratych RE, Goldsborough DC, Schuster MM. Psychological tests to predict long-term outcome of total abdominal colectomy for intractable constipation. *Am J Gastroenterol* 1995; **90**: 748-753
45 **Frexinos J**. Inertie colique primitive: mythe ou réalité? *Gastroenterol Clin Biol* 1987; **11**: 302-306
46 **Bassotti G**, Betti C, Pelli MA, Morelli A. Extensive investigation on colonic motility with pharmacological testing is useful for selecting surgical options in patients with inertia colica. *Am J Gastroenterol* 1992; **87**: 143-147
47 **Snape WJ**. Role of colonic motility in guiding therapy in patients with constipation. *Dig Dis* 1997; **15**(Suppl 1): 104-111
48 **Shafik A**, Shafik AA, El-Sibai O, Mostafa RM. Electric activity of the colon in subjects with constipation due to total colonic inertia: an electrophysiological study. *Arch Surg* 2003; **138**: 1007-1011
49 **Bassotti G**, Chiarioni G, Germani U, Battaglia E, Vantini I, Morelli A. Endoluminal instillation of bisacodyl in patients with severe (slow transity type) constipation is useful to test residual colonic propulsive activity. *Digestion* 1999; **60**: 69-73
50 **De Schryver AM**, Samsom M, Smout AI. Effects of a meal and bisacodyl on colonic motility in healthy volunteers and patients with slow-transit constipation. *Dig Dis Sci* 2003; **48**: 1206-1212
51 **Whitehead WE**, Wald A, Diamant NE, Enck P, Pemberton JH, Rao SS. Functional disorders of the anus and rectum. *Gut* 1999; **45**(Suppl II): II55-II59
52 Churchill's illustrated medical dictionary. *Churchill Livingstone New York* 1994

Edited by Zhu LH **Proofread by** Xu FM

PO Box 2345, Beijing 100023, China
Fax: +86-10-85381893
E-mail: wjg@wjgnet.com www.wjgnet.com

World J Gastroenterol 2004;10(17):2468-2471
World Journal of Gastroenterology
Copyright © 2004 by The WJG Press ISSN 1007-9327

• LIVER CANCER •

Advantages of assaying telomerase activity in ascites for diagnosis of digestive tract malignancies

Chung-Pin Li, Tze-Sing Huang, Yee Chao, Full-Young Chang, Jacquline Whang-Peng, Shou-Dong Lee

Chung-Pin Li, Full-Young Chang, Shou-Dong Lee, Division of Gastroenterology, Department of Medicine, Taipei Veterans General Hospital and Institute of Clinical Medicine, National Yang-Ming University School of Medicine, Taipei 11217, Taiwan, China
Tze-Sing Huang, Jacqueline Whang-Peng, Cancer Research Division, National Health Research Institutes and Institute of Clinical Medicine, National Yang-Ming University School of Medicine, Taipei 11217, Taiwan, China
Yee Chao, Cancer Center, Taipei Veterans General Hospital, Central Clinic Hospital, and National Yang-Ming University School of Medicine, Taipei 11217, Taiwan, China
Supported by the grant NSC89-2320-B-075-049 from the National Science Council, Taiwan
Correspondence to: Chung-Pin Li, M.D., Division of Gastroenterology, Department of Medicine, Taipei Veterans General Hospital, No. 201, Sec. 2, Shih-Pai Road, Taipei 11217, Taiwan, China. cpli@vghtpe.gov.tw
Telephone: +886-2-28757308 **Fax:** +886-2-28739318
Received: 2003-12-11 **Accepted:** 2004-02-24

Abstract

AIM: To evaluate the diagnostic value of assaying telomerase activity in ascites cells for the differential diagnosis of malignant and non-malignant ascites.

METHODS: Ascites from 40 patients with hepatocellular carcinoma (HCC), 31 with non-HCC gastrointestinal carcinoma (CA), and 24 with liver cirrhosis (LC) were analyzed for telomerase activity. The telomerase activities in cell pellets from ascites were measured according to the Telomeric Repeat Amplification Protocol (TRAP) and quantified with a densitometer.

RESULTS: Positive telomerase activity was detected in 16 of 31 (52%) CA patients, 10 of 40 (25%) HCC patients, and 1 of 24 (4%) LC patients ($P<0.001$). The telomerase activity was higher in the ascites of CA patients than in the ascites of HCC or LC patients (CA: 22.9±5.8, HCC: 6.7±2.5, LC: 1.3±1.3, $P = 0.001$). Cytology was positive in 18 CA patients (58%) and 1 HCC patient (2.5%), respectively. The positive telomerase activity was not related to patients' age, gender, and ascitic protein concentration, but to white blood count ($r = 0.31$, $P = 0.002$), neutrophil count ($r = 0.29$, $P = 0.005$), and the C-reactive protein level ($r = 0.29$, $P = 0.018$). When the results of both cytological examination and telomerase assay were considered together, the sensitivity increased to 77% for CA patients, 25% for HCC patients, and 48% for all 71 gastrointestinal cancer patients.

CONCLUSION: Combining cytological examination of ascites with telomerase activity assay significantly improves the differential diagnosis between malignant and non-malignant ascites.

Li CP, Huang TS, Chao Y, Chang FY, Whang-Peng J, Lee SD. Advantages of assaying telomerase activity in ascites for diagnosis of digestive tract malignancies. *World J Gastroenterol* 2004; 10(17): 2468-2471
http://www.wjgnet.com/1007-9327/10/2468.asp

INTRODUCTION

Ascites is a common complication of malignancy. Carcinoma of any organ can metastasize to the peritoneum. Gastric, colon, pancreatic, ovarian, breast, and lung carcinomas, as well as lymphoma, are the most common tumors associated with malignant ascites[1]. Hepatocellular carcinoma (HCC) is the leading cause of cancer mortality in Asia[2]. Ascites is also commonly seen in HCC patients, especially in terminal stage or when complicated with liver cirrhosis (LC). The pathophysiological mechanisms for the ascites production in LC are quite distinct from those for malignancy-related ascites[3]. The conventional diagnostic methods are sometimes inefficient and unsatisfactory to diagnose ascites as malignancy-related. For example, malignant ascites could be diagnosed by cytological examination of the ascitic fluids in only 50-70% of patients with ascites[1].

Telomeres (special DNA structures that contain TTAGGG repeats at the ends of all eukaryotic chromosomes) have important functions in protecting genomic DNA from degradation and deleterious recombination events[4]. Telomerase, an RNA-dependent DNA polymerase, can maintain the telomeric length by acting as a reverse transcriptase[4]. In humans, tumor cells escape programmed cell senescence through reactivation of telomerase[5]. These immortalized cells can compensate for telomeric shortening at each cell division, leading to progressive neoplastic evolution[5,6]. Telomerase re-expression was found in 85% of human malignant tumors[7-10]. The use of telomerase assay for cancer diagnosis might be possible because telomerase is thought to be re-expressed in malignant lesions but rarely in normal somatic cells[7-10]. Some studies also suggested that the telomerase activity of ascites could be a sensitive marker for differentiating malignancy-related ascites from nonmalignant ascites[11-13]. However, these studies included only small numbers of gastrointestinal tract cancer and HCC patients.

This study was to assess the diagnostic value of using telomerase activity assay to distinguish digestive tract cancer-derived ascites from benign ascites.

MATERIALS AND METHODS

Patients

Ninety-five patients with ascites undergoing a therapeutic or diagnostic paracentesis in Taipei Veterans General Hospital were enrolled prospectively into this study. These patients were divided into three groups on the basis of the cause of the ascites.

HCC Group consisted of 40 patients with HCC. The diagnoses were made by imaging studies (abdominal sonography and/or computed tomography and/or magnetic resonance imaging) and serum α-fetoprotein levels above 400 IU/mL in 34 patients, and were confirmed by liver biopsy in the remaining 6 patients.

CA Group consisted of 31 patients with non-HCC gastrointestinal carcinoma, including 10 gastric, 8 colon, 10 pancreatic cancers, and 3 cholangiocarcinomas (19 with liver metastasis and 12 without). All diagnoses were histologically confirmed.

LC Group comprised 24 patients with sterile uncomplicated cirrhotic ascites. Liver cirrhosis was diagnosed by typical clinical findings (splenomegaly, ascites and/or esophageal

varices), imaging studies (abdominal sonography and/or computed tomography and/or magnetic resonance imaging) and laboratory findings in 20 patients, and was confirmed by a liver biopsy in the remaining 4 patients. The serum α-fetoprotein level was <20 IU/mL, and an ultrasound showed no evidence of malignancy in each patient.

Ascitic fluids were subjected to routine assays, such as cell count and categorization, Gram's stain and culture, total proteins, albumin, and cytological examination. Blood samples for serum albumin determination were also taken at the same time as the above measurements to calculate the serum-ascites albumin gradient (SAAG). The ascites was also centrifuged and the sediment was detected with the Telomeric Repeat Amplification Protocol (TRAP). The samples were collected in heparinized containers and centrifuged at 2 000 r/min for 10 min at 4 °C. The supernatant was decanted. Cells were washed twice with ice-cold phosphate-buffered saline (PBS) and were stored in a 1.5-mL tube at -80 °C until assay. For bloody specimens, excessive RBCs were removed by Ficoll-Hypaque density-gradient centrifugation[14]. All samples were coded so that technicians running the assays were blinded as to the source of the samples.

Telomeric repeat amplification protocol (TRAP)

The telomerase activity was assayed according to the protocol described previously[15]. Cell lysates were prepared in 200 μL of lysis buffer consisting of 10 mmol/L Tris-HCl (pH 7.5), 5 g/L CHAPS, 1 mmol/L $MgCl_2$, 1 mmol/L EGTA, 100 mL/L glycerol, 0.1 mmol/L benzamidine, and 5 mmol/L β-mercaptoethanol. Aliquots of extracts were treated with or without RNase A (Sigma, St. Louis, MO) in a final concentration of 0.05 mg/mL for 30 min at 37 °C. Then, each TRAP reaction was performed at 30 °C for 30 min in 50 μL of reaction mixture containing 200 ng of cell lysates, 20 mmol/L Tris-HCl (pH 8.3), 0.5 g/L Tween-20, 1.5 mmol/L $MgCl_2$, 63 mmol/L KCl, 1 mmol/L EGTA, 250 μmol/L dNTPs, Primer Mix (Intergen Co., Purchase, NY), and 2 units of Taq polymerase (Roche Molecular Biochemicals, Indianapolis, IN), and followed by 33 cycles of PCR: at 94 °C for 0.5 min and 59 °C for 0.5 min. One half of each reaction mixture was resolved in a 125 g/L polyacrylamide gel, and after staining with SYBR® Green (Molecular Probes, Eugene, OR), the image of the telomeric repeat pattern was printed and quantified within a range from 50 to 100 base pairs by Alpha-InnoTech IS500 Digital Imaging System (Avery Dennison, CA). All samples were run in duplicate and the reproducibility was confirmed. All extracts that produced 6-base-pair ladders were tested for sensitivity to RNase A pretreatment, which is indicative of real telomerase activity.

The positive telomerase activity in the ascites cell pellet was calculated according to TPG (Total Product Generated) = $(X-X_0)$ C_R/C $(R-R_0)$ ×100, X: density of sample, X_0: density of heat- or RNase-treated sample, C: density of internal standard of the sample, C_R: density of internal standard of the control template, R: density of control template, and R_0: density of lysis buffer.

Statistical analysis

Results were expressed as mean±SE. Unpaired Student's *t*-test or one-way analysis of variance (ANOVA) was used to analyze continuous variables between groups. Chi-square test or Fisher's exact test was used for comparison of categorical variables. Pearson's correlation was performed to determine whether a relationship between two parameters was significant. Sensitivities and specificities were calculated in accordance with standard methods. Statistical analyses were performed using the SPSS software (SPSS 10.0, SPSS *Inc*., Chicago, IL). Results were considered statistically significant at $P<0.05$.

RESULTS

Patient characteristics

The composition of the patients' ascites is shown in Table 1. The ascites protein level was significantly higher in CA than in HCC and LC patients ($P<0.001$). In addition, the SAAG of HCC and LC relative to CA patients was significantly elevated ($P<0.01$). The white blood cells in the ascites consisted mainly of lymphocytes in all groups of patients (CA: 74±5%, HCC: 72±5%, LC: 86±4%). The high mean PMN count in HCC patients resulted from blood leakage due to tumor rupture in some HCC patients.

Cytological examination of ascites

Positive cytological examination of ascites was recorded in 18 of 31 (58%) CA patients and 1 of 40 (2.5%) HCC patients. As a control group, none of LC samples showed a positive cytological outcome (Table 2). For the totally 71 gastrointestinal cancer patients, the diagnostic specificity of our cytological examination reached 100%. Because a positive cytological result could make a diagnosis of malignancy, our data suggested that the conventional cytological examination had a sensitivity of 58% for diagnosing the ascites of CA patients, while the sensitivity was only 2.5% for the HCC ascites.

Telomerase activity in ascites

Ascitic telomerase activity was detected by TRAP assay. Representative examples of the results are shown in Figure 1. Positive telomerase activity was detected in 16 of 31 (52%) CA patients and 10 of 40 (25%) HCC patients (Table 2). Only one LC patient (4%) showed positive ascitic telomerase activity ($P<0.001$). Among CA patients, 5 of 10 gastric cancers (50%), 3 of 8 colon cancers (38%), 7 of 10 pancreatic cancers (70%), and 1 of 3 cholangiocarcinomas (33%) were positive for ascitic telomerase activity (Table 2).

Table 1 Clinical characteristics and ascitic fluid analyses

	CA	HCC	LC
Number of patients	31	40	24
Age (yr)	65±2	65±2	67±2
Sex: Male / Female	21 / 10	35 / 5	18 / 6
Protein (g / dL)	2.9±0.2	1.5±0.1[d]	1.5±0.2[d]
SAAG (g / dL)	1.1±0.1	2.0±0.2[b]	2.0±0.2[b]
WBC (cells / mm^3)	481±107	847±590	149±27
RBC (cells / mm^3)	13 093±7 975	192 633±104 982	3 730±1 515
PMN (cells / mm^3)	177±78	698±550	20±8
Lymphocytes (cells / mm^3)	305±77	149±46[a]	128±26[a]

Data are expressed as mean±SE. CA: non-HCC gastrointestinal carcinoma, HCC: hepatocellular carcinoma, LC: liver cirrhosis, SAAG: serum-ascites albumin gradient, WBC: white blood count, PMN: polymorphonuclear cells. [a]$P<0.05$, [b]$P<0.01$, [d]$P<0.001$ if compared with CA patients.

Table 2 Comparison of telomerase activity assay and cytological examination (*n*, %)

Group (*n*)	Underlying diseases (*n*)	Positive telomerase	Positive cytology
CA (31)		16 (52)	18 (58)
	Gastric cancer (10)	5 (50)	6 (60)
	Colon cancer (8)	3 (38)	4 (50)
	Pancreatic cancer (10)	7 (70)	8 (80)
	Cholangiocarcinoma (3)	1 (33)	0 (0)
HCC (40)		10 (25)	1 (2.5)
LC (24)		1 (4)	0 (0)

CA: non-HCC gastrointestinal carcinoma, HCC: hepatocellular carcinoma, LC: liver cirrhosis.

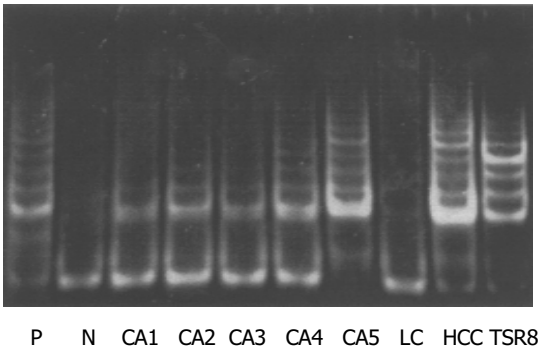

Figure 1 Representative results of ascitic telomerase activity assay. Lane P: positive control, Lane N: heat-inactivated sample, TSR8, quantitation control, CA: non-HCC gastrointestinal carcinoma, HCC: hepatocellular carcinoma, LC: liver cirrhosis.

It was noted that telomerase activity was higher in the ascites of CA patients than in the ascites of HCC and LC patients (CA: 22.9±5.8, HCC: 6.7±2.5, LC: 1.3±1.3, $P = 0.001$, Figure 2). In addition, as shown in Table 3, the telomerase activity was not related to patients' age, gender, serum albumin and ascitic protein amount, but to patients' white blood count ($r = 0.31$, $P = 0.002$), blood neutrophil count ($r = 0.29$, $P = 0.005$), and C-reactive protein level ($r = 0.29$, $P = 0.018$).

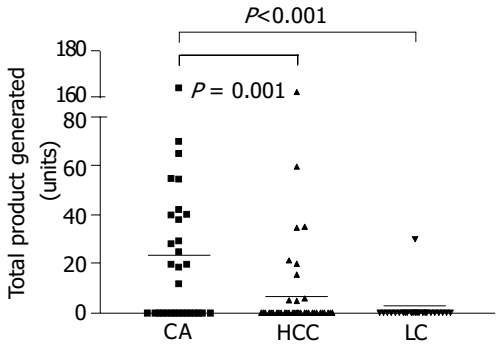

Figure 2 Individual and mean values of telomerase activities in CA, HCC and LC ascites.

When the results of both cytological examination and telomerase assay were combined together, the sensitivity increased to 77% (24/31) for CA patients, 25% (10/40) for HCC patients, and 48% (34/71) for the 71 gastrointestinal cancer patients. While cytological examination alone had a sensitivity of 27% (19/71) and telomerase assay alone had a sensitivity of 37% (26/71).

Table 3 Correlation between ascitic telomerase activity and clinical parameters

	r	*P*
Age (yr)	-0.05	0.65
Sex: Male/Female	-0.18	0.09
Serum albumin	-0.03	0.81
Ascites protein	0.08	0.44
Blood WBC	0.31	0.002
Blood neutrophil	0.29	0.005
Serum C-reactive protein	0.29	0.018

WBC: white blood count.

DISCUSSION

Diagnosis of cancer primarily depends on pathological examination. Ascites is a common complication of malignant neoplasms. The conventional cytological assessment of ascitic fluid can provide highly specific and accurate diagnoses of malignancies, but its unsatisfactory low sensitivity does not allow pathologists to early differentiate malignant ascites from non-malignant ascites[16]. Some studies have suggested that assay of telomerase activity in ascites might be an alternative method to improve the diagnosis[11,12]. However, only small numbers of patients with gastrointestinal tract cancers and HCC were included in those studies. The present study is the first one evaluating the value of telomerase activity assay in differential diagnosis of malignant and nonmalignant ascites of gastrointestinal cancers.

In our study, the sensitivity of telomerase activity assay of ascites from CA patients was 52%, comparable to that (58%) by cytological examination. This result is consistent with a previous report[11]. However, our TRAP sensitivity seemed to be less than that reported in another paper about ovarian cancers[17]. Although the average incidence of abnormal telomerase activity occurred in as high as 85% of human cancer patients, the incidence varied with different cancer types[8,18]. Among these, kidney, ovarian, and breast cancers showed the highest mean values of quantitatively assessed telomerase activities[19].

Ascites is commonly seen in HCC patients, especially in decompensated stages. Concomitant cirrhosis was present in more than 97% of HCC patients[20]. Not only the tumor growth, but also the underlying liver cirrhosis, led to ascites [20,21]. In analysis of our 24 LC and 40 HCC patients, only one HCC patient had a positive cytological diagnosis. This agrees with previously published data showing that malignant cells detected in ascites occurred in only 0-12% of the HCC patients[20-24], suggesting cytological examination is not an efficient tool for distinguishing HCC ascites from non-HCC LC ascites. Assay of telomerase activity (which was positive in 25% of HCC ascites samples were positive) is obviously better than the conventional cytological assessment.

Moreover, we speculated combining the results of both cytological examination and telomerase activity assay might improve diagnosis. We were able to identify malignancy in 77% of CA patients and 25% of HCC patients. For all 71 gastrointestinal cancer patients, the sensitivity of diagnosis increased to 48% (by the combination of both techniques) from 27% (by the cytological examination alone). Our study results thus indicate that TRAP assay is a useful tool for detecting cancer cells in ascites from gastrointestinal cancer patients.

Noteworthily, ascitic telomerase activity of gastrointestinal cancers is correlated with the increase in blood leukocytes and C-reactive protein. Leukocytosis and C-reactive protein are major markers of inflammation and cancer[25,26]. The source of

telomerase activity in ascitic cells could be cancer cells shed into the ascitic fluid or ascitic fluid leukocytes that were up-regulated by cancer-related cytokines[27-35]. Whatever the mechanism (s), assay of telomerase activity in ascitic cells may provide an adjunct to cytological examination in the diagnosis of digestive tract cancers.

REFERENCES

1 **Parsons SL,** Watson SA, Steele RJ. Malignant ascites. *Br J Surg* 1996; **83**: 6-14
2 **Tang ZY.** Hepatocellular carcinoma-cause, treatment and metastasis. *World J Gastroenterol* 2001; **7**: 445-454
3 **Runyon BA.** Care of patients with ascites. *N Engl J Med* 1994; **330**: 337-342
4 **Blackburn EH.** Structure and function of telomeres. *Nature* 1991; **350**: 569-573
5 **Shay JW.** Telomerase in human development and cancer. *J Cell Physiol* 1997; **173**: 266-270
6 **Wright WE,** Piatyszek MA, Rainey WE, Byrd W, Shay JW. Telomerase activity in human germline and embryonic tissues and cells. *Dev Genet* 1996; **18**: 173-179
7 **Kim NW,** Piatyszek MA, Prowse KR, Harley CB, West MD, Ho PL, Coviello GM, Wright WE, Weinrich SL, Shay JW. Specific association of human telomerase activity with immortal cells and cancer. *Science* 1994; **266**: 2011-2015
8 **Shay JW,** Wright WE. Telomerase activity in human cancer. *Curr Opin Oncol* 1996; **8**: 66-71
9 **Shay JW,** Bacchetti S. A survey of telomerase activity in human cancer. *Eur J Cancer* 1997; **33**: 787-791
10 **Yakoob J,** Hu GL, Fan XG, Zhang Z. Telomere, telomerase and digestive cancer. *World J Gastroenterol* 1999; **5**: 334-337
11 **Toshima S,** Arai T, Yasuda Y, Takaya T, Ito Y, Hayakawa K, Shibuya C, Yoshimi N, Shibayama M, Kashiki Y. Cytological diagnosis and telomerase activity of cells in effusions of body cavities. *Oncol Rep* 1999; **6**: 199-203
12 **Tangkijvanich P,** Tresukosol D, Sampatanukul P, Sakdikul S, Voravud N, Mahachai V, Mutirangura A. Telomerase assay for differentiating between malignancy-related and nonmalignant ascites. *Clin Cancer Res* 1999; **5**: 2470-2475
13 **Braunschweig R,** Yan P, Guilleret I, Delacretaz F, Bosman FT, Mihaescu A, Benhattar J. Detection of malignant effusions: comparison of a telomerase assay and cytologic examination. *Diagn Cytopathol* 2001; **24**: 174-180
14 **Boyum A.** Isolation of mononuclear cells and granulocytes from human blood. Isolation of monuclear cells by one centrifugation, and of granulocytes by combining centrifugation and sedimentation at 1 g. *Scand J Clin Lab Invest Suppl* 1968; **97**: 77-89
15 **Lee CC,** Huang TS. A novel topoisomerase II poison GL331 preferentially induces DNA cleavage at (C/G)T sites and can cause telomere DNA damage. *Pharm Res* 2001; **18**: 846-851
16 **Ehya H.** Effusion cytology. *Clin Lab Med* 1991; **11**: 443-467
17 **Duggan BD,** Wan M, Yu MC, Roman LD, Muderspach LI, Delgadillo E, Li WZ, Martin SE, Dubeau L. Detection of ovarian cancer cells: comparison of a telomerase assay and cytologic examination. *J Natl Cancer Inst* 1998; **90**: 238-242
18 **Kim NW.** Clinical implications of telomerase in cancer. *Eur J Cancer* 1997; **33**: 781-786
19 **Gelmini S,** Caldini A, Becherini L, Capaccioli S, Pazzagli M, Orlando C. Rapid, quantitative nonisotopic assay for telomerase activity in human tumors. *Clin Chem* 1998; **44**: 2133-2138
20 **Falconieri G,** Zanconati F, Colautti I, Dudine S, Bonifacio-Gori D, Di Bonito L. Effusion cytology of hepatocellular carcinoma. *Acta Cytol* 1995; **39**: 893-897
21 **Colli A,** Cocciolo M, Riva C, Marcassoli L, Pirola M, Di Gregorio P, Buccino G. Ascitic fluid analysis in hepatocellular carcinoma. *Cancer* 1993; **72**: 677-682
22 **Yuasa S,** Itoshima T, Nagashima H. Clinical studies of hepatocellular carcinoma with liver cirrhosis and ascites. *Acta Med Okayama* 1984; **38**: 291-299
23 **Runyon BA,** Hoefs JC, Morgan TR. Ascitic fluid analysis in malignancy-related ascites. *Hepatology* 1988; **8**: 1104-1109
24 **Nakashima T,** Okuda K, Kojiro M, Jimi A, Yamaguchi R, Sakamoto K, Ikari T. Pathology of hepatocellular carcinoma in Japan. 232 Consecutive cases autopsied in ten years. *Cancer* 1983; **51**: 863-877
25 **Toniatti C,** Arcone R, Majello B, Ganter U, Arpaia G, Ciliberto G. Regulation of the human C-reactive protein gene, a major marker of inflammation and cancer. *Mol Biol Med* 1990; **7**: 199-212
26 **Mahmoud FA,** Rivera NI. The role of C-reactive protein as a prognostic indicator in advanced cancer. *Curr Oncol Rep* 2002; **4**: 250-255
27 **Akiba J,** Yano H, Ogasawara S, Higaki K, Kojiro M. Expression and function of interleukin-8 in human hepatocellular carcinoma. *Int J Oncol* 2001; **18**: 257-264
28 **Chau GY,** Wu CW, Lui WY, Chang TJ, Kao HL, Wu LH, King KL, Loong CC, Hsia CY, Chi CW. Serum interleukin-10 but not interleukin-6 is related to clinical outcome in patients with resectable hepatocellular carcinoma. *Ann Surg* 2000; **231**: 552-558
29 **Price JA,** Kovach SJ, Johnson T, Koniaris LG, Cahill PA, Sitzmann JV, McKillop IH. Insulin-like growth factor I is a comitogen for hepatocyte growth factor in a rat model of hepatocellular carcinoma. *Hepatology* 2002; **36**: 1089-1097
30 **Su Q,** Liu YF, Zhang JF, Zhang SX, Li DF, Yang JJ. Expression of insulin-like growth factor II in hepatitis B, cirrhosis and hepatocellular carcinoma: its relationship with hepatitis B virus antigen expression. *Hepatology* 1994; **20**(4 Pt 1): 788-799
31 **Akiyama M,** Hideshima T, Hayashi T, Tai YT, Mitsiades CS, Mitsiades N, Chauhan D, Richardson P, Munshi NC, Anderson KC. Cytokines modulate telomerase activity in a human multiple myeloma cell line. *Cancer Res* 2002; **62**: 3876-3882
32 **Wilson J,** Balkwill F. The role of cytokines in the epithelial cancer microenvironment. *Semin Cancer Biol* 2002; **12**: 113-120
33 **Counter CM,** Gupta J, Harley CB, Leber B, Bacchetti S. Telomerase activity in normal leukocytes and in hematologic malignancies. *Blood* 1995; **85**: 2315-2320
34 **Hiyama K,** Hirai Y, Kyoizumi S, Akiyama M, Hiyama E, Piatyszek MA, Shay JW, Ishioka S, Yamakido M. Activation of telomerase in human lymphocytes and hematopoietic progenitor cells. *J Immunol* 1995; **155**: 3711-3715
35 **Weng NP,** Levine BL, June CH, Hodes RJ. Regulated expression of telomerase activity in human T lymphocyte development and activation. *J Exp Med* 1996; **183**: 2471-2479

Edited by Zhu LH and Xu FM

PO Box 2345, Beijing 100023, China
Fax: +86-10-85381893
E-mail: wjg@wjgnet.com www.wjgnet.com

World J Gastroenterol 2004;10(17):2472-2477
World Journal of Gastroenterology
Copyright © 2004 by The WJG Press ISSN 1007-9327

• LIVER CANCER •

Thrombocytosis: A paraneoplastic syndrome in patients with hepatocellular carcinoma

Shinn-Jang Hwang, Jiing-Chyuan Luo, Chung-Pin Li, Cheng-Wei Chu, Jaw-Ching Wu, Chiung-Ru Lai, Jen-Huei Chiang, Gar-Yang Chau, Wing-Yiu Lui, Chun-Chung Lee, Full-Young Chang, Shou-Dong Lee

Shinn-Jang Hwang, Department of Family Medicine, Taipei Veterans General Hospital and National Yang-Ming University School of Medicine, Taiwan, China
Shinn-Jang Hwang, Jiing-Chyuan Luo, Chung-Pin Li, Cheng-Wei Chu, Jaw-Ching Wu, Full-Young Chang, Shou-Dong Lee, Division of Gastroenterology, Department of Medicine, Taipei Veterans General Hospital and National Yang-Ming University School of Medicine, Taiwan, China
Chiung-Ru Lai, Department of Pathology, Taipei Veterans General Hospital and National Yang-Ming University School of Medicine, Taiwan, China
Jen-Huei Chiang, Department of Radiology, Taipei Veterans General Hospital and National Yang-Ming University School of Medicine, Taiwan, China
Gar-Yang Chau, Wing-Yiu Lui, Department of Surgery, Taipei Veterans General Hospital and National Yang-Ming University School of Medicine, Taiwan, China
Chun-Chung Lee, Central Laboratory, Shin Kong Wu Ho-Su Memorial Hospital, Taiwan, China
Shinn-Jang Hwang, Taipei Municipal Yang-Ming Hospital, Taipei, Taiwan, China
Supported by a grant from Taipei Veterans General Hospital, Taiwan, No. VGH88-299
Correspondence to: Shinn-Jang Hwang, M.D., F.A.C.G., Superintendent Office, Taipei Municipal Yang-Ming Hospital, 105 Yu-Sheng Street, Shih-Lin, Taipei, 111, Taiwan, China. sjhwang@vghtpe.gov.tw
Telephone: +886-2-28353461 **Fax**: +886-2-28347528
Received: 2004-02-06 **Accepted:** 2004-02-24

Abstract

AIM: Hepatocellular carcinoma (HCC) patients manifest a variety of paraneoplastic syndromes. Thrombocytosis was reported in children with hepatoblastoma. The aims of this study were to evaluate the prevalence and clinical significance of thrombocytosis in HCC patients and its relationships with serum thrombopoietin (TPO).

METHODS: We retrospectively reviewed clinical, biochemical and image data of 1 154 HCC patients. In addition, we measured platelet count and serum TPO in HCC patients with and without thrombocytosis, in patients with cirrhosis, chronic hepatitis and healthy subjects in a cross-sectional study.

RESULTS: Thirty-one (2.7%) of 1 154 HCC patients had thrombocytosis (platelet count >/=400 K/mm^3). HCC patients with thrombocytosis were significantly younger, had a higher serum α-fetoprotein, higher rate of main portal vein thrombosis, larger tumor volume, shorter survival, and were less likely to receive therapy than HCC patients without thrombocytosis. Multivariate logistic regression analyses showed that tumor volumes >/=30% and serum α-fetoprotein >/=140 000 ng/mL could significantly predict thrombocytosis. HCC patients with thrombocytosis had a significantly higher mean serum TPO than those without, as well as patients with cirrhosis, chronic hepatitis and healthy subjects. Platelet count and serum TPO dropped significantly after tumor resection in HCC patients with thrombocytosis and re-elevated after tumor recurred. Furthermore, the expression of TPO mRNA was found to be more in tumor tissues than in non-tumor tissues of liver in an HCC patient with thrombocytosis.

CONCLUSION: Thrombocytosis is a paraneoplastic syndrome of HCC patients due to the overproduction of TPO by HCC. It is frequently associated with a large tumor volume and high serum α-fetoprotein.

Hwang SJ, Luo JC, Li CP, Chu CW, Wu JC, Lai CR, Chiang JH, Chau GY, Lui WY, Lee CC, Chang FY, Lee SD. Thrombocytosis: A paraneoplastic syndrome in patients with hepatocellular carcinoma. *World J Gastroenterol* 2004; 10(17): 2472-2477
http://www.wjgnet.com/1007-9327/10/2472.asp

INTRODUCTION

Hepatocellular carcinoma (HCC) is the most common malignancy in Taiwan. During its clinical course, patients may manifest a variety of paraneoplastic syndromes, including hypercholesterolemia, hypoglycemia, hypercalcemia, and erythrocytosis[1]. According to our previous reports, the prevalence of paraneoplastic syndromes was 11.4-12.1% for hypercholesterolemia, 2.8-5.3% for hypoglycemia, 1.8-4.1% for hypercalcemia, and 2.5-3.1% for erythrocytosis[2-6]. Thrombocytosis has been found in children with hepatoblastoma and other malignancies[7-9]. The prevalence and clinical significance of thrombocytosis in adult patients with HCC have not been previously reported.

Human thrombopoietin (TPO), also known as megakaryocyte growth factor, is known to play a key role in the development of megakaryocytes[10,11]. TPO is secreted principally by hepatocytes and bone marrow stromal cells[10-14]. In addition, the expression of TPO gene has been found in both rat and human hepatoma cell lines [15,16]. The relationships between serum TPO levels and platelet counts in HCC patients, especially those associated with thrombocytosis, are of clinical interest. Our aim was to evaluate the prevalence of thrombocytosis in Chinese patients with HCC in a retrospective study. The clinical, biochemical and image characteristics of HCC patients with thrombocytosis were evaluated. Moreover, in order to evaluate the role of serum TPO in the manifestations of thrombocytosis in HCC patients, serum TPO levels were measured in HCC patients (with and without thrombocytosis), cirrhotic patients, chronic hepatitis patients, and normal subjects in a cross-sectional study.

MATERIALS AND METHODS

The clinical, laboratory and image data were retrospectively reviewed in 1 269 consecutive patients diagnosed with HCC at the Division of Gastroenterology, Taipei Veterans General Hospital, from January 1991 to December 1994[6]. Of these patients, 1 253 were enrolled in this study who met the following criteria: (1) histological proof of HCC; or (2) at least two typical HCC image findings (ultrasonography, computerized tomography, celiac angiography or magnetic resonance imaging) along with a serum AFP of more than 20 ng/mL. Among

the 1 253 patients, data of 1 197 cases were analyzed after excluding the patients with incomplete examination and data for analysis. Finally, data of 1 154 patients were selected for analyses in this study after excluding 43 patients with an evidence of acute infections or gastrointestinal bleeding. Patients with polycythemia vera were also excluded.

We defined hypercholesterolemia in HCC patients as a serum cholesterol level greater than 250 mg/dL (two standard deviations above the mean value of age-and-sex-matched healthy controls); hypoglycemia as plasma glucose less than 60 mg/dL; hypercalcemia as corrected serum calcium level more than 11.0 mg/dL; and erythrocytosis as a hemoglobin level greater than 16.7 gm/dL or hematocrit greater than 50% as in our previous reports[2-6]. Thrombocytosis was defined as having a platelet count greater than 400 K/mm^3.

To compare the serum TPO level, 18 consecutive HCC patients with thrombocytosis and 72 age-sex-tumor volume matched HCC patients without thrombocytosis were consecutively collected in a cross-sectional study from January 1999 to December 2000. In addition, 42 age-sex-matched cirrhotic patients and 66 chronic hepatitis patients were randomly selected for comparison. The etiologies of chronic hepatitis and cirrhosis were either viral hepatitis B or hepatitis C, which were all confirmed by liver biopsies. None of the patients with chronic hepatitis or cirrhosis received interferon or other anti-viral treatments before blood sampling. Alcoholic patients were not enrolled. Patients were also excluded if an acute infection or gastrointestinal bleeding was noted during enrollment. In addition, 62 healthy subjects who received their annual physical examinations at Taipei Veterans General Hospital, and whose age and sex were matched with the aforementioned 90 HCC patients, were randomly selected as healthy controls. Sera of the aforementioned subjects or patients were stored in aliquots at -70 °C until analyzed.

The underlying liver cirrhosis in HCC patients was diagnosed histologically or by characteristic image findings with the presence of ascites or esophageal varices. Patients with cirrhosis were given a score from 5-15 according to Child-Pugh's classification[17]. Tumor volume was calculated from computerized tomographic films and was expressed as percentages of tumor volume in total liver volume. The grade of differentiation and arrangement of tumor cells were assessed by a liver pathologist according to the classification of Edmondson and Steiner[18]. The pathologist was not given any clinical information pertaining to the biopsy specimens.

All clinical data of HCC patients including age, sex, Child-Pugh's scores, liver biochemistries (measured by a Hitachi Model 736 automatic analyzer, Tokyo, Japan), prothrombin time, and complete blood counts were recorded when an HCC was first diagnosed or at the time the thrombocytosis developed. Serum α-fetoprotein (AFP) was measured by a commercial kit (ELSA2-AFP, CIS bio-international, Cedex, France). Anti-HCV was measured by a second-generation enzyme immunoassay kit (Abbott Laboratories, Chicago, IL, USA). The serum markers of hepatitis B surface antigen (HBsAg) and antibody to hepatitis D virus (Abbott Laboratories) were recorded. Distant metastases to extrahepatic regional lymph nodes or other organs were evaluated by image studies. Methods of therapy for HCC, including surgical resection of tumors, transcatheter arterial chemoembolization (TACE), sono-guided percutaneous ethanol injection, or systemic chemotherapy and survival times were recorded in each patient. This study was approved by Taipei Veterans General Hospital, Taiwan.

Serum TPO levels were quantitatively measured by a solid phase enzyme immunoassay (Quantikine, R&D systems, Abingdon, UK). For the expression of TPO mRNA, an equal amount of fresh frozen tumors and non-tumor parts of the liver samples from a patient with thrombocytosis who received lobectomy for HCC were homogenized with a pestle. Total RNA was purified by TRIZOL reagent (Invitrogen and Life Technologies, Rockville, MD, USA). Reverse transcription-polymerase chain reaction (RT-PCR) was carried out to amplify 1 μg RNA using the First-strain cDNA Synthesis Kit (Amersham Pharmacia Biotech, Buckinghamshire, UK) according to the instruction manual. PCRs were carried out with 35 cycles at 94 °C for 1 min, at 60 °C for 1 min and at 72 °C for 1 min. Primer sequences were sense: 5'-TGCGTTTCCTGATGCTTGTAG-3' and anti-sense: '-AACCTTACCCTTCCTGAGACA-3'[12]. β-actin was used as an internal standard and diethyl pyrocarbonate-treated water was used as a negative control. The analysis of PCR products was performed by 20 g/L agarose gel electrophoresis. For quantitation of TPO mRNA, the PCR product was purified by the QIAquick Gel Extraction Kit (QIAGEN GmbH, Hilden, Germany) and $A_{260\ nm}$ was measured to estimate the DNA contents. Serial dilutions of this standard were then included in the following real-time PCR along with samples to produce a standard curve. Quantitative PCR was performed in 20 μL reaction capillaries using 1×DNA master SYBR Green I mix (Roche Diagnostics, Indianapolis, IN, USA), bovine serum albumin, 4 mmoL/L $MgCl_2$, 200 μmoL/L dNTPs, 0.4 U InViTaq-polymerase (InViTec; Berlin, Germany), 1 μL cDNA and 0.5 μmoL/L of the TPO-specific sense and antisense primers. DNA amplification, data collection and analyses were performed with LightCycler (Roche Diagnostics)[19]. The program was optimized and performed finally as denaturation at 94 °C for 30 s followed by 40 cycles of amplification (at 94 °C for 0.1 s, 60 °C for 0.1 s, 72 °C for 20 s). The temperature ramp rate was 20 °C/s. At the end of each extension step, the fluorescence of each sample was measured to allow the quantification of the PCR product. After the PCR was completed, the melting curve of the product was measured by a temperature gradient from 60 °C to 96 °C at 0.2 °C/s with continuous fluorescence monitoring to produce a melting profile of the primers. For normalization, the amount of TPO amplicon was divided by the amount of β-actin amplicon of the respective sample.

All data are expressed as mean±SD. Results were compared between groups using the Chi-square test, Fisher's exact test, Student's *t*-test, Mann-Whitney test or cross tabulation depending on the type of data analyzed. Survival adjusted for therapy was analyzed using the Kaplan-Meier method and was compared using the log rank method. Univariate and multivariate logistic regression using SPSS software (SPSS *Inc*., Chicago, IL, USA) were performed to evaluate the predictive values of the patients' clinical, laboratory, and tumor features associated with thrombocytosis. For all tests, only the results with *P* values less than 0.05 (two-tail test) were considered to be statistically significant.

RESULTS

Among the 1 154 HCC patients (1 005 males, 149 females, mean age 62.0±12.0 years, with a range of 13 to 84 years), 735 (63.7%) patients were HBsAg positive, 180 (15.6%) were anti-HCV positive, 49 (4.3%) were positive for both HBsAg and anti-HCV and 19 (1.6%) were positive for HBsAg and antibody to hepatitis D virus. The mean serum AFP level was 43 983±163 097 ng/mL (median 268 ng/mL, range 3-1 892 500 ng/mL).

Totally, 243 (21.1%) of 1 154 patients had paraneoplastic syndromes during the clinical course of HCC, in which 175 had a single paraneoplastic manifestation and 68 had multiple paraneoplastic manifestations. Thirty -one (2.7%) of 1 154 HCC patients had thrombocytosis (mean platelet count 484±87 K/mm^3, range 403-688 K/mm^3). The prevalence of hypercholesterolemia was 12.6%, hypoglycemia was 5.4%, hypercalcemia was 4.4%, and erythrocytosis was 3.2%. Eighteen of 31 HCC patients with thrombocytosis had other paraneoplastic manifestations

(11 with hypercholesterolemia, 1 with hypoglycemia, 4 with hypercholesterolemia and hypoglycemia, 1 with hypercholesterolemia and hypercalcemia, and 1 with hypercholesterolemia, hypoglycemia and hypercalcemia). Nine -hundred and eleven HCC patients were free of paraneoplastic manifestations.

In comparison of the clinical, laboratory data and tumor features between HCC patients with thrombocytosis and those without, HCC patients with thrombocytosis were significantly younger in age, had a higher mean serum AFP level, higher rate of main portal vein (MPV) thrombosis, bilobar tumor involvement, larger tumor volume, were less likely to receive or be suitable for HCC therapy, and had a shorter survival time than those without thrombocytosis (Table 1). HCC patients with thrombocytosis tended to have more extra-hepatic metastases than those without thrombocytosis (32% *vs* 19%, $P = 0.059$). There were no significant differences in sex distribution, viral etiologies, mean Child-Pugh's scores, and rates of cirrhosis between the two groups. Two hundred and fifty-eight (22%) of 1 154 HCC patients and 10 (32%) of 31 patients with thrombocytosis had their HCC tissues for histological analyses. Among the 10 HCC patients with thrombocytosis, tumor cell arrangement showed a trabecular pattern in 7 patients, and a mixed trabecular and acinar pattern in 3. Tumor cell differentiation revealed grade I in 3 patients, grade II in 4 patients, and grade III in 3 patients. The tumor cell arrangement and differentiation showed no significant differences between patients with and without thrombocytosis.

Age, sex, viral hepatitis markers, serum AFP, MPV thrombosis, metastases, bilobar tumor involvement, and tumor volumes were all selected as independent variables in logistic regression analyses, with the presence of thrombocytosis as the dependent variable. The continuous variables were transformed to categorical variables with the cut-off points determined by the Receiver Operating Characteristic Curve. In an univariate analysis, an age <60 years, serum AFP >140 000 ng/mL, tumor volume >30% of the total liver volume, bilobar tumor involvement, and MPV tumor thrombosis were significantly correlated with the presence of thrombocytosis (Table 2). In a stepwise multivariate analysis, a tumor volume >30% (odds ratio: 9.901, 95% confidence interval: 2.187-44.402, $P = 0.003$) and serum AFP >140 000 ng/mL (odds ratio: 2.660, 95% confidence interval: 1.090-6.487, $P = 0.031$) were significant predictive variables associated with the presence of thrombocytosis in HCC patients.

In the cross-sectional study, the mean platelet count was 440±43 K/mm^3 (range 401 to 540 K/mm^3) in 18 HCC patients with thrombocytosis, 174±100 K/mm^3 (range 102 to 396 K/mm^3) in 72 HCC patients without thrombocytosis, 72±29 K/mm^3 (range 18 to 154 K/mm^3) in 41 patients with cirrhosis, 178±48 K/mm^3 (range 105 to 300 K/mm^3) in 66 patients with chronic hepatitis, and 212±35 K/mm^3 (range 125 to 347 K/mm^3) in 62 healthy controls. The mean serum TPO level was significantly higher in HCC patients with thrombocytosis (404±196 pg/mL), when compared with HCC patients without thrombocytosis (181±85 pg/mL), cirrhotic patients (103±34 pg/mL), chronic hepatitis patients (113±46 pg/mL), and healthy subjects (123±53 pg/mL) (Figure 1). Serum TPO levels were positively correlated with platelet counts among 90 HCC patients ($r = 0.474$, $P<0.001$). Among the10 HCC patients with thrombocytosis, the

Table 1 Comparison of clinical and laboratory data, and tumor features between hepatocellular carcinoma (HCC) patients with and without thrombocytosis

	HCC patients with thrombocytosis (n = 31)	HCC patients without thrombocytosis (n = 1 123)	P value
Age (yr)	52±19	62±12	<0.001
Sex (male: female)	25:6	980:143	0.201
HBV: HCV: HBV+HCV-related	24:1:0	711:179:49	0.114
Mean Child-Pugh's scores	7.2±2.1	6.8±2.2	0.336
Mean platelet counts (k/mm^3)	484±87	154±80	<0.001
Median (range)	441 (403-688)	133 (11-396)	
Mean α-fetoprotein (ng/mL)	251 042±458 734	57 879±212 788	<0.001
Median (range)	4 859 (4-1 892 500)	252 (3-1 621 700)	
Cirrhosis (+:-)	23:8	913:210	0.445
MPV tumor thrombosis (+:-)	11:20	171:952	0.005
Tumor metastases (+:-)	10:21	196:927	0.059
Tumor volumes %	63.5±21.2	30.7±26.9	<0.001
Both lobes with tumor involvements (+:-)	22:9	439:684	<0.001
Therapy for HCC (+:-)	10:21	583:540	0.048
Mean survival (d)	144±208	373±521	<0.001
Median (range)	77 (4-852)	147(2-3 666)	

Data were expressed as mean±SD. HBV: hepatitis B virus, HCV: hepatitis C virus, MPV: main portal vein.

Table 2 Significant predictive variables in association with thrombocytosis in hepatocellular carcinoma patients using univariate logistic analyses

Variables	Odds ratio	95% confidence interval	P value
Age <60 yr	2.905	1.415-5.967	0.004
α-fetoprotein >140 000 ng/mL[1]	6.802	3.515-14.663	<0.001
Tumor volume >30%[1]	16.1	3.757-68.333	<0.001
Both lobes with tumor involvements	3.788	1.732-8.306	<0.001
Main portal vein tumor thrombosis	3.408	1.435-6.467	0.004

[1]Significantly predictive variables in multivariate analyses.

mean platelet count dropped significantly from 420±48 K/mm^3 to 278±38 K/mm^3 (P<0.001) after a surgical tumor resection or TACE, while the mean platelet count for HCC patients with thrombocytosis, who did not receive any therapy, showed a progressive increase during follow up.

Figure 2 illustrates the relationship of platelet counts with the serum levels of cholesterol, AFP and TPO in a 36-year-old HCC male patient. The serum AFP level was 164 000 ng/mL and serum HBsAg was positive. Image studies revealed a large tumor mass over the right lobe of liver with an invasion to the left medial segment. Hypercholesterolemia (serum cholesterol level 602 mg/dL) and thrombocytosis (platelet count 403 K/mm^3) were noted at the diagnosis of HCC. He received a surgical removal of tumors followed by chemotherapy with 5-fluorouracil for 12 wk. Platelet counts, serum levels of cholesterol and AFP dropped significantly after a surgical removal of the tumors. However, all re-elevated when the tumor recurred 18 wk after surgical treatment. Serum TPO level was 360 pg/mL before surgery (platelet count 403 K/mm^3), and fell to 130 pg/mL one week after operation (platelet count 120 K/mm^3). Figure 3 shows the qualitative expression of TPO mRNAs using RT-PCR in tumor and matched non-tumor tissues of the resected liver samples. The expression of TPO mRNAs was more intensive in tumor than in the non-tumor liver tissues. The results from the quantitative real-time PCR also revealed that the concentration of TPO mRNAs in tumors was 1.92 times greater than in matched non-tumor liver tissues.

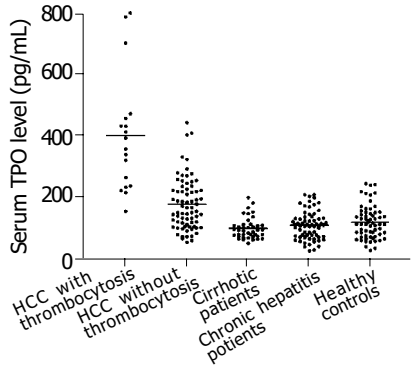

Figure 1 Distribution of serum thrombopoietin levels in hepatocellular carcinoma (HCC) patients with and without thrombocytosis, patients with cirrhosis, chronic hepatitis and healthy subjects. The mean serum thrombopoietin level in HCC patients with thrombocytosis was significantly higher than in HCC patients without thrombocytosis, patients with cirrhosis, chronic hepatitis and healthy subjects.

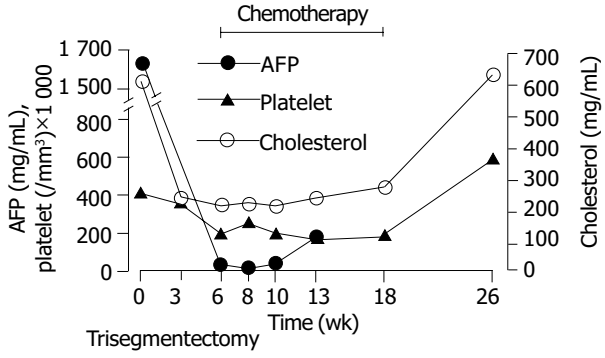

Figure 2 Clinical course of a hepatocellular carcinoma patient with thrombocytosis. The serum alfa-fetoprotein (AFP) level was 164 000 ng/mL before tumor resection. Hypercholesterolemia (serum cholesterol level: 602 mg/dL) and thrombocytosis (platelet count: 403 K/mm^3) were noted before operations. The platelet counts, serum levels of cholesterol and AFP fell significantly after a surgical removal of the tumors. However, all re-elevated when the tumor recurred 18 wk after surgical treatments.

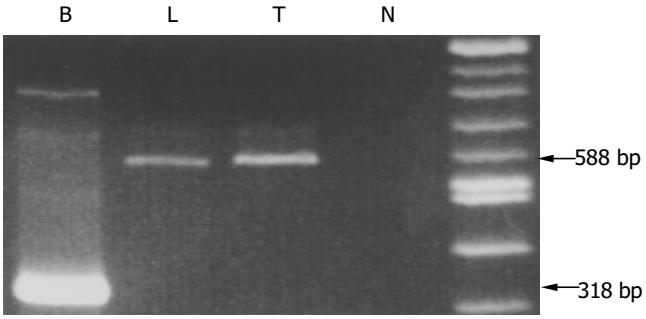

Figure 3 Analyses of thrombopoietin from tumor tissues (T) and non-tumor liver tissues (L) in a hepatocellular carcinoma patient with thrombocytosis using reverse-transcription polymerase chain reaction. β-actin was used as an internal standard (B). N: negative control. Results from an agarose gel electrophoresis showed a more intense density of thrombopoietin band from tumor tissues when compared with non-tumor liver tissues.

DISCUSSION

Common paraneoplastic syndromes seen in HCC patients include hypercholesterolemia, hypoglycemia, hypercalcemia, and erythrocytosis[1]. Thrombocytosis has been reported in children with hepatoblastoma[7-9]. The prevalence of thrombocytosis in HCC patients has not been previously reported. Our results showed that 2.7% of HCC patients hadthrombocytosis which was defined as a platelet count >400 K/mm^3. The prevalence of thrombocytosis might be underestimated because most HCC patients were associated with liver cirrhosis, and thrombocytopenia was frequently seen in these patients.

The clinical significance of thrombocytosis in HCC patients were similar to HCC patients with other paraneoplastic syndromes, including hypercholesterolemia, hypoglycemia, hypercalcemia, and erythrocytosis[2-6]. Large tumor volumes, high serum AFP, high rates of MPV tumor thrombosis, low rates of receiving therapy and poor prognosis have been identified in HCC patients with thrombocytosis. According to the multivariate logistic regression analyses, HCC patients with thrombocytosis were characterized by a large tumor volume and high serum AFP. HCC patients with thrombocytosis seemed to have a similar life expectancy as HCC patients with erythrocytosis or hypercholesterolemia, and had a better prognosis than patients with hypoglycemia and hypercalcemia which were usually pre-terminal events[6].

Before the cloning of TPO, the cause of thrombocytosis in children with hepatoblastoma and in other malignancies remains unclear. TPO, a glycoprotein hormone, is a potent stimulator of the growth and maturation of megakaryocytes and platelet production[10,11]. The main sites of TPO production are the liver and, to a lesser degree, the kidneys, bone marrow and spleen. Messenger RNA transcripts of TPO have been found mainly in the liver and released into circulation[14-16]. Most TPO is bound with and degraded by circulating platelets and megakaryocytes in the bone marrow, and the serum level is low. Circulating TPO levels are inversely correlated with the number of TPO receptors (c-Mpl-molecules) in regulating megakaryocytopoiesis and platelet production. When thrombocytopenia develops, binding receptors decrease and serum TPO levels increase. Elevated TPO levels stimulate megakaryocytopoiesis and result in increased platelet production[20-25]. This reverse relationship of platelet counts and serum TPO levels has been found in patients

with hematological diseases[26,27]. Patients with cirrhosis were frequently associated with low platelet counts. However, serum TPO levels in cirrhotic patients were found to be lower than chronic hepatitis patients or normal subjects due to inadequate TPO production by the diseased livers[28-32]. Serum TPO of cirrhotic patients increased after orthotopic liver transplantation, which was followed by an increase in platelet counts[14,33-35]. Our results revealed serum TPO levels were significantly lower in cirrhotic patients than in patients with chronic hepatitis or normal controls, and were consistent with previous reports.

Despite the fact that hepatoma cells have been found to express TPO *in vitro* and in animal models, the mechanisms by which thrombocytosis develops in HCC patients have not been studied. According to our results, HCC patients with thrombocytosis had a significantly higher mean serum TPO level than HCC patients without thrombocytosis. In addition, the platelet counts and serum TPO levels in HCC patients with thrombocytosis dropped after a surgical removal of the tumor or TACE, and re-elevated when a tumor recurred. Changes of platelet counts and serum TPO levels were parallel to the changes of serum AFP. Furthermore, by using the reverse transcription and real-time PCR methods, we demonstrated that the expression of TPO mRNA was more in tumor tissues than in matched non-tumor tissues in an HCC patient with thrombocytosis. Our results were consistent with the report that thrombocytosis in patients with hepatoblastoma was related to increased TPO production in tumors[9]. Thus, we speculate that thrombocytosis in HCC patients is due to the overproduction of TPO by tumors, and mostly in patients with a large tumor burden. The mechanisms of thrombocytosis in HCC patients are similar to those for other paraneoplastic manifestations. Hypoglycemia has been related to the overproduction of insulin-growth-factor II with insulin-like activities[2]. The cause of hypercalcemia has been related to overproduction of a parathyroid-related protein which interacts with parathyroid hormone receptors[4,36]. Elevation of serum erythropoietin has been seen in HCC patients with erythrocytosis[5,37].

In conclusion, thrombocytosis is one of the paraneoplastic syndromes in patients with HCC, due to the overproduction of TPO by HCC. HCC patients with thrombocytosis are associated with a large tumor volume and high serum AFP level.

REFERENCES

1 **Okuda K,** Kondo Y. Primary carcinomas of the liver. In: Haubrich WS, Schaffner F, Berk JE, eds. Gastroenterology Volume 3.5th ed. Philadelphia: W. B. *Saunders* 1995: 2467-2468

2 **Wu JC,** Daughaday WH, Lee SD, Hsiao TSY, Chou CK, Lin HD, Tsai YT, Chiang BN. Radioimmunoassay of serum IGF-I and IGF-II in patients with chronic liver diseases and hepatocellular carcinoma with or without hypoglycemia. *J Lab Clin Med* 1988; **112**: 589-594

3 **Hwang SJ,** Lee SD, Chang CF, Wu JC, Tsay SH, Lui WY, Chiang JH, Lo KJ. Hypercholesterolemia in patients with hepatocellular carcinoma. *J Gastroenterol Hepatol* 1992; **7**: 491-496

4 **Yen TC,** Hwang SJ, Wang CC, Lee SD, Yeh SH. Hypercalcemia and parathyroid hormone-related protein in hepatocellular carcinoma. *Liver* 1993; **13**: 311-315

5 **Hwang SJ,** Lee SD, Wu JC, Chang CF, Lu CL, Tsay SH, Lo KJ. Clinical evaluation of erythrocytosis in patients with hepatocellular carcinoma. *Chin Med J* 1994; **53**: 262-269

6 **Luo JC,** Hwang SJ, Li CP, Hsiao LT, Lai CR, Chiang JH, Lui WY, Chang FY, Lee SD. Paraneoplastic syndromes in patients with hepatocellular carcinoma in Taiwan. *Cancer* 1999; **86**: 799-804

7 **Nickerson HJ,** Silberman TL, McDonald TP. Hepatoblastoma, thrombocytosis, and increased thrombopoietin. *Cancer* 1980; **45**: 315-317

8 **Shafford EA,** Ritchard JP. Extreme thrombocytosis as a diagnostic clue to hepatoblastoma. *Arch Dis Child* 1993; **69**: 171-174

9 **Komura E,** Matsumura T, Kato T, Tahara T, Tsunoda Y, Sawada T. Thrombopoietin in patients with hepatoblastoma. *Stem Cells* 1998; **16**: 329-333

10 **de Sauvage FJ,** Hass PE, Spencer SD, Malloy BE, Gurney AL, Spencer SA, Darbonne WC, Henzel WJ, Wong SC, Kuang WJ, Oles KJ, Hultgren B Jr, Solberg LA, Goeddel DV, Eaton DL. Stimulation of megakaryocytopoiesis and thrombopoiesis by the c-Mpl ligand. *Nature* 1994; **369**: 533-538

11 **Lok S,** Kaushansky K, Holly RD, Kuijper JL, Lofton-Day CE, Oort PJ, Grant FJ, Helpel MD, Burkhead SK, Kramer JM, Bell LA, Sprecher CA, Blumberg H, Johnson R, Prunkard D, Ching AFT, Mathewes SL, Bailey MC, Forstrom JW, Buddle MM, Osborn SG, Evans SJ, Sheppard PO, Presnell SR, O'hara PJ, Hagen FS, Roth GJ, Foster DC. Cloning and expression of murine thrombopoietin cDNA and stimulation of platelet production *in vivo*. *Nature* 1994; **369**: 565-568

12 **Sungaran R,** Markovic B, Chong BH. Localization and regulation of thrombopoietin mRNA expression in human kidney, liver, bone marrow and spleen using *in situ* hybridization. *Blood* 1997; **89**: 101-107

13 **Nomura S,** Ogami K, Kawamura K, Tsukamoto I, Kudo Y, Kanakura Y, Kitamura Y, Miyazaki H, Kato T. Cellular localization of thrombopoietin mRNA in the liver by *in situ* hybridization. *Exp Hematol* 1997; **25**: 565-572

14 **Martin TG,** Somberg KA, Meng YG, Cohen RL, Heid CA, de Sauvage FJ, Shuman MA. Thrombopoietin levels in patients with cirrhosis before and after orthotopic liver transplantation. *Ann Intern Med* 1997; **127**: 285-288

15 **Shimada Y,** Kato T, Ogami K, Horie K, Kokubo A, Kudo Y, Maeda E, Sohma Y, Akahori H, Kawamura K, Miyazaki H. Production of thrombopoietin (TPO) by rat hepatocytes and hepatoma cell lines. *Exp Hematol* 1995; **23**: 1388-1396

16 **Hino M,** Nishizawa Y, Tagawa S, Yamane T, Morii H, Tatsumi N. Constitutive expression of the thrombopoietin gene in a human hepatoma cell line. *Biochem Biophys Res Commun* 1995; **217**: 475-481

17 **Pugh RN,** Murray-Lyon M, Dawson JL, Pietroni MC, Williams R. Transection of esophagus for bleeding esophageal varices. *Br J Surg* 1973; **60**: 646-649

18 **Okuda K,** Kondo Y. Primary carcinomas of the liver. In: Haubrich WS, Schaffner F, Berk JE, eds. Gastroenterology Volume 3. 5th ed. Philadelphia : W. B. *Saunders* 1995: 2462-2463

19 **Wittwer CT,** Ririe KM, Andrew RV, David DA, Gundry RA, Balis UJ. The LighCycler™ a microvolume multisample fluorimeter with rapid temperature control. *Biotechniques* 1997; **22**: 176-181

20 **McCarty JM,** Sprugel KH, Fox NE, Sabath DE, Kaushansky K. Murine thrombopoietin mRNA levels are modulated by platelet count. *Blood* 1995; **86**: 3668-3675

21 **Nichol JL,** Hokom MM, Hornkohl A, Sheridan WP, Ohashi H, Kato T, Li YS, Bartley TD, Choi E, Bogenberger J. Megakaryocyte growth and development factor. Analyses of *in vitro* effects on human megakaryopoiesis and endogenous serum levels during chemotherapy-induced thrombocytopenia. *J Clin Invest* 1995; **95**: 2973-2978

22 **Cohen-Solal K,** Villeval JL, Titeux M, Lok S, Vainchenker W, Wendling F. Constitutive expression of Mpl ligand transcripts during thrombocytopenia or thrombocytosis. *Blood* 1996; **88**: 2578-2584

23 **Stoffel R,** Wiestner A, Skoda RC. Thrombopoietin in thrombocytopenic mice: evidence against regulation at the mRNA level and for a direct regulatory role of platelets. *Blood* 1996; **87**: 567-573

24 **Emmons RV,** Reid DM, Cohen RL, Meng G,Young NS, Dunbar CE, Shulman NR. Human thrombopoietin levels are high when thrombocytopenia is due to increased platelet destruction. *Blood* 1996; **87**: 4068-4071

25 **Eaton DL,** de Sauvage FJ. Thrombopoietin: the primary regulator of megakaryocytopoiesis and thrombopoiesis. *Exp Hematol* 1997; **25**: 1-7

26 **Tahara T,** Usuki K, Sato H, Ohashi H, Morita H, Tsumura H, Matsumoto A, Miyazaki H, Urabe A, Kato A. A sensitive sandwich ELISA for measuring thrombopoietin in human serum: serum thrombopoietin levels in healthy volunteers and in patients with haemopoietic disorders. *Br J Haematology* 1996;

93: 783-788

27 **Tomita N,** Motomura S, Sakai R, Fujimaki K, Tanabe J, Fukawa H, Harano H, Kanamori H, Ogawa K, Mohri H, Marata A, Kodama F, Ishigatsubo Y, Tahara T, Kato T. Strong inverse correlation between serum TPO level and platelet count in essential thrombocythemia. *Am J Hematol* 2000; **63**: 131-135

28 **Peck-Radosavljevic M,** Zacherl J, Meng YG, Pidlich J, Lipinski E, Langle F, Steininger R, Muhlbacher F, Gang A. Is inadequate thrombopoietin production a major cause of thrombocytopenia in cirrhosis of the liver? *J Hepatol* 1997; **27**: 127-131

29 **Sezai S,** Kamisaka K, Ikegami F, Usuki M, Urabe A, Tahara T, Kato T, Miyazaki H. Regulation of hepatic thrombopoietin production by portal hemodynamics in liver cirrhosis. *Am J Gastroenterol* 1998; **93**: 80-82

30 **Wolber EM,** Ganschow R, Burdelski M, Jelkmann W. Hepatic thrombopoietin mRNA levels in acute and chronic liver failure of childhood. *Hepatology* 1999; **29**: 1739-1742

31 **Giannini E,** Borro P, Botta F, Fumagalli A, Malfatti F, Podesta E, Romagnoli P, Testa E, Chiarbonello B, Polegato S, Mamone M, Testa R. Serum thrombopoietin levels are linked to liver function in untreated patients with hepatitis C virus related chronic hepatitis. *J Hepatol* 2002; **37**: 572-577

32 **Koruk M,** Onuk MD, Akcay F, Savas MC. Serum thrombopoietin levels in patients with chronic hepatitis and liver cirrhosis, and its relationship with circulating thrombocyte counts. *Hepatogastroenterology* 2002; **49**: 1645-1648

33 **Goulis J,** Chau TN, Jordan S, Mehta AB, Watkinson A, Rolles K, Burroughs AK. Thrombopoietin concentrations are low in patients with cirrhosis and thrombocytopenia and are restored after orthotopic liver transplantation. *Gut* 1999; **44**: 754-758

34 **Faeh M,** Hauser SP, Nydegger UE. Transient thrombopoietin peak after liver transplantation for end stage liver disease. *Br J Haematol* 2001; **112**: 493-498

35 **Tsukahara A,** Sato Y, Yamamoto S, Szuki S, Nakatsuka H, Watanabe T, Kameyama H, Hatakeyama K. Thrombopoietin levels and peripheral platelet counts following living related donor liver transplantation. *Hepatogastroenterology* 2003; **50**: 227-230

36 **Suva LJ,** Winslow GA, Weltenhall RE, Hammonds RG, Moseley JM, Difenbach-Jagger H, Rodda CP, Kemp BE, Rodriguez H, Chen EY. A parathyroid hormone-related protein implicated in malignant hypercalcemia: cloning and expression. *Science* 1987; **237**: 893-896

37 **Kew MC,** Fisher JW. Serum erythropoietin concentrations in patients with hepatocellular carcinoma. *Cancer* 1986; **58**: 2485-2488

Edited by Zhu LH and Xu FM

PO Box 2345, Beijing 100023, China
Fax: +86-10-85381893
E-mail: wjg@wjgnet.com www.wjgnet.com

World J Gastroenterol 2004;10(17):2478-2481
World Journal of Gastroenterology
Copyright © 2004 by The WJG Press ISSN 1007-9327

• LIVER CANCER •

Potential involvement of leptin in carcinogenesis of hepatocellular carcinoma

Xiu-Jie Wang, Shu-Lan Yuan, Qing Lu, Yan-Rong Lu, Jie Zhang, Yan Liu, Wen-Dong Wang

Xiu-Jie Wang, Shu-Lan Yuan, Yan-Rong Lu, Jie Zhang, Division of Experimental Oncology, Key Laboratory of Biotherapy of Human Diseases of Ministry of Education, China, West China Hospital, Sichuan University, Chengdu 610041, Sichuan Province, China
Qing Lu, Yan Liu, Department of General Surgery, West China Hospital, Sichuan University, Chengdu 610041, Sichuan Province, China
Wen-Dong Wang, Pathology Department of West China Healthy College, Sichuan University, Chengdu 610041, Sichuan Province, China
Supported by the Grants From Sasakawa Medical Foundation of International Cooperation Department of Ministry of Public Health of China (054) and Science Foundation of West China University of Medical Sciences (L99016)
Correspondence to: Dr. Xiu-Jie Wang, Division of Experimental Oncology, Key Laboratory of Biotherapy of Human Diseases of Ministry of Education, China, West China Hospital, Sichuan University, Chengdu 610041, Sichuan Province, China. xiujiewang@yahoo.com
Telephone: +86-28-8423059 **Fax:** +86-28-85178772
Received: 2003-10-24 **Accepted:** 2003-12-29

Abstract

AIM: To investigate the potential involvement of leptin in carcinogenesis of hepatocellular carcinoma (HCC) and to elucidate the etiology, carcinogenesis and progress of HCC.

METHODS: Expressions of Ob gene product, leptin and its receptor, Ob-R were investigated in 36 cases of HCC specimens and corresponding adjacent non-tumorous liver tissues with immunohistochemical staining. The effect of leptin on proliferation of Chang liver cell line and liver cancer cell line SMMC-7721 was studied with cell proliferation assay (MTT).

RESULTS: Leptin expression was detected in 36 cases of adjacent non-tumorous liver tissues (36/36,100%) with moderate (++) to strong (+++) intensity; and in 72.22% (26/36) of HCC with weaker (+) intensity ($P<0.05$). Thirty of 36 (83.33%) cases of adjacent non-tumorous liver tissues were positive for Ob-R, with moderate (++) to strong (+++) intensity. In HCC, 11/36 (30.56%) cases were positive, with weak (+) intensity ($P<0.05$). In cell proliferation assay, leptin inhibited the proliferation of Chang liver cells. The cell survival rate was 10-13% lower than that of the untreated cells ($P>0.05$). Leptin had little effect on the proliferation of liver cancer cells ($P>0.05$).

CONCLUSION: High level expression and decreased or absent expression of leptin and its receptor in adjacent non-tumorous liver cells and HCC cells, inhibitory effect of leptin on the proliferation of normal Chang liver cells and no effect of leptin on proliferation of liver cancer cells, may provide new insights into the carcinogenesis and progression of human HCC. It could be assumed that leptin acting as an inhibitor and/or promoter, is involved in the process of carcinogenesis and progress of human HCC.

Wang XJ, Yuan SL, Lu Q, Lu YR, Zhang J, Liu Y, Wang WD. Potential involvement of leptin in carcinogenesis of hepatocellular carcinoma. *World J Gastroenterol* 2004; 10(17): 2478-2481
http://www.wjgnet.com/1007-9327/10/2478.asp

INTRODUCTION

Leptin, a circulating hormone secreted by adipocytes, is one of the major adipose cytokines acting as an important signaling molecule in energy regulation and food intake, and controls body weight homeostasis[1-3]. It modulates various physiological and pathophysiological states, including lipid metabolism, hematopoiesis, thermogenesis, obesity, and polycystic ovary syndrome[1,4]. Besides, leptin is also involved in obesity and carcinogenesis of some human cancers.

Recent studies suggested that leptin might play an important role in the process of initiation and progression of human cancers[2,3,5-12], but there were a difference and discordance among the results. Circulating levels of leptin were higher in cases of breast cancer[5], colorectal cancer[8], prostate cancer[6], eudiometrical cancer[13], and lower in cases of uterine leiomyomas than the controls[10], or had no difference in breast cancer[14]. One study showed that leptin might play a role in the development of prostate cancer[11]. Another study suggested plasma leptin was not associated with prostate cancer risk[10]. On the other hand, studies suggested that leptin expression was associated with invasive potential of functioning pituitary adenomas[15], and influenced cellular differentiation and the progression of prostate cancer[11]. *In vitr*o experimental studies, leptin not only stimulate proliferation of some human cancer cell lines, including breast cancer cell lines (ZR75-1, MCF-7, T-47D)[2,7,9,16-18], esophageal cancer cell lines (KYSE410, 150), prostate cancer cell lines (DU145 and PC-3)[2,3], acute myelogenous leukemia (AML)[19] cell lines, but also inhibited the growth of some human cancer cell lines, such as pancreas cancer cell lines (PANC-1, Mia-PaCa)[2]. The study results indicated that leptin had divergent effects on human cancer cell proliferation.

Hepatocellular carcinoma (HCC) is one of the most common malignancies in the world, and causes an estimated one million deaths annually. It has a poor prognosis due to its rapid infiltrating growth and complicating liver cirrhosis[20,21]. Epidemiological studies suggested that obesity was a risk factor of HCC complicated with alcoholic liver disease and cryptogenic cirrhosis[22,23]. Clinical investigations showed that serum leptin levels in alcoholic and post-hepatitis liver cirrhosis patients with or without HCC increased significantly compared with those in control subjects[24-30], suggesting that leptin is involved in the etiogenesis of hepatocellular carcinoma (HCC) in cirrhotic patients. Therefore, we hypotheses that leptin might be associated with the growth of liver cells and HCC cells, and played a role in carcinogenesis of hepatocellular carcinoma, but such a study has been reported. In order to confirm this hypothesis, the expression of leptin in human HCC and adjacent non-tumorous liver tissues was analyzed by immunohistochemical staining, and the effect of leptin on proliferation of normal liver cells and HCC cells *in vitro* was studied in this study.

MATERIALS AND METHODS

Immunohistochemical analysis of leptin and Ob-R expressions in human HCC and adjacent non-tumorous liver tissues

Patients and samples HCC specimens and corresponding adjacent non-tumorous liver tissues were collected from 36

patients surgically treated in West China Hospital of Sichuan University in China in 2000, all the patients were informed and consented to use their samples for this study. Of the 36 patients, 29 (80.56%) were males, 7 (19.44%) were females, their age ranged from 27 to 68 years (mean, 49.4 years), Twenty patients (20/36, 55.56%) were infected with HBV, 32 (32/36, 88.89%) were complicated with liver dysfunction, and 10 (10/36, 27.78%) with liver cirrhosis. None had any treatment before the surgical operation. All patients were diagnosed as HCC. The tissue specimens were routinely processed, formalin-fixed, and paraffin- embedded. Paraffinized sections were made for hematoxylin and eosin (HE) and immunohistochemical staining.

Reagents Ob (A-20) and Ob-R (H-300) rabbit anti-human polyclonal antibodies were purchased from Santa Cruz Biotechnology, USA. S-P immunohistochemical staining kit (SP9001) was purchased from Beijing Zhongshan Biological Technology Ltd.

Method Leptin protein and Ob-R were detected immunohitochemically with S-P method. Briefly, tissue sections were deparaffinized and rehydrated through graded alcohols. Antigen retrieval was performed by heating in microwave oven in 0.1 mol/L citrate buffer (pH 6). Then, endogenous peroxidase activity was blocked with 30 mL/L H_2O_2, and after treatment with normal goat serum, the sections were incubated with Ob (A-20) or Ob-R (H-300) rabbit anti-human polyclonal antibodies at a dilution of 1:100, overnight at 4°C, with biotinylated second antibody for 20 min, and with streptavidin/peroxidase for 30 min at room temperature. Subsequently, the sections were subjected to color reaction with 0.2 g/L 3,3 diaminobenzidine tetrahydrochloride containing 0.05 mL/L H_2O_2 in PBS (pH 7.4), and counterstained with hematoxylin lightly. In each staining run, a known leptin positive sample of fat tissue was added as a positive control, and a section of the same fat tissue incubated in PBS instead of Ob or Ob-R was included as a negative control.

Semi-quantitative evaluation was used to determine positively expressed cells by viewing 10 vision fields at ×400. Negative (-) indicated cells were stained less than 10%, mildly positive (+) showed 11-25% cells were stained, moderately positive (++) demonstrated 26-50% cells were stained, strongly positive (+++) revealed over 50% cells were stained. The intensity of staining in positive cells was compared with the negative control and scored as follows: negative (-), weak (+), moderate (++), strong (+++), the last three grades were all regarded as positive.

Proliferation assay in vitro

Reagents Chang liver cell line (ATCC CCL13) and liver cancer cell line SMMC-7721 were obtained from Shanghai Cell Biology Institute of Chinese Academy of Sciences. Human recombinant leptin was a product from Signa-Aldrich, Inc. USA. RPMI-1640 was the product of Gibco/BRL (Invitrogen Corporation, USA). Fetal bovine serum (FBS) was purchased from Huaxi Biology Institute (Chengdu, China). Trypsin, 3-(4, 5-dimethylthiazol-2-yl)-2, 5-diphenyltetrazolium bromide (MTT), and DMSO were purchased from the Sino-American Biotechnology Company of Beijing.

Cell culture Both Chang liver cell line and SMMC-7721 cell line were cultured in RPMI-1640 medium supplemented with 100 mL/L FBS, 100 U/mL penicillin, and 100 μg/mL streptomycin, at 37°C in a humidified atmosphere containing 50 mL/L CO_2.

Proliferation assay (MTT) Chang liver cells and SMMC-7721 cells were suspended at a concentration of 5×10^4/mL Then 200 μL of the cell suspension was placed in each well of a replicate 96-well microtiter plate. The cells were allowed to adhere overnight. Then different concentrations (10, 20, 40, 80, 160, 320 ng/mL) of leptin were added to each kind of cells. MTT assay was performed after 1-, 3-, 5-d growth. A 20 μL of 5 mg/mL of MTT was added to each well followed by incubation for 4 h at 37 . Formazan products were solubilized with DMSO; *A* values were read with an enzyme-linked immunosorbent assay reader (Bio-Tek, Houston, USA) at wavelength of 570 nm. All experiments were performed in triplicate. The effect of leptin on proliferation of Chang liver cells and SMMC-7721 cells were expressed as cell survival rates: *A* value of the treated group ÷*A* value of control group×100 %.

Statistics analysis

The data of immunohitochemical staining were analyzed with chi-square test. The data of cell proliferation assay were analyzed with variance analysis. $P<0.05$ was considered statistically significant.

RESULTS

Leptin expression in human HCC and adjacent non-tumorous liver tissues

The expressed Ob gene product, leptin was detected in all 36 specimen from adjacent non-tumorous liver tissues (36/36, 100%), with moderate (++) to strong (+++)intensity. The expression rate in HCC was 72.22% (26/36), but the intensity was weaker (+) than that in adjacent non-tumorous liver tissues (Figure 1), a significant difference in leptin expression was found between adjacent non-tumorous liver tissues and HCC ($P<0.05$). Ten of 36 specimens from HCC (10/36, 27.78%) even lost the expression of leptin, but Kupffer cells and vascular endothelial cells expressed high levels of leptin (Figure 2).

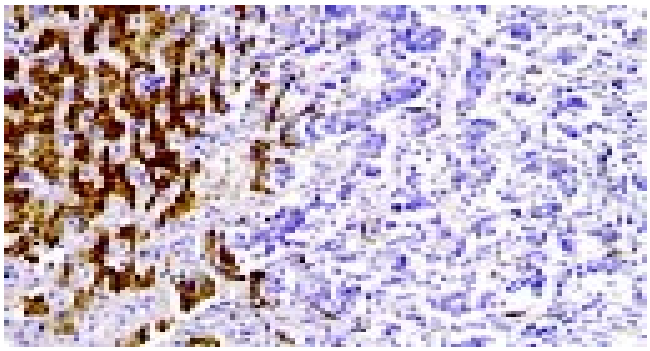

Figure 1 Expression of leptin in adjacent non-tumorous liver live cells (left) and absent expression in HCC cells (right). S-P immunohistochemical staining ×200.

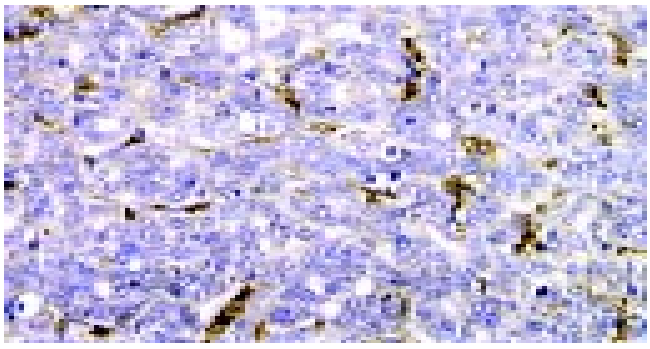

Figure 2 Absent expression of leptin in HCC cells, Kupffer cells and vascular endothelial cells expressed high levels of leptin. S-P immunohistochemical staining ×400.

Ob-R expression in human HCC and adjacent non-tumorous liver tissues

Thirty out of 36 specimens from adjacent non-tumorous liver tissues (30/36, 83.33%) were positive for Ob gene receptor product, with a moderate (++) to strong (+++) intensity. Only

11 of 36 specimens from HCC (11/36, 30.56%) were positive, with a weak (+) intensity. The expression of Ob-R was significantly lower than that of adjacent non-tumorous liver tissues ($P<0.05$).

Effect of leptin on the proliferation of Chang liver cells in vitro

Leptin inhibited the proliferation of Chang liver cells on the 5th d after leptin treatment at various concentrations. The cell survival rate was 10-13% lower than that of the untreated cells (Figure 3A), although without statistical significance ($P>0.05$).

Effect of leptin on proliferation of SMMC-7721 cells in vitro

Leptin had little effect on the proliferation of liver cancer cells (Figure 3B), the cell survival rate on each day after leptin treatment was lightly lower than that of the controls, but no statistical significance was found ($P>0.05$).

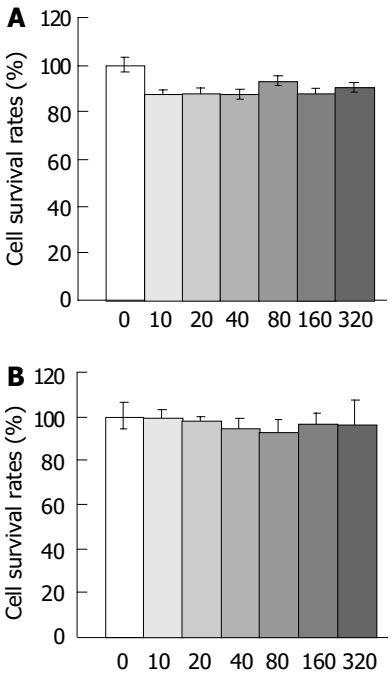

Figure 3 Effect of leptin at different concentrations (ng / mL) on proliferation of Chang liver cells and liver cancer cells on d 5 (MTT assay). A: Effect of leptin at different concentrations (ng / mL) on proliferation of Chang liver cells on d 5 (MTT assay), B: Effect of leptin at different concentrations (ng / mL) on proliferation of liver cancer cells on d 5 (MTT assay).

DISCUSSION

It has found that certain cancers are associated with obesity, including breast, prostate, colon, uterus, renal cell, pancreas carcinoma and esophagus adenocarcinoma[2,22,31]. Leptin, an Ob gene product, could control body weight homeostasis through food intake and energy expenditure, and was closely associated with obesity[1-3]. Although epidemiological observation showed that obesity was a risk factor of HCC complicated with alcoholic liver disease and cryptogenic cirrhosis[22,23,32], clinical investigations have identified that serum leptin levels in alcoholic and post-hepatitis liver cirrhosis patients with or without HCC are increased significantly in comparison with those in control subjects[22,24-30]. There was no study on the role of leptin in carcinogenesis of human hepatic cellular carcinoma[2,22-30].

The present study investigated the expression of leptin and its receptor Ob-R in both adjacent non-tumorous liver tissues and HCC tissues with immunohistochemical staining, and found that adjacent non-tumorous liver cells expressed higher levels of leptin and its receptor than corresponding HCC cells, about one fourth of HCC tissues lost the expression of leptin, and two thirds had no Ob-R expression (Figures 1, 2). These findings suggest that leptin could act *in vivo* as a paracrine/endocrine growth factor towards hepatocytes, and played a possible role in the process of initiation and progression of HCC, which could thus contribute to the explanation of the reasons why alcoholic and post-hepatitis liver cirrhosis patients with or without HCC had high levels of serum leptin[24-30] and the reasons why obesity was a risk factor of developing HCC[22,23].

In proliferation assay *in vitro*, leptin had differential effects on the proliferation of human cancer cells. Tt caused growth potentiation in breast, esophagus, and prostate cancer cells, but inhibited the proliferation of pancreatic cancer cells[2,19,32]. In MCF-7 cells, leptin and high glucose stimulated cell proliferation as demonstrated by the increases in DNA synthesis and expression of cdk2 and cyclin D1. However, they had no significant effect on the proliferation of multidrug-resistant human breast cancer NCI/ADR-RES cells[16]. In this study, leptin alone showed some inhibitory effect on the proliferation of normal Chang liver cells, and no effect on liver cancer SMMC-7721 cells. However, Chang liver cell line was originally thought to be derived from normal liver tissue, but was subsequently found on the basis of isoenzyme analysis, HeLa marker chromosomes, and DNA fingerprinting, to have HeLa cell contamination when it was established (www.atcc.org). Therefore, these findings *in vitro* might be associated with different biological characteristics of cancer cells to react to leptin treatment, and/or the organ derivation of cancer cell lines[2]. In addition, Chang liver cell line was not a good control of normal liver cells.

In vivo animal experiments findings showed that Leptin was a growth factor that could stimulate proliferation of colonic epithelial cells in mice[33]. It is also a profibrogenic cytokine and could play a key role in liver fibrosis[34]. *ob/ob* mice having a naturally occurring mutation in the *ob* gene that prevents the synthesis of leptin had an increased incidence of HCC[31]. This study showed that leptin had some inhibitory effect on the proliferation of normal Chang liver cells and no effect on the proliferating of on liver cancer SMMC-7721 cells (Figures 3A,3B), and adjacent non-tumorous liver tissues could express higher levels of leptin and its receptor than the corresponding HCC cells (Figure 1). It could be assumed that leptin acting as an inhibitor and/or promoter, was involved in the process of carcinogenesis and progression of human HCC. In addition, the high levels of leptin expression in Kupffer cells and vascular endothelial cells might be associated with liver cirrhosis[24,27,35,36], and angiogenesis of cancer tissues[1,14,37], because these lesions might deteriorate HCC.

In summary, a preliminary investigation of the possible involvement of leptin in carcinogenesis of human hepatocellular carcinoma was performed in this study to elucidate the etiology and carcinogenesis of HCC. To the best of our knowledge[2,20-30], this is the first report on involvement of leptin in HCC. The presence of leptin and its receptor in adjacent non-tumorous liver and HCC cells, and the effects of leptin on proliferation of normal Chang liver cells and liver cancer cells may provide new insights into the carcinogenesis and progression of human HCC.

REFERENCES

1 **Sierra-Honigmann MR,** Nath AK, Murakami C, Garcia-Cardena G, Papapetropoulos A, Sessa WC, Madge LA, Schechner JS, Schwabb MB, Polverini PJ, Flores-Riveros JR. Biological action of leptin as an angiogenic factor. *Science* 1998; **281:** 1683-1686

2 **Somasundar P,** Yu AK, Vona-Davis L, McFadden DW. Differential effects of leptin on cancer *in vitro*. *J Surg Res* 2003; **113**: 50-55

3 **Onuma M,** Bub JD, Rummel TL, Iwamoto Y. Prostate cancer cell-adipocyte interaction: Leptin mediates androgen-independent prostate cancer cell proliferation through c-Jun NH2-ter-

minal kinase. *J Biol Chem* 2003; **278**: 42660-42667
4 **Janeckova R**. The role of leptin in human physiology and pathophysiology. *Physiol Res* 2001; **50**: 443-459
5 **Stephenson GD,** Rose DP. Breast cancer and obesity: an update. *Nutr Cancer* 2003; **45**: 1-16
6 **Stattin P,** Kaaks R, Johansson R, Gislefoss R, Soderberg S, Alfthan H, Stenman UH, Jellum E, Olsson T. Plasma leptin is not associated with prostate cancer risk. *Cancer Epidemiol Biomarkers Prev* 2003; **12**: 474-475
7 **Catalano S,** Marsico S, Giordano C, Mauro L, Rizza P, Panno ML, Ando S. Leptin enhances, via AP-1, expression of aromatase in the MCF-7 cell line. *J Biol Chem* 2003; **278**: 28668-28676
8 **Stattin P,** Palmqvist R, Soderberg S, Biessy C, Ardnor B, Hallmans G, Kaaks R, Olsson T. Plasma leptin and colorectal cancer risk: a prospective study in Northern Sweden. *Oncol Rep* 2003; **10**: 2015-2021
9 **Hu X,** Juneja SC, Maihle NJ, Cleary MP. Leptin-a growth factor in normal and malignant breast cells and for normal mammary gland development. *J Natl Cancer Inst* 2002; **94**: 1704-1711
10 **Chan TF,** Su JH, Chung YF, Chang HL, Yuan SS. Decreased serum leptin levels in women with uterine leiomyomas. *Acta Obstet Gynecol Scand* 2003; **82**: 173-176
11 **Saglam K,** Aydur E, Yilmaz M, Goktas S. Leptin influences cellular differentiation and progression in prostate cancer. *J Urol* 2003; **169**: 1308-1311
12 **Kote-Jarai Z,** Singh R, Durocher F, Easton D, Edwards SM, Ardern-Jones A, Dearnaley DP, Houlston R, Kirby R, Eeles R. Association between leptin receptor gene polymorphisms and early-onset prostate cancer. *BJU Int* 2003; **92**: 109-112
13 **Petridou E,** Belechri M, Dessypris N, Koukoulomatis P, Diakomanolis E, Spanos E, Trichopoulos D. Leptin and body mass index in relation to endometrial cancer risk. *Ann Nutr Metab* 2002; **46**: 147-151
14 **Coskun U,** Gunel N, Toruner FB, Sancak B, Onuk E, Bayram O, Cengiz O, Yilmaz E, Elbeg S, Ozkan S. Serum leptin, prolactin and vascular endothelial growth factor (VEGF) levels in patients with breast cancer. *Neoplasma* 2003; **50**: 41-46
15 **Isono M,** Inoue R, Kamida T, Kobayashi H, Matsuyama J. Significance of leptin expression in invasive potential of pituitary adenomas. *Clin Neurol Neurosurg* 2003; **105**: 111-116
16 **Okumura M,** Yamamoto M, Sakuma H, Kojima T, Maruyama T, Jamali M, Cooper DR, Yasuda K. Leptin and high glucose stimulate cell proliferation in MCF-7 human breast cancer cells: reciprocal involvement of PKC-alpha and PPAR expression. *Biochim Biophys Acta* 2002; **1592**: 107-116
17 **Dieudonne MN,** Machinal-Quelin F, Serazin-Leroy V, Leneveu MC, Pecquery R, Giudicelli Y. Leptin mediates a proliferative response in human MCF7 breast cancer cells. *Biochem Biophys Res Commun* 2002; **293**: 622-628
18 **Laud K,** Gourdou I, Pessemesse L, Peyrat JP, Djiane J. Identification of leptin receptors in human breast cancer: functional activity in the T47-D breast cancer cell line. *Mol Cell Endocrinol* 2002; **188**: 219-226
19 **Bruserud O,** Huang TS, Glenjen N, Gjertsen BT, Foss B. Leptin in human acute myelogenous leukemia: studies of *in vivo* levels and *in vitro* effects on native functional leukemia blasts. *Haematologica* 2002; **87**: 584-595
20 **Qian J,** Feng GS, Vogl T. Combined interventional therapies of hepatocellular carcinoma. *World J Gastroenterol* 2003; **9**: 1885-1891
21 **Zhu AX.** Hepatocellular carcinoma: are we making progress? *Cancer Invest* 2003; **21**: 418-428
22 **Nair S,** Mason A, Eason J, Loss G, Perrillo RP. Is obesity an independent risk factor for hepatocellular carcinoma in cirrhosis? *Hepatology* 2002; **36**: 150-155
23 **Roth MJ,** Baer DJ, Albert PS, Castonguay TW, Dorgan JF, Dawsey SM, Brown ED, Hartman TJ, Campbell WS, Giffen CA, Judd JT, Taylor PR. Relationship between serum leptin levels and alcohol consumption in a controlled feeding and alcohol ingestion study. *J Natl Cancer Inst* 2003; **95**: 1722-1725
24 **Wang YY,** Lin SY. Leptin in relation to hepatocellular carcinoma in patients with liver cirrhosis. *Horm Res* 2003; **60**: 185-190
25 **Lin SY,** Wang YY, Sheu WH. Increased serum leptin concentrations correlate with soluble tumour necrosis factor receptor levels in patients with cirrhosis. *Clin Endocrinol* 2002; **57**: 805-811
26 **Testa R,** Franceschini R, Giannini E, Cataldi A, Botta F, Fasoli A, Tenerelli P, Rolandi E, Barreca T. Serum leptin levels in patients with viral chronic hepatitis or liver cirrhosis. *J Hepatol* 2000; **33**: 33-37
27 **Comlekci A,** Akpinar H, Yesil S, Okan I, Ellidokuz E, Okan A, Ersoz G, Tankurt E, Batur Y. Serum leptin levels in patients with liver cirrhosis and chronic viral hepatitis. *Scand J Gastroenterol* 2003; **38**: 779-786
28 **Greco AV,** Mingrone G, Favuzzi A, Capristo E, Gniuli D, Addolorato G, Brunani A, Cavagnin F, Gasbarrini G. Serum leptin levels in post-hepatitis liver cirrhosis. *J Hepatol* 2000; **33**: 38-42
29 **Campillo B,** Sherman E, Richardet JP, Bories PN. Serum leptin levels in alcoholic liver cirrhosis: relationship with gender, nutritional status, liver function and energy metabolism. *Eur J Clin Nutr* 2001; **55**: 980-988
30 **Serin E,** Ozer B, Gumurdulu Y, Kayaselcuk F, Kul K, Boyacioglu S. Serum leptin level can be a negative marker of hepatocyte damage in nonalcoholic fatty liver. *J Gastroenterol* 2003; **38**: 471-476
31 **Somasundar P,** Riggs D, Jackson B, Vona-Davis L, McFadden DW. Leptin stimulates esophageal adenocarcinoma growth by nonapoptotic mechanisms. *Am J Surg* 2003; **186**: 575-578
32 **Yang S,** Lin HZ, Hwang J, Chacko VP, Diehl AM. Hepatic hyperplasia in noncirrhotic fatty livers: is obesity-related hepatic steatosis a premalignant condition? *Cancer Res* 2001; **61**: 5016-5023
33 **Hardwick JC,** Van Den Brink GR, Offerhaus GJ, Van Deventer SJ, Peppelenbosch MP. Leptin is a growth factor for colonic epithelial cells. *Gastroenterology* 2001; **121**: 79-90
34 **Saxena NK,** Saliba G, Floyd JJ, Anania FA. Leptin induces increased alpha2(I) collagen gene expression in cultured rat hepatic stellate cells. *J Cell Biochem* 2003; **89**: 311-320
35 **Leclercq IA,** Farrell GC, Schriemer R, Robertson GR. Leptin is essential for the hepatic fibrogenic response to chronic liver injury. *J Hepatol* 2002; **37**: 206-213
36 **Shimizu H,** Kakizaki S, Tsuchiya T, Nagamine T, Takagi H, Takayama H, Kobayashi I, Mori M. An increase of circulating leptin in patients with liver cirrhosis. *Int J Obes Relat Metab Disord* 1998; **22**: 1234-1238
37 **Iversen PO,** Drevon CA, Reseland JE. Prevention of leptin binding to its receptor suppresses rat leukemic cell growth by inhibiting angiogenesis. *Blood* 2002; **100**: 4123-4128

Edited by Wang XL and Xu FM

PO Box 2345, Beijing 100023, China
Fax: +86-10-85381893
E-mail: wjg@wjgnet.com www.wjgnet.com

World J Gastroenterol 2004;10(17):2482-2487
World Journal of Gastroenterology
Copyright © 2004 by The WJG Press ISSN 1007-9327

• LIVER CANCER •

Function of oval cells in hepatocellular carcinoma in rats

Chi-Hua Fang, Jia-Qing Gong, Wei Zhang

Chi-Hua Fang, Jia-Qing Gong, Wei Zhang, Department of Hepatobiliary Surgery, Zhujiang Hospital, First Military Medical University, Guangzhou 510282, Guangdong Province, China
Supported by the Natural Science Foundation of Guangdong Province, No. 2001.010593, 2002.020097 and Key Science and Technology Research Project of Guangzhou, No. B012000-X-005-01-05
Correspondence to: Chi-Hua Fang, Department of Hepatobiliary Surgery, Zhujiang Hospital, First Military Medical University, Guangzhou 510282, Guangdong Province, China. fch58520@sina.com
Telephone: +86-20-84360607 **Fax:** +86-20-61643210
Received: 2003-06-05 **Accepted:** 2003-07-31

Abstract

AIM: To study oval cells' pathological characteristics and relationship with the occurrence of hepatocellular carcinoma (HCC); to observe the form and structural characteristics of oval cells; to explore the expression characteristics of C-kit, PCNA mRNA and *c-myc* gene during the occurrence and development of HCC and the effect of ulinastatin (UTI) on C-kit and PCNA expression.

METHODS: One hundred and twenty-five SD rats fed on 3,3'-diaminobenzidine (DAB) to construct HCC models were divided into control group, cancer-inducing group and UTI intervention group. In each group, rat liver samples were collected at weeks 2, 4, 6, 8, 10, 12, 14, 16, 18, 20, 22 and 24 respectively to study pathological distribution characteristics of oval cells in the process of carcinogenesis under optical microscope. Oval cells were separated by the methods of improved density gradient centrifugation and their structural characteristics were observed under optical microscope and electronic microscope respectively; the oval cells expressing C-kit and PCNA in the collected samples were observed by the methods of immunohistochemistry and image analysis and the expression of c-myc mRNA was also detected by reverse transcription polymerase chain reaction (RT-PCR).

RESULTS: Oval cells proliferated firstly in the portal area then gradually migrated into hepatic parenchyma in the inducing group and intervention group. The oval cells distributed inside and outside the carcinoma nodes. The oval cells presented the characteristics of undifferentiated cells: a high ratio of nucleolus and cellular plasm and obvious nucleoli, rare organelle in plasm. Only a few mitochondria and endoplasmic reticulum and some villus-like apophysis on surface of cells could be seen. Cells stained with C-kit and PCNA antibody were mainly oval cells distributed in the portal area. The expression of c-myc mRNA increased with the progression of HCC. However, in the intervention group, UTI could retard its increase.

CONCLUSION: Oval cells work throughout the development of HCC, and might play important roles in this process. *c-myc* gene may be a kind of promoter gene of HCC, and play a key role in hepatic injury and development of HCC. UTI could retard the occurrence of HCC.

Fang CH, Gong JQ, Zhang W. Function of oval cells in hepatocellular carcinoma in rats. *World J Gastroenterol* 2004; 10(17): 2482-2487
http://www.wjgnet.com/1007-9327/10/2482.asp

INTRODUCTION

HCC is one of the most common malignant carcinomas in China. Because of its high rate of metastasis and recurrence and lack of typical symptoms in early stage, HCC has the second mortality rate among all the malignant carcinomas[1,2]. Up to now, obvious progress has been made in the study of cell origin of HCC. One is that HCC is originated from abnormally differentiated oval cells, the other is that it results from dedifferentiation of mature liver cells. In order to probe the relationship between oval cells and HCC, we explored the pathologic distribution characteristics, structural features of oval cells in the pathogenesis of HCC in experimental SD rats and the expression characteristics of C-kit, PCNA and *c-myc* genes in oval cells.

MATERIALS AND METHODS

Materials

One hundred and twenty-five clearing SD rats (100±20 g) (Experimental Center of Zhongshan University) were fed in the environment of 18-28 °C and 40-70% humidity in Animal Feeding Unit, Zhujiang Hospital, First Military Medical University. DAB (Dako, Japan) was used as inducing drug for HCC in rat; proline, asparagic acid, serine phenylalanine, tyrosine pyruvate sodium, transferring, epidermal growth factor (EGF) (Sigma, USA) and F12, F12/DMEM (1:1) (Gibco, USA), and fetal bovine serum (Sijiqing Co, Hangzhou, China) were used for culture medium for oval cells. Collagenase VI and density gradient centrifugation (percoll) (Sigma) were used for separating oval cells. C-kit polyclonal antibody (Sigma), immunohistochemical kits (SABC methods) and poly-lysine for adhibiting section, neutral resin for envelop section (Boshide Co, Wuhan); PCNA immunohistochemical kits (SP methods), DAB dyeing reagent (Zhongshan Co, Beijing); c-myc mRNA kit, total RNA extraction kits, DNA marker (100 bp), primers for polymerase chain reaction(PCR) and RNAsin (Huamei Bioengineering Co), M-MLV reverse transcriptase (Promega USA), *Taq* DNA polymerase (Gibco), 4×dNTP (Sigma), amplification primer for reverse transcription polymerase chain reaction (RT-PCR) were synthesized by Shanghai Biotech Co. according to the GenBank database.

Methods

HCC model The method of constructing HCC model in the cancer-inducing group and inter group was according to the references[3,4]. After fed on DAB for 14 wk, rats were given normal drinking water, but in control group, the rats were fed on standard food. In the interference group, as soon as the DAB was administrated, UTI (2-10^4 U/kg) was injected into abdominal cavity, twice a week until wk14[5,6]. One hundred and twenty-five clearing SD rats were divided into control group (24 rats), cancer-inducing group (48 rats) and UTI interference group (48 rats), the other 5 rats were used to construct the

model of oval cells proliferation. Each group was divided into 12 sub-groups, and there were 2 rats in sub-group of the control group and the cancer-inducing group, 4 rats in sub-group of interference group. Two pieces of 1 cm×1 cm×1 cm tissue taken from the right liver lobe of each rat in sub-group were fixed in 40 g/L formaldehyde and 2-4 pieces of soybean-sized tissue taken from the left liver lobe of each rat in sub-group were placed respectively in the 0.5 mL centrifuge tube and preserved in a refrigerator at -80 °C at wk 2, 4, 6, 8, 10, 12, 14, 16, 18, 20, 22 and 24 respectively during construction of HCC model. The samples of right liver lobes were sliced serially to count cancerous nodes under low power microscope. Nodes more than 0.05 mm^2 were measured by the gridding ocular micrometer.

Separation of oval cells When the rats have been fed DAB for 4 wk, a large number of oval cells proliferated from the hepatic portal area, which could be identified by HE dyeing section analysis**.** Firstly, D-Hanks' solution was perfused through portal vein until the liver color turned yellow, then 1 g/L collagenase IV was affused to digest liver. The digested liver was put in a beaker, washed 3 times with Hank's solution, and minced thoroughly at the same time, then 0.6 g/L collagenase IV was added to further digest liver for 30 min at 37 °C. The cell suspension was filtrated through 100 holes/cm^2 sieve, then centrifuged at 300 r/min at 4 °C for 5 min, the cell suspension was extracted and centrifuged again at 2 000 r/min at 4 °C for 10 min. The upper layer solution abandoned, then cells were suspended again with 10 mL F12 solution. The density gradient centrifugation solution (percoll) was blended with 100 g/L NaCl at a ratio of 9:1 and diluted with F12 into the solution of 90%, 70% and 50%, respectively. Ten mL of each solution was put in a high-speed centrifugation tube of 50 mL, according to the concentration gradient of 90%, 70% and 50%. A 10 mL cell suspension was placed on the top of each tube, then centrifuged for 30 min at 4 °C, 12 000 *g* so that the oval cells were located between the centrifugation solution of 70% and 50%, then the oval cell suspension was extracted carefully to another tube, Hanks' solution was added with 5 kU/L benzylpenicillin and streptomycin A, then centrifuged at 1 000 r/min for 5 min, the precipitate was retained. Culture medium F12/DMEM (1:1) solution was added to suspend cells. Then the suspension was inoculated into 25 cm^3 plastic culture bottles, according to the density of 2×10^8/L, placed into incubating cabin with 5 mL/L CO_2 at 37 °C. After 24 h the culture solution was replaced and oval cells could be seen adhering to the bottle wall.

Culture of oval cells The culture medium consisted of 200 mL/L fetal bovine serum which was diluted with the solution of DMEM/F12(1:1) containing epidermal growth factor (20 μg/L), transferring (20 μg/L) and some kinds of amino acid. The culture medium was replaced every 2 or 3 d. When cells overgrew in the bottles, some parts of cells were transferred into another culture bottle. The culture medium in the bottles was extracted; F12 solution was added to clean the cells three times, then mixed with 2.5 g/L pancreatin to digest. The cells were observed under the microscope for about 1 min, then oval cells could be seen floating and then the culture medium was added to terminate digestion. After the cells were separated completely, they were inoculated into another bottle.

C-kit immunohistochemistry Carry sheet glasses were treated by polylysine. Paraffin sections (5 μm thick) were dewaxed by dimethylbenzene and alcohol respectively. After washed by 0.01 mol/L PBS for 2 min 3 times, the sections were incubated in 3 mL/L H_2O_2 solution for 10 min to inactivate endogenous peroxides, heated in citric acid sodium solution in microwave oven at 100 °C to retrieve antigen for 10 min and then cooled for 25 min. After washed with 0.1 mol/L PBS for 2 min 3 times, they were incubated with normal goat serum to block nonspecific binding of antibodies for 10 min at room temperature. The sections were then incubated with IgG of rabbit antiserum against mouse at 37 °C for 24 h or at 4 °C overnight, washed with 0.01 mol/L PBS for 3 times for 2 min each, then incubated with goat IgG anti-rabbit at 37 °Cfor 20 min, washed with 0.01 mol/L PBS for 2 min 3 times, Reagent SABC was added and incubated at 37 °C for 20 min, section were washed again with 0.01 mol/L PBS for 3 times. The immunoreacted cells were then visualized by using DAB kits as follows: a drop of reagent A, B and C was added into 1 mL distilled water, then they were blended completely and dripped on the sections. The sections were counterstained with hematoxylin for 50 s, then dehydrated and observed with light microscope.

PCNA immunohistochemistry (SP methods) The SABC reagent was replaced by the solution of streptoavidin marked with horse-radish peroxidase in the first steps and the other steps were the same as C-kit immunohistochemistry. C-kit protein was stained brown yellow. The localization of C-kit protein and its change in quantity were observed when the rats' livers were injured. PCNA protein was stained as brown yellow. The localization of PCNA positive cells in the hepatic lobule was observed and PCNA labeling index (proliferating index) was calculated by randomly observing 5 fields under high microscope in each section. The positive cells among 100 cells were counted in each field and mean values were taken.

RNA extraction and assessment The preserved 50-100 mg liver tissues were mixed and grinded evenly with 1 mL cold denaturant. A 1mL lysis liquid was added into a 2.0 mL centrifuge tube and then mixed with 0.1 mL sodium acetate (pH4.0). A 100 mL phenol/chloroform mixture was mixed with the above mentioned liquid and intensely vibrated for 10 s, then placed on ice for 10 min. The liquid was centrifuged at 4 °C. The top layer liquid was transferred into a 1.5-mL centrifuge tube and kept at -20 °C for 15 min after mixed with isopropanol of identical volume. White jelly-like precipitate after centrifugation at 10 000 *g* for 15 min at 4 °C was the total RNA. RNA was resolved completely by 1 mL lysis and RNA precipitate and wall of the tube liquid were washed with 250 mol/L alcohol. Resolved RNA in RNase-free water and preserved it at -20 °C. The absorbance (*A*) of total RNA was measured by ultraviolet spectrophotometer and the RNA concentration(g/L) was A_{260}×nucleic acid dilution times×40/1 000 (A_{260}/A_{280}) (if *A* of RNA >1.8, the RNA is pure enough to be used in the following experiment).

Agarose electrophoresis RNA solution 1 μL mixed with 2 μL bromphenol blue buffer was electrophored in the level electrophoresis chamber treated by RNase-free water at 100 V for 20 min then the gelatum was taken to be observed. Three RNA straps of 28 s, 18 s, and 5 s could be seen through gel electrophoresis.

cDNA synthesis and PCR reaction A 2 μL (1 μg) total RNA, 4 μL (20 pmoL) of c-myc downstream primer and 8 μL of RNA-free water were mixed well at the room temperature, put in water bath at 70 °C to degenerate for 5 min. Then they were put on ice for 1 min, centrifuged at 200 g for 30 s. A 5 μL M-MLV reverse transcriptase 5×Buffer, 5 μL dNTP (2.5 mmol/L), 5 μL rRNasin (20 U) and 5 μL M-MLV RT were added and the total reaction volume was 34 μL. The mixture was treated at 42 °C for 60 min and at 95 °C for 5 min to inactivate reverse transcriptase, then maintained at -30 °C. Sixteen μL of cDNA , 5 μL 10×Buffer (no $MgCl_2$), 3 μL solutions $MgCl_2$ (25 mmol/L), 4 μL (2.5 mmol/L) dNTP, 3 μL (15pmoL) of sense including target gene and mark gene repectively, 3 μL (15 pmoL) antisense including target gene and mark gene respectively, 1 μL (3U) *Taq* DNA enzyme and 9 μL RNA-free water were mixed totally at the room temperature, and the above total reactive volume was 50 μL. Then a drop of paraffin oil treated at high temperature was added onto the surface of mixture , and degenerated at 94 °Cfor 5 min. PCR cycle was at 94 °C, 50 °C and 72 °C respectively, for 1 min each. After 35 cycles, an extension at 72 °C was performed

for 5 min.

Agarose electrophoresis A 8 μL product of c-myc DNA was taken for caraphoresis in 20 g/L sepharose (containing small quantity EB), and two straps of 228-bp and 120-bp (the product of mark gene) were found under light. The caraphoresis strap of PCR was scanned and quantitatively analyzed with gel image analysis system.

Statistical analysis

Experiment results were analyzed with SPSS10.0 software. Data were analyzed with single-side analysis of variance and with LSD methods for inter-group analysis. Chi-squared test was used to compare rates between two groups. $P<0.05$ indicates significant difference.

RESULTS

Pathological characteristics

The rats' liver cells in the early period of cancer-inducing group showed balloon-like degeneration under light microscope (1-8 wk). Since the 2nd wk in the cancer-inducing group, the oval cells started to proliferate in portal area and gradually migrated into liver parenchyma (Figure 1). The pseudo-lobules formed in the liver and oval cells migrated into lobules in the middle period from the 15th to 24th wk. The cancer cell nucleus presented in different sizes and karyokinesis often occurred. Cancer cells infiltrated toward the periphery of liver tissue, and at the same time, focal bleeding and necrosis obviously occurred. Huge amounts of leucocytes infiltration could be seen in the peripheral area of nodes and portal area, and lots of oval cell proliferations were shown in portal area and in cancer nodes (Figure 2). Beginning from the 2nd wk of cancer induction, the proliferation of oval cells could be seen in portal area. Firstly oval cells appeared in the epithelial lining of bile duct of portal area and then gradually proliferated and migrated into liver parenchyma. In the fibrosis formation period, the proliferation of oval cells could be seen in portal area and in its peripheral area. The volume of oval cells was about as big as one third of normal liver cells, round or oval-shaped and its margin was unclear with scant cytoplasm and basophils. The cell nucleus was round or oval shaped, with slight stain, vague membrane and obvious nucleolus. Oval cells proliferated first in portal area and then in liver limiting plate, migrated along liver sinusoids and to the middle part of lobules. These cells often presented as two lines or branches, destroying the neighboring liver cord. The left lobe liver cells were scattered among the proliferated oval cells that distributed inside and mainly outside of the cancer nodes. Oval cells showed the characteristics of undifferentiated cells: a big ratio of nucleus and plasm and obvious nucleoi, rare organele in plasm, only a few mitochondria, endoplasmic reticulum and some villus-like apophysis on surface of cells could be seen under the electronic microscope (Figure 3).

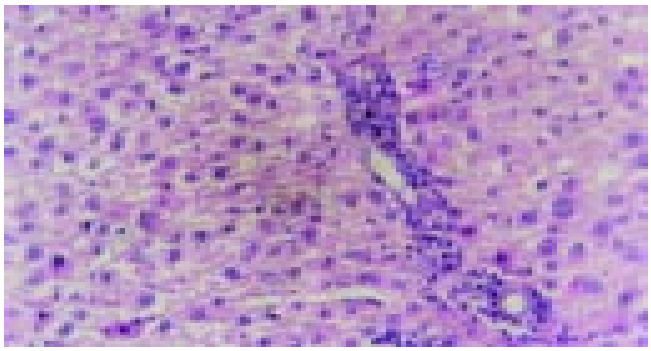

Figure 1 Early inflammatory liver tissues in cancer inducing group at the 2nd wk and the differentiation of oval cells in the portal area (HE staining, original magnification: ×200).

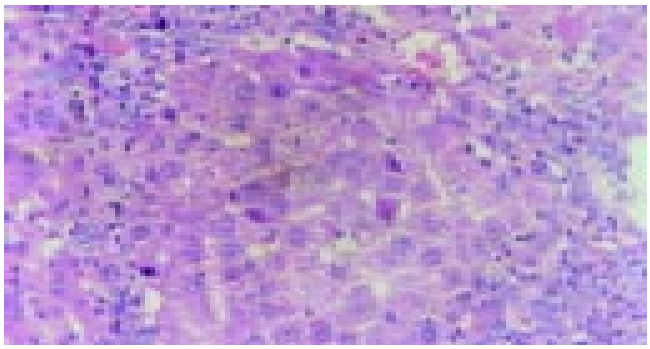

Figure 2 A large quantity of oval cells gathered around the cancer nodes in cancer inducing group at 20th wk (HE staining, original magnification: ×200).

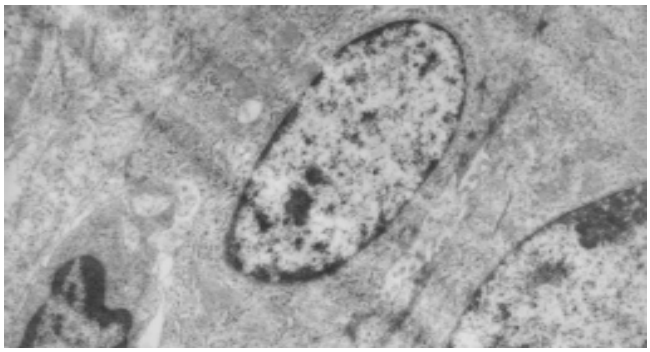

Figure 3 Electron microscopic observation showed: the volume of oval cell was about as big as one third of normal liver cell, round or oval shaped, scant cytoplasm with unclear cell margin.

The effect of UTI on cancer induction: in the early period, the balloon-like degeneration of liver cells was much milder than that of the liver cells in cancer-inducing group. The balloon-like degeneration of liver cells was obvious in the middle period and local liver cells became necrosis, liver lobes were destroyed and the liver fiber proliferated and the pseudo-lobues formed in the local area with a large amount of oval cell aggregating in the portal area and liver parenchyma could be seen. In the period of carcinoma formation, pseudo-lobues were seen apparently in large parts of liver parenchyma and a large number of oval cells aggregated to an extreme extent. Some liver cancer cells with column-like or glandular-like structure appeared in part of liver parenchyma and oval cells scattered among the cancer cells. The neoplasia nodes were counted as in Table 1.

Table 1 Number of cancerous nodes and cancer nodes' area in rat liver (mean±SD, n=8)

t/wk	Cases of hepatic cancer		Number of cancerous		Area of cancer nodes (mm^2)	
	A	B	A	B	A	B
2-4	0	0	0	0	0	0
6-8	0	0	0	0	0	0
10-12	2	0	4	0	9.5±8.2	0
14-16	6	2	15	5	10.7±8.7	5.8±4.5[a]
18-20	8	4	17	9	11.4±8.9	8.5±7.6
22-24	8	4	16	10	11.2±9.3	8.6±7.3

[a]$P<0.05$ *vs* group A; A: cancer- induction group; B: intervention group.

Characteristics of c-kit positive stain cells

C-kit positive stain localized in cell plasm in normal liver showed brown-yellow and was mainly in the mitotic and proliferating

liver cells. At the 2nd wk in the cancer-inducing group, some c-kit positive stain cells, mainly oval cells, appeared in the portal area and punctated positive pigmentations could be seen in liver lobules as well. At the 8th wk, oval cells in the portal area in the cancer-inducing group were obviously positively stained, with some positive pigmentation forming patches and some punctating in the rim of portal area (Figure 4). At the 14th wk, the normal liver structure was replaced by a lot of pseudolobule and still a large number of c-kit positive stain cells could be seen which mainly gathered in portal area. In the 22nd wk in the cancer-inducing group, a large number of cancerous nodes formed and some positive cells scattered among them (Figure 5). The characteristics of c-kit positive staining cells in the samples of intervention group was almost identical with that in cancer-inducing group.

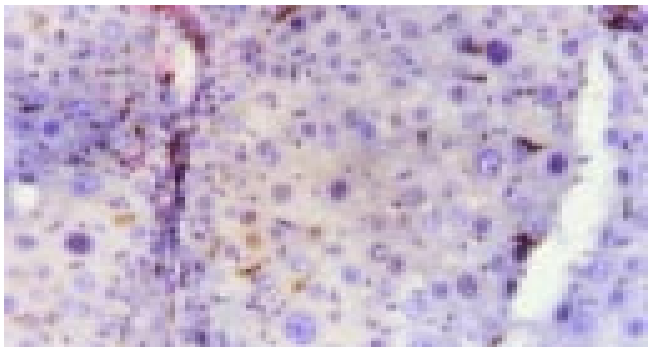

Figure 4 Expression of c-kit in liver tissue in cancer inducing group at the 8th wk. The oval cells were mainly stained in portal areas (Immunohistochemistry, ×200).

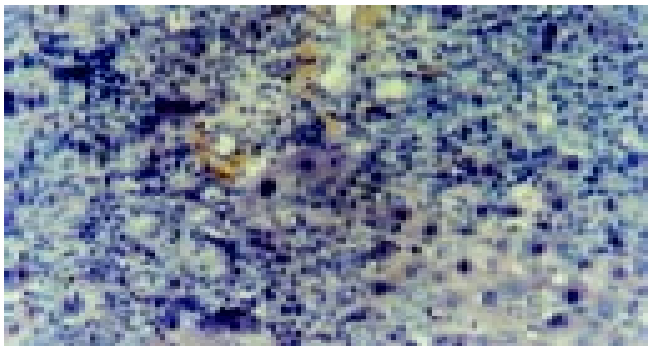

Figure 5 Expression of c-kit in the HCC tissue in cancer inducing group in the 24th wk (Immunohistochemistry, ×200).

Characteristics of PCNA positive cells

PCNA positive staining located in the nucleus, as granules or diffusively. Occasionally positive stains were seen in normal liver tissue. At the 2nd wk of the cancer-induction, the PCNA positive cells firstly appeared among the oval cells in the portal area. At the 4th wk, a lot of hepatic cells were positively stained, especially in central vein area. At the 6th wk, also the middle stage of inflammatory process, PCNA positive cells were seen all over the lobules of liver. At the 8th wk, the number of PCNA cells was comparatively decreased and nuclei of positive cells around the portal area tended to become larger gradually. From the 10th to 14th wk, some of the proliferating hepatic fibers were lightly stained and the oval cells in portal area still over expressed PCNA. From the 16th to 24th wk, a large number of cancerous nodes formed and PCNA over expressed in some cancerous nodes (Figure 6), while the number of positive cells was relatively fewer in necrotic cancerous nodes than in other areas and the number of dotted positive stain cells adjacent to the carcinoma tissue was apparently fewer than inside the carcinoma tissue. In the intervention group, PCNA positive stain cells firstly appeared among the oval cells in portal area, and then their number increased with the aggravation of hepatic intoxication by DAB. The PCNA positive stain rate and expression level reached the peak at the 10th wk in rat liver. The distribution characteristics of PCNA positive cells were similar to those in the cancer inducing group when HCC formed. The labeling index of PCNA positive stain cells is shown in Table 2.

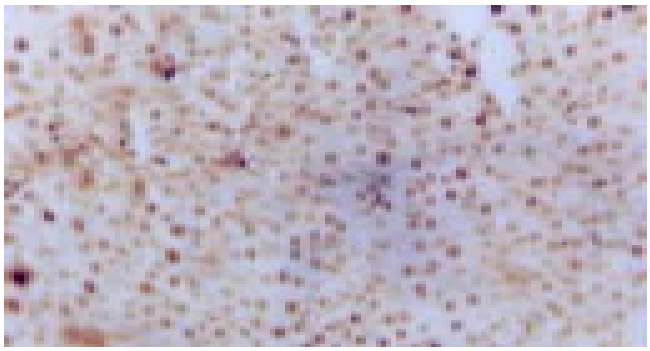

Figure 6 PCNA expression in HCC tissue in the cancer inducing group at the 24th wk (Immunohistochemistry, ×200).

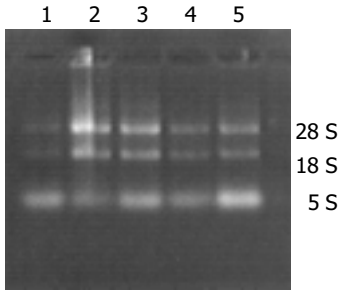

Figure 7 Electrophoresis image of total RNA in rat liver tissue.

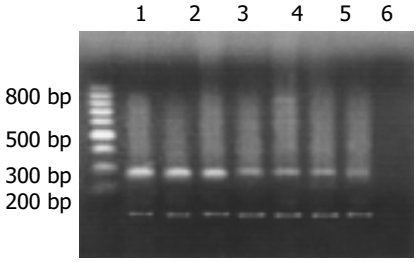

Figure 8 Products of RT-PCR of c-myc mRNA (up-strap: 228-bp c-myc; low-strap: 120-bp β-actin; Lanes1 and 2: Hepatocarcinoma tissue; Lane 3: Hepatocirrhosis tissue; Lanes 4-6: Inflammation tissue; Lane 7: Normal tissue).

Table 2 PCNA positive index and *c-myc* relative gray value in liver (mean±SD)

t/wk	Cancer induction (n = 8)		Intervention (n = 8)		Control (n = 4)	
	PCNA (%)	RGV	PCNA (%)	RGV	PCNA (%)	RGV
2-4	14.1±7.5[a]	1.3±1.0	7.6±3.3	1.2±0.6	3.0±1.2	1.0±0.3
6-8	48.2±15.5[b]	2.0±07	24.3±7.4[a]	1.5±0.7	2.9±1.5	1.1±0.4
10-12	23.7±9.6[a]	3.6±1.2[a]	35.1±6.5[b]	2.2±0.9	3.3±0.9	1.1±0.5
14-16	25.9±5.1[a]	5.7±1.4[a]	21.5±4.2[a]	3.5±1.0[a]	3.7±2.1	1.3±0.4
18-20	36.8±6.3[b]	7.8±1.4[a]	29.6±7.6[a]	6.5±1.1[a]	3.6±1.3	1.3±0.6
22-24	41.2±8.2[b]	8.2±2.2[b]	30.2±8.7[a]	8.0±1.3[b]	3.5±2.2	1.3±0.4

[a]P<0.05, [b]P<0.01 *vs* group C; RGV: Relative gray value.

c-myc gene expression

Expression of *c-myc* gene existed in normal rat liver tissue, but the expression quantity is relatively small. The expression of c-myc mRNA increased as soon as liver was intoxicated with DAB and its expression quantity tended to gradually increase with the aggravation of liver injury. In the period of carcinoma formation, c-myc mRNA expression level also gradually rose with the development of HCC (Table 2, Figures 7, 8). The intervention of UTI could not stop but could retard the increase of expression level of c-myc mRNA.

DISCUSSION

Oval cells are round or oval shaped with scant and basophilic cytoplasm, and round or oval shaped nucleus, small and clear light stained nucleolus and clear nuclear membrane. Because they can differentiate towards hepatic cells or bile duct epithelial cells when hepatic cells are severely injured or the proliferation is inhibited, oval cells are considered as a kind of progenitor cells with potential bilateral differentiation[7]. It is reported that the activation of Ito cells was probably a precondition for the activation of oval cells and stimulates oval cells in the portal areas to migrate towards the hepatic fibrosis area. Consequently, oval cells may participate in the formation of HCC[8-11].

There is no doubt that there are hepatic stem cells in hepatic tissues, but where do the hepatic stem cells come from? Some researchers thought that they were originated from the terminal biliary duct of portal area[12,13], but some insisted that they were from the canal of Hering[14-16], and some even found authentic evidence that the oval cells came from bone marrow stem cells[17-20]. In order to identify the origin of hepatic stem cells and the relationship between hepatic stem cells and the development of HCC, we carried out the study on the surface marker antigen c-kit with immunohistochemical methods, and found that: (1) In the early stage of hepatic injury, the c-kit positive stain cells firstly appeared among the oval cells in the portal area. (2) In the late stage of inflammatory lesion, c-kit was over expressed in the oval cells in the portal area and positive pigmentation presented as patches. (3) During the period of hepatic proliferation and fibrosis, positive expression of c-kit in portal area decreased compared with that in the late stage of inflammatory lesion. (4) In period of the formation of HCC, heteromorphisms of cancer cells were obvious and c-kit was still expressed in portal area. (5) At the beginning of inflammatory lesion, there were small quantities of c-kit positive cells in hepatic lobules with smaller nuclei and more were found near portal area. During the period of hepatic fibrosis, c-kit positive cells were rarely seen in hepatic lobules, but during the formation of HCC, c-kit positive cells appeared both inside and around the cancerous nodes. (6) In the normal hepatic tissues, c-kit-positive stain cells could be occasionally observed in the mitotic and proliferating hepatic cells. From these results, we can conclud that: (1) Oval cells had the highest expression level of c-kit in the portal area from hepatic injury to the occurrence and development of HCC. As it has been proved that the oval cells originate from bile duct epithelial cells in the portal area, we suggest that the terminal bile ducts are an important source of hepatic stem cells. (2) In the course of hepatic injury, c-kit positive cells could be found in hepatic lobules as well, especially near the portal area, which may be related to migration of oval cells along hepatic fibrosis into hepatic lobules. (3) C-kit was not only expressed in hepatic stem cells, but in the mitotic and proliferating hepatic cells, which indicated that c-kit might be a specific mark antigen for a type of juvenile cells, express only in a certain stage of mitotic and proliferation of hepatic cells. (4) C-kit positive stain cells played a role in the whole process of occurrence and development of HCC and appeared in cancerous nodes, so we thought that hepatic stem cells, just as was reported in literature, were involved in the occurrence and development of HCC.

PCNA is a type of M_r 36 000 nuclear protein which is only synthesized and expressed in proliferating cells. Cyto-dynamics shows that PCNA begins to increase in the late G_1 phase in the cell cycle, reaches the peak in the S phase and begins to decrease in the G_2-M phase, in this way it regulates the replication of DNA[21-23]. Therefore, PCNA can effectively reflect the proliferation ability of cells. In this experiment we found that the high level expression of PCNA appeared firstly in the oval cells in portal area at the early stage of inflammation, significantly higher than adjacent tissue. When the mitosis and proliferation of hepatic cells were inhibited, oval cells presented firstly with active proliferation and DNA was synthesized in a large amount in nucleus. The farther they were away from the portal area, the more mature the oval cells differentiated and the larger the size of nucleus tended to be. Thus the expression of PCNA distributed radiatively and regionally around the portal area and the regional predominance was kept for a long time in the process of carcinoma induction. Oval cells took part in the whole process of development of HCC, we could speculate that there might be close relationship between the development of HCC and the PCNA overexpressing oval cells.

c-myc gene is a maintaining gene for malignant tissue, coding for a protein located in nucleolus, a type of DNA conjugated protein with the function of transcription regulation[24-27]. This experiment suggested that the expression of *c-myc* gene increased slightly at the beginning of hepatic injury and the expression of c-myc mRNA increased progressively with the aggravation of hepatic injury. The expression of c-myc mRNA also tended to increase with the development of HCC. The above results indicated that: (1) As an oncogene, *c-myc* might be a promoter gene for HCC and played an important role in maintaining hepatic injury and hepatocyte carcinomatous change. (2) During the development of HCC, the expression level of *c-myc* continued to increase, indicating that *c-myc* was not only a maintaining gene for malignant carcinoma, but the quantity of its expression was a symbol for the degree of malignancy and progression of HCC.

UTI is a kind of broad-spectrum trypsin inhibitor extracted from human beings' urine. It has been found that UTI plays a prominent role in preventing cancer cells from spread. Some researchers pointed out that there were combination spots with UTI on the surface of nearly all kinds of cancer cells membrane and UTI could inhibit cancer cells to secrete granulocyte protein lyase, fibrinoclase, matrix metalloproteinase and collagenase[28,29], which can degrade peripheral matrix and lead tumor cells to spread, by combining with their receptors on the surface of cancer cell membrane. Some clinical reports showed that UTI could inhibit the cancer cells to combine with other anti-cancer drugs[30]. In this experiment, the interference of UTI throughout development of HCC and its effect on HCC were observed. It was found that from the 14th to 16th wk, the occurrence rate of HCC in the interference group was 25% (2/8), which was significantly different ($P<0.05$) from that of cancer induction group at the same time. During the 18th to 20th wk and the 22nd to 24th wk, the occurrence rate of HCC was both 50% (4/8), which was lower than that in the cancer inducing group at the same time. UTI's effect on inhibiting the occurrence of cancer was related to the following factors: (1) The occurrence of HCC needed certain micro-environment and UTI could inhibit some local cells from releasing inflammatory mediators by stabilizing lysosome membrane, then the inflammatory cells' chemotaxis was inhibited and local inflammation was relieved, thus it could inhibit the occurrence of tumor by stabilizing micro-environment. (2) Researches proved that UTI had fairly strong function to inhibit and clear away oxygen-derived free

radicals, while a lot of oxygen-derived free radical receptors existed on the surfaces of liver cells and oval cells, so possibly UTI could protect liver tissue from being damaged by oxygen-derived free radicals. Furthermore, during the whole process of cancer induction, the average cancer node area of liver rats in interference group was smaller than that of cancer inducing group at the same time points ($P<0.05$), especially at the early stage of carcinogenesis, which indicated that UTI could partly inhibit the growth and local spreading of tumor cells.

The results that interference of UTI could not stop but could retard the increase of the expression of c-myc mRNA indicate two points: (1) UTI can prevent the occurrence of hepatic injury and HCC to some extent, but can not inhibit the expression of *c-myc* gene, which might be related with inhibitory effect on hepatic tissue inflammation and protective effect on hepatocytes of UTI. (2) The expression of *c-myc* gene closely relates to the severity of hepatic injury.

REFERENCES

1 **Dominguez-Malagon H**, Gaytan-Graham S. Hepatocellular carcinoma: an update. *Ultrastruct Pathol* 2001; **25**: 497-516
2 **Hou L**, Li Y, Jia YH, Wang B, Xin Y, Ling MY, Lü S. Molecular mechanism about lymphogenous metastasis of hepatocarcinoma cells inmice. *World J Gastroenterol* 2001; **7**: 532-536
3 **Liu H**, Nobumoto K, Yamada Y, Higashi K, Hiai H. Modulation of genetic resistance to hepatocarcinogenesis in DRH rats by partial hepatectomy. *Cancer Lett* 2003; **196**: 13-16
4 **Karmakar R,** Banik S, Chatterjee M. Inhibitory effect of vitamin D3 on 3'methyl-4-dimethyl-amino-azobenzene-induced rat hepatocarcinogenesis: a study on antioxidant defense enzymes. *J Exp Ther Oncol* 2002; **2**: 193-199
5 **Biswas SJ**, Khuda-Bukhsh AR. Effect of a homeopathic drug, Chelidonium, in amelioration of p-DAB induced hepatocarcinogenesis in mice. *BMC Complement Altern Med* 2002; **2**: 4
6 **Koizumi R**, Kanai H, Maezawa A, Kanda T, Nojima Y, Naruse T. Therapeutic effects of uLinastatin on experimentaL crescentic gLomeruLonephritis in rats. *Nephron* 2000; **84**: 347-353
7 **Freitas I**, Fracchiolla S, Baronzio G, Griffini P, Bertone R, Sitar GM, Barni S, Gerzeli G, Sacco MG. Stem cell recruitment and liver de-differentiation in MMTV-neu (ErbB-2) transgenic mice. *Anticancer Res* 2003; **23**: 3783-3794
8 **Benedetti A,** Di Sario A, Casini A, Ridolfi F, Bendia E, Pigini P, Tonnini C, D'Ambrosio L, Feliciangeli G, Macarri G, Svegliati-Baroni G. Inhibition of the NA(+)/H(+) exchanger reduces rat hepatic stell ate cell activity and liver fibrosis: an *in vitro* and *in vivo* study. *Gastroenterology* 2001; **120**: 545-556
9 **Nakamura Y,** Trosko JE, Chang CC, Upham BL. Psyllium extracts decreased neoplastic phenotypes induced by the Ha-Ras oncogene transfected into a rat liver oval cell line. *Cancer Lett* 2004; **203**: 13-24
10 **Martel M**, Sarli D, Colecchia M, Coppa J, Romito R, Schiavo M, Mazzaferro V, Rosai J. Fibroblastic reticular cell tumor of the spleen: report of a case and review of the entity. *Hum Pathol* 2003; **34**: 954-957
11 **Shan CM,** Li J. Study of apoptosis in human liver cancers. *World J Gastroenterol* 2002; **8:** 247-252
12 **Paku S**, Schnur J, Nagy P, Thorgeirsson SS. Origin and structural evolution of the early proliferating oval cells in rat Liver. *Am J Pathol* 2001; **158**: 1313-1323
13 **Toshihior M**. Hepatic stem cells: form bone marrow cells to hepatocytes. *Biochem Biophys Res Commun* 2001; **281**: 1-5
14 **Vessey CJ**, de la Hall PM. Hepatic stem cells: a review. *Pathology* 2001; **33**: 130-141
15 **Badve S,** Logdberg L, Lal A, de Davila MT, Greco MA, Mitsudo S, Saxena R. Small cells in hepatoblastoma lack "oval" cell phenotype. *Mod Pathol* 2003; **16**: 930-936
16 **Okano J,** Shiota G, Matsumoto K, Yasui S, Kurimasa A, Hisatome I, Steinberg P, Murawaki Y. Hepatocyte growth factor exerts a proliferative effect on oval cells through the PI3K/AKT signaling pathway. *Biochem Biophys Res Commun* 2003; **309**: 298-304
17 **Laperche Y.** Oval cells and liver regeneration. *Med Sci* 2003; **19**: 697-698
18 **Hsu HC**, Ema H, Osawa M, Nakamura Y, Suda T, Nakauchi H. Hematopoietic stem cells express Tie-2 receptor in the murine fetaL liver. *Blood* 2000; **96**: 3757-3762
19 **Crosbie OM**, Reynolds M, McEntee G, Traynor O, Hegarty JE, O'Farrelly C. *In vitro* evidence for the presence of hematopoietic stem cells in the adult human liver. *Hepatology* 1999; **29**: 1193-1198
20 **Petersen BE**, Bowen WC, Patrene KD, Mars WM, Sullivan AK, Murase N, Boggs SS, Greenberger JS, Goff JP. Bone marrow as a potential source of hepatic oval cells. *Science* 1999; **284**: 1168-1170
21 **Arroyo MP**, Wang TS. Schizosaccharomyces pombe replication and repair proteins: proliferating cell nuclear antigen (PCNA). *Methods* 1999; **18**: 335-348
22 **Miura M**. Detection of chromatin-bound PCNA in mammaLian ceLLs and its use to study DNA excision require. *J Radiat Res* 1999; **40**: 1-12
23 **Gong Y**, Deng S, Zhang M, Wang G, Minuk GY, Burczynski F. A cyclin-dependent kinase inhibitor(p21(WAF1/CIP1)) affects thymidine incorporation in human liver cancer cells. *Br J Cancer* 2002; **86**: 625-629
24 **Jonas JC**, Laybutt DR, Steil GM, Trivedi N, Pertusa JG, Van de Casteele M, Weir GC, Henquin JC. High glucose stimulates early response gene c-Myc expression in rat pancreatic beta cells. *J Biol Chem* 2001; **276**: 35375-35381
25 **Deng CX**, Brodie SG. Roles of BRCA1 and its interacting proteins. *Bioessays* 2000; **22**: 728-737
26 **Fields WR**, Desiderio JG, Putnam KP, Bombick DW, Doolittle DJ. Quantification of changes in c-myc mRNA levels in normal human bronchial epithelial (NHBE) and lung adenocarcinoma (A549) cells following chemical treatment. *Toxicol Sci* 2001; **63**: 107-114
27 **Langa F**, Lafon I, Vandormael-Pournin S, Vidaud M, Babinet C, Morello D. Healthy mice with an altered c-myc gene: role of the 3' untranslated region revisited. *Oncogene* 2001; **20**: 4344-4353
28 **Kobayashi H**. Suppression of urokinase expression and tumor metastasis by bikunin overexpression (mini-review). *Hum Cell* 2001; **14**: 233-236
29 **Kobayashi H**, Suzuki M, Tanaka Y, Hirashima Y, Terao T. Suppression of urokinase expression and invasiveness by urinary trypsin inhibitor is mediated through inhibition of protein kinase C- and MEK/ERK/c-Jun-dependent signaling pathways. *J Biol Chem* 2001; **276**: 2015-2022
30 **Noie T,** Sugawara Y, Harihara Y, Takayama T, Kubota K, Ohashi Y, Makuuchi M. Kinetics of urinary trypsin inhibitor in patients undergoing partial hepatectomy. *Scand J Gastroenterol* 2001; **36**: 410-416

Edited by Zhu LH **Proofread by** Chen WW and Xu FM

PO Box 2345, Beijing 100023, China
Fax: +86-10-85381893
E-mail: wjg@wjgnet.com www.wjgnet.com

World J Gastroenterol 2004;10(17):2488-2492
World Journal of Gastroenterology
Copyright © 2004 by The WJG Press ISSN 1007-9327

• VIRAL HEPATITIS •

A candidate DNA vaccine elicits HCV specific humoral and cellular immune responses

Li-Xin Zhu, Jing Liu, Ye Ye, You-Hua Xie, Yu-Ying Kong, Guang-Di Li, Yuan Wang

Li-Xin Zhu, Jing Liu, Ye Ye, You-Hua Xie, Yu-Ying Kong, Guang-Di Li, Yuan Wang, State Key Laboratory of Molecular Biology, Institute of Biochemistry and Cell Biology, Shanghai Institutes for Biological Sciences, Chinese Academy of Sciences, Shanghai 200031, China
Supported by the National High Technology R&D Program of China, No. 2001AA215171
Correspondence to: Professor Yuan Wang, Institute of Biochemistry and Cell Biology, Shanghai Institutes for Biological Sciences, Chinese Academy of Sciences, Yue-Yang Road 320, Shanghai 200031, China. wangy@sibs.ac.cn
Telephone: +86-21-54921103 **Fax:** +86-21-54921011
Received: 2004-02-02 **Accepted:** 2004-02-21

Abstract

AIM: To investigate the immunogenicity of candidate DNA vaccine against hepatitis C virus (HCV) delivered by two plasmids expressing HCV envelope protein 1 (E1) and envelope protein 2 (E2) antigens respectively and to study the effect of CpG adjuvant on this candidate vaccine.

METHODS: Recombinant plasmids expressing HCV E1 and E2 antigens respectively were used to simultaneously inoculate mice with or without CpG adjuvant. Antisera were then collected and titers of anti-HCV antibodies were analyzed by ELISA. One month after the last injection, animals were sacrificed to prepare single-cell suspension of splenocytes. These cells were subjected to HCV antigen specific proliferation assays and cytokine secretion assays to evaluate the cellular immune responses of the vaccinated animals.

RESULTS: Antibody responses to HCV E1 and E2 antigens were detected in vaccinated animals. Animals receiving CpG adjuvant had slightly lower titers of anti-HCV antibodies in the sera, while the splenocytes from these animals showed higher HCV-antigen specific proliferation. Analysis of cytokine secretion from the splenocytes was consistent with the above results. While no antigen-specific IL-4 secretion was detected for all vaccinated animals, HCV antigen-specific INF-γ secretion was detected for the splenocytes of vaccinated animals. CpG adjuvant enhanced the secretion of INF-γ but did not change the profile of IL-4 secretion.

CONCLUSION: Vaccination of mice with plasmids encoding HCV E1 and E2 antigens induces humoral and cellular immune responses. CpG adjuvant significantly enhances the cellular immune response.

Zhu LX, Liu J, Ye Y, Xie YH, Kong YY, Li GD, Wang Y. A candidate DNA vaccine elicits HCV specific humoral and cellular immune responses. *World J Gastroenterol* 2004; 10(17): 2488-2492
http://www.wjgnet.com/1007-9327/10/2488.asp

INTRODUCTION

Hepatitis C virus (HCV) infection is a worldwide health problem[1]. Up to now, no effective medical treatment is available for the majority of HCV infected patients[2,3], while new infections are continuously emerging from blood transfusion, needle sharing, unprotected sex, close contact of HCV infected patient and other unidentified sources[4]. Thus to control the spread of HCV by vaccination becomes an urgent task, especially in developing countries including China, where there is a large infected population.

Various routes were taken to develop a vaccine against HCV infection. Recombinant HCV antigens purified from *E.coli*, yeast or insect cells could not protect the vaccinee from virus challenge[5], possibly due to the fact that post-translational modification of the virus antigens in mammalian cells is greatly different from that in the bacterial or yeast cells. So the study on vaccine development has been focused on mammalian systems. Although many efforts have been made in vaccine development and some encouraging results have been obtained[5-8], no effective vaccine is available.

The RNA genome of HCV has a high mutation rate, which explains the existence of many genotypes, subtypes and quasispecies[9-10]. Although there is still a possibility to develop a universal vaccine against HCV of all genotypes, the use of local HCV strain in vaccine study is preferred. Our laboratory has been focusing on DNA vaccine development[11] using an HCV strain isolated from a patient in northern China[12], since DNA vaccine is effective in eliciting cellular immune responses[13] which play key roles in viral clearance.

Envelope proteins were the first choice in the development of vaccines against virus infection. HCV envelope protein 2 has become the major target in HCV vaccine development not only because it is the putative major envelope protein[14], but also because E2 could mediate the binding of HCV particle to host cells[15] and is the ligand of the possible HCV receptor CD81 on the host cell surface[16]. It makes E2 an attractive choice for vaccine development as it has been shown to be a major target of immune response in HCV infected patients[17,18]. Previous studies also revealed multiple neutralizing epitopes in E2 proteins[19-22]. Another envelope protein of HCV, E1, is also desirable for vaccine development, since its possible role in maintaining the natural conformation of E2 protein (through E1-E2 complex)[23] and the possibility of its cooperation with E2 in mediating host cell binding and entry[24]. However, low expression levels of both E1 and E2 proteins were observed when they were expressed in a single open reading frame (data not shown). In this study, we expressed HCV E1 and E2 proteins separately and analyzed the immune responses of DNA vaccination delivered by two plasmids encoding HCV E1 and E2 proteins respectively.

Recent studies showed that the immune system responded to CpG motifs by activating potent Th1-like immune responses[23]. There have also been several reports demonstrating that CpG could enhance humoral immune responses elicited by DNA vaccination[24,25], possibly due to indirect effect of enhanced cellular immune responses. The effect of CpG adjuvant on the immune response elicited by the candidate DNA vaccine was also investigated in this study.

MATERIALS AND METHODS

Plasmids, CpG oligodeoxynucleotide (ODN) and cells

For the construction of pSecTagB/sE2, the fragment of HCV

E2 (aa. 384-661) was amplified using plasmid pUC18/E[12] as template with following primers: sense, 5'GGCGTTAAGCTTAA CACCTACGTG3' (HindIII site underlined); antisense, 5'CAG GAATTCTCACTCTGATCTATC3' (EcoRI site underlined). Insertion of the PCR product into pSecTagB (Invitrogen, California) resulted in pSecTagB/sE2, in which a secretion signal was provided at the N-terminal of E2 sequence. The recombinant plasmid was sequenced before further experiments.

HCV E1 encoding plasmid pSec-preS1-E1t340 (pSecTagB/sE1) was constructed as previously described[26]. CpG ODN1826 with phosphorothioate backbone was synthesized in Promega (Shanghai) according to the published sequence 5'TCCATGA CGTTCCTGACGTT3'[27]. The cell line used for transient expression of the recombinant plasmids, BHK-21, was maintained in DMEM supplemented with 50 mL/L FCS and antibiotics under 50 mL/L CO_2 in a humidified 37 °C incubator.

Transient expression

Transfection of BHK-21 cells with HCV-encoding plasmid or empty vector using lipofectAMINE (Invitrogen) was done according to the manuals of the manufacturer. Cells were harvested 48 h after transfection, lysed in SDS-PAGE loading buffer, and subjected to SDS-PAGE (10%). The resolved samples were then transferred onto nitrocellulose membrane and probed with polyclonal anti-E1 (Liu *et al*., unpublished data) or polyclonal anti-E2 antisera[28]. The signals were visualized with SuperSignal West Pico stable peroxide solution (Pierce, USA).

DNA immunization and sera preparation

Four groups of 5 female BALB/c mice (6-8 weeks old) purchased from the Shanghai Laboratory Animal Center were injected 3 times in quadriceps muscles: group 1, with 100 μg pSecTagB in 100 μL PBS; group 2, with 50 μg pSecTagB/sS1E1 and 50 μg pSecTagB/sE2 in a total volume of 100 μL PBS; group 3, with 100 μg pSecTagB together with 10 μg CpG in a total volume of 100 μL PBS; group 4, with 50 μg pSecTagB/sS1E1, 50 μg pSecTagB/sE2 and 10 μg CpG in a total volume of 100 μL PBS. Injections were performed at 0, 4 and 8 wk and blood samples were taken at -2, 2, 6 and 10 wk. Mice were bled under anesthesia through the retro-orbital plexus. Blood was incubated at room temperature for 4 h and centrifuged at 2 700 r/min at 4 °C for 10 min. Obtained sera were stored at -20 °C.

Anti-HCV antibody analysis

Enzyme-linked immunosorbent assay (ELISA) was used to determine the presence of antibodies against HCV E1 and E2 antigens in serum samples. *E. coli*-expressed HCV E1 (aa 192 to 315) or HCV E2 (aa 450 to 565[31]) was used to coat 96-well plates (MaxiSorp Surface, Nunc) at the concentration of 1 μg/mL. The antigens were suspended in PBS with 0.2 g/L sodium azide and incubated overnight at 4 °C. After the plates were washed with PBS plus 0.5 g/L Tween 20 (PBS-T) and blocked in blocking buffer (50 g/L fat-free milk powder in PBS-T), twofold serial dilutions of serum samples in blocking buffer were added and incubated for 2 h at 37 °C. After three wash steps with PBS-T, horseradish peroxidase (HRP) conjugated goat-anti-mouse IgG (Dako, Denmark; 1 000-fold diluted in blocking buffer) was added and incubated for 1 h at 37 °C. The plate was then developed with substrate buffer (50 mmol/L Na_2HPO_4, 25 mmol/L citric acid, 75 μg/mL 3,3',5,5'-tetramethylbenzidine, 0.15 mL/L H_2O_2). After 30 min of incubation at room temperature, the reaction was stopped by adding 0.5 mol/L H_2SO_4, and absorbance was measured at 450 nm on a microplate reader (Model 450, Bio-Rad Laboratories). Antibody titers were calculated as the highest dilution which gave a positive reading. The cutoff value was set as mean absorbency (*A*) of sera from the control mice vaccinated with non-recombinant plasmid multiplied by 2.

Preparation of splenocytes

Mice were sacrificed by cervical dislocation. Spleens from these mice were ground on metal mesh to prepare single-cell suspension in grinding media (RPMI1640 supplemented with 100 mL/L FCS, 1 mmol/L Sodium pyruvate and 50 μmol/L β-ME). Red blood cells were lysed by incubating the splenocyte preparations with lysis buffer (0.15 mol/L NH_4Cl, 10 mmol/L $KHCO_2$, 0.1 mmol/L EDTA, pH7.2-7.4) briefly and then washed with grinding media. The cells were resuspended in a small volume of grinding media and counted in the presence of Trypan blue. Splenocytes were immediately used for further experiments.

Assay for HCV antigen specific splenocyte proliferation

Splenocytes from vaccinated mice or naïve mice were diluted to 4×10^6/mL with grinding media and plated onto 24-well-plates at 2 mL/well. The cells were *in vitro* stimulated with 500 ng E2 (aa 450 to 565[31]) or mock stimulated for 3 d. The media were collected for cytokine assay. Fresh grinding medium with 0.5 μCi/mL [^{3}H] thymidine (Amersham Pharmacia Biotech) was added for another 24 h. Cells were then washed with PBS and 100 g/L trichloroacetic acid (TCA), incubated with 100 g/L TCA for 10 min at 37 °C. Afterwards, TCA was removed and cells were lysed with lysis buffer containing 0.33 mol/L NaOH and 10 g/L sodium dodecyl sulfate (SDS). [^{3}H] thymidine incorporation in the cell lysates was measured by liquid scintillation counting. Antigen specific proliferation was presented by stimulation index (SI): SI = cpm of the cells stimulated by antigen/cpm of mock stimulated cells. Splenocytes from naïve mice were used to monitor the specificity of this assay.

Analysis of HCV antigen specific cytokine secretion

Media from the *in vitro* stimulated splenocytes were collected and precleared by centrifugation at 10 000 *g* and 4 °C for 10 min. Concentration of INF-γ and IL-4 in the media was determined by ELISA using the mouse cytokine assay kits (Jingmei Biotech, Shenzhen) according to the protocols provided by the manufacturer. HCV E2 specific cytokine secretion was represented by stimulation index (SI): SI = cytokine secreted upon E2 stimulation/cytokine secreted upon mock stimulation. Splenocytes from naïve mice were used to monitor the specificity of this assay.

Statistical analysis

Statistical analysis was performed with unpaired 2-sided Student *t* test. Differences with P values <0.05 were considered significant.

RESULTS

Transient expression of HCV antigens in mammalian cells

Because the expression level was low when E1 and E2 were expressed in one open reading frame (data not shown), we expressed HCV E1 and E2 genes in separate plasmids in this study. To achieve high-level expression and proper post-translational modification of HCV envelope proteins, the pSecTagB vector with an efficient secretion signal of IgG molecules was chosen. Plasmid expressing HCV E2 was constructed as described in Materials and Methods. C-terminal hydrophobic sequence of E2 was truncated to facilitate the secretion of E2 and to obtain complex-type glycosylation modification, which was presented on the surface of HCV particles[29]. Secreted E2 protein was shown to have better antigenicity, possibly due to its proper modification by Golgi enzymes[30]. Plasmid pSecTagB/sE1 was taken as another component of the candidate DNA vaccine since high-level expression of E1 with this plasmid was observed previously in transiently and stably transfected NIH3T3 cells[26]. Before vaccination experiment, BHK-21 cells were transfected with pSecTagB/sE1 and pSecTagB/sE2, respectively, to check if they

would properly express the target HCV proteins in this cell line. By Western blot, both E1 and E2 were detected as glycosylated proteins with MW higher than those of polypeptide backbones, respectively (Figure 1). Secreted products were also detected for E1[26] and E2 (data not shown).

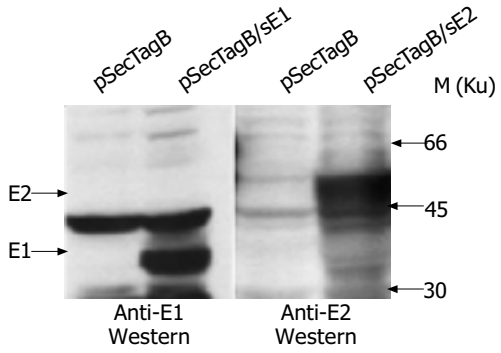

Figure 1 Transient expression with plasmids used in vaccination. Plasmids used for transfection are indicated at the top of each lanes. E1 and E2 products are indicated by arrowheads.

Humoral immune responses after DNA vaccination

DNA vaccination using the above characterized plasmids was carried out as described in Materials and Methods. After two injections, HCV E1 and E2 specific antibodies were detected in the sera of several mice. Without CpG adjuvant, the seroconversion rate was 2/5 for anti-E1 antibody, and 1/5 for anti-E2 antibody. When CpG was included as an adjuvant, the seroconversion rate was 3/4 for anti-E1 antibody and 2/4 for anti-E2 antibody. After the third injection, all animals became seroconverted to both anti-E1 and anti-E2 antibodies. The highest anti-E1 titer was 1:320 after the third injection for mice receiving plasmids only, while the highest titer for mice receiving plasmids with CpG was 80. The highest anti-E2 titers for both groups reached 1 280, but the average anti-E2 titer for mice receiving CpG was slightly lower than that for those receiving no CpG (Table 1).

E2 specific splenocyte proliferation

All the animals were sacrificed 30 d after the last injection to analyze cellular immune responses of the memory phase. Single-cell suspension of splenocytes was prepared for each individual animal. Splenocytes were immediately cultured in the presence of HCV E1 peptide or E2 protein. [^{3}H] thymidine was then added to the cells to measure HCV antigen specific proliferation. In our experiments, HCV E1 specific proliferation was not observed, neither was E1 specific cytokine secretion (data not shown), possibly due to insufficient stimulation. For E2 specific splenocyte proliferation, as shown in Figure 2, animals vaccinated with pSecTagB only or pSecTagB plus CpG had stimulation indexes similar to that of naïve mice. Some of the animals vaccinated with plasmids pSecTagB/sE1+pSecTagB/sE2 showed E2 specific splenocyte proliferation while the others did not. This gave an average SI slightly higher than that of pSecTagB vaccinated mice. Animals vaccinated with HCV gene encoding plasmids together with CpG all showed E2 specific splenocyte proliferation, which resulted in a significant difference ($P = 0.005$) of SI between animals injected with pSecTagB/sE1+pSecTagB/sE2+CpG and animals injected with pSecTagB+CpG.

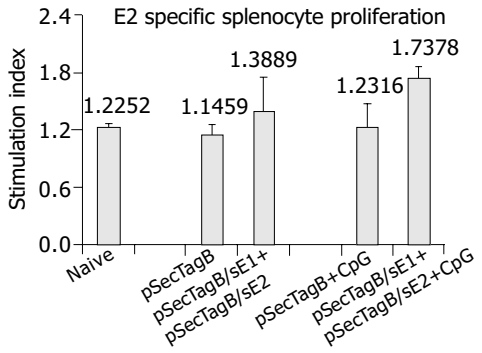

Figure 2 E2-specific splenocyte proliferation. Error bars represent the standard errors. Asterisk indicates the significant difference of the average SI between animals injected with (pSecTagB/sE1+pSecTagB/sE2+CpG) and animals injected with (pSecTagB+CpG) ($P = 0.005$).

E2 specific cytokine secretion

Cellular immune responses were also evaluated by cytokine secretion assay of the *in vitro* stimulated splenocytes from all vaccinated animals. INF-γ secretion is a marker of Th1 type antigen-specific cellular immune responses and plays key roles in fighting virus infection. Mice injected with pSecTagB/sE1+pSecTagB/sE2 showed heterogeneous cellular immune responses, some had E2 stimulated INF-γ secretion, while the rest did not. This resulted in a slightly higher average of SI compared to the control group injected with pSecTagB (Figure 3A). Mice injected with pSecTagB/sE1+pSecTagB/sE2+CpG all showed highly E2-specific INF-γ secretion, showing a SI higher than 3, while the control group injected with pSecTagB+CpG had an average SI similar to those of naïve mice and mice injected with pSecTagB alone. The difference of SI between the experiment group and its control group was very significant ($P = 0.0003$).

IL-4 secretion is a marker of Th2-like cellular immune responses. No significant difference in IL-4 secretion was detected between all groups receiving different inoculums (Figure 3B). IL-4 secretion of the vaccinated animals was similar to that of naïve mice, indicating that Th2-like cellular immune response was decreased to basal level, if there was ever a Th2-like response. In terms of IL-4 secretion, no effect of CpG was detected.

Table 1 Anti-HCV titers[1] after the third injection

Vaccine	Anti-E1 titers				
	1	2	3	4	5
pSecTagB/sE1+pSecTagB/sE2[2]	320	40	Dead animal	320	320
pSecTagB/sE1+pSecTagB/sE2+CpG[3]	80	80	Dead animal	80	80
			Anti-E2 titers		
	1	2	3	4	5
pSecTagB/sE1+pSecTagB/sE2[2]	160	160	Dead animal	1 280	1 280
pSecTagB/sE1+pSecTagB/sE2+CpG[3]	160	160	Dead animal	160	1 280

[1]Titers were determined as described in Materials and Methods. Serial dilution of anti-sera started from 1:40, thus titers lower than 40 were not determined and considered 0. [2]The cutoff value was established as mean *A* of sera from the control mice vaccinated with pSecTagB. [3]The cutoff value was established as mean *A* of sera from the control mice vaccinated with pSecTagB+CpG.

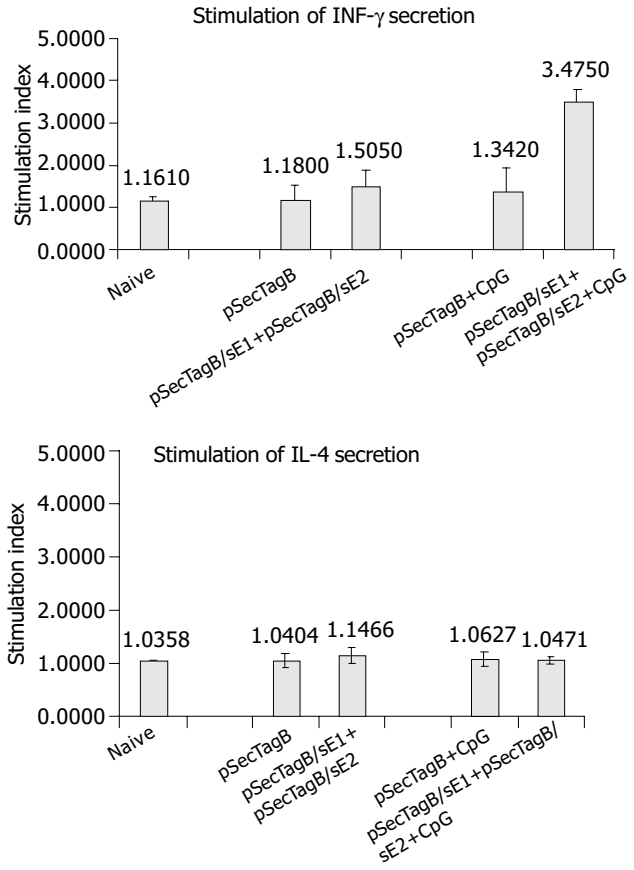

Figure 3 E2-specific cytokine secretion. Error bars represent the standard errors. Asterisk indicates the very significant difference of the average SI between animals injected with (pSecTagB / sE1+pSecTagB / sE2+CpG) and animals injected with (pSecTagB+CpG) in terms of INF-γ secretion (P = 0.0003).

DISCUSSION

In this study, target HCV antigens encoded by the DNA vaccine candidate, E1 and E2, were delivered by two separate plasmids that achieved higher-level expression and appropriate glycosylation of both antigens. DNA immunization results demonstrated that this DNA vaccine candidate could induce HCV specific humoral and cellular immune responses in mice. Anti-E2 titer obtained in this study was similar to our previous study[11], which was also comparable to the results from other laboratories[31-35]. We also detected comparable levels of anti-E1 antibodies in the sera of vaccinated mice, which together with anti-E2 antibodies, might be important in neutralizing the circulating HCV virus and preventing its spread in patients. HCV antigen specific splenocyte proliferation indicated that our candidate DNA vaccine was able to induce cellular immune response, which was critical in viral clearance. Cytokine secretion analysis revealed that the cellular immune response is Th1 type, which could activate CTL to remove cells with HCV antigen expression. Studies of HCV patients showed that protection against HCV infection was positively correlated with cellular immune responses[36,37], indicating that cellular immune responses might be more important in evaluating a candidate vaccine. The ability of our candidate vaccine to induce HCV specific cellular immune responses makes it a favorable choice in the development of prophylactic and therapeutic vaccine against HCV.

CpG motif, that is, CpG dinucleotide in particular base context (XCGY, where X is any base but C, and Y is any base but G), was first found to be immunoactive in activating B cells[38]. These CpG motifs are prevalent in bacterial and many viral DNAs but are heavily methylated and suppressed in vertebrate genomes[38,39]. Recent studies have shown that the immune system could respond to CpG motifs by activating potent Th1-like immune responses[23]. Several reports demonstrated that CpG could enhance humoral immune responses elicited by DNA vaccination[24,25], possibly due to indirect effect of enhanced cellular immune responses. In our vaccination experiment, we observed that after the second injection, the seroconversion rate for mice receiving CpG adjuvant was higher than that for those not receiving CpG. This enhanced humoral immune response at the early stage was likely due to the indirect positive effect of CpG on antigen presentation (via activation of antigen presenting cells by Th1). However, after the third injection, when all animals became seroconverted, those who received CpG as an adjuvant showed lower titers of both anti-E1 and anti-E2. This was consistent with the notion that when Th1-like response is the major immune response, Th2-like response is usually inhibited, followed by decreased antibody production. Further analysis of antigen specific cytokine secretion was consistent with this explanation. E2 specific INF-γ secretion was enhanced in splenocytes from those animals receiving CpG in vaccination, while this adjuvant did not change the E2 specific IL-4 secretion profile. These results indicated that CpG enhanced the Th1-like cellular immune response.

Apart from DNA vaccine, live virus vaccine and peptide vaccine are also efficient in inducing cellular immune response. Live virus vaccine using several different viral vectors has been under investigation[8,28,40], with continuous promising progresses. However, the interest in peptide vaccine is diminishing. The problem lies in the polymorphism of MHC molecules in the population. Certain individuals may have the MHC molecules necessary to bind a specific antigenic peptide, while others may not. Thus, the universality of a vaccine based on a specific peptide becomes a concern. Recently, combinational vaccination strategy with different species of vaccine components has been successful in laboratory in protecting against some elusive infectious reagents[41,42]. Combinational vaccination could reduce host immune responses against the viral vector itself, thus enhancing the efficiency of delivery. More importantly, combinational vaccination with different components could activate different components of the host immune surveillance system and result in enhanced immune responses. Our next effort will be focused on combinational vaccination with DNA vaccine descried above as one component.

ACKNOWLEDGEMENT

We thank Professor Yu Wang (Peking University) for providing HCV cDNA for this study.

REFERENCES

1 **Cohen JC**. The scientific challenge of hepatitis C. *Science* 1999; **285**: 26-30
2 **McHutchison JG**, Gordon SC, Schiff ER, Shiffman ML, Lee WM, Rustgi VK, Goodman ZD, Ling MH, Cort S, Albrecht JK. Interferon alfa-2b alone or in combination with ribavirin as initial treatment for chronic hepatitis C. Hepatitis Interventional Therapy Group. *N Engl J Med* 1998; **339**: 1485-1492
3 **Zein CO**, Zein NN. Advances in therapy for hepatitis C infection. *Microbes Infect* 2002; **4**: 1237-1246
4 **Williams I**. Epidemiology of hepatitis C in the United States. *Am J Med* 1999; **107**: 2S-9S
5 **Choo QL**, Kuo G, Ralston R, Weiner A, Chien D, Van Nest G, Han J, Berger K, Thudium K, Kuo C. Vaccination of chimpanzees against infection by the hepatitis C virus. *Proc Natl Acad Sci U S A* 1994; **91**: 1294-1298
6 **Fournillier A**, Depla E, Karayiannis P, Vidalin O, Maertens G, Trepo C, Inchauspe G. Expression of noncovalent hepatitis C virus envelope E1-E2 complexes is not required for the induction of antibodies with neutralizing properties following DNA immunization. *J Virol* 1999; **73**: 7497-7504

7 **Gordon EJ**, Bhat R, Liu Q, Wang YF, Tackney C, Prince AM. Immune responses to hepatitis C virus structural and nonstructural proteins induced by plasmid DNA immunizations. *J Infect Dis* 2000; **181**: 42-50

8 **Makimura M**, Miyake S, Akino N, Takamori K, Matsuura Y, Miyamura T, Saito I. Induction of antibodies against structural proteins of hepatitis C virus in mice using recombinant adenovirus. *Vaccine* 1996; **14**: 28-36

9 **Davis GL**. Hepatitis C virus genotypes and quasispecies. *Am J Med* 1999; **107**: 21S-26S

10 **Chen S**, Wang YM. Genetic evolution of structural region of hepatitis C virus in primary infection. *World J Gastroenterol* 2002; **8**: 686-693

11 **Zhu J**, Wang CL, Zhu LX, Kong YY, Wang Y, Li GD. DNA immunization with recombinant HCV E2 expression plasmids. *Shengwu Huaxue Yu Shengwu Wuli Xuebao* 2002; **34**: 445-451

12 **Wang Y**, Okamoto H, Tsuda F, Nagayama R, Tao QM, Mishiro S. Prevalence, genotypes, and an isolate (HC-C2) of hepatitis C virus in Chinese patients with liver disease. *J Med Virol* 1993; **40**: 254-260

13 **Gurunathan S**, Wu CY, Freidag BL, Seder RA. DNA vaccines: a key for inducing long-term cellular immunity. *Curr Opin Immunol* 2000; **12**: 442-447

14 **Hijikata M**, Kato N, Ootsuyama Y, Nakagawa M, Shimotohno K. Gene mapping of the putative structural region of the hepatitis C virus genome by *in vitro* processing analysis. *Proc Natl Acad Sci U S A* 1991; **88**: 5547-5551

15 **Rosa D**, Campagnoli S, Moretto C, Guenzi E, Cousens L, Chin M, Dong C, Weiner AJ, Lau JY, Choo QL, Chien D, Pileri P, Houghton M, Abrignani S. A quantitative test to estimate neutralizing antibodies to the hepatitis C virus: cytofluorimetric assessment of envelope glycoprotein 2 binding to target cells. *Proc Natl Acad Sci U S A* 1996; **93**: 1759-1763

16 **Pileri P**, Uematsu Y, Campagnoli S, Galli G, Falugi F, Petracca R, Weiner AJ, Houghton M, Rosa D, Grandi G, Abrignani S. Binding of hepatitis C virus to CD81. *Science* 1998; **282**: 938-941

17 **Zonaro A**, Ravaggi A, Puoti M, Kremsdorf D, Albertini A, Cariani E. Differential pattern of sequence heterogeneity in the hepatitis C virus E1 and E2/NS1 proteins. *J Hepatol* 1994; **21**: 858-865

18 **Shimizu YK**, Hijikata M, Iwamoto A, Alter HJ, Purcell RH, Yoshikura H. Neutralizing antibodies against hepatitis C virus and the emergence of neutralization escape mutant viruses. *J Virol* 1994; **68**: 1494-1500

19 **Zibert A**, Schreier E, Roggendorf M. Antibodies in human sera specific to hypervariable region 1 of hepatitis C virus can block viral attachment. *Virology* 1995; **208**: 653-661

20 **Lechner S**, Rispeter K, Meisel H, Kraas W, Jung G, Roggendorf M, Zibert A. Antibodies directed to envelope proteins of hepatitis C virus outside of hypervariable region 1. *Virology* 1998; **243**: 313-321

21 **Meunier JC**, Fournillier A, Choukhi A, Cahour A, Cocquerel L, Dubuisson J, Wychowski C. Analysis of the glycosylation sites of hepatitis C virus (HCV) glycoprotein E1 and the influence of E1 glycans on the formation of the HCV glycoprotein complex. *J Gen Virol* 1999; **80**(4 Pt 1): 887-896

22 **Meyer K**, Basu A, Ray R. Functional features of hepatitis C virus glycoproteins for pseudotype virus entry into mammalian cells. *Virology* 2000; **276**: 214-226

23 **Krieg AM**. CpG motifs in bacterial DNA and their immune effects. *Annu Rev Immunol* 2002; **20**: 709-760

24 **Moldoveanu Z**, Love-Homan L, Huang WQ, Krieg AM. CpG DNA, a novel immune enhancer for systemic and mucosal immunization with influenza virus. *Vaccine* 1998; **16**: 1216-1224

25 **Encke J**, zu Putlitz J, Stremmel W, Wands JR. CpG immunostimulatory motifs enhance humoral immune responses against hepatitis C virus core protein after DNA-based immunization. *Arch Virol* 2003; **148**: 435-448

26 **Zhu J**, Kong YY, Liu J, Zhang ZC, Wang Y, Li GD. Secretory expression of different C-terminal truncated HCV E1 proteins in mammalian cells and characterization of the expressed products. *Shengwu Huaxue Yu Shengwu Wuli Xuebao* 2001; **33**: 634-640

27 **Chu RS**, Targoni OS, Krieg AM, Lehmann PV, Harding CV. CpG oligodeoxynucleotides act as adjuvants that switch on T helper 1 (Th1) immunity. *J Exp Med* 1997; **186**: 1623-1631

28 **Liu J**, Zhu L, Zhang X, Lu M, Kong Y, Wang Y, Li G. Expression, purification, immunological characterization and application of *Escherichia coli*-derived hepatitis C virus E2 proteins. *Biotechnol Appl Biochem* 2001; **34**(Pt2): 109-119

29 **Sato K**, Okamoto H, Aihara S, Hoshi Y, Tanaka T, Mishiro S. Demonstration of sugar moiety on the surface of hepatitis C virions recovered from the circulation of infected humans. *Virology* 1993; **196**: 354-357

30 **Inudoh M**, Nyunoya H, Tanaka T, Hijikata M, Kato N, Shimotohno K. Antigenicity of hepatitis C virus envelope proteins expressed in Chinese hamster ovary cells. *Vaccine* 1996; **14**: 1590-1596

31 **Zucchelli S**, Capone S, Fattori E, Folgori A, Di Marco A, Casimiro D, Simon AJ, Laufer R, La Monica N, Cortese R, Nicosia A. Enhancing B- and T-cell immune response to a hepatitis C virus E2 DNA vaccine by intramuscular electrical gene transfer. *J Virol* 2000; **74**: 11598-11607

32 **Tedeschi V**, Akatsuka T, Shih JW, Battegay M, Feinstone SM. A specific antibody response to HCV E2 elicited in mice by intramuscular inoculation of plasmid DNA containing coding sequences for E2. *Hepatology* 1997; **25**: 459-462

33 **Ou-Yang P**, Hwang LH, Tao MH, Chiang BL, Chen DS. Co-delivery of GM-CSF gene enhances the immune responses of hepatitis C viral core protein-expressing DNA vaccine: role of dendritic cells. *J Med Virol* 2002; **66**: 320-328

34 **Encke J**, zu Putlitz J, Geissler M, Wands JR. Genetic immunization generates cellular and humoral immune responses against the nonstructural proteins of the hepatitis C virus in a murine model. *J Immunol* 1998; **161**: 4917-4923

35 **Dou J**, Liu K, Chen Z, Wo J, He N, Liu Y, Zhang M, Wang X, Xu C. Effect of immunization in mice with recombinant DNA encoding the hepatitis C virus structural protein. *Chin Med J* 1999; **112**: 1036-1039

36 **Cooper S**, Erickson AL, Adams EJ, Kansopon J, Weiner AJ, Chien DY, Houghton M, Parham P, Walker CM. Analysis of a successful immune response against hepatitis C virus. *Immunity* 1999; **10**: 439-449

37 **Lechner F**, Wong DK, Dunbar PR, Chapman R, Chung RT, Dohrenwend P, Robbins G, Phillips R, Klenerman P, Walker BD. Analysis of successful immune responses in persons infected with hepatitis C virus. *J Exp Med* 2000; **191**: 1499-1512

38 **Krieg AM**, Yi AK, Matson S, Waldschmidt TJ, Bishop GA, Teasdale R, Koretzky GA, Klinman DM. CpG motifs in bacterial DNA trigger direct B-cell activation. *Nature* 1995; **374**: 546-549

39 **Jones PA**. The DNA methylation paradox. *Trends Genet* 1999; **15**: 34-37

40 **Ezelle HJ**, Markovic D, Barber GN. Generation of hepatitis C virus-like particles by use of a recombinant vesicular stomatitis virus vector. *J Virol* 2002; **76**: 12325-12334

41 **Amara RR**, Villinger F, Altman JD, Lydy SL, O'Neil SP, Staprans SI, Montefiori DC, Xu Y, Herndon JG, Wyatt LS, Candido MA, Kozyr NL, Earl PL, Smith JM, Ma HL, Grimm BD, Hulsey ML, Miller J, McClure HM, McNicholl JM, Moss B, Robinson HL. Control of a mucosal challenge and prevention of AIDS by a multiprotein DNA/MVA vaccine. *Science* 2001; **292**: 69-74

42 **Haddad D**, Liljeqvist S, Stahl S, Hansson M, Perlmann P, Ahlborg N, Berzins K. Characterization of antibody responses to a Plasmodium falciparum blood- stage antigen induced by a DNA prime/protein boost immunization protocol. *Scand J Immunol* 1999; **49**: 506-514

Edited by Zhang JZ and Wang XL **Proofread by** Xu FM

PO Box 2345, Beijing 100023, China
Fax: +86-10-85381893
E-mail: wjg@wjgnet.com www.wjgnet.com

World J Gastroenterol 2004;10(17):2493-2497
World Journal of Gastroenterology
Copyright © 2004 by The WJG Press ISSN 1007-9327

Helicobacter pylori cagA, *iceA* and *vacA* genotypes in patients with gastric cancer in Taiwan

Hwai-Jeng Lin, Chin-Lin Perng, Wen-Ching Lo, Chew-Wun Wu, Guan-Ying Tseng, Anna Fen-Yau Li, I-Chen Sun, Yueh-Hsing Ou

Hwai-Jeng Lin, I-Chen Sun, Division of Gastroenterology, Department of Medicine, VGH-TAIPEI, Taiwan, China
Chin-Lin Perng, I-Lan Hospital, Department of health, Taiwan, China
Wen-Ching Lo, Zhongxiao Municipal Hospital, Taipei, Taiwan, China
Chew-Wun Wu, Division of General Surgery, Department of Surgery, VGH-TAIPEI, Taiwan, China
Guan-Ying Tseng, Ton-Yen General Hospital, Hsin-Chu, Taiwan, China
Anna Fen-Yau Li, Department of Pathology, VGH-TAIPEI, Taiwan, China
Yueh-Hsing Ou, Institute of Biotechnology in Medicine, School of Medical Technology and Engineering, and School of Medicine, National Yang-Ming University, Taiwan, China
Supported by VGH 91-274, NSC 91-2314-B075-127
Correspondence to: Professor Hwai-Jeng Lin, Division of Gastroenterology, Department of Medicine, VGH-TAIPEI, Shih-Pai Rd, Sec 2, Taipei, 11217, Taiwan, China. hjlin@vghtpe.gov.tw
Telephone: +886-2-28712121 Ext. 2015 **Fax:** +886-2-28739318
Received: 2003-11-12 **Accepted:** 2003-12-15

Abstract

AIM: *Helicobacter pylori* (*H pylori*) has been linked to chronic gastritis, peptic ulcer, gastric cancer and MALT-lymphoma. The link of genotypes of *H pylori* to gastric cancer remains controversial. The aim of this study was to investigate the *H pylori vacA* alleles, *cagA* and *iceA* in patients with gastric cancer in Taiwan.

METHODS: Patients with gastric cancer, peptic ulcer and chronic gastritis were enrolled in this study. We obtained biopsy specimens from the stomach at least 2 cm away from the tumor margin in patients with gastric cancer, and from the antrum of stomach in patients with peptic ulcer or chronic gastritis. DNA extraction and polymerase chain reaction were used to detect the presence or absence of *cagA* and to assess the polymorphism of *vacA* and *iceA*.

RESULTS: A total of 168 patients (gastric ulcer: 77, duodenal ulcer: 66, and chronic gastritis: 25) were found to have positive PCR results of the biopsy specimens from patients with peptic ulcer and chronic gastritis. We found positive *cagA* (139/168, 83%), m2 (84/168, 50%) and *iceA1* (125/168, 74%) strains in the majority of patients. In patients with gastric cancer, the *vacA* s1a and s1c subtypes were less commonly found than those in non-cancer patients (35/66 *vs* 127/168, $P = 0.0001$ for s1a and 13/66 *vs* 93/168, $P < 0.0001$ for s1c). In the middle region, the m1T strain in patients with gastric cancer was more than that of non-cancer patients (23/66 *vs* 33/168, $P = 0.02$).

CONCLUSION: In Taiwan, *H pylori* with positive *vacA* s1a, *cagA* and *iceA1* strains are found in the majority of patients with gastric cancer or non-cancer patients. In patients with gastric cancer, the *vacA* s1a and s1c subtypes are less and m1T is more than in patients with peptic ulcer and chronic gastritis.

Lin HJ, Perng CL, Lo WC, Wu CW, Tseng GY, Li AFY, Sun IC, Ou YH. *Helicobacter pylori cagA*, *iceA* and *vacA* genotypes in patients with gastric cancer in Taiwan. *World J Gastroenterol* 2004; 10(17): 2493-2497
http://www.wjgnet.com/1007-9327/10/2493.asp

INTRODUCTION

Helicobacter pylori (*H pylori*) is one of the most common bacterial infections of humans[1]. It has been closely linked to chronic gastritis, peptic ulcer, gastric cancer and MALT-lymphoma[2,3]. It has heterogeneous genotypes and phenotypes[4,5].

The International Agency for Research on Cancer of the World Health Organization recommends that *H pylori* be classified as a group I carcinogen [6]. In a long-term follow-up study, gastric cancers developed in 36 (2.9%) of the 1 246 infected and none of the 280 uninfected patients ($P<0.001$)[7]. Enomoto *et al.* and Uemura *et al.* also confirmed that very few patients who had gastric cancer were not infected with *H pylori*[7,8].

The clinical outcome of *H pylori* infection was supposed to be linked to certain strains, *e.g.* vacuolating cytotoxin (*vacA*) and the cytotoxin-associated gene (*cagA*)[9,10]. However, controversy exists concerning the relationship between *H pylori* and gastric cancer. It is now evident that approximately 25-50% of the world's population is infected by *H pylori*. Why, then, did only a minority of them develop gastric cancer? A report of an epidemiological study in Africa suggested that *H pylori* infection did not always directly correlate with the risk for gastric cancer[11]. The same phenomenon occurred in southern Asia[12]. The prevalence of *H pylori* is high in India and Bangladesh, but low gastric cancer rates have been reported. In addition, Louw et al did not find difference in the prevalence of *H pylori* infection when comparing gastric cancer cases with matched controls[13].

How could the above phenomenon be explained? Although *H pylori* infection is very common, there is geographic distribution of different subtypes[14]. Is it possible that different subtypes of *H pylori* cause different outcomes? In Taiwan, specific genotypes of *H pylori* have been found in patients with peptic ulcer or non-ulcer dyspepsia[15,16]. There is no report concerning the genotype of gastric cancer in Taiwan so far. The aim of this study was to determine the *vacA*, *cagA*, and *iceA* genotypes of *H pylori* in patients with gastric cancer as compared with those in patients with peptic ulcer or chronic gastritis in Taiwan.

MATERIALS AND METHODS

Patients with gastric cancer, peptic ulcers (gastric ulcer or duodenal ulcer, at least 5 mm in diameter) or chronic gastritis were invited to enter the study. Patients with pregnancy, bleeding tendency (platelet count less than 50 000/mm^3, prothrombin time less than 30%, or taking anti-coagulants), age under 10, or over 90 years, and inability to cooperate were excluded from the study. The study was approved by the Clinical Research Committee of the Veterans General Hospital, Taipei.

Endoscopic examination and biopsy were performed after informed consent was obtained. In patients with peptic ulcer or chronic gastritis, we took one specimen from the antrum of

each patient for rapid urease test, one specimen from the gastric antrum for DNA extraction and PCR assay. In patients with gastric cancer, we took two specimens from the stomach at least 2 cm from the cancer part for rapid urease test and DNA extraction and PCR assay. Lysates of gastric mucosa biopsy specimens were used for PCR. DNA of gastric biopsy specimens was extracted according to the method described by Boom[17]. Briefly, biopsy specimens were homogenized in guanidinium isothiocyanate, using a sterile micropestle. DNA was extracted, washed and eluted in 100 μL of 10 mnol/L Tris-HCL (pH 8.3). Two microliters of the eluted DNA were used for each PCR reaction.

All pathological samples from patients with gastric cancer were evaluated by a single experienced pathologist, and classified in accordance with the Lauren classification as diffuse, intestinal or mixed types[18]. The description of advanced gastric cancer was based on Borrmann's classification[19]. The morphological subtypes of early gastric cancer were classified according to the guidelines of Japanese Endoscopy Society[20].

Oligonucleotide primers for PCR amplification of specific segments are shown in Table 1[15,21,22]. For *vacA* evaluation, the PCR program comprised 35 cycles of denaturation (at 94 °C for 1 min), annealing (at 56 °C for 2 min, extension at 72 °C for 1 min), and one final extension (at 72 °C for 10 min). For *cagA*, amplification was performed with 35 cycles of denaturation (at 94 °C for 1 min, annealing at 56 °C for 2 min, extension at 72 °C for 1 min), and one final extension (at 72 °C for 5 min). For *iceA* amplification, amplifications were performed with 40 cycles of denaturation (at 95 °C for 30 s), annealing (at 50 °C for 45 s), extension (at 72 °C for 45 s) and one final extension (at 72 °C for 10 min).

The association between *H pylori* genotypes and clinical diseases was determined using the chi-square test with Yates' correction or Fisher's exact test when appropriate. A *P* value less than 0.05 was considered statistically significant.

RESULTS

Patients with peptic ulcer and chronic gastritis

Between January 2002 and Feburary 2003, a total of 278 patients with peptic ulcer or chronic gastritis were included in this study. There were 200 males and 78 females with a mean age of 62.1 years, 95% C.I.: 61.1-64.3 years. One hundred and forty patients had gastric ulcers, 101 patients had duodenal ulcers, 37 patients had chronic gastritis. Among these patients, 168 patients (65.9%) (comprising 25 patients with chronic gastritis, 77 patients with gastric ulcer, and 66 patients with duodenal ulcer) were found to have positive PCR (Table 2). Of them, the urease test was found to be positive in 152 patients (90.5%). There was no significant difference in age of the patients with chronic gastritis (mean: 51 years, 95% CI : 42.8-59.2 years), gastric ulcer (65.3 years, 62.3-68.9), duodenal ulcer (58.9 years, 54.7-63.1) and gastric cancer (69 years, 67-91).

In the s-region, *vacA* s1a was most frequently found (76%, 127/168, $P<0.001$ *vs* s1b, s1c and s2) followed by s1c (93/168, 55%), s1b (9/168, 5%), and s2 (2/168, 1%) (Table 3). In the m-region, m2 was most frequently found (84/168, 50%) ($P<0.0001$ *vs* m1T and m1), followed by m1T (33/168, 20%) and m1 (2/168, 2%). *CagA* was found in 139 patients (83%). *IceA1* was found most commonly in comparison with *ice A2* (125 *vs* 29, $P<0.0001$).

Patients with gastric cancer

A total of 167 patients with gastric cancers were enrolled in this study (mean age: 69 y/o, 95% CI: 67.0-91.0, sex M/F: 130/37). We obtained specimens through endoscopic biopsy from 66 patients and surgery from 101 patients. After PCR assessment of gastric specimens, a total of 66 patients (39.5%) were found to be positive (24 patients from endoscopic biopsy and 42 patients from surgical specimens) (Table 3). We found early gastric cancer in seven patients (type IIc: 2, IIc+III: 5) and advanced gastric cancer in 59 patients (Borrmann type I: 7, II: 28, III: 14, IV: 10) (Table 4).

Among these patients, 35 (53%) were found to have *vacA* s1a ($P<0.001$ *vs* s1c, s1b, and s2), followed by s1c (13 patients, 20%) ($P<0.001$ *vs* s1b and s2) and s1b (1 patient, 2%), s2 (1 patient, 2%) (Table 3). In the m-region, m2 was most commonly found (32 patients, 48%) ($P<0.0001$ *vs* m1) followed by m1T (23 patients, 35%) and m1 (1 patient, 2%). In the *iceA* subtypes, *iceA1* was most commonly found (39 patients, 59%) followed by *ice A2* (15 patients, 23%) ($P<0.0001$). *CagA* was found in 76% (50/66) of the patients.

The genotypes between early gastric cancer and advanced gastric cancer were similar (Table 4). There was no difference of genotypes according to Borrmann's classification (Table 5). Regarding the histological classification, there was no difference of genotypes among the diffuse type, intestinal type and mixed types (Table 6).

Table 1 Oligonucleotide primers used for *cagA*, *vacA* and *iceA* genotyping

Region detected	Primer designation	Primer sequence	Size of PCR product (bp)	References
s1 and s2	VA1-F	5'ATGGAAATACAACAAACACACC3'	259/286	14
	VA1-R	5'CTGCTTGAATGCGCCAAACTTTATC3'		
s1a	SS1-F	5'GTCAGCATCACACCGCAAC3'	190	20
s1b	SS3-F	5'AGCGCCATACCGCAAGAG3'	187	20
s1c	S1C-F	5'CTYGCTTTAGTRGGGYTA3'	213	26
M1	VA3-F	5'GGTCAAAATGCGGTCATGG3'	290	20
	VA3-R	5'CCATTGGTACCTGTAGAAAC3'		
M1T	m1T-F	5'GGTCAAAATGCGGTCATGG3'	290	14
	m1T-R	5'CTCTTAGTGCCTAAAGAAACA3'		
M2	VA4-F	5'GGAGCCCCAGGAAACATTG3'	352	20
	VA4-R	5'CATAACTAGCGCCTTGCAC3'		
iceA1	iceA1F	5'GTGTTTTTAACCAAAGTATC3'	247	21
	iceA1R	5'CTATAGCCASTYTCTTTGCA3'		
iceA2	iceA2F	5'GTTGGGTATATCACAATTTAT3'	229	21
	iceA2R	5'TTRCCCTATTTTCTAGTAGGT3'		
lcagA	lcagAD008	5'ATAATGCTAAATTAGACAACTTGAGCGA3'	297	8
	lcagAR008	5'TTAGAATAATCAACAAACATCACGCCAT3'		

Table 2 Genotypes of *H pylori* in patients with non-gastric cancer (chronic gastritis, gastric ulcer and duodenal ulcer) (%)

Diagnosis	No of Patients	s1a	s1b	s1c	s2	s1a +s1c	s1as +s1b	s1b +s2	s1a+ s1b+s1c	m1	m1T	m2	m1T +m2	cagA	iceA1	iceA2	iceA1 +iceA2
Chronic gastritis	25	21 (84)	0 (0)	14 (56)	0 (0)	11 (44)	0 (0)	0 (0)	0 (0)	0 (0)	8 (32)	12 (48)	2 (8)	22 (88)	22 (88)	2 (8)	0 (0)
Gastritic ulcer	77	59 (77)	1 (1)	42 (55)	0 (0)	36 (47)	0 (0)	0 (0)	0 (0)	0 (0)	11 (14)	45 (58)	1 (1)	63 (82)	54 (70)	17 (22)	3 (4)
Duodenal ulcer	66	47 (71)	8 (12)	37 (56)	2 (3)	30 (45)	7 (11)	2 (3)	4 (6)	2 (3)	14 (21)	27 (41)	7 (11)	54 (82)	49 (74)	10 (15)	3 (5)

P>0.05 for all genotypes among three groups.

Table 3 Genotypes of *H pylori* in patients with gastric cancer (GC) and non-gastric cancer (non-GC) (%)

Diagnosis	No of Patients	s1a	s1b	s1c	s2	s1a+s1c	s1a+ s1b+s2	s1a+ s1b+s1c	m1	m1T	m2	m1T +m2	cagA	iceA1	iceA2	iceA1 +iceA2
GC	66	35[b] (53)	1 (2)	13[l] (20)	1 (2)	7 (11)	1 (2)	0 (0)	1 (2)	23[a] (35)	32[h] (48)	4 (6)	50 (76)	39[f] (59)	15 (23)	2 (3)
Non-GC	168	127[d] (76)	9 (5)	93[l] (55)	2 (1)	77 (46)	2 (2)	4 (2)	2 (2)	33[a] (20)	84[j] (50)	10 (6)	139 (83)	125[f] (74)	29 (17)	6 (4)

[b]P<0.001 *vs* s1b, s1c and s2 of non-GC, [d]P<0.0001 *vs* m1T, m1 of non-GC, [f]P<0.0001 *vs* ice A2 of non-GC, [h]P<0.001 *vs* s1c, s1b and s2 of GC, [j]P<0.0001 *vs* m1 of GC, [l]P<0.0001, [a]P = 0.02.

Table 4 Genotypes of *H pylori* in patients with early or advanced gastric cancer (%)

Diagnosis	No of Patients	s1a	s1b	s1c	s2	s1a+s1c	s1a+ s1b+s2	m1	m1T	m2	m1T+m2	cagA	iceA1	iceA2	iceA1 +iceA2
EGC	7	4 (57)	0 (0)	2 (29)	0 (0)	1 (14)	0 (0)	0 (0)	1 (14)	3 (43)	0 (0)	6 (86)	4 (57)	1 (4)	0 (0)
AGC	59	31 (53)	1 (2)	11 (19)	1 (2)	6 (10)	1 (2)	1 (2)	22 (37)	29 (49)	4 (7)	44 (75)	35 (59)	14 (24)	2 (3)

Table 5 Genotypes of *H pylori* in patients with advanced gastric cancer according to Borrmann's classification (%)

Diagnosis	No of Patients	s1a	s1b	s1c	s2	s1a+s1c	s1a+ s1b+s2	m1	m1T	m2	m1T+m2	cagA	iceA1	iceA2	iceA1 +iceA2
I	7	4 (57)	0 (0)	2 (29)	0 (0)	1 (14)	0 (0)	0 (0)	5 (71)	1 (14)	0 (0)	5 (71)	5 (71)	1 (14)	0 (0)
II	28	15 (54)	1 (4)	3 (11)	1 (4)	3 (11)	1 (4)	1 (4)	8 (29)	13 (46)	1 (4)	20 (71)	17 (61)	6 (21)	1 (4)
III	13	6 (46)	0 (0)	5 (38)	0 (0)	2 (15)	0 (0)	0 (0)	3 (23)	8 (62)	1 (8)	11 (85)	8 (62)	3 (23)	0 (0)
IV	10	5 (50)	0 (0)	1 (10)	0 (0)	0 (0)	0 (0)	0 (0)	5 (50)	7 (70)	2 (20)	8 (80)	5 (50)	4 (40)	1 (10)

Table 6 Genotypes of *H pylori* in patients with gastric cancer according to histological classification. (%)

Diagnosis	No of Patients	s1a	s1b	s1c	s2	s1a+s1c	s1a+ s1b+s2	m1	m1T	m2	m1T+m2	cagA	iceA1	iceA2	iceA1 +iceA2
Intestinal	28	15 (54)	0 (0)	5 (18)	0 (0)	3 (5)	0 (0)	0 (0)	7 (25)	16 (57)	2 (7)	21 (75)	16 (57)	8 (29)	1 (4)
Diffuse	24	12 (50)	1 (4)	4 (17)	1 (4)	2 (8)	1 (4)	0 (0)	9 (38)	10 (42)	1 (4)	18 (75)	15 (63)	4 (17)	1 (4)
mixed	11	5 (45)	0 (0)	3 (27)	0 (0)	1 (9)	0 (0)	1 (9)	5 (45)	5 (45)	1 (9)	9 (82)	6 (55)	3 (27)	0 (0)

Comparison of gastric cancer patient with non-cancer (peptic ulcer and chronic gastritis) patients

In patients with gastric cancer, the *vacA* s1a and s1c subtypes were less commonly found than those in non-cancer patients (35/66 *vs* 127/168, P<0.001 for s1a and 13/66 *vs* 93/168, P<0.0001 for s1c) (Table 3). In the middle region, the m1T in patients with gastric cancer was more than that in non-cancer patients (23/66 *vs* 33/168, P = 0.02). There was no difference in *iceA* and *cagA* between patients with gastric cancer and non-cancer status.

DISCUSSION

This is the first sudy to investigate the allelic variations of *H pylori vacA*, *cagA* and *iceA1* in gastric cancer patients in Taiwan. The results showed *vacA* s1a, m2, and *iceA1* predominated in patients with gastric cancer and those without.

H pylori has become a world-wide infective agent ranging from 25% in developed countries to more than 80% in the developing world[23]. Not all individuals infected with *H pylori* developed gastric illness and this might be related to various factors such as environmental factors, host genetic factors, and bacterial virulent ability[24]. Certain genotypes (*e.g*. *cagA*, *vacA* s1a) have been closely related to severe clinical outcome and response to anti- *H pylori* therapy[25,26]. However, these findings were not supported by other studies[27].

Different genotypes of *H pylori* have been confirmed in patients with peptic ulcer or non-ulcer dyspepsia from diverse geographic areas[14,23]. For example, in Northern and Eastern Europe, 89% strains were *vacA* s1a. *VacA* s1a and s1b were equally present in France and Italy. In Spain and Portugal, 89% of the strains were *vacA* s1b. While in north America, s1a and s1b were equally prevalent. *VacA* s1c was only found in East Asia. In Taiwan, *H pylori* with *vacA* s1a was the major strain[15,16]. Because of this diversity, it is interesting to analyze the genotypes in different areas.

In this study, predominance of *vacA* s1a was found in patients with gastric cancer (53%) and non-cancer status (76%). Our findings were similar to those reported by other authors in patients with peptic ulcer or non-ulcer dyspepsia[15,16]. In Hong Kong and Korea, a low incidence of *vacA* s1a subtype was found[28,29]. The previous Taiwan reports gave no data concerning *vacA* s1c[6,15]. *VacA* s1c was frequently found (20% in gastric cancer and 55% in non-cancer) in this study. In contrast, *vacA* s1b and s2 were rare. Our findings were compatible with those

in mainland China[30]. A high incidence of *vacA* s1c in this study was similar to the reports of Hong Kong[28], Korea[29], and Japan[31], but different from those of the Western world[14].

Concerning the m-region of *vacA*, m1 strains predominated in most Western reports[14,23]. However, there were few m1 subtypes (2% in cancer and 2% in non-cancer) in this study. We used a modified primer (m1T)[15] and found that some patients (35% in gastric cancer, 20% in non-cancer) with *H pylori* infection contained this genotype. M2 strains predominated (48% in gastric cancer and 50% in non-cancer) in this study. Our findings were consistent with reports from our previous experience[32], other studies in Taiwan[15,16], Hong Kong[28], and mainland China[30]. In contrast, Japan and Korea had a much lower incidence of m2 strain[27,29]. We could not detect the m-region in some patients (15% in gastric cancer and 28% in non-cancer). This indicates a great variation in the *vacA* region in Taiwan, particularly in the mid-region locus. *H pylori* may have a different geographic evolution in Taiwan even compared with other East Asian countries.

IceA1 has been suggested to be related to peptic ulcer disease[22,33]. But, like other authors, we doubted this finding[27-29,32]. It has been found that *IceA1* is the predominant subtype of *ice* in the East Asia, while *iceA2* is the predominant subtype in the USA and Columbia[27]. In this study, we found *iceA1* was the predominant subtype and showed no difference in patients with gastric cancer and non-cancer status.

The clinical relevance of putative virulence-associated genes of *H pylori* in patients with gastric cancer is a matter of controversy. Enomoto *et al*. found that 98% of patients with gastric cancer were *H pylori*-positive[12]. Many studies suggested the strong association of certain genotypes of *H pylori* with gastric cancer[34-38]. A significant association (o.r. 2.94) between *cagA* and gastric cancer was found in young Italian patients[34]. Miehlke *et al*. suggested a significant association between the *H pylori vacA* s1, m1, *cagA* and gastric cancer[35]. Kidd *et al*. confirmed that the *vacA* s1b, m1 and *iceA1* were closely linked to gastric cancer in South Africa[36]. van Doorn *et al.* found a significant association between the presence of ulcers or gastric cancer and the presence of *vacA* s1 and *cagA*[37]. Basso *et al* and Qiao *et al*. also concluded that *H pylori* infection caused by *cagA* positive/*vacA* s1 was a frequent finding in patients with gastric cancer[38,39].

However, some authors have presented different observations. Mitchell *et al*. compared serum antibody to *cagA* antigen in patients with gastric cancer and normal subjects[40]. They found no association between *cagA* and gastric cancer in Chinese subjects. Other authors also confirmed no relationship between *cagA* status and the risk of gastric cancer[41]. Some Japanese studies did not support the link of *vacA* and *cagA* with gastric cancer[42,43]. In these Japanese studies, the majority of the controls had positive *vacA* and *cagA*. Therefore, they obtained a different result as compared with those of the Western studies. In addition, the case number was small in their series. Increased number is needed to avoid bias. In this study, we found no difference in *cagA* between gastric cancer and non-cancer status. But, we found less *vacA* s1a, s1c and more m1T in patients with gastric cancer.

There is a paucity of *iceA* allele data in isolates from patients with gastric cancer. Gastric cancer isolates from Japan and Korea were distinguished by the prevalence of *iceA1* (67%) while 75% of isolates from the USA were *iceA2*[27]. In this study, we found that iceA1 predominated (59%) in patients with gastric cancer.

Patients with histologic findings of severe gastric atrophy, corpus-predominant gastritis or intestinal metaplasia are at an increased risk for gastric cancer. *H pylori* carrying the *cagA* gene might have promoted the atrophic metaplastic mucosal lesions that represent the pathway in multistep intestinal type gastric oncogenesis[25,44]. Correa *et al*. and Uremura *et al*. found that severe atrophic gastritis accompanying intestinal metaplasia caused by persistent *H pylori* infection was closely related to the development of intestinal type gastric cancer[9,45]. But, some authors present different results. No significant relationship was found between *H pylori* and diffuse type gastric cancer because atrophic change was not evident in these patients[46,47]. In addition, other authors did not support this finding due to epidemiological and pathological evidence[48,49]. In this study, we found no difference in genotypes among diffuse, intestinal and mixed types of gastric cancer. In addition, there was no difference of genotypes in patients with early and advanced gastric cancer. However, the case number should be increased to avoid type II error.

In conclusion, *vacA* s1a, m2, and *iceA1* predominate in patients with gastric cancer. As compared with those of non-cancer patients, patients with gastric cancer have less *vacA* s1a, s1c and more m1T subtypes. Genotypes are similar according to morphological and pathological classification.

REFERENCES

1 **Blaser MJ**. Ecology of *Helicobacter pylori* in the human stomach. *J Clin Invest* 1997; **100**: 759-762
2 **Dunn BE**, Cohen H, Blaser MJ. *Helicobacter pylori*. *Clin Microbiol Rev* 1997; **10**: 720-741
3 **Wang RT**, Wang T, Chen K, Wang JY, Zhang JP, Lin SR, Zhu YM, Zhang WM, Cao YX, Zhu CW, Yu H, Cong YJ, Zheng S, Wu BQ. *Helicobacter pylori* infection and gastric cancer: evidence from a retrospective cohort study and nested case-control study in China. *World J Gastroenterol* 2002; **8**: 1103-1107
4 **Akopyranz N**, Bukanov NO, Westblom TU, Kresovich S, Berg DE. DNA diversity among clinical isolates of *Helicobacter pylori* detected by PCR-based RAPD fingerprinting. *Nucleic Acids Res* 1992; **20**: 5137-5142
5 **Foxall PA**, Hu LT, Mobley HL. Use of polymerase chain reaction-amplified *Helicobacter pylori* urease structural genes for differentiation of isolates. *J Clin Microbiol* 1992; **30**: 739-741
6 International Agency for Research on Cancer. Schistosomes, liver flukes and *Helicobacter pylori* IARC Monographs on the Evaluation of Carcinogenic Risks to Humans. 61. *Lyon, France: IARC* 1994
7 **Uemura N**, Okamoto S, Yamamoto S, Matsumura N, Yamaguchi S, Yamakido M, Taniyama K. *Helicobacter pylori* infection and the development of gastric cancer. *N Engl J Med* 2001; **345**: 784-789
8 **Enomoto H**, Watanabe H, Nishikura K, Umezawa H, Asakura H. Topographic distribution of *Helicobacter pylori* in the resected stomach. *Eur J Gastroenterol Hepatol* 1998; **10**: 473-478
9 **Covacci A**, Censini S, Bugnoli M, Petracca R, Burroni D, Macchia G, Massone A, Papini E, Xiang Z, Figura N. Molecular characterization of the 128-kDa immunodominant antigen of *Helicobacter pylori* associated with cytotoxicity and duodenal ulcer. *Proct Natl Acad Sci U S A* 1993; **90**: 5791-5795
10 **Cover TL**. The vacuolating cytotoxin of *Helicobacter pylori*. *Mol Microbiol* 1996; **20**: 241-246
11 **Holcombe C**. *Helicobacter pylori*: The African enigma. *Gut* 1992; **33**: 429-431
12 **Miwa H**, Go MF, Sato N. *H pylori* and gastric cancer: The Asian enigma. *Am J Gastroenterol* 2002; **97**: 1106-1112
13 **Louw JA**, Kidd MSG, Kummer AF, Taylor K, Kotze U, Hanslo D. The relationship between *Helicobacter pylori* infection, the virulence genotypes of the infecting strain and gastric cancer in the African setting. *Helicobacter* 2001; **6**: 268-273
14 **van Doorn LJ**, Figueiredo C, Megráud F, Pena S, Midolo P, Queiroz DM, Carneiro F, Vanderborght B, Pegado MD, Sanna R, De Boer W, Schneeberger PM, Correa P, Ng EK, Atherton J, Blaser MJ, Quint WG. Geographic distribution of *vacA* allelic types of *Helicobacter pylori*. *Gastroenterology* 1999; **116**: 823-830
15 **Wang HJ**, Kuo CH, Yeh AAM, Chang PCL, Wang WC. Vacuolating toxin production in clinical isolates of *Helicobacter pylori* with different vacA genotypes. *J Inf Dis* 1998; **178**: 207-212
16 **Lin CW**, Wu SC, Lee SC, Cheng KS. Genetic analysis and

clinical evaluation of vacuolating cytotoxin gene A and cytotoxin-associated gene A in Taiwanese *Helicobacter pylori* isolated from peptic ulcer patients. *Scand J Infect Dis* 2000; **32**: 51-57
17 **Boom R**. Sol CJ, Salimans MM, Jansen CL, Mertheim-van Dillen PM, van der Noordaa J. Rapid and simple method for purification of nucleic acids. *J Clin Microbiol* 1990; **28**: 495-503
18 **Lauren P**. The two histological main types of gastric carcinoma: Diffuse and the so-called intestinal type caricinoma. *Acta Path Microbiol Scand* 1965; **64**: 31-49
19 **Borrmann R**. (1926) Handbuch der spezielen Pathologisch Anatomie und Histologie, Vol 4/1, (ed) Henke F and Lubarsch 0, ch C, pt5. *Berlin Springer*
20 Japanese Research Society for Gastric Cancer. The general rules for the Gastric Cancer Study in Surgery and Pathology. Part I, clinical classification and Part II, histological classification of gastric cancer. *Jpn J Surg* 1981; **11**: 127-145
21 **Atherton JC**, Cao P, Peek RM, Tummuru MKR, Blaser M, Cover TL. Mosaicism in vacuolating cytotoxin alleles of *Helicobacter pylori*. *J Biol Chem* 1995; **270**: 17771-17777
22 **van Doorn LJ**, Figueiredo C, Sanna R, Plaisier A, Schneeberger P, de Boer W, Quint W. Clinical relevance of the cagA, vacA and iceA status of *Helicobacter pylori*. *Gastroenterology* 1998; **115**: 58-66
23 **Pounder RE**. The prevalence of *Helicobacter pylori* in different countries. *Aliment Pharmacol Ther* 1995; **9**(Suppl 2): 33-40
24 **Malaty HM**, Graham DY. Importance of childhood socioeconomic status on the current prevalence of *Helicobacter pylori* infection. *Gut* 1994; **35**: 742-745
25 **Parsonnet J**, Friedman GD, Orentreich N, Vogelman H. Risk for gastric cancer in people with cagA positive or cagA negative *Helicobacter pylori* infection. *Gut* 1997; **40**: 297-301
26 **Atherton JC**. The clinical relevance of strain types of *Helicobacter pylori*. *Gut* 1997; **40**: 701
27 **Yamaoka Y**, Kodama T, Gutierrez O, Kim JG, Kashima K, Graham DY. Relationship between *Helicobacter pylori iceA*, *cagA*, and *vacA* status and clinical outcome: studies in four different countries. *J Clin Microbiol* 1999; **37**: 2274-2279
28 **Wong BC**, Yin Y, Berg DE, Xia HHX, Zhang JZ, Wang WH, Wong WH, Huang XR, Tang VS, Lam SK. Distribution of distinct vacA, agA and iceA alleles in *Helicobacter pylori* in Hong Kong. *Helicobacter pylori* 2001; **6**: 317-324
29 **Kim SY**, Woo CW, Lee YM, Son BR, Kim JW, Chae HB, Youn SJ, Park SM. Genotyping *cagA*, *vacA* subtype, *iceA1*, and *BabA* of *Helicobacter pylori* isolates from Korean patients, and their association with gastroduodenal diseases. *J Korean Med Sci* 2001; **16**: 579-584
30 **Pan ZJ**, Berg DE, van der Hulst RWM, Su WW, Raudonikiene A, Xiao SD, Dankert J, Tytgat GN, van der Ende A. Prevalence of vacuolating cytotoxin production and distribution of distinct vacA alleles in *Helicobacter pylori* from China. *J Infect Dis* 1998; **178**: 220-226
31 **Fukuta K**, Azuma T, Ito Y, Suto H, Keida Y, Wakabayashi H, Watamabe A, Kuriyama M. Clinical relevance of caeE gene from *Helicobacter pylori* strains in Japan. *Dig Dis Sci* 2002; **47**: 667-674
32 **Perng CL**, Lin HJ, Sun IC, Tseng GY, Chang FY, Lee SD. *Helicobacter pylori cagA*, *iceA* and *vacA* status in Taiwan patients with peptic ulcer and gastritis. *J Gastroenterol Hepatol* 2003; **18**: 1244-1249
33 **Figura N**, Vindigni C, Covacci A, Presenti L, Burroni D, Vernillo R, Banducci T, Roviello F, Marrelli D, Bicontri M, Kristodhullu S, Gennari C, Vaira D. CagA positive and negative *Helicobacter pylori* strains are simultaneously present in the stomach of most patients with non-ulcer dyspepsia: relevance to histological damage. *Gut* 1998; **42**: 772-778
34 **Rugge M**, Busatto G, Cassaro M, Shiao YH, Russo V, Leandro G, Avellini C, Fabiano A, Sidoni A, Covacci A. Patients younger than 40 years with gastric carcinoma: *Helicobacter pylori* genotype and associated gastritis phenotype. *Cancer* 1999; **85**: 2506-2511
35 **Miehlke S**, Kirsch C, Agha-Amiri K, Gunther T, Lehn N, Malfertheiner P, Stolte M, Ehninger G, Bayerdorffer E. The *Helicobacter pylori* vacA s1, m1 genotype and cagA are associated with gastric carcinoma in Germany. *Int J Cancer* 2000; **87**: 322-327
36 **Kidd M**, Peek RM, Lastovica AJ, Israel DA, Kummer AF, Louw JA. Analysis of *iceA* genotypes in South African *Helicobacter pylori* strains and relationship to clinically significant disease. *Gut* 2001; **49**: 629-635
37 **van Doorn LJ**, Figueiredo C, Rossau R, Jannes G, van Asbroeck M, Sousa JC, Carneiro F, Quint WG. Typing of *Helicobacter pylori vacA* gene and detection of *cagA* gene by PCR and reverse hybridization. *J Clin Microbiol* 1998; **36**: 1271-1276
38 **Basso D**, Navaglia F, Brigate L, Piva MG, Toma A, Greco E, Di Mario F, Galeotti F, Roveroni G, Corsini A, Plebani M. Analysis of *Helicobacter pylori vacA* and *cagA* genotypes and serum antibody profile in benign and malignant gastroduodenal diseases. *Gut* 1998; **43**: 182-186
39 **Qiao W**, Hu JL, Xiao B, Wu KC, Peng DR, Atherton JC, Xue H. *cagA* and *vacA* genotype of *Helicobacter pylori* associated with gastric disease in Xi'an area. *World J Gastroenterol* 2003; **9**: 1762-1766
40 **Mitchell HM**, Hazell SL, Li YY, Hu PJ. Serological response to specific *Helicobacter pylori* antigens: antibody against *cagA* antigen is not predictive of gastric cancer in a developing country. *Am J Gastroenterol* 1996; **91**: 1785-1788
41 **Kikuchi S**, Crabtree JE, Forman D, Kurosawa M. Association between infections with cagA-positive or –negative strains of *Helicobacter pylori* and risk for gastric cancer in young adults. *Am J Gastroenterol* 1999; **94**: 3455-3459
42 **Shimoyama T**, Yoshimura T, Mikami T, Fukuda S, Crabtee JE, Munakata A. Evaluation of *Helicobacter pylori vacA* genotypes in Japanese patients with gastric cancer. *J Clin Pathol* 1998; **51**: 299-301
43 **Maeda S**, Ogura K, Yoshida H, Kanai F, Ikenoue T, Kato N, Shiratori Y, Omata M. Major virulence factors, *vacA* and *cagA* are commonly positive in *Helicobacter pylori* isolates in Japan. *Gut* 1998; **42**: 338-343
44 **Rugge M**, Cassaro M, Farinati F, Saggioro A, Di Mario F. *Helicobacter pylori* and atrophic gastritis: importance of cag-A status. *J Natl Cancer Inst* 1996; **88**: 762-764
45 **Correa P**. Human gastric carcinogenesis: a multistep and multifactorial process-First American Cancer Society Award Lecture on Cancer Epidemiology and Prevention. *Cancer Res* 1992; **52**: 6735-6740
46 **Sipponen M**, Kosunen TU, Valle J, Riihela M, Seppala K. *Helicobacter pylori* infection and chronic gastritis in gastric cancer. *J Clin Pathol* 1992; **45**: 319-323
47 **Solcia E**, Fiocca R, Luinetti O, Villani L, Padovan L, Calistri D, Ranzani GN, Chiaravalli A, Capella C. Intestinal and diffuse gastric cancers arise in a different background of *Helicobacter pylori* gastritis through different gene involvement. *Am J Surg Pathol* 1996; **20**(Suppl 1): 8-22
48 **Kikuchi S**, Wada O, Nakajima T, Kobayashi O, Konishi T, Inaba Y. Serum anti-*Helicobacter pylori* antibody and gastric carcinoma among young adults. *Cancer* 1995; **75**: 2789-2793
49 **Kokkola A**, Valle J, Haapiainen R, Sipponen P, Kivilaakso E, Puolakkainen P. *Helicobacter pylori* infection in young patients with gastric carcinoma. *Scand J Gastroenterol* 1996; **31**: 643-647

Edited by Wang XL and Xu FM

PO Box 2345, Beijing 100023, China
Fax: +86-10-85381893
E-mail: wjg@wjgnet.com www.wjgnet.com

World J Gastroenterol 2004;10(17):2498-2502
World Journal of Gastroenterology
Copyright © 2004 by The WJG Press ISSN 1007-9327

Construction of attenuated Salmonella typhimurium Strain expressing *Helicobacter pylori* conservative region of adhesin antigen and its immunogenicity

Yang Bai, Ya-Li Zhang, Ji-De Wang, Zhao-Shan Zhang, Dian-Yuan Zhou

Yang Bai, Ya-Li Zhang, Ji-De Wang, Dian-Yuan Zhou, PLA Institute for Digestive Medicine, Nanfang Hospital, the First Military Medical University, Guangzhou 510515, Guangdong Province, China
Zhao-Shan Zhang, Institute of Biotechnology, Academy of Military Medical Sciences, Beijing 100071, China
Supported by the National Natural Science Foundation of China, No. 30270078
Correspondence to: Dr. Yang Bai , PLA Institute for Digestive Medicine, Nanfang Hospital, the First Military Medical University, Guangzhou 510515, Guangdong Province, China. baiyang1030@hotmail.com
Telephone: +86-20-61641532
Received: 2003-11-04 **Accepted:** 2004-01-12

Abstract

AIM: To construct a non-resistant and attenuated *Salmonella typhimurium* (*S. typhimurium*) strain which expresses conservative region of adhesion AB of *Helicobacter pylori* (*H pylori*) and evaluate its immunogenicity.

METHODS: The AB gene amplified by PCR was inserted into the expression vector pYA248 containing *asd* gene and through two transformations introduced into the delta *Cya*, delta *Crp*, delta *Asd* attenuated Salmonella typhimurium strain, constructing balanced lethal attenuated Salmonella typhimurium strains X4072 (pYA248-AB). Bridged ELISA method was used to measure the expression of AB antigen in sonicate and culture supernatant. According to the method described by Meacock, stability of the recombinant was evaluated. Semi-lethal capacity test was used to evaluate the safety of recombinant. The immunogenicity of recombinant was evaluated with animal experiments.

RESULTS: The attenuated *S. typhimurium* X4072 (pYA248-AB) which expresses AB was successfully constructed. Furthermore, bridged ELISA assay showed that the content of AB in recombinant X4072 (pYA248- AB) culture supernatant was higher than that was in thallus lytic liquor. And after recombinant X4072 (pYA248- AB) was cultured for 100 generations without selection pressure, the entire recombinant bacteria selected randomly could grow, and the AB antigen was defected positive by ELISA. The growth curve of the recombinant bacteria showed that the growth states of X4072 (pYA248) and X4072 (pYA248-AB) were basically consistent. The survival rate of C57BL/6 was still 100%, at 30 d after mice taking X4072 (pYA248-AB) 1.0×10^{10} cfu orally. Oral immunization of mice with X4072 (pYA248-AB) induced a specific immune response.

CONCLUSION: *In vitro* recombinant plasmid appears to be stable and experiments on animals showed that the recombinant strains were safe and immunogenic *in vitro*, which providing a new live oral vaccine candidate for protection and care of *H pylori* infection.

Bai Y, Zhang YL, Wang JD, Zhang ZS, Zhou DY. Construction of attenuated Salmonella typhimurium Strain expressing *Helicobacter pylori* conservative region of adhesin antigen and its immunogenicity. *World J Gastroenterol* 2004; 10 (17): 2498-2502
http://www.wjgnet.com/1007-9327/10/2498.asp

INTRODUCTION

The discovery of *Helicobacter pylori* (*H pylori*) has brought about a revolution in the research of etiological factor and prevention and cure of chronic gastritis, peptic ulcer and the associated diseases[1,2]. It has been confirmed that *H pylori* is the main cause of chronic gastritis and peptic ulcer, and an important factor for the infection of gastric cancer and mucosa-associated lymphoid tissue (MALT) lymphoma and primary gastric non-Hodgkin's lymphoma[3-7]. In 1994, the World Health Organization has defined it as a class 1 carcinogen, and direct evidence of its carcinogenesis has recently been demonstrated in an animal model and a retrospective cohort study and nested case-control study in China[8,9]. Data of epidemiology showed that 50 percent of the population all over the world is infected with *H pylori*, and China has a high infection rate[10]. Based on it, eradication of *H pylori* is one of the main methods for preventing and treating the above-mentioned diseases. At present, the widely used method for eradication of *H pylori* in clinical practice is the antibiotic treatment, though high the eradication rate is, such problems as high expenses, yearly reduced eradication rate resulting from gradually increasing drug-resistant strains, side effects of drugs and low patient compliance have still not been solved[11-13]. Immunization against *H pylori* infection has been one of the most prospective treatments. In view of the fact that the conservative region of four confirmed adhesins is outer membrane protein and porin type component, outer membrane protein and porin are the excellent candidate components vaccination[14-16]. In addition, the attenuated Salmonella typhimurium strain expressing foreign antigen is a very hopeful new-generation of vaccine. Experiments on human body indicated that the attenuated Salmonella typhimurium strain has very good endurence and immunogenicity, which can be used to transmit foreign antigen, therefore, the problem of adjuvant as well as the problem of high cost for taking subunit protein vaccine orally are solved. At present, the research of attenuated Salmonella typhimurium strain in application to *H pylori* vaccine has been done, but non-resistant and attenuated Salmonella typhimurium strain containing the balanced lethal system has not yet been applied to the research and production of *H pylori* vaccine. We attempted to construct the non-resistance and attenuated Salmonella typhimurium strain expressing AB, and to study its biological properties to pave the way for further research of biological treatment.

MATERIALS AND METHODS

Materials

The strains and plasmids used in the experimental processes are showed in Table 1.

Table 1 Strain (plasmid) and genotype

Strain (plasmid)		Genotype	Source
E coli X6097		*Asd*$^-$	Dr. Roy Curtiss
Salmonella			
typhimurium	X3181	Wild strain	Institute for the control of biological product, Ministry of Health
	X3730	*GalE*$^-$, *hsd*$^-$, *asd*$^-$	Dr. Roy Curtiss
	X4072	*Cya*$^-$, *Crp*$^-$, *Asd*$^-$	Dr. Roy Curtiss
pET-22b (+)-AB		Amp^r, *AB*	Construction in the previous research[17-20], Dr. Roy Curtiss
pYA248		*Asd*$^+$	Construction in the research
pYA248-AB		*AB*	

Thirty specific-pathogen free male C57BL/6 mice, aged 4 wk, were purchased from Animal Center of our institute. Restriction enzymes, such as *EcoR* I, *Sal* I *etc*. and T4 DNA ligase, Vent DNA polymerase *etc*. were purchased from New England Biolabs corporation, Promega corporation and Sino-American Hua Mei Biotechnology Company, respectively. The goat anti-rabbit IgG-HRP and IgA-HRP were purchased from Sino-American Hua Mei Biotechnology Company. Our institute provided anti-AB antibody and AB antigen. DAP (50 mg/L) was purchased from Sigma corporation. Other reagents were analytically pure reagents produced in China.

Recombinant DNA techniques

The alkaline lysis method was chosen for rapid and large-scale preparations of plasmid DNA as described previously[21]. In accordance with the the gene sequence in conservative region, we designed specific primers and added appropriate restriction enzyme sites on its 5' termini, which was synthesized by Shanghai Boya *Co*. The sequences of primers were as follows: conservative region 1: 5'-CCG GAA TTC AAC GCG CTC AAC AAT CAG-3'; conservative region 2, 5'-CAC GTC GAC CTA GAA TGA ATA CCC ATA AG-3'. Conservative region 1 and conservative region 2 contained *Eco*R I and *Sal* I sites, respectively. The template was pET-22b (+) -AB. PCR was performed by the hot start method. The PCR condition was that after initial denaturing at 95 °C for 30 s, each cycle of amplification consisted of denaturation at 95 °C for 30 s, annealing at 55 °C for 30 s and polymerization at 72 °C for 30 s, and a further polymerization for 10 min after 35 amplication cycles. PCR products were separated by electrophoresis analysis on a 8 g/L agarose gel. The PCR product was harvested from agarose gel, digested with *Eco*R I and *Sal* I, and inserted into the *Eco*R I and *Sal* I restriction fragments of the expression vector pYA248 using T4 DNA ligase. The resulting plasmids pYA248-AB were transformed into *E.coli* X6097, Salmonella typhimurium X3730 and X4072 one by one and positive clone was screened through assay of double restriction enzyme digestion. DNA sequence was performed with the DNA automatic sequencer.

Assay of AB protein expressed by recombiant strain

Recombinant strain S typhimurium X4072 (pYA248-AB) cells, after being inoculated in the culture medium of LB liquids, were cultured with shaking at 37 °C for 15-16 h, and then centrifuged, to collect thallus and supernatant. Thallus, after being washed with saline once and centrifuged, suspended with deionized water. The suspension was sonicated on ice for three min, and centrifuged, to obtain the supernatant. Bridged ELISA was used to measure the expression of AB artigen in sonicate and culture supernatant.

Assay of stability of recombinant strain

The experiment testing stability of recombinant strain was performed according to the method described by Meacock[37,38]. Ten percent of thallus, incubated with shaking at 37 °C overnight, was inoculated in LB culture medium containing DAP and was further cultured for 12 h, from which the another 10 percent was inoculated in LB culture medium containing DAP and cultured for another 12 h, which was continued in the same way for up to 50 h. By this time, recombinant X4072 (pYA248-AB) cells had been cultured for 100 generations, and then it was diluted to 10^6-fold. A total volume of 100 μL of the diluted solution was taken and paved on LB agar plate containing DAP. After being cultured overnight, 100 single thalluses were randomly selected and transferred on LB agar plate without containing DAP. Bacteria could not grow on agar plate without containing DAP liquids, means plasmid loss; through this method stability of recombinant plasmid was verified. Meanwhile, ELISA was used to measure the expression of AB antigen in the culture supernatant of these 100 thalluses.

Assay of growth curve of recombinant strain

Single clone *S.typhimurium* X4072 (pYA248) and *S.typhimurium* X4072 (pYA248-AB) were selected and inoculated in culture medium of LB liquid, respectively. After being cultured with shaking at 37 °C for 10 h, 50 μL of it was inoculated in 5 mL culture medium of LB liquid, followed by culture with shaking at 37 °C. The value of A_{60} was measured once every other hour, from which growth curve was drawn.

Assay of immunology of recombinant strain

Three groups of 5 mice including controls were used as follows: (1) PBS control group was non-immunized mice that received PBS; (2)Salmonella control group was immunized with attenuated *S. typhimurium* X4072 (pYA248) strain; (3) The vaccine group was immunized with *S. typhimurium* X4072 (pYA248-AB) strain expressing AB. Prior to immunizations ,the mice were left overnight without solid food and 4 h without water. A total volume of 100 μL of 30 g/L sodium bicarbonate were given orally using a stainless steel catheter tube to neutralize the stomach pH. Immediately after stomach neutralization, mice from PBS control group received 100 μL PBS, and mice from the Salmonella control group and Salmonella vaccine group, received 1.0×10^9 colony forming units (c.f.u) of *S. typhimurium* strain X4072 (pYA248) and *S. typhimurium* strain X4072 (pYA248-AB), respectively, in a total volume of 100 μL. Water and food were returned to the mice after immunization. At 4 wk after immunization, mice were sacrificed by terminal cardiac puncture under metoxyfluorance anesthesia and the small intestines were taken from mice to prepare intestine fluid. Indirect ELISA was used to evaluate serum samples and intestine fluid from mice for AB-specific IgG or IgA. Purified *H pylori* AB was used as the coating antigen in ELISA immunoassays.

RESULTS

Construction of recombinant plasmid containing asd gene and encoding AB gene

The size of plasmid pYA248 was 3.0 kb. Promotor was Ptrc and multiclonal points included *Eco*R I *Hin* d III and *Sal* I *etc*. and pYA248 was digested with *Eco*R I and *Sal* I, and large E-S

sequences were recovered as vector. The same enzymes were used to completely digest AB PCR product and mixed with vector for connection after being recovered, and then transformed into *E. coli* X6097 by the means of $CaCL_2$. Transformer could grew on LB agar plate without containing DAP and further extracted plasmid for verification. The results of double restriction enzyme digestion of recombinant plasmid pYA248-AB are showed in Figure 1.

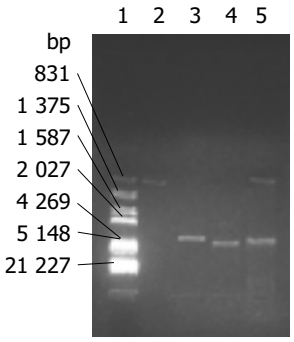

Figure 1 Double restriction enzyme digestion map of recombinant plasmid PYA248-AB. Lane1: DNA marker; Lane2: PCR product; lane3: pYA248 / *Eco*RI; lane4: pYA248-AB / *Eco*RI; lane5: pYA248-AB / *Eco*RI+*Sal*I.

Construction of recombinant strain

Recombinant plasmid extracted from *E.coli* X6097 (pYA248-AB) was transformed into *S.typhimurium* X3730 and X4072 by the transformation of electricity one by one. Owing to the difference between two kinds of *S.typhimurium*, the best transformational conditions were worked out. By adopting the first condition: cuvette gap 0.2 cm, voltage 2.5 kV, field strength 12.5 E, capacitor 25 μF, resistor 200 Ω, time constant 4.5-5.0 ms, recombinant plasmid was transformed into *S.typhimurium* X3730 and then separated from it. By adopting the second condition: cuvette gap 0.2 cm, voltage 2.4 kV, field strength 12.0 E, capacitor 25 μF, resistor 400 Ω, time constant 9-13 ms, recombinant plasmid was transformed into *S. typhimurium* X4072, from which recombinant strain *S.typhimurium* X4072 (pYA248-AB) was obtained.

Assay of AB protein expressed in recombinant strain

The results of AB expressed in X4072 (pYA248-AB) culture and sonicate supernatant assayed by bridged ELISA are shown in Table 2. The fact that the content of AB in recombinant germ X4072 (pYA248-AB) culture supernatant was higher than that in sonicate supernatant indicated that AB existed mainly in culture supernatant was expressed in the form of secretion.

Table 2 Expression of AB in X4072 (PYA248-AB) assayed by bridged ELISA

Sample	A_{492nm}	P / N
Negtive control of X4072 (pYA248) culture supernatant	0.04	
Negtive control of X4072 (pYA248) sonicate supernatant	0.04	
Positive control of BL21 (pET-AB) periplasm	1.08	27.0
X4072 (pYA248-AB) culture supernatant	0.96	24.0
X4072 (pYA248-AB) sonicate supernatant	0.78	19.5

Assay of stability of AB antigen expressed in recombinant strain

After recombinant germ pYA248-AB was cultured 100 generations, 100 bacteria were randomly selected and then transferred onto LB agar plate containing DAP. All of them could grow and the AB antigen was detected positive by ELISA. For the recombinant the mean of the value of A_{492nm} plus or minus standard deviation was 0.979±0.052, and the value of A_{492nm} of negative control X4072 (pYA248) was 0.040, which indicated that recombinant germ, after seeing cultured for 100 generations, could stably exist in attenuated *S.typhimurium* strain.

Growth curve of recombinant strain

Single clone X4072 (pYA248) and X4072 (pYA248-AB) were selected and then inoculated in the culture medium of LB liquid. After being cultured at 37 °C overnight, 50 μL of it was inoculated in 5 mL culture medium of LB liquid and then cultured with shaking at 37 °C. The value of A_{600} was measured and recorded once every other hour, from which growth curve (Figure 2) was drawn. It can be discovered from Figure 2 that the growth states of all bacteria were basically consistent, that is, metabolism of the bacteria were basically unaffected by transforming recombinant plasmid into attenuated *S. typhimurium* strain.

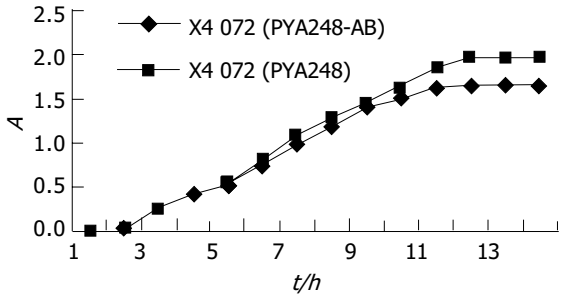

Figure 2 A growing curve of X4072 (PYA248) and X4072 (PYA248-AB).

Safety of recombinant strain

The results of experiments testing safety of C57BL/6 mice taking recombinant strain orally are shown in Table 3. After taking virulent strain X3181×10^7 c.f.u, all the mice died within 5 d, but after taking recombinant strain X4072 (pYA248-AB) 1.0×10^{10} c.f.u, the survival rate was still 100 percent. It can be noticed from the table that the number of live bacteria of C57BL/6 mice taking recombinant strain orally was 10^3 fold more than that of the lethal dose of virulent strain X3181.

Table 3 Survival of mice after oral inoculation with virulent and recombinant *S.typhimurium* strains

Strain	Relevant phenotype	Inoculating dose (c.f.u)	Observation intervals (d)	Survial (live / total)
X3181	wild type	1.0×10^7	5	0 / 5
		2.6×10^5	30	2 / 5
X4072 (PYA248-AB)	$Cya^-Crp^-AB^+$	1.0×10^{10}	30	5 / 5

Immunology of recombinant strain

The positive results defected by ELISA had colors, but the negative results had no colors, or weak colors. The five mice (group 3) serums and intestinal fluid immuned with vaccine *S. typhimurium* X4072 (pYA248-AB) showed positive results. In contrast, the mice serums and intestinal fluid of PBS control group and Salmonella control group showed negative results. It indicated *S.typhimurium* X4072 (pYA248-AB) could enable the organism to generate specific mucous membrane and humoral immunity.

DISCUSSION

S. typhimurium strain, through adhesion, invasion and inhabitation in intestine-associated lymph tissue, can be phagocyted by macrophage and M cells in Peyer node and through mesentery

lymph node reaches liver and spleen, which further stimulate other organs and tissue to develop mucous membrane, cell and body fluid immunization responses effectively. In recent few years, the research and production of gastrointestinal tract vaccine with attenuated *S. typhimurium* strain as the release system have become a new trend in the research of a new-type recombinant live vaccine taken orally. In it, attenuated *S.typhimurium* strain as a kind of vaccine carrier carrying foreign antigen is, up to now, the most widely used strain. This is mainly due to the fact that the model of mice infected by *S.typhimurium* strain is basically consistent with the organism of man infected by typhoid, and the virulence factor of *S. typhimurium* strain has been deeply researched[25,26]. The genes of virulence which have already been used in attenuated mutation of *S. typhimurium* strain include: *aro* gene controlling synthesis of aromatic compound[22]; gal E gene affecting synthesis of lipopolysaccharide[23]; *cya, crp* gene adjusting metabolic level of cyclic adenosine monophosphate(cAMP)[24], *pur* gene controlling sythesis of purine organism[25]; non-specific acid phosphoric acid enzyme *phoP* gene manipulating transcripition of gene and omp gene adjusting porin expression *etc*[26,27]. Many laboratories have successfully constructed attenuated and immunity *S.typhimurium* strain by mutating relative genes, which have been proved to be safe through experiments on animals, such as mice, cattle, and pig and even on human volunteers[28-33]. But when these attenuated *S.typhimurium* strains are used to express foreign protective antigen, genes encoding protective antigen are usually cloned on a vector containing drug resistance gene. In order to make sure of the stability of plasmid, antibiotic must be used as selection pressure. According to the rules stipulated in American Food and Drug Administration, drug resistance plasmid can not exist in live vaccine and the stability of recombinant plasmid can not be maintained in human beings and animals by antibiotic[28].

In order that foreign protective antigen can be stably expressed in attenuated *S.typhimurium* strain without antibiotic, a new type of plasmid vector system has been now developed, that is, the vector-host balanced lethal system. Host strain in the vector-host balanced lethal system is a type of chromosome mutant, and the mutated gene is housing keeping gene. Because the product of its encoding catalysed the genetic metabolic reaction of bacteria, the defects of the gene will certainly result in nutritious deficiency of bacteria, therefore, it can not grow in normal culture medium. Under this condition, plasmid must be necessary for the existence of bacteria. Once the transformed plasmid is lost, bacteria will not synthesize the essential substance so as not to grow in normal culture medium. Therefore, all bacteria that can grow in normal culture medium certainly contain recombinant plasmid, so as to construct the balanced lethal system. In this system, foreign protective antigen can be stably expressed without antibiotic in host stain. And the balanced lethal system constructed by *asd* gene has been widely used, for example, Redman *et al*.[34] cloned the surface protein antigen gene of *streptococcus* to plasmid with *asd*, and then transformed it to △*cya*△*crp*△*asd* defective *S. typhimurium* strains which were taken by mice orally. The results showed that recombinant strain could induce mice to produce continuous reaction of antibody response[34]. Scholars experimented △*cya*△(*crp cdt*)△*asd* expressing hepatitis B virus core pre S protein on adult women volunteers, showing that the strain could stimulate organism to develop system and mucous immunity response, and produce a unique secreted antibody (sIgA) in urinary and reproductive tract and intestinal tract[35].

By adopting the system as described above, we successfully carried out the construction of attenuated *S. typhimurium* strain expressing AB. Because the cell wall of *S. typhimurium* strain is thick and so hard to be transformed, *E.coli* X6097 with knocked out *asd* gene was used as host strain for screening recombinant clone. The screened recombinant plasmid was transformed electrically to host *S. typhimurium* X3730. X3730 with knocked out gene *asd* is the gene *galE* mutated strain of *S. typhimurium* strain LT-2 and loses the effect of restriction but possess the effect of modification, because of which plasmid transformed into *S. typhimurium* strain can obtain the methylated model of *S. typhimurium* strain and thus stably exists in *S.typhimurium* strain. Recombinant plasmid with methylated model extracted from X3730 was transformed into final *S.typhimurium* strain X4072 without restriction and so the construction work was finished.

Experiment on animals has proved that recombinant strain is safe. It was found by ELISA that AB protein was expressed mainly in the form of secretion, but the expression level was comparatively low. For recombinant strain with vaccine construction as the aim, however, a more important issue than high level expression is the stability of expressing foreign gene, because only when engineering bacteria can exist in body for a relatively long period and stably release antigen, it can effectively stimulate the immune system response of organism and expression with too high level may destroy the biological and chemical balance of strain as a complete organism which makes it hard for *S .typhimurium* strain to maintain the stable expression of foreign gene. The recombinant strain we constructed possessed a good stability, and under the condition without selection pressure,we recombinant plasmid could exist stably, and the foreign gene could also be expressed stably whose growth curve showed no obvious changes for expression of foreign gene. The main reason for it is probably that the expression level of foreign gene is suitable to *S. typhimurium* strain. In addition, according to Sutton etal's[36] principle of immunization protection and cure of *H pylori* "less is best", that is, low dose of antigen has better immunization effect, and maybe this *S. typhimurium* strain live vaccine expressing *H pylori* antigen with a low but stable level can create better immunization effect. In this study, the serums and intestine fluid from the mice immunized with *S.typhimurium* X4072 (pYA248-AB) expressed specific antibody aimed to AB, but the serums and intestine fluid from the mice in the control group failed to express. These results suggest that *S. typhimurium* X4072 (pYA248-AB) might be a good candidate as a vaccine. However, whether it can be used as a vaccine or not need be researched further. To achieve his goal we are carrying out the associated experiments on animals now.

REFERENCES

1 **Janowitz HD**, Abittan CS, Fiedler LM. A gastroenterological list for the millennium. *J Clin Gastroenterol* 1999; **29**: 336-338
2 **Kirsner JB**. The origin of 20th century discoveries transforming clinical gastroenterology. *Am J Gastroenterol* 1998; **93**: 862-871
3 **Bai Y**, Zhang YL, Jin JF, Wang JD, Zhang ZS, Zhou DY. Recombinant *Helicobacter pylori* catalase. *World J Gastroenterol* 2003; **9**: 1119-1122
4 **Blaser MJ**. Polymorphic bacteria persisting in polymorphic hosts: assessing *Helicobacter pylori*-related risks for gastric cancer. *J Natl Cancer Inst* 2002; **94**: 1662-1663
5 **Bai Y**, Zhang YL, Wang JD, Zhang ZS, Zhou DY. Construction of the non-resistant attenuated Salmonella typhimurium strain expressing *Helicobacter pylori* catalase. *Diyi Junyi Daxue Xuebao* 2003; **23**: 101-105
6 **Fireman Z**, Trost L, Kopelman Y, Segal A, Sternberg A. *Helicobacter pylori*: seroprevalence and colorectal cancer. *Isr Med Assoc J* 2000; **2**: 6-9
7 **Bai Y,** Zhang YL, Wang JD, Yang YS, Chen Y, Zhang ZS, Zhou DY. Study on the cloning, expression and the immunogenicity of *Helicobacter pylori* heat shock protein 60 gene. *Diyi Junyi Daxue Xuebao* 2002; **22**: 3-5
8 **Parsonnet J**, Friedman GD, Vandersteen DP, Chang Y, Vogelman JH, Orentreich N, Sibley RK. *Helicobacter pylori* infec-

tion and the risk of gastric carcinoma. *N Engl J Med* 1991; **325**: 1127-1131

9 **Parsonnet J**, Hansen S, Rodriguez L, Gelb AB, Warnke RA, Jellum E, Orentreich N, Vogelman JH, Friedman GD. *Helicobacter pylori* infection and gastric lymphoma. *N Engl J Med* 1994; **330**: 1267-1271

10 **Bai Y**, Chen Y, Lin HJ, Wang JD, Chang SH, Zhou DY, Zhang YL. *In vitro* evaluation of the safety and biological activity of recombinant *Helicobacter pylori* blood group antigen-binding adhesin. *Diyi Junyi Daxue Xuebao* 2003; **23**: 882-884

11 **Michetti P**. Vaccine against *Helicobacter pylori*: fact or fiction? *Gut* 1997; **41**: 728-730

12 **Lahaie RG**, Chiba N, Fallone C. Meeting review-*Helicobacter pylori*: basic mechanisms to clinical cure 2000. *Can J Gastroenterol* 2000; **14**: 856-861

13 **Bai Y,** Chang SH, Wang JD, Chen Y, Zhang ZS, Zhang YL. Construction of the *E.coli* clone expressing adhesin BabA of *Helicobacter pylori* and evaluation of the adherence activity of BabA. *Diyi Junyi Daxue Xuebao* 2003; **23**: 293-295

14 **Tomb JF**, White O, Kerlavage AR, Clayton RA, Sutton GG, Fleischmann RD, Ketchum KA, Klenk HP, Gill S, Dougherty BA, Nelson K, Quackenbush J, Zhou L, Kirkness EF, Peterson S, Loftus B, Richardson D, Dodson R, Khalak HG, Glodek A, McKenney K, Fitzegerald LM, Lee N, Adams MD, Venter JC. The complete genome sequence of the gastric pathogen *Helicobacter pylori*. *Nature* 1997; **388**: 539-547

15 **Doig P**, Trust TJ. Identification of surface-exposed outer membrane antigens of *Helicobacter pylori*. *Infect Immun* 1994; **62**: 4526-4533

16 **Rijpkema SG**. Prospects for therapeutic *Helicobacter pylori* vaccines. *J Med Microbiol* 1999; **48**: 1-3

17 **Bai Y**, Zhang YL, Wang JD, Lin HJ, Zhang ZS, Zhou DY. Conservative region of the genes encoding four adhesins of *Helicobacter pylori*: cloning, sequence analysis and biological information analysis. *Diyi Junyi Daxue Xuebao* 2002; **22**: 869-871

18 **Bai Y**, Dan HL, Wang JD, Zhang ZS, Odenbreit S, Zhou DY, Zhang YL. Cloning, expression, purification and identification of conservative region of four *Helicobacter pylori* adhesin genes in AlpA gene. *Prog Biochen Biophys* 2002; **29**: 922-926

19 **Bai Y**, Zhany YL, Chen Y, Wang JD, Zhou DY. Study of Immunogenicity and safety and adherence of conservative region of four *Helicobacter pylori* adhesin *in vitro*. *Prog Biochen Biophys* 2003; **30**: 422-426

20 **Bai Y**, Zhang YL, Wang JD, Zhang ZS, Zhou DY. Cloning and immunogenicity of conservative region of adhesin gene of *Helicobacter pylori*. *Zhonghua Yixue Zazhi* 2003; **83**:736-739

21 **Sambrook J**, Fritsch EF, Maniatis T. Molecular cloning: a laboratory manual. New York: *Cold Spring Harbor Laboratory Press* 1989

22 **Stocker BA**. Auxotrophic Salmonella typhi as live vaccine. *Vaccine* 1988; **6**: 141-145

23 **Hone D**, Morona R, Attridge S, Hackett J. Construction of defined galE mutants of Salmonella for use as vaccines. *J Infect Dis* 1987; **156**: 167-174

24 **Curtiss R 3rd**, Kelly SM. *Salmonella typhimurium* deletion mutants lacking adenylate cyclase and cyclic AMP receptor protein are avirulent and immunogenic. *Infect Immun* 1987; **55**: 3035-3043

25 **McFarland WC**, Stocker BA. Effect of different purine auxotrophic mutations on mouse-virulence of a Vi-positive strain of *Salmonella dublin* and of two strains of *Salmonella typhimurium*. *Microb Pathog* 1987; **3**: 129-141

26 **Hohmann EL**, Oletta CA, Miller SI. Evaluation of a phoP/phoQ-deleted, aroA-deleted live oral *Salmonella typhi* vaccine strain in human volunteers. *Vaccine* 1996; **14**: 19-24

27 **Dorman CJ**, Chatfield S, Higgins CF, Hayward C, Dougan G. Characterization of porin and ompR mutants of a virulent strain of *Salmonella typhimurium*: ompR mutants are attenuated *in vivo*. *Infect Immun* 1989; **57**: 2136-2140

28 **Curtiss R 3rd**, Galan JE, Nakayama K, Kelly SM. Stabilization of recombinant avirulent vaccine strains *in vivo*. *Res Microbiol* 1990; **141**: 797-805

29 **Maskell DJ**, Sweeney KJ, O'Callaghan D, Hormaeche CE, Liew FY, Dougan G. *Salmonella typhimurium* aroA mutants as carriers of the *Escherichia coli* heat-labile enterotoxin B subunit to the murine secretory and systemic immune systems. *Microb Pathog* 1987; **2**: 211-221

30 **Clements JD**, El-Morshidy S. Construction of a potential live oral bivalent vaccine for typhoid fever and *cholera-Escherichia coli*-related diarrheas. *Infect Immun* 1984; **46**: 564-569

31 **Giron JA**, Xu JG, Gonzalez CR, Hone D, Kaper JB, Levine MM. Simultaneous expression of CFA/I and CS3 colonization factor antigens of enterotoxigenic *Escherichia coli* by delta aroC, delta aroD Salmonella typhi vaccine strain CVD 908. *Vaccine* 1995; **13**: 939-946

32 **Formal SB**, Baron LS, Kopecko DJ, Washington O, Powell C, Life CA. Construction of a potential bivalent vaccine strain: introduction of *Shigella sonnei* form I antigen genes into the galE *Salmonella typhi* Ty21a typhoid vaccine strain. *Infect Immun* 1981; **34**: 746-750

33 **Hone DM**, Harris AM, Chatfield S, Dougan G, Levine MM. Construction of genetically defined double aro mutants of *Salmonella typhi*.*Vaccine* 1991; **9**: 810-816

34 **Redman TK**, Harmon CC, Michalek SM. Oral immunization with recombinant *Salmonella typhimurium* expressing surface protein antigen A (SpaA) of *Streptococcus sobrinus*: effects of the *Salmonella* virulence plasmid on the induction of protective and sustained humoral responses in rats.*Vaccine* 1996; **14**: 868-878

35 **Nardelli-Haefliger D**, Benyacoub J, Lemoine R, Hopkins-Donaldson S, Potts A, Hartman F, Kraehenbuhl JP, De Grandi P. Nasal vaccination with attenuated *Salmonella typhimurium* strains expressing the *Hepatitis B* nucleocapsid: dose response analysis. *Vaccine* 2001; **19**: 2854-2861

36 **Sutton P**, Wilson J, Lee A. Further development of the *Helicobacter pylori* mouse vaccination model. *Vaccine* 2000; **18**: 2677-2685

37 **Meacock PA**, Cohen SN. Partitioning of bacterial plasmids during cell division: a cis-acting locus that accomplishes stable plasmid inheritance. *Cell* 1980; **20**: 529-542

38 **Meacock PA**, Cohen SN. Genetic analysis of the inter-relationship between plasmid replication and incompatibility. *Mol Gen Genet* 1979; **174**: 135-147

Edited by Kumar M **Proofread by** Xu FM

PO Box 2345, Beijing 100023, China
Fax: +86-10-85381893
E-mail: wjg@wjgnet.com www.wjgnet.com

World J Gastroenterol 2004;10(17):2503-2508
World Journal of Gastroenterology
Copyright © 2004 by The WJG Press ISSN 1007-9327

• BASIC RESEARCH •

Adaptive cytoprotection through modulation of nitric oxide in ethanol-evoked gastritis

Joshua Ka-Shun Ko, Chi-Hin Cho, Shiu-Kum Lam

Joshua Ka-Shun Ko, School of Chinese Medicine, Hong Kong Baptist University, Hong Kong, China
Chi-Hin Cho, Department of Pharmacology, Faculty of Medicine, The University of Hong Kong, Hong Kong, China
Shiu-Kum Lam, Department of Medicine, Faculty of Medicine, The University of Hong Kong, Hong Kong, China
Correspondence to: Dr. Joshua Ka-Shun Ko, 4/F, School of Chinese Medicine Building, 7 Hong Kong Baptist University Road, Hong Kong, China. jksko@hkbu.edu.hk
Telephone: +852-3411 2907 **Fax:** +852-3411 2461
Received: 2004-02-02 **Accepted:** 2004-03-24

Abstract

AIM: To assess the mechanisms of protective action by different mild irritants through maintenance of gastric mucosal integrity and modulation of mucosal nitric oxide (NO) in experimental gastritis rats.

METHODS: Either 200 mL/L ethanol, 50 g/L NaCl or 0.3 mol/L HCl was pretreated to normal or 800 mL/L ethanol-induced acute gastritis Sprague-Dawley rats before a subsequent challenge with 500 mL/L ethanol. Both macroscopic lesion areas and histological damage scores were determined in the gastric mucosa of each group of animals. Besides, gastric mucosal activities of NO synthase isoforms and of superoxide dismutase, along with mucosal level of leukotriene $(LT)C_4$ were measured.

RESULTS: Macroscopic mucosal damages were protected by 200 mL/L ethanol and 50 g/L NaCl in gastritis rats. However, although 200 mL/L ethanol could protect the surface layers of mucosal cells in normal animals (protection attenuated by N^G-nitro-L-arginine methyl ester), no cytoprotection against deeper histological damages was found in gastritis rats. Besides, inducible NO synthase activity was increased in the mucosa of gastritis animals and unaltered by mild irritants. Nevertheless, the elevation in mucosal LTC_4 level following 500 mL/L ethanol administration and under gastritis condition was significantly reduced by pretreatment of all three mild irritants in both normal and gastritis animals.

CONCLUSION: These findings suggest that the aggravated 500 mL/L ethanol-evoked mucosal damages under gastritis condition could be due to increased inducible NO and LTC_4 production in the gastric mucosa. Only 200 mL/L ethanol is truly "cytoprotective" at the surface glandular level of non-gastritis mucosa. Furthermore, the macroscopic protection of the three mild irritants involves reduction of LTC_4 level in both normal and gastritis mucosa, implicating preservation of the vasculature.

Ko JKS, Cho CH, Lam SK. Adaptive cytoprotection through modulation of nitric oxide in ethanol-evoked gastritis. *World J Gastroenterol* 2004; 10(17): 2503-2508
http://www.wjgnet.com/1007-9327/10/2503.asp

INTRODUCTION

Excessive ethanol ingestion can result in gastritis characterized by mucosal edema, subepithelial hemorrhages, cellular exfoliation and inflammatory cell infiltration[1]. Alcohol has been shown to affect the mucosal barrier and histology[2]. Morphologically, alcohol-induced gastric superficial injury involves mostly the inter-foveolar epithelium and gastric pits, and heals rapidly by restitution[3]. On the other hand, the deeper lesions involve intramucosal hemorrhage and vascular engorgement[4]. As a consequence of damage to microvessels, leakage of inflammatory mediators occurs, and vasoconstriction of submucosal arteries would result in ischemia. Eventually, these events would enhance the formation of more severe necrotic mucosal injury. Several products of arachidonate metabolism have been implicated to participate in the pathogenesis of ethanol-induced gastric mucosal damage[5].

It is known that neuronal modulating processes such as the release of vasoactive mediators are crucial for the gastric mucosa to resist the continual onslaught of aggressive agents[6]. Previous findings have suggested that there are interactions between the endothelium-derived vasodilator mediators, including that prostaglandins (PG), can regulate gastric mucosal microcirculation and integrity[7]. Endothelial cells also release a highly labile humoral vasodilator substance, now known to be nitric oxide (NO), that mediates the vascular relaxation induced by vagal stimulation[8]. Nonetheless, it should be noted that the production of NO from a calcium-independent (inducible) form of the enzyme could lead to cell injury in the endothelium[9]. Thus, the induction of NO synthesis may not always be beneficial. For instance, formation and interaction between superoxide and NO radicals are the key elements of oxidative challenges in the gastric mucosa.

There are some endogenous proinflammatory mediators that could be activated during the aggressive attack of noxious agents or severe tissue trauma. Leukotriene $(LT)C_4$ is one of these substances which would lead to microcirculatory disturbances and severe mucosal tissue injury[10]. Such a detrimental action may somehow involve the generation of reactive oxygen free radicals. In other words, these effects could be modulated by enzyme systems of the oxygen-handling cells, such as superoxide dismutase (SOD), which are able to protect cells against the toxic effects caused by oxygen species[11].

Acute hemorrhagic gastritis patients have underlying predisposing conditions such as alcohol abuse or use of NSAID. Besides endoscopic and surgical therapy, the focus on pharmacotherapy would be the enhancement of mucosal defense mechanisms so as to accelerate healing and prevent relapses[12]. The present study attempted to illustrate that different mild irritants had differential modes of action in the adaptive cytoprotection against ethanol-induced gastric mucosal damage in animals under gastritis condition, whereas some of these involved modulation of eicosanoids and NO biosynthesis in the gastric mucosa. These data may also provide the explanation why gastritis can predispose the stomach to ulceration.

MATERIALS AND METHODS

Animals

Male Sprague-Dawley rats (240-260 g) were used after

acclimatization for at least three days in a controlled room with constant temperature (22±1 °C) and humidity (65-70%). They were fed a standard diet of laboratory chow (Ralston Purina, USA) and had free access to tap water *ad libitum*. All experimental animals were deprived of food in individual wired cages 24 h beforehand.

Treatments and induction of gastritis

Animals in the "normal" (non-gastritis) groups received oral administration (10 mL/kg) of either distilled water or one of the three mild irritants, 200 mL/L ethanol, 50 g/L NaCl and 0.3 mol/L HCl via a stainless steel orogastric tube, 15 min before the administration of 500 mL/L ethanol (10 mL/kg). For animals that were used to demonstrate the action of mild irritants alone (basal), distilled water was given instead of 500 mL/L ethanol. All animals were sacrificed 30 min later.

To induce gastritis, 800 mL/L ethanol was given to the rats orally (10 mL/kg). The treated animals were returned to their home cages with provision of food and tap water. After 24 h, all the 800 mL/L ethanol-treated animals were deprived of food again, with tap water supply only. Similar experiments as those of the "normal" animals were performed using these gastritis rats 24 h following starvation (i.e. the experiments were carried out 48 h after the induction of gastritis). Our preliminary study showed that at this time point the gastritis animals were free from any gross macroscopic lesion or erosion, but the deeper mucosal cells comprising more than 800 mL/L of the total mucosal thickness were damaged or morphologically changed when observed microscopically.

In order to investigate the participation of the endogenous vasoactive mediator during the processes, N^G-nitro-L-arginine methyl ester (L-NAME, 12.5 mg/kg, i.v.) was pretreated 15 min before the administration of mild irritants to inhibit endogenous NO production[13].

Macroscopic evaluation of gastric mucosal damage

The animals were sacrificed by a sharp blow behind the head and followed by cervical dislocation. Their stomachs were removed and opened along the greater curvature. After thoroughly rinsed in ice-cold saline solution and blotted dry, the area of macroscopic lesions on the mucosa was traced onto a glass slide, and measured by transparent 1-mm^2 grids[14]. A section of each stomach tissue was removed and preserved for subsequent microscopic studies. Finally, the glandular mucosa of the rest of stomach tissue was scrapped by using a glass slide, weighed and immediately frozen in liquid nitrogen. The mucosal samples were stored at -70 °C until assayed for various endogenous mediators.

Histological evaluation of gastric mucosal damage

Within a week of formalin fixation, the gastric tissues were processed for paraffin embedding. A (1.0× 0.5×0.3) cm^3 block of gastric tissue was dehydrated by immersion in progressively increasing concentrations of ethanol. Slices of 6-μm thick sections were stained by the periodic acid-Schiff technique, and counterstained by Harris' hematoxylin solution. The stained sections were then left in the fume-cupboard overnight.

An Olympus microscope (200×) with a scaled eyepiece was used for the morphometric study. Any histological damage in a section was quantified according to the method from O'Brien and coworkers[15]. The criteria for damage were the absence of gastric mucosal cells or the presence of grossly disrupted cells. The standards for evaluation of the severity of microscopic mucosal damage were as follows: type I damage-length of luminal surface mucous cells damaged or vacuolated, type II damage-extensive luminal surface cell damage with disrupted and exfoliated cells lining the gastric pits, type III damage-disrupted cells of the gastric glands beneath the damaged surface and gastric pit cells. For each tissue sample, four measurements of the total mucosal length as well as the length with damaged or disrupted mucosal cells were examined (in mm) and averaged. The final index for the degree of histological damage was represented by the percentage of the damaged mucosal length in terms of the total length of the gastric mucosa.

Determination of NO synthase activity in gastric mucosa

A mucosal sample was placed in a buffer solution (pH 7.2) containing 10 mmol/L HEPES, 0.32 mol/L sucrose, 0.1 mmol/L EDTA, 1 mmol/L DL-dithiothreitol, 10 μg/mL of soybean trypsin inhibitor, 10 μg/mL of leupeptin, 2 μg/mL of aprotinin, and 1 mg/mL of phenyl-methanesulfonyl fluoride. The sample was homogenized for 20 s under ice-cold condition, and then centrifuged at 22 000 *g* for 30 min at 4 °C. An aliquot of 100 μL from the supernatant was withdrawn for protein assay[16].

The NO synthase activity was determined from the conversion of [^{3}H] L-arginine to the NO co-product citrulline[17]. The supernatant was passed over a 0.75-mL column containing Dowex AG50WX-8 resins to remove any endogenous arginine[18]. The reaction mixture comprised 100 μL of the supernatant and 150 μL of buffered solution (pH 7.2) containing 10 mmol/L HEPES, 0.7 mmol/L NADPH, 150 μmol/L $CaCl_2$, 7 mmol/L L-valine to inhibit any arginase[19], and 1 μCi of [^{3}H] L-arginine. The amount of [^{3}H] L-citrulline formed in this reaction mixture represented the total NO synthase activity. A similar reaction mixture was also prepared, with the addition of 1 mmol/L EGTA, which removed Ca^{2+} ions from the system[13]. Product formation that remained persistent in this system determined the inducible NO synthase activity. Incubation of the mixtures with or without EGTA was continued for 30 min at 37 °C. The reaction was terminated by adding 50 μL of 200 mL/L perchloric acid, and the solution mixture was neutralized by 160 μL of 1 mol/L NaOH[20]. This was followed by the dilution with 540 μL of deionized water containing 1 mmol/L L-arginine and 1 mmol/L citrulline. Subsequently, the resulting 1 mL mixture in each reaction tube was applied onto a chromatographic column containing 0.5 g of Dowex AG50WX-8 resins[21]. Following the separation from unreacted [^{3}H] L-arginine by cation-exchange chromatography, the product [^{3}H] L-citrulline was eluted through the column by 1 mL of deionized water and collected into a scintillation vial. The samples were counted for the amount of radioactivity using a liquid scintillation counter (2 000 CA, Packard, USA). The data obtained were corrected for background counts obtained by a similar procedure but with heat-inactivated mucosal tissue. The final results were represented as cpm/min/mg protein. Constitutive NO synthase activity was obtained by subtracting the inducible NO synthase activity by the total NO synthase activity.

Determination of LTC_4 level in gastric mucosa

The pre-weighed mucosal samples were homogenized for 15 s under ice-cold condition in phosphate buffer (50 mmol/L, pH 7.4) with indomethacin (28 μmol/L), to prevent any neoformation of cyclooxygenase products during the extraction process. The homogenized samples were then centrifuged at 1 400 r/min for 15 min at 4 °C. An aliquot of 100 μL from the supernatant was withdrawn for protein assay[16]. The assay was carried out by using a LTC_4 [^{3}H] RIA kit (NEN Dupont, USA.). A standard curve was constructed with a range of 0.025-1.6 ng/100 μL. The final values of the samples obtained were represented as pg/mg protein.

Determination of SOD activity in gastric mucosa

The pre-weighed mucosal samples were homogenized for 20 s under ice-cold condition in phosphate buffer (50 mmol/L, pH 7.4). The homogenized samples were then centrifuged at 20 000 *g* for 15 min at 4 °C. An aliquot of 100 μL from the supernatant was withdrawn for protein assay[16].

The SOD activity in tissue homogenates was determined by the NBT reaction[22]. A 10 μL of the homogenates was added to a solution mixture containing 150 μL each of 2 mmol/L xanthine, 2 mmol/L EDTA and 0.5 mmol/L NBT, 500 μL of Na_2CO_3 and 75 μg/mL of BSA. After being made up to a 2.85 mL solution with phosphate buffer, the mixture was incubated for 3 min in a 25 °C bath. Following that, 150 μL of 0.12 μmol/L xanthine oxidase was added to the mixture and 3 mL solution was incubated further at 25 °C for 20 min. The reaction was terminated by adding 1 mL of 0.8 mmol/L $CuCl_2$ solution to each tube. The inhibition of NBT reduction in each sample was determined spectrophotometrically at 560 nm and the final value of SOD activity was represented as units/mg protein.

Drugs

[^{3}H] L-arginine (specific activity = 36.1 Ci/mmoL) and the [^{3}H] LTC_4 RIA kit were purchased from NEN DuPont (Boston, MA, USA.). L-NAME, DL-dithiothreitol, soybean trypsin inhibitor, leupeptin, aprotinin, phenylmethanesulfonyl fluoride, L-valine, L-arginine and DL-citrulline were all products of Sigma Chemicals (St. Louis, MO, USA.).

Statistical analysis

All the results were expressed as mean±SE of 6 animals per group. The means were compared by the analysis of variance followed by unpaired Student's *t* test. Differences were considered statistically significant if the *P* value was less than 0.05.

RESULTS

Adaptive cytoprotection of mild irritants against 50% ethanol-induced macroscopic lesion formation in gastritis rats (Table 1)

Under gastritis condition, there was a general aggravating effect on the macroscopic ethanol-evoked gastric mucosal damage in all experimental groups, when compared with the damaging effects of 500 mL/L ethanol in normal animals. The degree of protection by 200 mL/L ethanol and 50 g/L NaCl in gastritis rats was lessened when compared to that in normal animals, while the gastroprotection of 0.3 mol/L HCl was completely relieved in gastritis animals. As in normal animals, L-NAME pretreatment alleviated the protective action of 200 mL/L ethanol in gastritis animals. Nonetheless, the protective action of 50 g/L NaCl was preserved under gastritis condition.

Table 1 Effect of mild irritants on 500 mL/L ethanol-induced macroscopic lesion formation in gastric mucosa of normal and gastritis rats, and modulation by pretreatment with L-NAME

Pretreatment	Macroscopic lesion areas (mm^2)	
	Normal	Gastritis
H_2O (Control)	41.17±7.85	134.17±19.23^{d}
200 mL/L EtOH	2.00±0.93^{b}	31.33±5.96^{b,f}
50 g/L NaCl	0±0^{b}	15.00±3.80^{b,f}
0.3 mol/L HCl	0±0^{b}	124.33±20.60^{f}
L-NAME+H_2O	42.50±10.65	125.40±17.75^{f}
L-NAME+200 mL/L EtOH	32.33±9.95^{a}	98.83±7.22^{h,f}
L-NAME+50 g/L NaCl	0±0^{b}	32.25±7.49^{b,f}
L-NAME+0.3 mol/L HCl	0±0^{b}	104.25±12.20^{h}

Values are mean±SE (n = 6), ^{b}P<0.001 *vs* corresponding H_2O group without mild irritant. ^{a}P<0.05, ^{f}P<0.001*vs* corresponding group without drug pretreatment. ^{d}P<0.01, ^{h}P<0.001 *vs* corresponding group without gastritis (Normal).

Adaptive cytoprotection of mild irritants against 50% ethanol-induced histological damage in gastritis rats (Table 2)

The type II and type III histological damages induced by 500 mL/L ethanol were generally aggravated in the gastric mucosa of gastritis animals. In addition, the histological cytoprotection of 200 mL/L ethanol that could be observed in normal animals (the total, type I and type II histological damages, which was alleviated by the pretreatment with L-NAME) was completely

Table 2 Effect of mild irritants on 500 mL/L ethanol-induced histological damage in gastric mucosa of normal and gastritis rats, and modulation of protective action of 200 mL/L ethanol by pretreatment with L-NAME

Treatment	Histological damage (% total mucosal thickness)							
	Normal				Gastritis			
	Total	Type I	Type II	Type III	Total	Type I	Type II	Type III
H_2O (Control)	70.80±1.26	16.23±1.07	21.92±1.01	31.36±1.67	91.13±4.31^{f}	14.99±1.14	27.37±1.83^{e}	48.77±3.69^{f}
200 mL/L EtOH	59.61±2.04^{b}	11.12±0.97^{h}	15.27±1.10^{h}	33.20±1.80	92.23±3.89^{j}	14.17±1.26	25.06±1.77^{j}	53.00±3.16^{j}
50 g/L NaCl	73.16±1.82	15.37±1.26	22.64±1.54	35.15±2.07	90.73±3.15^{f}	12.11±1.02	28.33±1.60^{e}	50.29±3.40^{f}
0.3 mmol/L HCl	66.37±2.21	18.20±1.55	20.01±1.98	28.16±3.04	89.83±3.71^{f}	13.72±1.33	25.69±1.52^{e}	50.40±2.56^{j}
L-NAME+H_2O	74.2±1.96	16.41±1.72	21.19±1.70	36.62±3.21	94.27±3.06^{f}	15.21±1.31	29.61±1.97^{f}	49.42±3.90^{e}
L-NAME+200 mL/L EtOH	69.75±2.11^{d}	15.55±1.41^{a}	20.48±1.88^{c}	33.71±2.86	95.10±3.62^{f}	13.78±1.56	27.49±1.81^{e}	53.82±4.11^{f}

Values are mean±SE (n = 6), ^{h}P<0.01, ^{b}P<0.001 *vs* corresponding H_2O group without mild irritant. ^{a}P<0.05, ^{d}P<0.01 *vs* corresponding group without drug pretreatment. ^{e}P<0.05, ^{f}P<0.01, ^{j}P<0.001 *vs* corresponding group without gastritis (Normal).

Table 3 Effect of mild irritants and/or 500 mL/L ethanol on constitutive and inducible nitric oxide synthase activity in gastric mucosa of normal and gastritis rats

	Nitric oxide synthase activity (cpm/min/mg protein)							
	H_2O		200 mL/L EtOH		50 g/L NaCl		0.3 mol/L HCl	
	Constitutive	Inducible	Constitutive	Inducible	Constitutive	Inducible	Constitutive	Inducible
Basal normal	266.01±22.10	96.97±12.72	768.98±93.17^{b}	107.66±17.17	734.68±74.67^{b}	84.13±19.26	328.77±48.23	97.52±16.12
500 mL/L EtOH normal	132.18±16.49^{d}	106.55±13.19	326.54±33.43^{a,h}	143.51±15.71	282.67±23.86^{a,d}	109.67±12.32^{a}	160.86±25.07	137.24±16.13
Basal gastritis	31.56±7.20^{f}	856.58±93.82^{f}	31.13±10.47^{f}	746.05±94.07^{f}	41.26±11.64^{f}	649.89±81.83^{f}	22.27±8.01^{f}	949.87±106.22^{f}
500 mL/L EtOH gastritis	56.21±8.64^{j}	972.29±123.73^{f}	39.12±3.09^{f}	888.88±129.36^{f}	42.72±10.29^{f}	853.36±103.64^{f}	49.82±10.58^{j}	875.24±122.44^{f}

Values are mean±SE (n = 6), ^{b}P<0.001 *vs* corresponding H_2O group without mild irritant treatment. ^{a}P<0.05, ^{h}P<0.01, ^{d}P<0.001 *vs* corresponding group without 500 mL/L EtOH treatment (Basal). ^{j}P<0.01, ^{f}P<0.001 *vs* corresponding group without gastritis (Normal).

Table 4 Effect of mild irritants and / or 50% ethanol on superoxide dismutase (SOD) activity in gastric mucosa of normal and gastritis rats

	SOD activity (units / mg protein)			
	H_2O	200 mL / L EtOH	50 g / L NaCl	0.3 mol / L HCl
Basal normal	32.08±2.20	36.07±3.18	38.01±1.55	37.53±3.06
500 mL / L EtOH normal	37.20±2.51	41.14±1.82	40.48±0.99	41.33±3.78
Basal gastritis	41.92±2.42[a]	47.51±3.27[a]	48.03±2.06[b]	50.56±3.88[a]
500 mL / L EtOH gastritis	50.85±4.46[a]	49.76±3.36[a]	57.68±6.04[a]	54.92±4.74[a]

Values are mean±SE (n = 6), [a]P<0.05, [b]P<0.01 *vs* corresponding group without gastritis (Normal).

Table 5 Effect of mild irritants and / or 50% ethanol on leukotriene C_4 (LTC_4) level in gastric mucosa of normal and gastritis rats

	LTC_4 level (pg / mg protein)			
	H_2O	200 mL / L EtOH	50 g / L NaCl	0.3 mol / L HCl
Basal normal	13.33±3.08	5.77±0.86[a]	4.19±0.67[a]	4.28±0.81[a]
500 mL / L EtOH normal	29.28±5.46[c]	10.01±1.87[b]	9.15±3.05[b]	8.17±2.42[b]
Basal gastritis	35.08±6.28[e]	17.05±4.22[a,e]	12.88±3.68[a,e]	14.86±3.60[a,e]
500 mL / L EtOH gastritis	43.84±3.79	18.86±4.66[b]	17.70±3.06[d]	21.28±6.33[a]

Values are mean±SE (n = 6), [a]P<0.05, [b]P<0.01, [d]P<0.001 *vs* corresponding H_2O group without mild irritant. [c]P<0.05 *vs* corresponding group without 500 mL / L EtOH treatment (Basal). [e]P<0.05 *vs* corresponding group without gastritis (Normal).

relieved. Five percent NaCl and 0.3 mol/L HCl did not exert any cytoprotective action in the histological level whatsoever.

Effects of mild irritants on NO synthase activity in gastric mucosa of gastritis rats, during basal condition or followed by 500 mL/L ethanol challenge (Table 3)

The condition of gastritis caused a profound elevation of inducible NO synthase activity as well as a reduction of constitutive NO synthase activity in all experimental groups. The elevation of constitutive NO synthase activity induced by 200 mL/L ethanol or 50 g/L NaCl was also alleviated in gastritis rats, with the inducible NO synthase activity remained unaltered by mild irritants. On the other hand, the overall inhibitory effect of 500 mL/L ethanol on mucosal constitutive NO synthase activity was relieved in gastritis animals, of which the activation of the constitutive isozyme by 200 mL/L ethanol and 50 g/L NaCl was also completely prevented.

Effects of mild irritants on SOD activity in gastric mucosa of gastritis rats, during basal condition or followed by 500 mL/L ethanol challenge (Table 4)

SOD activity was significantly increased in all gastritis animals, when compared to normal rats. On the other hand, neither the mild irritants nor 500 mL/L ethanol significantly altered SOD activity in the gastric mucosa.

Effects of mild irritants on LTC_4 level in gastric mucosa of gastritis rats, at basal condition or followed by 500 mL/L ethanol challenge (Table 5)

In general, there was a higher LTC_4 level in the gastric mucosa of all gastritis animals. Nevertheless, all three mild irritants significantly reduced the level of LTC_4 in the gastric mucosa of both normal and gastritis rats. Fifty percent ethanol significantly increased the amount of mucosal LTC_4 in normal animals, but not in gastritis animals. The ability of mild irritants to reduce mucosal LTC_4 level remained persistent in all 500 mL/L-ethanol-treated groups.

DISCUSSION

Previous studies investigating on the phenomenon of gastric adaptive cytoprotection were conducted in normal animals. The present investigation demonstrated the adaptive cytoprotection of mild irritants in gastritis rats. It is known that after deep mucosal injury involving extensive hemorrhage and tissue destruction, as in the case of gastritis induced by 80% ethanol, epithelial restitution still occurred[23]. The term "hemorrhagic gastritis" is a term used to describe the appearance of subepithelial hemorrhage in the stomach. Some patients with gastric subepithelial hemorrhage could be expected to have associated histologic gastritis. Hence, histological protection and the preservation of vascular integrity were the two main criteria of gastroprotection[24]. Our findings indicated that the gross macroscopic protective actions of 200 mL/L ethanol and 50 g/L NaCl remained persistent in the gastritis stomach. The loss of protective effect of 0.3 mol/L HCl under gastritis condition implied that a normal functional mucosa could be essential for the protective mechanism of the mild acid. We previously reported that adaptive cytoprotection by 0.3 mol/L HCl was completely blocked by vagotomy, implicating that innervation of an intact vagus nerve was one of the prerequisites of this mild irritant to induce physiological responses in the mucosal oxyntic cells[25]. Similarly, normal integrity of the mucosa that was interfered under gastritis condition may also be important for the protective action of HCl. Apart from that,50 g/L NaCl and 0.3 mol/L HCl failed to preserve the mucosal cells histologically, even in non-gastritis normal animals, leaving 200 mL/L ethanol to be the only agent that could exert "true cytoprotection" at the surface glandular level. Nevertheless, the loss of histological protective ability of 200 mL/L ethanol during gastritis condition also suggests that the initiation of its histologic adaptive cytoprotection may also require an intact glandular mucosa to operate. Clinically, the histologic gastritis that attributed to ethanol was somehow related to the underlying presence of *H pylori*, although ethanol did not seem to initiate *H pylori*-associated histologic gastritis directly[26]. Treatment of *H pylori* was associated with almost complete normalization of histologic findings[27]. In other words, 200 mL/L ethanol may only be responsible for the improvement of macroscopic gastric mucosal lesion formation by surface epithelial restitution, while *H pylori* eradication is capable of restoring the deep subepithelial mucosa in histologic gastritis.

In general, inflammatory reactions were initiated and amplified by proinflammatory mediators from injured tissues as well as those being synthesized during the process[28]. These substances could result in further local tissue injury by release and activation of destructive enzymes as well as production of oxygen-derived free radicals. Thus, removal of oxygen-derived free radicals could stimulate the healing of ethanol-induced acute gastric mucosal injury in rats[29]. Increased superoxide generation was resulted from activation of polymorphonuclear leukocytes and macrophages, which were the stimuli that induced the production of NO by inducible NO synthase[30]. NO produced in a relatively high concentration by this inducible enzyme might react with oxygen or superoxide to yield more reactive oxidants, such as the peroxynitrite[31]. These secondary oxidants are believed to be responsible for most biological oxidative damages, and are often the targets of antioxidant defense. In the present study, inducible NO synthase activity was significantly increased for many folds in gastritis animals, which could be correlated with the aggravation in 500 mL/L ethanol-induced mucosal damage and the alleviation of the histological cytoprotection induced by 200 mL/L ethanol. Although the administration of 500 mL/L ethanol to normal rats did not cause any significant activation of inducible NO synthase activity, the activity of constitutive NO isozyme was inhibited. Production of NO from the calcium-dependent constitutive enzyme has been known to play a role in the modulation of gastric mucosal integrity[32]. The general suppression of this constitutive isozyme in gastritis mucosa could be due to the loss of endothelial integrity. Alternatively, the gastroprotection caused by 200 mL/L ethanol and 50 g/L NaCl, which concurrently maintained the constitutive NO synthase activity following 500 mL/L ethanol challenge in normal animals, must be due to the preservation of endothelium and hence to maintain vascular integrity. However, L-NAME pretreatment only reversed the protective action of 200 mL/L ethanol but not that of 50 g/L NaCl, suggesting that the involvement of NO from the constitutive form in the anti-lesion action of NaCl is still uncertain. Nevertheless, the suppression of constitutive NO synthase activity and the loss of its activation by 200 mL/L ethanol in the gastritis mucosa may explain why gastritis provoked ethanol ulceration and attenuated the protective action of 200 mL/L ethanol, respectively[33]. In addition, the damaged mucosa could activate the inducible NO isozyme and trigger the release of more free radicals, thus producing extensive tissue necrosis under gastritis condition.

Local SOD has been shown to abolish the gastric mucosal injury induced by the cytotoxic level of NO, possibly due to the prevention of peroxynitrite formation from interaction between superoxide and cytotoxic NO[34]. Our results demonstrated that under gastritis condition, SOD activity was significantly elevated. This could be a defensive mechanism of the gastric mucosa that would be activated when a tremendous amount of superoxide and other free radicals was produced following severe tissue injury. Indeed, acute administration of either mild irritants or 500 mL/L ethanol did not induce a similar increase in SOD activity in the gastric mucosa. Hence, the acute protective action of mild irritants in both normal and gastritis rats did not seem to involve the modulation of mucosal SOD activity.

It was reported in a human study that the basal release of PGE_2 and LTC_4 in alcoholics was higher than that in healthy volunteers, and that alcohol administration could cause an increase in PGE_2 and LTC_4 in healthy volunteers[35]. In addition, by using a rat model, the same group of investigators further proposed that the anti-lesion effect of some gastroprotective agents was related to the inhibition of LTC_4 formation and an increase in PGE_2 biosynthesis in the gastric mucosa[36]. Our findings in fact indicated that LTC_4 level in the mucosa was significantly increased in gastritis rats, which was similar to the state in alcoholics. Moreover, the challenge with 500 mL/L ethanol also stimulated an increase in LTC_4 level, as in the case of healthy volunteers. In fact, increased synthesis of mucosal PGE_2 in alcoholics could also indicate a defensive mechanism of the mucosa, mainly to counteract with the proinflammatory action of LTC_4 generated from the tissue. In the present study, mild irritants were able to induce a significant inhibition on the release of LTC_4 in both normal and gastritis mucosa. Reduction of this autacoid would attenuate vascular disturbances and decrease hemorrhagic lesions in the gastric mucosa[37].

In summary, aggravation in 500 mL/L ethanol-induced gastric mucosal damages under gastritis condition can be due to increased mucosal biosynthesis of inducible NO and LTC_4. The protective action of 200 mL/L ethanol could be restricted to the surface mucosal cells, thus having no effect on deeper histologic lesions. In general, deep histologic protection by mild irritants could not be found in gastritis animals. On the other hand, mild irritants could also act by reducing gastric mucosal LTC_4 level, which can lessen gross vascular injury and subsequently reduce hemorrhagic lesion even in gastritis mucosa.

REFERENCES

1 **Guslandi M.** Effect of ethanol on the gastric mucosa. *Dig Dis Sci* 1987; **5:** 21-32
2 **Laine L,** Weinatein WM. Histology of alcoholic hemorrhagic "gastritis": a prospective evaluation. *Gastroenterology* 1988; **94:** 1254-1262
3 **Lacy ER,** Morris GP, Cohen MM. Rapid repair of the surface epithelium in human gastric mucosa after acute superficial injury. *J Clin Gastroenterol* 1993; **17**(Suppl 1): S125-S135
4 **Guth PH,** Paulsen G, Nagata H. Histologic and microcirculatory changes in alcohol-induced gastric lesions in the rat: effect of prostaglandin cytoprotection. *Gastroenterology* 1984; **87:** 1083-1090
5 **Peskar BM,** Lange K, Hoppe U, Peskar BA. Ethanol stimulates formation of leukotriene C_4 in rat gastric mucosa. *Prostaglandins* 1986; **31:** 283-293
6 **Yonei Y,** Holzer P, Guth PH. Laparotomy-induced gastric protection against ethanol injury is mediated by capsaicin-sensitive sensory neurons. *Gastroenterology* 1990; **99:** 3-9
7 **Whittle BJR,** Lopez-Belmonte J, Moncada S. Regulation of gastric mucosal integrity by endogenous nitric oxide: interaction with prostanoids and sensory neuropeptides in the rat. *Br J Pharmacol* 1990; **99:** 607-611
8 **Palmer RMJ,** Ferrige AG, Moncada S. Nitric oxide release accounts for the biological activity of endothelium-derived relaxing factor. *Nature* 1987; **327:** 524-526
9 **Palmer RMJ,** Bridge L, Foxwell NA, Moncada S. The role of nitric oxide in endothelial cell damage and its inhibition by glucocorticoids. *Br J Pharmacol* 1992; **105:** 11-12
10 **Tsuji S,** Kawano S, Sato N, Kamada T. Mucosal blood flow stasis and hypoxemia as the pathogenesis of acute gastric mucosal injury: role of endogenous leukotrienes and prostaglandins. *J Clin Gastroenterol* 1990; **12**(Suppl 1): S85-S91
11 **Szelenyi I,** Brune K. Possible role of oxygen free radicals in ethanol-induced gastric mucosal damage in rats. *Dig Dis Sci* 1988; **33:** 865-871
12 **Chamberlain CE.** Acute hemorrhagic gastritis. *Gastroenterol Clin North Am* 1993; **22:** 843-873
13 **Tepperman BL,** Soper BD. Interaction of nitric oxide and salivary gland epidermal growth factor in the modulation of rat gastric mucosal integrity. *Br J Pharmacol* 1993; **110:** 229-234
14 **Cho CH,** Chen BW, Hui WM, Luk CT, Lam SK. Endogenous prostaglandins: its role in gastric mucosal blood flow and ethanol ulceration in rats. *Prostaglandins* 1990; **40:** 397-403
15 **O'Brien P,** Schultz C, Gannon B. An evaluation of the phenomenon of cytoprotection using quantitative histological criteria. *J Gastroenterol Hepatol* 1987; **2:** 113-121
16 **Read SM,** Northcote DH. Minimization of variation in the response to different proteins of the Coomassie Blue G-binding assay for protein. *Anal Biochem* 1981; **116:** 53-58
17 **Knowles RG,** Palacios M, Palmer RM, Moncada S. Formation

of nitric oxide from L-arginine in the central nervous system: a transduction mechanism for stimulation of the soluble guanylate cyclase. *Proc Natl Acad Sci U S A* 1989; **86:** 5159-5162

18 **Bredt DS,** Snyder SH. Nitric oxide mediates glutamate-linked enhancement of cGMP levels in the cerebellum. *Proc Natl Acad Sci U S A* 1989; **86:** 9030-9033

19 **Tepperman BL,** Vozzolo BL, Soper BD. Effect of neutropenia on gastric mucosal integrity and mucosal nitric oxide synthesis in the rat. *Dig Dis Sci* 1993; **38:** 2056-2061

20 **Rees DD,** Palmer RMJ, Schulz R, Hodson HF, Moncada S. Characterization of three inhibitors of endothelial nitric oxide synthase *in vitro* and *in vivo*. *Br J Pharmacol* 1990; **101:** 746-752

21 **Kostka P,** Jang E, Watson EG, Stewart JL, Daniel EE. Nitric oxide synthase in the autonomic nervous system of canine ileum. *J Pharmacol Exp Ther* 1993; **264:** 34-39

22 **Beauchamp C,** Fridovich I. Superoxide dismutase: improved assays and an assay applicable acrylamide gels. *Anal Biochem* 1971; **44:** 276-287

23 **Lacy ER.** Epithelial restitution in the gastrointestinal tract. *J Clin Gastroenterol* 1988; **10**(Suppl 1): S72-S77

24 **Ko JKS**, Ching CK, Chow JYC, Zhang ST, Lam SK, Cho CH. The vascular and glandular organoprotective properties of metronidazole in the rodent stomach. *Aliment Pharmacol Ther* 1997; **11:** 811-819

25 **Ko JKS,** Cho CH. Adaptive gastric mucosal cytoprotection in rats: different modes of action by three mild irritants. *Digestion* 1996; **57:** 54-59

26 **Laine L.** *Helicobacter pylori*, gastric ulcer, and agents noxious to the gastric mucosa. *Gastroenterol Clin North Am* 1993; **22:** 117-125

27 **Uppal R,** Lateef SK, Korsten MA, Paronetto F, Lieber CS. Chronic alcoholic gastritis. Roles of alcohol and *Helicobacter pylori*. *Arch Intern Med* 1991; **151:** 760-764

28 **Kozol RA,** Downes RJ, Kreutzer DL, Wentzel S, Rossomando E, Elgebaly SA. Release of neutrophil chemotactic factors from gastric tissue. Initial biochemical characterization. *Dig Dis Sci* 1989; **34:** 681-687

29 **Salim AS.** Removing oxygen-derived free radicals stimulates healing of ethanol-induced erosive gastritis in the rat. *Digestion* 1990; **47:** 24-28

30 **Morris SM Jr,** Billiar TR. New insights into the regulation of inducible nitric oxide synthesis. *Am J Physiol* 1994; **266:** E829-E839

31 **Mannick EE,** Bravo LE, Zarama G, Realpe JL, Zhang XJ, Ruiz B, Fontham ET, Mera R, Miller MJ, Correa P. Inducible nitric oxide synthase, nitrotyrosine, and apoptosis in *Helicobacter pylori* gastritis: effect of antibiotics and antioxidants. *Cancer Res* 1996; **56:** 3238-3243

32 **Tepperman BL,** Whittle BJR. Endogenous nitric oxide and sensory neuropeptides interact in the modulation of the rat gastric microcirculation. *Br J Pharmacol* 1992; **105:** 171-175

33 **Palmer RMJ,** Reed DD, Ashton DS, Moncada S. L-Arginine is the physiological precursor for the formation of nitric oxide in endothelial-dependent relaxation. *Biochem Biophys Res Commun* 1988; **153:** 1251-1255

34 **Lamarque D,** Whittle BJR. Role of oxygen-derived metabolites in the rat gastric mucosal injury induced by nitric oxide donors. *Eur J Pharmacol* 1995; **277:** 187-194

35 **Franco L,** Cavallini G, Bovo P, Marcori M, Orlandi PG, Moltrer F, Vetturi B, Velo GP. Gastric eicosanoid synthesis in normal subjects and alcoholics after ethanol stimulation. *Ital J Gastroenterol* 1995; **27:** 244-247

36 **Franco L,** Velo GP. Eicosanoid and gastroprotection by copper derivatives and NDGA. *Inflamm Res* 1995; **44:** 139-142

37 **Ko JKS,** Ma JJ, Chow JYC, Ma L, Cho CH. The correlation of the weakening effect on gastric mucosal integrity by 5-HT with neutrophil activation. *Free Rad Biol Med* 1998; **24:** 1007-1014

Edited by Wang XL and Xu FM

PO Box 2345, Beijing 100023, China
Fax: +86-10-85381893
E-mail: wjg@wjgnet.com www.wjgnet.com

World J Gastroenterol 2004;10(17):2509-2513
World Journal of Gastroenterology
Copyright © 2004 by The WJG Press ISSN 1007-9327

• BASIC RESEARCH •

Effects of motilin and ursodeoxycholic acid on gastrointestinal myoelectric activity of different origins in fasted rats

Ping Fang, Lei Dong, Jin-Yan Luo, Xiao-Long Wan, Ke-Xin Du, Ning-Li Chai

Ping Fang, Lei Dong, Jin-Yan Luo, Xiao-Long Wan, Ning-Li Chai, Department of Gastroenterology, Second Hospital of Xi'an Jiaotong University, Xi'an 710004, Shaanxi Province, China
Ke-Xin Du, Functional Center, Medical School, Xi'an Jiaotong University, Xi'an 710004, Shaanxi Province, China
Supported by the National Natural Science Foundation of China, No. 30170414
Correspondence to: Professor Lei Dong, Department of Gastroenterology, Second Hospital of Xi'an Jiaotong University, Xi'an 710004, Shaanxi Province, China. pingf7613@sina.com
Telephone: +86-29-83098317 **Fax:** +86-29-87231758
Received: 2003-10-27 **Accepted:** 2003-12-29

Abstract

AIM: To investigate gastrointestinal migrating myoelectric complex (MMC) and the effects of porcine motilin and ursodeoxycholic acid (UDCA) on MMC of gastrointestinal tract of different origins in fasted rats.

METHODS: Three bipolar silver electrodes were chronically implanted on the antrum, duodenum and jejunum. Seven days later 24 experimental rats were divided into 2 groups. One group was injected with porcine motilin *via* sublingual vein at a dose of 20 μg/kg, the other group was perfused into stomach with UDCA. The gastrointestinal myoelectric activity was recorded 1 h before and 2 h after the test substance infusions into the rats.

RESULTS: In all fasted rats a typical pattern of MMC was observed. Among the totally 68 activity fronts recorded in fasted rats under control, 67% started in duodenum, and 33% in antrum. MMC cycle duration and duration of phase III of antral origin were longer than those of duodenal origin. Administration of 20 μg/kg porcine motilin induced a premature antral phase III of antral origin. But perfusion into stomach with UDCA resulted in shorter MMC cycle duration, longer duration of phase III of duodenal origin, which were followed with shorter cycle duration and duration of antral phase III.

CONCLUSION: In fasted rats, MMC could originate from antrum and duodenum respectively. The characteristics of MMC of different origins may contribute to the large variations within subjects. The mechanisms of different origins of phase III may be different. Porcine motilin and UDCA could affect MMC of different origins of the gastrointestinal tract in fasted state, respectively.

Fang P, Dong L, Luo JY, Wan XL, Du KX, Chai NL. Effects of motilin and ursodeoxycholic acid on gastrointestinal myoelectric activity of different origins in fasted rats. *World J Gastroenterol* 2004; 10(17): 2509-2513
http://www.wjgnet.com/1007-9327/10/2509.asp

INTRODUCTION

The migrating myoelectric complex (MMC) is a distinct pattern of electromechanical activity observed in gastrointestinal tract during fasting. It is thought to serve a housekeeping role and sweep undigested residual through the digestive tract. Phase III of MMC originates at variable sites in the gut from the esophagus (especially from antrum and duodenum) to proximal ileum. Large variations in MMC characteristics were described both within subjects and between subjects. The reason for the large variation in MMC characteristics is unknown. However, regarding the supposed differences in mechanisms that regulate the phase III of MMC of antral or duodenal origins, different origin of phase III within subject could be a basis for the differences in MMC characteristics[1,2].

Motilin, a 22 amino acid peptide secreted by endocrinocytes in the mucosa of the proximal small intestine, participates in controlling the pattern of smooth muscle contractions in the upper gastrointestinal tract. These bursts of motilin secretion are temporarily related to the onset of housekeeping contractions, which sweep the undigested material of stomach and small intestine[3]. Previous studies showed that the enterohepatic circulation of bile acids and interdigestive motility must somehow be associated with each other. Phase III of MMC played an important role in the transport of bile acids from the proximal duodenum to the distal small intestine, where bile acids were absorbed for transport back to the liver.

The purpose of the present study was to investigate the gastrointestinal MMC characteristics with respect to the different origin of phase III in fasted rats. Furthermore, the effects of exogenous porcine motilin and UDCA on the interdigestive myoelectric activity were investigated and the relationship between the above two drugs and the MMCs of different origin in conscious rats were studied.

MATERIALS AND METHODS

Animal preparation

Twenty-four healthy Sprague-Dawley rats (15 male and 9 female) weighing 200-250 g were fed with a dry rat food, and tap water for drinking *ad libitum*. After fasted for one night, the rats were intraperitoneally anesthetized with sodium pentobarbital 30 mg/kg. The hair on the skull and abdomen was shaved. The surgery was done with sterile instruments, and under strict aseptic conditions. The abdominal musculature and peritoneum were opened through the linea alba. Three bipolar insulated silver electrodes made by Teflon-coated wire (0.5 mm in outer diameter, 20 cm in length) were implanted into the muscular layer of the bowel with a needle as a trocar. One millimeter of the wire was exposed near the implanted end, and the interval between pairs of electrodes should be 2.0-3.0 mm. The electrodes were placed on the gastric antrum at 5 mm proximal to the pylorus, on the duodenum and jejunum respectively at 1 cm and 15 cm distal to the pylorus. The bundled electrode wires were grasped by the clamp through a silastic tube (2.4 mm in diameter), which then passed through the subcutaneous tunnel from the abdominal incision to the back of the shoulder exit. During operation the intestine was kept moist with sterile 9 g/L NaCl solution, and 4 mL of this solution was applied intraperitoneally before closure of the abdomen to compensate for intraoperative fluid loss. The abdominal wall was closed in three layers with

running Vicryl 4-0 sutures. The rats were kept in a humidified incubator at 37 °C for 2 to 4 h after operation. Following this, they were individually housed with free access to water and food. Housing conditions were kept constant with temperature at 22 °C, humidity of 60% and a 12-h light/dark cycle. The rats were allowed to adjust to these conditions for 1 wk before experiment.

Motility recordings

Rats were fasted for 16 h with free access to water. The experiments were performed in conscious rats. The gastrointestinal myoelectric activity recordings were monitored by using an electrical swivel mechanism to a computerized, multichannel recorde (RM-6280C, Chengdu, China). Myoelectric activity was sampled at a rate of 1 kHz. The signals were amplified and bandpass filtered (frequencies above 0.3 Hz and below 100 Hz were cut off). The amplitudes of contractions were recorded in μV.

Experimental procedures

A randomized, placebo-controlled experiment was performed. The rats were coded and divided into 2 groups, 12 in each group. On each experimental day, at the beginning of the experiments, the gastrointestinal myoelectric activity was recorded for 1 h for each rat, and during this period at least 2 or 3 MMCs appeared. The substances were dissolved immediately before use in normal saline. In each group, 4 rats were placed as control that received placebo (vehicle), 0.2 mL saline containing 250 μg bovine serum albumin (BSA, Sigma). One group was injected with porcine motilin (Sigma) *via* sublingual vein at a dose of 20 μg/kg, and the other group was perfused into stomach with UDCA (Pharmaceutical Factory of Changzhou City) respectively. After the substances were used, the gastrointestinal myoelectric activity of the rats was continuously recorded at least for 2 h. After the conversion from analog to digital, the signals were stored on optical disk for later analysis.

Statistical analysis

All variables followed a normal distribution and are expressed as mean±SD unless otherwise stated. The presented means are unweighted means, *i.e.*, means of all subjects after first calculating the mean within each subject separately. The MMC characteristics such as MMC cycle duration, duration of phase III, mean amplitude and frequency of phase III were examined by using the ANOVA model, both before and after discrimination for antral or duodenal phase III origin effects. The homogeneity of variance for each variable, after being divided into antral and duodenal phase III origin effects, was tested and appeared equal. Within-subject and between-subject effects were analyzed by the ANOVA model. For the MMC cycle duration, the corresponding variance components between and within individuals were used to calculate the variance between individuals as a percentage of the total variance. To explain the importance of the factor preceding phase III origin in the total variance, the sum of squares of the factor preceding phase III origin was calculated as a percentage of the total sum of squares in the ANOVA model. The effects of unfamiliarity with gastrointestinal catheter studies on MMC cycle duration was examined using the ANOVA model. Student's *t* test was used to compare the different paired values before and after the test substances administration in the above 2 groups. Statistical significance was defined as two-tailed $P<0.05$.

RESULTS

MMC characteristics of different origin

In all fasted rats typical pattern of MMCs were observed. The total number of MMC cycles recorded was 68. The mean MMC cycle duration was 746±140 s. In total, phase III cycles were observed with 23 (33%) of antral origin and 45 (67%) of duodenal origin. Fifty-nine percent of the total variance in MMC cycle duration was explained by the within-subject variance. The duration and the amplitude of phase III were significantly different between subjects ($P<0.05$; Table 1). The large variation in MMC cycle duration is visible in Figure 1. The MMC cycle duration following a phase III of antral origin was significantly longer than those of duodenal origin ($P<0.05$; Table 2). When the factor preceding phase III origin was included in our model, this factor contributed significantly to the total variation in MMC cycle duration; 31% of the total sum of squares was explained by the factor preceding phase III in comparison to 36% explained by the between-subject variance. The duration of phase III for duodenum was significantly longer when it started in the antrum than in the duodenum ($P<0.05$). The other characteristics of MMC for duodenum were not significantly different between the phase III of the above two origins.

Table 1 MMC characteristics in 24 normal rats

MMC characteristics	mean±SD
MMC cycle duration/s	746±140[a]
Duration of phase III/s	214±53[a]
Amplitude of phase III/μV	287±23[a]
Frequency of phase III/(bursts/min)	11.4±0.3

Values are shown for duodenum. [a]$P<0.05$ *vs* between subjects.

Table 2 MMC characteristics of different origin of ongoing phase III (n = 24, mean±SD)

MMC characteristics	After phase III of antral origin	After phase III of duodenal origin
MMC cycle duration/s	901±74	667±91[a]
Duration of phase III/s	271±30	186±35[a]
Amplitude of phase III/μV	292±17	284±25
Frequency of phase III/(bursts/min)	11.2±0.5	11.6±0.2

Values are shown for duodenum. [a]$P<0.05$ *vs* antral.

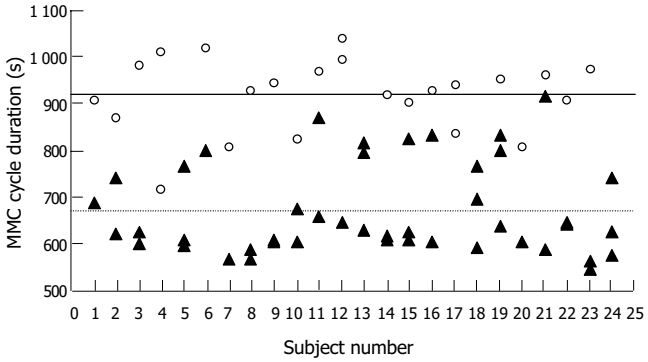

Figure 1 MMC cycle duration of all subjects following phase III. ○, antral origin; ▲, duodenal origin; Solid line: antral mean MMC cycle duration (746.3); Dotted line: duodenal mean MMC cycle duration (667.0).

Effects of porcine motilin and UDCA

The effects of porcine motilin on the interdigestive gastrointestinal myoelectric activity were established within 1 to 2 min after the injection *via* sublingual vein at a dose of 20 μg/kg. A premature antral phase III which did not migrate caudad to the duodenum and jejunum was observed. And one injection only induced

one premature antral phase III. The characteristics of premature antral phase III were different significantly from those of normal antral phase III. The shorter duration and higher amplitude of premature antral phase III appeared (Figure 2). The effects of UDCA on the interdigestive gastrointestinal myoelectric activity were established within 3 to 4 min after the stomach was perfused of UDCA. The shorter MMC cycle duration, and the longer duration of phase III of duodenal origin, followed by the shorter cycle duration and duration of antral phase III were observed. There was no significant difference in the other parameters of MMC of antrum and duodenum before and after the treatment (Figure 3, Table 3). Furthermore, there was no significant difference in the MMC characteristics before and after placebo treatment in the above 2 experiments.

Table 3 Effects of UDCA on the interdigestive gastrointestinal myoelectric activity (n = 8, mean±SD)

MMC characteristics	Antrum		Duodenum	
	Before	After	Before	After
The number of MMC	7	11	11	21
MMC cycle duration/s	885±106	800±48[a]	780±45	602±78[a]
Duration of phase III/s	161±13	113±19[a]	156±9	241±20[a]
Amplitude of phase III/μV	297±11	284±20	288±22	285±19
Frequency of phase III/(bursts/min)	3.1±0.5	3.2±0.6	11.2±1.6	11.5±1.8

[a]P<0.05 *vs* before treatment.

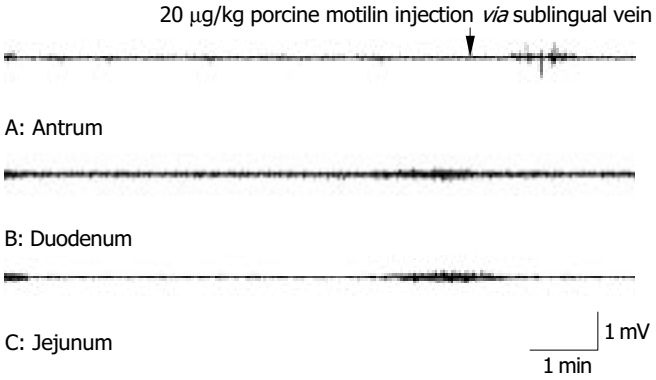

Figure 2 Effects of porcine motilin on the interdigestive gastrointestinal myoelectric activity in one case.

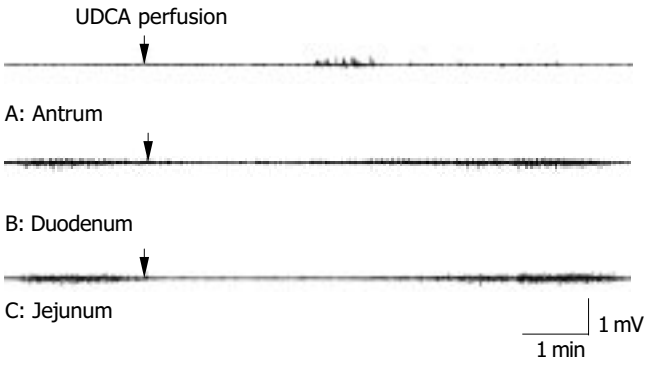

Figure 3 Effects of UDCA on the interdigestive gastrointestinal myoelectrical activity in one case.

DISCUSSION

Gastrointestinal motility pattern could mainly be divided into the interdigestive and digestive states. The interdigestive state is characterized by the cyclical occurrence of activity front, phase III contractions, which could occur in the antrum, duodenum and migrate to the small intestine. The digestive state is characterized by sustained contractions with different amplitude in the gastric antrum and small intestine. In our experiments, a typical pattern of MMC in interdigestive state was observed in all rats. The phases of the MMC can be distinguished: phase III, motor quiescence, phase III, a period of irregular contractile activity and phase III, a period of rhythmic contractions. The MMC pattern was disrupted by feeding, and irregular contractions with different amplitude were sustained in the antrum, duodenum and jejunum for at least 30 min after feeding. MMC was firstly described in the small intestine of fasting dogs and observed in the overall gastrointestinal tract of several species, including rats[4-6]. In our study they have also been found in gastric antrum and small intestine. A method that could record the gastrointestinal myoelectrical activities in physiological conditions was established in our experiment. The model we have developed seemed to be suitable for studying the gastrointestinal myoelectric activities. The effects we obtained could be attributed to neither sedatives nor operative stress because of the method unable to record the gastrointestinal motility without the use of anesthesia. Furthermore, the surgical operations were well tolerated by the animals, especially by small animals. At present the method of stationary manometry was used in most of the experiments of this field[7,8]. But it is not suitable for small animal experiments. Our method was simple, easy and successful. Few tissue was injured. Several pairs of electrodes could be implanted and work stably and repeatedly. The experimental techniques would be helpful for further studying the mechanisms of gastrointestinal motility.

A typical pattern of MMC was observed in all fasted rats. Among the totally 68 activity fronts recorded in them under control, 67% started in the duodenum, and 33% in the antrum. The MMC cycle duration and duration of phase III of antral origin were longer than those of duodenal origin. The MMCs were subject to large variations in its characteristics, both between subjects and within subjects. The reason for this wide variation is unknown. Our results contributed to a better understanding of this variation. Our study showed that MMC characteristics had close relationship with the origin of phase III. But Gregersen *et al*. described a positive correlation between the duration of phase III in the duodenum and the duration of the next MMC cycle[9]. They could not attribute this to a difference in origin of phase III, most likely due to the limited number of observations within each subject. The percentages of antral and duodenal originated phase III observed within a subject would strongly affect the mean MMC cycle duration of this subject as well as the overall mean of a group of subjects[10,11]. An explanation for the differences in MMC cycle duration and duration of phase III was that it might imply differences in the mechanism controlling interdigestive motility in antrum and small intestine. This may reflect functional differences existing in the hormonal mechanisms involved in the regulation of antral and duodenal phase III. It was thought that a difference might exist in the refractory period between the gastric antrum and small intestine, with a shorter refractory period in the duodenum compared with the antrum. Another possible reason may be the anatomic structure of rats. Because there is no gallbladder in rats, bile acids secreted to duodenum directly. In addition, our study could not explain why the density and the sensitivity of receptor in gastrointestinal tract changed[12,13].

The mechanisms regulating MMC is not understood completely. Previous study showed that the area postrema of medulla oblongata, vagal innervation, enteric nervous system and gastrointestinal hormone could regulate the MMC. Among them motilin in plasma plays a very critical role in the initiation of MMC. Motilin is one of the gastrointestinal hormones. It

belongs to gut-brain peptide and distributes in the brain and gastrointestinal tract[14-22]. Plasma levels of the motilin fluctuate in synchrony with the different phase of MMC. Motilin could stimulate the gastrointestinal motility of many animals, and there were species differences in its effects[23]. After duodenectomy, no obvious phase III contractions were seen in the gastric antrum, but the contractile response of the stomach to exogenous motilin was similar to that of intact dogs[24]. This experiment showed that endogenous motilin was released from duodenum. One research showed that the motilin could activate calcium current in human and canine jejunal circular smooth muscle. Furthermore, the density and sensitivity of motilin receptor of different parts of gastrointestinal tract were different. But recently the close relationship between motilin and MMC of antral but not duodenal origin was found[25]. Porcine motilin could influence the MMC of antral origin in our experiment. Administration of 20 μg/kg porcine motilin could induce a premature antral phase III in rats. The characteristics of it were different significantly from those of normal antral phase III. But the results of our experiments were coincident with previous studies. Maybe the density and sensitivity of motilin receptor of antrum were higher than those of other parts of gastrointestinal tract[12,13]. Some studies showed that duodenal pH governed interdigestive motility in humans. But neither duodenal acidification nor increases in motilin concentration were necessary to initiate MMC in man[26]. Administration of a low dose of erythromycin induced an MMC that started from the gastric antrum, unaccompanied by a motilin peak. These findings showed that the activation of motilin receptor triggered the MMC.

Another important factor influencing MMC is enterohepatic cycle of bile acids. The enterohepatic cycle of bile acids had close relationship with MMC. The possible explanation was that the development of MMC of duodenal origin was not autonomous but dependent on the stimulation of bile acids to the local mucous of duodenum. Furthermore, duodenum, possibly by releasing endogenous motilin, might recruit and further augment the gastric response to initiation of the MMC of antral origin[27-29]. So there are maybe two mechanisms for initiation of MMC in the stomach and duodenum. In our experiment perfusion into stomach of rats with UDCA could shorten the MMC cycle duration and elongate the duration of phase III of duodenal origin, which was followed by the contractions of antrum within a short time. We suggest that UDCA may drain into the duodenum influencing the MMC of duodenal origin and stimulate the release of endogenous motilin from the mucous of duodenum, because crushing the gallbladder of patient during operation could eject the bile acids and induce a higher level of plasma motilin. On the contrary, some researchers thought that bile aids in duodenum could not induce the release of motilin and affect the MMC[30]. In the study of patients with gallstone, the motilin in plasma did not decrease obviously *vs* control group. But according to the above supposition, we could infer that the motilin in plasma should decrease obviously compared with control group because the motility of gallbladder decreased in most of the patients. The results obtained from this experiment did not coincident with those of previous experiments. Another research showed that the kinetics of duodenum did not change significantly after cholecystectomy. So these studies did not support the local stimulatory theory[31,32]. But one study showed that the occurrence of MMC had close relationship with the increase of the plasma concentration of motilin and bile acids. Maybe it could explain the contradiction in this respect to some extent[33]. But our study could not draw this conclusion.

Gastrointestinal motility disorder is common in clinical practice, and studying the mechanisms of it is very important to its diagnosis and therapy. Our study showed that the mechanisms of different origin of phase III may be different and porcine motilin and UDCA could affect the MMC of different origin of the gastrointestinal tract in fasting state respectively. This may provide novel treatments for patients with disturbed gut motility.

REFERENCES

1 **Gielkens HA,** Nieuwenhuizen A, Biemond I, Lamers CB, Masclee AA. Interdigestive antroduodenal motility and gastric acid secretion. *Aliment Pharmacol Ther* 1998; **12**: 27-33

2 **Bush TG,** Spencer NJ, Watters N, Sanders KM, Smith TK. Spontaneous migrating motor complexes occur in both the terminal ileum and colon of the C57BL/6 mouse *in vitro*. *Auton Neurosci* 2000; **84:** 162-168

3 **Suzuki H,** Mochiki E, Haga N, Satoh M, Mizumoto A, Itoh Z. Motilin controls cyclic release of insulin through vagal cholinergic muscarinic pathways in fasted dogs. *Am J Physiol* 1998; **274**(1 Pt 1): G87-95

4 **Powell AK,** Fida R, Bywater RA. Motility in the isolated mouse colon: migrating motor complexes, myoelectric complexes and pressure waves. *Neurogastroenterol Motil* 2003; **15:** 257-266

5 **Kaji T,** Takamatsu H, Kajiya H. Motility of the gastrointestinal tract and gallbladder during long-term total parenteral nutrition in dogs. *J Parenter Enteral Nutr* 2002; **26:** 198-204

6 **Romanski KW,** Rudnicki J, Slawuta P. The myoelectric activity of ileum in fasted and fed young pigs. *J Physiol Pharmacol* 2001; **52**(4 Pt 2): 851-861

7 **Matsunaga H,** Tanaka M, Takahata S, Ogawa Y, Naritomi G, Yokohata K, Yamaguchi K, Chijiiwa K. Manometric evidence of improved early gastric stasis by erythromycin after pylorus-preserving pancreatoduodenectomy. *World J Surg* 2000; **24:** 1236-1241

8 **Andrews JM,** O'donovan DG, Hebbard GS, Malbert CH, Doran SM, Dent J. Human duodenal phase III migrating motor complex activity is predominantly antegrade, as revealed by high-resolution manometry and colour pressure plots. *Neurogastroenterol Motil* 2002; **14**: 331-338

9 **Gregersen H,** Rittig S, Vinter-Jensen L, Kraglund K. The relation between antral contractile activity and the duodenal component of the migrating motility complex. *Scand J Gastroenterol Suppl* 1988; **152**: 36-41

10 **Qian LW,** Pasricha PJ, Chen JD. Origins and patterns of spontaneous and drug-induced canine gastric myoelectrical dysrhythmia. *Dig Dis Sci* 2003; **48**: 508-515

11 **Luiking YC,** Akkermans LM, van der Reijden AC, Peeters TL, van Berge-Henegouwen GP. Differential effects of motilin on interdigestive motility of the human gastric antrum, pylorus, small intestine and gallbladder. *Neurogastroenterol Motil* 2003; **15**: 103-111

12 **Koenig JB,** Cote N, LaMarre J, Harris WH, Trout DR, Kenney DG, Monteith G. Binding of radiolabeled porcine motilin and erythromycin lactobionate to smooth muscle membranes *in various* segments of the equine gastrointestinal tract. *Am J Vet Res* 2002; **63**: 1545-1550

13 **Depoortere I.** Motilin and motilin receptors: characterization and functional significance. *Verh K Acad Geneeskd Belg* 2001; **63**: 511-529

14 **Wang L,** Zhou L, Tian R. Role of the area postrema of medulla oblongata in the regulation of canine interdigestive migrating motor complex. *Chin Med J* 2002; **115**: 384-388

15 **Wang L,** Zhou L, Tian R. Effect of electrical lesion of the area postrema on gastrointestinal interdigestive migrating motor complex in conscious dogs. *Zhonghua Yixue Zazhi* 2000; **80**: 764-768

16 **Hashmonai M,** Szurszewski JH. Effect of cerebroventricular perfusion of bombesin on gastrointestinal myoelectric activity. *Am J Physiol* 1998; **274**(4 Pt 1): G677-686

17 **Guan Y,** Tang M, Jiang Z, Peeters TL. Excitatory effects of motilin in the hippocampus on gastric motility in rats. *Brain Res* 2003; **984**: 33-41

18 **Tang M,** Zhang HY, Jiang ZY, Xu L, Peeters TL. Effect of central administration of motilin on the activity of gastric-related neurons in brain stem and gastric motility of rats. *Shengli*

Xuebao 2000; **52**: 416-420
19 **Romanski KW.** Influence of various feeding conditions, the migrating myoelectric complex and cholinergic drugs on antral slow waves in sheep. *Arch Tierernahr* 2002; **56**: 393-408
20 **Tanaka T,** Kendrick ML, Zyromski NJ, Meile T, Sarr MG. Vagal innervation modulates motor pattern but not initiation of canine gastric migrating motor complex. *Am J Physiol Gastrointest Liver Physiol* 2001; **281**: G283-G292
21 **Tanaka T,** VanKlompenberg LH, Sarr MG. Selective role of vagal and nonvagal innervation in initiation and coordination of gastric and small bowel patterns of interdigestive and postprandial motility. *J Gastrointest Surg* 2001; **5**: 418-433
22 **Tanaka T,** Zyromski NJ, Libsch KD, Kendrick ML, Sarr MG. Canine ileal motor activity after a model of jejunoileal autotransplantation. *Ann Surg* 2003; **237**: 192-200
23 **Sasaki N,** Yoshihara T. The effect of motilin on the regulation mechanism of intestinal motility in conscious horses. *J Vet Med Sci* 1999; **61**: 167-170
24 **Suzuki H,** Mochiki E, Haga N, Shimura T, Itoh Z, Kuwano H. Effect of duodenectomy on gastric motility and gastric hormones in dogs. *Ann Surg* 2001; **233:** 353-359
25 **Luiking YC,** Peeters TL, Stolk MF, Nieuwenhuijs VB, Portincasa P, Depoortere I, van Berge Henegouwen GP, Akkermans LM. Motilin induces gall bladder emptying and antral contractions in the fasted state in humans. *Gut* 1998; **42**: 830-835
26 **Tomita R,** Fujisaki S, Tanjoh K, Fukuzawa M. Studies on gastrointestinal hormone and jejunal interdigestive migrating motor complex in patients with or without early dumping syndrome after total gastrectomy with Roux-en-Y reconstruction for early gastric cancer. *Am J Surg* 2003; **185**: 354-359
27 **Kajiyama Y,** Irie M, Enjoji A, Ozeki K, Ura K, Kanematsu T. Role of bile acids in duodenal migrating motor complexes in dogs. *Dig Dis Sci* 1998; **43**: 2278-2283
28 **Van Ooteghem NA,** Van Erpecum KJ, Van Berge-Henegouwen GP. Effects of ileal bile salts on fasting small intestinal and gallbladder motility. *Neurogastroenterol Motil* 2002; **14:** 527-533
29 **Einarsson C,** Ellis E, Abrahamsson A, Ericzon BG, Bjorkhem I, Axelson M. Bile acid formation in primary human hepatocytes. *World J Gastroenterol* 2000; **6**: 522-525
30 **van Ooteghem NA,** Moschetta A, Rehfeld JF, Samsom M, van Erpecum KJ, van Berge-Henegouwen GP. Intraduodenal conjugated bile salts exert negative feedback control on gallbladder emptying in the fasting state without affecting cholecystokinin release or antroduodenal motility. *Gut* 2002; **50**: 669-674
31 **Stolk MF,** Van Erpecum KJ, Peeters TL, Samsom M, Smout AJ, Akkermans LM, Vanberge-Henegouwen GP. Interdigestive gallbladder emptying, antroduodenal motility, and motilin release patterns are altered in cholesterol gallstone patients. *Dig Dis Sci* 2001; **46:** 1328-1334
32 **Andersen PV,** Mortensen J, Oster-Jorgensen E, Rasmussen L, Pedersen SA, Qvist N. Cholecystectomy in patients with normal gallbladder function did not alter characteristics in duodenal motility which was not correlated to size of bile acid pool. *Dig Dis Sci* 1999; **44:** 2443-2448
33 **Portincasa P,** Peeters TL, van Berge-Henegouwen GP, van Solinge WW, Palasciano G, van Erpecum KJ. Acute intraduodenal bile salt depletion leads to strong gallbladder contraction, altered antroduodenal motility and high plasma motilin levels in humans. *Neurogastroenterol Motil* 2000; **12:** 421-430

Edited by Zhu LH and Chen WW **Proofread by** Xu FM

PO Box 2345, Beijing 100023, China
Fax: +86-10-85381893
E-mail: wjg@wjgnet.com www.wjgnet.com

World J Gastroenterol 2004;10(17):2514-2518
World Journal of Gastroenterology
Copyright © 2004 by The WJG Press ISSN 1007-9327

• BASIC RESEARCH •

Improvement of barrier function and stimulation of colonic epithelial anion secretion by *Menoease Pills*

Jin-Xia Zhu, Ning Yang, Gui-Hong Zhang, Lai-Ling Tsang, Yu-Lin Gou, Hau-Yan Connie Wong, Yiu-Wa Chung, Hsiao-Chang Chan

Jin-Xia Zhu, Lai-Ling Tsang, Yu-Lin Gou, Hau-Yan Connie Wong, Yiu-Wa Chung, Hsiao-Chang Chan, Epithelial Cell Biology Research Center, Department of Physiology, Faculty of Medicine, The Chinese University of Hong Kong, Shatin, Hong Kong, China
Jin-Xia Zhu, Ning Yang, Gui-Hong Zhang, Department of Physiology, Medical School, Zhengzhou University, Zhengzhou 450052, Henan Province, China
Supported by a fund from the Innovation and Technology Commission of Hong Kong, SAR
Correspondence to: Professor Hsiao-Chang Chan, Epithelial Cell Biology Research Center, Department of Physiology, Faculty of Medicine, The Chinese University of Hong Kong, Shatin, NT, Hong Kong, China. hsiaocchan@cuhk.edu.hk
Telephone: +852-26096839 **Fax:** +852-26035022
Received: 2004-02-02 **Accepted:** 2004-03-04

Abstract

AIM: *Menoease Pills* (MP), a Chinese medicine-based new formula for postmenopausal women, has been shown to modulate the endocrine and immune systems[1]. The present study investigated the effects of MP and one of its active ingredients, *ligustrazine*, on epithelial barrier and ion transport function in a human colonic cell line, T_{84}.

METHODS: Colonic transepithelial electrophysiological characteristics and colonic anion secretion were studied using the short circuit current (I_{SC}) technique. RT-PCR was used to examine the expression of cytoplasmic proteins associated with the tight junctions, *ZO-1* (zonula occludens-1) and *ZO-2* (zonula occludens-2).

RESULTS: Pretreatment of T_{84} cells with MP (15 μg/mL) for 72 h significantly increased basal potential difference, transepithelial resistance and basal I_{SC}. RT-PCR results showed that the expressions of *ZO-1* and *ZO-2* were significantly increased after MP treatment, consistent with improved epithelial barrier function. Results of acute stimulation showed that apical addition of MP produced a concentration-dependent (10-5 000 μg/mL, EC_{50} = 293.9 μg/mL) increase in I_{SC}. MP-induced I_{SC} was inhibited by basolateral treatment with bumetanide (100 μmol/L), an inhibitor of the Na^+-K^+-$2Cl^-$ cotransporter, apical addition of Cl^- channel blockers, diphenylamine-2, 2′-dicarboxylic acid (1 mmol/L) or glibenclamide (1 mmol/L), but not 4, 4′-diisothiocyanostilbene-2, 2′-disulfonic acid or epithelial Na+ channel blocker, amiloride. The effect of MP on *ZO-1* and *ZO-2* was mimicked by *Ligustrazine* and the *ligustrazine*-induced I_{SC} was also blocked by basolateral application of bumetanide and apical addition of diphenylamine-2, 2′-dicarboxylic acid or glibenclamide, and reduced by a removal of extracellular Cl^-.

CONCLUSION: The results of the present study suggest that MP and *lligustrazine* may improve epithelial barrier function and exert a stimulatory effect on colonic anion secretion, indicating the potential use of MP and its active ingredients for improvement of GI tract host defense and alleviation of constipation often seen in the elderly.

Zhu JX, Yang N, Zhang GH, Tsang LL, Gou YL, Wong HYC, Chung YW, Chan HC. Improvement of barrier function and stimulation of colonic epithelial anion secretion by *Menoease Pills. World J Gastroenterol* 2004; 10(17): 2514-2518
http://www.wjgnet.com/1007-9327/10/2514.asp

INTRODUCTION

It is well known that the gastrointestinal (GI) epithelium of the host, as the first defense line, plays an important role in protecting enteric epithelia from invasion of most pathogens. Intestinal epithelial barrier function regulates epithelial ions and nutrient transport as well as host defense mechanisms. Epithelial membrane pumps, ion channels and tight junctions tightly control epithelial transcellular and paracellular fluxes[2,3]. Cl^- secretion also provides an essential driving force for lubrication of intestinal contents during regular bowel movements or flushing of microbial organisms or artificial irritants in host defense responses[4,5]. Epithelial Cl^- channels play an important role in regulation and maintenance of normal GI physiological functions. Abnormal regulation of Cl^- channels may result in diarrhea[6-8] or constipation[9,10]. While the later represents one of the frequently encountered conditions in aged people, few remedies are available for alleviation of the condition in the elderly.

Menoease Pills (Modified *Bak Foong Pills*, MP), a newly developed formula based on traditional Chinese medicine *Bak Foong Pills* (*BFP*, also known as Baifeng Wan)[11-17], has been designed for the use of postmenopausal women. It has been demonstrated that MP can regulate hormonal profiles (Gou *et al*, unpublished data) and immune system in the elderly[1], indicating its beneficial effects for postmenopausal or elderly women. Since our previous studies have demonstrated that *BFP* could increase colonic epithelial Cl^- and pancreatic duct epithelial HCO_3^- secretion[11,15,16] and both *BFP* and MP have a common active ingredient, *ligustrazine*, we undertook the present study to examine whether MP and *ligustrazine* exerted any effect on Cl^- secretion and epithelial electrophysiological characteristics using human colonic T_{84} cells in conjunction with the short-circuit current technique and RT-PCR.

MATERIALS AND METHODS

Chemicals and solutions

Dulbecco's Modified Eagle's medium (DMEM)/F12, Hank's balanced salt solution (HBSS), and fetal bovine serum were from Gibco Laboratories (New York, NY). 4, 4'-diisothiocyanostilbene-2, 2'-disulfonic acid (DIDS) and glibenclamide were from Sigma (St. Louis, MO). MP was obtained from Eu Yan Sang Ltd (Hong Kong). Diphenylamine-2, 2'-dicarboxylic acid (DPC) was purchased from Riedel-de Haen Chemicals (Hannover, Germany). Calbiochem (San Diego, CA) was the source for amiloride hydrochloride and bumetanide. Krebs-Henseit (K-H) solution had the following composition (mmol/L): NaCl, 117; KCl, 4.5; $CaCl_2$, 2.5; $MgCl_2$, 1.2; $NaHCO_3$, 24.8; KH_2PO_4, 1.2; glucose, 11.1. The solution was gassed with 950 mL/L O_2 and 50 mL/L CO_2, at pH 7.4.

MP extraction

Five hundred gram of MP powder in 700 mL/L ethanol at a ratio of 1 to 10 (g/mL) was put in round-bottomed flask and boiled under reflux for 2 h . The mixture was filtered and the residues of MP were subject to the same treatment for a second time. The filtrates from the two treatment procedures were collected and put in the vacuum rotary evaporator for concentration. The extracts were collected and lyophilized by a freeze dryer.

Cell culture

Human colonic T_{84} cells were purchased from American Type Culture Collection (Rockville, MD). The cells were grown in DMEM/F12 with 100 mL/L fetal bovine serum. For I_{SC} recording the cells ($2\text{-}3\times10^5$/mL) were plated onto each floating permeable support, which was made of a Millipore filter with a silicone rubber ring attached on top of it for confining the cells (culture area 0.45 cm^2). For the RT-PCR analysis, cells were seeded on the Millipore filter with a confined culture area of 4.5 cm^2. Cultures were incubated at 37 °C in 950 mL/L O_2 and 50 mL/L CO_2 for 6 d before experiments. For the experiments of MP and *ligustrazine* pretreatments, MP (15 μg/mL) or *ligustrazine* (100 μmol/L) was added into the culture medium at 72 h before experiments, when the cells became semi-confluent.

Short-circuit current measurement

The measurement of I_{SC} has been described previously[18]. Monolayers grown on permeable supports were clamped vertically between two halves of the Ussing chamber. The monolayers were bathed in both sides with Krebs-Henseit solution, which was maintained at 37°C by a water jacket enclosing the reservoir. The Krebs-Henseit solution was bubbled with 950 mL/L O_2 and 50 mL/L CO_2 to maintain the pH of the solution at 7.4. Drugs could be added directly to apical or basal side of the epithelium. Usually, the epithelia exhibited a basal transepithelial potential difference for every monolayer examined, which was measured by the Ag/AgCl reference electrodes (World Precision Instruction) connected to a preamplifier which was in turn connected to a voltage-clamp amplifier (World Precision Instruction, DVC-1000). In most of the experiments, the change in I_{SC} was defined as the maximal rise in I_{SC} following agonist stimulation and it was normalized to current change per unit area of the epithelial monolayer (μA/cm^2). The total charges transported for 15 min (the area under the curve of the agonist-induced I_{SC} responses) were also used to describe the agonist-induced responses (μC/cm^2). In each experiment, a transepithelial potential difference was 0.1 mV. The change in current in response to the applied potential was used to calculate the transepithelial resistance (TER) of the monolayer using Ohm's Law. Experiments were normally repeated in different batches of culture to ensure that the data were reproducible.

Reverse transcription PCR (RT-PCR) analysis

Total RNA (15 μg) was extracted from the T_{84} (control, MP and *ligustrazine* pretreated). Expressions of *ZO-1* and *ZO-2* were analyzed by competitive RT-PCR. The specific oligo nucleotide primers for *ZO-1* was CGGTCCTCTGAGCCTGTAAG for sense and GGA TCTACATGCGACGACAA for antisense corresponding to nucleotides 3 100-3 470 with an expected cDNA of 371 bp[19], and for ZO-2 was GCCAAAACCCAGAACAAAGA for sense and ACTGCTCTCTCCCACCTCCT for antisense corresponding to nucleotides 3 018-3 283 with an expected cDNA of 212 bp[19]. GAPDH was used as an internal marker for semi-quantitative analysis of expressions of *ZO-1* and *ZO-2* of T_{84} cells. The specific oligonucleotide primers for GAPDH were TCC CAT CAC CAT CTT CCA G for sense and TCC ACC ACT GAC ACG TTG for antisense corresponding to nucleotides 249-764 bp with an expected cDNA of 515 bp[20].

Data analysis

Results were expressed as mean±SD. The number of experiments represents independent measurements on separate monolayers. Comparisons between groups of data were made by Student's *t*-test. A *P* value less than 0.05 was considered statistically significant. EC_{50} values were determined by nonlinear regression using GraphPad Prism software.

RESULTS

Effect of pretreatment with MP on electrophysiological characteristics

Pretreatment of T_{84} cells with MP 15 μg/mL (n = 15) for 72 h significantly increased the basal transepithelial potential difference from 0.39±0.07 to 2.27±0.59 mV (Figure 1A, P<0.01), basal I_{SC} from 3.05±0.44 to 7.14±1.80 μA/cm^2 (Figure 1B, P<0.05) and transepithelial resistance (TER) from 0.14±0.01 to 0.37±0.04 μC/cm^2 (Figure 1C, P<0.001).

Effect of pretreatment with MP on expressions of ZO-1 and ZO-2

In order to see weather MP-induced TER increase was related to the cytoplasmic proteins associated with tight junctions, *ZO-1* (zonula occludens-1) and *ZO-2* (zonula occludens-2), we used RT-PCR analysis to examine the expression levels of *ZO-1* and *ZO-2* in T_{84} cells (Figure 2A). Semi-quantitative analyses showed that the expression levels of both *ZO-1* and *ZO-2* after MP pretreatment were significantly elevated, the ratio of *ZO-1* to GAPDH was from 0.46±0.08 to 0.81±0.10 (n = 6, P<0.05, Figure 2B), and the ratio of *ZO-2* to GAPDH was from 0.76±0.12 to 1. 27±0.12 (n = 4, P<0.001, Figure 2C), indicating the enhancement of epithelial barrier function.

MP-induced I_{SC} response

As shown in Figure 3, apical addition of MP (10-5000 μg/mL) produced an I_{SC} increase which was concentration-dependent (Figure 3A) with an apparent EC_{50} of about 293.9 μg/mL (Figure 3B). MP-induced changes in I_{SC} were calculated as total charges transported for 15 min (μC/cm^2, the area under the curve of the MP-induced I_{SC} responses for the given time period) since the current kinetics did not sustain. MP at 10, 50, 100, 500, 1 000 and 5 000 μg/mL produced I_{SC} increases of 306.7±25.5 (n = 4), 673.3±91.3 (n = 4), 1380.0±119.4 (n = 4), 7624.0±309.7 (n = 5), 9580.0±734.9 (n = 6) and 10053.3±979.1 μC/cm^2 (n = 4), respectively.

Anion dependence of MP-induced I_{SC}

In order to study the ion species involved in mediating MP-induced I_{SC}, a Na^+ channel blocker, amiloride and a couple of Cl^- channel blockers, DPC, glibenclamide and DIDS were examined (Figure 4). The change in I_{SC} was defined as the maximal rise in I_{SC} following MP stimulation and it was normalized to current change per unit area of the epithelial monolayer (μA/cm^2). DPC (1 mmol/L, n = 4, Figure 4A) or glibenclamide (1 mmol/L, n = 5) added to the apical side reduced MP (500 μg/mL)-induced responses from 10.0±0.97 μA/cm^2 to 1.78±0.18 μA/cm^2 (P<0.01) or from 9.44±0.49 μA/cm 2 to 1.39±0.5 μA/cm^2 (P<0.001) respectively, but apical addition of amiloride (10 μmol/L, n = 4) or DIDS (100 μmol/L, n = 4) had no significant effects (Figure 4B). Basolateral addition of bumetanide (100 μmol/L, n = 6), a strong inhibitor of the Na^+-K^+-$2Cl^-$ cotransporter reduced the MP-induced I_{SC} from 9.33±0.64 to 2.31±0.74 μA/cm^2 (Figure 4B, P<0.01).

Mimicking effects of MP by ligustrazine

Similar to the effects of pretreatment with MP, treating T_{84} cells with *ligustrazine*, one of the active ingredients of MP, for 72 h also increased the levels of *ZO-1* and *ZO-2*, the ratio of *ZO-1* to GAPDH was raised from 0.46±0.08 to 0.65±0.11 (n = 6, Figure 2B)

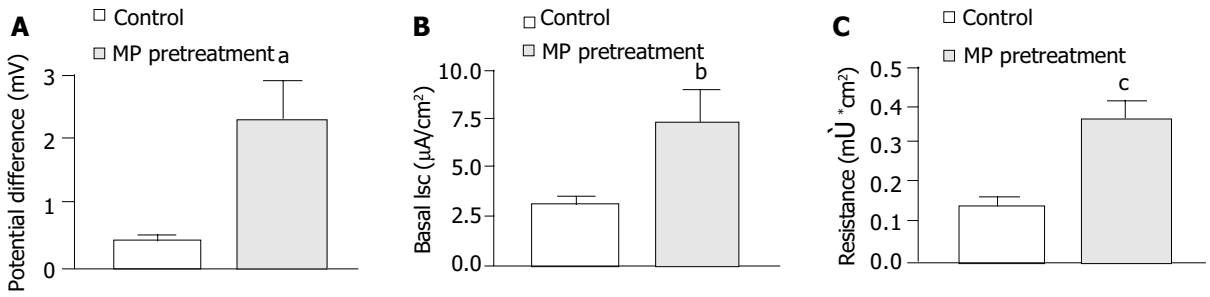

Figure 1 Effects of *MP* pretreatment on transepithelial electrophysiological characteristics. Comparison of potential difference (A) transepithelial I_{SC} (B) and transepithelial resistance (C) in T_{84} cells with and without MP (15 μg / mL, 72 h) pretreatment. Values are mean±SE; $^{a(b)}P<0.01$; $^{b(a)}P<0.05$; $^{c(d)}P<0.001$.

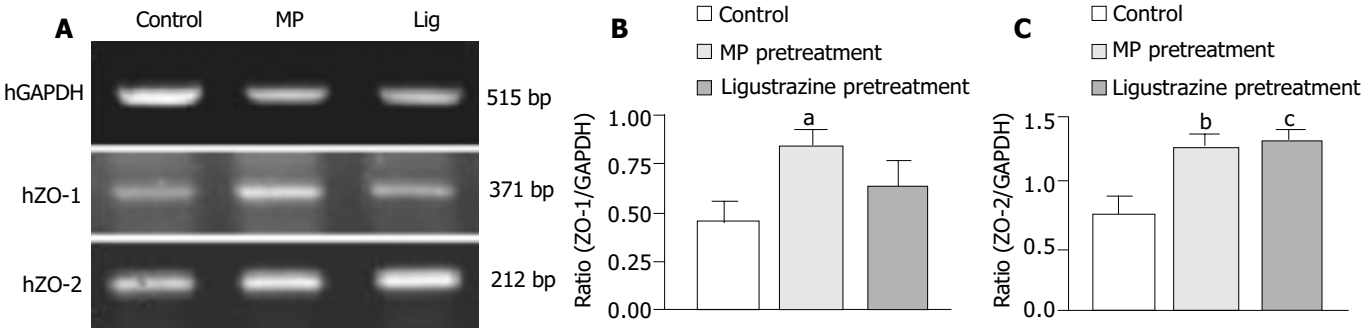

Figure 2 RT-PCR analyses of mRNA expressions of *ZO-1* and *ZO-2* in T_{84} cells. (A) RT-PCR results with products as expected of *ZO-1* and *ZO-2* found in control, MP pretreatment and *ligustrazine* pretreatment. Semi-quantitative analyses of *ZO-1* (B) and ZO-2 (C) expressions in T_{84} cells without and with MP or *ligustrazine* pretreatment, which were shown in ratio of *ZO-1* or *ZO-2* to GAPDH (internal marker). Values are mean±SE; ^{a}P and $^{b(c)}P<0.05$; $^{c(d)}P<0.001$.

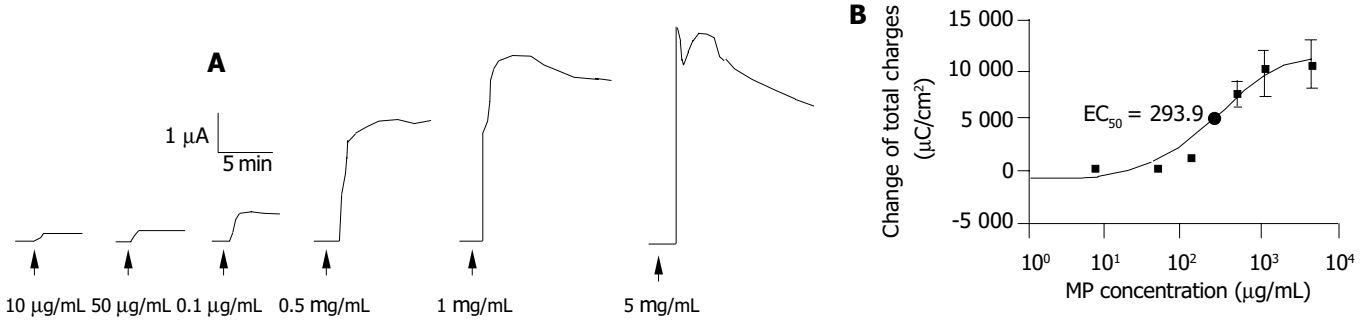

Figure 3 MP-induced I_{SC} in T_{84} cell lines. A: Representative I_{SC} recordings in response to MP (10, 50, 100, 500, 1 000 and 5 000 μg / mL) added to the apical side. Arrowheads indicate the time of MP addition. B: The concentration-response curve for MP-induced responses. Different concentrations of MP were added to the apical side and each data was obtained from at least 3 individual experiments. Values are mean±SE of maximal I_{SC} increase.

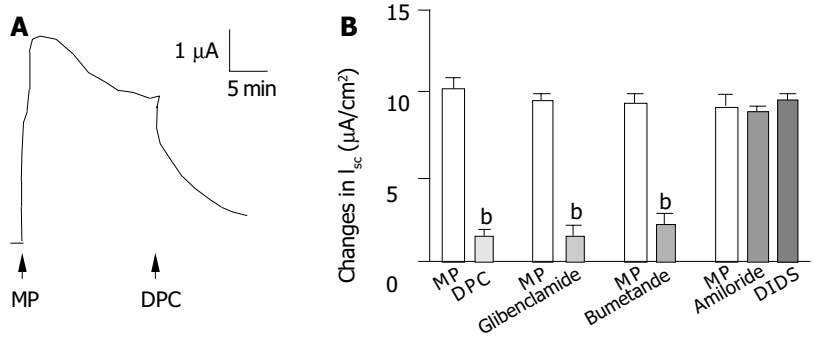

Figure 4 Anion dependence of MP-induced I_{SC}. A: Representative I_{SC} recording with arrows indicating the time for apical addition of MP (500 μg / mL) and DPC (1 mmol / L). B: Summary of the effects of DPC (1 mmol / L, apical), glibenclamide (1 mmol / L, apical), bumetanide (100 μmol / L, basolateral), amiloride (10 μmol / L, apical) and DIDS (100 μmol / L, apical) on MP-induced I_{SC}. Values are mean±SE; $^{b}P<0.01$.

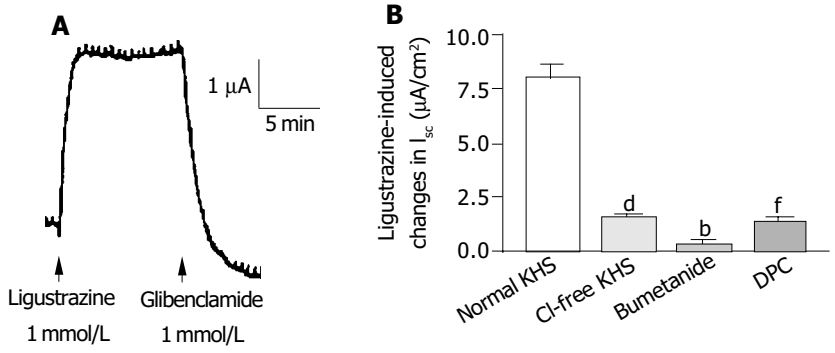

Figure 5 Anion dependence of *ligustrazine*-induced I_{SC}. A: Representative I_{SC} recording with arrows indicating the time for apical addition of *ligustrazine* (1 mmol/L) and glibemclamide (1 mmol/L). B: Summary of the effects of removal of extracellular Cl^-, basolateral addition of bumetanide (100 μmol/L) and apical addition of DPC (1 mmol/L) on *ligustrazine*-induced I_{SC}. Values are mean±SE; ^dP, ^bP and ^fP<0.001.

and the ratio of *ZO-2* to GAPDH was from 0.76±0.12 to 1.33±0.07 (n = 4, P<0.001) (Figure 2C).

Acute stimulation with *ligustrazine* (1 mmol/L, apical side) produced a current increase which was similar to that induced by acute addition of MP (0.5 mg/mL, apical) (n = 6, Figure 5A). Removal of Cl^- from KHS (n = 4), apical addition of DPC or glibenclamide (1 mmol/L) (n = 3) and basolateral administration of bumetanide (100 mmol/L) (n = 3) reduced *ligustrazine*-induced current increases by 79.9% (P<0.001), 82.4% (P<0.001) and 96.2% (P<0.001), respectively (Figure 5B).

DISCUSSION

The present study has provided scientific evidence for the pharmacological action of MP, a Chinese medicine-based formula for postmenopausal women, on the GI tract. The results demonstrated that MP could stimulate Cl^- secretion in human colonic epithelial cell line T_{84}. The supporting evidence includes: MP-induced responses were insensitive to Na^+ channel blockers; the response was inhibited by Cl^- channel blockers; and substantially inhibited by the Na^+-K^+-2Cl^- cotransporter inhibitors. The stimulatory effects of MP on colonic anion secretion were mimicked by its active ingredient, *ligustrazine*. Since *ligustrazine* is an active ingredient common in both MP and *BFP*, a traditional formula previously shown to stimulate anion secretion by GI tract epithelia[11,15,16], the present results suggest that *Ligustrazine* may be one of the responsible ingredients involved in mediating the secretory effects of both MP and *BFP*.

Apart from its acute stimulatory effects on colonic anion secretion, MP, by treating T_{84} cells for 72 h, was also demonstrated to significantly alter the electrophysiological characteristics of the colonic epithelia. Increases in transepithelial potential and basal I_{SC} may represent an increased driving force for anion secretion and basal secretion, respectively. These results indicate long-term treatment of MP can promote colonic anion secretion, consistent with its acute effects. On the other hand, pretreatment of T_{84} cells with MP also increased the transepithelial resistance, indicating its effect on improving epithelial barrier function. This was confirmed by RT-PCR results, which showed that pretreatment with MP significantly up-regulated gene expressions of tight junction related proteins, *ZO-1* and ZO-2. Similar results were obtained using *Ligustrazine*, suggesting that *ligustrazine* was able to improve barrier function in addition to colonic secretion. It has been reported that an elevation of intracellular calcium could decrease the tight junction resistance in T_{84} monolayers[21]. Since *Ligustrazine* has been shown to decrease intracellular Ca^{2+} by inhibiting Ca^{2+} entry and/or Ca^{2+} release[22,23], *ligustrazine* as well as *ligustrazine*-containing MP may strengthen tight junctions, thereby enhancing transepithelial resistance. In fact, we have found that intracellular calcium could also be reduced by an apical addition of MP (data not shown), indicating a possible mechanism for improving barrier function. Further studies may be required to understand the detailed mechanisms.

Taken together, the present results have demonstrated that MP and *Ligustrazine* exert a stimulatory effect on gastrointestinal Cl^- secretion and improvement of epithelial barrier function. Since MP is designed for postmenopausal or elderly women, its demonstrated effects on the colonic epithelia, in addition to its beneficial effect on endocrine (Gou *et al*., unpublished data) and immune systems previously shown[1], suggest that MP and its active ingredient, *ligustrazine*, may be used to alleviate some of the GI tract disorders, such as infection and constipation, often seen in the elderly.

REFERENCES

1 **Ho AL**, Gou YL, Rowlands DK, Chung YW, Chan HC. Effects of Bak Foong Pills and Menoease Pills on white blood cell distribution in old age female rats. *Biol Pharm Bull* 2003; **26**: 1748-1753
2 **Baumgart DC**, Dignass AU. Intestinal barrier function. *Curr Opin Clin Nutr Metab Care* 2002; **5**: 685-694
3 **Balkovetz DF**, Katz J. Bacterial invasion by a paracellular route: divide and conquer. *Microbes Infect* 2003; **5**: 613-619
4 **Hosoda Y**, Winarto A, Iwanaga T, Kuwahara A. Mode of action of ANG II on ion transport in guinea pig distal colon. *Am J Physiol Gastrointest Liver Physiol* 2000; **278**: G625-634
5 **Albanese CT**, Cardona M, Smith SD, Watkins S, Kurkchubasche AG, Ulman I, Simmons RL, Rowe MI. Role of intestinal mucus in transepithelial passage of bacteria across the intact ileum *in vitro*. *Surgery* 1994; **116**: 76-82
6 **Forte LR**, Thorne PK, Eber SL, Krause WJ, Freeman RH, Francis SH, Corbin JD. Stimulation of intestinal Cl- transport by heat-stable enterotoxin: activation of cAMP-dependent protein kinase by cGMP. *Am J Physiol* 1992; **263**(3 Pt 1): C607-615
7 **Grondahl ML**, Jensen GM, Nielsen CG, Skadhauge E, Olsen JE, Hansen MB. Secretory pathways in Salmonella Typhimurium-induced fluid accumulation in the porcine small intestine. *J Med Microbiol* 1998; **47**: 151-157
8 **Lencer WI**, Delp C, Neutra MR, Madara JL. Mechanism of cholera toxin action on a polarized human intestinal epithelial cell line: role of vesicular traffic. *J Cell Biol* 1992; **117**: 1197-1209
9 **Tenore A**, Fasano A, Gasparini N, Sandomenico ML, Ferrara A, Di Carlo A, Guandalini S. Thyroxine effect on intestinal Cl-/HCO3- exchange in hypo- and hyperthyroid rats. *J Endocrinol* 1996; **151**: 431-437
10 **Ewe K**. Intestinal transport in constipation and diarrhoea. *Pharmacology* 1988; **36**(Suppl 1): 73-84
11 **Tang N**, Zhu JX, Zhao WC, Xing Y, Gou YL, Rowlands DK, Chung YW, Chan HC. Effect of Bak Foong pills on exocrine pancreatic-bile secretion. *Biol Pharm Bull* 2003; **26**: 1384-1387
12 **Zhou Q**, Rowlands DK, Gou YL, Tsang LL, Chung YW, Chan HC. Cardiovascular protective effects of traditional Chinese

medicine Bak Foong pills in spontaneously hypertensive rats. *Biol Pharm Bull* 2003; **26**: 1095-1099

13 **Liu B**, Dong XL, Xie JX, Gou YL, Rowlands DK, Chan HC. Effect of Bak Foong pills on enhancing dopamine release from the amygdala of female rats. *Biol Pharm Bull* 2003; **26**: 1028-1030

14 **Gou YL**, Ho AL, Rowlands DK, Chung YW, Chan HC. Effects of Bak Foong Pill on blood coagulation and platelet aggregation. *Biol Pharm Bull* 2003; **26**: 241-246

15 **Zhu JX**, Chan YM, Tsang LL, Chan LN, Zhou Q, Zhou CX, Chan HC. Cellular signaling mechanisms underlying pharmacological action of Bak Foong Pills on gastrointestinal secretion. *Jpn J Physiol* 2002; **52**: 129-134

16 **Zhu JX**, Lo PS, Zhao WC, Tang N, Zhou Q, Rowlands DK, Gou YL, Chung YW, Chan HC. Bak Foong Pills stimulate anion secretion across normal and cystic fibrosis pancreatic duct epithelia. *Cell Biol Int* 2002; **26**: 1011-1018

17 **Rowlands DK**, Tsang LL, Cui YG, Chung YW, Chan LN, Liu CQ, James T, Chan HC. Upregulation of cystic fibrosis transmembrane conductance regulator expression by oestrogen and Bak Foong Pill in mouse uteri. *Cell Biol Int* 2001; **25**: 1033-1035

18 **Ussing HH**, Zerahn K. Active transport of sodium as the source of electric current in the short-circuited isolated frog skin. Reprinted from Acta. Physiol. Scand. **23**: 110-127, 1951. *J Am Soc Nephrol* 1999; **10**: 2056-2065

19 **Youakim A,** Ahdieh M. Interferon-gamma decreases barrier function in T_{84} cells by reducing *ZO-1* levels and disrupting apical actin. *Am J Physiol* 1999; **276**(5 Pt 1): G1279-1288

20 **Usui T**, Hara M, Satoh H, Moriyama N, Kagaya H, Amano S, Oshika T, Ishii Y, Ibaraki N, Hara C, Kunimi M, Noiri E, Tsukamoto K, Inatomi J, Kawakami H, Endou H, Igarashi T, Goto A, Fujita T, Araie M, Seki G. Molecular basis of ocular abnormalities associated with proximal renal tubular acidosis. *J Clin Invest* 2001; **108**: 107-115

21 **Tai YH**, Flick J, Levine SA, Madara JL, Sharp GW, Donowitz M. Regulation of tight junction resistance in T_{84} monolayers by elevation in intracellular Ca^{2+}: a protein kinase C effect. *J Membr Biol* 1996; **149**: 71-79

22 **Pang PK**, Shan JJ, Chiu KW. Tetramethylpyrazine, a calcium antagonist. *Planta Med* 1996; **62**: 431-435

23 **Liu SY**, Sylvester DM. Antiplatelet activity of tetramethylpyrazine. *Thromb Res* 1994; **75**: 51-62

Edited by Zhu LH and Xu FM

PO Box 2345, Beijing 100023, China
Fax: +86-10-85381893
E-mail: wjg@wjgnet.com www.wjgnet.com

World J Gastroenterol 2004;10(17):2519-2523
World Journal of Gastroenterology
Copyright © 2004 by The WJG Press ISSN 1007-9327

• BASIC RESEARCH •

Morphologic and biomechanical changes of rat oesophagus in experimental diabetes

Yan-Jun Zeng, Jian Yang, Jing-Bo Zhao, Dong-Hua Liao, En-Ping Zhang, Hans Gregersen, Xiao-Hu Xu, Hong Xu, Chuan-Qing Xu

Yan-Jun Zeng, Xiao-Hu Xu, Hong Xu, Chuan-Qing Xu, Forensic Medicine Department, Medical College, Santou University, Santou 515031, Guangdong Province, China
Jian Yang, En-Ping Zhang, Beijing University of Technology, Beijing 100022, China
Jing-Bo Zhao, Dong-Hua Liao, Hans Gregersen, Department of Gastrointestinal Surgery, Aalborg University, Denmark
Correspondence to: Yan-Jun Zeng, Forensic Medicine Department, Medical College, Shantou University, Shantou 515031, Guangdong Province, China. yjzeng@bjut.edu.cn
Telephone: +86-10-67391685 **Fax:** +86-10-67391738
Received: 2003-8-26 **Accepted:** 2003-10-22

Abstract

AIM: To study morphologic and biomechanical changes of oesophagus in diabetes rats.

METHODS: Diabetes was induced by a single injection of streptozotocin (STZ). The type of diabetes mellitus induced by parenteral STZ administration in rats was insulin-dependent (type I). The samples were excised and studied *in vitro* using a self-developed biomaterial test machine.

RESULTS: The body mass was decreased after 4 d with STZ treatment. The length of esophagus shortened after 4, 7, 14 d. The opening angle increased after 14 d. The shear, longitudinal and circumferential stiffness were obviously raised after 28 d of STZ treatment.

CONCLUSION: The changes of passive biomechanical properties reflect intra-structural alteration of tissue to a certain extent. This alteration will lead to some dysfunction of movement. For example, tension of esophageal wall will change due to some obstructive disease.

Zeng YJ, Yang J, Zhao JB, Liao DH, Zhang EP, Gregersen H, Xu XH, Xu H, Xu CQ. Morphologic and biomechanical changes of rat oesophagus in experimental diabetes. *World J Gastroenterol* 2004; 10(17): 2519-2523
http://www.wjgnet.com/1007-9327/10/2519.asp

INTRODUCTION

Esophagus is a distensible muscular tube that connects pharynx and stomach. The function of the esophagus is to transport food by peristaltic movement, which is the result of the interaction of the tissue forces in the esophageal wall and the hydrodynamic forces in the food bolus. Esophagus has been studied by radiography[1], concurrent videofluoroscopy and manometry[2,3], high-frequency ultrasonography[4-6], and endoscopic sclerotherapy[7,8]. Motility disorders[9], bolus transport[10,11], systemic sclerosis[12], pain[13], wall distensibility[8], impedance planimetric characterization[14] and the effects of epidermal growth factor[15] on esophagus have been reported in many papers. Since the function of esophagus is mainly mechanical, our work was focused on providing quantitative measurement of passive biomechanical properties of esophagus. Many investigations on biomechanics of esophagus are available in the literature[16,17]. Gregersen *et al*. studied strain distribution in the layered wall[18,19], relation between pressure and cross-sectional area[20] and other biomechanical properties[21-23] of esophagus. A more recent work used a novel ultrasound technique to study the biomechanics of the human esophagus *in vivo*[24]. Patel represented biomechanical and sensory parameters of the human esophagus at four levels[25]. Researchers have done a lot biomechanical studies on gastrointestinal tract such as intestine[26,27], small intestine[28-32], ileum[33], duodenum[34] and large intestine[35,36].

Most previous studies have explained the relationship between the diabetes and gastrointestinal tract function[37,38]. Some researches studied relationship between esophageal dysfunction and neuropathy[39], oesophagus scintigraphy[40] and the relationship between esophageal motility and transit[41] in diabetic patients. More recently, Jorgensen reported tension-strain relations and morphometry of rat small intestine in experimental diabetes[42]. Zhao introduced the remodeling of zero-stress state of small intestine in streptozotocin-induced diabetic rats[43].

This paper presents the effect of experimental diabetes on the morphologic and biomechanical properties of the esophagus. The result of this study indicated that experimental type I diabetes caused significant changes in the passive biomechanical properties in the rat esophagus.

MATERIALS AND METHODS

Materials

Diabetes was induced by a single injection of streptozotocin (STZ). The form of diabetes mellitus induced by parenteral STZ administration in rats is insulin-dependent (type I). Twenty-seven rats were divided into 4 groups according to the survival time after STZ treatment: 4 d (n = 7), 7 d (n = 7), 14 d (n = 7), 28 d (n = 6). Another 8 rats were used as normal controls. The samples were taken from the middle part of esophagus. Two rings were cut from each end of the sample to measure the geometric parameters of the no-load state and the opening angle at zero-stress state. The remaining part was excised and studied *in vitro* using a self-developed biomaterial test machine.

Methods

Using this machine, the esophagus was stepwise elongated and inflated and continuously twisted in circumferential-longitudinal direction. In the normal controls and 28 d of diabetes group, after the intact esophagus was tested, the mucosa and muscle layers were separated using microsurgery and tested in the same loading procedure as mentioned above. The esophagus was treated as a membrane when the stress and strain were calculated, the longitudinal and circumferential stresses were considered to be evenly distributed along the wall thickness while the radial stress and other transverse shear stresses were

ignored. The torque *vs* twist-angle relation was approximately linear at a specified pressure and longitudinal stretch ratio. Thus, the shear modulus can be computed by the torque, twist angle and polar moment of inertial at this state. However, the shear modulus varied greatly with the changing inflation pressure and longitudinal stretch ratio.

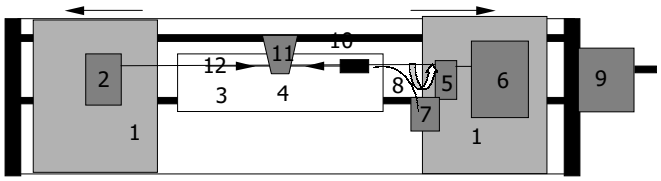

Figure 1 Simplified diagram of biomaterial test machine.1: Linear stage, 2: Torque transducer, 3: Organ bath, 4: Specimen, 5: Force transducer, 6: Motor for axial rotation, 7: Pressure transducer, 8: Infusion channel, 9: Motor for linear stage, 10: Rails for linear stage, 11: CCD camera, 12: Plastic rod.

RESULTS

Type I diabetes could induce the following effect on the biomechanical and morphologic properties of esophagus: body weight and morphology, shear modulus, circumferential and longitudinal stress-strain relationship, stress-strain relationship of muscle layer and mucosa layer.

Body weight and morphology

The body mass kept a steady increase in the control rats. But it went down after 4 d in the diabetes rat (Figure 2A). The length of esophagus *in vivo* obviously declined after 4, 7, 14 d, but it would return to normal level after 28 d (Figure 2B). The mass per unit lengh *in vitro* changed little (Figure 2C). In the intact esophagus, the opening angle increased after 14 d of STZ treatment (Figure 2D).

Shear modulus

Changes of elastic shear moduli in the course of diabetes development at longitudinal stretch ratio λ_{zz} = 1.5 and various transmural pressure are shown in Figure 3A. Elastic shear modulus would rise with increased transmural pressure. Especially when transmural pressure was more than 0.25 kPa, the shear moduli for various transmural pressure were remarkably different. And diabetes has notably affected the shear modulus. This effect showed that shear moduli are obviously increased after 28 d.

Changes of elastic shear modulus in the course of diabetes development at transmural pressure P = 1 kPa and various longitudinal stretch ratio are pictured in Figure 3B. Elastic shear modulus would rise with increased longitudinal stretch ratio. Shear moduli were remarkably different at various longitudinal stretch ratios. And diabetes has notably affected the shear modulus. This effect demonstrated that shear moduli were obviously increased after 28 d of STZ treatment.

Circumferential and longitudinal stress-strain relationship

Figure 4A shows the changes of circumferential stress-strain relationship in the course of diabetes development at longitudinal stretch ratio λ_{zz} = 1.5 and various transmural pressure. All curves of experimental group inclined to left side except that after 4 d. The curve after 28 d was on the most left side. The circumferential stiffness increased after 7, 14, 28 d of diabetes.

The changes of longitudinal stress-strain relationship in the course of diabetes development at transmural pressure P = 0.25 kPa and various longitudinal stretch ratio are pictured in Figure 4B. The stress-strain curve after 28 d was obviously inclined to left side. So the longitudinal stiffness notably increased after 28 d.

Stress-strain relationship of muscle layer and mucosa layer

The circumferential stress-strain relationship of muscle layer and mucosa layer in the process of inflation at a longitudinal stretch ratio of 1.5 is pictured in Figure 5A. And the experimental diabetes was after 28 d. For muscle layer, there was no obvious difference between the control and diabetes groups. For mucosa layer, the stress-strain curve moved to left side in parallel. So circumferential stiffness of mucosa layer with diabetes was larger than that of control.

Figure 5B shows longitudinal stress-strain relationship of muscle layer and mucosa layer in the process of elongation at a transmural pressure of 0.25 kPa. For muscle layer, there was no obvious difference between control and diabetes groups. There was no notable difference for mucosa layer either.

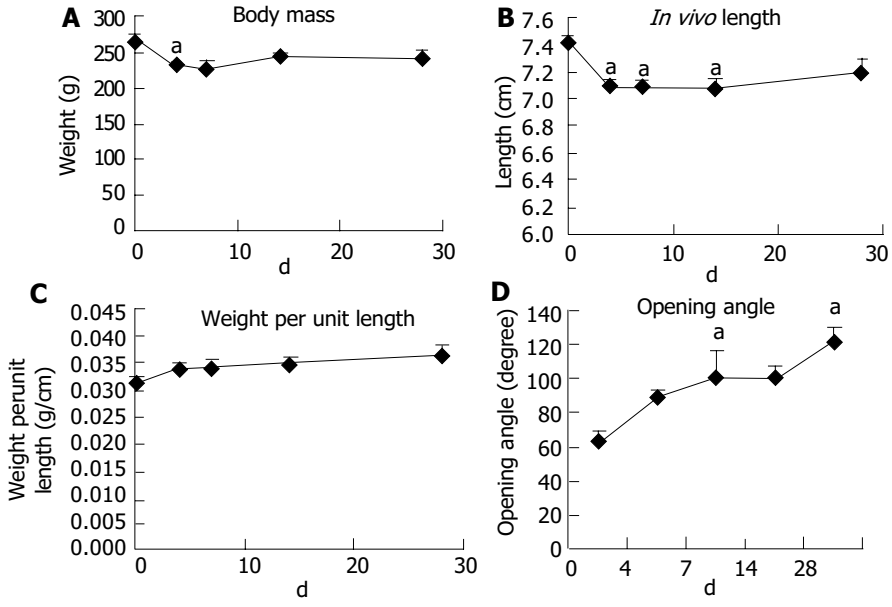

Figure 2 Changes of body mass and esophagus morphology and opening angle at zero-stress state in the process of diabetes development. Dunner's test result: significant difference *vs* normal control (^aP<0.05). A: Change of body mass, B: Change of *in vivo* length, C: Change of mass per unit length, D: Change of opening angle.

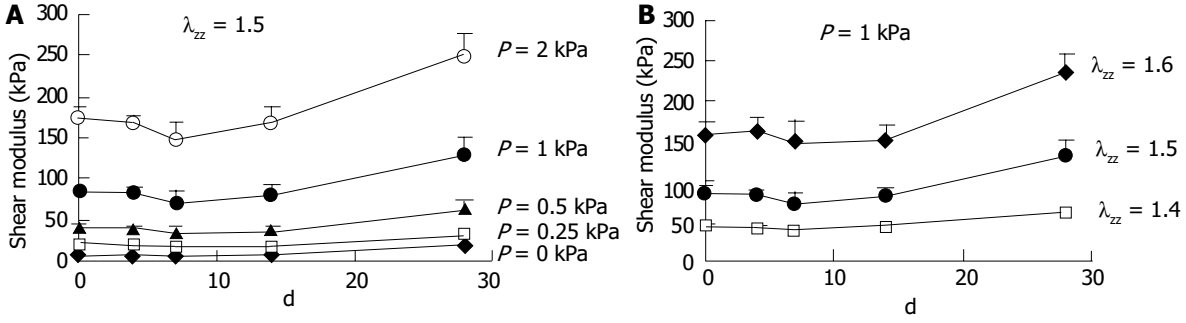

Figure 3 Change of elastic shear modulus in the process of diabetes development. A: Change at λ_{zz} = 1.5 and various transmural pressure, B: Change at P = 1 kPa and various longitudinal stretch ratio.

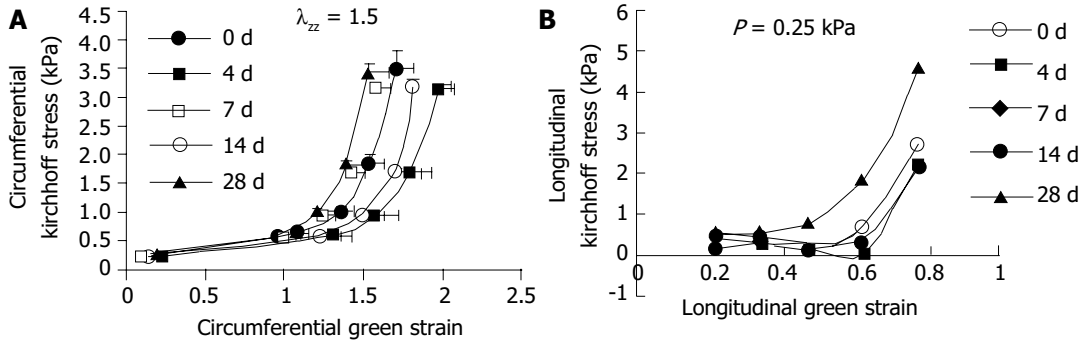

Figure 4 A: Change of circumferential stress-strain relation in the course of diabetes development at λ_{zz} = 1.5 and various transmural pressure. B: Change of longitudinal stress-strain relation in the course of diabetes development at P = 0.25 kPa and various longitudinal stretch ratio.

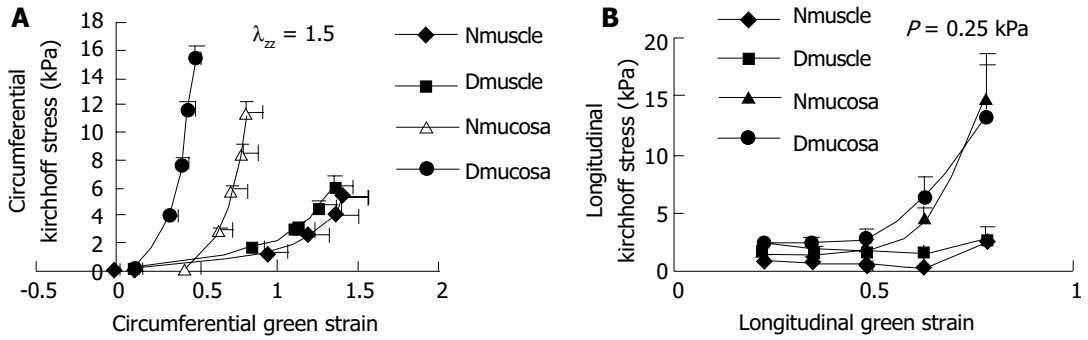

Figure 5 A: Circumferential stress-strain relation between muscle layer and mucosa layer in the process of inflation at a longitudinal stretch ratio of 1.5. N: Normal control, D: 28 d of diabetes. B: Longitudinal stress-strain relation between muscle layer and mucosa layer in the process of elongation at a transmural pressure of 0.25 kPa. N: Normal control, D: 28 d of diabetes.

DISCUSSION

A large number of studies have discovered that diabetes can affect the movement of oesophagus. Transportation of oesophagus may delay or slow down, and movement of esophagus can not coordinate.

This dysfunction of movement can be a result of muscle and nerve cooperative failure[39-41,44-47]. Histologic research has proved that diabetes can destroy vagus nerve[48]. Though there are many papers on movement and function of oesophagus in diabetes, few data on morphologic and passive biomechanical properties are seen. The change of passive biomechanical properties reflects intra-structural alteration of tissue to a certain extent. This alteration will result in some dysfunction of movement, for example, tension of esophageal wall will change due to some obstructive disease[49,50], and therefore, it is necessary to study biomechanics and morphology together.

The body mass is decreased in rat with diabetes. This is consistent with other studies[43,51]. Diabetes will lead to hyperplasia of some organs. Hyperplasia of esophagus is less frequent than that of small intestine[52,53]. Diabetes has caused rise of the opening angle of small intestine[44], also it is seen for esophagus.

In this paper, the shear, longitudinal and circumferential stiffnesses were obviously elevated after 28 d with STZ treatment. Jorrensen[42], Liu[54] and Zhao[51] have discovered that stiffness is raised in diabetes in small intestine, blood vessel and arterial wall.

We can draw a conclusion that the changes of passive biomechanical properties reflect intra-structural alteration of tissue to a certain extent. This alteration will lead to some dysfunction of movement.

REFERENCES

1 **Grishaw EK,** Ott DJ, Frederick MG, Gelfand DW, Chen MY. Functional abnormalities of the esophagus: a prospective analysis of radiographic findings relative to age and symptoms. *Am*

J Roentgenol 1996; **167:** 719-723
2 **Pouderoux P**, Shi G, Tatum RP, Kahrilas PJ. Esophageal solid bolus transit: studies using concurrent videofluoroscopy and manometry. *Am J Gastroenterol* 1999; **94**: 1457-1463
3 **Narawane NM**, Bhatia SJ, Mistry FP, Abraham P, Dherai AJ. Manometric mapping of normal esophagus and definition of the transition zone. *Indian J Gastroenterol* 1998; **17:** 55-57
4 **Nicosia MA**, Brasseur JG, Liu JB, Miller LS. Local longitudinal muscle shortening of the human esophagus from high-frequency ultrasonography. *Am J Physiol Gastrointest Liver Physiol* 2001; **281:** G1022-1033
5 **Pehlivanov N,** Liu J, Kassab GS, Puckett JL, Mittal RK. Relationship between esophageal muscle thickness and intraluminal pressure: an ultrasonographic study. *Am J Physiol Gastrointest Liver Physiol* 2001; **280:** G1093-1098
6 **Assentoft JE,** Gregersen H, O'Brien WD Jr. Determination of biomechanical properties in guinea pig esophagus by means of high frequency ultrasound and impedance planimetry. *Dig Dis Sci* 2000; **45:** 1260-1266
7 **Juhl CO,** Vinter-Jensen L, Djurhuus JC, Gregersen H, Dajani EZ. Biomechanical properties of the oesophagus damaged by endoscopic sclerotherapy. An impedance planimetric study in minipigs. *Scand J Gastroenterol* 1994; **29:** 867-873
8 **Petersen JA,** Djurhuus C, Koff J, Vinter-Jensen L, Gregersen H. Endoscopic sclerotherapy in porcine esophagus changes luminal cross-sectional area and wall distensibility dose- and time-dependently. *Dig Dis Sci* 1998; **43:** 521-528
9 **Hewson EG,** Ott DJ, Dalton CB, Chen YM, Wu WC, Richter JE. Manometry and radiology. Complementary studies in the assessment of esophageal motility disorders. *Gastroenterology* 1990; **98:** 626-632
10 **Nicosia MA,** Brasseur JG. A mathematical model for estimating muscle tension *in vivo* during esophageal bolus transport. *J Theor Biol* 2002; **219:** 235-255
11 **Ren J,** Massey BT, Dodds WJ, Kern MK, Brasseur JG, Shaker R, Harrington SS, Hogan WJ, Arndorfer RC. Determinants of intrabolus pressure during esophageal peristaltic bolus transport. *Am J Physiol* 1993; **264**(3 Pt 1)**:** G407-413
12 **Villadsen GE,** Storkholm J, Zachariae H, Hendel L, Bendtsen F, Gregersen H. Oesophageal pressure-cross-sectional area distributions and secondary peristalsis in relation to subclassification of systemic sclerosis. *Neurogastroenterol Motil* 2001; **13:** 199-210
13 **Drewes AM,** Schipper KP, Dimcevski G, Petersen P, Andersen OK, Gregersen H, Arendt-Nielsen L. Multimodal assessment of pain in the esophagus: a new experimental model. *Am J Physiol Gastrointest Liver Physiol* 2002; **283:** G95-103
14 **Gregersen H,** Vinter-Jensen L, Juhl CO, Dajani EZ. Impedance planimetric characterization of the distal oesophagus in the goettingen minipig. *J Biomech* 1996; **29:** 63-68
15 **Vinter-Jensen L,** Juhl CO, Eika B, Gregersen H, Dajani EZ. Epidermal growth factor attenuates the sclerotherapy-induced biomechanical properties of the oesophagus. An experimental study in minipigs. *Scand J Gastroenterol* 1995; **30:** 614-619
16 **Gregersen H,** Weis SM, McCulloch AD. Oesophageal morphometry and residual strain in a mouse model of osteogenesis imperfecta. *Neurogastroenterol Motil* 2001; **13:** 457-464
17 **Gregersen H,** Lee TC, Chien S, Skalak R, Fung YC. Strain distribution in the layered wall of the esophagus. *J Biomech Eng* 1999; **121:** 442-448
18 **Lu X,** Gregersen H. Regional distribution of axial strain and circumferential residual strain in the layered rabbit oesophagus. *J Biomech* 2001; **34:** 225-233
19 **Liao D,** Fan Y, Zeng Y, Gregersen H. Stress distribution in the layered wall of the rat oesophagus. *Med Eng Phys* 2003; **25**: 731-738
20 **Gregersen H,** Christensen LL. Pressure-cross-sectional area relations and elasticity in the rabbit oesophagus *in vivo. Digestion* 1996; **57:** 174-179
21 **Orvar KB,** Gregersen H, Christensen J. Biomechanical characteristics of the human esophagus. *Dig Dis Sci* 1993; **38:** 197-205
22 **Barlow JD,** Gregersen H, Thompson DG. Identification of the biomechanical factors associated with the perception of distension in the human esophagus. *Am J Physiol Gastrointest Liver Physiol* 2002; **282:** G683-689
23 **Drewes AM,** Pedersen J, Liu W, Arendt-Nielsen L, Gregersen H. Controlled mechanical distension of the human oesophagus: sensory and biomechanical findings. *Scand J Gastroenterol* 2003; **38:** 27-35
24 **Takeda T,** Kassab G, Liu J, Puckett JL, Mittal RR, Mittal RK. A novel ultrasound technique to study the biomechanics of the human esophagus *in vivo*. *Am J Physiol Gastrointest Liver Physiol* 2002; **282:** G785-793
25 **Patel RS,** Rao SS. Biomechanical and sensory parameters of the human esophagus at four levels. *Am J Physiol* 1998; **275**(2 Pt 1): G187-191
26 **Dou Y,** Lu X, Zhao J, Gregersen H. Morphometric and biomechanical remodelling in the intestine after small bowel resection in the rat. *Neurogastroenterol Motil* 2002; **14:** 43-53
27 **Dou Y,** Gregersen S, Zhao J, Zhuang F, Gregersen H. Morphometric and biomechanical intestinal remodeling induced by fasting in rats. *Dig Dis Sci* 2002; **47:** 1158-1168
28 **Dou Y,** Gregersen S, Zhao J, Zhuang F, Gregersen H. Effect of re-feeding after starvation on biomechanical properties in rat small intestine. *Med Eng Phys* 2001; **23:** 557-566
29 **Zhao J,** Yang J, Vinter-Jensen L, Zhuang F, Gregersen H. The morphometry and biomechanical properties of the rat small intestine after systemic treatment with epidermal growth factor. *Biorheology* 2002; **39:** 719-733
30 **Liao D**, Yang J, Zhao J, Zeng Y, Vinter-Jensen L, Gregersen H. The effect of epidermal growth factor on the incremental Young's moduli in the rat small intestine. *Med Eng Phys* 2003; **25**: 413-418
31 **Zhao J,** Yang J, Vinter-Jensen L, Zhuang F, Gregersen H. Biomechanical properties of esophagus during systemic treatment with epidermal growth factor in rats. *Ann Biomed Eng* 2003; **31:** 700-709
32 **Zeng YJ,** Qiao AK, Yu JD, Zhao JB, Liao DH, Xu XH, Hans G. Collagen fiber angle in the submucosa of small intestine and its application in Gastroenterology. *World J Gastroenterol* 2003; **9**: 804-807
33 **Yang J,** Zhao JB, Zeng YJ, Gregersen H. Biomechanical properties of ileum after systemic treatment with epithelial growth factor. *World J Gastroenterol* 2003; **9:** 2278-2283
34 **Gao C**, Zhao J, Gregersen H. Histomorphometry and strain distribution in pig duodenum with reference to zero-stress state. *Dig Dis Sci* 2000; **45:** 1500-1508
35 **Gao C,** Gregersen H. Biomechanical and morphological properties in rat large intestine. *J Biomech* 2000; **33:** 1089-1097
36 **Yang J,** Zhao J, Zeng Y, Vinter-Jensen L, Gregersen H. Morphological properties of zero- stress state in large intestine during systemic EGF treatment. *Dig Dis Sci* 2003; **48:** 442-448
37 **Murtagh JE.** Diabetes mellitus: the general practitioner's perspective. *Clin Exp Optom* 1999; **82:** 74-79
38 **Verne GN,** Sninsky CA. Diabetes and the gastrointestinal tract. *Gastroenterol Clin North Am* 1998; **27:** 861-874
39 **Kinekawa F,** Kubo F, Matsuda K, Fujita Y, Tomita T, Uchida Y, Nishioka M. Relationship between esophageal dysfunction and neuropathy in diabetic patients. *Am J Gastroenterol* 2001; **96:** 2026-2032
40 **Westin L,** Lilja B, Sundkvist G. Oesophagus scintigraphy in patients with diabetes mellitus. *Scand J Gastroenterol* 1986; **21:** 1200-1204
41 **Holloway RH,** Tippet MD, Horowitz M, Maddox AF, Moten J, Russo A. Relationship between esophageal motility and transit in patients with type I diabetes mellitus. *Am J Gastroenterol* 1999; **94:** 3150-3157
42 **Jorgensen CS,** Ahrensberg JM, Gregersen H, Flyvberg A. Tension-strain relations and morphometry of rat small intestine in experimental diabetes. *Dig Dis Sci* 2001; **46:** 960-967
43 **Zhao J,** Sha H, Zhou S, Tong X, Zhuang FY, Gregersen H. Remodelling of zero-stress state of small intestine in streptozotocin-induced diabetic rats. Effect of gliclazide. *Dig Liver Dis* 2002; **34:** 707-716
44 **Karayalcin B,** Karayalcin U, Aburano T, Nakajima K, Hisada K, Morise T, Okada T, Takeda R. Esophageal clearance scintigraphy, in diabetic patients-a preliminary study. *Ann Nucl*

Med 1992; **6:** 89-93
45 **Sundkvist G,** Hillarp B, Lilja B, Ekberg O. Esophageal motor function evaluated by scintigraphy, video-radiography and manometry in diabetic patients. *Acta Radiol* 1989; **30:** 17-19
46 **Clouse RE,** Lustman PJ, Reidel WL. Correlation of esophageal motility abnormalities with neuropsychiatric status in diabetics. *Gastroenterology* 1986; **90**(5 Pt 1): 1146-1154
47 **Rathmann W,** Enck P, Frieling T, Gries FA. Visceral afferent neuropathy in diabetic gastroparesis. *Diabetes Care* 1991; **14:** 1086-1089
48 **Smith B.** Neuropathology of the oesophagus in diabetes mellitus. *J Neurol Neurosurg Psychiatry* 1974; **37:** 1151-1154
49 **Gregersen H,** Giversen IM, Rasmussen LM, Tottrup A. Biomechanical wall properties and collagen content in the partially obstructed opossum esophagus. *Gastroenterology* 1992; **103:** 1547-1551
50 **Mittal RK,** Ren J, McCallum RW, Shaffer HA Jr, Sluss J. Modulation of feline esophageal contractions by bolus volume and outflow obstruction. *Am J Physiol* 1990; **258**(2 Pt 1): G208-215
51 **Zhao J,** Lu X, Zhuang F, Gregersen H. Biomechanical and morphometric properties of the arterial wall referenced to the zero-stress state in experimental diabetes. *Biorheology* 2000; **37:** 385-400
52 **Mayhew TM,** Carson FL, Sharma AK. Small intestinal morphology in experimental diabetic rats: a stereological study on the effects of an aldose reductase inhibitor (ponalrestat) given with or without conventional insulin therapy. *Diabetologia* 1989; **32:** 649-654
53 **Zoubi SA,** Williams MD, Mayhew TM, Sparrow RA. Number and ultrastructure of epithelial cells in crypts and villi along the streptozotocin-diabetic small intestine: a quantitative study on the effects of insulin and aldose reductase inhibition. *Virchows Arch* 1995; **427:** 187-193
54 **Liu SQ,** Fung YC. Changes in the rheological properties of blood vessel tissue remodeling in the course of development of diabetes. *Biorheology* 1992; **29:** 443-457

Edited by Zhu LH **Proofread by** Chen WW and Xu FM

PO Box 2345, Beijing 100023, China
Fax: +86-10-85381893
E-mail: wjg@wjgnet.com www.wjgnet.com

World J Gastroenterol 2004;10(17):2524-2528
World Journal of Gastroenterology
Copyright © 2004 by The WJG Press ISSN 1007-9327

• BASIC RESEARCH •

Angiogenic synergistic effect of basic fibroblast growth factor and vascular endothelial growth factor in an *in vitro* quantitative microcarrier-based three-dimensional fibrin angiogenesis system

Xi-Tai Sun, Yi-Tao Ding, Xiao-Gui Yan, Ling-Yun Wu, Qiang Li, Ni Cheng, Yu-Dong Qiu, Min-Yue Zhang

Xi-Tai Sun, Yi-Tao Ding, Xiao-Gui Yan, Qiang Li, Yu-Dong Qiu, Department of Hepatobiliary Surgery, Affiliated Gu Lou Hospital of Medical College, Hepatobiliary Research Institute, Nanjing University, Nanjing 210008, Jiangsu Province China
Ling-Yun Wu, Ni Cheng, State Key Laboratory of Pharmaceutical Biotechnology, Department of Biochemistry, Nanjing University, Nanjing 210093, Jiangsu Province China
Min-Yue Zhang, State Key Laboratory of Pharmaceutical Biotechnology, Model Animal Research Center, Department of Biochemistry, Nanjing University, Nanjing 210093, Jiangsu Province, China
Correspondence to: Dr. Min-Yue Zhang, State Key Laboratory of Pharmaceutical Biotechnology, Model Animal Research Center, Department of Biochemistry, Nanjing University, 10 Jinyin Street, Nanjing 210093, Jiangsu Province, China. zmy@nju.edu.cn
Telephone: +86-25-83595108 **Fax:** +86-25-83595108
Received: 2003-12-10 **Accepted:** 2004-01-12

Abstract

AIM: To develop an *in vitro* three-dimensional (3-D) angiogenesis system to analyse the capillary sprouts induced in response to the concentration ranges of basic fibroblast growth factor (bFGF) and vascular endothelial growth factor (VEGF) and to quantify their synergistic activity.

METHODS: Microcarriers (MCs) coated with human microvascular endothelial cells (HMVECs) were embedded in fibrin gel and cultured in 24-well plates with assay media. The growth factors bFGF, or VEGF, or both were added to the system. The wells (n = 8/group) were digitally photographed and the average length of capillary-like sprouts (ALS) from each microcarrier was quantitated.

RESULTS: In aprotinin-stabilized fibrin matrix, human microvascular endothelial cells on the MCs invaded fibrin, forming sprouts and capillary networks with lumina. The angiogenic effects of bFGF or VEGF were dose-dependent in the range from 10 to 40 ng/mL. At d 1, 10 ng/mL of bFGF and VEGF induced angiogenesis with an ALS of 32.13±16.6 μm and 43.75±27.92 μm, respectively, which were significantly higher than that of the control (5.88±4.45 μm, P<0.01), and the differences became more significant as the time increased. In addition, the combination of 10 ng/mL of bFGF and VEGF each induced a more significant effect than the summed effects of bFGF (10 ng/mL) alone and VEGF (10 ng/mL) alone when analyzed using SPSS system for general linear model (GLM) (P = 0.011), and that also exceeded the effects by 20 ng/mL of either bFGF or VEGF.

CONCLUSION: A microcarrier-based *in vitro* three-dimensional angiogenesis model can be developed in fibrin. It offers a unique system for quantitative analysis of angiogenesis. Both bFGF and VEGF exert their angiogenic effects on HMVECs synergistically and in a dose-dependent manner.

Sun XT, Ding YT, Yan XG, Wu LY, Li Q, Cheng N, Qiu YD, Zhang MY. Angiogenic synergistic effect of basic fibroblast growth factor and vascular endothelial growth factor in an *in vitro* quantitative microcarrier-based three-dimensional fibrin angiogenesis system. *World J Gastroenterol* 2004; 10 (17): 2524-2528
http://www.wjgnet.com/1007-9327/10/2524.asp

INTRODUCTION

Angiogenesis is a process by which new capillaries develop from an existing microvascular network. It is associated with a number of physiologic and pathologic conditions including malignancies, diabetic retinopathy, and rheumatoid arthritis. Angiogenesis in fibrin-based matrix is especially interesting because it is essential in tumor angiogenesis and wound healing.

Angiogenesis was first observed *in vitro* by Folkman and Haudenschild 20 years ago[1]. After culture of endothelial cells, these cells organize spontaneously into capillary-like structures (CLS) with the presence of lumina. From a physiological point of view, an ideal *in vitro* system would take into account all the representative steps of *in vivo* angiogenesis, from detachment of endothelial cells from the vascular wall to final tubular morphogenesis and vascular network formation. It should be also rapid, easy to use, reproducible, and easily quantifiable. Depending on the way the cells reorganize, the *in vitro* models of angiogenesis described to date can be roughly classified into two categories: two-dimensional (2-D) and three-dimensional (3-D). While 2-D angiogenesis models lack the third dimension and obviously do not reflect all physiological steps, the 3-D models are closer to the *in vivo* environment, because they consider more steps of angiogenesis[2].

A variety of 3-D *in vitro* models of angiogenesis have been developed in the past few years[3-7] and have thus significantly increased our understanding of the roles of endothelial cells, extracellular matrix (ECM), growth factors and other bioactive molecules in angiogenesis.

In this study, we described an *in vitro* system of angiogenesis, which was based on microcarriers (MCs), human microvascular endothelial cells (HMVECs) and fibrin extracellular matrix. With this system, the angiogenic effect of basic fibroblast growth factor (bFGF) and vascular endothelial growth factor (VEGF) and their synergism were tested.

MATERIALS AND METHODS

Cell isolation and culture

HMVECs were isolated from juvenile foreskin as described previously[8, 9]. Briefly, the foreskin was cut into small pieces, washed with PBS and incubated with 15-20 mL of 2 g/L dispase in DMEM (Gibco BRL Cat# 11885-084) overnight (18-24 h) at 4 °C. The tissue pieces were transferred into DMEM and scratched with a scalpel. The remnants were discarded and the resulting cell suspension (containing HMVEC and other contaminating cell types) was centrifuged at 1 000 r/min for 5 min. The pellet was re-suspended in 10-15 mL of endothelial growth medium

(EGM) consisting of endothelial basal medium (EBM) (Clonetics, San Diego, CA), supplemented with 10 ng/mL epidermal growth factor (EGF) (Clonetics), 12 μg/mL bovine brain extract (BBE) (Clonetics), 1.0 μg/mL hydrocortisone (Clonetics), 100 U/mL penicillin (Clonetics), and 100 mg/mL streptomycin (Clonetics) in the presence of 150 mL/L normal human serum and seeded into a gelatin-coated 75-cm^2 tissue culture flask. Culture medium was changed every 2-3 d. Before the cultures were confluent (normally 5-7 d after seeding), the HMVECs were separated from the other cells in culture by immuno-magnetic isolation with CD31-Dynabeads following the manufacturer's instructions (Dynal A.S, Oslo, Norway). Endothelial cell cultures were characterized and determined to be >99% pure on the basis of the formation of typical cobblestone monolayer in culture and positive immuno-staining for factor VIII-related antigen (Beijing Zhongshan Biotechnology Co., Ltd). The purified HMVECs were cultured in EGM at 37 °C (50 mL/L CO_2) on gelatin-coated cell culture surfaces. All assays were conducted with cells in passages 6 to 8.

Microcarrier cell culture

Gelatin-coated cytodex-3 microcarriers (MCs) (Amersham Pharmacia Biotech, Piscataway, NJ) were prepared according to the recommendations of the supplier. Freshly autoclaved MCs were suspended in EGM and endothelial cells were added to a final density of 50-80 cells/MC. The cells were allowed to attach to the MCs in a 1.5 mL Eppendorf tube for 4 h at 37 °C. The MCs were then re-suspended in a larger volume of medium and cultivated for another 24-48 h at 37 °C (50 mL/L CO_2). MCs were gently agitated to prevent aggregation of individual MCs. MCs were used for angiogenesis assay when the endothelial cells on the MCs reached confluence[10, 11].

Microcarrier-based fibrin gel angiogenesis assay

The microcarrier-based fibrin gel angiogenesis assay was performed as described[10] with some modifications. Working solution of fibrinogen (Shanghai Raas Blood Product Co., Ltd) was prepared by dissolving the stock solution of fibrinogen (20 mg/mL in PBS) in EBM to a concentration of 1.0 mg/mL, supplemented with EGF and hydrocortisone at 10 ng/mL and 1.0 μg/mL, respectively. The 24-well plates were used for the assay. The bottom of each well was first covered with 250 μL fibrinogen solution, and the clotting was induced by addition of thrombin (0.5 U/mL). After 30 min of polymerization, another 250 μL of fibrinogen solution containing about 250 EC-coated MCs was added. The MCs were evenly distributed in the fibrinogen by gently shaking the culture plates, and polymerization was induced as described above. After complete polymerization, 1.0 mL of EBM supplemented with 10 ng/mL of EGF, 1.0 μg/mL of hydrocortisone and 50 mL/L adult human serum was added on the gel. To prevent excess fibrinolysis by fibrin-embedded cells, aprotinin was added to the growth media at 200 KIU/mL. For the experiments, which required bFGF (PeproTech EC Ltd) and/or VEGF (PeproTech EC Ltd), the components were added to both of the fibrinogen solution and the supernatant medium at the desired concentrations.

Quantification and statistics

At the time point of interest, six random fields of vision for every well were digitally photographed under inverted microscope, and the pictures were transferred to a computer. The quantification of capillary-like structure formation was performed as described by Xue and Greisler with some modifications[12]. Briefly, a special grid was made by dividing a circle with radially oriented lines around 360 degrees with 10-degree intervals using Photoshop (version 6.0; Adobe Systems Inc). The digital photographs were transparently layered with the grid. For each photographed microcarrier, the lengths of sprouts were measured on each of the grid lines and summed (Figure 1). The lengths of sprouts from each MC were averaged in each well. The average lengths of sprouts (ALS) from 8 replicate wells of each testing group were analyzed and expressed as mean±SD. SPSS system for one-way ANOVA was used to compare the differences during the time courses and the General Liner Model (GLM) was used to determine the synergism. $P<0.05$ was considered statistically significant.

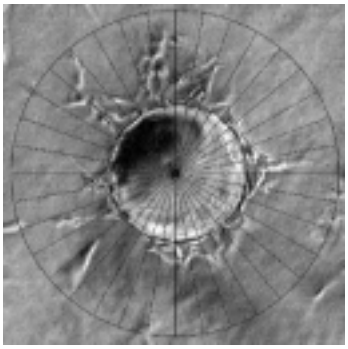

Figure 1 Quantification of angiogenesis. Each MC in random photographed fields was overlaid with a grid that was equally divided around 360° at 10-degree intervals (original magnification ×100). For each photographed microcarrier, the lengths of sprouts were measured on each of the grid lines and summed. The lengths of sprouts from each MC were averaged in each well. The average lengths of sprouts (ALS) from 8 replicate wells of each testing group were analyzed. Bar: 100 μm.

RESULTS

Sequential steps of capillary formation

In 1995, Nehls and Herrmann described a microcarrier-based *in vitro* model of angiogenesis[9]. In their model, the endothelial cells coated on the microcarriers invaded the fibrin gel, forming elongated capillary-like structure in a response to angiogenic factors. However, this model was performed with large vascular endothelial cells of calf pulmonary artery origin. Although in later studies, they used human microvascular endothelial cells to investigate their response to the co-cultured tumor cells, but no positive result was found[13]. In the present study, by modifying the system, we successfully established the microcarrier-based *in vitro* model of angiogenesis with human microvascular endothelial cells in fibrin.

In the early stages of capillary growth (about 16 h after polymerization of the fibrin gel), the HMVECs on microcarriers migrated into fibrin matrix to form sprouts without detectable lumina. At about 16-48 h, sprouts elongated, and small intracellular or intercellular lumina was formed. Usually, broad lumina developed at the base of the sprouts. The lumina frequently contained cellular debris, which could be seen to float by shaking the culture dishes, indicating that lumina contents had liquefied. The tips of capillary sprouts were generally solid or showed only primitive, slit-like lumina, which in later stages anastomosed to other sprouts, and finally formed capillary-like network (at about 5-7 d) (Figure 2). This result was not consistent with what was observed by Nehls and Herrmann, who assumed that due to the presence of serum, anastomosis of capillary sprouts occurred rarely[14].

Capillary sprout formation induced by bFGF and VEGF

In the absence of growth factors, capillary sprout formation in our model was minimal. Both bFGF and VEGF induced obvious EC sprouting. The curves for both cytokines increase significantly with time. The angiogenic effects of both cytokines were dose-dependent over the range from 10 to 40 ng/mL. At d 1, 10 ng/mL

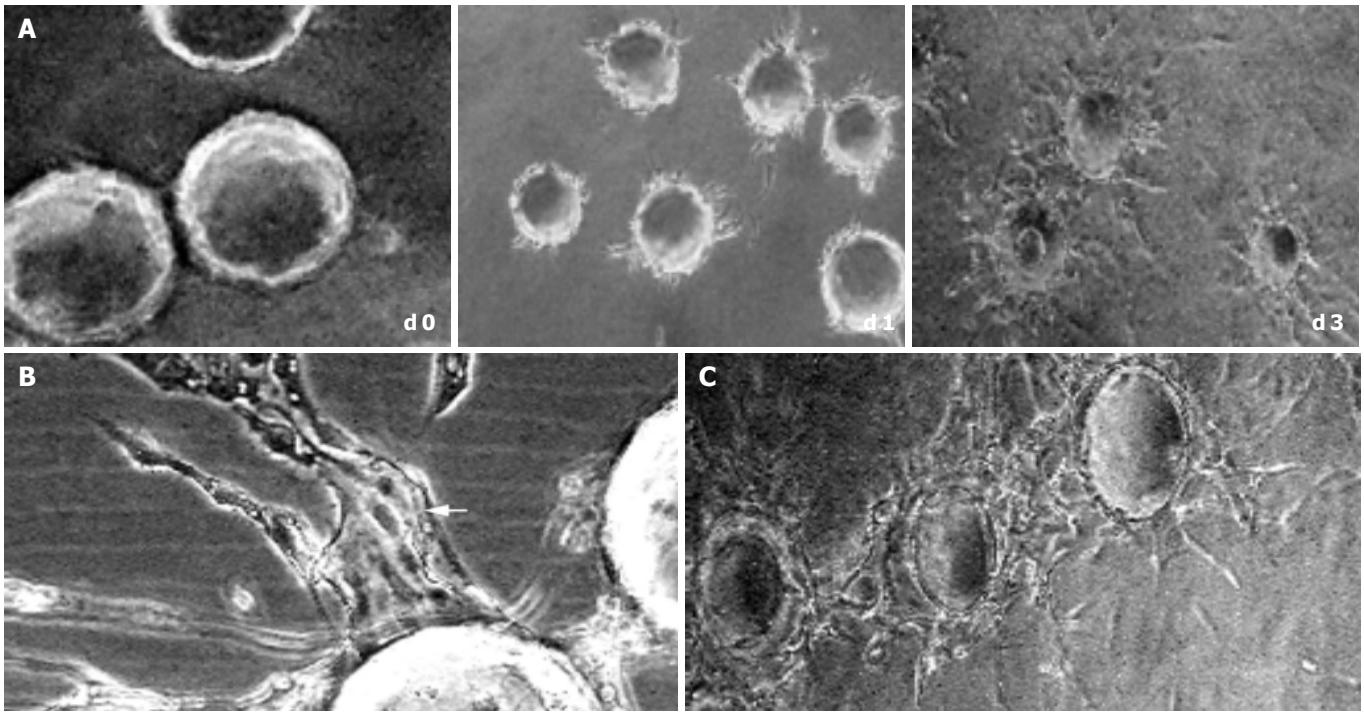

Figure 2 Sequential steps of capillary formation. During 3 d after polymerization of the fibrin gel, the HMVECs (bFGF 40 ng / mL) on microcarriers migrated into fibrin matrix to form sprouts, which elongated (A) with intracellular or intercellular lumina formed (bFGF 40 ng / mL). The lumina frequently contained cellular debris, which can be seen to float by shaking the culture dishes, indicating that lumina contents had liquefied (B, arrow). In the late stage (d 5), the capillary sprouts anastomosed to each other, and finally formed capillary-like network (C) (original magnification ×100).

of bFGF and VEGF induced angiogenesis with an ALS of 32.13±16.6 μm and 43.75±27.92 μm, respectively, which was significantly higher than that of the control (5.88±4.45 μm, $P<0.01$). With the time going, on the difference became more significant (Figure 3). Within the dose range, angiogenesis increased correspondingly in both extent and rapidity as the concentration increased (Figure 4).

Exposure of ECs to both bFGF and VEGF in combination stimulated an angiogenic response that was greater than sum of their individual effects, and that occurred more rapidly than the response to either growth factor. The ALS induced by 10 ng/mL of bFGF plus 10 ng/mL of VEGF in combination was 590.75±289.15 μm, which was greater than the total effects of 10 ng/mL of bFGF (124.00±62.12 μm) and 10 ng/mL of VEGF (171.38±119.42 μm) and also greater than that induced by 20 ng/mL of either bFGF (187.25 ± 98.14 μm) or VEGF (280.5±198.23 μm) (Figure 5). The synergism of bFGF and VEGF was confirmed by the GLM test, which showed that the effect of the combination of bFGF plus VEGF was greater than the sum of the individual effects of bFGF and VEGF alone ($P = 0.011$) (Figure 5).

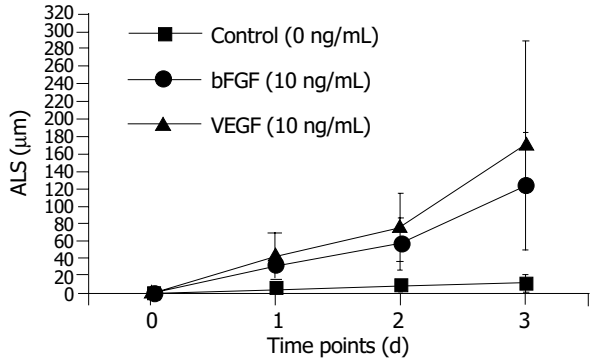

Figure 3 Time course of HMVEC angiogenesis in fibrin. Microcarriers coated with HMVECs were embedded in fibrin. The angiogenic effects of either bFGF or VEGF were dose-dependent over the range from 10 to 40 ng / mL. At day 1, 10 ng / mL of bFGF and VEGF induced angiogenesis with an ALS of 32.13±16.6 μm and 43.75±27.92 μm, respectively, which were significantly higher than that of the control (5.88±4.45 μm, $P<0.01$). The difference became more significant, as the time increased.

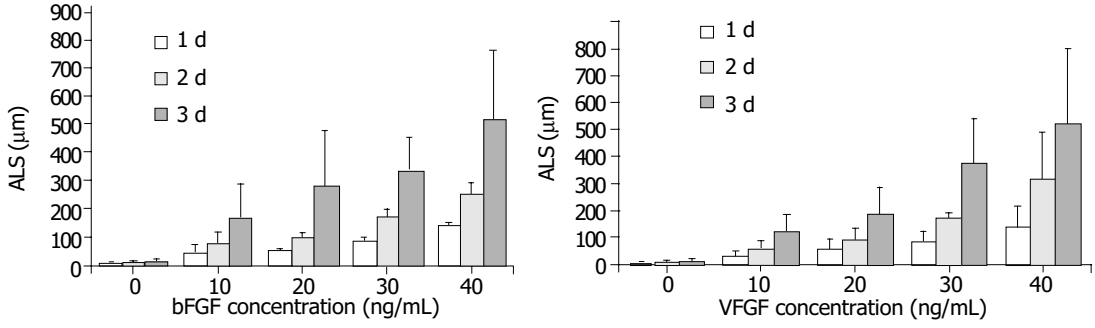

Figure 4 Dose responses of bFGF and VEGF on angiogenesis. Both bFGF and VEGF exhibited dose-dependent angiogenic effects in the range from 10 to 40 ng / mL. At d 1, 10 ng / mL of bFGF and VEGF induced angiogenesis with an ALS of 32.13±16.6 μm and 43.75±27.92 μm, respectively, which were significantly higher than that of the control (5.88±4.45 μm, $P<0.01$). With the concentration increasing, the difference became more significant.

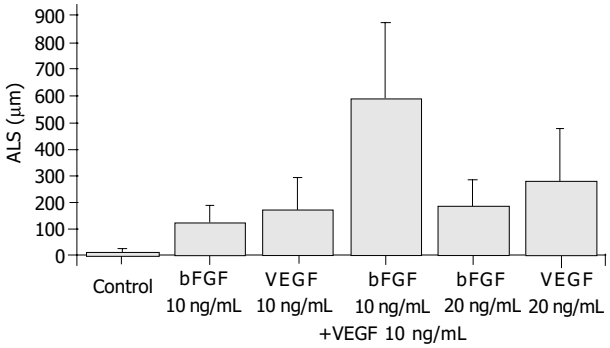

Figure 5 Synergism of bFGF and VEGF. The samples were quantitated at d 3. The combination of 10 ng / mL bFGF and 10 ng / mL VEGF induced an angiogenic response that was greater than the sum of the effects by each cytokine alone at the same dose (P = 0.011).

DISCUSSION

Three-dimensional angiogenesis assays are based on the capacity of activated endothelial cells to invade 3-D substrates. The matrix may consist of collagen gels, plasma clot, purified fibrin, matrigel, or a mixture of these proteins with others. The culture medium may be added to the gel before polymerization or on top of the gel. Depending on the culture medium composition (percentage of serum, addition of cytokines), cells can be induced to sprout, proliferate, migrate, differentiate, and tubular endothelial cell phenotypes in the 3-D configuration. Thus, one can *in vitro* observe the morphogenic responses of isolated ECs, which characterize the *in vivo* angiogenesis. In fact, a variety of 3-D angiogenesis models have provided great advances in the understanding of angiogenesis and the investigation of angiogenic/anti-angiogenic factors[2].

In 3-D angiogenesis models, the ECs were usually reorganized in the following ways: directly overlaid by gels[15, 16], sandwiched between two gel layers[17], seeded dispersedly[18] or clustered as spheroids in gels[3, 4], or attached onto microcarrier beads. Microcarrier-based angiogenesis model was firstly developed by Nehls and Drenckhan[10], who suggested, in their later studies, that in the presence of serum, the anastomosis of capillary sprouts occurred only rarely[14].

In this study, we also established an *in vitro* angiogenesis system based on microcarrier, but it was with human dermal microvascular endothelial cells (HMVECs). With this system, we observed all of the angiogenic steps that characterize the *in vivo* angiogenesis, including sprouting (16-24 h), branching (24-48 h), and capillary network formation (after 72 h), as described above. However, not in agreement with the observation by Nehls and Drenckhan, we found that the anastomosis of capillary sprouts occurred commonly in the later stage (3-5 d), even in the presence of up to 100 mL/L serum in our system (data not shown). After 5 d, the capillary-like network could be seen around/between MCs.

Since one of our goals was to characterize the gene expression patterns at the different steps of angiogenesis including sprouting, branching and networking, our 3-D angiogenesis model thus gave a good supporting. However, because of the morphological complexity, the capillary-like network at the late stage of the model was difficult to be quantified. So, we confined our observation to the first 3 d of the culture for the angiogenic quantification of the growth factors.

Angiogenesis in physiological conditions is characterized by strict regulation and occurs mostly through a collagen-rich extracellular matrix and leads to the formation of an organized capillary network. In contrast, in different pathological conditions as they are associated with tumor growth or wound healing, capillary sprouting processes are known to primarily occur in a fibrin-rich matrix and the stimulation of new vessels is exaggerated, leading to the formation of a disorganized[4, 19], capillary network. As one of the native ECM components involved in angiogenesis, fibrin is formed by the polymerization of fibrinogen after the proteolytic cleavage by thrombin. This scenario naturally takes place at sites of wound healing and tumor under the stimulation of VEGF and other factors, and leads to the deposition and stabilization of local fibrin clots. These fibrin clots serve as a temporary matrix that provides a solid support for invading cells, such as fibroblasts and endothelial cells.

In vitro angiogenesis in fibrin is affected by EC fibrinolysis involving both plasmin and metalloproteinase systems and the spatial structure of the gel[20, 21]. Cell surface fibrinolytic activity is crucial for EC invasion and migration in fibrin[22, 23]. The presence of aprotinin is necessary to maintain the integrity of fibrin. In the absence of aprotinin, fibrin was unable to support EC angiogenesis because it would be degraded before capillary-like structure formation. The configuration and mechanical properties of fibrin were determined by the conditions in which it polymerized. Various factors, including pH, ionic strength, fibrinogen and thrombin concentrations could affect the structural feature of fibrin[24]. It is thus important to prepare fibrin at a well-controlled condition when performing fibrin matrix-based angiogenic experiments, and to avoid any modification between the groups when comparing the potency of different angiogenic factors.

Many growth factors have been found to have angiogenic effects. FGFs and VEGFs are the best characterized among them. FGFs and VEGFs bind with high specificity to their cognate receptor tyrosine kinases, inducing activation of the intrinsic enzymatic activity of these receptors. This activity leads to tyrosine phosphorylation of the receptors, as well as of substrates for the kinases. In some cases, growth factors may induce angiogenesis by regulating the expression of some other growth factors and their receptors[19]. It is noteworthy that FGF and VEGF may act synergistically in induction of angiogenesis. Synergy of these growth factors in *in vivo* angiogenesis has been reported[25], and combination of the two factors also yielded a synergistic response in collagen-based *in vitro* system[26, 27]. The mechanisms responsible for this synergism are that these two growth factors closely interact with each other in angiogenic process. bFGF could induce expression of endogenous VEGF and its receptors in ECs[28-30], and VEGF-receptor antagonists inhibited bFGF-induced angiogenesis in spite of its lack of activities against bFGF receptors[31]. The capacity of VEGF to induce u-PA-plasmin activity and angiogenesis depended on endogenous bFGF produced by ECs[32]. In our fibrin and microcarrier-based angiogenesis model, we also found that both bFGF and VEGF demonstrated angiogenic effects on HMVECs in a dose-depended manner, and when applied in combination these two factors also acted synergistically.

In conclusion, we have successfully established a microcarrier-based *in vitro* three-dimensional angiogenesis model that offers a unique system for quantitative analysis of angiogenesis. The model is especially applicable to *in vitro* evaluation and screening of novel angiogenic or angiostatic factors. It may also shed light on the study of molecular mechanism of angiogenesis.

REFERENCES

1 **Folkman J**, Haudenschild C. Angiogenesis *in vitro. Nature* 1980; **288**: 551-556

2 **Vailhe B**, Vittet D, Feige JJ. *In vitro* models of vasculogenesis and angiogenesis. *Lab Invest* 2001; **81**: 439-452

3 **Korff T**, Augustin HG. Integration of endothelial cells in multicellular spheroids prevents apoptosis and induces differentiation. *J Cell Biol* 1998; **143**: 1341-1352

4 **Korff T**, Augustin HG. Tensional forces in fibrillar extracellular matrices control directional capillary sprouting. *J Cell Sci*

1999; **112**(Pt 19): 3249-3258
5 **Vernon RB**, Sage EH. A novel, quantitative model for study of endothelial cell migration and sprout formation within three-dimensional collagen matrices. *Microvasc Res* 1999; **57**: 118-133
6 **Bell SE**, Mavila A, Salazar R, Bayless KJ, Kanagala S, Maxwell SA, Davis GE. Differential gene expression during capillary morphogenesis in 3D collagen matrices: regulated expression of genes involved in basement membrane matrix assembly, cell cycle progression, cellular differentiation and G-protein signaling. *J Cell Sci* 2001; **114**(Pt 15): 2755-2773
7 **Vailhe B**, Ronot X, Lecomte M, Wiernsperger N, Tranqui L. Description of an in vitro angiogenesis model designed to test antiangiogenic molecules. *Cell Biol Toxicol* 1996; **12**: 341-344
8 **Peters K**, Schmidt H, Unger RE, Otto M, Kamp G, Kirkpatrick CJ. Software-supported image quantification of angiogenesis in an *in vitro* culture system: application to studies of biocompatibility. *Biomaterials* 2002; **23**: 3413-3419
9 **Kubota Y**, Kleinman HK, Martin GR, Lawley TJ. Role of laminin and basement membrane in the morphological differentiation of human endothelial cells into capillary-like structures. *J Cell Biol* 1988; **107**: 1589-1598
10 **Nehls V**, Drenckhahn D. A novel, microcarrier-based *in vitro* assay for rapid and reliable quantification of three-dimensional cell migration and angiogenesis. *Microvasc Res* 1995; **50**: 311-322
11 **Nehls V**, Drenckhahn D. A microcarrier-based cocultivation system for the investigation of factors and cells involved in angiogenesis in three-dimensional fibrin matrices *in vitro*. *Histochem Cell Biol* 1995; **104**: 459-466
12 **Xue L**, Greisler HP. Angiogenic effect of fibroblast growth factor-1 and vascular endothelial growth factor and their synergism in a novel *in vitro* quantitative fibrin-based 3-dimensional angiogenesis system. *Surgery* 2002; **132**: 259-267
13 **von Bulow C**, Hayen W, Hartmann A, Mueller-Klieser W, Allolio B, Nehls V. Endothelial capillaries chemotactically attract tumour cells. *J Pathol* 2001; **193**: 367-376
14 **Nehls V**, Herrmann R, Huhnken M. Guided migration as a novel mechanism of capillary network remodeling is regulated by basic fibroblast growth factor. *Histochem Cell Biol* 1998; **109**: 319-329
15 **Schor AM**, Schor SL, Allen TD. Effects of culture conditions on the proliferation, morphology and migration of bovine aortic endothelial cells. *J Cell Sci* 1983; **62**: 267-285
16 **Montesano R**, Orci L, Vassalli P. *In vitro* rapid organization of endothelial cells into capillary-like networks is promoted by collagen matrices. *J Cell Biol* 1983; **97**(5 Pt 1): 1648-1652
17 **Chalupowicz DG**, Chowdhury ZA, Bach TL, Barsigian C, Martinez J. Fibrin II induces endothelial cell capillary tube formation. *J Cell Biol* 1995; **130**: 207-215
18 **Bayless KJ**, Salazar R, Davis GE. RGD-dependent vacuolation and lumen formation observed during endothelial cell morphogenesis in three-dimensional fibrin matrices involves the alpha(v) beta(3) and alpha(5) beta(1) integrins. *Am J Pathol* 2000;**156**: 1673-1683
19 **Gerwins P**, Skoldenberg E, Claesson-Welsh L. Function of fibroblast growth factors and vascular endothelial growth factors and their receptors in angiogenesis. *Crit Rev Oncol Hematol* 2000; **34**: 185-194
20 **Vailhe B**, Lecomte M, Wiernsperger N, Tranqui L. The formation of tubular structures by endothelial cells is under the control of fibrinolysis and mechanical factors. *Angiogenesis* 1998; **2**: 331-344
21 **van Hinsbergh VW**, Collen A, Koolwijk P. Role of fibrin matrix in angiogenesis. *Ann N Y Acad Sci* 2001; **936**: 426-437
22 **Koolwijk P**, van Erck MG, de Vree WJ, Vermeer MA, Weich HA, Hanemaaijer R, van Hinsbergh VW. Cooperative effect of TNFα, bFGF, and VEGF on the formation of tubular structures of human microvascular endothelial cells in a fibrin matrix. Role of urokinase activity. *J Cell Biol* 1996; **132**: 1177-1188
23 **Hiraoka N**, Allen E, Apel IJ, Gyetko MR, Weiss SJ. Matrix metalloproteinases regulate neovascularization by acting as pericellular fibrinolysins. *Cell* 1998; **95**: 365-377
24 **Nehls V**, Herrmann R. The configuration of fibrin clots determines capillary morphogenesis and endothelial cell migration. *Microvasc Res* 1996; **51**: 347-364
25 **Asahara T**, Bauters C, Zheng LP, Takeshita S, Bunting S, Ferrara N, Symes JF, Isner JM. Synergistic effect of vascular endothelial growth factor and basic fibroblast growth factor on angiogenesis *in vivo*. *Circulation* 1995; **92**(9 Suppl): II365-371
26 **Pepper MS**, Ferrara N, Orci L, Montesano R. Potent synergism between vascular endothelial growth factor and basic fibroblast growth factor in the induction of angiogenesis *in vitro*. *Biochem Biophys Res Commun* 1992; **189**: 824-831
27 **Goto F**, Goto K, Weindel K, Folkman J. Synergistic effects of vascular endothelial growth factor and basic fibroblast growth factor on the proliferation and cord formation of bovine capillary endothelial cells within collagen gels. *Lab Invest* 1993; **69**: 508-517
28 **Seghezzi G**, Patel S, Ren CJ, Gualandris A, Pintucci G, Robbins ES, Shapiro RL, Galloway AC, Rifkin DB, Mignatti P. Fibroblast growth factor-2 (FGF-2) induces vascular endothelial growth factor (VEGF) expression in the endothelial cells of forming capillaries: an autocrine mechanism contributing to angiogenesis. *J Cell Biol* 1998; **141**: 1659-1673
29 **Pepper MS**, Mandriota SJ, Jeltsch M, Kumar V, Alitalo K. Vascular endothelial growth factor (VEGF)-C synergizes with basic fibroblast growth factor and VEGF in the induction of angiogenesis *in vitro* and alters endothelial cell extracellular proteolytic activity. *J Cell Physiol* 1998; **177**: 439-452
30 **Pepper MS**, Mandriota SJ. Regulation of vascular endothelial growth factor receptor-2 (Flk-1) expression in vascular endothelial cells. *Exp Cell Res* 1998; **241**: 414-425
31 **Tille JC**, Wood J, Mandriota SJ, Schnell C, Ferrari S, Mestan J, Zhu Z, Witte L, Pepper MS. Vascular endothelial growth factor (VEGF) receptor-2 antagonists inhibit VEGF- and basic fibroblast growth factor-induced angiogenesis *in vivo* and *in vitro*. *J Pharmacol Exp Ther* 2001; **299**; 1073-1085
32 **Mandriota SJ**, Pepper MS. Vascular endothelial growth factor-induced *in vitro* angiogenesis and plasminogen activator expression are dependent on endogenous basic fibroblast growth factor. *J Cell Sci* 1997; **110**(Pt 18): 2293-2302

Edited by Kumar M **Proofread by** Zhu LH and Xu FM

PO Box 2345, Beijing 100023, China
Fax: +86-10-85381893
E-mail: wjg@wjgnet.com www.wjgnet.com

World J Gastroenterol 2004;10(17):2529-2534
World Journal of Gastroenterology
Copyright © 2004 by The WJG Press ISSN 1007-9327

• CLINICAL RESEARCH •

Hematotesticular barrier is altered from early stages of liver cirrhosis: Effect of insulin-like growth factor 1

Inma Castilla-Cortázar, Nieves Diez, María García-Fernández, Juan Enrique Puche, Fernando Diez-Caballero, Jorge Quiroga, Matías Díaz-Sánchez, Alberto Castilla, Amelia Díaz Casares, Isabel Varela-Nieto, Jesús Prieto, Salvador González-Barón

Inma Castilla-Cortázar, Nieves Diez, María García-Fernández, Fernando Diez-Caballero, Matías Díaz-Sánchez, Department of Human Physiology, University of Navarra, Pamplona, Navarra, Spain
Jorge Quiroga, Jesús Prieto, Department of Internal Medicine, Liver Unit, University of Navarra, Pamplona, Navarra, Spain
Inma Castilla-Cortázar, María García-Fernández, Juan Enrique Puche, Amelia Díaz Casares, Salvador González-Barón, Department of Human Physiology, School of Medicine, University of Málaga, Malaga, Spain
Alberto Castilla, Department of Internal Medicine, Hospital Sierrallana, Tollelavega and School of Medicine, University of the Basque Country-Vitoria-Gasteiz, Spain
Isabel Varela-Nieto, Instituto de Investigaciones Biomédicas "Alberto Sols", Consejo Superior de Investigaciones Cientificas-Universidad Autónoma de Madrid (CSIC-UAM), Madrid, Spain
Supported by the Spanish Program I+D, SAF 99/0072 and SAF 2001/1672
Correspondence to: Inma Castilla-Cortázar, MD, PhD, Department of Human Physiology, School of Medicine, University of Málaga, Campus Teatinos 29080, Málaga, Spain. iccortazar@uma.es
Telephone: +34-952131577 **Fax:** +34-952131650
Received: 2004-02-06 **Accepted:** 2004-03-04

Abstract

AIM: The pathogenesis of hypogonadism in liver cirrhosis is not well understood. Previous results from our laboratory showed that IGF-1 deficiency might play a pathogenetic role in hypogonadism of cirrhosis. The administration of IGF-1 for a short period of time reverted the testicular atrophy associated with advanced experimental cirrhosis. The aim of this study was to establish the historical progression of the described alterations in the testes, explore testicular morphology, histopathology, cellular proliferation, integrity of testicular barrier and hypophysogonadal axis in rats with no ascitic cirrhosis.

METHODS: Male Wistar rats with histologically-proven cirrhosis induced with carbon tetrachloride (CCl_4) for 11 wk, were allocated into two groups (n = 12, each) to receive recombinant IGF-1 (2 μg/100 g·d, sc) for two weeks or vehicle. Healthy rats receiving vehicle were used as control group (n = 12).

RESULTS: Compared to controls, rats with compensated cirrhosis showed a normal testicular size and weight and very few histopathological testicular abnormalities. However, these animals showed a significant diminution of cellular proliferation and a reduction of testicular transferrin expression. In addition, pituitary-gonadal axis was altered, with significant higher levels of FSH (P<0.001 *vs* controls) and increased levels of LH in untreated cirrhotic animals. Interestingly, IGF-1 treatment normalized testicular transferrin expression and cellular proliferation and reduced serum levels of LH (P = ns *vs* controls, and P<0.01 *vs* untreated cirrhotic group).

CONCLUSION: The testicular barrier is altered from an early stage of cirrhosis, shown by a reduction of transferrin expression in Sertoli cells, a diminished cellular proliferation and an altered gonadal axis. The treatment with IGF-1 could be also useful in this initial stage of testicular disorder associated with compensated cirrhosis.

Castilla-Cortázar I, Diez N, García-Fernández M, Puche JE, Diez-Caballero F, Quiroga J, Díaz-Sánchez M, Castilla A, Casares AD, Varela-Nieto I, Prieto J, González-Barón S. Hematotesticular barrier is altered from early stages of liver cirrhosis: Effect of insulin-like growth factor 1. *World J Gastroenterol* 2004; 10 (17): 2529-2534
http://www.wjgnet.com/1007-9327/10/2529.asp

INTRODUCTION

Hypogonadism (characterized by low testosterone levels and relative hyperestrogenism, loss of libido, sexual impotence and feminine body features in men) is a common complication of advanced liver cirrhosis[1]. Previous data demonstrated that rats with advanced cirrhosis showed reduced testicular size and weight and severe histopathological testicular abnormalities, including reduced tubular diameters, loss of the germinal line, and diminutions in cellular proliferation and spermatogenesis and testicular transferrin expression, a good marker of the integrity of blood-testis barrier[2]. In addition, low serum testosterone and high serum LH were present in cirrhotic animals, as well as decreased levels of serum IGF-1. Interestingly, the administration of IGF-1 at low doses for a short period of time reverted the testicular atrophy and improved the altered pituitary-testicular axis in these animals[2]. In cirrhotic patients, hypogonadism has been attributed to a variety of mechanisms including gonadal toxicities of alcohol, malnutrition and increased production of estrogens from androgens in peripheral tissues due to the existence of portal systemic shunting[3-9].

Insulin-like growth factor-1 (IGF-1) is an anabolic hormone produced in different tissues although the liver accounts for 90% of the circulating hormone, which is synthesized in response to growth hormone (GH) stimulation[10,11]. In cirrhosis the reduction of receptors for GH in hepatocytes and the diminished synthesizing ability of the liver parenchyma caused a progressive fall of serum IGF-1 levels[11-14]. Although in an early stage of cirrhosis serum levels of IGF-1 were normal, its bio-availability seemed to be diminished[15]. The clinical impact of the reduced production or availability of IGF-1 in cirrhosis was largely unknown[11-14]. Recent studies from our laboratory have demonstrated that short courses of treatment with low doses of IGF-1 were able to induce marked improvements in nutritional state[15], nitrogen retention[16], intestinal absorption[17-19], osteopenia[20,21], liver function reducing fibrogenesis[22,23], and restore the reduced somatostatinergic tone[24] in rats with experimental cirrhosis. These data suggest that IGF-1 deficiency plays a pathogenetic role in several systemic complications occurring in cirrhosis.

It is well known that IGF-1 stimulates testosterone synthesis and spermatogenesis[25-32]. Its deficiency could contribute to the development of hypogonadism associated with cirrhosis as

the previous data supported[2]. Since the pathogenesis of hypogonadism in cirrhosis is not yet well understood, the aim of the present study was to study the chronological progression of the described alterations in testes[2] in advanced cirrhosis, explore testicular morphology, histopathology, cellular proliferation, integrity of testicular barrier and hypophyso-gonadal axis in rats with cirrhosis in an early stage, without ascites.

MATERIALS AND METHODS

Induction of liver cirrhosis

All experimental procedures were performed in conformity with The Guiding Principles for Research Involving Animals[33]. Cirrhosis was induced as previously described[15,16]. Briefly, male Wistar rats (3-week-old, 130-150 g) were subjected to CCl_4 inhalation (Merck, Darmstadt, Germany) twice a week for 11 wk with a progressively increasing exposure time from 1 to 5 min. During the whole period of cirrhosis induction animals received Phenobarbital (Luminal, Bayer, Leverkusen, Germany) in the drinking water (400 mg/L). Both food (standard semipurified diet for rodents; B.K. Universal, Sant Vicent del Horts, Spain) and water were given *ad libitum*. Healthy, age and sex-matched control rats were maintained under the same conditions but receiving neither CCl_4 nor Phenobarbital.

Study design

The treatment was administrated for 2 wk after stopping of CCl_4 exposure. In the morning of d 0, animals were weighed and blood samples were drawn from the retroocular venous plexus from all rats with capillary tubes (Marienfeld, Germany) and stored at -20 °C until used for analytical purposes. Cirrhotic rats were randomly assigned to receive either vehicle (saline) (group CI, $n = 12$) or recombinant human IGF-1 (Pharmacia-Uppsala, Sweden) (2 μg/100 g·d in two divided doses, subcutaneously) (group CI+IGF, $n = 12$) for two weeks. Control rats (group CO, $n = 10$) received saline during the same period.

In the morning of the 15th d, rats were weighed, blood was obtained from the retroocular plexus and animals were killed by decapitation. After the abdominal cavity was opened, the liver and testes were dissected and weighed. Samples from the left major liver lobe and testes were processed for histological examination (fixed in Bouin's solution). The testicular diameters (AP and LM) were measured using a precision calliper, Mituyoto® (±0.05 mm). Ascites was ruled out by direct exploration of abdominal cavity in all cirrhotic animals.

Liver histopathology

Bouin-fixed tissues were processed and sections (4-μm) were stained with Haematoxylin and Eosin and Masson's trichrome. Livers were scored (1 to 4) as previously reported[15,22]. Preestablished criteria for inclusion of cirrhotic (CI) animals in the final analysis were the presence of: (1) altered baseline biochemical data of liver function; and (2) in retrospect, histologically proven liver cirrhosis (scores 3 or 4 of the classification) in CCl_4-treated-animals. All animals had compensated cirrhosis without ascites.

Testicular histopathology and PCNA and transferrin immunohistochemistry

For histopathological evaluation of testes, 30 seminiferous tubules from each rat of the three groups were blindly evaluated by two observers and the arithmetic mean of the scores was taken as the final result. Transverse sections of seminiferous tubuli were examined and evaluation of histological changes was made using a light projection microscope (Micro Promar Leitz GMBH, Wetzlar, Germany) at 150× magnification. The following parameters were studied: tubular diameter, quantitation of the presence of different types of cells in tubuli, presence of peritubular fibrosis, and the number of proliferating cells. For general purposes haematoxylin & eosin stain and Masson's trichrome stain were used. Specific techniques for other purposes are specified in the corresponding paragraphs.

Changes in tubuli were classified into 5 categories (Category I: highest damage to Category V: full normality). Category I: presence of only Sertoli cells; category II: Sertoli cells plus spermatids; category III: Sertoli cells, plus spermatides, and spermatocytes; category IV: presence of all kinds of cells but showing some morphological alterations (i.e.: severe vacuolization, aberrant cells); category V: presence of all kinds of cells without morphological alterations. The presence of peritubular fibrosis was evaluated in Masson's trichrome preparations according to the thickness of the staining of collagen deposition surrounding tubuli. Proliferating cells were identified by immunostaining of proliferating cellular nuclear antigen (PCNA) using an avidin-biotin peroxidase method[34] with retrieval of antigen by means of microwave irradiation. Specific anti-PCNA antibody (mouse anti-PCNA, clone PC 10, DAKO, Denmark) biotinylated rabbit anti-mouse IgG (DAKO, Denmark) were used and the avidin-biotin complex technique (ABC, DAKO kit) was performed. The bound antibodies were visualized by means of 3,3'-diaminobenzidine tetrahydrochloride (Sigma Chemical Company, St. Louis, MO) with nickel enhancement[34]. Finally, samples were slightly counterstained (10 s) in hematoxylin, dehydrated, and mounted in DPX. Controls were performed by substitution of the primary antibody by TBS. The number of PCNA positive cells was recorded. The result was expressed as stained cells per tubuli (arithmetic mean of 30 screened tubuli).

In addition, the expression of transferrin[35] in tubuli was evaluated by immunostaining using similar technique as for PCNA with specific anti-transferrin antibody (obtained from rabbit, RARa/TRf, Nordic Immunological Laboratories, Teknovas, The Netherland). Transferrin expression was scored from 0 to 4 points. If 30 tubuli expressed transferrin normally all over the germinal epithelium, it was scored 0 points. The remaining scores were obtained according to the following formula: (30-tubuli showing expression of transferrin all over the germinal epithelium) ×0.075.

Analytical methods

Serum levels of albumin, total proteins, glucose, cholesterol, bilirubin, alkaline phosphatase, transferrin and aminotransferases (AST and ALT) were determined by routine laboratory methods using a Hitachi 747 autoanalyzer (Boerhringer-Mannheim, Germany). Serum levels of the different hormones were assessed by RIA in a GammaChen 9612 Plus (Serono Diagnostics, Roma, Italy) using specific commercial assay systems: total and free testosterone and estradiol-6, Coat-a-Count, DPC (Diagnostic Products Corporation, Los Angeles, CA); rat luteinizing hormone (rLH) and rat follicle stimulating hormone (rFSH) from Amersham International Plc (Little Chalfont Buckinghamshire, England HP7 9NA); IGF-1 by extraction (Nichols Institute Diagnostics, San Juan Capistrano, CA, USA).

Lipid peroxidation assessment of testicular homogenates

Malondyaldehyde (MDA) was assessed after heating samples at 45 for 60 min in acid medium. It was quantitated by a colorimetric assay using LPO-586 (Bioxytech; OXIS International *Inc*., Portland, OR, USA), which after reacting with MDA, generated a stable chromophore that could be measured at 586 nm (Hitachi U2 000 Spectro; Roche).

Statistical analysis

Data are expressed as mean±SE. To assess the homogeneity between the three groups of rats a Kruskall-Wallis test was

used, followed by multiple post-hoc comparisons using Mann-Withney *U* tests (two tailed) with Bonferroni adjustment. A regression model was fitted considering histopathological score, PCNA or transferrin expression scores and IGF-1 plasma concentration as the dependent and independent variables respectively. Within group differences between pre-and post-treatment values were assessed by means of Wilcoxon matched pairs signed rank sum test. Any *P* value less than 0.05 was considered to be statistically significant. Calculations were performed by SPSS Win v.6.0. program.

RESULTS

At baseline, CI groups showed abnormal values compared to controls (CO) in serum levels of alanine aminotransferase (CO = 26±2; CI = 273±49 IU/L, $P<0.01$), aspartate aminotransferase (CO = 55±5; CI = 297±49 IU/L, $P<0.001$), cholesterol (CO = 82±4; CI = 115±5 mg/dL, $P<0.05$), alkaline phosphatase (CO = 310±43; CI = 701±146 IU/L, $P<0.05$), bilirubin (CO = 0.4±0.0; CI = 1.2±0.3 mg/dL, $P<0.05$), total proteins (CO = 6.9±0.1; CI = 6.4±0.2 g/dL, $P<0.05$) and albumin (CO = 3.6±0.1; CI = 3.1±0.2 g/dL, $P<0.05$). No differences were found between cirrhotic groups.

At the end of the experimental period, all rats from groups CI and CI+IGF showed established cirrhosis (mixed micro-macronodular cirrhosis in liver histopathology) with some signs of portal hypertension (spleen weight, g, CO = 0.8±0.0; CI = 1.4±0.2; CI+IGF = 1.4±0.1, $P<0.001$ both cirrhotic groups *vs* controls). Ascites was absent in all of the cirrhotic animals.

Testicular morphology and morphometry

The testicular size and volume were normal in the cirrhotic groups as compared to controls. Morphometric study showed reduction in testicular weight (in absolute values but not if it was corrected by body mass) in untreated cirrhotic group as compared to controls and CI+IGF group. Findings regarding longitudinal and transverse testicular diameters were similar to those in testicular weight. Morphometric data in the three groups are summarized in Table 1.

Testicular histopathology

Figure 1 shows testicular morphology in the three experimental groups. Testicular histological section of normal rat (CO) demonstrated active spermatogenesis in normal-size seminiferous tubuli with thin basement membranes and minimal peritubular fibrosis. Leydig cells were scarce, being widely separated by seminiferous tubuli. No evidence of peritubular fibrosis and other alterations was found in cirrhotic groups. Cellular analyses (see Methods) in 30 seminiferous tubuli were performed in each preparation and summarized in Table 2. No relevant findings were obtained in this morphologic study.

Testicular cellular proliferation, as evaluated by PCNA[35], was significantly reduced in CI rats while CI+IGF rats showed values similar to controls (CO: 66±2, CI: 57±1, CI+IGF: 61±1, $P<0.001$ untreated cirrhotic group *vs* controls and $P<0.05$ CI+IGF *vs* controls and CI group). Figure 2 shows PCNA immunohistochemistry (PCNA+cells) in the three groups.

Testicular transferrin, a marker of the integrity of hemato-testicular barrier[36-38], was evaluated from 0 to 4 points by immunohistochemistry in testicular slices (see Methods). Transferrin expression was decreased in CI rats (3.40±0.03 points, $P<0.001$ *vs* CO and CI+IGF groups) as compared to controls (3.98±0.04 points) and to cirrhotic rats receiving IGF-1 (3.76±0.05 points). Figure 3 shows transferrin expression in the three experimental groups.

Testicular levels of MDA in order to study the likely direct damage of CCl_4 to testes, MDA levels, an index of lipid peroxidation[39], were assessed in testicular homogenates. No differences were found between the three experimental groups in testicular MDA content (nmoL/mg protein, CO = 9.1±0.8, CI = 13.0±3.2, CI+IGF = 8.9±1.6).

Pituitary-gonadal axis

Serum levels of sexual hormones are summarized in Table 3. No significant differences were found between groups, either in total and free testosterone, or estradiol, or in the ratio of estradiol/testosterone. However, a significant increase of FSH ($P<0.001$ *vs* controls) and also high levels of LH ($P = 0.06$ *vs* controls) were observed in untreated rats with compensated cirrhosis, suggesting an altered negative feed-back since this early stage of the cirrhosis. On the other hand, LH concentrations were moved towards normal values in IGF-1 treated cirrhotic group (P = ns *vs* controls, and $P<0.01$ *vs* untreated cirrhotic rats).

Serum levels of IGF-1

At the time of animal sacrifice (d 15), no significant differences between the three groups were found in serum levels of IGF-1 (CO: 1030±67, CI: 1165±58, CI+IGF: 1030±38 ng/mL), similar to those described previously in early stage of cirrhosis[16-18,24].

Table 1 Body mass and parameters of testicular size and weight in the three experimental groups (d 15)

	Healthy control rats (CO, n = 12)	Untreated cirrhotic rats (CI, n = 12)	Cirrhotic rats treated with IGF-1 (CI+IGF, n=12)
Body mass (g)	545.0±1.0	460.0±1.0[d]	458.0±9.0[d]
Right testis (g)	2.0±0.0	1.6±0.1[d]	1.7±0.1[d]
(×100 g/bm)	(0.4±0.0)	(0.3±0.0)	(0.4±0.0)
External testicular diameters (mm)			
• Longitudina	20.4±0.26	18.56±0.22[d]	18.37±0.34[d]
• Transversal	10.3±0.24	9.41±0.23[b]	9.64±0.14[a]

[a]$P<0.05$; [b]$P<0.01$; [d]$P<0.001$ *vs* CO group.

Table 2 Cellular analysis: Thirty seminiferous tubuli were examined in each preparation. The table summarizes the number of tubuli in each category: category I, only Sertoli s cells; category II, I+spermatids; category III, II+spermatocytes; category IV, all types of cells but with some alterations; category V, all types of cells with normal features

Category	I	II	III	IV	V
Controls (CO) (n = 10)×30 tubuli	0	0	0	2	298
Untreated cirrhotic rats (CI) (n = 10)×30 tubuli	0	0	5	20	275
IGF-treated cirrhotic rats (CI+IGF) (n = 10)×30 tubuli	0	0	0	8	292
Statistical analysis (P)	ns	ns	ns	[a]$P<0.05$	ns

[a]$P<0.05$, CI *vs* CO group.

Table 3 The pituitary-gonadal axis (on d 15) in the three experimental groups

	Healthy control rats (CO, *n* = 12)	Untreated cirrhotic rats (CI, *n* = 12)	IGF-1-treated cirrhotic rats (CI+IGF, *n* = 12)
Total testosterone (ng/dL)	62±13	77±17	64±7
Free testosterone (pg/mL)	0.36±0.09	0.36±0.10	0.41±0.05
Estradiol (pg/mL)	31±2	33±2	29±1
Estradiol/Total testosterone	0.5±0.1	0.5±0.1	0.6±0.1
LH (ng/mL)	4.8±0.6	6.0±0.5	3.8±0.7[d]
FSH (ng/mL)	22±8	27±1[f]	26±4[b]

[b]$P<0.01$CI+IGF *vs* CO group; [d]$P<0.01$ CI+IGF *vs* CI group; [f]$P<0.001$ CI *vs* CO group.

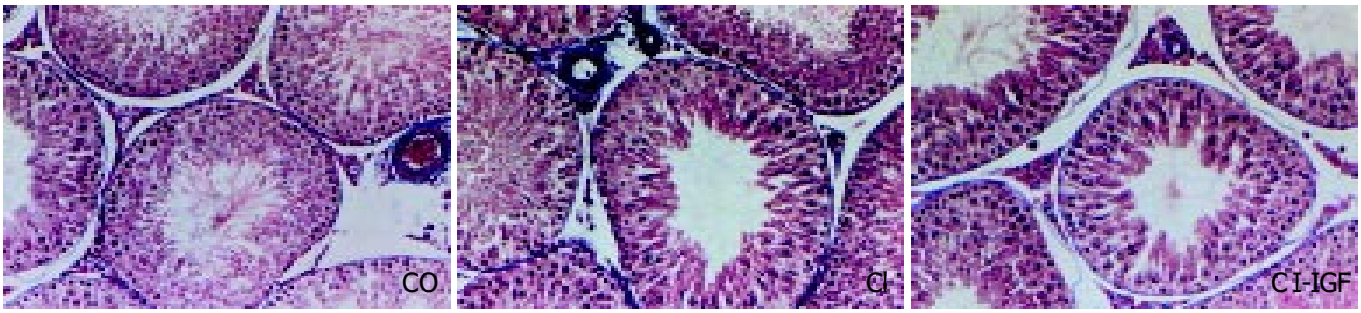

Figure 1 Microscopy of testes (×150 magnification, Masson's stain). Testicular histological sections of normal rat (CO) demonstrated active spermatogenesis in normal-size seminiferous tubuli with thin basement membranes and minimal peritubular fibrosis. Leydig cells were scarce, being widely separated by seminiferous tubuli. No evidence of peritubular fibrosis and other alterations were found in testes from cirrhotic animals.

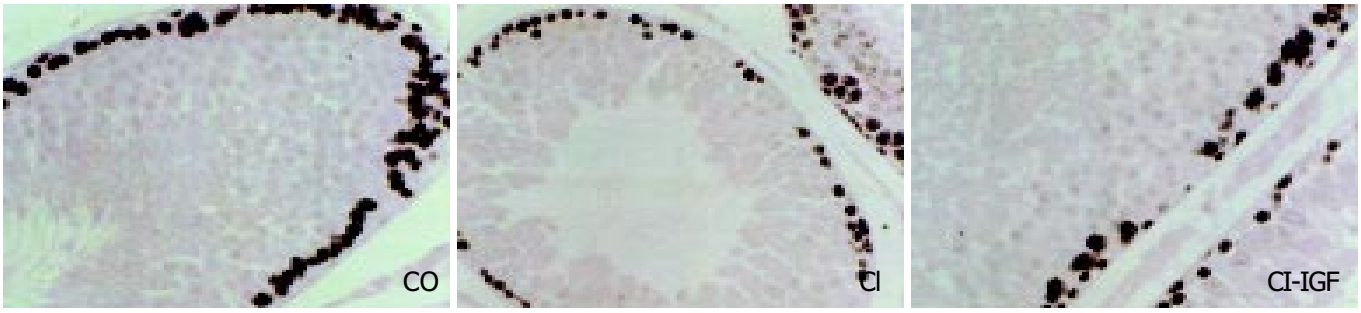

Figure 2 Study of proliferative activity, assessed by PCNA immunostaining. A significant reduction of cellular proliferation were observed in rats with compensated cirrhosis. This reduction was normalized in IGF-1 treated cirrhotic group (CI+IGF). (×200 magnification, in the three pictures).

Figure 3 Immunohistochemistry for testicular transferrin in seminiferous tubuli. Transferrin immunostaining was observed at the level of Sertoli cells and in germ cells in normal rats (CO) and in cirrhotic rats treated with IGF-1 (CI+IGF) but a lower or absent transferrin immunostaining was observed in several tubuli of untreated cirrhotic rats (CI) (score, CI: 3.40±0.03, CO: 3.98±0.04, CI+IGF-1: 3.76±0.05).

DISCUSSION

This study demonstrates that rats with compensated CCl_4-induced cirrhosis show some testicular alterations and gonadal dysfunction, from early stages of liver cirrhosis. The main finding of this study is that there is an altered hemato-testicular barrier, probably responsible for the reduction of cellular proliferation, as well as a paradoxical response of pituitary-testicular axis.

The occurrence of testicular atrophy and gonadal dysfunction in advanced cirrhosis is a well known clinical event[1,3-9]. Both testicular histopathological abnormalities and low levels of serum testosterone have been described in patients with

alcoholic and nonalcoholic cirrhosis several years ago[3-9]. Previous experimental data[2] showed that severe testicular atrophy and gonadal insufficiency treated with low doses of IGF-1 recovered to normal in a very short time (21 d). Data regarding experimentally induced cirrhosis are, however, scarce. Our previous data showed a severe testicular damage[2] as manifested by macroscopic testicular atrophy and a variety of histopathological abnormalities including a reduction in tubular diameters, presence of aberrant cells in tubular lumen, peritubular fibrosis, loss of the germinal line and a marked reduction in cellular proliferation. These alterations resembled those found in necropsic studies in alcoholic cirrhotics[1] and those reported in experimental models of testicular damage such as chronic testicular ischemia[35].

The mechanisms responsible for the described alterations are not fully understood, although the relationship between IGF-1 deficiency and testicular damage in cirrhosis was demonstrated in the mentioned work[2]. In cirrhotic rats included in the current work, no IGF-1 deficiency was present but there was a reduced availability of this hormone as it has been suggested previously[16-18,22]. Moreover, we have previously demonstrated that the changes induced by cirrhosis in the serum profile of IGF-1 binding proteins further reduce bio-availability of IGF-1 in cirrhotic rats[16]. In fact, exogenous administration of IGF-1 was able to reverse several abnormalities (decreased food utility and intestinal absorption of nutrients, and somatostatinergic tone and osteopenia) associated with cirrhosis in animals with normal serum levels of this hormone[16-20,22-24].

On the other hand, a direct effect of IGF-1 on testes seemed to be the most important factor to explain previous findings[2]. This idea is supported by the existence of receptors for IGF-1 in Sertoli cells, germ cells and Leydig cells[25-27] and by findings demonstrating a direct effect of IGF-1 on testes[27-31]. Since IGF-1 is a well recognized trophic factor for testis, its deficiency could be a contributing factor to testicular damage in cirrhosis.

The present work was designed in order to gain more insights into the mechanisms involved in the pathogenesis of hypogonadism associated with liver cirrhosis. In fact, many factors that have been involved in this process, such as portal systemic shunting[1,39,40] or undernutrition[1,41] were minimized in this early stage of the liver disease. Specifically, this study was targeted to establish the historical progression of the described testicular alterations[2].

The blood-testis barrier is considered nearly as specific as the blood-brain barrier[42]. Although all cells require irons from serum transferrin produced by hepatocytes, cells that create a blood barrier such as Sertoli cells in the testis and choroid plexus epithelium in the brain also express the transferrin gene to provide irons to cells sequestered within the serum-free environment. Testicular transferrin expression was a good marker of the integrity of the hemato-testicular barrier[36,37]. A major finding of this work was that transferrin expression by Sertoli cells was reduced in untreated cirrhotic rats. The medical bioavailability of IGF-1 could be due to the mechanism of testicular transferrin reduction. IGF-1 treatment increased the expression of this protein in Sertoli cells of cirrhotic rats (Figure 3). This possibility seemed to be plausible since several metabolic functions of Sertoli cells were also influenced by IGF-1[32,43-45]. Interestingly, the recovery of transferrin expression in Sertoli cells observed in our study suggested a role for IGF-1 in maintaining the integrity of the hematotesticular barrier[2,33-38].

The first step of the pathogenesis of testicular atrophy occurring in advanced cirrhosis seems to be the decreased expression of transferrin, showing a dysfunction of Sertoli cells and consequently the disruption in blood-testis barrier integrity. Therefore, the observed reduction of cellular proliferation finally affecting spermatogenesis[2,46] would be its logical consequence.

A question arises as to whether direct toxicity of CCl_4 on testicular tissue could contribute to testicular injury. Alcohol was known to produce oxidative damage and to be able to pass across testicular barrier[47,48]. This toxic possibility has been reasonably ruled out by the presence of similar levels of MDA, a marker of lipid peroxidation[39], in testicular homogenates from the three experimental groups. Certainly, a slight increase of testicular MDA was found in untreated cirrhotic rats, but this did not reach statistical significance.

In the early stage of cirrhosis, testosterone levels were normal. However, both FSH and LH were increased in untreated cirrhotic animals. This abnormal response of the negative feedback could be an initial hormonal reaction of primary hypogonadism. In advanced stages of cirrhosis, we found increased levels of serum LH associated with a significant reduction of total and free serum testosterone defining a picture of primary hypogonadism, thus ruling out hypothalamic-pituitary dysfunction as the responsible mechanism[2]. Interestingly, LH levels were reduced by IGF-1 treatment in this series with compensated cirrhosis and an incipient gonadal dysfunction. The significant increase of FSH could be related to the observed reduction of cellular proliferation in cirrhotic rats. Since a close relationship has been reported between IGF-1 and gonadotropins[49-51], our findings require further investigation.

In summary, this study shows an altered hemato-testicular barrier from an early stage of cirrhosis and suggests that the reduction of IGF-1 bioavailability may play a critical role in the beginning stage of testicular damage and hypogonadism associated with liver cirrhosis. In addition, these results support the conclusion that the exogenous administration of IGF-1 may be useful for the treatment of testicular alterations in cirrhotic patients.

ACKNOWLEDGEMENTS

The authors wish to express their gratitude to Dr. Bruce Scharschmidt, Chiron, for generously granting the rhIGF-1 used in this study. We are as well deeply indebted to the "Real Academia de Medicina de Cataluña" (Barcelona) and Mrs.C. Alonso-Borrás and Mr. J. Celaya for financial collaboration.

RREFERENCES

1 **Van Thiel DH**. Endocrine function. In The liver: biology and pathobiology. *Raven Press* 1982; 717-912
2 **Castilla-Cortázar I**, García M, Quiroga J. Insulin-like growth factor-I reverts testicular atrophy in rats with advanced cirrhosis. *Hepatology* 2000; **31**: 592-600
3 **Van Thiel** GH, Gavaler JS, Slone FL. Is feminization in alcoholic men due in part to portal hypertension?: a rat model. *Gastroenterology* 1980; **78**: 81-91
4 **Bennett HS**, Baggenstoss AH, Butt H. The testis, breast and prostate of men who die of cirrhosis of the liver. *Am J Clin Pathol* 1950; **20**: 814-828
5 **Van Steenbergen W**. Alcohol, liver cirrhosis and disorders in sex hormone metabolism. *Acta Clin Belg* 1993; **48**: 269-283
6 **Galvao-Teles A**, Monteiro E, Gavaler JS. Gonadal consequences of alcohol abuse: lessons from the liver. *Hepatology* 1986; **6**: 123-128
7 **Guechot J**, Vaubourdolle M, Ballet F. Hepatic uptake of sex steroids in men with alcoholic cirrhosis. *Gastroenterology* 1987; **92**: 203-207
8 **Bannister P**, Handley T, Chapman C, Losowsky MS. Hypogonadism in chronic liver disease: impaired release of luteinising hormone. *Brit Med* 1986; **293**: 1191-1193
9 **Pajarinen J**T, Karhunden PJ. Spermatogenic arrest and "Sertoli cell-only" syndrome-common alcohol-induced disorders of the human testis. *Int J Androl* 1994; **17**: 292-299
10 **Sara VR**, Hall K. Insulin-like growth factors and their binding proteins. *Physiol Rev* 1990; **70**: 591-613
11 **Schimpf RM**, Lebrec D, Donadieu M. Somatomedin production in normal adults and cirrhotic patients. *Acta Endocrinol* 1977; **86**: 355-362

12 **Hattori N**, Kurahachi H, Ikekubo K. Serum growth hormone-binding protein, insulin-like growth factor-I, and growth hormone in patients with liver cirrhosis. *Metab Clin Exp* 1992; **41**: 377-381
13 **Moller S**, Becker U, Juul A, Skakkebæk NE, Christensen E. Prognostic value of insulinlike growth factorI and its binding proteins in patients with alcohol-induced liver disease. *Hepatology* 1996; **23**: 1073-1078
14 **Moller S**, Gronbaek M, Main K, Becker U, Skakkebaek NE. Urinary growth hormone (U-GH) excretion and serum insulin-like growth factor 1 (IGF-1) in patients with alcoholic cirrhosis. *J Hepatol* 1993; **17**: 315-320
15 **Caufriez A**, Reding P, Urbain D, Goldstein J, Copinschi G. Insulin-like growth factor-I: a good indicator of functional hepatocellular capacity in alcoholic liver cirrhosis. *J Endocrinol Invest* 1991; **14**: 317-321
16 **Picardi A**, Costa de Oliveira A, Muguerza B, Tosar A, Quiroga J, Castilla-Cortázar I, Santidrián S, Prieto J. Low doses of insulin-like growth factor-I improve nitrogen retention and food efficiency in rats with early Cirrhosis. *J Hepatol* 1997; **24**: 267-279
17 **Castilla-Cortázar I**, Prieto J, Urdaneta E, Pascual M, Nuñez M, Zudaire E, García M, Quiroga J, Santidrián S. Impaired intestinal sugar transport in cirrhotic rats: correction by low doses of insulin-like growth factor I. *Gastroenterology* 1997; **113**: 1180-1187
18 **Castilla-Cortázar I**, Picardi A, Tosar A, Ainzua J, Urdaneta E, García M, Pascual M, Quiroga J, Prieto J. Effect of insulin-like growth factor I on *in vivo* intestinal absorption of D-galactose in cirrhotic rats. *Am J Physiol* 1999; **276**(1 Pt 1): G37-G42
19 **Pascual M**, Castilla-Cortázar I, Urdaneta E, Quiroga J, García M, Picardi A, Prieto J. Altered intestinal transport of amino acids in cirrhotic rats: the effect of insulin-like growth factor-I. A*m J Physiology* 2000; **279**: G319-G324
20 **Cemborain A**, Castilla-Cortázar I, García M, Quiroga J, Muguerza B, Picardi A, Santidrián S, Prieto J. Osteopenia in rats with liver cirrhosis: beneficial effects of IGF-1 treatment. *J Hepatol* 1998; **28**: 122-131
21 **Cemborain A**, Castilla-Cortázar I, García M, Muguerza B, Delgado G, Díaz-Sánchez M, Picardi A. Effects of IGF-1 treatment on osteopenia in rats with advanced liver cirrhosis. J *Physiol Biochem* 2000; **56**: 91-99
22 **Castilla-Cortázar I**, García M, Muguerza B, Pérez R, Quiroga J, Santidrián S, Prieto J. Hepatoprotective effects of insulin-like growth factor-I in rats with carbon-tetrachloride-induced cirrhosis. *Gastroenterology* 1997; **113**: 1682-1691
23 **Muguerza B**, Castilla-Cortázar I, García M, Quiroga J, Santidrián S, Prieto J. Antifibrogenic effect *in vivo* of low doses of Insulin-like growth factor-I (IGF-1) in cirrhotic rats. *BBA* 2001; **1536**: 185-195
24 **Castilla-Cortázar I**, Aliaga-Montilla MA, Salvador J, García M, Quiroga J, Delgado G, González-Barón S, Prieto J. Insulin-like growth factor-I restores the reduced somatostatinergic tone controlling GH secretion in cirrhotic rats. *Liver* 2001; **37**: 215-219
25 **Tajima Y**, Watanabe D, Koshimizu U, Matsuzawa T, Nishimune Y. Insulin-like growth factor-I and transforming growth factor-alpha stimulate differentiation of type A spermatogonia in organ culture of adult mouse cryptorchid testes. *Int J Androl* 1995; **18**: 8-12
26 **Spiteri-grech J**, Weinbauer GF, Bolze P, Chandolia RK, Bartlett JM, Nieschlag E. Effects of FSH and testosterone on intratesticular insulin-like growth factor-I and specific germ cell populations in rats treated with gonadotrophin-releasing hormone antagonist. *J Endocrinol* 1993; **137**: 81-89
27 **Zhou J**, Bondy C. Anatomy of the insulin-like growth factor system in the human testis. *Fertil Steril* 1993; **60**: 897-904
28 **Dubois W**, Gallard GV. Culture of intact Sertoli/germ cell units and isolated Sertoli cells from Squalus testis. II. Stimulatory effects of insulin and IGF-1 on DNA synthesis in premeiotic stages. *J Exp Zool* 1993; **267**: 233-244
29 **Moore A**, Morris JD. The involvement of insulin-like growth factor-I in local control of steroidogenesis and DNA synthesis of Leydig cells in the rat testicular interstitium. *J Endocrinol* 1993; **138**: 107-114
30 **Grizard G**. IGF(s) and testicular function. Secretion and action of IGF-1 on Leydig cells. *Contracept Fertil Sex* 1994; **22**: 551-555
31 **Lin T**, Wang D, Nagpal ML, Shimasaki S, Ling N. Expression and regulation of insulin-like growth factor-binding protein -1, -2, -3 and -4 messenger ribonucleic acids in purified rat Leydig cells and their biological effects. *Endocrinology* 1993; **132**: 1898-1904
32 **Rappaport MS,** Smith EP. Insulin-like growth factor (IGF) binding protein 3 in the rat testis: follicle-stimulating hormone dependence of mRNA expression and inhibition of IGF-1 action on cultured Sertoli cells. *Biol Reprod* 1995; **52**: 419-425
33 The Guiding Principles for Research Involving Animals. National Academy of Sciences and published by *the National Institute of Health* -NIH-, revised in 1991
34 **Shu SY**, Ju G, Fan LZ. The glucose oxidase-DAB-nickel method in peroxidase histochemistry of the nervous system. *Neurosci Lett* 1988; **85**: 169-171
35 **Santamaria L**, Martin R, Codesal J, Paniagua R. Myoid cell proliferation in rat seminiferous tubules after ischaemic testicula atrophy induced by epinephrine. Morphometric and immunohistochemical (bromo-deoxyuridine and PCNA) studies. *Int J Androl* 1995; **18**: 13-22
36 **Skinner MK**, Cosand WL, Griswold MD. Purification and characterization of testicular transferrin secreted by rat Sertoli cells. *Biochem J* 1984; **218**: 313-320
37 **Chaudhary J**, Skinner MK. Comparative sequence analysis of the mouse and human transferrin promoters: hormonal regulation of the transferrin promoter in sertoli cells. *Mol Reprod Dev* 1998; **50**: 273-283
38 **Gutteridge JMC.** Lipid peroxidation and antioxidants as biomarkers of tissue damage. *Clin Chem* 1995; **41**: 1819-1828
39 **Zaitoun AM**, Apelqvist G, Wikell C, Al-Mardini H, Bengtsson F, Record CO. Quantitative studies of testicular atrophy following portacaval shunt in rats. *Hepatology* 1998; **28**: 1461-1466
40 **Smanik EJ**, Mullen KD, Giroski WG, McCullough AJ. The influence of portacaval anastomosis on gonadal and anterior pituitary hormones in a rat model standardized for gender, food intake, and time after surgery. *Steroids* 1991; **56**: 237-241
41 **Mezey E**. Liver disease and nutrition. *Gastroenterology* 1978; **74**: 770-783
42 **Ghabriel MN**, Lu JJ, Hermanis G, Zhu C, Setchell BP. Expression of a blood-brain barrier-specific antigen in the reproductive tract of the male rat. *Reproduction* 2002; **123**: 389-397
43 **Itoh N**, Nanbu A, Tachiki H, Akagashi K, Nitta T, Mikuma N, Tsukamoto T, Kumamoto Y. Restoration of testicular transferrin, insulin-like growth factor I (IGF-1), and spermatogenesis by exogenously administered purified FSH and testosterone in medically hypophysectomized rats. *Arch Androl* 1994; **33**: 169-177
44 **Rappaport MS**, Smith EP. Insulin-like growth factor-I inhibits aromatization induced by follice-stimulating hormone in rat Sertoli cell culture. *Biol Reprod* 1996; **54**: 446-452
45 **Prati M**, Palmero S, de Marco P, Trucchi P, Fugassa E. Effect of insulin-like growth factor-I on sertoli cell metabolism in the pubescent rats. *Boll Soc Ital Biol Sper* 1992; **68**: 121-128
46 **Waites GM**, Gladwell RT. Physiological significance of fluid secretion in the testis and blood-testis barrier. *Physiol Rev* 1982; **62**: 624-671
47 **Farghali H**, Williams DS, Gavaler J, Van Thiel DH. Effect of short-term ethanol feeding on rat testes as assessed by 31P NMR spectroscopy, 1H NMR imaging, and biochemical methods. *Alcohol Clin Exp Res* 1991; **15**: 1018-1023
48 **Salonen J**, Eriksson CJ. Penetration of ethanol into the male reproductive tract. *Alcohol Clin Exp Res* 1989; **13**: 746-751
49 **Adam CL**, Gadd TS, Findlay PA, Wathes DC. IGF-1 stimulation of LH secretion, IGF—binding proteins (IGFBPs) and expression of mRNAs for IGFs, IGF receptors and IGFBPs in the ovine pituitary gland. *J Endocrinol* 2000; **166**: 247-254
50 **Carneiro G**, Lorenzo P, Pimentel C, Pegoraro L, Bertolini M, Ball B, Anderson G, Liu I. Influence of IGF-1 and its interaction with gonadotropins, estradiol, and fetal calf serum on *in vitro* maturation and parthenogenic development in equine oocytes. *Biol Reprod* 2001; **65**: 899-905
51 **Xia YX**, Weiss JM, Polack S, Diedrich K, Ortmann O. Interactions of IGF-1, insulin and estradiol with GnRH-stimulated luteinizing hormone release from female rat gonadotrophs. *Eur J Endocrinol* 2001; **144**: 73-79

Edited by Zhu LH and Xu FM

PO Box 2345, Beijing 100023, China
Fax: +86-10-85381893
E-mail: wjg@wjgnet.com www.wjgnet.com

World J Gastroenterol 2004;10(17):2535-2539
World Journal of Gastroenterology
Copyright © 2004 by The WJG Press ISSN 1007-9327

• CLINICAL RESEARCH •

Enterobius vermicularis infection among population of General Mansilla, Argentina

Betina C Pezzani, Marta C Minvielle, María M de Luca, María A Córdoba, María C Apezteguía, Juan A Basualdo

Betina C Pezzani, Marta C Minvielle, María M de Luca, María A Córdoba, Juan A Basualdo, Cátedra de Microbiología y Parasitología, Facultad de Ciencias Médicas, Universidad Nacional de La Plata1900, Argentina
María C Apezteguía, Comisión de Investigaciones Científicas de la provincia de Buenos Aires
Supported by the Agencia Nacional de Promoción Científica y Técnica de la Argentina, the Alberto J. Roemmers Foundation, and the Universidad Nacional de La Plata, and it was declared of Municipal Interest by the town of Magdalena, Province of Buenos Aires, Argentina
Correspondence to: Juan A Basualdo, Cátedra de Microbiología y Parasitología, Facultad de Ciencias Médicas, Universidad Nacional de La Plata, Calle 60 y 120 s/n, La Plata 1900, Argentina. jabasua@atlas.med.unlp.edu.ar
Telephone: +54-221-4258987 **Fax:** +54-221-4258987
Received: 2004-02-28 **Accepted:** 2004-04-29

Abstract

AIM: To evaluate the relationships between the personal, sociocultural, and environmental characteristics, and the presence or absence of symptoms with the detection of *Enterobius vermicularis* (*E. vermicularis*) in a population sample in our region (General Mansilla, Province of Buenos Aires, Argentina), by individual and familiar analyses.

METHODS: *E. vermicularis* was diagnosed in 309 people from 70 family units residing in the urban area and the rural area of the city of General Mansilla. Each of them was surveyed so as to register personal, environmental and sociocultural data. Questions about the presence or absence of anal itch, abdominal pain and sleeping disorder were also asked. Significant associations were determined by square chi tests. Logistic regression models were adjusted by using a backward conditional stepwise method to determine the presence of this parasite in the individuals and in the families.

RESULTS: The parasites were found in 29.12% (90/309) of the individuals, with a frequency of 14.28% (20/140) among the heads of the families and of 41.42% (70/169) among the children. The only variables showing a significant association were affiliation, where the risk category was "being the son/daughter of", and the symptoms were abdominal pain, sleeping disorder, and anal itch. Families with a member infected with parasite were considered Positive Families (PF) and they were 40/70 (57.14%), only 5% (2/40) of the PF had 100% of their members infected with the parasite. The logistic regression models applied showed that the risk categories were mainly affiliation (son/daughter) and housing (satisfactory) among others.

CONCLUSION: The presence of *E. vermicularis* was proved in one third of the studied population. The frequency of families with all their members infected with the parasite was very low. Most of the studied personal, sociocultural, and environmental variables did not turn out to be significantly associated with the presence of the parasite. An association with the category of "son/daughter" and housing classified as "satisfactory" was determined. The latter may be due to the fact that the people living in that category of housing have hygienic practices at home that favour the distribution of the eggs in the environment. The presence of the analysed symptoms was associated with the presence of the parasite, thus strengthening the need of periodical control of the population showing at least one of these symptoms.

Pezzani BC, Minvielle MC, de Luca MM, Córdoba MA, Apezteguía MC, Basualdo JA. *Enterobius vermicularis* infection among population of General Mansilla, Argentina. *World J Gastroenterol* 2004; 10(17): 2535-2539
http://www.wjgnet.com/1007-9327/10/2535.asp

INTRODUCTION

Enterobius vermicularis (*E. vermicularis*) is a small whitish nematode whose evolution cycle differs from other intestinal helminths in the biological peculiarities[1].

Enterobiosis is a cosmopolitan parasitosis. The peculiar biology of *E. vermicularis* contributes to the creation of contamination foci around the infected resident and the re-infections. The intra-family or cohabitating members' infection is very frequent. The most important infection routes are through oral and respiratory tract. The oral infection included the anus-hand-mouth route, onychophagia and/or ingestion of contaminated food. The respiratory tract infection would be from inhaling dust contaminated with the parasite eggs[2].

The main source of contamination inside the house is found in the environmental dust and carried by children. This would be one of the infection routes for the family units.

It has been reported that no sex difference existed in the infection rates. The teen-age, however, infection rates remain unchanged in boys but decrease among girls, since girls start observing hygienic practices with higher precocity than boys[3,4]. Among adults, the infection frequency is similar in both sexes, but it was commonly observed that many adults seemed not to get infected even when subjected to contaminated environments due to personal hygiene[1-5].

Waste disposal little affects the distribution of the infection, since the oxyurus eggs are not found in excrement. Several groups in the population may be infected without depending on the socioeconomic conditions and environmental hygiene due to the biological characteristics of this parasite[6,7].

Generally, this parasitosis is an asymptomatic illness, and in those cases where clinical manifestations are present, anal itch is the most frequent symptom. Indirectly, and mainly in children, it produces insomnia, fatigue and irritability, and sometimes abdominal pain[2-8,9].

The objective of this study was to evaluate the relationship between the personal, socio-cultural and environmental characteristics, presence or absence of symptoms, and the detection of *E. vermicularis* in a sample population in our region (Province of Buenos Aires, Argentina), through individual and family analysis.

MATERIALS AND METHODS

Study area

The city of General Mansilla is located in the northeast of the Province of Buenos Aires, in the central-western area of the Argentine Republic (South America), 96 km from the city of Buenos Aires. Population is 2 300 in the urban area and 1 700 in the rural area. The urban area covers 250 hectares and the rural population is settled in a 15 km range around it (Figure 1).

Population

A total of 309 people constituting 70 family units, made up by mother, father and children (1 to 6 per family), were studied. Fifty families were analyzed from the urban area (221 people) and 20 from the rural area (88 people). Each member of the family was surveyed to record personal, environmental and socio-cultural data. The following variables were assessed: a) personal: sex, age, affiliation of each member, and number of children in each family; b) socio-cultural and environmental: habitat (urban area - rural area), water supply (water pump - running water), disposal of waste (sewer - no sewer), housing (satisfactory - unsatisfactory), home garbage (collected - not collected), bathroom (existent - non-existent), and overcrowding (yes - no). Housing was considered satisfactory when built of masonry with cement floors, and unsatisfactory when built of wood and/or metal with dirt floors. Overcrowding was considered when more than three individuals slept together in the same room. Besides, questions were asked about the presence or absence of the following symptoms: anal itch, abdominal pain and sleeping disorders, since they are considered to be typical of this parasitosis.

Parasitological analysis

A perianal swab method was performed to each surveyed individual for the detection of *E. vermicularis*. Each surveyed person was given five 10 cm×10 cm gauze pads and a bottle of 5% formaldehyde. At the same time, they were explained the procedure for sample taking. In the case of minors, instructions were given to their parents. Each of the testee collected the sample before getting up for 5 consecutive days, each day rubbing a gauze pad previously imbibed in water, on the perianal margins. Then, they put the sample in the container with formaldehyde and sent it to the lab.

Statistical analysis

The association between each of the variables studied and the presence of *E. vermicularis* was analyzed by means of the chi square test. In the case of finding statistically significant associations, the odds ratio (OR) was calculated.

Logistic regression models were adjusted by using backward conditional stepwise method to determine the presence of *E. vermicularis* in individuals and in families. In the case of individuals (total, rural and urban), socio-cultural and environmental characteristics, symptoms, age and sex were used as (independent) explanatory variables. In the case of families, only socio-cultural and environmental characteristics and affiliation were used. The logistic regression model predicts the probability of being infected with *E.vermicularis* according to the explanatory variables. From this prediction, individuals are classified according to their risk of infection as: high risk (when the probability is higher than 0.5), and low risk (when the probability is lower than 0.5). For this classification, sensitivity (S), specificity (E), positive predictive value and negative predictive value, and global adjustment (total percentage of correct predictions) in each of the models were estimated. The model can be used to obtain OR estimators for each variable. SPSS (Statistical Package for the Social Sciences) software version 11.5 was used.

RESULTS

The frequency of infected people in the total studied population (309) was 29.12% (90/309). Among the parents, it was 14.28% (20/140) and 41.42% (70/169) among the children.

Families with at least one infected member were called positive families (PF) and the rest, negative families (NF). The number of PF was 40/70 (57.14%). Of these, 8 families presented less than 25% of their members with the parasite, 20 had 26-50%, 6 between 51% and 75%, 4 between 76% and 99% and only two had 100% of their members infected.

The mean age of parents from PF and NF was 32.3 and 33.6, respectively. The mean age for children from PF and NF was 8.48 and 7.71, respectively. The mean age of positive children was 6.85. Thirty percent (12/40) of the mothers from PF were infected while only 20% (8/40) of the fathers were infected. Prevalence for adults from PF was 25% (20/80).

The number of children from PF was 103. Of these, 67.96% (70/103) were positive and 52.85% (37/70) were male. The number of children from NF was 66, 48.48% (32/66) of which were male.

The results obtained from socio-cultural and environmental aspects both from PF and NF and their statistical analysis are shown in Table 1.

Table 1 Sociocultural and environmental factors studied in 70 *E. vermicularis* infected and non-infected families in General Mansilla, Province of Buenos Aires, Argentina (*n*, %)

Variable		PF (n = 40)	FN (n = 30)	P
Habitat	Urban	29 (72.5)	21 (70)	0.8188
	Rural	11 (27.5)	9 (30)	
Water supply	Water pump	12 (30)	13 (43.33)	0.2493
	Running water	28 (70)	17 (56.66)	
Disposal of waste	Sewer	14 (35)	8 (26.66)	0.4573
	No sewer	26 (65)	22 (73.33)	
[1]Housing	Satisfactory	30 (75)	20 (66.66)	0.4450
	Unsatisfactory	10 (25)	10 (33.33)	
Garbage	Collected	28 (70)	21 (70)	1.0000
	Not collected	12 (30)	9 (30)	
Bathroom	Existent	25 (62.5)	22 (73.33)	0.3396
	Non-existent	15 (37.5)	8 (26.66)	
[2]Overcrowding	Yes	17 (42.5)	9 (30)	0.2841
	No	23 (57.5)	21 (60)	

PF: Families with some member infected with *E. vermicularis*; NF: Families with no member infected with *E. vermicularis*. [1]Satisfactory housing: With cement floors and masonry walls; unsatisfactory housing: Dirt floors and wood or metal walls. [2]Overcrowding: Yes: when more than three people sleep in a room; No: When less than three people sleep in a room.

When analyzing the association between the presence of *E.vermicularis* and each variable separately, the only one showing statistically significant association was affiliation, where the risk category was being the son/daughter (P = 0.000, OR = 4.242), and the symptoms of abdominal pain (P = 0.001, OR = 2.680), sleeping disorders (P = 0.003, OR = 2.339), and anal itch (P = 0.001, OR = 2.662).

Table 2 (a, b, c and d) shows the results from the logistic regression models built for the total of individuals, those residing in the urban area, those living in the rural area, and the families.

(1) In the whole population, the affiliation variable was the most significant, that is, children had greater probability of being infected than parents. In order of importance, the variables garbage collection and type of housing followed. Type of water supply and symptoms of abdominal pain and sleeping disorders

turned out to be of lesser importance. This model classified 22.2% of the infected individuals (S) and 92.2% of the non-infected individuals (E) correctly. Globally, it classified 71.8% of the individuals correctly.

(2) Among the rural population the affiliation variable had an even higher significance degree. It also turned out to be important age variable. This continuous variable had a positive coefficient, which implies that at an older age there is more risk to be infected. But being the affiliation variable present, older children are those with the higher risk of being infected. In order of importance, the symptom of sleeping disorders, type of housing and no bathroom available followed. This model classified 53.8% of the positive individuals (S), and 93.3% of the non-infected individuals (E) correctly. Globally, it classified 81.4% of the individuals correctly.

(3) Among the urban population, the affiliation variable was also the most significant. The symptom of abdominal pain, type of water supply and type of housing followed. This model classified 23.4% of the infected individuals (S) and 89.3% of the non-infected individuals (E) correctly. Globally, it classified 70.4% of the individuals correctly.

(4) Among the positive families, the variables of garbage collection, housing, water supply and bathroom had a similar degree of significance. This model classified 95% of the infected families (S) and 23% of the non-infected families (E) correctly. Globally, it classified 64.3% of the families correctly.

Table 2 Logistic regression models for the presence of *E. vermicularis* in 309 (88 rural and 221 urban) individuals, both individually and grouped into 70 families in General Mansilla, Argentina

Variable	Risk category	Coefficient	Odds Ratio
For the total of individuals, *n* = 309			
Affiliation	Son / daughter	1.267	3.550
Housing	Satisfactory	0.829	2.288
Garbage	Not collected	1.372	3.944
Water	Running	0.951	2.591
Abdominal pain	Present	0.555	1.742
Sleeping disorders	Present	0.561	1.752
Constant	-1.825		
For rural individuals, *n* = 88			
Affiliation	Son / daughter	10.246	28 167
Housing	Satisfactory	2.857	17.5
Age (yr)	Eldest son / daughter	0.316	1.372
Bathroom	Non-existent	2.160	8.670
Sleeping disorders	Present	1.967	7.151
Constant	-12.493		
For urban individuals, *n* = 221			
Affiliation	Son / daughter	1.176	3.241
Housing	Satisfactory	0.917	2.5
Water	Running	1.372	3.937
Abdominal pain	Present	0.690	1.993
Constant	-1.612		
For positive families, *n* = 40			
Housing	Satisfactory	2.749	15.625
Water	Running	2.614	13.699
Garbage	Not collected	2.75	15.636
Bathroom	Non-existent	2.403	11.056
Constant	0.338		

Regarding the three studied symptoms, the analysis showed anal itch in 19.41% (60/309) of the people. Of them, 27/60 (45%) were positive for *E. vermicularis* ($P = 0.0026$, OR = 2.42), 12/60 (20%) were negative but belonged to a PF, and 21/60 (35%) were negative from NF. The presence of sleeping disorders was shown in 22.65% (79/309) of the studied population, 30/70 (42.85%) ($P = 0.0040$, OR = 2.24) of which were parasite infected, 17/70 (24.28%) showed no parasites but belonged to a PF, and 23/70 (32.85%) were negative from NF.

Abdominal pain was detected in 19.41% (60/309) of the testees, 28/60 (46.66%) ($P = 0.009$, OR = 2.64) of which were parasite infected individuals, 12/60 (20%) were negative for the parasite test but belonged to a PF, and 20/60 (33.33%) were negative from NF.

Figure 1 Geographical location of General Mansilla city in Argentina.

DISCUSSION

In the present study a high frequency of infection was found for *E. vermicularis*, going from 29.12% in the total population up to 41.42% if only the child population considered. These percentages are higher than those published in other countries. In Korea, a prevalence of this parasitosis was reported in 9.8% of school children[10], 9.2% in pre-schoolers[3], 14.8 in kindergarten children[11], 12.6% in school children in the rural area[4], and 9.8% in children of school age[12]. In the town of Chennai, India, a prevalence of 0.50% was reported[13] in school age children. In Thailand, in 5- to 10-year-old children, the prevalence was 21.91%[7]. In Taiwan it was 11% in school age children[14]. A prevalence of 10.5% was found for children between 7 and 13 years old in Turkey[15]. A study carried out in 18- to 35-year-old adults in Malaysia, Kuala Lumpur, reported a frequency of 9.2%[16,17]. In Poland, the frequency among 7-year-old children was 16.45%[19]. And in Sweden, it was 21% in children from primary care centres[18].

In America, a study carried out in New York (United States) on the prevalence of *E.vermicularis* in mentally and developmentally retarded children showed a prevalence of 4.5%[19]. In Venezuela, the prevalence found in 5- to 14-year-old children was 19.1%[20], and in Peru it was 1.1% in adults and children from different communities[21]. In Argentina, a study carried out in two aboriginal communities from the province of Misiones, a prevalence of 0% and 5% for *E. vermicularis* was shown[22]. In the Province of La Rioja, a percentage of 14.8% was reported in middle-class children[23], and in the city of Buenos Aires, 20.50% was reported in hospital population[24]. In Neuquen (Patagonia), 18.8% was reported in adults and children from deprived neighbourhoods[25].

However, the high frequency shown in our study is similar to that reported by Norhayati *et al*.[26] in 1994 in Malaysia (40.4%), Nithikathkul *et al*.[6] in 2001 in Thailand (38.82%), Bahader *et al*.[27] in 1995 in Egypt (43.8%), Gilman *et al*.[28] in 1991 in Peru

(42.0%), and Mercado *et al*.[29] in 1996 in Chile (35.2%) on studies done in diverse populations.

This study did not show significant sex and age differences regarding parasite infected parents, but there was a higher frequency among the mothers, probably due to the greater daily contact with their parasite infected children (regular behaviour among the inhabitants of this region).

The children had a higher probability of being infected than the parents. As to the infected children, no statistically verifiable differences could be found regarding sex or age but, unlike the parents, the highest level of infected people were male, probably in association with different hygienic practices for each sex. This difference agrees with Yoon *et al*'s[3] report about 10.1% of boys and 8.1% of girls with parasites, and Kim *et al*'s[10] about 10.8% in male and 8.7% in female schoolchildren. However, Kim[10] reports 7.1% and 12.5% positive values for male and female kindergarten children, respectively. In our study, parasite infected kindergarten infantile population, sex distribution was 50% (13/26).

Among the PF there was a high percentage of non-infected parents and only 5% of these families had all of their members infected. With these results we could infer that when someone is detected to have parasites, the treatment of all the members of his/her family is not necessary, especially if we take into account that the cost of the treatment has to be afforded by each family in our region. This would make a regular control of the population so as to detect positive cases and treat them appropriately and thus reduce the prevalence of this parasitosis.

Socio-cultural and environmental factors studied in this study showed no statistically significant associations between PF and NF, which are in agreement with Nithikathkul *et al*.[7] not with Kim *et al*.[10].

Overcrowding was significantly associated for Acosta *et al*[1] ($P<0.001$) with this parasitosis in children in Venezuela, but this association could not be shown in our study, in agreement with Norhayati *et al*.'s findings in children in Malaysia[26].

In this study, a significant association was proved by the presence of anal itch, sleeping disorders and abdominal pain, and the detection of this parasite. But these symptoms were not exclusive for the parasite-infected population since 20% to 35% of the non-parasite infected people showed at least one of these symptoms. Venezuela[1] reported that 53.9% of the parasite-infected population showed anal itch.

As a conclusion of this work we point out that enterobiosis was present in a percentage close to 30% of the general population and over 40% in children in our region (Province of Buenos Aires, Argentina).

Contrary to what was expected, the risk of getting this helminthosis was not related to age, sex, or most of the socio-cultural and environmental factors studied (habitat, consumption water, disposal of waste, garbage collection, bathroom characteristics and overcrowding). An association was determined between the variable affiliations, where the risk category was "being the son/daughter of".

The type of housing categorized as "satisfactory" was also related to this parasitosis. This contradictory situation could be due to the fact that people living in this type of housing show hygienic practices in the home favouring the distribution of eggs in the atmosphere (*e.g.*, shaking the sheets, using a feather dust for cleaning, *etc*.)

These results also strengthen the need of regular control of the population reporting at least one of these symptoms: anal itch, sleeping disorders, and/or abdominal pain.

ACKNOWLEDGEMENTS

The authors wish to thank Dr. Roberto Zungri for his permanent "field work" contribution to this study.

REFERENCES

1 **Acosta M**, Cazorla D, Garvett M. Enterobiasis among school-children in a rural population from Estado Falcon, Venezuela, and its relation with socioeconomic level. *Invest Clin* 2002; **43:** 173-181
2 **Atias A.** Enterobiosis u Oxiuriosis. In: Atías A, ed. Parasitología Médica. *Editorial Mediterráneo, Santiago, Chile* 1999: 188-193
3 **Yoon HJ**, Choi YJ, Lee SU, Park HY, Huh S, Yang YS. Enterobius vermicularis egg positive rate of pre-school children in Chunchon, Korea (1999). *Korean J Parasitol* 2000; **38:** 279-281
4 **Kim BJ**, Yeon JW, Ock MS. Infection rates of Enterobius vermicularis and Clonorchis sinensis of primary school children in Hamyang-gun, Gyeongsangnam-do (province), Korea. *Korean J Parasitol* 2001; **39:** 323-325
5 **Smolyakov R**, Talalay B, Yanai-Inbar I, Pak I, Alkan M. Enterobius vermicularis infection of female genital tract: a report of three cases and review of literature. *Eur J Obstet Gynecol Reprod Biol* 2003; **107:** 220-222
6 **Nithikathkul C,** Changsap B, Wannapinyosheep S, Poister C, Boontan P. The prevalence of Enterobius vermicularis among primary school students in Samut Prakan Province, Thailand. *Southeast Asian J Trop Med Public Health* 2001; **32**(Suppl 2)**:** 133-137
7 **Nithikathkul C**, Changsap B, Wannapinyosheep S, Poister C, Boontan P. The prevalence of enterobiasis in children attending mobile health clinic of Huachiew Chalermprakiet University. *Southeast Asian J Trop Med Public Health* 2001; **32** (Suppl 2): 138-142
8 **Grencis RK**, Cooper ES. Enterobius, trichuris, capillaria, and hookworm including ancylostoma caninum. *Gastroenterol Clin North Am* 1996; **25:** 579-597
9 **Nokes C**, Bundiy DA. Compliance and absenteeism in school children: implications for helminth control. *Trans R Soc Trop Med Hyg* 1993; **87**: 148-152
10 **Kim BJ**, Lee BY, Chung HK, Lee YS, Lee KH, Chung HJ, Ock MS. Egg positive rate of Enterobius vermicularis of primary school children in Geoje island. *Korean J Parasitol* 2003; **41:** 75-77
11 **Lee KJ**, Lee IY, Im K. Enterobius vermicularis egg positive rate in a primary school in Chungchongnam-do (province) in Korea. *Korean J Parasitol* 2000; **38:** 177-178
12 **Lee KJ**, Ahn YK, Ryang YS. Enterobius vermicularis egg positive rates in primary school children in Gangwon-do (province), Korea. *Korean J Parasitol* 2001; **39:** 327-328
13 **Fernandez MC**, Verghese S, Bhuvaneswari R, Elizabeth SJ, Mathew T, Anitha A, Chitra AK. A comparative study of the intestinal parasites prevalent among children living in rural and urban settings in and around Chennai. *J Commun Dis* 2002; **34:** 35-39
14 **Fan PC**. Review of enterobiasis in Taiwan and offshore islands. *J Microbiol Immunol Infect* 1998; **31:** 203-210
15 **Gurses N**, Ozkan Y, Peksen Y, Uysal S, Aydin M. Intestinal parasites in primary schools of different socioeconomic status and environmental conditions. *Mikrobiyol Bul* 1991; **25:** 57-62
16 **Oothuman P**, Noor Hayati MI, Mastura MH, Rampal L, Jeffery J, Rubiah M, Ismail G, Fatmah MS. Prevalence of Enterobius vermicularis amongst adults living in hostels by six successive day examination. *Southeast Asian J Trop Med Public Health* 1992; **23**: 82-86
17 **Plonka W**, Dzbenski TH. The occurrence of intestinal parasites among children attending first classes of the elementary schools in Poland in the school year 1997/1998. *Przegl Epidemiol* 1999; **53:** 331-338
18 **Herrstrom P**, Fristrom A, Karlsson A, Hogstedt B. Enterobius vermicularis and finger sucking in young Swedish children. *Scand J Prim Health Care* 1997; **15:** 146-148
19 **Schupf N**, Ortiz M, Kapell D, Kiely M, Rudelli RD. Prevalence of intestinal parasite infections among individuals with mental retardation in New York State. *Ment Retard* 1995; **33:** 84-89
20 **Devera R**, Perez C, Ramos Y. Enterobiasis in students from Ciudad Bolivar, Venezuela. *Bol Chil Parasitol* 1998; **53:** 14-18
21 **Maco Flores V**, Marcos Raymundo LA, Terashima Iwashita A, Samalvides Cuba F, Gotuzzo Herencia E. Distribution of

entero-parasitic infections in the Peruvian Highland: study carried out in six rural communities of the department of Puno, Peru. *Rev Gastroenterol Peru* 2002; **22**: 304-309

22 **Ilkow C**, Digiani MC, Navone GT. Prevalencias y cargas parasitarias intestinales en dos comunidades mbya guaraní (provincia de Misiones, Argentina). [Intestinal prevalences and burden in two mbya guaraní communities- province of Misiones, Argentina)] 3º Congreso Argentino de Parasitología 2000. *Libro de Resúmenes. Tomo II,* p 393

23 **Flores J,** Páez S, Toro A, Bellegarde E, Córdoba P. Prevalencia de *Enterobius vermicularis* en la capital de la provincia de la rioja. [Prevalence of Enterobius vermicularis in the capital city of La Rioja´s province] 3º Congreso Argentino de Parasitologia 2002. *Libro de Resúmenes. Tomo II, p* 418

24 **Menghi C**, Clementel V, Zadcovich S, Gatta C, Fernández GG, Szmulewicz G, Mendez O. Enteroparasitosis halladas en una población asistida en un hospital de la ciudad de Buenos Aires. [Enteroparasitoses in hospital population of Buenos Aires city] 3º Congreso Argentino de Parasitología 2000. *Libro de Resúmenes. Tomo II, p* 425

25 **Soriano SV**, Barbieri LM, Pierangeli NB, Giayetto AL, Manacorda AM, Castronovo E, Pezzani BC, Minvielle M, Basualdo JA. Intestinal parasites and the environment: Frequency of intestinal parasites in children of Neuquen, Patagonia, Argentina. *Rev Latinoam Microbiol* 2001; **43**: 96-101

26 **Norhayati M**, Hayati MI, Oothuman P, Azizi O, Fatmah MS, Ismail G, Minudin YM. Enterobius vermicularis infection among children aged 1-8 years in a rural area in Malaysia. *Southeast Asian J Trop Med Public Health* 1994; **25**: 494-497

27 **Bahader SM**, Ali GS, Shaalan AH, Khalil HM, Khalil NM. Effects of Enterobius vermicularis infection on intelligence quotient (I.Q) and anthropometric measurements of Egyptian rural children. *J Egypt Soc Parasitol* 1995; **25:** 183-194

28 **Gilman RH**, Marquis GS, Miranda E. Prevalence and symptoms of *Enterobius vermicularis* infections in a Peruvian shanty town. *Trans R Soc Trop Med Hyg* 1991; **85:** 761-764

29 **Mercado R**, García M. Various epidemiological aspects of *enterobius vermicularis* infection inpatients served at public outpatient clinics and hospitals from the northern section of Santiago, Chile, 1995. *Bol Chil Parasitol* 1996; **51:** 91-94

Edited by Chen WW **Proofread by** Xu FM

PO Box 2345, Beijing 100023, China
Fax: +86-10-85381893
E-mail: wjg@wjgnet.com www.wjgnet.com

World J Gastroenterol 2004;10(17):2540-2543
World Journal of Gastroenterology
Copyright © 2004 by The WJG Press ISSN 1007-9327

• CLINICAL RESEARCH •

Possible causes of central pontine myelinolysis after liver transplantation

Jun Yu, Shu-Sen Zheng, Ting-Bo Liang, Yan Shen, Wei-Lin Wang, Qing-Hong Ke

Jun Yu, Shu-Sen Zheng, Ting-Bo Liang, Yan Shen, Wei-Lin Wang, Qing-Hong Ke, Department of Hepatobiliary Surgery, the First Affiliated Hospital, Medical School of Zhejiang University, Hangzhou 310003, Zhejiang Province, China
Correspondence to: Professor Shu-Sen Zheng, Department of Hepatobiliary Surgery, the First Affiliated Hospital, Medical School of Zhejiang University,Hangzhou 310003, Zhejiang Province, China. zhengss@mail.hz.zj.cn
Telephone: +86-571-87236616
Received: 2003-10-24 **Accepted:** 2003-12-22

Abstract

AIM: To sum up the clinical characteristics of patients with central pontine myelinolysis (CPM) after orthotopic liver transplantation (OLT) and to document the possible causes of CPM.

METHODS: Data of 142 patients undergoing OLT between January 1999 to May 2003 were analyzed retrospectively. Following risk factors during perioperation were analyzed in patients with and without CPM: primary liver disease, preoperative serum sodium level, magnesium level and plasma osmolality, fluctuation degree of serum sodium concentration, and immunosuppressive drug level, *etc*.

RESULTS: A total of 13 (9.2%) neurologic symptoms appeared in 142 patients post-operation including 5 cases (3.5%) with CPM and 8 cases (5.6%) with cerebral hemorrhage or infarct. Two patients developing CPM after OLT had a hyponatremia history before operation (serum sodium<130 mmol/L), their mean serum sodium level was 130.6±5.54 mmol/L. The serum sodium level was significantly lower in CPM patients than in patients without neurologic complications or with cerebral hemorrhage/infarct (P<0.05). The increase in serum sodiumduring perioperative 48 h after OLT in patients with CPM was significantly greater than that in patients with cerebral hemorrhage/infarct but without neurologic complications (19.5±6.54 mmol/L, 10.1±6.43 mmol/L, 4.5±4.34 mmol/L, respectively, P<0.05). Plasma osmolality was greatly increased postoperation in patients with CPM. Hypomagnesemia was noted in all patients perioperation, but there were no significant differences between groups. The duration of operation on patients with CPM was longer than that on others (492±190.05 min, P<0.05). Cyclosporin A (CsA) levels were normal in all patients, but there were significant differences between patients with or without neurologic complications (P<0.05).

CONCLUSION: CPM may be more prevalent following liver transplantation. Although the diagnosis of CPM after OLT can be made by overall neurologic evaluations including magnetic resonance imaging (MRI) of the head, the mortality is still very high. The occurance of CPM may be associated with such factors as hyponatremia, rapid rise of serum sodium concentration, plasma osmolality increase postoperation, the duration of operation, and high CsA levels.

Yu J, Zheng SS, Liang TB, Shen Y, Wang WL, Ke QH. Possible causes of central pontine myelinolysis after liver transplantation. *World J Gastroenterol* 2004; 10(17): 2540-2543
http://www.wjgnet.com/1007-9327/10/2540.asp

INTRODUCTION

The morbidity and mortality of central nervous system (CNS) complications after orthotopic liver transplantation (OLT) was 19% and 47% respectively[1]. Central pontine myelinolysis (CPM)[2] is the most serious CNS complication that could be seen after OLT, and represents an important source of mortality early after OLT[3]. CPM following liver transplantation was reported more and more in foreign literatures[4,5], but it was rarely reported in our country[6,7].

In this paper, we studied retrospectively 142 patients undergoing OLT in our center. Fifteen patients had CNS complications after OLT including 5 patients with CPM. The clinical features and possible causes of CPM after liver transplantation were analyzed.

MATERIALS AND METHODS

Clinical data

Between January 1999 to May 2003, consecutive OLT was performed on 142 patients at our center. Medical records and clinical data of the patients were retrospectively investigated. Of them 117 were males and 25 females, age from 19 to 65 years, their age was 45±8.9 years. Indications for OLT included severe hepatitis 28 cases, hepatic cirrhosis (32 cases), liver carcinoma (53 cases), polycystic liver (3 cases), and others (24 cases). Operative procedures were performed with the standard technique and UW preservation solution. All patients had similar perioperative intensive care and received cyclosporin A (CsA) and methylprednisolone-based induction immunosuppression.

Observational indicators

Patients who developed posttransplant abnormal neurological symptoms underwent overall neurological evaluation. Magnetic resonance imaging (MRI) of head was performed in selected cases. CPM was diagnosed based on: (1) patients who had a variety of signs including mental status changes, quadriparesis, pseudobulbar palsy, and drowsiness, *etc*; (2) MRI showed a hypointense signal in T1-weighted images and a hyperintense signal in T2-weighted images in the central pontine. The signal of T2 was slightly increased after contrast administration.

Following risk factors during perioperation were analyzed between patients with and without CPM: age, gender, primary liver disease, pretransplant serum sodium , magnesium levels, plasma osmolality, fluctuation degree of serum sodium and plasma osmolality 48 h after transplantation, duration of operation, and CsA level. Hyponatremia was defined as serum sodium <130 mmol/L. Hypomagnesium was defined as serum magnesium <1.5 mg/L.

Statistical analysis

Data were expressed as mean±SD. Comparisons of group

means were made with ANOVA for unpaired data, and Chi-Square test for enumeration data. $P<0.05$ and $P<0.01$ were considered statistically significant.

RESULTS

Clinical features of patients with CNS complications

Fifty-eight of 142 patients undergoing OLT developed abnormal neurological symptoms such as mania, tremor, confusion, drowsiness, and diminished state of responsiveness. Thirteen patients were diagnosed having CNS complications based on clinical features and MRI. The demographic characteristics of the patients are outlined in Table 1. There were 10 males and 3 females aged 40-55 years. Primary diseases included severe hepatitis in 6 cases; hepatic cirrhosis in 4 cases; liver carcinoma, drug liver failure, IgA nephropathy, and polycystic liver in 1 case, respectively. Patients developed neurological complications in the early postoperative period including cerebral hemorrhage/infarct in 8 cases, CPM in 5 cases. The incidence of cerebral hemorrhage/infarct and CPM was 5.6% (8/142) and 3.5% (5/142), respectively. The extent of CPM on MRI was variable, showing a hypointensity signal of T1-weighted images in the pontine without space occupying sign (Figure 1A), and increased signal intensity of T2-weighted images in central pontine (Figure 2A, 2B). None of the patients showed extrapontine myelinolysis. CNS complications occurred two weeks after liver transplantation, ranged from 2 to 18 d. The median time of survival of patients with CPM after OLT was 24±16.1 d, ranged 7 to 48 d. The patients who were complicated with cerebral hemorrhage or infarct survived 2 to 96 d after transplantation, the mean time was 33±30.7 d.

Comparison of clinical characteristics in patients with and without CPM (Table 2)

Pretransplant hyponatremia was present in all symptomatic patients with CPM. Two patients developing CPM after OLT had a severe hyponatremia history before operation (serum sodium level <130 mmol/L). The average serum sodium level was 130.6±5.54 mmol/L. The serum sodium level was significantly lower in patients with CPM than in patients without neurologic complications or with cerebral hemorrhage/infarct ($P<0.05$). The average increase of perioperative serum sodium 48 h after OLT in patients with CPM, cerebral hemorrhage/infarct, and without CNS complications was 19.5±6.54 mmol/L, 10.1±6.43 mmol/L, 4.5±4.34 mmol/L, respectively ($P<0.01$). Plasma osmolarity was greatly increased 48 h postoperation in patients with CPM. Despite this, the plasma osmolality was normal in patients without CPM, but no significant difference was noted between patient who had complication of cerebral hemorrhage/infarct and patients who had no CNS complication. Hypomagnesemia was noted in all patients perioperation, but there were no significant differences between groups. The operation time for patients with CPM was longer than that for others ($P<0.05$). But no significant difference was found in operation time between patients who had complication of cerebral hemorrhage/infarct and those who had no CNS complication. Following transplantation, all patients received CsA-based induction immunosuppression. Though the mean CsA level in all patients was normal, the average CsA level was greatly higher in patients with CNS complications than in patients without CNS complications. Age, gender, primary liver disease were similar among three groups.

Table 1 Clinical characteristics of patients with CNS complications

Patient NO.	Hospital NO.	Age (yr)	Gender	Primary disease	CNS complication	Timing of onset (d)	Timing of survival (d)
1	287206	40	Male	Severe hepatitis	Cerebral hemorrhage	6	11
2	286967	48	Male	Severe hepatitis	CPM	10	15
3	291172	41	Female	Severe hepatitis	Cerebral hemorrhage	8	26
4	299921	54	Male	Severe hepatitis	CPM	6	23
5	306331	53	Female	polycystic liver	Cerebral infarct	4	28
6	312075	51	Male	Hepatic cirrhosis	Cerebral hemorrhage	2	9
7	314112	53	Male	Severe hepatitis	CPM	18	48
8	325113	49	Male	Liver carcinoma	Cerebral hemorrhage	2	2
9	315349	41	Male	Hepatic cirrhosis	CPM	3	20
10	328762	46	Male	Drug liver failure IgA nephropathy	CPM	5	7
11	351480	55	Female	Hepatic cirrhosis	Cerebral hemorrhage	14	56
12	362960	52	Male	Hepatic cirrhosis	Cerebral hemorrhage	3	36
13	363980	46	Male	Severe hepatitis	Cerebral hemorrhage	14	96

Table 2 Comparison of Clinical characteristics in patients with and without CPM

Index	CNS Complications		NO CNS Complication
	CPM	Cerebral hemorrhage /cerebral infarct	
Preoperative serum sodium (mmol/L)	130.6±5.54[bc]	135.9±2.61	137.4±3.83
Preoperative serum magnesium (mg/L)	0.8±0.19	0.9±0.20	1.0±0.21
Preoperative sosm (mOsm/kg H_2O)	274.3±33.09	290.2±22.12	292.5±26.05
Change in serum sodium After 48 h (mmol/L)	19.5±6.54[bd]	10.1±6.43[b]	4.5±4.34
Postoperative sosm (mOsm/kg H_2O)	341.6±14.99[bc]	317.9±29.76	308.8±16.89
Surgery time (min)	492.0±190.05[a]	450.0±93.50	399.9±76.07
CsA level (ng/dL)	301.3±9.23[b]	273.8±28.55[a]	247.2±35.44

Abbreviations: Sosm: Serum Osmolarity [a]$P<0.05$ (0.016, 0.037), [b]$P<0.01$ (0.000, 0.001) compared with no CNS complications; [c]$P<0.05$ (0.017, 0.02), [d]$P<0.01$ (0.000) compared with cerebral hemorrhage/infarct.

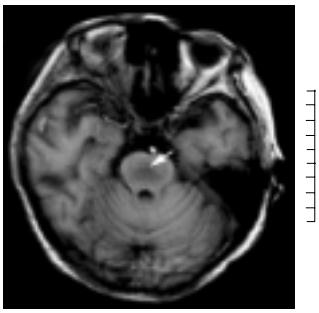

Figure 1 T1-Weighted axial magnetic resonance imaging scan shows symmetric area of hypointensity in the pons. (arrow).

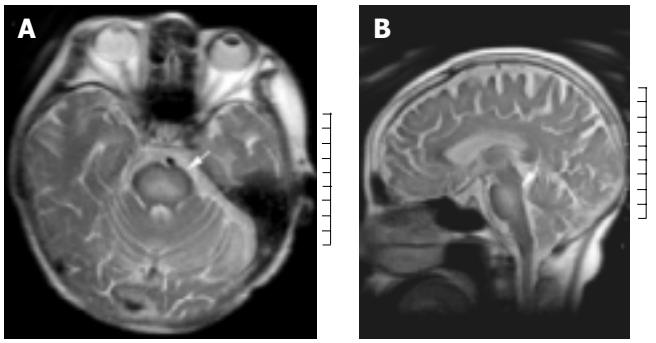

Figure 2 A: T2-Weighted axial magnetic resonance imaging shows bilaterally symmetric high-signal intensity is seen in the central pons. (arrow) B: T2-Weighted sagittal magnetic resonance imaging demonstrates hyperintensity area in central pons. (arrow).

DISCUSSION

CPM was first described in 1959 by Adams. CPM after OLT was first reported by Starzl[8] in 1978. CPM[9,10] was characterized by symmetrical loss of myelin in the pontine basalis, with relatively well-preserved axons and neuronal cell bodies. Acute CPM often occurred and had a variety of signs including quadriparesis, pseudobulbar palsy, and locked-in syndrome. As a severe neurological complication, the progress of CPM was usually dismal, with a high mortality rate[11]. Most cases of CPM were diagnosed post-morten. With the recognition of CPM and the development in MRI technology, more cases of CPM could be diagnosed while patients were alive. Liver transplant recipients constituted a high risk group for developing CPM. The incidence of CPM after OLT varied from 5-10%[12-14], which was higher than that in other patients (0.16-5.8%)[15]. The exact etiology of CPM is uncertain, the rapid correction of hyponatremia might be an important factor. However, controversy has been going on[16-20].

Pathogenesis of CPM after OLT

End-stage hepatic insufficiency was a common feature of pretransplanted patients. Advanced liver failure was always associated with some degree of renal insufficiency. So almost all hyponatremic states associated with liver disease were chronic and difficult to be corrected[21]. Input for patients after OLT was considerably increased as a consequence of bleeding during operation. The sodium content for fresh frozen plasma was around 165 mmol/L, 150 mmol/L for albumin solution, and 140 mmol/L for red blood cells, significantly higher than the serum sodium of patients with hyponatremia. Correction of blood loss would thus inevitably lead to a rapid rise in serum sodium concentration. A multicenter study showed[22] that rapid correction of hyponatremia exceeding 18 mmol/L in the first 48 h was significantly associated with CPM. The present study demonstrated that not all patients with hyponatremia developed CPM. But increase of serum sodium 48 h after OLT in patients with CPM was 19.5±6.54 mmol/L, which was significantly higher than that in patients without CPM. Plasma osmolality was also greatly increased 48 h postoperation. The results of our study suggested that rapid correction of hyponatremia and abrupt change of plasma osmolality might account for the development of CPM. Liver failure might lead to disruption of astrocyte metabolism with resulting abnormalities of blood-brain barrier function and a decreased ability to generate new intracellular osmoles in response to osmotic changes. Thus, patients with liver transplantation were particularly susceptible to CPM[23,24]. Lien *et al*.[25] suggested that rapid correction of hyponatremia might produce acute dehydration of edematous brain, leading to high ion to organic osmolyte ratio, osmotic endothelial injury, and endothelial cell shrinkage with loosening of tight junctions. Subsequently, transvascular transport increased and myelinotoxic factors released. Because of an extensive gray-white matter admixture in the pontine, this anatomic arrangement could provide a suitable environment wherein myelinotoxic factors, chiefly derived from the richly vascular gray matter, could interact with surrounding bundles of myelin-containing white matter, then lead to demyelination viz development of CPM.

Dunn *et al*.[26] demonstrated the neurotoxicity of CsA in transplanted patients. Three cases developing CsA associated akinetic mutism after liver transplantation were reported by Bird *et al*.[27], two of three were identified by MRI. The CsA level in all patients was monitored and controlled in normal range. Although the mean in-hospital CsA level in CPM group was not different with that in cerebral hemorrhage/infarct group, the CsA leves in patients with CNS complications was higher than that in patients without CNS complications. In this study, pretransplant hypomagnesemia was noted in all patients after OLT. Previous study suggested[28] that CsA neurotoxicity could lead to massive white matter lesions. Hypomagnesemia might contribute to CsA neurotoxicity and was associated with development of CPM after OLT, although the mechanism of CPM is unclear.

The results of our study also suggested that operation time in patients with CPM was significantly longer than that in patients without CNS complications. But there were no differences in operation time between patients with cerebral hemorrhage/infarct and without CNS complications, indicating that CNS lesions in liver transplant recipients may be related with intraoperative bleeding, prolonged low blood perfusion.

Prevention and therapy of CPM after OLT

To our knowledge, at present there is no definitive therapy for CPM. Therefore, prevention of this condition has become crucial[29]. Slower correction of perioperative hyponatremia may be critical for patients undergoing OLT. The rate of correction should not exceed 15 mmol/L/24 h or 18 mmol/L/48 h. Major fluctuations in serum sodium during surgery should be avoided. Plasma osmolality level should be remained within normal reference, and aggressive magnesium replacement should be initiated for hypomagnesemia. To decrease the duration of operation and intraoperative bleeding, no veno-venous bypass should be recommended. Immunosuppressive agent concentrations should be carefully monitored and controlled to avoid neurotoxicity[30]. MRI of head should be performed when patients occurred neurologic and psychiatric symptoms after OLT[31,32]. The best way of preventing CPM was to perform transplantation at an early stage of the disease. More recently, subclinical CPM after OLT was reported[33], the patients were nearly asymptomatic, but MRI showed marked lesions in the pontine. According to these we suggest that the diagnosis of CPM should be considered in patients undergoing OLT with major electrolyte fluctuations, and high

immunosuppressive agent levels. MRI is currently the best modality available to identify CPM. Support treatment is very important for patients with CPM. It was reported that cortical hormonel, vitamin, and serum replacement were used in CPM[34]. Whether these therapies play a role in CPM remains to be determined.

Prognosis of CPM after OLT

A previous study showed[35] that the occurrence of CPM after OLT varied from 2 to 11 d, average 7 d. The prognosis of CPM is usually dismal, with a high mortality rate. The results of the present study demonstrated that CPM occurred 3 to 18 d OLT. The median time of survival after OLT was 24.6±16.13 d, ranged 7 to 48 d, the mortality was 100%. These liver transplant recipients with CPM were associated with the following aspects. (1) Patients with CPM often had other complications[36], such as infection, hemorrhage of digestive tract, and multi-organ failure. (2) Inadequate water intake and electrolyte derangements were not corrected due to CPM. (3) Venovenous bypass was used in part of transplantations[37,38], which led to the increase in operation time, interoperative bleeding, time of low perfusion. The limited number of patients in this study may account for the high mortality of CPM after OLT.

REFERENCES

1 **Bonham CA,** Dominguez EA, Fukui MB, Paterson DL, Pankey GA, Wagener MM, Fung JJ, Singh N. Central nervous system lesions in liver transplant recipients: prospective assessment of indications for biopsy and implications for management. *Transplantation* 1998; **66:** 1596-1604

2 **Kaiys-Wyllie M.** Central pontine myelinolysis: a multidisciplinary approach to care. *J Neurosci Nurs* 1994; **26:** 36-41

3 **Lampl C,** Yazdi K. Central pontine myelinolysis. *Eur Neurol* 2002; **47:** 3-7

4 **Singh N,** Yu VL, Gayowski T. Central nervous system lesions in adult liver transplant recipients: Clinical review with implications for management. *Medicine* 1994; **73:** 110-118

5 **Fryer JP,** Fortier MV, Metrakos P, Verran DJ, Asfar SK, Pelz DM, Wall WJ, Grant DR, Ghent CN. Central pontine myelinolysis and cyclosporine neurotoxicity following liver transplantation. *Transplantation* 1996; **61**: 658-661

6 **Xia SS.** Current status of liver transplantation in China. *Shijie Huaren Xiaohua Zazhi* 1999; **7**: 645-646

7 **Qian YB,** Cheng GH, Huang JF. Multivariate regression analysis on early mortality after orthotopic liver transplantion. *World J Gastroenterol* 2002; **8:** 128-130

8 **Starzl TE,** Schneck SA, Mazzoni G, Aldrete JA, Porter KA, Schroter GPJ, Koep LJ, Putnam CW. Acute neurological complications after liver transplantation with particular reference to intraoperative cerebral air embolus. *Ann Surg* 1978; **187:** 236-240

9 **Ferreiro JA,** Robert MA, Townsend J, Vinters HV. Neuropathologic findings after liver transplantation. *Acta Neuropathol* 1992; **84:** 1-14

10 **Wijdicks EF,** Blue PR, Steers JL, Wiesner RH. Central pontine myelinolysis with stupor alone after orthotopic liver transplantation. *Liver Transplant Surg* 1996; **2:** 14-16

11 **Menger H,** Jorg J. Outcome of central pontine and extrapontine myelindysis (*n* = 44). *J Neurol* 1999; **246:** 700-705

12 **Boon AP,** Carey MP, Adams DH, Buckels J, McMaster P. Central pontine myelinolysis in liver transplantation. *J Clin Pathol* 1991; **44:** 909-914

13 **Estol CJ,** Faris AA, Martinez AJ, Ahdab-Barmada M. Central pontine myelinolysis after liver transplantation. *Neurology* 1989; **39:** 493-498

14 **Bramhall SR,** Minford E, Gunson B, Buckels JAC. Liver transplantation in the UK. *World J Gastroenterol* 2001; **7:** 602-611

15 **Kleinschmidt-DeMasters BK,** Norenberg MD. Rapid correction of hyponatremia causes demyelination: relation to central pontine myelinolysis. *Science* 1981; **211**: 1068-1070

16 **Tien R,** Arieff AI, Kucharczyk W, Wasik A, Kucharczyk J. Hyponatremic encephalopathy: is central pontine myelinolysis a component? *Am J Med* 1992; **92:** 513-522

17 **Mast H,** Gordon PH, Mohr JP, Tatemichi TK. Central pontine myelinolysis: clinical syndrome with normal serum sodium. *Eur J Med Res* 1995; **1:** 168-170

18 **Oh MS,** Choi KC, Uribarri J, Sher J, Rao C, Carroll HJ. Prevention of myelinolysis in rats by dexamethasone or colchicine. *Am J Nephrol* 1990; **10:** 158-160

19 **Wszolek ZK,** McComb RD, Pfeiffer RF, Steg RE, Wood RP, Shaw BW Jr, Markin RS. Pontine and extrapontine myelinolysis following liver transplantation. Relationship to serum sodium. *Transplantation* 1989; **48:** 1006-1012

20 **Soni BM,** Vaidyanthan S, Watt JW, Krishnan KR. A retrospective study of hyponatremia in tetraplegic/paraplegic patients with a review of the literature. *Paraplegia* 1994; **32:** 597-607

21 **Palmer BF,** Gates JR, Lader M. Causes and management of hyponatremia. *Pharmacother* 2003; **37:** 1694-1702

22 **Sterns RH**, Cappuccio JD, Silver SM, Cohen EP. Neurologic sequelae after treatment of severe hyponatremia: a multicenter perspective. *J Am Soc Nephrol* 1994; **4:** 1522-1533

23 **Mueller AR,** Platz KP, Bechstein WO, Schattenfroh N, Stoltenburg-Didinger G, Blumhardt G, Christe W, Neuhaus P. Neurotoxicity after orthotopic liver transplantation. A comparison between cyclosporine and FK506. *Transplantation* 1994; **58:** 155-170

24 **Kanwal F,** Chen D, Ting L, Gornbein J, Saab S, Durazo F, Yersiz H, Farmer D, Ghobrial RM, Busuttil RW, Han SH. A model to predict the development of mental status changes of unclear cause after liver transplantation. *Liver Transpl* 2003; **9:** 1312-1319

25 **Lien YH.** Role of organic osmolytes in myelinolysis. A topographic study in rats after rapid correction of hyponatremia. *J Clin Invest* 1995; **95:** 1579-1586

26 **Dunn CJ,** Wagstaff AJ, Perry CM, Plosker GL, Goa KL. Cyclosporin: an updated review of the pharmacokinetic properties, clinical efficacy and tolerability of a microemulsion-based formulation (neoral) 1 in organ transplantation. *Drugs* 2001; **61:** 1957-2016

27 **Bird GL,** Meadows J, Goka J, Polson R, Williams R. Cyclosporin-associated akinetic mutism and extrapyramidal syndrome after liver transplantation. *J Neurol Neurosurg Psychiatry* 1990; **53:** 1068-1071

28 **Abbasoglu O,** Goldstein RM, Vodapally MS, Jennings LW, Levy MF, Husberg BS, Klintmalm GB. Liver transplantation in hyponatremic patients with emphasis on central pontine myelinolysis. *Clinical Transplantation* 1998; **12:** 263-269

29 **Harris CP,** Townsend JJ, Baringer JR. Symptomatic hyponatraemia: can myelinolysis be prevented by treatment? *J Neurol Neurosurg Psychiatry* 1993; **56:** 626-632

30 **Rodriguez J,** Benito-Leon J, Molina JA, Ramos A, Bermejo F. Central pontine myelinolysis associated with cyclosporin in liver transplantation. *Neurologia* 1998; **13:** 437-440

31 **Bernsen HJ,** Prick MJ. Improvement of central pontine myelinolysis as demonstrated by repeated magnetic resonance Imaging in a patient without evidence of hyponatremia. *Acta Neurol Belg* 1999; **99:** 189-193

32 **Bekiesinska-Figatowska M,** Bulski T, Rozyczka I, Furmanek M, Walecki J. MR imaging of seven presumed cases of central pontine and extrapontine myelinolysis. *Acta Neurobiol Exp* 2001; **61:** 141-144

33 **Kato T,** Hattori H, Nagato M, Kiuchi T, Uemoto S, Nakahata T, Tanaka K. Subclinical central pontine myelinolysis following liver transplantation. *Brain Dev* 2002; **24:** 179-182

34 **Soupart A,** Ngassa M, Decaux G. Therapeutic relowering of the serum sodium in a patient after excessive correction of hyponatremia. *Clin Nephrol* 1999; **51:** 383-386

35 **Bronster DJ,** Emre S, Boccagni P, Sheiner PA, Schwartz ME, Miller CM. Central nervous system complications in liver transplant recipients-incidence, timing, and long-term follow-up. *Clin Transplant* 2000; **14:** 1-7

36 **Zheng SS,** Liang TB, Xu X, Wang WL, Shen Y, Zhang M, Huang DS. Ten year's experience on liver transplantation in a single organ transplantation center. *Zhonghua Putong Waike Zazhi* 2003; **18:** 71-73

37 **Kokudo N,** Sugawara Y, Imamura H, Sano K, Makuuchi M. Sling suspension of the liver in donor operation: a gradual tape-repositioning technique. *Transplantation* 2003; **76:** 803-807

38 **Yan LN,** Wang W, Li B, Lu SC, Wen TF, Zeng Y, Cheng NS, Zhao JC, Lin QY, Chen XL, Wu XD, Jia QB, Zhou Y, Tu B, Wu YT. Venovenous byApass ahead of mobilization of the liver in orthotopic liver transplantation. *Hepatobiliary Pancreat Dis Int* 2003; **2:** 44-47

Edited by Wang XL and Xu FM

PO Box 2345, Beijing 100023, China
Fax: +86-10-85381893
E-mail: wjg@wjgnet.com www.wjgnet.com

World J Gastroenterol 2004;10(17):2544-2546
World Journal of Gastroenterology
Copyright © 2004 by The WJG Press ISSN 1007-9327

• BRIEF REPORTS •

Ecologic study of serum selenium and upper gastrointestinal cancers in Iran

Mehdi Nouraie, Akram Pourshams, Farin Kamangar, Masood Sotoudeh, Mohammad Hossein Derakhshan, Mohammad Reza Akbari, Hafez Fakheri, Mohammad Javad Zahedi, Kathleen Caldwell, Christian C. Abnet, Philip R. Taylor, Reza Malekzadeh, Sanford M. Dawsey

Mehdi Nouarie, Akram Pourshams, Masood Sotoudeh, Mohammad Hossein Derakhshan, Mohammad Reza Akbari, Hafez Fakheri, Mohammad Javad Zahedi, Reza Malekzadeh, Digestive Disease Research Center, Tehran University of Medical Sciences, Tehran, Iran
Farin Kamangar, Christian C. Abnet, Philip R. Taylor, Sanford M. Dawsey, National Cancer Institute, NIH, Bethesda, MD20895-8314, USA
Kathleen Caldwell, Centers for Disease Control, Atlanta, Georgia, USA
Correspondence to: Dr. Sanford M. Dawsey, Senior Investigator, Cancer Prevention Studies Branch, CCR, NCI, 6116 Executive Blvd., Suite 705, Bethesda, MD 20895-8314, USA. dawseys@mail.nih.gov
Telephone: +1-301-594-2930 **Fax:** +1-301-435-8644
Received: 2004-03-06 **Accepted:** 2004-04-28

Abstract

AIM: Both observational and experimental studies have shown that higher selenium status reduces the risk of upper gastrointestinal cancers in selenium deficient populations. Recent cancer registry data have shown very different rates of esophageal cancer (EC) and gastric cancer (GC) in four Provinces of Iran, namely Ardabil, Mazandaran, Golestan, and Kerman. The aim of this study was to have a preliminary assessment of the hypothesis that high rates of EC in Golestan and high rates of GC in Ardabil may be partly attributable to selenium deficiency.

METHODS: We measured serum selenium in 300 healthy adults from Ardabil (n = 100), Mazandaran (n = 50), Golestan (n = 100), and Kerman (n = 50), using inductively coupled plasma, with dynamic reaction cell, mass spectrometry (ICP-DRC-MS) at the US Centers for Disease Control (Atlanta, Georgia).

RESULTS: The median serum selenium concentrations were very different in the four Provinces. The medians (IQR) for selenium in Ardabil, Mazandarn, Golestan, and Kerman were 82 (75-94), 123 (111-132), 155 (141-173), and 119 (110-128) μg/L, respectively (P<0.001). The results of linear regression showed that the Province variable, by itself, explained 76% of the variance in log selenium (r^2 = 0.76). The proportion of the populations with a serum selenium more than 90 μg/L (the concentration at which serum selenoproteins are saturated) was 100% in Golestan, Kerman, and Mazandaran but only 29% in Ardabil.

CONCLUSION: Our findings suggest that selenium deficiency is not a major contributor to the high incidence of EC seen in northeastern Iran, but it may play a role in the high incidence of GC in Ardabil Province.

Nouarie M, Pourshams A, Kamangar F, Sotoudeh M, Derakhshan MH, Akbari MR, Fakheri H, Zahedi MJ, Caldwell K, Abnet CC, Taylor PR, Malekzadeh R, Dawsey SM. Ecologic study of serum selenium and upper gastrointestinal cancers in Iran. *World J Gastroenterol* 2004; 10(17): 2544-2546
http://www.wjgnet.com/1007-9327/10/2544.asp

INTRODUCTION

Esophageal cancer (EC) and gastric cancer (GC), collectively known as upper gastrointestinal (UGI) cancers, constitute 16% of all cancer deaths worldwide and are responsible for approximately one million deaths each year[1].

Both observational and experimental studies have shown that higher selenium status reduces the risk of UGI cancers in selenium deficient populations[2-5]. In a large-scale, prospective cohort study conducted in Finland, a low selenium region prior to a current supplementation program, Knekt and colleagues found a lower risk of stomach cancer in individuals with higher baseline serum selenium concentrations[3]. In another large cohort study, Mark and colleagues also found a reduced risk of esophageal cancer and gastric cardia cancer among individuals with higher initial serum selenium concentrations in a selenium deficient population in Linxian, China[4]. A double-blind, randomized clinical trial in this same Chinese population showed a reduced risk of both cardia and non-cardia gastric cancers in individuals supplemented with a combination of selenium, beta-carotene, and alpha-tocopherol[2].

Iran also has high rates of both EC and GC[6-8], and these cancers are the two most common causes of cancer death in Iran[9]. However, recent cancer registry data showed highly varying rates of EC and GC in four Provinces of Iran, namely Ardabil[7], Mazandaran, Golestan, and Kerman (unpublished data). The annual age-standardized incidence rates (ASRs) for EC were 15, 19, 40, and 3 per 10^5, and ASRs for GC were 38, 22, 18, and 8 per 10^5 in these four Provinces, respectively.

We hypothesized that differences in serum selenium may partly explain the highly varying rates of EC and GC in Iran. Here, we present the results of an ecologic study that compared serum selenium concentrations in randomly selected healthy subjects from Ardabil, Mazandaran, Golestan, and Kerman Provinces.

MATERIALS AND METHODS

Serum samples from 300 healthy adults were selected for this study. These subjects had all been recruited for previous studies. Ardabil serum samples (100 samples) were selected from participants in an endoscopic survey of gastric precancerous lesions conducted among rural and urban subjects ⩾40 years old[10]. These subjects were selected using simple random sampling, and all resided in Meshkinshahr, a major city in Ardabil, or its surrounding villages. Mazandaran and Kerman serum samples (50 samples each) were selected from participants in a survey of the prevalence of celiac disease among urban inhabitants ⩾18 years old in these two Provinces. These subjects were selected randomly from the entire urban

population of Sari and Kerman, the two major cities of these Provinces. In Golestan, 100 serum samples were selected from urban and rural individuals ⩾40 years of age who were recruited during the pilot phase of a cohort study of UGI cancers. In all of these studies, the only inclusion criteria were residence, age, and lack of life-threatening conditions. All samples were collected in the years 2002 and 2003. From these subjects, we selected our study samples such that they represented male and female participants equally (Table 1). Samples from Ardabil and Golestan included both urban and rural populations, but samples from Kerman and Mazandaran represented only urban subjects.

A single blood sample was collected from each person. Serum was separated and frozen in -20 ℃ freezers in plastic vials, and the samples were transported to the U.S. Centers for Disease Control (Atlanta, Georgia) on dry ice, where serum selenium was measured using inductively coupled plasma, with dynamic reaction cell, mass spectrometry (ICP-DRC-MS). The analytical limit of detection for assessment was 5.2 μg/L with a reference range of 80-300 μg/L[11]. We pooled samples to make an internal quality control serum, and 20 quality control samples were randomly inserted among the other serum samples. The coefficient of variation in these samples was 0.04.

The distribution of serum selenium in the four Provinces was not normal. Therefore we used medians and interquartile ranges (IQRs) to present the descriptive results and the Kruskal-Wallis test to test the differences in serum selenium ranks among provinces, between males and females, and between urban and rural participants. The distribution of the natural logarithm of selenium (log selenium) in each province did not deviate from normal. Therefore we used linear regression to test the effect of age on log selenium values. We also used linear regression to find the proportion of variance of log selenium that was explained by the province. All statistical analyses were done using STATA® Software, version 8 (Stata Corporation, Tx).

RESULTS

The median age of all the study subjects was 45 years. Half of the subjects from each area (a total of 150) were males (Table 1). Half of the subjects from Ardabil and Golestan (n = 100) and all of the subjects from Mazandaran and Kerman (n = 100) were from urban areas.

The median serum selenium concentrations were very different in the four Provinces. The medians (IQR) for selenium in Ardabil, Mazandarn, Golestan, and Kerman were 82 (75-94), 123 (111-132), 155 (141-173), and 119 (110-128) μg/L, respectively (P<0.001). The results of linear regression showed that the province variable, by itself, explained 76% of the variance in log selenium (r^2 = 0.76). The proportion of these populations with serum selenium concentrations more than 90 μg/L (the concentration at which serum selenoproteins are saturated[12]) was 100% in Golestan, Kerman, and Mazandaran, but only 29% in Ardabil.

The median (IQR) serum selenium concentrations in males and females were 124 (95-145) and 116 (92-143) μg/L, respectively (P = 0.49).

Simple linear regression did not show a significant effect of age on log selenium in any of the four Provinces. The correlation coefficient between selenium and age in all samples combined was very low (r = 0.006).

Median (IQR) serum selenium concentrations in the urban and rural samples of Ardabil were 81 (76-86) and 83 (74-96) μg/L, respectively (P = 0.57). Median (IQR) serum selenium concentrations in urban and rural samples from Golestan were 150 (135-165) and 161 (144-183) μg/L (P = 0.003).

DISCUSSION

Shamberger and Frost first suggested a role for selenium in the prevention of cancer in 1969, when they observed an inverse association between the geographic distribution of selenium in forage crops and cancer mortality rates in the United States[13]. A growing body of evidence, from both laboratory and epidemiologic studies, has since shown that selenium may have anticarcinogenic effects, especially against cancers of the lung, prostate, skin, and gastrointestinal system[14,15].

In this study, we measured serum selenium in 300 Iranian adults from four provinces with varying risks of EC and GC to have a preliminary assessment of the hypothesis that the high rates of EC in Golestan and GC in Ardabil may be partly attributable to selenium deficiency. The proportion of the populations with a serum selenium more than 90 μg/L (the concentration at which the serum selenoproteins are saturated) was 100% in Golestan, Kerman, and Mazandaran, and these three provinces had medium to high concentrations of serum selenium compared with the other areas of the world. Therefore, it is unlikely that high incidence of EC in Golestan and Mazandaran is due to selenium deficiency. This is consistent with a case-control study in Mazandaran that did not find any difference in hair selenium between EC cases and controls[16]. In Ardabil, however, only 29% of the population had a serum selenium concentration above 90 μg/L. This suggests that the high incidence of GC and pre-neoplastic gastric lesions in Ardabil[10] could be partly due to selenium deficiency.

This is the first study that has examined serum selenium concentrations in different Iranian populations. Median serum selenium ranged widely, from 82 μg/L in Ardabil to 155 μg/L in Golestan. The median serum selenium concentration in these four provinces combined, weighted for the population of each province, was 123 μg/L. For comparison, median serum selenium in other areas of the world varies from very low concentrations (<50 μg/L) in some parts of China and Serbia to very high concentrations (>200 μg/L) in parts of the USA and some other regions of China. However, the majority of median serum selenium concentrations in the world range from 80-120 μg/L[17].

The wide range of serum selenium concentrations among the four provinces and its small range within each province was an interesting finding. The major predictor of serum selenium is dietary intake[14,17], and the observed differences

Table 1 Distribution of age, sex, location, and serum selenium in study sample

Province	Number of samples	Median age (yr)	Male (%)	Urban (%)	Annual incidence of EC / 10^5	Annual incidence of GC / 10^5	Median serum selenium (IQR) in μg / L
Ardabil	100	49	49 (49)	49 (49)	15	38	82 (75-94)
Mazandaran	50	35	24 (48)	50 (100)	19	22	123 (111-132)
Golestan	100	50	51 (51)	51 (51)	40	18	155 (141-173)
Kerman	50	33	26 (52)	50 (100)	3	8	119 (110-128)
Total	300	45	150 (50)	200 (67)	-	-	123[1]

[1]A weighted median based on the total population of each province.

among the provinces are most likely due to variation in the selenium content of their diets.

We plan to conduct further observational studies to confirm or refute the association of selenium intake and the risk of GC in Ardabil.

REFERENCES

1 **Parkin DM**, Bray F, Ferlay J, Pisani P. Estimating the world cancer burden: Globocan 2000. *Int J Cancer* 2001; **94**: 153-156

2 **Blot WJ**, Li JY, Taylor PR, Guo W, Dawsey S, Wang GQ, Yang CS, Zheng SF, Gail M, Li GY. Nutrition intervention trials in Linxian, China: supplementation with specific vitamin / mineral combinations, cancer incidence, and disease-specific mortality in the general population. *J Natl Cancer Inst* 1993; **85**: 1483-1492

3 **Knekt P**, Aromaa A, Maatela J, Alfthan G, Aaran RK, Hakama M, Hakulinen T, Peto R, Teppo L. Serum selenium and subsequent risk of cancer among finnish men and women. *J Natl Cancer Inst* 1990; **82**: 864-868

4 **Mark SD**, Qiao YL, Dawsey SM, Wu YP, Katki H, Gunter EW, Fraumeni JF Jr, Blot WJ, Dong ZW, Taylor PR. Prospective study of serum selenium levels and incident esophageal and gastric cancers. *J Natl Cancer Inst* 2000; **92**: 1753-1763

5 **Wei WQ**, Abnet CC, Qiao YL, Dawsey SM, Dong ZW, Sun XD, Fan JH, Gunter EW, Taylor PR, Mark SD. Prospective study of serum selenium concentrations and esophageal and gastric cardia cancer, heart disease, stroke, and total death. *Am J Clin Nutr* 2004; **79**: 80-85

6 **Mahboubi E**, Kmet J, Cook PJ, Day NE, Ghadirian P, Salmasizadeh S. Oesophageal cancer studies in the Caspian Littoral of Iran: the caspian cancer registry. *Br J Cancer* 1973; **28**: 197-214

7 **Sadjadi A**, Malekzadeh R, Derakhshan MH, Sepehr A, Nouraie M, Sotoudeh M, Yazdanbod A, Shokoohi B, Mashayekhi A, Arshi S, Majidpour A, Babaei M, Mosavi A, Mohagheghi MM, Alimohammadian M. Cancer occurrence in Ardabil: Results of a population-based cancer registry from Iran. *Int J Cancer* 2003; **107**: 113-118

8 **Saidi F**, Sepehr A, Fahimi S, Farahvash MJ, Salehian P, Esmailzadeh A, Keshoofy M, Pirmoazen N, Yazdanbod M, Roshan MK. Oesophageal cancer among the turkomans of northeast Iran. *Br J Cancer* 2000; **83**: 1249-1254

9 Iranian Disease Prevention and Control Department. Cancer Incidence in Iran. Tehran: *Ministry of Health and Medical Education* 2000: 6

10 **Malekzadeh R**, Sotoudeh M, Derakhshan MH, Mikaeli J, Yazdanbod A, Merat S, Yoonessi A, Tavangar M, Abedi BA, Sotoudehmanesh R, Pourshams A, Asgari AA, Doulatshahi S, Alizadeh BZ, Arshi S, Madjidpoor A, Mir MS, Fleischer DE. Prevalence of gastric precancerous lesions in Ardabil, a high incidence province for gastric adenocarcinoma in the northwest of Iran. *J Clin Pathol* 2004; **57**: 37-42

11 Agency for Toxic Substance and Disease Registry. Toxicological Profile for Selenium. Atlanta, GA: *U.S. Department of Health and Human Services* 2001

12 Panel of dietary antioxidants and related compounds. Selenium. In: Panel of dietary antioxidants and related compounds, eds. Dietary reference intakes for vitamin C, vitamin E, selenium, and carotenoids. Washington DC: *National Academy Press* 2000: 284-324

13 **Shamberger RJ**, Frost DV. Possible protective effect of selenium against human cancer. *Can Med Assoc J* 1969; **100**: 682

14 **Combs GF Jr**, Gray WP. Chemopreventive agents: selenium. *Pharmacol Ther* 1998; **79**: 179-192

15 **Combs GF Jr**, Lü JX. Selenium as a cancer preventive agent. In: Hatfield DL, ed. Selenium: Its molecular biology and role in human health. Norwell, MA: *Kluwer Adademic Publishers* 2001: 205-217

16 **Azin F**, Raie RM, Mahmoudi MM. Correlation between the levels of certain carcinogenic and anticarcinogenic trace elements and esophageal cancer in northern Iran. *Ecotoxicol Environ Saf* 1998; **39**: 179-184

17 **Alfthan G**, Neve J. Reference values for serum selenium *in various* areas-evaluated according to the TRACY protocol. *J Trace Elem Med Biol* 1996; **10**: 77-87

Edited by Chen WW **Proofread by** Xu FM

PO Box 2345, Beijing 100023, China
Fax: +86-10-85381893
E-mail: wjg@wjgnet.com www.wjgnet.com

World J Gastroenterol 2004;10(17):2547-2549
World Journal of Gastroenterology
Copyright © 2004 by The WJG Press ISSN 1007-9327

• BRIEF REPORTS •

Changes of mRNA expression of enkephalin and prodynorphin in hippocampus of rats with chronic immobilization stress

Jia-Xu Chen, Wei Li, Xin Zhao, Jian-Xin Yang, Hong-Yan Xu, Zhu-Feng Wang, Guang-Xin Yue

Jia-Xu Chen, Wei Li, Xin Zhao, Jian-Xin Yang, Hong-Yan Xu, Zhu-Feng Wang, Guang-Xin Yue, School of Basic Medical Science, Beijing University of Traditional Chinese Medicine, Beijing 100029, China
Supported by the National Natural Science Foundation of China, No. 30000216, Teaching and Research Award Program for Outstanding Young Teachers in Higher Education Institutes of Ministry of Education, China, Foundation for the Authors of National Excellent Doctoral Dissertations of China, No. 200059, and Fok Ying Tong Education Foundation, No. 81037
Correspondence to: Dr. Jia-Xu Chen, Deputy of TCM Diagnosis Department, Beijing University of Traditional Chinese Medicine, Beijing 100029, China. chenjiaxu@hotmail.com
Telephone: +86-10-64287074
Received: 2003-12-23 **Accepted:** 2004-01-16

Abstract

AIM: To observe the changes of enkephalin mRNA and prodynorphin mRNA in hippocampus of rats induced by chronic immobilization stress.

METHODS: Thirty rats were randomly divided into three groups of 10 each: the normal control group (group A), the group induced by chronic immobilization stress for 7 d (group B) and the group induced by chronic immobilization stress for 21 d (group C). The changes of the enkephalin mRNA and prodynorphin mRNA in the rat hippocampus were detected by reverse transcription-polymerase chain reaction (RT-PCR).

RESULTS: Expression levels of enkephalin mRNA and prodynorphin mRNA in rat hippocampus were significantly increased under chronic immobilization stress, and the expression of prodynorphin mRNA in the rat hippocampus in group C was remarkably higher than that in group B (0.624±0.026; $n = 5$; $P<0.01$).

CONCLUSION: The increased enkephalin mRNA and prodynorphin mRNA gene expressions in rat hippocampus were involved in chronic stress.

Chen JX, Li W, Zhao X, Yang JX, Xu HY, Wang ZF, Yue GX. Changes of mRNA expression of enkephalin and prodynorphin in hippocampus of rats with chronic immobilization stress. *World J Gastroenterol* 2004; 10(17): 2547-2549
http://www.wjgnet.com/1007-9327/10/2547.asp

INTRODUCTION

It is known that exposure to a variety of stressors can lead to the increase of plasma β-endorphin up to 10-15 times higher than normal. β-endorphin, enkephalin and dynorphin are termed as opioid peptides that are likely to exert influence on emotional and psychological state. Endogenous opioid peptides are extensively involved in the modulation of stress[1] and regulation between central nervous system and immune system. We found that immune function was changed markedly (IL-1_β in serum was increased, while IL-2 and IL-6 in serum were decreased) in rats under chronic immobilization stress[2]. The average optical density of glucocorticoid receptor (GR) in hippocampus CA_1 and parietal lobe cortex was markedly increased after 7 d immobilization stress (180 min daily) exposure in comparison with normal control, but it was declined to the normal level after 21 d of stress exposure; the level of plasma adrenocorticotropin (ACTH) and serum cortisol had similar changes to that of GR[3]. Are the opioid peptides in hippocampus implicated for the regulation of immune and internal secretion function under restrain stress? Here, we used animal models induced by chronic immobilization stress to observe the characteristic changes of expression of enkephalin mRNA and prodynorphin mRNA with reverse transcription-polymerase chain reaction (RT-PCR) in rat hippocampus.

MATERIALS AND METHODS

Subjects

Thirty male, Sprague-Dawley rats, weighing 180-220 g, were supplied by the Research Center of Experimental Animals "Weitong Lihua" in Beijing, with qualified certification No: SCXK-BJ2002-0003. They were randomly divided into three groups of 10 each: the normal control group (group A), the model group of 7 d (group B) and the model group of 21 d (group C). The rats were housed in groups of 5 rats in each cage and provided free access to food and water (20-24 °C, relative humidity of 30-40%).

All experiments conformed to the guidelines of NIH on the ethical use of animals. All efforts were made to minimize the animal suffering and maintain the number of animals necessary to produce reliable data.

Modeling methods

A T-form bound brace (self-made) was used: A frame with length of 20 cm and width of 10 cm and thickness of 2.8 cm was prepared. Its upper platform was of 22 cm in length and 6.6 cm in its widest part. A small frame for fixing the rat's head at the front end and grooves for rat's limbs were adapted. In the upper platform three adaptable soft bands, of which two are wide and one is thin, for fixing the rat in the head and neck, chest and loins, loins and back respectively were added. Means of chronic binding were applied in order to create stress models of rats. The rats were immobilized in the above-noted binding brace for 3 h daily and for either 7 or 21 consecutive days.

Extraction and measurement of total RNA

Extraction of total RNA of rat hippocampus: Rats were decapitated at the end of modeling and hippocampus tissues were rapidly taken bilaterally out and placed on the ice-plate. The tissues of 50-100 mg were mixed with 1 mL pre-cold TRIzol (Gibcol) and were sufficiently ground in the appliance for grinding tissue. The homogenates produced were thereafter placed in ice for 5 min. Homogenates of hippocampus were added into 0.2 mL chloroform and drastically agitated for 15 s and placed in ice for 2-3 min. The resulting solution was then centrifuged at 12 000 *g* for 15 min. Supernatant was taken out and mixed with 0.5 mL isopropanol and placed for 5-10 min at room temperature. The resulting solution was then centrifuged at 12 000 *g* for 10 min at 4 °C and the supernatant produced was then removed. The

sediment was rinsed with 0.5 mL of 750 mL/L freshly made alcohol solution and centrifuged at 7 500 r/min for 5 min at 4 °C and the resulting supernatant was then removed. The sediment was dried at room temperature and then dissolved by 1 g/L diethyl pyrocarbonate (Sigma), in order to produce a concentration at which 1 μg RNA was resolved in 1 mL water.

Total RNA detection by electrophoresis

A 2-μL sample of the total RNA extracted was demonstrated by electrophoresis on 10 g/L agarose gel under constant voltage for 20 min. The strips of 28S, 18S and 5S were observed in the gel image system.

Quantification and purity identification of RNA

Certain amount of RNA sample was diluted (10- or 20- fold) and its concentration and purity were measured by ultraviolet spectrophotometer. Measurement of absorbance A_{260} was chosen to count the concentration of RNA (μg/μL) and ratios of A_{260}/A_{280} were chosen for its purity which was required as 1.8-2.0. Therefore, RNA with ratios less than 1.7 was deserted.

PCR primer design

Primers of β-actin, enkephalin and prodynorphin, of which β-actin was taken as inner-control of quasi-quantification PCR, were respectively designed by the software of Primer 5.0 according to the sequence of GenBank and synthesized by Sanboyuanzhi Company. Sequences of primers were as follows: β-actin: Primer of the upper stream: 5'-CATCTCTTGCTCGAAG TCCA-3', Primer of the down stream: 5'-ATCATGTTTGAGAC CTTCAACA-3'. Enkephalin: Primer of the upper stream: 5'-ATGGCGTTCCTGAGACTTTGA-3', Primer of the down stream: 5'-TAGAGTTTTGGCGTATTTCGGAGGC-3'. Prodynorphin: Primer of the upper stream: 5'-ATGGCGTGGTCCAGGCTGATGC-3', Primer of the down stream: 5'-AGTTTGTAGATTTA GAAGCCTTATCC-3'. Genes of enkephalin (810 bp) and prodynorphin (747 bp) were respectively amplified.

Reverse transcription reaction

A sample of RNA was kept at constant temperature of 70 °C for 10 min, centrifuged for several seconds and then placed in a water-bath. The following reaction (20 μL) happened in the centrifugal tube of PCR of 0.5 mL: 1 μL random primer 50 ng/μL; 1 μL dNTP (10 mmol/L) (Promega); 4 μL 5×RT buffer; 1 μL mixed solution of reverse transcriptase; 2 μL RNA sample; 1 μL DEPC-ddH_2O. The above-noted reaction system was placed at room temperature for 10 min and kept at constant temperature of 37 °C for 30 min, at 95 °C for 5 min, and then at 4 °C for 3 min prior to next procedures.

Amplification of target DNA by PCR

Enkephalin and prodynorphin were respectively amplified by PCR (PCT-100TM Programmable Thermal Controller, product of MJ RESEARCH, INC, America). The following materials were included in a 50 μL reaction system: 6 μL RT reaction product; 4.5 μL 10×PCR buffer; 1 μL dNTP (10 mmol/L); 1 μL (50 pmoL) sense primer (enkephalin or prodynorphin); 1 μL (50 pmoL) antisense primer (enkephalin or prodynorphin); 1 μL *Taq* DNA polymerase (Promega); 35.5 μL DEPC-ddH2O. In the meantime, primer of enkephalin or prodynorphin was replaced by β-actin to perform PCR reaction with the rest reaction system noted above. The above systems were sufficiently mixed and centrifuged, then PCR reactions performed after adding 50 μL light mineral oil.

Temperatures of 46, 52 and 58 °C were respectively chosen as annealing temperature, so that three of them would be able to be used for amplification, while non-specific DNA segments would not occur. The last condition of optimized reaction was as follows: pre-degeneration at 94 °C for 3 min, tempering at 52 °C and extension at 72 °C, for 30 cycles, thereafter extension at 72 °C for another 15 min.

Amplified product was detected with 10 g/L agarose gel electrophoresis and analyzed with gel image analysis system FIT-5000 (Sweden). Ratio of optical density of the target genes and ratio of optical density of β-actin, which can be expressed as a stable value in the tissue (and it was therefore taken as interior control strip), were employed as data for quasi-quantified analysis.

Statistical analysis

Data were expressed as mean±SD and software of SPSS was applied for statistical analysis. ANOVA was performed for comparison among groups and followed by a post-hoc test. Significance was accepted at $P<0.05$.

RESULTS

General state of rats

Rats manifested symptoms such as lassitude, fewer activities, no gloss in hair, decreased food intake and loose stools.

Electrophoresis of total RNA

Three strips of 28S, 18S and 5S were observed after the extraction of the total RNA from the rat hippocampus with TRIzol RNA and electrophoresis.

Results of PCR amplification

Corresponding strips of target DNA were obtained via reverse transcription and PCR. The length of the strip of β-actin DNA was 300 bp, that of the enkephalin was 810 bp and that of the prodynorphin was 747 bp.

The expression of enkephalin mRNA was mildly increased in the rat hippocampus of group A, and significantly increased in the rat hippocampus of group C ($P<0.01$, $P<0.05$) when compared with rats in group A and B, respectively. The expression of prodynorphin mRNA was significantly increased in the rat hippocampus of group B and C when compared with rats in group A ($P<0.01$). The expression of prodynorphin mRNA in the rat hippocampus in group C was remarkably higher than that in group B ($P<0.01$). The results are shown in Table 1.

Table 1 Expression of enkephalin mRNA and prodynorphin mRNA in rat hippocampus (n = 5, mean ±SD)

Group	Enkephalin mRNA	Prodynorphin mRNA
A	0.284±0.013	0.360±0.017
B	0.308±0.018	0.492±0.036[b]
C	0.352±0.028[bc]	0.624±0.026[bd]

Statistical analyses were performed by analysis of variance and post-hoc test. [b]$P<0.01$ *vs* group A; [c]$P<0.05$, [d]$P<0.01$ *vs* group B.

DISCUSSION

Endogenous opioid peptides, which mainly include enkephalin family (methionine enkephalin and leucine enkephalin), endorphin family (α-endorphin, β-endorphin and γ-endorphin) and dynorphin family (dynorphin A and dynorphin B), are one class of matters with opioid action, naturally generated in the brain of mammals. It has been reported that endogenous opioid peptides are extensively involved in the regulation of stress and exert important effect on mediating the central nervous system and immune system[4-7].

The increased expression of opioid peptides including enkephalin mRNA and prodynorphin mRNA in our study, may influence hippocampal function and facilitate long-term depression (LTD) of the Schaffer collateral input to CA1 pyramidal neurons[8]. Chronic stress increased the synthesis

of opioid peptides in the nervous system and increased plasma glucocorticoid[9] .

Enkephalin is extensively distributed inside the brain as a kind of endogenous opioid peptides. It plays several roles in analgesia, cardiovascular, respiratory and body temperature regulation via receptors of endogenous opioid peptides including widespread immunity modulation after it is generated and released. In addition, enkephalin can exert its effect on regulating the immune functions of body under both normal and stress conditions. Both methionine enkephalin and leucine enkephalin can influence the activity and the formation rate of rosettes of T lymphocyte, as well as the activity of natural killer cells in the body under physiological conditions[6,10]. The mechanism of enkephalin involved in regulating immunity under physiological conditions has yet to be clarified. More researches have focused on the mechanism of enkephalin in regulating immunity in different stress situations. Researches suggested that methionine enkephalin and leucine enkephalin could markedly inhibit the cytotoxic action that can be stopped by naloxone, a substance that is produced by the natural killer cells, under the stress induced by electric shock in rats. Therefore, endogenous opioid peptides played an important role in immune regulation stimulated by stress[11,12].

Hippocampus is a crucial structure is which enkephalin can regulate immune function via IL-1α. A spleen lymphocyte proliferation reaction stimulated by Canavalia protein A could be markedly reinforced by microinjection of methionine enkephalin and leucine enkephalin into rat hippocampus (similar result obtained in the experiment of mice)[13]. The inhibitive effect of enkephalin on IL-1 gene expression of the glia cell in hippocampus may shed lights on the mechanisms involved in the immunological amplification by microinjection of enkephalin, which inhibits gene expression of IL-1α via opioid receptors in glia cells of hippocampus or in certain nerve cell membranes that possess the capacity of generating IL-1α, and result in decreased activating effect of IL-1α on the hypothalamus-pituitary-adrenal axis together with decreased synthesis of IL-1α inside the brain, and simultaneous strengthening of the immune function of body by decreasing the blood plasma corticoid[14-16].

It was demonstrated in the present study that expression of enkephalin mRNA was mildly increased after 7 d and significantly increased after 21 d under the conditions of chronic immobilization. In general, increase of enkephalin will result in poorer immune function. In line with our former research[2], the substantial decrease of the transforming function of the spleen lymphocytes in rats most likely originated from the indirect inhibitive action of enkephalin. It means that the increase of enkephalin would inhibit gene expression of central IL-1α and is likely to result in lower IL-1α inside the brain.

Prodynorphin, containing the sequence of leucine enkephalin at N-terminal which was considered as its precursor at first, is another member of the endogenous opioid peptides with analogous distribution inside the brain in striatum, hippocampus and hypothalamus.It also exists in adrenal glands and genital organs. The splitting process of prodynorphin is complicated and its main products include dynorphin A_{1-17}, dynorphin B_{1-29}, dynorphin A_{1-8} and neo-endorphin. In addition, generation of prodynorphin mRNA is affected by multiple factors in many regions of brain. For instance, gamma-aminobutyric acid (GABA) can decrease its generation in neo-striatum.

With dual action, dynorphin can not only protect, but also damage the nerve cells in some cases. It was indicated that the expression of prodynorphin in rat hippocampus was significantly increased and its change was likely to be earlier than that of enkephalin under the condition of chronic immobilization stress. Taken together our previous and current experiments, increase of dynorphin is likely to result in certain nerve damage as fewer numbers of brain-derived neurotrophic factors (BDNF) and neurotrophin 3 (NT_3) might exert fewer protective effects on the nervous system under chronic immobilization stress. Whether and how dynorphin correlates with neurotrophins have yet to be established.

ACKNOWLEDGEMENTS

We greatly thank Qing-Hong Chen and Ioannis Solos for their kindly correcting grammar, spelling and punctuation of the manuscript.

REFERENCES

1 **Vaccarino AL**, Kastin AJ. Endogenous opiates: 1999. *Peptides* 2000; **21**: 1975-2034

2 **Li W,** Chen JX, Yang JX, Zhao X, Tang YT, Liu XL, Xu HY. The effect of compounds of soothing liver, invigorating spleen, tonifying kidney on the praxiology and immunological function of chronic immobilization stressed rats. *Acta Laboratorium Animalis Scientia Sinica* 2003; **11**: 33-37

3 **Tang YT,** Chen JX. Regulative effects of three TCM formulas on hypothalamus-pituitary-adrenal axis in the rats with chronic restrained stress. *J Beijing Univ Traditional Chine Med* 2002; **25**: 23-26

4 **Harbuz MS,** Lightman SL. Responses of hypothalamic and pituitary mRNA to physical and psychological stress in the rat. *J Endocrinol* 1989; **122**: 705-711

5 **Lightman SL,** Young WS 3rd. Influence of steroids on the hypothalamic corticotropin-releasing factor and preproenkephalin mRNA responses to stress. *Proc Natl Acad Sci U S A* 1989; **86**: 4306-4310

6 **Plotnikoff NP,** Murgo AJ, Miller GC, Corder CN, Faith RE. Enkephalins: immunomodulators. *Fed Proc* 1985; **44**: 118-122

7 **Kurumaji A,** Takashima M, Shibuya H. Cold and immobilization stress-induced changes in pain responsiveness and brain Met-enkephalin-like immunoreactivity in the rat. *Peptides* 1987; **8**: 355-359

8 **Wagner J,** Etemad LR, Thompson AM. Opioid- mediated facilitation of long-term depression in rat hippocampus. *J Pharmacol Exp Ther* 2001; **296**: 776-781

9 **Ahima RS,** Garcia MM, Harlan RE. Glucocorticoid regulation of preproenkephalin gene expression in the rat forebrain. *Brain Res Mol Brain Res* 1992; **16**: 119-127

10 **Miller GC,** Murgo AJ, Plotnikoff NP. Enkephalins-enhancement of active T-cell rosettes from normal volunteers. *Clin Immunol Immunopathol* 1984; **31**: 132-137

11 **Devi RS,** Namasivayam A, Prabhakaran K. Modulation of non-specific immunity by hippocampal stimulation. *J Neuroimmunol* 1993; **42**: 193-197

12 **Shavit Y,** Lewis JW, Terman GW, Gale RP, Liebeskind JC. Opioid peptides mediate the suppressive effect of stress on natural killer cell cytotoxicity. *Science* 1984; **223**: 188-190

13 **Ban E,** Milon G, Prudhomme N, Fillion G, Haour F. Receptors for interleukin-1 (alpha and beta) in mouse brain: mapping and neuronal localization in hippocampus. *Neuroscience* 1991; **43**: 21-30

14 **Blalock JE.** The syntax of immune-neuroendocrine communication. *Immunol Today* 1994; **11**: 504-511

15 **Payne LC,** Weigent DA, Blalock JE. Induction of pituitary sensitivity to interleukin-1: a new function for corticotropin-releasing hormone. *Biochem Biophys Res Commun* 1994; **198**: 480-484

16 **Wang AJ,** Yang YZ, Wu YM, Xie H, Hu MX, Gao N, Hong J, Sun CL. Effect of intrahippocampal microinjection of enkephalin on cellular immune function and brain IL-1 alpha gene expression in rat. *Acta Physiologica Sinica* 1996; **48**: 348-354

Edited by Chen WW and Zhu LH **Proofread by** Xu FM

PO Box 2345, Beijing 100023, China
Fax: +86-10-85381893
E-mail: wjg@wjgnet.com www.wjgnet.com

World J Gastroenterol 2004;10(17):2550-2552
World Journal of Gastroenterology
Copyright © 2004 by The WJG Press ISSN 1007-9327

• BRIEF REPORTS •

Differentiation of dermis-derived multipotent cells into insulin-producing pancreatic cells *in vitro*

Chun-Meng Shi, Tian-Min Cheng

Chun-Meng Shi, Tian-Min Cheng, Institute of Combined Injury, Third Military Medical University, 30 Gaotanyan street, 400038, Chongqing City, China
Supported by the National Key Basic Research Project, No. 1999054205
Correspondence to: Dr. Chun-Meng Shi, Institute of Combined Injury, Third Military Medical University, Gaotanyan 400038, Chongqing City, China. shicm@sina.com
Telephone: +86-23-68752355 **Fax:** +86-23-68752279
Received: 2003-12-28 **Accepted:** 2004-01-15

Abstract

AIM: To observe the plasticity of whether dermis-derived multipotent cells to differentiate into insulin-producing pancreatic cells *in vitro*.

METHODS: A clonal population of dermis-derived multipotent stem cells (DMCs) from newborn rat with the capacity to produce osteocytes, chondrocytes, adipocytes and neurons was used. The gene expression of cultured DMCs was assessed by DNA microarray using rat RGU34A gene expression probe arrays. DMCs were further cultured in the presence of insulin complex components (Insulin-transferrin-selenium, ITS) to observe whether DMCs could be induced into insulin-producing pancreatic cells *in vitro*.

RESULTS: DNA microarray analysis showed that cultured DMCs simultaneously expressed several genes associated with pancreatic cell, neural cell, epithelial cell and hepatocyte, widening its transcriptomic repertoire. When cultured in the specific induction medium containing ITS for pancreatic cells, DMCs differentiated into epithelioid cells that were positive for insulin detected by immunohistochemistry.

CONCLUSION: Our data indicate that dermal multipotent cells may serve as a source of stem/progenitor cells for insulin-producing pancreatic cells.

Shi CM, Cheng TM. Differentiation of dermis-derived multipotent cells into insulin-producing pancreatic cells *in vitro*. *World J Gastroenterol* 2004; 10(17): 2550-2552
http://www.wjgnet.com/1007-9327/10/2550.asp

INTRODUCTION

Organ-specific stem cells possess plasticity that can permit differentiation along new lineages and have significant implications for future therapies of diabetes. The production of endocrine pancreas and insulin-secreting beta cells from adult nonpancreatic stem cells and hepatic oval stem cell has been demonstrated[1,2]. Zulewski *et al*. also showed that pancreatic islets contained a heretofore unrecognized distinct population of cells that expressed the neural stem cell-specific marker nestin. The nestin-positive islet-derived progenitor (NIP) cells are a distinct population of cells that reside within pancreatic islets and may participate in the neogenesis of islet endocrine cells[2]. According to this result, liver stem cells have been proved to differentiate into pancreatic islet-like cells[3]. Dermis is a highly accessible tissue source for adult stem cells. Nestin-positive skin-derived stem cells have been isolated from dermis by Toma *et al*[4]. In our previous study, we isolated a clonal population of dermal multipotent cells by their adherence to tissue culture plastic (termed as plastic adherent DMCs) from newborn rat dermis. These cells showed the differentiation capacity to produce nestin-positive cells[5]. In this study, we aimed to investigate whether plastic adherent DMCs had the differentiation capacity to produce insulin-producing pancreatic cells *in vitro*.

MATERIALS AND METHODS

Materials

A clonal population of dermis-derived multipotent stem cells (DMCs) was used in the experiments. The clonal population of DMCs were isolated and identified from primary dermal cells of male newborn Wistar rat as previously described[5]. All tissue culture reagents, including Iscove's Modified Dulbecco's Medium (IMDM), ITS (insulin-transferrin selenium), epidermal growth factor, basic fibroblast growth factor, were purchased from Sigma (St. Louis, CA, USA). Fetal bovine serum (FBS) was purchased from Hyclone (Logan, UT, USA). The rat RGU34A gene expression probe arrays were purchased from Affymetrix (Santa Clara, CA). Mouse anti-insulin monoclonal antibody was purchased from Sigma (St. Louis, CA, USA). Horseradish peroxidase (HRP)-labeled goat anti-mouse IgG antibody was purchased from Boster (Wuhan, China).

Methods

Cell culture The DMCs were cultured in IMDM medium containing 10 mL/L fetal bovine serum and 100 U/mL penicillin and 100 μg/mL streptomycin. Cultures were maintained at 37 °C in a humidified atmosphere containing 50 mL/L CO_2. For differentiation induction, DMCs were transferred into specific inducing medium containing 10 μg/mL of keratocyte growth factor (KGF), 20 ng/mL of epidermal growth factor (EGF), 10 mmol/L of nicotinamide, and 1 mg/mL of ITS. The differentiated cells were examined for the insulin expression by immunohistochemistry.

DNA Microarray analysis Total RNA from cultured DMCs was isolated using QIAGEN's RNeasy total RNA isolation kit (Rneasy, Qiagen) following the manufacture's instructions, and quantified. Transcript profiling was conducted by means of rat RGU34A gene expression probe arrays, containing 8 799 probe sets, interrogating primarily annotated genes. The experiment was conducted according to the recommendations of the manufacturer (Affymetrix GeneChip expression analysis manual). The resulting "data-file" was processed further using the microarray analysis suite 5 software package (Affymetrix). According to the statistical expression analysis algorithm, the presence of a gene within a given sample was determined at a detection P value of <0.05 and was graded as absent (A), marginal (M), or present/positive (P).

Immunocytochemistry Immunocytochemistry study with peroxidase-labeled streptavidin biotin method was performed to detect the expression of insulin in differentiated cells. Before

detection, the cells were washed three times for 20 min with phosphate-buffered saline (PBS, PH = 7.2) to exclude the pollution of exogenous insulin in the culture medium. After washing, the cells were blocked for 30 min with 100 mL/L normal goat serum in PBS and were incubated with mouse anti-insulin antibody (1:100) at 4 °C for 24 h. Incubation at room temperature with anti-mouse secondary antibody and avidin-biotinylated peroxidase complexes was performed for 2 h. The specimens were washed for 15 min with 0.01 mol/L PBS between all steps. The reaction product was developed with 0.5 g/L 3'3-diaminobenzine tetrahydrochloride (DAB). After staining, the result was observed microscopically. PBS was used as a substitute for primary antibody as negative control.

RESULTS

Biological properties of DMCs

Most adherent DMCs were of spindle-shaped cells (Figure 1). Phenotype analysis showed that DMCs were negative for some lineage-specific surface markers, including pan-cytokeratin, cytokeratin19, factor VIII, CD31, CD45, CD34, α-smooth muscle actin (α-SMA), desmin, collagen II and nestin, but were positive for CD59, CD90, CD44, vascular cell adhesion molecule-1 (VCAM-1) and intercellular adhesion molecule-1 (ICAM-1). The doubling time of cultured DMCs was about 40 h. Following induction, DMCs had the capacity to differentiate into cells with phenotypic characteristics of osteocytes (alkaline phosphatase activity and alizarin red staining), adipocytes (oil red staining), chondrocytes (collagen II and Alcian blue staining) and neurons (nestin and NF-200 staining) in specific induction media.

Figure 1 Morphology of cultured DMCs. (Inverted microscope, ×100).

Gene expression profile of plastic-adherent DMCs

The gene expression of DMCs was assessed by DNA microarray analysis and the harbinger of a potential cell type was viewed by simultaneous expression of a panel of lineage-related genes. The result revealed that the cultured DMCs simultaneously expressed genes associated with pancreatic cells (Table 1). DMCs also simultaneously expressed transcripts for epithelial cell, neural cell, and hepatocyte as well (Table 1). These transcripts were developmentally related with pancreatic tissue and further widened the transcriptomic repertoire of DMCs. To confirm the data by DNA microarray, several genes were further tested by RT-PCR and the result was consistent with the result from microarray (data not shown).

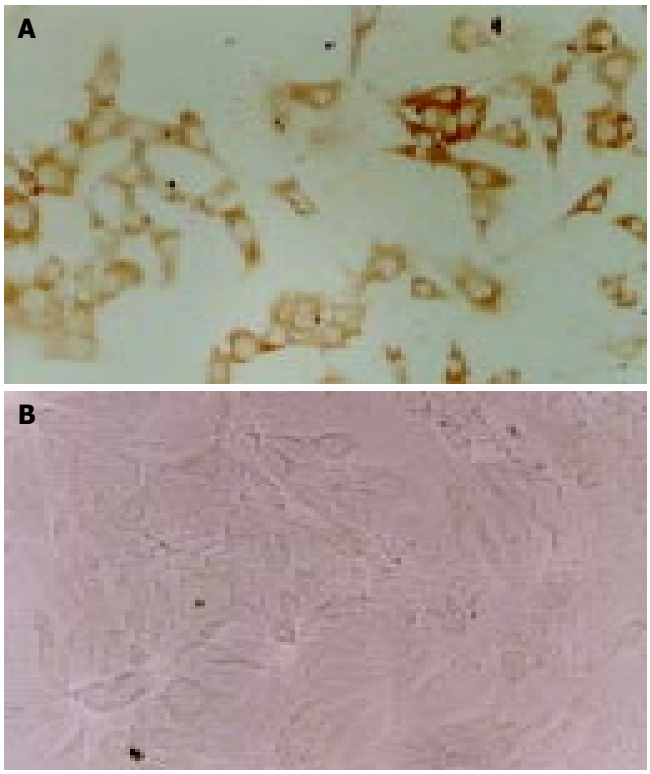

Figure 2 Differentiation of DMCs into insulin-producing cells. A: After induction in the medium containing ITS for 4 wk, cells were positive for insulin; B: Negative control (SP, ×200).

Table 1 DMC gene lists (partial) associated with diverse cellular lineages

Cell lineage	Representative examples of associated genes
A: Pancreatic cell	Pancreatic eukaryotic initiation factor 2 alpha-subunit kinase (PEK), pancreatic secretory trypsin inhibitor-like protein (PSTI), pancreatic islet cDNA Rattus norvegicus cDNA similar to rapamycin-binding protein FKBp-13, insulin II gene, IRS-1 mRNA for insulin-receptor, mRNA for glucose-dependent insulinotropic polypeptide
B: Neural cell	Neural visinin-like Ca2+-binding protein type 3, neuron-specific enolase, neuronal nitric oxide synthase, GABA receptor-associated proteins, NCAM, brain-derived neurotrophic factor (BDNF), syntaxin 7, glial fibrillary acidic protein (GFAP), adrenomedullin, myelin protein SR13 (growth-arrest-specific Gas-3 homolog), neurotrimin; secretogranin II, synapse-associated protein 102, latexin, kexin-like protease PC7A, N-methyl-D-aspartate (NMDA) receptor
C: Epithelial cell	Epithelial membrane protein 1, epithelial cell transmembrane protein antigen precursor, epidermal growth factor precursor, heparin-binding EGF-like growth factor , mucin, parathymosin and thy mosin 4 and 10
D: Hepatocyte	Liver glycogen phosphorylase enzyme, liver IL-6 receptor ligand binding chain, liver specifc tran scription factor LF-B, liver nuclear protein P47, liver aL-Fucosidase, hepatocyte nuclear factor 3α (HNF-3beta)

Expression of a single gene can't define the phenotype of a particular cell type. Simultaneous expression of a panel of lineage-related genes in single isolated cell was viewed as the harbinger of a potential cell type. Representative examples of genes corresponding to each cell lineage are outlined in the above table.

Differentiation of DMCs into insulin-producing pancreatic cells

DMCs were further tested for their capacity to produce pancreatic cells in the inducing medium containing ITS. The morphology of DMCs were changed into epithelial cells-like cells when cultured in medium containing ITS for 2 wk and immunohistochemistry showed that a proportion of cells (less than 10 %) were positive for insulin when cultured in medium containing ITS for 4 wk (Figure 2). The negative control cells showed no positive staining for insulin. This result further indicated that DMCs could undergo differentiation to form insulin-producing cells.

DISCUSSION

Replacement of the insulin-producing pancreatic islet âcells represents the ultimate treatment for type I diabetes. Recent advances in islet transplantation underscore the urgent need for developing alternatives to human tissue donors, which are scarce. The generation of insulin-producing cells from adult stem cells is one possible approach[6-9]. Recent studies have suggested that there are closely developmental relationship between the nestin positive progenitors and the pancreatic cells[10-13]. In addition to liver stem cells and neural stem cells, multipotent stem cells from dermis have been proved to have the capacity to produce nestin positive cells[4, 5]. In this study, we further reported that dermis-derived multipotent stem cells also showed a remarkable flexibility to differentiate into insulin-producing cells, when the appropriate stimuli were given. Since dermal cells are relatively easy to access and they also can be used for autologous use that may represent a safety advantage, dermis-derived multipotent cells may serve as a source of stem/progenitor cells for β cells.

Nevertheless, the efficiency of adult stem cells to differentiate into insulin-producing cells *in vitro* is low at present and expansion with large scale is needed for application. Genetic manipulation in tissue culture may be a choice and it is possible that new insights into endocrine pancreas development will lead to the manipulation of progenitor cell fate towards the β cell phenotype of insulin production, storage and regulated secretion[14, 15]. If successful, these approaches could lead to widespread cell replacement therapy for type I diabetes.

REFERENCES

1 **Suzuki A**, Zheng Yw YW, Kaneko S, Onodera M, Fukao K, Nakauchi H, Taniguchi H. Clonal identification and characterization of self-renewing pluripotent stem cells in the developing liver. *J Cell Biol* 2002; **156**: 173-184

2 **Zulewski H**, Abraham EJ, Gerlach MJ, Daniel PB, Moritz W, Muller B, Vallejo M, Thomas MK, Habener JF. Multipotential nestin-positive stem cells isolated from adult pancreatic islets differentiate *ex vivo* into pancreatic endocrine, exocrine, and hepatic phenotypes. *Diabetes* 2001; **50**: 521-533

3 **Meivar-Levy I**, Ferber S. New organs from our own tissues: liver-to-pancreas transdifferentiation. *Trends Endocrinol Metab* 2003; **14**: 460-466

4 **Toma JG**, Akhavan M, Fernandes KJ, Barnabe-Heider F, Sadikot A, Kaplan DR, Miller FD. Isolation of multipotent adult stem cells from the dermis of mammalian skin. *Nat Cell Biol* 2001; **3**: 778-784

5 **Shi C**, Cheng T. Effects of acute wound environment on neonatal rat dermal multipotent cells. *Cells Tissues Organs* 2003: **175**; 177-185

6 **Street CN**, Rajotte RV, Korbutt GS. Stem cells: a promising source of pancreatic islets for transplantation in type 1 diabetes. *Curr Top Dev Biol* 2003; **58**: 111-136

7 **Scharfmann R**. Alternative sources of beta cells for cell therapy of diabetes. *Eur J Clin Invest* 2003; **33**: 595-600

8 **Soria B**, Skoudy A, Martin F. From stem cells to beta cells: new strategies in cell therapy of diabetes mellitus. *Diabetologia* 2001; **44**: 407-415

9 **Pattou F**, Kerr-Conte J, Gmyr V, Vandewalle B, Vantyghem MC, Lecomte-Houcke M, Proye C, Lefebvre J. Human pancreatic stem cell and diabetes cell therapy. *Bull Acad Natl Med* 2000; **184**: 1887-1899

10 **Delacour A**, Nepote V, Trumpp A, Herrera PL. Nestin expression in pancreatic exocrine cell lineages. *Mech Dev* 2004; **121**: 3-14

11 **Esni F**, Stoffers DA, Takeuchi T, Leach SD. Origin of exocrine pancreatic cells from nestin-positive precursors in developing mouse pancreas. *Mech Dev* 2004; **121**: 15-25

12 **Humphrey RK**, Bucay N, Beattie GM, Lopez A, Messam CA, Cirulli V, Hayek A. Characterization and isolation of promoter-defined nestin-positive cells from the human fetal pancreas. *Diabetes* 2003; **52**: 2519-2525

13 **Lardon J**, Rooman I, Bouwens L. Nestin expression in pancreatic stellate cells and angiogenic endothelial cells. *Histochem Cell Biol* 2002; **117**: 535-540

14 **Suzuki T**, Kadoya Y, Sato Y, Handa K, Takahashi T, Kakita A, Yamashina S. The expression of pancreatic endocrine markers in centroacinar cells of the normal and regenerating rat pancreas: their possible transformation to endocrine cells. *Arch Histol Cytol* 2003; **66**: 347-358

15 **Ferber S,** Halkin A, Cohen H, Ber I, Einav Y, Goldberg I, Barshack I, Seijffers R, Kopolovic J, Kaiser N, Karasik A. Pancreatic and duodenal homeobox gene 1 induces expression of insulin genes in liver and ameliorates streptozotocin-induced hyperglycemia. *Nat Med* 2000; **6**: 568-572

Edited by Kumar M **Proofread by** Xu FM

PO Box 2345, Beijing 100023, China
Fax: +86-10-85381893
E-mail: wjg@wjgnet.com www.wjgnet.com

World J Gastroenterol 2004;10(17):2553-2556
World Journal of Gastroenterology
Copyright © 2004 by The WJG Press ISSN 1007-9327

• BRIEF REPORTS •

Heparin improves organ microcirculatory disturbances in caerulein-induced acute pancreatitis in rats

Marek Dobosz, Lucjanna Mionskowska, Stanislaw Haæ, Sebastian Dobrowolski, Dariusz Dymecki, Zdzislaw Wajda

Marek Dobosz, Lucjanna Mionskowska, Department of General and Gastroenterological Surgery, St. Vincent a'Paulo Hospital, Gdynia, Poland
Stanislaw Haæ, Sebastian Dobrowolski, Dariusz Dymecki, Zdzislaw Wajda, Department of General, Transplant and Endocrine Surgery, Medical University of Gdañsk, Poland
Supported by Medical University of Gdañsk, grant W-120, Poland
Correspondence to: Marek Dobosz, M.D., Ph.D., ul. Kossaka 2/7, 80-249 Gdañsk, Poland. marek-dobosz@wp.pl
Telephone: +48-58-6665540 **Fax:** +48-58-6665540
Received: 2004-02-06 **Accepted:** 2004-03-02

Abstract

AIM: Microcirculatory disturbances are important early pathophysiological events in various organs during acute pancreatitis. The aim of the study was to evaluate changes in microperfusion of the pancreas, liver, kidney, stomach, colon, skeletal muscle, and to investigate the influence of heparin on the organ microcirculation in caerulein-induced experimental acute pancreatitis.

METHODS: Acute pancreatitis was induced by 4 intraperitoneal injections of caerulein (Cn) (15 μg/kg). The organ microcirculation was measured by laser Doppler flowmetry. Serum interleukin 6 and hematocrit levels were analysed.

RESULTS: Acute pancreatitis resulted in a significant drop of microperfusion in all examined organs. Heparin administration (2×2.5 mg/kg) improved the microcirculation in pancreas (36.9±4% *vs* 75.9±10%), liver (56.6±6% *vs* 75.2±16%), kidney (45.1±6% *vs* 79.3±5%), stomach (65.2±8% *vs* 78.1±19%), colon (69.8±6% *vs* 102.5±19%), and skeletal muscle (59.2±6% *vs* 77.9±13%). Heparin treatment lowered IL-6 (359.0±66 U/mL *vs* 288.5±58 U/mL) and hematocrit level (53±4% *vs* 46±3%).

CONCLUSION: Heparin administration has a positive influence on organ microcirculatory disturbances accompanying experimental Cn-induced acute pancreatitis.

Dobosz M, Mionskowska L, Haæ S, Dobrowolski S, Dymecki D, Wajda Z. Heparin improves organ microcirculatory disturbances in caerulein-induced acute pancreatitis in rats. *World J Gastroenterol* 2004; 10(17): 2553-2556
http://www.wjgnet.com/1007-9327/10/2553.asp

INTRODUCTION

Pathophysiolsogy of acute pancreatitis (AP) is heterogeneous and involves a complex cascade of events. Impaired tissue perfusion within the pancreatic gland is one of the early disorders accompanying the disease[1,2]. Prolonged ischaemia and impaired tissue oxygenation, resulting from vasoconstriction, hemoconcentration, hypercoagulation, leukocyte adherence, increased vascular permeability, and interstitial oedema, play an important role in the progression of the disease, leading to the development of pancreatic necrosis[2-4]. Besides the pancreas, the microcirculatory disturbances, as a consequence of hypovolemia and systemic inflammatory response, are also observed in other organs[1,5-8].

Although the hypovolemia and impairment of cardiac output can be normalized easily by vigorous fluid replacement, microcirculatory disturbances may be prevented merely by adequate fluid therapy, even though the cardiovascular parameters are stabilized at the baseline level[9]. Various vasoactive mediators, as bradykinin, endothelin, thromboxan, platelet activating factor, and nitric oxide participate in the development of microcirculatory failure[3,8]. In the last decade, the beneficial effect of therapeutic strategies in acute pancreatitis, affecting vasoactive mediators, is confirmed in several experimental studies.

One of the possible therapeutic agents, influencing microcirculatory disturbances by means of its anticoagulant and antiinflammatory properties, which could be applied in acute pancreatitis, is heparin. Some reports underlined beneficial impact of this well known polysaccharide on the course of the disease[10-12]. In this study we examined whether heparin influenced splanchnic malperfusion in experimental caerulein-induced acute pancreatitis in rats.

MATERIALS AND METHODS

Animal models

The study was carried out on 34 male Wistar rats weighing 180-200 g. The rats were kept on a standard rat chow and fasted overnight before the experiment with water *ad libitum.* Acute pancreatitis was induced by four intraperitoneal injections of caerulein (Cn) (Sigma, St. Louis, USA) (15 μg/kg) in 1 mL of saline at 1h intervals: at the begining, and consecutively after the first, second, and third hour of the experiment. Five hours after the first caerulein injection, rats were anaesthetized with pentobarbital sodium (40 mg/kg). Following the anaesthesia, a laparotomy was performed, and a fiberoptic probe of laser Doppler flowmeter (Periflux 4 001, Perimed Jarfalla, Sweden) was positioned against the surface of the pancreas, liver, kidney, stomach, colon, and skeletal muscle of thigh in order to estimate the organs' perfusion. Blood flow was measured in three different portions of each organ, the mean values were calculated, and presented as percent changes from basal values obtained in control rats (100%). After the measurements, blood was aspirated from the inferior caval vein for hematocrit and interleukin 6 tests, the pancreas was removed for microscopic evaluation, and the animals were exsanquinated.

The animals were randomly allocated into three groups: Group I (n=10), control; Group II (n=12), Cn-induced pacreatitis without treatment; and Group III (n=12), Cn-induced pancreatitis treated with heparin (Polfa, Warszawa, Poland) 2×2.5 mg/kg, given in the 3rd and 4th hafter the first Cn injection.

This study was approved by the Ethical Committee of the Medical University of Gdañsk.

Interleukin-6 functional assay

The IL-6 bioassay was performed using the IL-6 dependent

mouse hybridoma cell line B9 obtained from Dr. Lucien Aarden, Netherland Red Cross, Amsterdam. B9 cells were cultured in flat bottomed microtitre plates (10 000 cells/well) in the presence of serial dilutions of test sera. Starting serum dilutions were 1:10 for all specimens. After 48 h of incubation, proliferation of the B9 cells was measured using a rapid colorimetric MTT (tetrazolium) assay. The concentration of recombinant IL-6 producing half maximal proliferation was defined as one unit of activity, and the quantity of IL-6 in a serum sample was calculated by reference to a standard curve. Polyclonal anti-IL-6 antibody (Boehringer-Mannheim) was added into selected wells at concentrations: 1:10, 1:20, 1:50 in order to confirm the specificity of the assay. The antibody completely blocked IL-6 activity.

Statistical analysis

Data are presented as mean±SD. The differences between the groups were analysed by means of ANOVA test. Probability values less than 0.05 were considered significant.

RESULTS

Four intraperitoneal caerulein injections resulted in marked pancreatic oedema in all the rats. The microscopic examination revealed oedematous form of acute pancreatitis, with inter-and intralobular oedema, vacuolisation of parenchymal cells, and leukocyte infiltration within the pancreatic gland. No parenchymal necrosis was detected.

Microcirculatory values

Caerulein induced acute pancreatitis resulted in a significant drop of pancreatic microperfusion to 36.9±4% of basal values. Administration of heparin significantly improved the microcirculation of the pancreas up to 75.9±13%. Hepatic perfusion in rats with pancreatitis receiving no treatment was decreased to 56.6±6%, heparin injection raised this parameter to 75.2±16%. Renal blood flow in group II with pancreatitis was diminished to 45.1±6%, which was improved significantly with heparin treatment up to 79.3±15%. Microcirculatory values of stomach and colon wall in acute pancreatitis group were reduced to 65.2±8% and 69.8±6% respectively. Intraperitoneal injection of heparin caused improvement in the blood flow in stomach to 78.1±19%, and especially in colon to 102.55±19%. Similarly, skeletal muscle perfusion in rats with pancreatitis was significantly ameliorated after heparin administration from 59.2±3% to 77.9±13% (Figure 1).

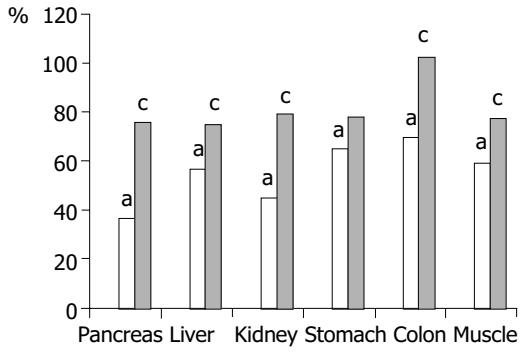

Figure 1 Microcirculatory parameters of pancreas, liver, kidney, stomach, colon and muscle (Mean values). Legend: grey bars: - control, white bars: - AP, black bars: - AP+heparin, [a]*P*<0.05 *vs* control, [c]*P*<0.05 *vs* AP group.

Serum interleukin 6 assay

Cn-induced acute pancreatitis caused a significant increase of serum IL-6 activity from 37.7±21 U/mL up to 359.0±66 U/mL in control rats. The heparin administration significantly diminished IL-6 level to 288.5±58 U/mL (Table 1).

Hematocrit measurements

The mean hematocrit level of the control group without pancreatitis was 41±3%. In group II with Cn-induced pancreatitis the hematocrit was significantly increased to 53±4%. Heparin administration in animals with pancreatitis of group III significantly reduced the hematocrit to 46±3% (Table 1).

Table 1 Interleukin 6 and hematocrit levels in the three groups

Group	Interleukin 6(U / mL)	Hematocrit (%)
Control	37.7±21	41±3
Acute pancreatitis	359.0±66[a]	53±4[a]
Acute pancreatitis + heparin	288.5±58[c]	46±3[c]

[a]*P*<0.05 *vs* control, [c]*P*<0.05 *vs* acute pancreatitis group.

DISCUSSION

Caerulein-induced experimental pancreatitis was adopted by many authors to investigate microcirculatory changes of AP. The present study indicated that in Cn-induced acute pancreatitis the microperfusion of the pancreas decreased to 36.9% of basal values. These observations are in accordance with other investigations, which revealed the drop of local pancreatic blood flow in Cn induced pancreatitis[2,13,14], although a majority of microcirculatory studies did not report such an obvious deterioration of the pancreatic perfusion as observed in the current study. Such a sharp decline of the pancreatic microperfusion might be influenced by the fact that the animals did not receive i.v. fluid administration, and could be elucidated also by an additional stress resulted from six i.p. injections of the drugs in conscious animals. In Liu's study[14], the water immersion stress in rats with Cn-induced pancreatitis caused further pancreatic ischemia, diminishing the pancreatic blood flow to 37% of the normal value, and was considered as an aggravating factor in AP.

In contrast to these observations, the Heidelberg group described increased pancreatic capillary flow in experimental oedematous pancreatitis[15,16]. The discrepancy of the results may be explained by various techniques of microcirculatory measurements and i.v. fluid administration. On the other hand, in the model of necrotizing pancreatitis, the authors observed a significant decrease of the pancreatic capillary flow[16].

The disturbances of microcirculation in acute pancreatitis were not only confined to pancreatic capillary bed but were also observed in other organs[5-8]. It was suggested that diffused microcirculatory disorders might play a crucial role in the development of the pancreatitis-associated multiorgan dysfunction syndrome[7], some authors even defined severe AP as a systemic dysfunction syndrome[7,17].

The present study confirmed these data. Besides the pancreas, reduced capillary perfusion was observed in liver, kidney, stomach, colon, and skeletal muscles, however the drop in perfusion of other organs was not so remarkable as in the pancreas. This suggests that in pancreatitis, pancreatic gland is especially susceptible to microcirculatory disorders. Kinnala *et al*. found that splanchnic malperfusion seemed to begin with pancreatic hypoperfusion before disturbances in gut microcirculation[1]. On the other hand, Hotz *et al.* noted that in mild pancreatitis, pancreatic capillary perfusion remained unchanged, whereas mucosal and subserosal colonic capillary blood flow was significantly reduced. It was also shown in their experiment that severe pancreatitis was associated with a marked reduction in both pancreatic and colonic capillary perfusion[18].

Microcirculatory disturbances in AP comprised many

components: decreased capillary blood flow and capillary density, increased capillary permeability, and enhanced leukocyte-endothelial interaction[7]. It still remains unclear which of these factors is the initiating one or the most important. It seems to be logical that any effort to improve the microcirculation may be beneficial for all organs, irrespective of the underlying initiating factors.

Many studies documented positive impacts of various treatments on improving microcirculation in acute pancreatitis. In studies by Konturek *et al*. and Liu *et al*. pancreatic microperfusion was ameliorated with L-arginine (nitric oxide donor) treatment[13,14]. Improvement of impaired pancreatic microcirculation by isovolemic hemodilution with dextran was observed by Klar *et al*.[19]. Rheologic properties of pentoxifylline, its antiinflammatory effect, reduction of thrombus formation, and lowering of blood viscosity had a positive influence on Cn-induced pancreatitis in study of Gomez-Cambronero *et al*.[20]. An advantageous effect of ICAM-1 antibodies on microcirculation in AP was shown by Foitzik *et al*.[21], and Werner *et al*.[22]. A single i.v. injection of bovine hemoglobin in an experiment by Strate *et al*. reduced microcirculatory dysfunction and pancreatic tissue damage in rodent pancreatitis[4]. In a study by Zhao *et al*. Chinese natural medicines: Yuanhu (YHI) and Huoxuehuayu (HHI-I) had a positive impact on acute pancreatitis development, including pancreatic malperfusion and serum IL-6 level. Recently, it was shown that endothelin receptor blockade might be a promising therapeutic approach in AP, resulting in improvement of microcirculation, decreased capillary permeability and tissue injury[7,23,24].

Intraperitoneal heparin administration in the current study significantly improved blood perfusion of examined organs. The beneficial effect of heparin on pancreatic microcirculation may in theory have an influence on severity of the disease, it could prevent or restrict the development of pancreatic necrosis. It was shown in our recent publication that heparin treatment in oedematous pancreatitis ameliorated the microscopic alterations of the pancreas: reduced leukocyte infiltration and diminished pancreatic oedema[25].

By improving hepatic capillary blood flow, heparin could influence phagocytic Kupffer cell function in the liver which is important for eliminating antigens and toxic substances in acute pancreatitis. The study of Forgacs *et al*. showed a close relationship between liver phagocytic function and hepatic microperfusion in the early stage of experimental pancreatitis[26]. On the other hand, Chen *et al*. revealed that a significant number of adherent leukocytes was observed in hepatic microcirculation 2 h after the induction of AP[27]. This could impair hepatic perfusion, and might be a potential target for heparin treatment. In another study, Chen *et al*. observed beneficial effects of protease inhibitor gabexate mesilate on pancreatic and hepatic microcirculation[8].

The pathophysiology of renal insufficiency, often observed as a complication of acute pancreatitis, is heterogeneous. The improvement of renal blood flow observed after heparin treatment in the rats with pancreatitis could also prevent this complication. Foitzik *et al*. using endothelin receptor blockers in severe acute pancreatitis, besides the enhancement of pancreatic perfusion, observed improved renal function[7].

It was shown that decreased capillary blood flow in the colonic mucosa was associated with impaired gut barrier function and increased translocation of live bacteria through the morphologically intact colonic wall[28]. The present study revealed that heparin treatment in the group with pancreatitis led the altered microperfusion of the colonic wall to the normal level. It suggests that heparin administration may play a role in prevention of secondary pancreatic infection.

Besides the organ microcirculatory improvement, heparin administration significantly decreased interleukin 6 activity, and reduced hematocrit level. IL-6 was a reliable predictor of acute pancreatitis severity[29]. Diminished IL-6 activity in the group with AP treated with heparin may indicate that this therapy could limit inflammatory response observed in AP. Beneficial influence of heparin on hematocrit level, observed in group III, may also suggest that heparin reduces capillary permeability, not just in the pancreatic gland, and prevent the fluid to the third space. Therefore heparin therapy may reduce the need for vigorous fluid resuscitation as applied in patients with AP.

The improvement of systemic microperfusion after heparin administration in rats with AP might be explained by its anticoagulatory effect which diminished blood viscosity and facilitated capillary blood flow. Besides its anticoagulant properties, heparin may play a positive role in AP treatment due to its antiinflammatory effects: TNF inhibition[30], protection from oxygen free radicals[31], the blockade of complement activity[32] and histamine release[33]. It was also shown that heparin prevented post-ischemic endothelial cell dysfunction[34], neutrophil adhesion[35], and had an inhibitory effect on the biosynthesis and release of endothelin-1, a very potent endogenous vasoconstrictor[36,37].

In conclusion, heparin counteracts microcirculatory disorders, not only within the pancreas but also in other organs. The preservation of organ microperfusion with this treatment may be significant for diminishing and treating local and systemic complications in AP.

REFERENCES

1 **Kinnala PJ**, Kuttila KT, Gronroos JM, Havia TV, Nevalainen TJ, Niinikoski JH. Splanchnic and pancreatic tissue perfusion in experimental acute pancreatitis. *Scand J Gastroenterol* 2002; **37**: 845-849

2 **Zhou ZG**, Chen YD, Sun W, Chen Z. Pancreatic microcirculatory impairment in experimental acute pancreatitis in rats. *World J Gastroenterol* 2002; **8**: 933-936

3 **Zhou ZG**, Chen YD. Influencing factors of pancreatic microcirculatory impairment in acute panceatitis. *World J Gastroenterol* 2002; **8**: 406-412

4 **Strate T**, Mann O, Kleinhans H, Schneider C, Knoefel WT, Yekebas E, Standl T, Bloechle C, Izbicki JR. Systemic intravenous infusion of bovine hemoglobin significantly reduces microcirculatory dysfunction in experimentally induced pancreatitis in the rat. *Ann Surg* 2003; **238**: 765-771

5 **Foitzik T**, Eibl G, Hotz B, Hotz H, Kahrau S, Kasten C, Schneider P, Buhr HJ. Persistent multiple organ microcirculatory disorders in severe acute pancreatitis: experimental findings and clinical implications. *Dig Dis Sci* 2002; **47**: 130-138

6 **Skoromnyi AN**, Starosek VN. Hemodynamic changes in the liver, kidney, small intestine and pancreas in experimental acute pancreatitis. *Klin Khir* 1998; **12**: 46-48

7 **Foitzik T**, Eibl G, Hotz HG, Faulhaber J, Kirchengast M, Buhr HJ. Endothelin receptor blockade in severe acute pancreatitis leads to systemic enhancement of microcirculation, stabilization of capillary permeability, and improved survival rates. *Surgery* 2000; **128**: 399-407

8 **Chen HM**, Hwang TL, Chen MF. The effect of gabexate mesilate on pancreatic and hepatic microcirculation in acute experimental pancreatitis in rats. *J Surg Res* 1996; **66**: 147-153

9 **Knol JA**, Inman MG, Strodel WE, Eckhauser FE. Pancreatic response to crystalloid resuscitation in experimental pancreatitis. *J Surg Res* 1987; **43**: 387-392

10 **Gabryelewicz A**, Kosidlo S, Prokopowicz J, Podkowicz K. Does heparin modify protease-antiprotease balance in acute experimental pancreatitis in rats. *Hepatogastroenterology* 1986; **33**: 79-82

11 **Goulbourne IA,** Watson H, Davies GC. 111In-platelet and 125I-fibrinogen deposition in the lungs in experimental acute pancreatitis. *J Surg Res* 1987; **43**: 521-526

12 **Rabenstein T**, Roggenbuck S, Framke B, Martus P, Fischer B, Nusko G, Muehldorfer S, Hochberger J, Ell C, Hahn EG, Schneider HT. Complications of endoscopic sphincterotomy:

can heparin prevent acute pancreatitis after ERCP? *Gastrointest Endosc* 2002; **55**: 476-483

13 **Konturek SJ**, Szlachcic A, Dembinski A, Warzecha Z, Jaworek J, Stachura J. Nitric oxide in pancreatic secretion and hormone-induced pancreatitis in rats. *Int J Pancreatol* 1994; **15**: 19-28

14 **Liu X**, Nakano I, Yamaguchi H, Ito T, Goto M, Koyanagi S, Kinjoh M, Nawata H. Protective effect of nitric oxide on development of acute pancreatitis in rats. *Dig Dis Sci* 1995; **40**: 2162-2169

15 **Klar E**, Schratt W, Foitzik T, Buhr H, Herfarth C, Messmer K. Impact of microcirculatory flow pattern changes on the development of acute edematous and necrotizing pancreatitis in rabbit pancreas. *Dig Dis Sci* 1994; **39**: 2639-2644

16 **Schmidt J**, Ebeling D, Ryschich E, Werner J, Gebhard MM, Klar E. Pancreatic capillary blood flow in an improved model of necrotizing pancreatitis in the rat. *Surg Res* 2002; **106**: 335-341

17 **Gullo A**, Berlot G. Ingredients of organ dysfunction or failure. *World J Surg* 1996; **20**: 430-436

18 **Hotz HG**, Foitzik T, Rohweder J, Schulzke JD, Fromm M, Runkel NS, Buhr HJ. Intestinal microcirculation and gut permeability in acute pancreatitis: early changes and therapeutic implications. *J Gastrointest Surg* 1998; **2**: 518-525

19 **Klar E**, Mall G, Messmer K, Herfarth C, Rattner DW, Warshaw AL. Improvement of impaired pancreatic microcirculation by isovolemic hemodilution protects pancreatic morphology in acute biliary pancreatitis. *Surg Gynecol Obstet* 1993; **176**: 144-150

20 **Gomez-Cambronero L**, Camps B, de La Asuncion JG, Cerda M, Pellin A, Pallardo FV, Calvete J, Sweiry JH, Mann GE, Vina J, Sastre J. Pentoxifylline ameliorates cerulein-induced pancreatitis in rats: role of glutathione and nitric oxide. *J Pharmacol Exp Ther* 2000; **293**: 670-676

21 **Foitzik T**, Eibl G, Buhr HJ. Therapy for microcirculatory disorders in severe acute pancreatitis: comparison of dalayed therapy with ICAM-1 antibodies and a specific endothelin A receptor antagonist. *J Gastrointest Surg* 2000; **4**: 240-246

22 **Werner J**, Hartwig W, Schmidt E, Gebhard MM, Herfarth C, Klar E. Reduction of local and systemic complications of acute pancreatitis by monoclonal antibody to ICAM-1. *Langenbecks Arch Chir Suppl Kongressbd*. 1998; **115** (Suppl I): 725-729

23 **Foitzik T**, Hotz HG, Eibl G, Faulhaber J, Kirchengast M, Buhr HJ. Endothelin receptor block in acute pancreatitis –improvement of microcirculation and decrease of capillary permeability also distant from the pancreas. *Langenbecks Arch Chir Suppl Kongressbd* 1998; **115**(Suppl I): 427-429

24 **Plusczyk T**, Witzel B, Menger MD, Schilling M. ETA and ETB receptor function in pancreatitis-associated microcirculatory failure, inflammation, and parenchymal injury. *Am J Physiol Gastrointest Liver Physiol* 2003; **285**: G145-153

25 **Dobosz M**, Wajda Z, Hac S, Myœliwska J, Bryl E, Mionskowska L, Roszkiewicz A, Mysliwski A. Nitric oxide, heparin and procaine treatment in experimental ceruleine-induced acute pancreatitis in rats. *Arch Immunol Ther Exp* 1999; **47**: 155-160

26 **Forgacs B**, Eibl G, Wudel E, Franke J, Faulhaber J, Kahrau S, Buhr HJ, Foitzik T. RES function and liver microcirculation in the early stage of acute experimental pancreatitis. *Hepatogastroenterology* 2003; **50**: 861-866

27 **Chen HM**, Sunamura M, Shibuya K, Yamauchi JI, Sakai Y, Fukuyama S, Mikami Y, Takeda K, Matsuno S. Early microcirculatory derangement in mild and severe pancreatitis models in mice. *Surg Today* 2001; **31**: 634-642

28 **Foitzik T**, Stufler M, Hotz HG, Klinnert J, Wagner J, Warshaw AL, Schulzke JD, Fromm M, Buhr HJ. Glutamine stabilizes intestinal permeability and reduces pancreatic infection in acute experimental pancreatitis. *J Gastrointest Surg* 1997; **1**: 40-47

29 **Bhatia M**, Brady M, Shokuhi S, Christmas S, Neoptolemos JP, Slavin J. Inflammatory mediators in acute pancreatitis. *J Pathol* 2000; **190**: 117-125

30 **Lantz M**, Thysell H, Nilsson E, Olsson I. On the binding of tumor necrosis factor (TNF) to heparin and the release *in vivo* of the TNF-binding protein I by heparin. *J Clin Invest* 1991; **88**: 2026-2031

31 **Hiebert LM**, Liu JM. Heparin protects cultured arterial endothelial cells from damage by toxic oxygen metabolites. *Atherosclerosis* 1990; **83**: 47-51

32 **Weiler JM**, Edens RE, Linhardt RJ, Kapelanski DP. Heparin and modified heparin inhibit complement activation *in vivo*. *J Immunol* 1992; **148**: 3210-3215

33 **Lucio J**, D'Brot J, Guo CB, Abraham WM, Lichtenstein LM, Kagey-Sobotka A, Ahmed T. Immunologic mast cell-mediated responses and histamine release are attenuated by heparin. *J Appl Physiol* 1992; **73**: 1093-1101

34 **Sternbergh WC 3rd**, Makhoul RG, Adelman B. Heparin prevents postischemic endothelial cell dysfunction by a mechanism independent of its anticoagulant activity. *J Vasc Surg* 1993; **17**: 318-327

35 **Leculier C**, Benzerara O, Couprie N, Francina A, Lasne Y, Archimbaud E, Fiere D. Specific binding between human neutrophils and heparin. *Br J Haematol* 1992; **81**: 81-85

36 **Imai T**, Hirata Y, Emori T, Marumo F. Heparin has an inhibitory effect on endothelin-1 synthesis and release by endothelial cells. *Hypertension* 1993; **21**: 353-358

37 **Inoue K**, Hirota M, Kimura Y, Kuwata K, Ohmuraya M, Ogawa M. Further evidence for endothelin as an important mediator of pancreatic and intestinal ischemia in severe acute pancreatitis. *Pancreas* 2003; **26**: 218-223

Edited by Zhu LH and Xu FM

PO Box 2345, Beijing 100023, China
Fax: +86-10-85381893
E-mail: wjg@wjgnet.com www.wjgnet.com

World J Gastroenterol 2004;10(17):2557-2559
World Journal of Gastroenterology
Copyright © 2004 by The WJG Press ISSN 1007-9327

• BRIEF REPORTS •

Helicobacter pylori in gastric corpus of patients 20 years after partial gastric resection

Christian Kirsch, Ahmed Madisch, Petja Piehler, Ekkehard Bayerdörffer, Manfred Stolte, Stephan Miehlke

Christian Kirsch, Ahmed Madisch, Stephan Miehlke, Medical Department I, Technical University Hospital, Dresden, Germany
Petja Piehler, Community Hospital, Kitzbühl, Germany
Ekkehard Bayerdörffer, Department of Internal Medicine, University Hospital, Marburg, Germany
Manfred Stolte, Institute of Pathology, Klinikum Bayreuth, Germany
Correspondence to: Dr. Stephan Miehlke, Medical Department I, Technical University Hospital Carl Gustav Carus, Fetscherstraße 74, D-01307 Dresden, Germany. miehlke@mk1.med.tu-dresden.de
Telephone: +49-351-4585645 **Fax:** +49-351-4584394
Received: 2004-03-23 **Accepted:** 2004-04-29

Abstract

AIM: To determine the long-term prevalence of *Helicobacter pylori* (*H pylori*) gastritis in patients after partial gastric resection due to peptic ulcer, and to compare the severity of *H pylori*-positive gastritis in the corpus mucosa between partial gastrectomy patients and matched controls.

METHODS: Endoscopic biopsies were obtained from 57 patients after partial gastric resection for histological examination using hematoxylin/eosin and Warthin-Starry staining. Gastritis was graded according to the updated Sydney system. Severity of corpus gastritis was compared between *H pylori*-positive partial gastrectomy patients and *H pylori*-positive duodenal ulcer patients matched for age and gender.

RESULTS: In partial gastrectomy patients, surgery was performed 20 years (median) prior to evaluation. In 25 patients (43.8%) *H pylori* was detected histologically in the gastric remnant. Gastric atrophy was more common in *H pylori*-positive compared to *H pylori*-negative partial gastrectomy patients ($P<0.05$). The severity of corpus gastritis was significantly lower in *H pylori*-positive partial gastrectomy patients compared to duodenal ulcer patients ($P<0.01$). There were no significant differences in the activity of gastritis, atrophy and intestinal metaplasia between the two groups.

CONCLUSION: The long-term prevalence of *H pylori* gastritis in the gastric corpus of patients who underwent partial gastric resection due to peptic ulcer disease is comparable to the general population. The expression of *H pylori* gastritis in the gastric remnant does not resemble the gastric cancer phenotype.

Kirsch C, Madisch A, Piehler P, Bayerdörffer E, Stolte M, Miehlke S. *Helicobacter pylori* in gastric corpus of patients 20 years after partial gastric resection. *World J Gastroenterol* 2004; 10(17): 2557-2559
http://www.wjgnet.com/1007-9327/10/2557.asp

INTRODUCTION

Helicobacter pylori (*H pylori*) is the major etiological factor for peptic ulcer disease and gastric MALT lymphoma, and is strongly linked to the development of gastric carcinoma[1-3]. Recently, a gastric cancer phenotype of *H pylori* gastritis has been proposed, which is characterized by an increased inflammation of the corpus mucosa[4]. This phenotype of *H pylori* gastritis is significantly more common in patients with early gastric cancer, and also in those with advanced stages of gastric cancer[4,5]. An increased severity of corpus inflammation has also been described in particular risk groups for gastric cancer, such as first-degree relatives of gastric cancer patients[6]. In contrast, patients with duodenal ulcer disease are characterized by a severe gastritis in the antrum, but a mild gastritis in the corpus[7]. The risk for gastric cancer in duodenal ulcer patients is low compared to the general population[8].

Patients underwent partial gastric resection for peptic ulcer are at high risk for developing cancer in the gastric remnant[9]. Several mechanisms have been proposed for this phenomenon. It has been suggested that stump cancers uniformly develop upon a background of chronic mucosal changes in the gastric remnant[10-12]. Factors that may contribute to cancer of the gastric remnant include enterogastric pancreaticobiliary reflux, hypochlorhydria, microflora, and N-nitroso compounds[13,14].

The role of *H pylori* gastritis with respect to cancer risk in patients underwent partial gastric resection for benign peptic ulcer disease is not clearly defined. Assuming that the majority of peptic ulcer patients were *H pylori*-infected at the time of surgery, persisting *H pylori* infection and long-term inflammation of the gastric corpus mucosa might contribute to carcinogenesis in these patients.

The aim of our study was therefore to determine the prevalence of *H pylori* gastritis in the gastric remnant of patients who underwent partial gastric resection, and to test the hypothesis that *H pylori*-positive patients with partial gastric resection may have a more severe corpus gastritis resembling the gastric cancer phenotype of *H pylori* gastritis.

MATERIALS AND METHODS

The study included consecutive patients who were admitted to our institution for surveillance endoscopy after partial gastric resection due to peptic ulcer disease. Exclusion criteria included previous surgery for gastric cancer, previous treatment for *H pylori* infection, and a present ulcer or tumor under endoscopy. Further exclusion criteria included pretreatment with antibiotics, proton-pump inhibitors, non-steroidal anti-inflammatory within the 4 wk before study entry.

Endoscopic biopsies were routinely obtained in 4 quadrants from the anastomosis, or from any suspicious macroscopic lesion. In addition, 2 biopsies were obtained from the middle of the remnant corpus and 2 from the cardia for assessing prevalence, severity of *H pylori* gastritis, and gastric atrophy. All biopsy specimens were fixed in 40 g/L formaldehyde and embedded in paraffin. Sections were stained with hematoxylin and eosin and Warthin-Starry. The presence of *H pylori* colonization as well as intestinal metaplasia and atrophy were judged as positive or negative. The grade of gastritis (infiltration of lymphocytes and plasma cells), the activity of gastritis (infiltration of neutrophil granulocytes), and the replacement of foveolar epithelium by regenerative epithelium were assessed by a semiquantitative

scale (grade 0 = negative, grade 1 = mild, grade 2 = moderate, grade 3 = severe) in accordance with the updated Sydney system[15].

The control group consisted of *H pylori*-positive patients with duodenal ulcer disease who participated in previous clinical trials[7] and who were age- and gender-matched. In these patients, endoscopic biopsies have been obtained from the antrum and the corpus, and were processed as described above. All histological slides were assessed by a single pathologist.

Data analysis was performed using the statistical software package SPSS 10.0 for Windows. The Chi-square test or Fisher exact test was used when appropriate. $P<0.05$ was considered statistically significant.

RESULTS

A total of 57 patients with partial gastric resection were included into the study (19 males and 38 females, median age 64 years, range 26-92 years). The time period between surgery and histology assessment ranged from 8 to 47 years with a median of 20 years. None of the intraepithelial neoplasia was detected at the gastric anastomosis. In 25 patients (43.9%) *H pylori* was detected histologically in the gastric remnant.

Table 1 summarizes the histological features in the corpus and cardia of partial gastrectomy patients. For analysis purposes, patients with grade 0 and 1, and patients with grade 2 and 3 were combined, respectively. There was a higher proportion of patients with moderate or severe activity of gastritis in the corpus ($P<0.0005$) and cardia ($P = 0.007$) among *H pylori*-positive patients compared to *H pylori*-negative partial gastrectomy patients. In addition, the proportion of patients with atrophy in the corpus mucosa was significantly higher among *H pylori*-positive compared to *H pylori*-negative patients ($P = 0.047$). No significant differences were found with regard to grade of gastritis, regenerative epithelium and the presence of intestinal metaplasia between *H pylori*-positive and *H pylori*-negative partial gastrectomy patients.

The comparison of corpus gastritis between *H pylori*-positive partial gastrectomy patients and *H pylori*-positive duodenal ulcer patients is summarized in Table 2. The proportion of patients with moderate or severe grade of gastritis in the corpus ($P = 0.001$) and with moderate or severe regenerative epithelium ($P = 0.004$) was significantly lower in *H pylori*-positive partial gastrectomy patients than that in *H pylori*-positive duodenal ulcer patients, respectively. A similar trend was observed for the activity of gastritis in the corpus, however the differences were not statistically significant. The prevalence of intestinal metaplasia in the corpus mucosa was similar in both groups. The prevalence of atrophy in the corpus mucosa was higher in partial gastrectomy patients, however the difference did not reach statistical significance.

Table 2 Severity of corpus gastritis in *H pylori*-positive partial gastrectomy patients and *H pylori*-positive duodenal ulcer patients matched by age and gender

	Partial gastrectomy (n = 25)	Duodenal ulcer (n = 25)	P
Grade of gastritis			
Grade 0 or 1, *n* (%)	24 (96)	13 (52)	
Grade 2 or 3, *n* (%)	1 (4)	12 (48)	0.001
Activity of gastritis			
Grade 0 or 1, *n* (%)	16 (64)	11 (44)	
Grade 2 or 3, *n* (%)	9 (36)	14 (56)	0.256
Regenerative epithelium			
Grade 0 or 1, *n* (%)	25 (100)	17 (68)	
Grade 2 or 3, *n* (%)	0 (0)	8 (32)	0.004
Intestinal metaplasia			
Present, *n* (%)	5 (20)	5 (20)	1.00
Atrophy			
Present, *n* (%)	11 (44)	5 (20)	0.128

DISCUSSION

In the present study the prevalence of *H pylori* gastritis in patients underwent partial gastrectomy was 43.9% which is comparable to the average population in Germany and which is within the range of other studies on the *H pylori* prevalence in partial gastrectomy patients[16-20].

An association between *H pylori* infection and an increased acute and chronic inflammatory response and a higher prevalence of chronic atrophic gastritis and intestinal metaplasia in the gastric remnant mucosa has been described[16,18] while others were non-confirmatory[20]. Our study suggests that *H pylori* leads to a higher proportion of atrophy in the corpus of the gastric remnant compared to *H pylori*-negative partial gastrectomy patients.

Several studies have shown that a severe although non-atrophic gastritis in the corpus mucosa is a particular risk factor for gastric cancer among those individuals infected with *H pylori*[4-7]. These findings were recently confirmed by a prospective observational study from Japan where gastric cancer developed only in those patients infected with *H pylori*[21] and where a

Table 1 Histology in the corpus and cardia of partial gastrectomy patients

	Corpus			Cardia		
	HP + n = 25	HP − n = 32	P	HP + n = 25	HP − n = 32	P
Grade of gastritis						
Grade 0 or 1, *n* (%)	24 (96)	32 (100)	-	24 (96)	32 (100)	-
Grade 2 or 3, *n* (%)	1 (4)	0	0.439	1 (4)	0	0.439
Activity of gastritis						
Grade 0 or 1, *n* (%)	16 (64)	32 (100)	-	16 (64)	32 (100)	-
Grade 2 or 3, *n* (%)	9 (36)	0	<0.0005	9 (36)	0	0.007
Regenerative epithelium						
Grade 0 or 1, *n* (%)	25 (100)	32 (100)	-	24 (96)	32 (100)	-
Grade 2 or 3, *n* (%)	0	0	-	1 (4)	0	0.439
Intestinal metaplasia						
Present, *n* (%)	5 (20)	7 (22)	1.00	4 (16)	4 (12.5)	0.720
Atrophy						
Present, *n* (%)	11 (44)	6 (19)	0.047	0	3 (9.5)	0.248

No partial gastrectomy patient had a grade 2 or 3 regenerative type of epithelium in the corpus. Based upon this result a statistical analysis with regard to regenerative type of epithelium in the corpus was not appropriate.

corpus-dominant gastritis or pangastritis was associated with an 34-fold increased risk for gastric cancer. Based upon the increased risk for gastric cancer in the presence of severe corpus gastritis we hypothesized that patients with partial gastrectomy due to ulcer disease may develop a corpus-dominant phenotype of *H pylori* gastritis, which may contribute as a risk factor for cancer in these patients. Surprisingly, we found a significant lower grade of gastritis in the corpus of *H pylori*-positive partial gastrectomy patients compared to the control group consisting of *H pylori*-positive duodenal ulcer patients. Possible explanation for this finding might include that in some patients the infection may have disappeared spontaneously due to an altered gastric milieu, or that some of the patients may have been operated due to *H pylori*-negative ulcer caused by nonsteroidal anti-inflammatory drugs. Other patients may have received antibiotic therapy for other indications that *H pylori* infection potentially leads to coincident eradication of the bacteria. Nevertheless, we conclude that partial gastrectomy patients should be tested for *H pylori* infection, and, if diagnosed positive, eradication therapy should be initiated to reduce the risk of ulcer relapse[22].

Other factors than *H pylori* have been implicated in the pathogenesis of the mucosa alterations in partial gastrectomy patients, including enterogastric reflux, achlorhydria and increased mucosal proliferation, effects of vagotomy and dietary factors[23-26]. Bile reflux may play a promotional role by increasing permeability to initiating carcinogens. This enterogastric reflux has been reported to be more pronounced after a gastrojejunostomy than after a gastroduodenostomy, which may explain the higher stomach cancer risk after a Billroth II operation[27-29].

In conclusion, our study suggests that the *H pylori* prevalence in partial gastrectomy patients (former peptic ulcer patients) is comparable to the general population. *H pylori*-positive partial gastrectomy patients appear not to develop a corpus-dominant gastritis resembling the gastric cancer phenotype of *H pylori* gastritis.

REFERENCES

1 **Graham DY.** *Helicobacter pylori* infection in the pathogenesis of duodenal ulcer and gastric cancer: a model. *Gastroenterology* 1997; **113**; 1983-1991

2 **Bayerdörffer E,** Miehlke S, Neubauer A, Stolte M. Gastric MALT -lymphoma and *Helicobacter pylori* infection. *Aliment Pharmacol Ther* 1997; **11**(Suppl 1): 89-94

3 Schistosomes, liver flukes and *Helicobacter pylori*. IARC Working group on the evaluation of carcinogenic risks to humans. Lyon, 7-14 June 1994. *IARC Monogr Eval Carcinog Risks Hum* 1994; **61**: 1-241

4 **Meining A**, Bayerdörffer E, Müller P, Miehlke S, Lehn N, Hölzel D, Hatz R, Stolte M. Gastric carcinoma risk index in patients infected with *Helicobacter pylori*. *Virchows Arch* 1998; **432**: 311-314

5 **Miehlke S,** Hackelsberger A, Meining A, Hatz R, Lehn N, Malfertheiner P, Stolte M, Bayerdörffer E. Severe expression of corpus gastritis is characteristic in gastric cancer patients infected with *Helicobacter pylori*. *Br J Cancer* 1998; **78**: 263-266

6 **Meining AG,** Bayerdorffer E, Stolte M. *Helicobacter pylori* gastritis of the gastric cancer phenotype in relatives of gastric carcinoma patients. *Eur J Gastroenterol Hepatol* 1999; **11**: 717-720

7 **Meining A,** Stolte M, Hatz R, Lehn N, Miehlke S, Morgner A, Bayerdörffer E. Differing degree and distribution of gastritis in *Helicobacter pylori* -associated diseases. *Virchows Arch* 1997; **431**: 11-15

8 **Hansson LE,** Nyren O, Hsing AW, Bergström R, Josefsson S, Chow WH, Fraumeni JF Jr, Adami HO. The risk of stomach cancer in patients with gastric or duodenal ulcer disease. *N Engl J Med* 1996; **335**: 242-249

9 **Safatle-Ribeiro AV,** Ribeiro U Jr, Reynolds JC. Gastric stump cancer: what is the risk? *Dig Dis* 1998; **16**: 159-168

10 **Safatle-Ribeiro AV,** Ribeiro Junior U, Reynolds JC, Gama-Rodrigues JJ, Iriya K, Kim R, Bakker A, Swalsky PA, Pinotti HW, Finkelstein SD. Morphologic, histologic, and molecular similarities between adenocarcinomas arising in the gastric stump and the intact stomach. *Cancer* 1996; **78**: 2288-2299

11 **Kaminishi M,** Shimizu N, Yamaguchi H, Hashimoto M, Sakai S, Oohara T. Different carcinogenesis in the gastric remnant after gastrectomy for gastric cancer. *Cancer* 1996; **77**(8 Suppl): 1646-1653

12 **Bajtai A,** Hidvegi J. The role of gastric mucosal dysplasia in the development of gastric carcinoma. *Pathol Oncol Res* 1998; **4**: 297-300

13 **Langhans P,** Bues M, Bunte H. Morphological changes in the operated stomach under the influence of duodenogastric reflux. Clinical follow-up over 20 years. *Scand J Gastroenterol Suppl* 1984; **92**: 145-148

14 **Sobala GM,** Pignatelli B, Schorah CJ, Bartsch H, Sanderson M, Dixon MF, Shires S, King RF, Axon AT. Levels of nitrite, nitrate, N-nitroso compounds, ascorbic acid, and total bile acids in gastric juice of patients with and without precancerous conditions of the stomach. *Carcinogenesis* 1991; **12**: 193-198

15 **Dixon MF,** Genta RM, Yardley JH, Correa P. Classification and grading of gastritis. The updated Sydney System. International Workshop on the Histopathology of Gastritis, Houston 1994. *Am J Surg Pathol* 1996; **20**: 1161-1181

16 **Leung WK,** Lee YT, Choi CL, Chan FK, Ching J, Sung JJ. Diagnosis of *Helicobacter pylori* infection after gastric surgery for peptic ulcer: is the rapid urease test useful? *Scand J Gastroenterol* 1998; **33**: 586-589

17 **Ludtke FE,** Maierhof S, Kohler H, Bauer FE, Tegeler R, Schauer A, Lepsien G. *Helicobacter pylori* colonization in surgical patients. *Chirurg* 1991; **62**: 732-738

18 **Leivonen MK,** Haglund CH, Nordling SF. *Helicobacter pylori* infection after partial gastrectomy for peptic ulcer and its role in relapsing disease. *Eur J Gastroenterol Hepatol* 1997; **9**: 371-374

19 **Nagahata Y,** Kawakita N, Azumi Y, Numata N, Yano M, Saitoh Y. Etiological involvement of *Helicobacter pylori* in "reflux" gastritis after gastrectomy. *Am J Gastroenterol* 1996; **91**: 2130-2134

20 **Rino Y,** Imada T, Shiozawa M, Takahashi M, Fukuzawa K, Hasuo K, Nagano A, Tanaka J, Hatori S, Amano T, Kondo J. *Helicobacter pylori* of the remnant stomach and its eradication. *Hepatogastroenterology* 1999; **46**: 2069-2073

21 **Uemura N,** Okamoto S, Yamamoto S, Matsumura N, Yamaguchi S, Yamakido M, Taniyama K, Sasaki N, Schlemper RJ. *Helicobacter pylori* infection and the development of gastric cancer. *N Engl J Med* 2001; **345**: 784-789

22 **Lee YT,** Sung JJ, Choi CL, Chan FK, Ng EK, Ching JY, Leung WK, Chung SC. Ulcer recurrence after gastric surgery: is *Helicobacter pylori* the culprit? *Am J Gastroenterol* 1998; **93**: 928-931

23 **Offerhaus GJ,** Rieu PN, Jansen JB, Joosten HJ, Lamers CB. Prospective comparative study of the influence of postoperative bile reflux on gastric mucosal histology and *Campylobacter pylori* infection. *Gut* 1989; **30**: 1552-1557

24 **Fukuzawa K,** Noguchi Y, Matsumoto A. Alterations in DNA proliferation in gastric stump mucosa with special reference to topography. *Surgery* 1996; **119**: 191-197

25 **Ikeguchi M,** Kondou A, Oka A, Tsujitani S, Maeta M, Kaibara N. Flow cytometric analysis of the DNA content of tumor cells in cases of gastric cancer in the upper third of the stomach and in the remnant stomach. *Oncology* 1995; **52**: 116-122

26 **Kaminishi M,** Shimizu N, Shimoyama S, Yamaguchi H, Tsuji E, Aoki F, Nomura S, Yoshikawa A, Kuramoto S, Oohara T, Inada K, Tatematsu M. Denervation promotes the development of cancer-related lesions in the gastric remnant. *J Clin Gastroenterol* 1997; **25**(Suppl 1): S129-134

27 **Clarke MR,** Safatle-Ribeiro AV, Ribeiro U, Sakai P, Reynolds JC. Bcl-2 protein expression in gastric remnant mucosa and gastric cancer 15 or more years after partial gastrectomy. *Mod Pathol* 1997; **10**: 1021-1027

28 **Kodera Y,** Yamamura Y, Torii A, Uesaka K, Hirai T, Yasui K, Morimoto T, Kato T, Kito T. Gastric stump carcinoma after partial gastrectomy for benign gastric lesion: what is feasible as standard surgical treatment? *J Surg Oncol* 1996; **63**: 119-124

29 **Leivonen M,** Nordling S, Haglund C. Does *Helicobacter pylori* in the gastric stump increase the cancer risk after certain reconstruction types? *Anticancer Res* 1997; **17**: 3893-3896

Edited by Chen WW **Proofread by** Xu FM

PO Box 2345, Beijing 100023, China
Fax: +86-10-85381893
E-mail: wjg@wjgnet.com www.wjgnet.com

World J Gastroenterol 2004;10(17):2560-2562
World Journal of Gastroenterology
Copyright © 2004 by The WJG Press ISSN 1007-9327

• BRIEF REPORTS •

Cloning and expression and immunogenicity of *Helicobacter pylori* $BabA_2$ gene

Yang Bai, Ya-Li Zhang, Ye Chen, Jian-Feng Jin, Zhao-Shan Zhang, Dian-Yuan Zhou

Yang Bai, Ya-Li Zhang, Ye Chen, Dian-Yuan Zhou, PLA Institute for Digestive Medicine, Nanfang Hospital, the First Military Medical University, Guangzhou 510515, Guangdong Province, China
Jian-Feng Jin, Chemistry university of Beijing, Beijing 100071, China
Zhao-Shan Zhang, Institute of Biotechnology, Academy of Military Medical Sciences, Beijing 100071, China
Supported by the National Natural Science Foundation of China, No. 30270078
Correspondence to: Dr. Yang Bai, PLA Institute for Digestive Medicine, Nanfang Hospital, the First Military Medical University, Guangzhou 510515, Guangdong Province, China. Baiyang1030@hotmail.com
Telephone: +86-20-61641532
Received: 2003-08-06 **Accepted:** 2003-10-07

Abstract

AIM: To construct a recombinant strain which expresses BabA of *Helicobacter pylori* (*H pylori*) and to study the immunogenicity of BabA.

METHODS: $BabA_2$ DNA was amplified by PCR and inserted into the prokaryotie expression vector pET-22b (+) and expressed in the BL21 (DE3) *E.coli* strain. Furthermore, BabA immunogenicity was studied by animal test.

RESULTS: DNA sequence analysis showed the sequence of $BabA_2$ DNA was the same as the one published by GenBank. The BabA recombinant protein accounted for 34.8% of the total bacterial protein. The serum from *H pylori* infected patients and Balb/c miced immunized with BabA itself could recognize rBabA.

CONCLUSION: BabA recombinant protein may be an potential vaccine for control and treatment of *H pylori* infection.

Bai Y, Zhang YL, Chen Y, Jin JF, Zhang ZS, Zhou DY. Cloning and expression and immunogenicity of *Helicobacter pylori* $BabA_2$ gene. *World J Gastroenterol* 2004; 10(17): 2560-2562
http://www.wjgnet.com/1007-9327/10/2560.asp

INTRODUCTION

Helicobacter pylori (*H pylori*), a human-specific gastric pathogen, was first isolated in 1982 and has emerged as the causative agent of chronic active gastritis and peptic ulcer disease[1-11]. Most infected individuals show no clinical symptoms, implicating additional factors, such as genetic predisposition and genotype of the infecting strain, are involved in disease pathogenesis. Chronic infection is associated with the development of gastric adenocarcinoma, one of the most common types of cancer in humans, and *H pylori* was recently defined as a class 1 carcinogen. In addition, seroprevalence studies indicate that *H pylori* infection is also associated with cardiovascular, respiratory, extra-gastroduodenal digestive, autoimmune disease. At present the main treatment to eradicate *H pylori* is combined antibiotics, but the cost of combination therapy and the emergency of antibiotic resistance provide further incentives for vaccine development.

In the development of *H pylori* vaccine, candidate vaccine antigens adopted currently such as urease, vacuolating cytotoxin, catalase, *etc.* basically focus on blocking toxicity factors of *H pylori* while considerably few candidate vaccine antigens focus on adhesins which are closely associated with *H pylori* colonizing human gastric mucosa by adhering to mucous epithelial cells and mucus layer lining the gastric epithelium. BabA is the only adhesin gene whose receptor has been confirmed. Studies indicate that BabA gene contains two alleles: $BabA_1$ and $BabA_2$. Gene $BabA_1$ is different from $BabA_2$ in the presence of a 10 bp repeat motif and in lack of Leb antigen-binding activity. No concerned study has been reported to date about $BabA_2$ in China. So in this study, recombinant plasmid of *H pylori* $BabA_2$ gene was constructed and expressed for development of *H pylori* vaccine.

MATERIALS AND METHODS

Materials

Bacterial strain BL21 (DE3) and plasmid pET-22 b (+) were provided by Institute of Biotechnology, Academy of Military Medical Sciences. *H pylori* SS1 was preserved in this research institute. Restriction enzyme *Not* I, *Nco* I and T4 DNA ligase, Vent DNA polymerase, isopropyl-β-D-thiogalactopyranoside (IPTG) were purchased from New England Biolabs Company. DNA molecular weight standard λ DNA/*Eco*RI+*Hin*dIII, goat anti-mouse and goat anti-human IgG-HRP were purchased from Huamei Bioengineering Company and His-Tag precolumn from Invitrogen Company. Specific-pathogen-free, female BALB/c mice were housed according to Health Research Council of China guidelines and allowed free access to food and water. Eight *H pylori* positive sera (which were detected positive by the urease test, pathological dying and germiculture) and three *H pylori* negative sera (which were detected negative by the above-mentioned three examinations) were from patients treated in the Endoscope Center of this institute. Other reagents were analytically pure reagents produced in China.

Recombinant DNA techniques

Unless otherwise stated, plasmid and chromosomal DNA extractions, resctriction enzyme digests, DNA ligations, transformations into *E.coli* and other common DNA manipulations were performed by standard procedures. Genome of *H pylori* was prepared from the cells collected from the colonies on the agar plate. The gene of *H pylori* $BabA_2$ was amplified from the genome of *H pylori* by PCR using the primers $BabA_2$1 (5'-TG GCC ATG GAT AAA AAA CAC ATC CTT TCA-3') as upstream primer and $BabA_2$2 (5'-AG TGC GGC CGC ATA AGC GAA CAC ATA G-3') as downstream primer as described in the literature[33]. $BabA_2$1 and $BabA_2$2 contained *Nco* I and *Not* I sites, respectively. PCR was performed with the hot start method. PCR condition was that after initial denaturing at 95 °C for 30 s, each cycle of amplification consisted of denaturing at 95 °C for 30 s, annealing at 55 °C for 30 s and polymerization at 72 °C for 60 s and further polymerization for 10 min after 35 PCR cycles. The PCR product was harvested from agarose gel, digested with *Nco* I and *Not* I, and inserted into the *Nco* I and *Not* I restriction fragment of the expression vector pET-22b(+) using T4 DNA ligase. The

resulting plasmid pET- BabA was transformed into competent *E.coli* BL21 (DE3) cells using ampicillin resistance for selection. The alkaline lysis method was chosen for large-scale preparations of recombinant plasmids which were identified by restriction enzymes. DNA sequence was performed with a DNA automatic sequencer.

Induced expression, purification and SDS-polyacrylamide gel electrophoresis

The recombinant strains were incubated overnight at 37 °C and shaked in 5 mL LB with 100 μg/mL ampicillin. A 50 mL LB was inoculated and the cells grew until the optical density at 600 nm reached 0.4-0.6. Isopropyl-β-D-thiogalactopyranoside (IPTG) was added to a final concentration of 0.1, 0.2, 0.4, 0.6, 0.8, 1.0 mmol/L, respectively. *E.coli* cells from a 50 mL growth 3 h or 5 h after induction were harvested by centrifugation at 12 000 *g* for 10 min and the pellet was resuspended in 1 mL 30 mmol/L Tris buffer (pH8.0) containing 1 mmol/L EDTA (pH8.0), 200 g/L sucrose. The suspension was put on ice for 10 min, and then centrifuged for 10 min at 12 000 *g*, and the resulting suspernatant contained proteins from the periplasm. The resulting pellet was resuspended in 5 mL 50 mmol/L Tris buffer (pH8.0) containing 2 mmol/L EDTA, 0.1 mg/mL lysozyme and 10 g/L Triton X-100. The suspension was incubated at 30 °C for 20 min and then sonicated on ice until it became clarified. The lysate was centrifuged at 12 000 *g* for 15 min at 4 °C, then the resulting supernatant containing proteins from the cytoplasm was purified with Ni-NTA column. Whole-cell lysates, sonicated supernatant,osmotic shock liquid of recombinant strains expressing *H pylori* BabA2 genes and the purified rBabA were analyzed by electrophoresis analysis in a 100 g/L polyacrylamide gel.

Immunization of mice

Sixty-eight-week-old mice were immunized 4 times by hypodermic injection in the back of mice at weekly intervals. Each dose consisted of 20 μg of *H pylori* rBabA protein and 200 μg of adjuvant aluminum hydroxide gel. Age-matched control mice were not immunized. Four weeks after the last immunization, blood samples were taken from the retro-orbital sinus to measure the anti BabA systemic immune responses and stored at -20 °C until assay.

Serum antibody responses

Indirect ELISA as described previously evaluated serum samples from mice and patients for BabA-specific IgG. Purified *H pylori* rBabA was used as the coating antigen in ELISA immunoassays.

RESULTS

PCR amplification of H pylori BabA$_2$ gene

According to the literature, the gene encoding the BabA protein, was amplified by PCR with chromosomal DNA of *H pylori* Sydeny strain (ss1) as the templates. The cloning products were electrophoresed and visualized on 8 g/L agarose gel (Figure 1). It revealed that BabA$_2$ DNA fragment amplified by PCR contained a gene of approximately 2 226 nucleotides, which was compatible with the previous reports.

Construction of recombinant plasmid and restriction enzyme confirmation

After the PCR products and pET-22 b (+) plasmid were cut by *Not* I and *Nco* I, directional cloning was performed, resulting in a recombinant plasmid named pET-22 b (+)/BabA. The recombinant plasmids pET-22 b (+)/BabA were all digested by *Not* I or *Nco* I, and by *Not* I and *Nco* I simultaneously, then digestive products were visualized on 8 g/L agarose gel eletrophoresis (Figure 2). It demonstrated that recombinant plasmid contained the objective gene.

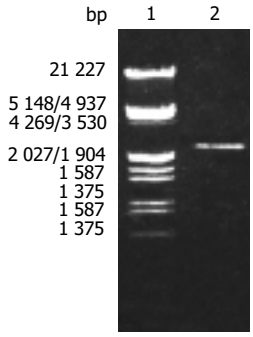

Figure 1 BabA$_2$ DNA fragment amplified by PCR from *Helicobacter pylori* electrophoresed on 8 g / L agarose gel. Lane 1: Nucleotide marker; Lane 2: PCR products.

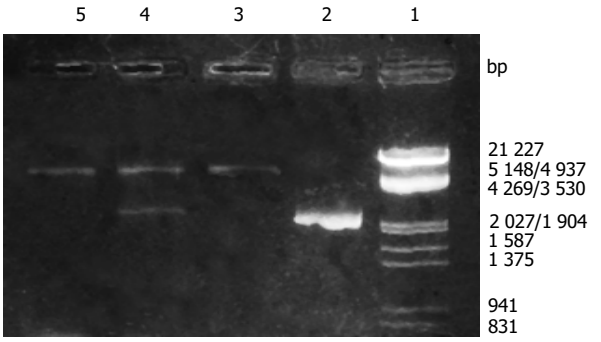

Figure 2 Identification of recombinant plasmid by restriction enzyme digestion. Lane 1: Nucleotide marker; Lane 2: PCR products; Lane 3: Recombinant plasmid / *Not* I; Lane 4: Recombinant plasmid / *Not* I and *Nco* I; Lane5: pET22b(+) / *Not* I.

Sequence analysis of cloned BabA$_2$ nucleotide

The nucleotide sequence of cloned genes inserted in pET22 b(+) was analyzed by automatic sequencing across the cloning junction, using the universal primer T7. The results showed that cloned genes contained 2 226 nucleotides with a promoter and a start codon coding a putative protein of 741 amino acid residues with a calculated molecular mass of BabA. As compared with previously reports, the homogeneity was 100% between them.

Expression and purification of BabA$_2$ gene in Escherichia coli

Whole-cell lysate, sonicated supernatant, osmotic shock liquid of recombinant strains expressing *H pylori* BabA$_2$ genes and the purified rBabA were analyzed by electrophoresis analysis in a 100 g/L polyacrylamide gel for detection of fusion proteins (Figure 3). The result showed that the clearly identifiable band was 78 000 u highly expressed fusion proteins, which was similar to that predicted. Gel automatic scan analysis showed that it was 0.6 at D value and the final concentration of IPTG was 0.1 mmol/L and the expression of BabA rose remarkably after 5 h of induction, which accounted for 34.8% of total bacterial proteins. Among them, soluble substance accounted for 15. 0% of supernatant. BabA was further analyzed with Ni-NTA column and finally BabA whose purity was 90%.

Antigenicity study of recombinant fusion protein

The postive results by the test of ELISA had colours, but the negtive results had no colours, or weak colours. Serum from the eight mice serums immuned with rBabA showed positive results. In contrast, serum from the eight mice in the control group showed negtive results. At the same time, serums from patients also showed the same results. *H pylori* positive serum from the eight patients showed positive results and *H pylori* negative serum from the three patients showed postive results.

It showed that anti-BabA antibody existed in the serum of infected patients and rBabA could enable the organism to generate specific humoral immunity.

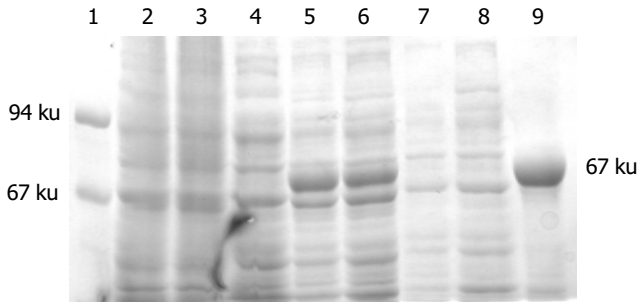

Figure 3 The 100 g/L SDS-PAGE analysis of fusion protein expressed in BL21 (DE3). Lane 1: Molecular mass marker (67, 94) $\times 10^3$; Lane 2: control strain BL21 (pET) before induction; Lane 3: control strain BL21 (pET) after 5-h induction with IPTG; Lane 4: BL21 (pET-BabA) cells before induction; Lane 5: BL21(pET- BabA) cells after 3-h induction with IPTG; Lane 6: BL21(pET- BabA) cells after 5-h induction with IPTG; Lane 7: BL21(pET- BabA) cells periplasm protein after 3-h induction with IPTG; Lane 8: sonicated supernatant of BL21 (pET-BabA) cells after 3-h induction with IPTG; Lane 9: recombinant protein BabA purified.

DISCUSSION

At first Wadstr *et al*. suspected that the resting or slow growing cells of *H pylori* could interact with Lewis blood group substances in gastric mucin layer and on epithelium to facilitate initial colonization. Afterwards Iiver *et al*. used receptor activity-directed affinity tagging to purify a kind of adhesin which mediated adherence of *H pylori* to human gastric epithelial cells by interacting with fucosylated Lewis b (Leb) histo-blood group antigen and named the adhesion BabA. Immunogold electron microscopy found BabA adhesin was located on the bacterial cell outer membrane by probing the Leb antigen. Receptor displacement analyses showed that receptor-adhesin complex was formed under conditions of equilibrium. Most of the cells (>90%) of the bacterial exhibited BAB activity, as determined by confocal microscopy and fluorescent Leb antigen. The Ka value for formation of the Leb antigen-BabA complex was -1×10^{10} mol/L. The number of Leb glycoconjugate molecules bound to BabA was calculated as -500 per bacterial cell. In addition, the prevalence of blood group antigen-binding activity was also assessed among 95 recent clinical isolates of *H pylori*, and 66% (63 isolates) were bound to the Leb antigen. Bosch *et al*. investigated the effects of acute stress on the salivary levels of the carbohydrate structure sulfo-Lewis (sulfo-Le). The results showed the stressor induced a strong increase in salivary sulfo-Le concentration (U/mL), sulfo-Le output (U/min), sulfo-Le/total protein ratio (U/mg protein), and saliva-mediated adherence (*ex vivo*) of *H pylori*. As expected, sulfo-Le concentration correlated with the adherence of *H pylori* ($r = 0.72$, $P<0.05$). In a word, the adhesin BabA and its receptor Leb played an important role in the adherence mechanism of *H pylori*, especially when people were in the state of acute stress.

Isolates of *H pylori* differed in virulence and from individuals with peptic ulcers most often were type I strains that expressed vacuolating cytotoxin A (VacA) and cytotoxin-associated gene A (CagA) protein. By definition, type II strains could express neither marker. The bacterial Leb-binding phenotype was associated with the presence of the cag pathogenicity island among clinical isolates of *H pylori*. A vaccine strategy based on the BabA adhesin might serve as a means to target the virulent type I strains of *H pylori*. So we selected *H pylori* ss1 chromosome DNA as a template, which has strong adhesin and is capable of coloning firmly in the stomach of a mouse, designed specific primers and successfully screened the genes of $BabA_2$. To facilitate the expression and purification at the next stage, we cloned it into a fusion expression vector with 6 hercynine tails. The restriction enzyme digestion and the sequencing results showed that one open reading frame had the size of 2 226 bp. SDS-PAGE and scan analysis showed that the molecular mass of BabA was 78 ku and recombinant protein accounted for 34.8% of the total bacterial protein. Considering that the recombinant protein with bio-activity tended to preserve more integral and positive antigenicity, we selected supernatant of ultrasound disrupted live *E.coli* and performed repeated purification of rBabA with Ni-NTA resin, thus obtaining rBabA with activity whose purity was 90%. This has laid a foundation for further research on immune protection and molecular adhesin mechanism. In this study, serum from the mice immuned with purified recombinant protein BabA could be used to detect specific antibody against BabA, but serum from the mice in the control group could not. Serum from patients also showed the same results. These results suggest that BabA of *H pylori* maybe a good candidate as a vaccine component.

REFERENCES

1 **Bai Y**, Zhang YL, Wang JD, Lin HJ, Zhang ZS, Zhou DY. Conservative region of the genes encoding four adhesins of *Helicobacter pylori*: cloning, sequence analysis and biological information analysis. *Diyi Junyi Daxue Xuebao* 2002; **22**: 869-871

2 **Vandenplas Y**. *Helicobacter pylori* infection. *World J Gastroenterol* 2000; **6**: 20-31

3 **Bai Y,** Chang SH, Wang JD, Chen Y, Zhang ZS, Zhang YL. Construction of the *E.coli* clone expressing adhesin BabA of *Helicobacter pylori* and evaluation of the adherence activity of BabA. *Diyi Junyi Daxue Xuebao* 2003; **23**: 293-295

4 **Morgner A**, Miehlke S, Stolte M, Neubauer A, Alpen B, Thiede C, Klann H, Hierlmeier FX, Ell C, Ehninger G, Bayerdörffer E. Development of early gastric cancer 4 and 5 years after complete remission of *Helicobacter pylori* -associated gastric low - grade marginal zone B-cell lymphoma of MALT type. *World J Gastroenterol* 2001; **7**: 248-253

5 **Bai Y**, Zhang YL, Wang JD, Zhang ZS, Zhou DY. Construction of the non-resistant attenuated salmonella typhimurium strain expressing *Helicobacter pylori* catalase. *Diyi Junyi Daxue Xuebao* 2003; **23**: 101-105

6 **Solnick JV**, Canfield DR, Hansen LM, Torabian SZ. Immunization with recombinant *Helicobacter pylori* urease in specific-pathogen-free rhesus monkys (Macaca mulatta). *Infect Immun* 2000; **68**: 2560-2565

7 **Ilver D**, Arnqvist A, Ogren J, Frick IM, Kersulyte D, Incecik ET, Berg DE, Covacci A, Engstrand L, Boren T. *Helicobacter pylori* adhesin binding fucosylated histo-blood group antigens revealed by retagging. *Science* 1998; **279**: 373-377

8 **Sambrook J**, Fritsch EF, Maniatis T. Molecular cloning: a laboratory manual. 2nd ed. New York: *Cold Spring Harbor Laboratory Press* 1989: 35-400

9 **Wadstrom T**, Hirmo S, Boren T. Biochemical aspects of *Helicobacter pylori* colonization of the human gastric mucosa. *Aliment Pharmacol Ther* 1996; **10**(Suppl 1): 17-27

10 **Bosch JA**, de Geus EJ, Ligtenberg TJ, Nazmi K, Veerman EC, Hoogstraten J, Amerongen AV. Salivary MUC5B-mediated adherence (*ex vivo*) of *Helicobacter pylori* during acute stress. *Psychosom Med* 2000; **62**: 40-49

11 **Covacci A**, Censini S, Bugnoli M, Petracca R, Burroni D, Macchia G, Massone A, Papini E, Xiang Z, Figura N. Molecular characterization of the 128-kDa immunodominant antigen of *Helicobacter pylori* associated with cytotoxicity and duodenal ulcer. *Proc Natl Acad Sci U S A* 1993; **90**: 5791-5795

Edited by Hu DK and Wang XL **Proofread by** Xu FM

PO Box 2345, Beijing 100023, China
Fax: +86-10-85381893
E-mail: wjg@wjgnet.com www.wjgnet.com

World J Gastroenterol 2004;10(17):2563-2566
World Journal of Gastroenterology
Copyright © 2004 by The WJG Press ISSN 1007-9327

• BRIEF REPORTS •

Antisense imaging of colon cancer-bearing nude mice with liposome-entrapped 99m-technetium-labeled antisense oligonucleotides of *c-myc* mRNA

Jian-Guo Zheng, Tian-Zhi Tan

Jian-Guo Zheng, Department of Nuclear Medicine, Beijing Hospital, Beijing 100730, China
Tian-Zhi Tan, Department of Nuclear Medicine, West China Hospital, Sichuan University, Chengdu 610041, Sichuan Province, China
Supported by Natural Scientific Foundations of China, No: 39870200
Correspondence to: Tian-Zhi Tan, Department of Nuclear Medicine, West China Hospital, Sichuan University, Chengdu 610041, Sichuan Province, China. ttz@mcwcums.com
Telephone: +86-28-85422696 **Fax:** +86-28-85422696
Received: 2004-02-14 **Accepted:** 2004-02-24

Abstract

AIM: To investigate the feasibility for antisense imaging of the colon cancer with liposome-entrapped 99 m-technetium labeled antisense oligonucleotides as tracers.

METHODS: Fifteen mer single-stranded aminolinked phosphorothioate antisense oligonucleotides of *c-myc* mRNA were labeled with ^{99m}Tc-pertechnetate, then purified and finally entrapped with liposomes to form the labeling compounds, liposome-entrapped ^{99m}Tc-labeled antisense oligonucleotides. The LS-174-T cells (colon of adenocarcinoma cell line) were incubated with the labeling compounds to test the uptake rates of LS-174-T cells. Later on, a model of 30 tumor bearing nude mice was constructed by inoculating with 5×10^6 of LS-174-T cells at right flank of each nude mouse. About 10 d later, the model were adminstered by intravenous injection of the liposome-entrapped ^{99m}Tc-labeled antisense oligonucleotides. Then some of the tumour bearing nude mice were sacrificed at 0.5, 1, 2, and 4 h after intravenous injection, and proper quantity of liver, spleen, tumor, *etc*. was obtained. The tissues were counted in a gamma counter, and after correction for decay and background activity, expressed as a percentage of the injected dose. The others whose anterior and posterior whole-body scans were obtained at 1, 1.5, 2, 4, 6 and 24 h with a dual-head bodyscan camera equipped with parallel-hole low-energy collimaters. The ratios of radioactive counts in tumor to that in contralateral equivalent region of abdomen were calculated.

RESULTS: The uptake rates of LS-174-T cells for liposome-entrapped ^{99m}Tc-labeled antisense oligonucleotides increased as time prolonged and reach the peak (17.77±2.41%) at 7 h. The biodistributions showed that the rdioactivity in the tumor (13.46±0.20%) of injected dose was the highest at 2 h of intravenous injection of liposome-entrapped ^{99m}Tc-labeled antisense oligonucleotides, and then decreased sharply to 4.58±0.45% at 4 h. The tumor was shown clearly in the whole-body scan at 2 h of intravenous injection. The ratios, radioactive counts in tumor to that in contralateral equivalent region of abdomen (1.7332±0.2537), was the highest one at 2 h after intravenous injection of liposome-entrapped ^{99m}Tc-labeled antisense oligonucleotides.

CONCLUSION: The liposome-entrapped ^{99m}Tc-labeled antisense oligonucleotides deserve being developed into radiopharmaceutics for the colon cancer imaging.

Zheng JG, Tan TZ. Antisense imaging of colon cancer-bearing nude mice with liposome-entrapped 99m-technetium-labeled antisense oligonucleotides of *c-myc* mRNA. *World J Gastroenterol* 2004; 10(17): 2563-2566
http://www.wjgnet.com/1007-9327/10/2563.asp

INTRODUCTION

Antisense imaging was referred to that antisense oligonucleotides of a gene were labeled with radionuclide, then administered to a organism to show its focus, especially the tumor[1]. Colon cancer is a malignant tumor that seriously threatens human health. Its main oncogene, *c-myc*, whose overexpression can reach 30 times, is a target gene for antisense imaging[2]. The oligonucleotides that are complementary to *c-myc* mRNA can prohibit many kinds of cancer cells from growing[3]. Many nuclear medicine researchers are interested in this oncogene[4,5]. At present, the antisense oligonucleotides of *c-myc* mRNA have been successfully labeled with ^{99m}Tc[6,7]. However, to the author's knowledge, their application in experimental researches on antisense imaging has not been reported as yet. Is the uptake rate of tumor tissue too small and the background too high to indicate the tumor? How can the uptake rates of tumor cells be increased? Do these limit the application of ^{99m}Tc-labeled antisense oligonucleotides? In order to explore the feasibility for antisense imaging of the colon carcinoma, develop a new radiolabeled-gene-pharmaceutics, and promote the progress in the molecular nuclear medicine, the primary experimental studies, antisense imaging, on liposome-entrapped ^{99m}Tc-labeled antisense phosphorothioate oligonucleotides as a tracer were carried out.

MATERIALS AND METHODS

Materials

Fifteen mer, single-stranded phosphorothioate oligonucleotides, aminolinked, antisense oligonucleotides targeted at the translation initiation codon of *c-myc* mRNA were purchased from Gibco-BRL, US. Their base sequences were 5'-NH_2-FACGTTGAGGGGCAT-3' (F stood for phosphorothioate A). The molecular mass of the chain was about 300 u. These oligonucleotides were used directly without further purification, and generally handled under sterile conditions. All solutions were sterilized by terminal filtration through a 0.22 μm filter. All pipettes and tubes were autoclaved prior to use. The oligonucleotides were dissolved at a concentration of 4 mg/mL in sterile water and stored at -20 °C.

The hydrazino nicotinamide derivatives were synthesized elsewhere. 99 m-pertechnetate was obtained from a ^{99}Mo-^{99m}Tc radionuclide generator made by the Chinese Atomic Energy Institute. Tricine, $Sncl_2\cdot2H_2O$ and Dimethyl sulfoxide were

supplied by Sigma Company, US, lipofectamin reagent by Gibco-BRL, US, EDTA by Boehringer Mannheim Company, Germany, and Sep-Pak (C_{18}) reverse column by Waters Company, US.

The oligonucleotides were bound to hydrazino nicotinamide derivatives and then labeled with ^{99m}Tc following the methods described by Hnatowich *et al*[8]. The ^{99m}Tc-labeled oligonucleotides were entrapped with liposome according to the manufacturer's protocols.

The cellular uptake rates of oligonucleotides

The LS-174-T cells were grown by adherent culture in media (RPMI-1 640, Gibco-BRL, US), supplemented with 100 mL/L fetal bovine serum at 37 °C, 50 mL/L CO_2. Thirty-six culture plates with diameter of 33 mm each was inoculated with about 1×10^5 LS-174-T cells and cultured at 37 °C for 48 h. After the cells were grown to about 50% confluence in regular culture media, they were transfected using lipofectamin with 2 μg of freshly prepared liposome-entrapped ^{99m}Tc-labeled antisense oligonucleotides with radioactivity of about 29.60 MBq according to the manufacturer's protocols. The cellular uptake rates were determined at 1, 2, 5 and 7 h, and the testing steps were as follows: The cells were detached by 2.5 g/L trypsin to form suspension, then washed three times with the media by centrifugation (2 500 r/min, 10 min). The supernatant was collected into a 50 mL volumetric cylinder and the precipitation remained in the centrifugation tube. Then the radioactive counts in the precipitation and supernatant were counted in an automatic gamma well counter after correction for decay and background activity separately, and the cellular uptake rates were expressed as a percentage of the total counts. The uptake rate = radioactive counts in precipitation/the total counts in precipitation and supernatant ×100%.

The biodistribution of the antisense oligonucleotides in tumor-bearing nude mice

At first, the tumor model was constructed. Large-scale of LS-174-T cells collected by digestion, centrifugation and washing, were diluted with culture medium without serum and antibiotic to the concerntration of 5×10^6 cells per 0.2 mL. Thirty male nude mice, aged about 2 mo, were purchased from Experimental Animal Center of Sichuan University. The mice were maintained in a specific pathogen-free environment and cared in accordance with the institutional guidelines. Each of them was inoculated with 5×10^6 cells at right flank. The tumor was allowed to grow for 10 d until diameter reached about 1 cm. Thus the tumor model was constructed successfully.

Biodistribution of liposome-entrapped ^{99m}Tc-labeled antisense oligonucleotides was determined in the 20 tumor-bearing nude mice. Each mouse received 0.3 mL of saline containing 3 to 5 μg (0.259 MBq) of liposome-entrapped ^{99m}Tc-labeled antisense oligonucleotides by tail vein administration. Meanwhile, the same injected dose of liposome-entrapped ^{99m}Tc-labeled antisense oligonucleotides was stored in a tube as standard, and double assays were carried out. Five mice were used at each time point of 0.5, 1, 2 and 4 h. After being bled from eye, they were sacrificed by cervical dislocation, and proper quantity of liver, spleen, kidney, lung, heart, bone, muscle, stomach, intestines, brain and tumor obtained. The tissues were washed cleanly with cool physiological saline and weighted by electronic balance (Denver, US). The tissues were counted against appropriate standards of known dilution in an automatic gamma well counter, and after correction for decay and background activity, expressed as a percentage of the injected dose.

Antisense imaging

The liposome-entrapped ^{99m}Tc-labeled antisense oligonucleotides containing oligonucleotides from 30 to 90 μg at the concentration of 37 MBq/mL were freshly prepared. The 6 tumor-bearing nude mice were administered with 0.3 mL of the above products through tail vein. When these mice anesthetized with pentobarbital, anterior and posterior whole-body scans were obtained at 1, 1.5, 2, 4, 6 and 24 h with a dual-head bodyscan camera (Elcint Apex Helix, Israel) equipped with parallel-hole low-energy collimaters. The ratios of radioactive counts in tumor to that in the contralateral equivalent region of abdomen were calculated.

RESULTS

The cellular uptake rates of oligonucleotides

The most important thing for antisense imaging is how much oligonucleotides are able to enter cells. High uptake rate is the key to success. The celluar uptake rates are as follows: 7.21±1.23% at 1 h, 15.19±2.81% at 2 h, 16.13±2.54% at 5 h, and 17.77±2.41% at 7 h. Within 7 h, the cellular uptake rate increased as the time prolonged, and reached the peak at 7 h. It was significantly higher than that at 1 and 2 h. However, the uptake rate at 7 h was not significantly higher than that at 5 h.

The biodistribution of liposome-entrapped ^{99m}Tc-labeled antisense oligonucleotides

The biodistribution of liposome-entrapped ^{99m}Tc-labeled antisense oligonucleotides are shown in Table 1. The endothelial system played a main role in biodistribution, and accumulated the greater part of the injected dose. The radioactive counts in the tumor tissue increased within 2 h and gradually reached the peak at 2 h, then dropped down sharply.

Table 1 Course of biodistribution of liposome-entrapped ^{99m}Tc-labeled antisense oligonucleotides in tumor-bearing nude mice (mean±SD, percent of injected dose, n = 5 mice for each time)

Tissue	0.5 h	1 h	2 h	4 h
Liver	8.78±0.63	9.16±1.14	7.92±0.38^c	8.97±0.12^c
Spleen	6.78±0.37^c	8.86±0.60	7.37±0.64^c	8.02±0.23^c
Kidney	4.89±0.67^a	2.90±1.19^a	3.07±0.18^{ac}	0.47±0.02^{ac}
Lung	10.23±1.02	13.37±0.84	12.21±0.42^a	10.20±0.50^c
Heart	7.18±0.13	8.78±1.01	7.25±0.18	5.28±0.45^{ac}
Blood	5.51±0.24^a	4.55±0.15	2.81±0.11^{ac}	2.61±0.06^{ac}
Bone	1.84±0.64^a	3.14±1.04^a	1.43±0.24^{ac}	1.02±0.32^{ac}
Muscle	2.27±0.37^a	1.36±0.60^{ac}	1.69±0.91^{ac}	2.85±0.26^a
Stomach	12.45±0.62^a	13.77±0.38	10.63±0.35	6.70±0.44^{ac}
Intestines	4.54±0.42^a	6.68±4.14	7.76±0.34^c	8.44±0.63^c
Brain	2.24±0.42^a	2.16±2.10^{ac}	0.68±0.06^{ac}	0.52±0.06^{ac}
Tumor	6.12±0.31^a	8.09±0.86	13.46±0.20^a	4.58±0.45^a

$^aP<0.05$ *vs* that of liver tissue $^cP<0.05$ *vs* that of tumor tissue.

Antisense imaging

Anterior imaging at 1 h after intravenous injection of liposome-entrapped ^{99m}Tc-labeled antisense oligonucleotides showed that little accumulation of radioactivity might be seen in the right middle flank which was the place of tumor. Anterior imaging demonstrated a little accumulation of radioactivity in tumor site at 1.5 h (Figure 1), and a circular abnormal accumulation focus of radioactivity in the location of tumor at 2 h (Figure 2), but no accumulation of radioactivity in the location of tumor at 24 h.

The ratios of radioactive counts in tumor tissue to that in the contralateral equivalent region

The ratio was the highest one (1.7332±0.2537) at 2 h after intravenous injection of liposome-entrapped ^{99m}Tc-labeled antisense oligonucleotides. It was significantly higher than

that at 4 and 6 h ($P<0.05$). Although it was higher than that at 1.0 and 1.5 h, there was no statistical difference. These ratios are shown in Table 2.

Table 2 Ratios of the radioactive counts in tumor to that in the contralateral equivalent region of abdomen (mean±SD, $n = 5$ for each time point)

Time point (h)	Ratios
1.0	1.2266±0.1259
1.5	1.5597±0.0190
2.0	1.7332±0.2537
4.0	1.0182±0.0495[a]
6.0	1.0199±0.0131[a]

[a]$P<0.05$ *vs* ratio of 2.0 h.

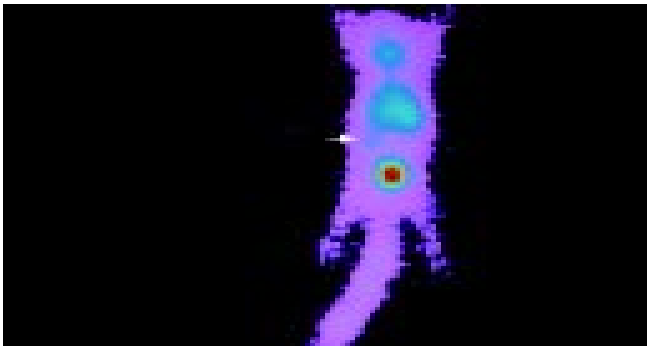

Figure 1 Anterior imaging at 1.5 h after intravenous injection of liposome-entrapped ^{99m}Tc-labeled antisense oligonucleotides. A little accumulation of radioactivity in tumor site, the right middle flank (arrow) could be observed.

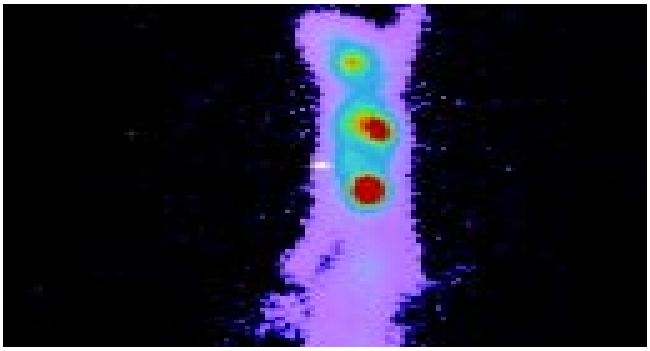

Figure 2 Anterior imaging at 2 h after intravenous injection of liposome-entrapped ^{99m}Tc-labeled antisense oligonucleotides. A circular abnormal accumulation focus was observed in the location of tumor (arrow).

DISCUSSION

The possible advantages of delivering oligonucleotides into cells by liposomes are not only to increase the uptake rates of dividing and mitostatic cells, but also protect the oligonucleotides against degeneration by nucleases. It has been confirmed that the amount of oligonucleotides used can be decreased greatly as liposomes are adopted as vectors *in vitro*[9-13].

The cellular uptake rates of the liposome-entrapped ^{99m}Tc-labeled antisense oligonucleotides are the key parameter to antisense imaging. The maxium cellular uptake rate of the LS-174-T (17.77±2.41%) was plenty enough for the experimental or clinical use, and could be applied for the following experiments: biodistribution and antisense imaging.

The biodistribution assay showed that the radioactive counts per gram of the tumor tissue was in the middle level at 0.5 h after injection, increased as time prolonged within 2 h, and reached the peak at 2 h. The proportion of radioactive counts per gram of the tumor tissue to the total was 13.46±0.20%, which was significantly higher than that of the liver, spleen, kidney, blood, bone, muscle, intestines and brain. The ratio of radioactive counts in the tumor to that in the blood was 4.79, and to that in the muscle was 7.96. It was thus evident that enough liposome-entrapped ^{99m}Tc-labeled antisense oligonucleotides were accumulated in the tumor tissue. The tumor could be observed clearly so long as radioactivity in the tissues around it was comparatively low.

Delong *et al*[14]. studied the biodistribution of ^{99m}Tc-labeled phosphorothioate oligonucleotides without using liposomes as carriers. Their investigation demonstrated that radioactivity in the tumor tissue was only 2% to 3%. However, in our study, liposomes were used as vectors, and 4.58% to 13.46% of the total radioactivity could be accumulated in the tumor. Radioactivity was 2.29 to 4.49 times higher than that reported by Delong *et al*[14]. Thus, the uptake rates of the tumor tissue can be increasee greatly by using liposomes as carriers. Accordingly, liposome is an effective vector in antisense imaging.

The whole body scan in the tumor bearing nude mice showed that the tumor was observed clearly at 2 h after intravenous injection of the liposome-entrapped ^{99m}Tc-labeled antisense oligonucleotides. It was evident that the imaging of the liver above the tumor and the bladder below the tumor was more clear than that of the tumor. They could influence the imaging of the tumor. However, the interference of the bladder can easily be decreased by diuretic or drinking a certain quantity of water, which is a routine clinical method of whole body bone scan. But the influence of the liver needs further investigation.

Although the imaging of the liver will influence the quality of the antisense imaging, our primary success on the tumor-bearing nude mice with ^{99m}Tc-labeled antisense oligonuceotides may contribute to the molecular nuclear medicine progress.

In conclusion, liposome-entrapped ^{99m}Tc-labeled antisense oligonucleotides with high cellular uptake rates can be accumulated by tumor in the tumor bearing-nude mice, and be able to show the colon carcinoma accurately, was worthy of being developed into a new radiopharmaceutics for diagnosis[15]. This will provide a new strategy for the early diagnosis of the colon carcinoma.

REFERENCES

1 **Gauchez AS**, Du Moulinet D'Hardemare A, Lunardi J, Vuillez JP, Fagret D. Potential use of radiolabeled antisense oligonucleotides in oncology. *Anticancer Res* 1999; **19**: 4989-4997

2 **Zheng J**, Tan T. The application of radionuclide antisense therapy for malignant tumours. *Nucl Med Commun* 2001; **22**: 469-472

3 **Kang Y**, Cortina R, Perry RR. Role of *c-myc* in tamoxifen-induced apoptosis estrogen-independent breast cancer cells. *J Natl Cancer Inst* 1996; **88**: 279-284

4 **Dewanjee MK**, Ghafouripour AK, Kapadvanjwala M, Dewanjee S, Serafini AN, Lopez DM, Sfakianakis GN. Noninvasive imaging of *c-myc* oncogene messenger RNA with indium-111-antisense probes in a mammary tumor-bearing mouse model. *J Nucl Med* 1994; **35**: 1054-1063

5 **Hjelstuen OK**, Tonnesen HH, Bremer PO, Verbruggen AM. 3'-99mTc-labeling and biodistribution of a CAPL antisense oligodeoxynucleotide. *Nucl Med Biol* 1998; **25**: 651-657

6 **Zhang YM**, Rusckowski M, Liu N, Liu C, Hnatowich DJ. Cationic liposomes enhance cellular / nuclear localization of 99mTc-antisense oligonucleotides in target tumor cells. *Cancer Biother Radiopharm* 2001; **16**: 411-419

7 **Liu G**, Zhang S, He J, Liu N, Gupta S, Rusckowski M, Hnatowich DJ. The influence of chain length and base sequence on the pharmacokinetic behavior of 99mTc-morpholinos in mice.

Q J Nucl Med 2002; **46**: 233-243

8 **Hnatowich DJ**, Mardirossian G, Fogarasi M, Sano T, Smith CL, Cantor CR, Rusckowski M, Winnard P Jr. Comparative properties of a technetium-99m-labeled single-stranded natural DNA and a phosphorothioate derivative *in vitro* and in mice. *J Pharmacol Exp Ther* 1996; **276**: 326-334

9 **Ma DD**, Wei AQ. Enhanced delivery of synthetic oligonucleotides to human leukaemic cells by liposomes and immunoliposomes. *Leuk Res* 1996; **20**: 925-930

10 **Ropert C**, Lavignon M, Dubernet C, Couvreur P, Malvy C. Oligonucleotides encapsulated in pH sensitive liposomes are efficient toward Friend retrovirus. *Biochem Biophys Res Commun* 1992; **183**: 879-885

11 **Zelphati O**, Zon G, Leserman L. Inhibition of HIV-1 replication in cultured cells with antisense oligonucleotides encapsulated in immunoliposomes. *Antisense Res Dev* 1993; **3**: 323-338

12 **Kanamaru T**, Takagi T, Takakura Y, Hashida M. Biological effects and cellular uptake of *c-myc* antisense oligonucleotides and their cationic liposome complexes. *J Drug Target* 1998; **5**: 235-246

13 **Moreira JN**, Hansen CB, Gaspar R, Allen TM. A growth factor antagonist as a targeting agent for sterically stabilized liposomes in human small cell lung cancer. *Biochim Biophys Acta* 2001; **1514**: 303-317

14 **Delong RK**, Nolting A, Fisher M, Chen Q, Wickstrom E, Kligshteyn M, Demirdji S, Caruthers M, Juliano RL. Comparative pharmacokinetics, tissue distribution, and tumor accumulation of phosphorothioate, phosphorodithioate, and methylphosphonate oligonucleotides in nude mice. *Antisense Nucleic Acid Drug Dev* 1997; **7**: 71-77

15 Z**heng J**, Tan T, Zhang C, Li Y, Liang Z, Tu J. Preparation of liposome-mediated 99m-technetium-labeled antisense oligonucleotides of *c-myc* mRNA. *Shengwu Yixue Gongchengxue Zazhi* 2003; **20**: 704-707

Edited by Kumar M **Proofread by** Xu FM

PO Box 2345, Beijing 100023, China
Fax: +86-10-85381893
E-mail: wjg@wjgnet.com www.wjgnet.com

World J Gastroenterol 2004;10(17):2567-2570
World Journal of Gastroenterology
Copyright © 2004 by The WJG Press ISSN 1007-9327

• BRIEF REPORTS •

Inhibition of mouse hepatocyte apoptosis via anti-Fas ribozyme

Min Zhang, Wei He, Fang Liu, Ping Zou, Juan Xiao, Zhao-Dong Zhong, Zhong-Bo Hu

Min Zhang, Wei He, Fang Liu, Ping Zou, Juan Xiao, Zhao-Dong Zhong, Zhong-Bo Hu, Institute of Hematology, Union Hospital, Tongji Medical College, Huazhong University of Science and Technology, Wuhan 430022, Hubei Province, China
Supported by the National Natural ScienceFoundation of China, No. 30240022
Correspondence to: Professor Ping Zou, Institute of Hematology, Union Hospital, Tongji Medical College, Huazhong University of Science and Technology, Wuhan 430022, Hubei Province, China. zhangmin35@yahoo.com.cn
Telephone: +86-27-85726880
Received: 2003-10-10 **Accepted:** 2003-12-16

Abstract

AIM: To investigate the effects of anti-Fas ribozyme on Fas expression and apoptosis in primary cultured mouse hepatocytes.

METHODS: Mouse hepatocytes were isolated by using collagenase irrigation. A hammerhead ribozyme targeting the Fas mRNA was constructed, and transfected into mouse hepatocytes via Effectene. Then Fas expression in mouse hepatocytes was detected by RT-PCR and western blotting. After being treated with anti-Fas antibody (JO_2), hepatocytes viability was measured with MTT assay. Caspase-3 proteolytic activity was detected, and cell apoptosis was measured according to Annexin V-FITC apoptosis detection kit.

RESULTS: Fas expressed in primary mouse hepatocytes. Fas expression in hepatocytes transfected with anti-Fas ribozyme was decreased remarkably and correlated with the resistance to Fas-mediated apoptosis as determined by flow cytometry and caspase-3 proteolytic activity.

CONCLUSION: Anti-Fas ribozyme can remarkably decrease the Fas expression in mouse hepatocytes, thus inhibit Fas-mediated apoptosis in hepatocytes. It is suggested that anti-Fas ribozyme could significantly increase the resistance of transplanted hepatocytes to apoptosis and improve the survival of transplanted hepatocytes.

Zhang M, He W, Liu F, Zou P, Xiao J, Zhong ZD, Hu ZB. Inhibition of mouse hepatocyte apoptosis via anti-Fas ribozyme. *World J Gastroenterol* 2004; 10(17): 2567-2570
http://www.wjgnet.com/1007-9327/10/2567.asp

INTRODUCTION

Liver transplantation is one of the efficient ways to treat liver function failure and liver necrosis induced by all kinds of diseases[1,2]. But Fas expresses in hepatocytes and Fas-mediated apoptosis significantly impairs graft survival[3-7]. Anti-Fas hammerhead ribozyme was designed and synthesized to target directly at position 596 of the Fas RNA, and cloned into a eukaryotic vector, which was transfected into primary cultured mouse hepatocytes via a vector named Effectene different from usual Lipofectamine reagents[8]. Then the effects of anti-Fas ribozyme on Fas expression and apoptosis of mouse hepatocytes were investigated.

MATERIALS AND METHODS

Reagents and materials

E.coli DH-5α was a kind gift from Department of Immunology, Tongji Medical College. Prokaryotic vector pBSKU6 and green fluorescent protein pEGFPC1 were given as presents by Dr. Kongxinjuan. All restriction endonucleases and T_4 DNA ligase were products of Promega Company. Mini plasmid DNA extraction kit, gel DNA purification kit and DL-2000 DNA marker were purchased from TaKaRa Company. Transfection reagent Effectene was purchased from Qiagen Company. Reverse transcriptional kit, dNTP, Taq DNA polymerase were products of MBI Company. Fluorescein isothiocyanate (FITC)-conjugated Annexin V kit was product of Bender Company (purchased from Jingmei Company). FITC-conjugated anti-mouse Fas antibody (JO_2) was product of PharMingen Company. Caspase-3 activity detection kit was product of Clontech Company. MTT reagent was purchased from Sigma Company.

Synthesis and cloning of ribozyme

GUA triplets located at 596 of the mouse Fas RNA were selected as the cleavage site of ribozyme[9], two small nucleotide sequences complementary to flanks of the cleavage site of target RNA were located before and after hammerhead structure-the conservative core catalytic sequence of ribozyme, which can form typical active cleavage structure through complementation[10]. The cDNAs encoding the anti-Fas ribozyme were composed of two complementary strands each about 50 nt, which were terminated with *Bam*H I and *Xba* I: a 5' TCTAGAGATATATAAACTGATGAGTCCGTGAGGA CGAA ACAAGTG GATCC 3', b 5' GGATC CACTTGT TTC GTCCTCACGGACTCATCAG TTTATATATC TCTAGA 3'. All cDNAs were synthesized by Shanghai Shenggong Company. The ribozyme was cloned into the *Bam*H I and *Xba* I sites of the pBSKU6, which was named as U6-RZ596, and digested and sequenced to be correct. Then this recombinant plasmid was used as templete to get a fragment including U6 promoter and ribozyme by using PCR. The fragment was subcloned into the *Mlu* I site of the pEGFPC1, which was named as pU6-RZ596, and testified to be correct.

Isolation, cultivation and transfection of primary mouse hepatocytes

Healthy adult mice were spiled via portal vein after being anaesthetized and irrigated with a constant flux at about 9 mL/min. First Hanks solution was used without Ca^{2+} and Mg^{2+}, then 0.2 g/L collagenase solution for 8 min[11,12]. At last liver tissues were lacerated bluntly and digested vibrantly for 15 min in 37 °C bath water, and filtrated through nylon net and washed with PBS twice. Cells were resuspended in RPMI 1640 supplemented with 100 mL/L FBS and counted. Cell viability was 90-92%. Cell count was adjusted to 2×10^6/mL and cells were cultured in a humidified 50 mL/L CO_2 atmosphere at 37 °C. Cells were collected and grouped as following: empty control; cells transfected with pEGFPC1; cells transfected with pU6-RZ596. Transfection was performed according to the instructions of Effectene reagent. Cells were cultured for 48 h, the stably transfected cells were selected by culturing in medium containing G418 (600 μg/mL).

Detection of Fas mRNA expressed in hepatocytes by using RT-PCR

Total RNA was extracted from all above-mentioned groups by using TriZol reagent. After cDNA was synthesized, PCR reaction was performed, β-actin was used as control. The employed primers were as follows: Fas sense primer 5'-GCTGCAGACATG CTGTGGATC-3' and anti-sense primer 5'-TCACAGCCAGGA GAATCGCAG-3', β-actin sense primer 5'-GACGATGATATTG CCGCACT-3' and anti-sense primer 5'-GATACCACGCTTGC TCTGAG-3'. Reaction conditions for PCR were: pre-denaturation for 3 min at 95 °C, 30 cycles of denaturation for 30 s at 95 °C, annealing for 45 s at 58 °C, extension for 45 s at 72 °C, and extension for 3 min at 72 °C. PCR products were run on 15 g/L agarose gel.

Detection of Fas protein expressed in hepatocytes by western blot

Three groups of cells were collected regularly and lysed in soluble buffer, then the proteins were measured as 0.4 μg/μL, and electrophoresed in 100 g/L SDS-polyacrylamide minigels. The first antibody was rabbit anti-mouse-Fas antibody (1:200). The second antibody was goat anti-rabbit-IgG (1:5 000). At last the color was developed by ECL system.

Detection of caspase-3 protease activity

Treated with JO_2 (5 μg/mL) for 24 h under common growth condition, apoptosis of three-groups of cells were induced. Meanwhile the negative control without apoptosis and apoptosis cells treated with caspase-3 inhibitor (DEVD-fmk) were established. After being collected, cells were treated with cell lysis buffer sufficiently. The supernatant was retained (including protein needed), and then the procedure was performed according to the instructions of caspase-3 activity detection kit. The optical density (*A*) was measured at 405 nm.

Detection of cell viability via MTT assay

Grouped and treated as above, cells were inoculated into 96-well plates at a concentration about 10^5/mL (100 μL/well). After incubation with 10 μL MTT(0.5 mg/mL) for 4 h at 37 °C, the formazan crystals were dissolved in 100 μL DMSO, then the *A* was measured at 570 nm.

Detection of apoptosis through FACS

Three groups of cells treated with anti-Fas antibody JO_2 and the empty control were conjugated with Annexin V-FITC and PI respectively. Cell apoptosis was analyzed by flow cytometry.

RESULTS

Effects of ribozyme on Fas expression

Fas and β-actin PCR amplification generated amplicons of 419 bp and 186 bp respectively. Through scanning the luminescence, the ratio of Fas/β-actin was analyzed by using gel image analysis system. The negative control was 1.1; mouse hepatocytes transfected with pEGFPC1 was 0.98; hepatocytes transfected with pU6-RZ596 was 0.43. It was clear that Fas mRNA expression in cells transfected with anti-Fas ribozyme was lower than that in control and cells transfected with empty vector (Figure 1).

Western blotting displayed Fas protein expressed in cells transfected with pU6-RZ596 was much lower than that expressed in control and cells transfected with pEGFPC1, which was consistent with the results of RT-PCR (Figure 2).

Effect of anti-Fas ribozyme on caspase-3 activity

After 24 h of stimulation with JO_2, caspase-3 activity of mouse hepatocytes was specifically inhibited by a caspase-3 inhibitor. Compared with negative control, caspase-3 activities of other groups transfected with pEGFPC1 and pU6-RZ596 were 95% and 45% respectively (Figure 3).

Effect of anti-Fas ribozyme on cell viability

After induction of apoptosis of mouse hepatocytes through stimulation with JO_2, cell viability was detected by MTT assay. Compared with negative control, cell viabilities of other groups transfected with pEGFPC1 and pU6-RZ596 were 98% and 208% respectively (Figure 4).

Inhibition of Fas-mediated apoptosis in mouse hepatocytes

Cell apoptosis was induced as the method mentioned above. Apoptosis rates of cells in control, mock-transfected and pU6-RZ596-transfected groups were 86%, 87% and 35%, respectively (Figure 5).

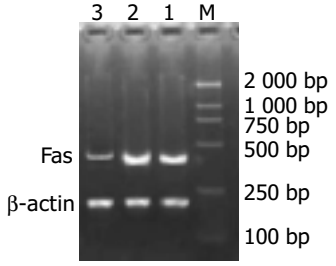

Figure 1 *Fas* gene transcription in all groups. M: DL-2000 DNA marker, Lanes 1-3: Empty control, mock-transfected group and pU6-RZ596-transfected group.

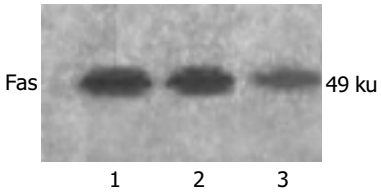

Figure 2 Fas protein expression in all groups. M: Marker; Lanes 1-3: Empty control, mock-transfected group and pU6-RZ596-transfected group.

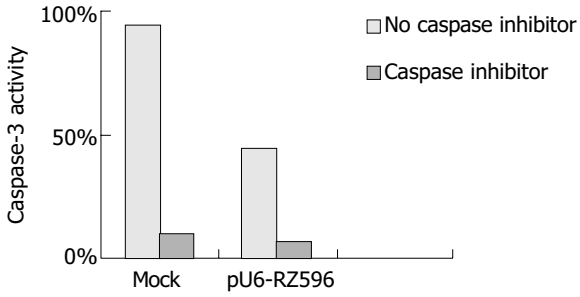

Figure 3 Detection of caspase-3 activity in all groups.

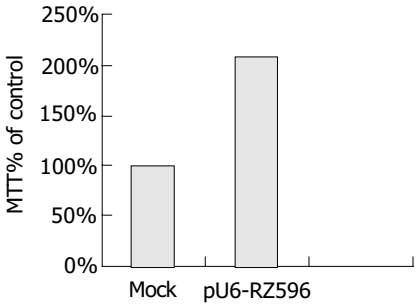

Figure 4 Stimulated with JO_2 for 24 h, cells viabilities of control, mock-transfected and pU6-RZ596-transfected groups were detected by MTT assay.

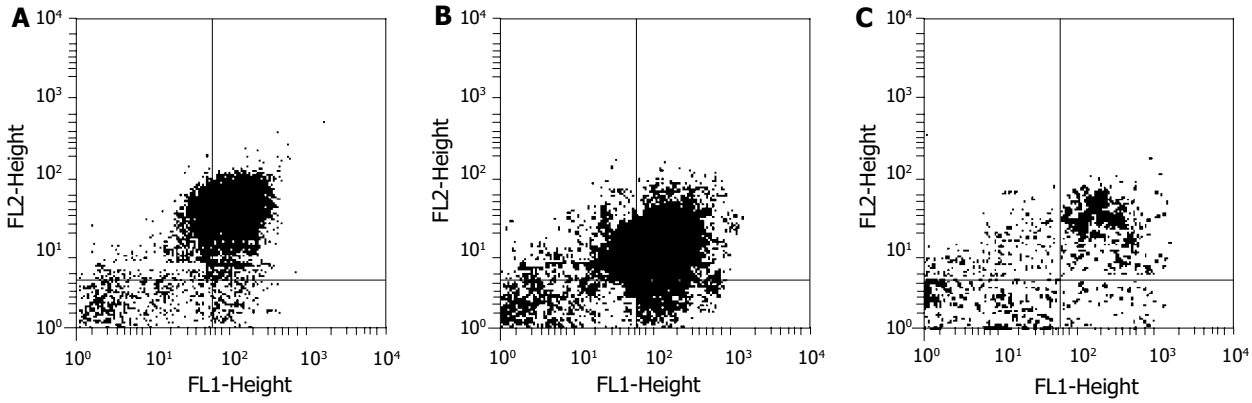

Figure 5 Detection of apoptosis of hepatocytes through cytometry. A: Apoptosis rate of control group was 86%; B: Apoptosis rate of mock-transfected cells was 87%; C: Apoptosis rate of pU6-RZ596-transfected cells was 35%.

DISCUSSION

Usually in clinic the hepatocytes of patients with acute or chronic liver failure show denaturation, necrosis and function failure. Existing pathogenic therapy and usual allopathy can not compensate functions of hepatocytes[12,13]. Now, the most efficient way is liver transplantation, but grafts survival is one of the important factors to affect whether liver transplantation is successful.

Primary mouse hepatocytes were isolated through two-step irrigation method[14], in which Fas expression was detected by RT-PCR and Western bloting. Treated with anti-Fas antibody JO_2, apoptosis of hepatocytes was induced with decreased viability. So hammerhead ribozyme targeting directly at 596 GUA triplets of Fas mRNA was constructed to efficiently block out Fas gene and decrease apoptosis of hepatocytes. As an RNA molecule with catalysis function[15], ribozyme can bind and cleave target RNA to inhibit gene expression. Hammerhead ribozyme is widely used in gene therapy because of its many superiorities[16], including small molecule weight, easy to design and synthesis, *etc.* Anti-Fas ribozyme was transfected into mouse hepatocytes by using Effectene reagent, then the stable clone was selected to investigate the inhibition action of ribozyme on Fas-mediated apoptosis. Results displayed that expression of Fas mRNA and protein in cells transfected with anti-Fas ribozyme was remarkably lower than that in control and mock-transfected cells. After stimulation with apoptosis inducer JO_2 (imitating the role of FasL *in vivo*) for 24 h, apoptosis rate of cells transfected with anti-Fas ribozyme was obviously lower than that of negative control and mock-transfected cells. Accordingly, caspase-3 activity of ribozyme-transfected cells was much lower than that of other groups, but cell viability was higher than the other two groups.

Apoptosis activates a series of proteases to induce programmed death of target cells through two ways including death receptor way and mitochondria way[17,18]. The final effect of the two ways is activity of caspase-3, that is to say caspase-3 is the common channel of two apoptosis ways[19]. Therefore, caspase-3 activity was increased in apoptosis and correlated with apoptosis rate positively. Anti-Fas ribozyme could not only decrease Fas expression but also weaken caspase-3 activity to reduce apoptosis induced by anti-Fas antibody. It is clear that hammerhead ribozyme targeting at 596 site of Fas RNA in this research can efficiently cleave Fas mRNA, which decreases not only the Fas expression but also its function. In existence of factors inducing apoptosis, ability of hepatocytes transfected with ribozyme against apoptosis was enhanced and cell viability was increased, which was coincident with study results of Dagmer about primary mouse islet β cells and insulinoma cells[20,21].

In short, anti-Fas ribozyme not only prevents Fas expression in mouse hepatocytes but also inhibits Fas-mediated apoptosis to improve cell survival after being transfected into hepatocytes, which afford strong assurance for successful liver transplantation. Further research should be focused on clinical application of anti-Fas ribozyme and selection of more efficient, highly specific and low toxic vectors[22-24].

REFERENCES

1 **Sato Y**, Yamamoto S, Takeishi T, Nakatsuka H, Kokai H, Hatakeyama K. New hepatic vein reconstruction by double expansion of outflow capacity of left-sided liver graft in living-donor liver transplantation. *Transplantation* 2003; **76:** 882-884

2 **Akamatsu N,** Sugawara Y, Kaneko J, Sano K, Imamura H, Kokudo N, Makuuchi M. Effects of middle hepatic vein reconstruction on right liver graft regeneration. *Transplantation* 2003; **76:** 832-837

3 **Sorom AJ**, Nyberg SL, Gores GJ. Keratin, fas, and cryptogenic liver failure. *Liver Transpl* 2002; **8:** 1195-1197

4 **Rivero M**, Crespo J, Mayorga M, Fabrega E, Casafont F, Pons-Romero F. Involvement of the Fas system in liver allograft rejection. *Am J Gastroenterol* 2002; **97:** 1501-1506

5 **Uchiyama H**, Kishihara K, Minagawa R, Hashimoto K, Sugimachi K, Nomoto K. Crucial Fas-Fas ligand interaction in spontaneous acceptance of hepatic allografts in mice. *Immunology* 2002; **105:** 450-457

6 **Wang H**, Chen XP, Qiu FZ. Overcoming multi-drug resistance by anti-MDR1 ribozyme. *World J Gastroenterol* 2003; **9:** 1444-1449

7 **Dunham CM**, Murray JB, Scott WG. A Helical twist-induced conformational switch activates cleavage in the hammerhead ribozyme. *J Mol Biol* 2003; **332:** 327-336

8 **Nikcevic G**, Kovacevic-Grujicic N, Stevanovic M. Improved transfection efficiency of cultured human cells. *Cell Biol Int* 2003; **27:** 735-737

9 **Persson T**, Hartmann RK, Eckstein F. Selection of hammerhead ribozyme variants with low Mg2+ requirement: importance of stem-loop II. *Chembiochem* 2002; **3:** 1066-1071

10 **Murray JB**, Dunham CM, Scott WG. A pH-dependent conformational change, rather than the chemical step, appears to be rate-limiting in the hammerhead ribozyme cleavage reaction. *J Mol Biol* 2002; **315:** 121-130

11 **Azuma H**, Hirose T, Fujii H, Oe S, Yasuchika K, Fujikawa T, Yamaoka Y. Enrichment of hepatic progenitor cells from adult mouse liver. *Hepatology* 2003; **37:** 1385-1394

12 **Tanimizu N**, Nishikawa M, Saito H, Tsujimura T, Miyajima A. Isolation of hepatoblasts based on the expression of Dlk/Pref-1. *J Cell Sci* 2003; **116**(pt 9)**:** 1775-1786

13 **Wagner M**, Kaufmann P, Fickert P, Trauner M, Lackner C, Stauber RE. Successful conservative management of acute hepatic failure following exertional heatstroke. *Eur J Gastroenterol*

Hepatol 2003; **15:** 1135-1139
14 **Crossin JD**, Muradali D, Wilson SR. US of liver transplants: normal and abnormal. *Radiographics* 2003; **23:** 1093-1114
15 **Heneghan MA**, Zolfino T, Muiesan P, Portmann BC, Rela M, Heaton ND, O'grady JG. An evaluation of long-term outcomes after liver transplantation for cryptogenic cirrhosis. *Liver Transpl* 2003; **9:** 921-928
16 **Musallam L**, Ethier C, Haddad PS, Denizeau F, Bilodeau M. Resistance to Fas-induced apoptosis in hepatocytes: role of GSH depletion by cell isolation and culture. *Am J Physiol Gastrointest Liver Physiol* 2002; **283:** G709-718
17 **Steitz TA**, Moore PB. RNA, the first macromolecular catalyst: the ribosome is a ribozyme. *Trends Biochem Sci* 2003; **28:** 411-418
18 **Khan AU**, Lal SK. Ribozymes: a modern tool in medicine. *J Biomed Sci* 2003; **10:** 457-467
19 **Shi G**, Wu Y, Zhang J, Wu J. Death decoy receptor TR6/DcR3 inhibits T cell chemotaxis *in vitro* and *in vivo*. *J Immunol* 2003; **171**: 3407-3414
20 **Curtin JF**, Cotter TG. Live and let die: regulatory mechanisms in Fas-mediated apoptosis. *Cell Signal* 2003; **15:** 983-992
21 **Ientile R**, Campisi A, Raciti G, Caccamo D, Curro M, Cannavo G, Li Volti G, Macaione S, Vanella A. Cystamine inhibits transglutaminase and caspase-3 cleavage in glutamate-exposed astroglial cells. *J Neurosci Res* 2003; **74:** 52-59
22 **Klein D**, Denis M, Ricordi C, Pastori RL. Assessment of ribozyme cleavage efficiency using reverse transcriptase real-time PCR. *Mol Biotechnol* 2000; **14:** 189-195
23 **Klein D**, Ricordi C, Pugliese A, Pastori RL. Inhibition of Fas-mediated apoptosis in mouse insulinoma betaTC-3 cells via an anti-Fas ribozyme. *Hum Gene Ther* 2000; **11:** 1033-1045
24 **Mergia A**, Heinkelein M. Foamy virus vectors. *Curr Top Microbiol Immunol* 2003; **277:** 131-159

Edited by Zhu LH and Chen WW **Proofread by** Xu FM

PO Box 2345, Beijing 100023, China
Fax: +86-10-85381893
E-mail: wjg@wjgnet.com www.wjgnet.com

World J Gastroenterol 2004;10(17):2571-2573
World Journal of Gastroenterology
Copyright © 2004 by The WJG Press ISSN 1007-9327

• BRIEF REPORTS •

A novel process for production of hepatitis A virus in Vero cells grown on microcarriers in bioreactor

Ming-Bo Sun, Yan-Jun Jiang, Wei-Dong Li, Ping-Zhong Li, Guo-Liang Li, Shu-De Jiang, Guo-Yang Liao

Ming-Bo Sun, Yan-Jun Jiang, Wei-Dong Li, Ping-Zhong Li, Guo-Liang Li, Shu-De Jiang, Guo-Yang Liao, Institute of Medical Biology, Chinese Academy of Medical Sciences, Peking Union Medical College, Kunming 650118, Yunnan Province, China
Supported by the Natural Science Foundation of Yunnan Province, No.1999C0023Q
Correspondence to: Guo-yang Liao, Institute of Medical Biology, Chinese Academy of Medical Sciences, 379 Jiaoling Road, Kunming 650118, Yunnan Province, China. liaogy@21cn.com
Telephone: +86-871-8334330
Received: 2003-12-28 **Accepted:** 2004-01-08

Abstract

AIM: To develop a novel process for production of HAV in Vero cells grown on microcarriers in a bioreactor.

METHODS: Vero cells infected with HAV strain W were seeded at an initial density of 1×10^5 cells/mL into a 7-L bioreactor containing Cytodex-I microcarriers. During the stage of cell proliferation, the following conditions were applied: pH 7.2±0.2, temperature 37±0.2 °C, dissolved oxygen 40% of air saturation and agitation rate 40 r/min . After the stage of virus culture started, the culture conditions were altered to pH 7.2±0.2, temperature 35±0.2 °C, dissolved oxygen 25% of air saturation, agitation rate 50 r/min and perfusion of fresh medium at a flux of 20 mL/h. During the course of fermentation, cell density, HAV antigen titre, glucose, lactate and ammonia levels were monitored. A control experiment using conventional static culture was conducted in the T150 flask.

RESULTS: After a 28-d cultivation, cell density increased to 14.0×10^5 cells/mL in the bioreactor, 5.6×10^9 viable cells and 4 000 mL virus suspension with a titre of 1:64 were harvested. The viral antigen output per cell unit in the bioreactor was 3-fold higher than that in the T150 flask. Meanwhile the metabolic mode of Vero cells did not change after the infection with HAV strain W.

CONCLUSION: The process for production of HAV in Vero cells grown on microcarriers in a bioreactor is a novel, efficient and practical way to obtain virus antigen for vaccine purpose. This approach produces more cells and HAV antigen than the conventional static culture. With futher improvement, it is possible to be used for the production of hepatitis A vaccine.

Sun MB, Jiang YJ, Li WD, Li PZ, Li GL, Jiang SD, Liao GY. A novel process for production of hepatitis A virus in Vero cells grown on microcarriers in bioreactor. *World J Gastroenterol* 2004; 10(17): 2571-2573
http://www.wjgnet.com/1007-9327/10/2571.asp

INTRODUCTION

Hepatitis A continues to be one of the most frequently reported infectious diseases with a worldwide distribution, and the continued occurrence of extensive community wide outbreaks indicates that hepatitis A remains a major public health problem. The availability of hepatitis A vaccine provides the opportunity to substantially lower disease incidence and potentially eliminate infection[1,2]. Several inactivated and live-attenuated hepatitis A vaccines have been developed. Due to the high protective efficacy, immunogenicity and safety, the inactivated vaccines are more favored[3-6]. At present several inactivated hepatitis A vaccines such as HAVRIX^R, VAQTA^R, AVAXIM^R and EPAXAL^R are commercially available[7-9]. Inactivated hepatitis A vaccine is prepared by methods similar to those used for inactivated poliovirus vaccines. Cell-culture-adapted virus is propagated in human fibroblast cells, usually in MRC-5 cells, purified from cell lysates by ultrafiltration and exclusion gel chromatography or other methods, inactivated with formalin, and absorbed to an aluminum hydroxide adjuvant. Compared with the production of live- attenuated vaccines, much larger quantities of HAV antigen are required for the production of inactivated vaccines. Thus the production of inactivated hepatitis A vaccines is usually hampered by the difficulty of preparation of large amounts of virus antigens in the conventional static flask or roller bottle cultures. The technique of microcarrier cell culture was first developed in the late 1960 s and has been used successfully for the production of rabies and poliomyelitis vaccines. One definite advantage of microcarrier cell culture is the ability to offer a high product output, which may help to solve the shortage of virus antigens for production of inactivated hepatitis A vaccines[10-13].

As mentioned above, most hepatitis A vaccines are commonly prepared by cultivation of HAV in human fibroblast cells including MRC-5 cells. No vaccine is produced by microcarrier technology due to the unsuitability of growth for MRC-5 cells on microcarriers. For HAV production in a microcarrier system it is necessary to establish suitable cells on microcarriers. Vero cells can grow well on microcarriers. But HAV is very difficult to adapt to grow in Vero cells. There are few reports about the isolation and adaptation of HAV in Vero cells. Until recently, no report about the production of hepatitis A vaccines in Vero cells grown on microcarriers in bioreactor is available. To verify the feasibility of this approach, HAV strain W was isolated and adapted in Vero cells in our previous work. This study described the production of HAV strain W in Vero cells grown on Cytodex-I microcarriers in a 7-L bioreactor.

MATERIALS AND METHODS

Bioreactor

A 7-L cell bioreactor (Applikon. Co., Holland) was used. Its work volume is 4 L. The value of dissolved oxygen was regulated by importing air mixture with different ratios of O_2, N_2, CO_2 and air. The value of pH was controlled by addition of $NaHCO_3$.

Microcarrier

Cytodex-I microcarrier (Pharmacia Fine Chemicals, Uppsala, Sweden) was used.

Medium

Cells were grown in minimum essential medium (MEM; Gibco, Glasgow, UK) supplemented with 100 U/mL penicillin, 10 mmol/L

of glucose, 5 mmol/L of glutamine and 100 mL/L bovine calf serum. In both virus culture medium and the feeding medium, bovine calf serum was reduced to 2 %.

Cell line and virus

Vero cell line was obtained from ATCC and preserved at our laboratory. Vero cells were used between passages 142 and 146 in this study. HAV strain W was isolated and adapted in Vero cells at our laboratory. The antigen titre of HAV used for inoculation was 1:128.

Virus adsorption

Vero cells were seeded into the T150 flasks at the concentration allowing for the formation of a confluent monolayer in 4-5 d. The monolayer cells were trypinsized and collected to make cell suspension in a Bellco agitation bottle. The cell suspension was inoculated with HAV strain W and incubated at 35 °C with a stirring of 30 rpm for 6 h.

Bioreactor culture

Bioreactor culture was divided into two stages including cell proliferation and virus culture. Infected Vero cells were seeded into the 7-L bioreactor at an initial density of 1×10^5 cells/mL. During the stage of cell proliferation, the following conditions were applied: pH 7.2±0.2, temperature 37±0.2 °C, dissolved oxygen 40% of air saturation and agitation rate 40 r/min. After the cell density reached to 1×10^6 cells/mL, stage of virus culture started and the used medium was replaced with maintenance medium. The culture conditions were altered to: pH 7.2±0.2, temperature 35±0.2 °C, dissolved oxygen 25% of air saturation and agitation rate 50 r/min. Meanwhile, perfusion was started and the perfusion rate was modulated to 20 mL/h. After a 28-d culture, infected cells were trypinsized and collected for the harvest of HAV antigen.

In a further study, M199 medium was used instead of MEM during virus culture. A circulating equipment was used to increase the dissolved oxygen in the feeding medium.

Conventional static culture

Infected Vero cells were seeded at an initial density of 1×10^5 cells/mL into the T150 flask containing 150 mL MEM medium. The cultures were incubated at 35 °C and the medium was replaced each week. After a 28-d culture, infected cells were trypinsized and collected for the harvest of HAV antigen.

Metabolite analysis

Samples taken from the cultures in the bioreactor were centrifuged at 1 500 r/min for 10 min. The supernatants were stored at -20 °C until tested. Glucose, ammonia and lactate concentrations were monitored by enzymatic assays, using specific assay kits (16-UV, 171-UV and 826-UV for glucose, ammonia and lactate respectively; Sigma, St. Louis, USA).

HAV antigen titre assay

Harvested cells were applied to three cycles of freezing and thawing following ultrasonication. After centrifugation at 1 500 r/min for 10 min, HAV antigen titre in the supernatant was determined by ELISA.

RESULTS

Growth and metabolism of infected Vero cells in bioreactor

Seventy-eight hours after the seeding, infected Vero cell density increased from 1×10^5 cells/mL to 11.17×10^5 cells/mL. At this point, the mode of bioreactor culture was switched from cell proliferation to virus culture. During the stage of virus culture, the cell density was kept above 1×10^6 cells/mL, reaching a maximum of 15.60×10^5 cells/mL at 402 h. It achieved 14.0×10^5 cells/mL at the end of virus culture, indicating a 14-fold increase over the initial cell density. The initial concentration of glucose was 7.8 mmol/L at the beginning of cell proliferation stage. As the cell density increased, the concentration declined. The rate of declination gradually became slow as a result of the feeding of fresh medium. The residual glucose concentration was 0.63 mmol/L at the end of virus culture. The initial concentrations of lactate and ammonia were 1.27 mmol/L and 0.18 mmol/L respectively at the beginning of cell proliferation and increased along with the increasing of cell density. The lactate level increased from 3.87 mmol/L to 12.68 mmol/L and ammonia level from 1.19 mmol/L to 2.68 mmol/L during the stage of virus culture. The rate of accumulation also became slow due to the feeding of fresh medium at the end of virus culture. Figure 1 shows the variations of cell density, glucose, lactate, and ammonia levels.

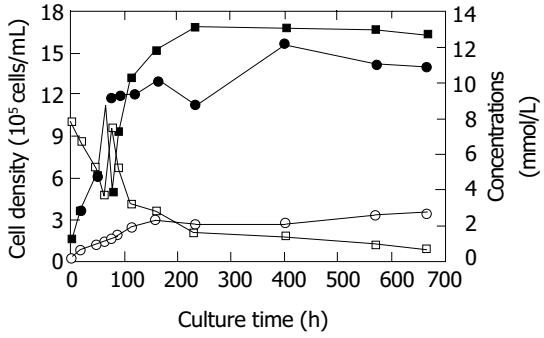

Figure 1 Growth and metabolism curves of Vero cells infected with HAV strain W. (●) Viable cell density (10^5 cells / mL), (□)Glucose (mmol / L), (■) Lactate (mmol / L), (○) Ammonia (mmol / L).

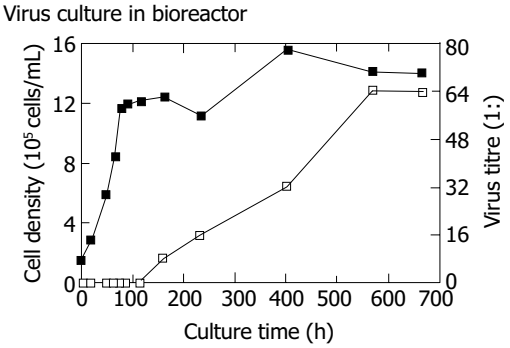

Figure 2 Production of HAV antigens by Vero cells grown on Cytodex-I microcarriers in a 7-litre bioreactor. (■) Viable cell density (10^5 cells / mL), (□) HAV antigen titre (1:).

Virus culture in bioreactor

No HAV antigen was detected during the stage of cell proliferation and at the early stage of virus culture. At 160 h, HAV antigen was first detected with a titre of 1:8 and achieved a maximum of 1:64 at 570 h (Figure 2). Four thousand mililitres of virus suspension with a titre of 1:64 was obtained at the end of virus culture.

Cell and antigen yields in flask

After a 28-d cultivation, 4×10^7 viable cells and 5 mL virus suspension with a titre of 1:128 were obtained from a T150 flask.

Improvement of virus culture in bioreactor

MEM medium was replaced by M199 medium, which contained richer nutriments and was more suitable for virus growth in cells. A circulating equipment was added to increase the dissolved oxygen in the feeding medium. With these

modifications, antigen titre achieved 1:128 in the harvested suspension.

DISCUSSION

In this study the growth kinetics and metabolic properties of Vero cells infected with HAV strain W were investigated. The results were similar to those of uninfected Vero cells in our previous work (Data not shown) and other studies[14,15]. This indicated that the metabolic mode of Vero cells did not change after infection with HAV strain W.

The yield of viable cells was 5.6×10^9 in the bioreactor whereas 4×10^7 in the T150 flask. The former was 140-fold higher than the latter. The yield of HAV antigens was 4 000 mL with a titre of 1:64 in the bioreactor and equaled to the yield from 400 T150 flasks. Furthermore, per 10^5 cells produced 1 mL HAV antigens with a titre of 1:4.57 in a bioreactor compared with only a titre of 1:1.6 in the T150 flask, that is the antigen output per cell unit in the bioreactor was 3-fold higher than that in the T150 flask. The findings mentioned above demonstrated this process for the production of HAV in Vero cells grown on microcarriers in a bioreactor could provide much higher yields of viable cells and virus antigens than that in conventional static culture. The antigen output per cell unit was also apparently higher. The technique of microcarrier culture in a bioreactor could offer numerous advantages over traditional techniques, such as a high ratio of surface area to volume, an efficient monitoring and control of key process parameters including temperature, pH and dissolved oxygen. Moreover, the culture substrate conditions could be controlled exactly and regulated in batch or fed-batch operation. The optimal metabolism and physiological status of cells could be achieved through the feeding of fresh medium and removal of toxic metabolites. Thus a high cell density and product output rate could be easily achieved[15-18].

In conclusion, the process for production of HAV in Vero cells grown on microcarriers in a bioreactor is a novel, efficient and practical way to obtain virus antigens for vaccine purpose. This approach produces more cells and HAV antigens than the conventional static culture. The optimal growth conditions for Vero cells and HAV strain W in a bioreactor are being further investigated to enhance the yield of virus antigens.

REFERENCES

1 **Zamir C**, Rishpon S, Zamir D, Leventhal A, Rimon N, Ben-Porath E. Control of a community-wide outbreak of hepatitis A by mass vaccination with inactivated hepatitis A vaccine. *Eur J Clin Microbiol Infect Dis* 2001; **20**: 185-187

2 **Van Damme P**, Banatvala J, Fay O, Iwarson S, McMahon B, Van Herck K, Shouval D, Bonanni P, Connor B, Cooksley G, Leroux-Roels G, von Sonnenburg F. Hepatitis A booster vaccination: is there a need? *Lancet* 2003; **362**: 1065-1071

3 **Demicheli V**, Tiberti D. The effectiveness and safety of hepatitis A vaccine: a systematic review. *Vaccine* 2003; **21**: 2242-2245

4 **Xu ZY**, Wang XY, Li RC, Meng ZD, Zhang Y, Gong J, Ma JC, Li YT, Zhao SJ, Li YP, Zhao YL, Huang QC, Lou D, Xia JL, Liu HB, Liu XL, Ouyang PY. Immunogenicity and efficacy of two live attenuated hepatitis A vaccines (H_2 strains and LA-1 strains). *Zhonghua Yixue Zazhi* 2002; **82**: 678-681

5 **Ren AG**, Ma JR, Feng FM, Xu YJ, Liu CB. Safety and immunogenicity of a new inactivated hepatitis A vaccine. *Zhonghua Shiyan He Linchuangbingduxue Zazhi* 2001; **15**: 357-359

6 **Ren YH**, Chen JT, Wu WT, Gong XJ, Zhang YC, Xue WH, Ren YF, Han LJ, Kang WX, Li SP, Liu CB. The study on the 0, 12 month vaccination schedule' of Healive inactivated hepatitis A vaccine in children. *Zhonghua Liuxingbingxue Zazhi* 2003; **24**: 1013-1015

7 **Huang GB**, Wang ZG, Li RC. The investigation on the safety and immunogenicity of inactived hepatitis A vaccine AVAXIM. *Zhonghua Liuxingbingxue Zazhi* 2000; **21**: 287-288

8 **Linglöf T**, Van Hattum J, Kaplan KM, Corrigan J, Duval I, Jensen E, Kuter B. An open study of subcutaneous administration of inactivated hepatitis A vaccine (VAQTA®) in adults: safety, tolerability, and immunogenicity. *Vaccine* 2001; **19**: 3968-3971

9 **Usonis V**, Bakasénas V, Valentelis R, Katiliene G, Vidzeniene D, Herzog C. Antibody titres after primary and booster vaccination of infants and young children with a virosomal hepatitis A vaccine(Epaxal®). *Vaccine* 2003; **21**: 4588-4592

10 **Williams JL**, Bruden DA, Cagle HH, McMahon BJ, Negus SE, Christensen CJ, Snowball MM, Bulkow LR, Fox-Leyva LK. Hepatitis A vaccine: immunogenicity following administration of a delayed immunization schedule in infants, children and adults. *Vaccine* 2003; **21**: 3208-3211

11 **Franco E**, Vitiello G. Vaccination strategies against hepatitis A in southern Europe. *Vaccine* 2003; **21**: 696-697

12 **Hennessey JP Jr**, Oswald CB, Dong ZY, Lewis JA, Sitrin RD. Evaluation of the purity of a purified, inactivated hepatitis A vaccine (VAQTA™). *Vaccine* 1999; **17**: 2830-2835

13 **Murdoch DL,** Goa K, Figgitt DP. Combined hepatitis A and B vaccines: a review of their immunogenicity and tolerability. *Drugs* 2003; **63**: 2625-2649

14 **Sun MB**, Zhang LJ, Liao GY, Li GL, Jiang SD. Physiology of Vero, CHO and Hybridoma cells cultured in bioreactor. *Zhongguo Shengwuzhipinxue Zazhi* 2001; **14**: 213-216

15 **Guan YH**, Kemp RB. Detection of the changing substrate requirements of cultured animal cells by stoichiometric growth equations validated by enthalpy balances. *J Biotechnol* 1999; **69**: 95-114

16 **Voigt A**, Zintl F. Hybridoma cell growth and anti-neuroblastoma monoclonal antibody production in spinner flasks using a protein-free medium with microcarriers. *J Biotechnol* 1999; **68**: 213-226

17 **Kallel H**, Rourou S, Majoul S, Loukil H. A novel process for the production of a veterinary rabies vaccine in BHK-21 cells grown on microcarriers in a 20-l bioreactor. *Appl Microbiol Biotechnol* 2003; **61**: 441-446

18 **Dürrschmid M**, Landauer K, Simic G, Blüml G, Doblhoff-Dier O. Scalable inoculation strategies for microcarrier-based animal cell bioprocesses. *Biotechnol bioeng* 2003; **83**: 681-686

Edited by Zhang JZ and Wang XL **Proofread by** Xu FM

PO Box 2345, Beijing 100023, China
Fax: +86-10-85381893
E-mail: wjg@wjgnet.com www.wjgnet.com

World J Gastroenterol 2004;10(17):2574-2579
World Journal of Gastroenterology
Copyright © 2004 by The WJG Press ISSN 1007-9327

• BRIEF REPORTS •

Effect of interleukin-10 and platelet-derived growth factor on expressions of matrix metalloproteinases-2 and tissue inhibitor of metalloproteinases-1 in rat fibrotic liver and cultured hepatic stellate cells

Li-Juan Zhang, Yun-Xin Chen, Zhi-Xin Chen, Yue-Hong Huang, Jie-Ping Yu, Xiao-Zhong Wang

Li-Juan Zhang, Jie-Ping Yu, Department of Gastroenterology, People's Hospital, Medical School of Wuhan University, Wuhan 430060, Hubei Province, China
Yun-Xin Chen, Zhi-Xin Chen, **Yue-Hong Huang, Xiao-Zhong Wang,** Department of Gastroenterology, Union Hospital of Fujian Medical University, Fuzhou 350001, Fujian Province, China
Supported by the Science and Technology Fund of Fujian Province, No.2003D05
Correspondence to: Xiao-Zhong Wang, Department of Gastroenterology, Union Hospital of Fujian Medical University, Fuzhou 350001, Fujian Province, China. drwangxz@pub6.fz.fj.cn
Telephone: +86-591-3357896
Received: 2004-01-02 **Accepted:** 2004-01-12

Abstract

AIM: To examine the expressions of matrix metalloproteinases-2 (MMP-2) and tissue inhibitor of metalloproteinases-1 (TIMP-1) in rat fibrotic liver and in normal rat hepatic stellate cells, and to investigate the changes in their expressions in response to treatment with interleukin-10 (IL-10) and platelet-derived growth factor (PDGF).

METHODS: Rat models of CCl_4-induced hepatic fibrosis were established and the liver tissues were sampled from the rats with or without IL-10 treatment, and also from the control rats. The expressions of MMP-2 and TIMP-1 in liver tissues were detected by S-P immunohistochemistry, and their expression intensities were evaluated in different groups. Hepatic stellate cells (HSCs) were isolated from normal rat and cultured *in vitro* prior to exposure to PDGF treatment or co-treatment with IL-10 and PDGF. MMP-2 and TIMP-1 levels were measured by semi-quantitative reverse transcriptional polymerase chain reaction (RT-PCR).

RESULTS: CCl_4- induced rat hepatic fibrosis models were successfully established. The positive expressions of MMP-2 and TIMP-1 increased obviously with the development of hepatic fibrosis, especially in untreated model group (84.0% and 92.0%, $P<0.01$). The positive signals decreased significantly following IL-10 treatment (39.3% and 71.4%, $P<0.01$ and $P<0.05$) in a time-dependent manner. TIMP-1 mRNA in PDGF-treated group was significantly increased time-dependently in comparison with that of the control group, but PDGF did not obviously affect MMP-2 expression. No difference was noted in TIMP-1 and MMP-2 expressions in HSCs after IL-10 and PDGF treatment ($P>0.05$).

CONCLUSION: MMP-2 and TIMP-1 expressions increase in liver tissues with the development of fibrosis, which can be inhibited by exogenous IL-10 inhibitor. PDGF induces the up-regulation of TIMP-1 but not MMP-2 in the HSCs. IL-10 inhibits TIMP-1 and MMP-2 expressions in HSCs induced by PDGF.

Zhang LJ, Chen YX, Chen ZX, Huang YH, Yu JP, Wang XZ. Effect of interleukin-10 and platelet-derived growth factor on expressions of matrix metalloproteinases-2 and tissue inhibitor of metalloproteinases-1 in rat fibrotic liver and cultured hepatic stellate cells. *World J Gastroenterol* 2004; 10(17): 2574-2579
http://www.wjgnet.com/1007-9327/10/2574.asp

INTRODUCTION

Liver fibrosis and its end-stage sequelae cirrhosis represent a major worldwide health problem. By definition progressive fibrosis occurs when the rate of matrix synthesis exceeds matrix degradation[1]. Considerable evidence suggests that the hepatic stellate cells (HSCs) are central to the fibrotic process. HSCs are normally located in the perisinusoidal space as quiescent vitamin A-storing cells secreting low levels of extracellular matrix (ECM). Following liver injury, increased synthesis of extracellular matrix constituents occurs in combination with other phenotypic changes (also called activation) of HSCs into myofibroblast-like cells. It has been demonstrated by the analysis of freshly isolated HSCs that a number of these phenotypic changes take place, including increased expression of extracellular matrix constituents and the expression of α-SMA[2,3]. This activated phenotype of HSCs subsequently becomes the major source of the interstitial collagens[4-6]. It has been suggested that HSCs are also a source of matrix-degrading metalloproteinases (MMPs), indicating their participation in matrix remodeling[7-9]. As a family of neutral proteinases, MMPs act on a variety of substrates[10]. Different expression profiles of MMPs influence the outcome of ECM components, resulting in preferential accumulation of interstitial collagens, type I in particular, in the fibrotic liver. MMPs are tightly regulated at the levels of transcription, secretion, and proteolytic activation, and their activities are governed by tissue-derived inhibitors[11]. The expression of tissue inhibitors of MMPs (TIMP) has also been demonstrated in human fibrotic liver disease and animal models of liver fibrosis[12]. At present, 4 TIMPs have been characterized[13], all being low-molecular-weight proteins sharing structural similarities. Individual members of the TIMP family display selective affinities for different members of the MMP family[14]. TIMP-1 controls mostly the activity of MMP, particularly MMP-1, whereas TIMP-2 is the major inhibitor of MMP-2[15]. MMP/TIMP balance is thought to play a pivotal role in the development of liver fibrosis, but their direct interaction *in vivo* has not yet been clarified. In the present study, the expressions of MMP-2 and TIMP-1 in rat fibrotic liver and in HSCs were examined and their changes were investigated in the presence of interleukin (IL)-10 and PDGF.

MATERIALS AND METHODS

Materials

One hundred clean male Sprague-Dawley rats weighing 140-180 g

(provided by Shanghai Experimental Animal Center) were divided randomly into control group (n = 24), model group (n = 40) and IL-10 treatment group (n = 36). All the rats were bred under routine condition (room temperature of 22±2 °C, humidity of 55±5%, with light/dark alternating every 12 h and free access to water and food. The feed was provided by BK Company in Shanghai, China).

Preparation of rats

Rats in control group were given intraperitoneal injection with saline at 2 mL/kg twice a week, and those in model and IL-10 treatment groups received intraperitoneal injection with 500 mL/L CCl_4 (dissolved in castor oil) at 2 mL/kg twice a week. From the third week, rats in treatment group were given intraperitoneal injection with IL-10 at 4 μg/kg (dissolved in saline) 20 min prior to CCl_4 injection. All injections were performed on Mondays and Thursdays after measurement of the rats' body weight. In the 5th wk, 3 rats in model group and 2 in treatment group died; in the 7th wk, 8 and 4 rats in these two groups died, respectively, and in the 9th week, another 10 and 6 died. At this time point, 3 rats in control group also died. In the 5th, 7th and 9th wk, 7 to 10 rats in each group were sacrificed to collect their liver samples, which were fixed in 40 g/L formaldehyde and embedded with paraffin.

Immunohistochemistry

Rat liver tissues were sectioned at the thickness of 4 μm. After deparaffinization with xylene and dehydration with graded ethanol, the sections were incubated in PBS containing 30 mL/L H_2O_2 to remove endogenous peroxidases and then in PBS containing 0.1 mol/L citrate to saturate the nonspecific binding sites. After incubation with goat anti-rat MMP-2 and TIMP-1 monoclonal antibodies, the sections were treated with instant S-P immunohistochemical reagents (American Zymed Company) and then incubated in a buffer solution containing 3,3-diaminobenzidine tetrahydrochloride (DAB) and H_2O_2 for visualization, followed by dehydration and mounting procedures. Microscopic examination of the sections was then performed.

Result assessment

Reactions were graded and scored according to their intensities and percentage of the positive cells respectively as follows: Zero score for negative reaction, 1 score for pale yellowish staining, and 2 scores for dense yellow or brown staining; 0 score for a percentage of positive cells below 5%, 1 score for one between 6% and 25%, 2 scores for one between 26% and 50%, and 3 for one over 50%. The eventual score of the section was derived from the product of the 2 scores for staining intensity and positive cell percentage, and graded as negative (-) result for a score lower than 1, positive result (+) for one between 2 and 3, and strong positive result (++) for one over 4. Ridit analysis was utilized to assess the difference between the groups.

Hepatic stellate cells isolation and culture

Male Sprague-Dawley rats weighing 450-500 g were used for isolation of HSCs. Rat liver nonparenchymal cells were isolated by means of sequential perfusion with collagenase and pronase E as described previously[16]. Buoyant HSCs were separated from the resulted cell suspension by elutriation over a Nycodenz gradient centrifugation. Desmin immunocytochemistry demonstrated a purity of isolated HSCs over 95%. The HSCs were then seeded into plastic tissue culture flask at the density of 1×10^6/mL in DMEM containing 100 mL/L fetal calf serum (FCS), and incubated at 37 °C with 50 mL/L CO_2. The culture medium was replaced 24 h after plating and every 48-72 h thereafter. The subsequent passages of HSCs were diluted to 5×10^4/mL before seeded into 50 mL culture flask containing DMEM medium supplemented with FCS.

PDGF treatment of HSCs

The cultured HSCs were divided into 6 groups: the first and sixth groups serving as control were cultured in 3 mL DMEM medium for 2 and 24 h, respectively, with the second, third, fourth and fifth groups cultured in 3 mL DMEM medium in the presence of 20 ng/mL PDGF for 2, 4, 8 and 24 h, respectively. The cells were then harvested for reverse transcriptional-PCR (RT-PCR).

Co-treatment of HSCs with IL-10 and PDGF

Cultured HSCs were divided into 8 groups: the first and second groups (blank control) were cultured in 3 mL DMEM medium for 2 and 24 h, respectively, and the third, fifth and seventh groups (negative control) cultured in 3 mL DMEM medium containing 20 ng/mL PDGF for 2, 12 and 24 h, respectively, while the fourth, sixth and eighth groups were cultured in 3 mL DMEM medium containing both 20 ng/mL IL-10 and 20 ng/mL PDGF for 2, 12 h and 24 h, respectively. The cells were then harvested for RT-PCR.

RT-PCR for MMP-2 and TIMP-1

Total RNA was isolated from HSCs using Gentra reagent (USA) according to the protocol provided by the manufacturer. The A_{260}/A_{280} of total RNA ranged between 1.8 and 2.0. After treatment with Dnase-I (1-2 μg), total RNA was reversely transcribed into complementary DNA (cDNA) with oligo (dT) using cDNA synthesis kit, and 2 μL cDNA product was then used as the template to amplify specific fragments in a 25 μL reaction system. PCRs using *Taq* polymerase reaction were carried out with an initial denaturation at 95 °C for 5 min, followed by 25 cycles at 94 °C for 45 s, annealing at 60 °C for 30 s, at 72 °C for 60 s, with a final extension at 72 °C for 7 min. The primer sequences used for MMP-2 were 5'-GTGCTGAAGGACACCCTCAAGAAGA-3' (sense) and 5'-TTGCCGTCCTTCTCAAAGTTGTACG-3' (antisense), and those for TIMP-1 were 5'-GCCATGGAGAGCCTCTGTGG-3' (sense) and 5'-GCAGGCAGGCAAAGTGATCG-3' (antisense); the primers for β-actin as the internal control were 5'-GAGCTATGAGCTGCCTGACG-3' (sense) and 5'-AGCACTTGCGGTCCACGATG-3' (antisense).

Electrophoresis and semi-quantitative analysis

PCR products underwent 2% agarose gel electrophoresis and were visualized with ethidium bromide. The expected products' sizes were 604 bp for MMP-2, 310 bp for TIMP-1 and 410 bp for β-actin. Bio Imagine System was applied to detect the density of the bands of PCR products. The expression levels of MMP-2 and TIMP-1 were calculated by the ratio of their band densities of PCR products to that of β-actin. Semi-quantitative detection was repeated for 5 times. SPSS 10.0 software was used to analyze the difference between the groups.

RESULTS

MMP-2 and TIMP-1 expressions in liver tissues

The positive rate of MMP-2 in control group, model group and IL-10 treatment group was 9.5%, 84.0% and 39.3%, respectively, and that of TIMP-1 was 23.8%, 92.0% and 71.4%, respectively. The granular positive products were localized in the cytoplasm of hepatocytes and biliary epithelial cells. In control group, the positive expressions of MMP-2 and TIMP-1 were weak and found mainly in endothelial cells and hepatic cells. In model group, positive expressions increased obviously with the development of hepatic fibrosis, distributing in biliary epithelial cells, fibroblasts and muscular cells. In treatment group the

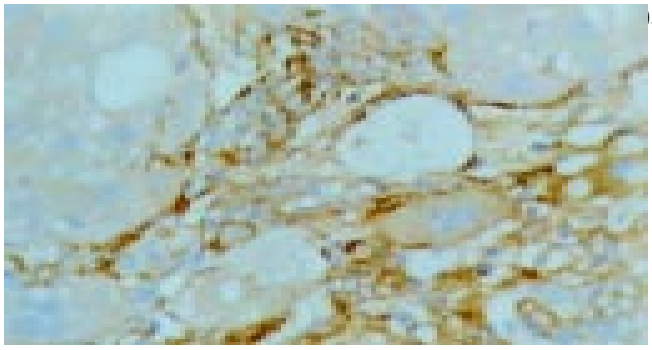

Figure 1 MMP-2-positive cells in the model group (S-P method, ×200).

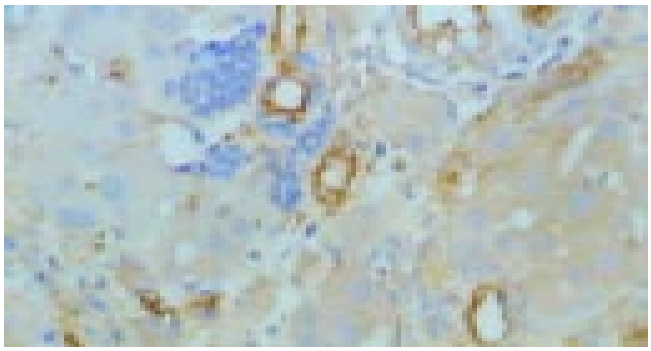

Figure 2 MMP-2-positive cells in IL-10 treatment group (S-P method, ×200).

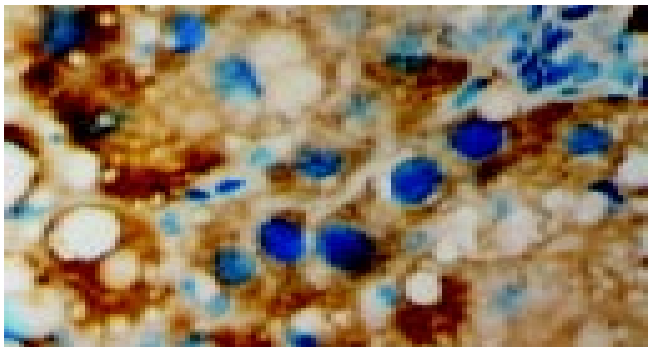

Figure 3 TIMP-1-positive cells in the model group (S-P method,

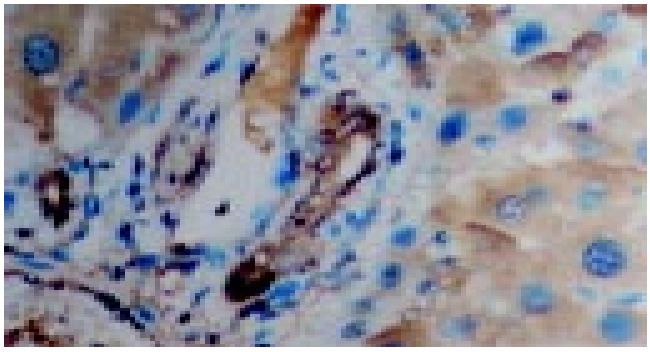

Figure 4 TIMP-1-positive cells in IL-10 treatment group (S-P method, ×400).

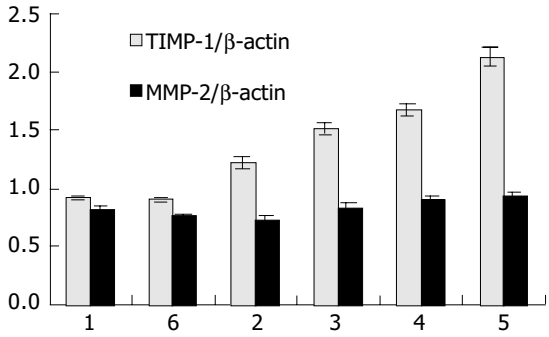

Figure 5 Effects of PDGF on TIMP-1 and MMP-2 expressions in HSCs. 1: Control group (2 h); 2: PDGF-treated group (2 h); 3: PDGF-treated group (4 h); 4: PDGF-treated group (8 h); 5: PDGF-treated group (24 h); 6: Control group (24 h).

Intensities of MMP-2 and TIMP-1 immunoreactivities

Comparison of MMP-2 and TIMP-1 positive expression levels between the 3 groups is shown in Table 1. Ridit analysis showed significant difference between the 3 groups ($P<0.01$). Higher expression levels of MMP-2 and TIMP-1 in model group were detected than in control group ($P<0.01$). In treatment group, IL-10 treatment resulted in decreased immunoreactivities for MMP-2 and TIMP-1 ($P<0.01$ and $P<0.05$ respectively). The expression levels of MMP-2 and TIMP-1 in different phases of hepatic fibrosis are listed in Table 2. With the development of hepatic fibrosis, the intensities of MMP-2 and TIMP-1 immunoreactivities increased gradually, and the difference was

Table 1 Comparison of MMP-2 and TIMP-1 immunoreactivities between control, model and treatment groups

Group	MMP-2					TIMP-1			
	n	-	+	++	Ridit value	-	+	++	Ridit value
Control	21	19	2	0	0.312	16	5	0	0.277[b]
Model	25	4	13	8	0.712[d]	2	14	9	0.684[d]
Treatment	28	17	10	1	0.451[e]	8	18	2	0.503[g]

[b]$P<0.01$ *vs* treatment group; [c]$P<0.05$; [d]$P<0.01$ *vs* control group; [e]$P>0.05$ *vs* control group; [g]$P<0.05$ *vs* model group.

Table 2 Comparison of MMP-2 and TIMP-1 immunoreactivities measured at different time points in model group

Wk	*n*	MMP-2				TIMP-1			
		-	+	++	Ridit value	-	+	++	Ridit value
5	8	1	7	0	0.378	1	6	1	0.36[ab]
7	8	2	5	1	0.388	1	5	2	0.418[e]
9	9	1	1	7	0.709	0	2	7	0.698[c]

[b]$P<0.01$ *vs* wk 7 and 9; [a]$P<0.05$ *vs* wk 9; [c]$P<0.05$ *vs* wk 7; [e]$P>0.05$ *vs* wk 5.

significant (P<0.05).

Relative quantities of MMP-2 and TIMP-1 mRNA in HSCs

Expression of TIMP-1 in PDGF-treated HSCs was significantly increased time-dependently as compared with that in control cells (P<0.01). There was no difference in MMP-2 expression between PDGF-treated HSCs and control cells (Figure 5). After treatment with IL-10 and PDGF, expressions of TIMP-1 and MMP-2 in HSCs were similar to those in negative control groups (P>0.05), without changes over time (Figure 6).

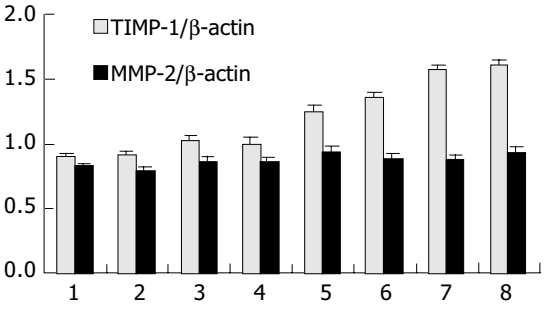

Figure 6 Effects of IL-10 and PDGF on TIMP-1 and MMP-2 expressions in HSCs. 1: Blank control group (2 h); 2: Blank control group (24 h); 3: Negative control group (2 h); 4: Treatment group (2 h); 5: Negative control group (12 h); 6: Treatment group (12 h); 7: Negative control group (24 h); 8: Treatment group (24 h).

DISCUSSION

Liver fibrosis is thought to be a progressive pathological process that leads ultimately to deposition of excess matrix proteins in extracellular space[17], and destroys normal liver architecture to finally result in cirrhosis. In extracellular space, matrix degradation occurs predominantly consequent to the action of a family of enzymes known as matrix metalloproteinases[18]. These enzymes are secreted by cells into extracellular space as proenzymes, which are then activated by a number of specific mechanisms. MMP-2 (gelatinase A) produced by activated HSCs, as demonstrated by immunohistochemistry and *in situ* hybridization[19,20], plays an important role in remodeling the basement membranes as it degrades several of the collagen components including collagen IV, laminin and fibronectin[21]. In other tissues, such as lung, kidney and heart, MMP-2 expression is also increased during fibrogenesis[22-25]. Recent studies showed that inhibition of MMP-2 activity[26] or blockade of MMP-2 synthesis[21] might effectively prevent mesangial cell proliferation and collagen I synthesis *in vitro*, indicating the possible role of MMP-2 as a growth factor and activator for mesangial cells, performed probably through an autocrine pathway[27]. In human liver fibrosis or in rat models of CCl_4-induced liver fibrosis, the expression of MMP-2 mRNA was increased by several fold, and HSCs expressed MMP-2 when activated by *in vitro* culture[27,28], as is consistent with our findings in this study.

TIMPs are the most important family of molecules involved in regulation of extracellular MMP activity[29-32]. TIMPs are produced by a wide variety of cells and often cosecreted with MMPs, providing local autoregulation of MMP activity. Recognized now as a multifunctional protein, TIMP-1 has been reported to stimulate steroidogenesis, inhibit angiogenesis, and induce changes in cell morphology[11,33]. It has been shown that TIMP-1, but not TIMP-2, can enter the nuclei of several types of cells, which further suggests that TIMP-1 may also act as a transcription factor[34,35]. We found that during the development of liver fibrosis, TIMP-1 expression in the liver was markedly up-regulated. Increased serum TIMP-1 levels have been documented in patients with chronic active liver disease in correlation with histological degree of human liver fibrosis[36]. Liver TIMP-1 protein levels are also closely correlated with the histological degree of liver fibrosis. The above findings suggest that TIMP-1 plays an important role in the development of liver fibrosis[12,30,37]. Recent findings indicate that HOE077, a prolyl-4-hydroxylase inhibitor, may prevent fibrosis by inhibiting the expression of liver type I procollagen and TIMP-1 mRNAs as well as proline hydroxylation and stellate cell activation, resulting in reduced expression of procollagen and TIMP-1 mRNAs[38]. Experiments with liver-targeted TIMP-1 transgenic (TIMP-Tg) mouse have shown significantly attenuated ability of reversing spontaneous liver fibrosis in TIMP-Tg mice as compared with the control mice[39]. But the exact role of TIMP-1 in liver fibrogenesis has not yet been clarified. In another experiment with TIMP-Tg mice, the direct effect of TIMP-1 overexpression on CCl_4-induced liver fibrosis was examined, it was found that TIMP-1 did not induce liver fibrosis by itself, but strongly promoted liver fibrosis development, in other words, TIMP-1 behaved not as the initiation factor, but as a strong promoter of liver fibrosis[40].

PDGF is a major mitogen for connective tissue cells and some other cell types. This dimeric molecule consists of disulfide-bonded, structurally similar A- and B-polypeptide chains that combine to form homo- and hetero-dimers, and is involved in autocrine and paracrine stimulation of cell growth in several different pathological conditions. Evidence showed that recombinant PDGF stimulated proliferation of nonconfluent myofibroblasts and collagen production in confluent cultures of myofibroblasts without increasing cell number, demonstrating the importance of PDGF in pathogenesis of liver fibrosis[41-45]. It has been established that human and rat HSCs are able to migrate according to the concentration gradients of chemotactic factors[46-48]. The best characterized chemotactic factor for HSCs identified so far is PDGF-BB[46,47,49], known also as the most potent mitogen for HSCs and overexpression during active hepatic fibrogenesis[50]. Our findings in this study showed that after PDGF treatment, the expression of TIMP-1 increased significantly in HSCs possibly because PDGF-promoted HSC proliferation and activation, indicating the importance of PDGF in pathogenesis of liver fibrosis. We also found that the expression of MMP-2 did not increase in HSCs after PDGF treatment, which is suggestive of the irrelevance of MMP-2 in fibrogenesis induced by PDGF.

IL-10, originally isolated from mouse helper T cells, is a cytokine that regulates a number of interleukins. It inhibits synthesis of several cytokines by T lymphocytes and activates monocytes, and was therefore originally named cytokine synthesis inhibitory factor[51]. Recent studies showed that IL-10 also acted on connective tissue cells such as fibroblasts, inducing, for instance, transcriptional inhibition of the expression of type I collagen, which is the major component of extracellular matrix[52]. IL-10 also possesses antifibrogenic properties by down-regulating profibrogenic cytokines like TGF-β_1 and TNF-α[53,54]. Our previous studies indicated that IL-10 could produce antifibrogenesis effect on CCl_4-induced rat hepatic fibrosis. In this study, we found that IL-10 down-regulated expression of MMP-2 and TIMP-1 in rat fibrotic liver, possibly another way that IL-10 exerts its effect of antifibrogenesis. In our previous study, PDGF was found to markedly promote the contraction and proliferation of HSCs and expressions of collagen type I and III as well as TGF-β_1 in HSCs, which was significantly inhibited by IL-10[55]. But results of the present experiment showed that at the dose of 20 ng/mL, IL-10 did not inhibit TIMP-1 and MMP-2 expressions in PDGF-treated HSCs, indicating that the inhibitory effects of IL-10 on HSCs may not involve TIMP-1 and MMP-2.

In summary, the present study demonstrates that positive

expressions of MMP-2 and TIMP-1 in rat liver tissue increase with the development of hepatic fibrosis, and MMP-2 and TIMP-1 play an important role during the development of liver fibrosis. Exogenous IL-10 decreases the expression of MMP-2 and TIMP-1 in liver tissues. PDGF increases the expression of TIMP-1 in HSCs, possibly through promoting HSC proliferation and activation, and this effect is not inhibited by IL-10.

REFERENCES

1 **Bedossa P,** Paradis V. Liver extracellular matrix in health and disease. *J Pathol* 2003; **200**: 504-515
2 **Rockey DC.** The cell and molecular biology of hepatic fibrogenesis. Clinical and therapeutic implications. *Clin Liver Dis* 2000; **4**: 319-355
3 **Bataller R,** Brenner DA. Hepatic stellate cells as a target for the treatment of liver fibrosis. *Semin Liver Dis* 2001; **21**: 437-451
4 **Safadi R,** Friedman SL. Hepatic fibrosis-role of hepatic stellate cell activation. *Med Gen Med* 2002; **4**: 27
5 **Reeves HL,** Friedman SL. Activation of hepatic stellate cells-a key issue in liver fibrosis. *Front Biosci* 2002; **7**: d808-826
6 **Iredale JP.** Hepatic stellate cell behavior during resolution of liver injury. *Semin Liver Dis* 2001; **21**: 427-436
7 **Imai K,** Sato T, Senoo H. Adhesion between cells and extracellular matrix with special reference to hepatic stellate cell adhesion to three-dimensional collagen fibers. *Cell Struct Funct* 2000; **25**: 329-336
8 **Neubauer K,** Saile B, Ramadori G. Liver fibrosis and altered matrix synthesis. *Can J Gastroenterol* 2001; **15**: 187-193
9 **Benyon RC,** Arthur MJ. Extracellular matrix degradation and the role of hepatic stellate cells. *Semin Liver Dis* 2001; **21**: 373-384
10 **Okazaki I,** Watanabe T, Hozawa S, Arai M, Maruyama K. Molecular mechanism of the reversibility of hepatic fibrosis: with special reference to the role of matrix metalloproteinases. *J Gastroenterol Hepatol* 2000; **15**(Suppl): D26-32
11 **Will H,** Atkinson SJ, Butler GS, Smith B, Murphy G. The soluble catalytic domain of membrane type 1 matrix metalloproteinase cleaves the propeptide of progelatinase A and initiates autoproteolytic activation. Regulation by TIMP-2 and TIMP-3. *J Biol Chem* 1996; **271**: 17119-17123
12 **McCrudden R,** Iredale JP. Liver fibrosis, the hepatic stellate cell and tissue inhibitors of metalloproteinases. *Histol Histopathol* 2000; **15**: 1159-1168
13 **Gomez DE,** Alonso DF, Yoshiji H, Thorgeirsson UP. Tissue inhibitors of metalloproteinases: structure, regulation and biological functions. *Eur J Cell Biol* 1997; **74**: 111-122
14 **Arthur MJ.** Fibrogenesis II. Metalloproteinases and their inhibitors in liver fibrosis. *Am J Physiol Gastrointest Liver Physiol* 2000; **279**: G245-249
15 **Senoo H,** Imai K, Matano Y, Sato M. Molecular mechanisms in the reversible regulation of morphology, proliferation and collagen metabolism in hepatic stellate cells by the three-dimensional structure of the extracellular matrix. *J Gastroenterol Hepatol* 1998; **13**(Suppl): S19-32
16 **Ramm GA**. Isolation and culture of rat hepatic stellate cells. *J Gastroenterol Hepatol* 1998; **13**: 846-851
17 **Iredale JP**. Tissue inhibitors of metalloproteinases in liver fibrosis. *Int J Biochem Cell Biol* 1997; **29**: 43-54
18 **Benyon RC,** Arthur MJ. Extracellular matrix degradation and the role of hepatic stellate cells. *Semin Liver Dis* 2001; **21**: 373-384
19 **Takahara T,** Furui K, Yata Y, Jin B, Zhang LP, Nambu S, Sato H, Seiki M, Watanabe A. Dual expression of matrix metalloproteinase-2 and membrane-type 1-matrix metalloproteinase in fibrotic human livers. *Hepatology* 1997; **26**: 1521-1529
20 **Takahara T,** Furui K, Funaki J, Nakayama Y, Itoh H, Miyabayashi C, Sato H, Seiki M, Ooshima A, Watanabe A. Increased expression of matrix metalloproteinase-II in experimental liver fibrosis in rats. *Hepatology* 1995; **21**: 787-795
21 **Turck J,** Pollock AS, Lee LK, Marti HP, Lovett DH. Matrix metalloproteinase 2 (gelatinase A) regulates glomerular mesangial cell proliferation and differentiation. *J Biol Chem* 1996; **271**: 15074-15083
22 **Swiderski RE,** Dencoff JE, Floerchinger CS, Shapiro SD, Hunninghake GW. Differential expression of extracellular matrix remodeling genes in a murine model of bleomycin-induced pulmonary fibrosis. *Am J Pathol* 1998; **152**: 821-828
23 **Fukuda Y,** Ishizaki M, Kudoh S, Kitaichi M, Yamanaka N. Localization of matrix metalloproteinases-1, -2, and -9 and tissue inhibitor of metalloproteinase-2 in interstitial lung diseases. *Lab Invest* 1998; **78**: 687-698
24 **Shimizu T,** Kuroda T, Hata S, Fukagawa M, Margolin SB, Kurokawa K. Pirfenidone improves renal function and fibrosis in the post-obstructed kidney. *Kidney Int* 1998; **54**: 99-109
25 **Bakowska J,** Adamson IY. Collagenase and gelatinase activities in bronchoalveolar lavage fluids during bleomycin-induced lung injury. *J Pathol* 1998; **185**: 319-323
26 **Steinmann-Niggli K,** Ziswiler R, Kung M, Marti HP. Inhibition of matrix metalloproteinases attenuates anti-Thy1.1 nephritis. *J Am Soc Nephrol* 1998; **9**: 397-407
27 **Benyon RC,** Hovell CJ, Da Gaca M, Jones EH, Iredale JP, Arthur MJ. Progelatinase A is produced and activated by rat hepatic stellate cells and promotes their proliferation. *Hepatology* 1999; **30**: 977-986
28 **Arthur MJ,** Stanley A, Iredale JP, Rafferty JA, Hembry RM, Friedman SL. Secretion of 72 kDa type IV collagenase / gelatinase by cultured human lipocytes. Analysis of gene expression, protein synthesis and proteinase activity. *Biochem J* 1992; **287**(Pt 3): 701-707
29 **Arthur MJ,** Iredale JP, Mann DA. Tissue inhibitors of metalloproteinases: role in liver fibrosis and alcoholic liver disease. *Alcohol Clin Exp Res* 1999; **23**: 940-943
30 **Arthur MJ,** Mann DA, Iredale JP. Tissue inhibitors of metalloproteinases, hepatic stellate cells and liver fibrosis. *J Gastroenterol Hepatol* 1998; **13**(Suppl): S33-38
31 **Murphy FR,** Issa R, Zhou X, Ratnarajah S, Nagase H, Arthur MJ, Benyon C, Iredale JP. Inhibition of apoptosis of activated hepatic stellate cells by tissue inhibitor of metalloproteinase-1 is mediated via effects on matrix metalloproteinase inhibition: implications for reversibility of liver fibrosis. *J Biol Chem* 2002; **277**: 11069-11076
32 **Bahr MJ,** Vincent KJ, Arthur MJ, Fowler AV, Smart DE, Wright MC, Clark IM, Benyon RC, Iredale JP, Mann DA. Control of the tissue inhibitor of metalloproteinases-1 promoter in culture-activated rat hepatic stellate cells: regulation by activator protein-1 DNA binding proteins. *Hepatology* 1999; **29**: 839-848
33 **Thorgeirsson UP,** Yoshiji H, Sinha CC, Gomez DE. Breast cancer; tumor neovasculature and the effect of tissue inhibitor of metalloproteinases-1 (TIMP-1) on angiogenesis. *In Vivo* 1996; **10**: 137-144
34 **Zhao WQ,** Li H, Yamashita K, Guo XK, Hoshino T, Yoshida S, Shinya T, Hayakawa T. Cell cycle-associated accumulation of tissue inhibitor of metalloproteinases-1 (TIMP-1) in the nuclei of human gingival fibroblasts. *J Cell Sci* 1998; **111**(Pt 9): 1147-1153
35 **Ritter LM,** Garfield SH, Thorgeirsson UP. Tissue inhibitor of metalloproteinases-1 (TIMP-1) binds to the cell surface and translocates to the nucleus of human MCF-7 breast carcinoma cells. *Biochem Biophys Res Commun* 1999; **257**: 494-499
36 **Iredale JP,** Benyon RC, Pickering J, McCullen M, Northrop M, Pawley S, Hovell C, Arthur MJ. Mechanisms of spontaneous resolution of rat liver fibrosis. Hepatic stellate cell apoptosis and reduced hepatic expression of metalloproteinase inhibitors. *J Clin Invest* 1998; **102**: 538-549
37 **Herbst H,** Wege T, Milani S, Pellegrini G, Orzechowski HD, Bechstein WO, Neuhaus P, Gressner AM, Schuppan D. Tissue inhibitor of metalloproteinase-1 and -2 RNA expression in rat and human liver fibrosis. *Am J Pathol* 1997; **150**: 1647-1659
38 **Sakaida I,** Uchida K, Hironaka K, Okita K. Prolyl 4-hydroxylase inhibitor (HOE 077) prevents TIMP-1 gene expression in rat liver fibrosis.*J Gastroenterol* 1999; **34**: 376-377
39 **Yoshiji H,** Kuriyama S, Yoshii J, Ikenaka Y, Noguchi R, Nakatani T, Tsujinoue H, Yanase K, Namisaki T, Imazu H, Fukui H. Tissue inhibitor of metalloproteinases-1 attenuates spontaneous liver fibrosis resolution in the transgenic mouse. *Hepatology* 2002; **36**(4 Pt 1): 850-860

40 **Yoshiji H,** Kuriyama S, Miyamoto Y, Thorgeirsson UP, Gomez DE, Kawata M, Yoshii J, Ikenaka Y, Noguchi R, Tsujinoue H, Nakatani T, Thorgeirsson SS, Fukui H. Tissue inhibitor of metalloproteinases-1 promotes liver fibrosis development in a transgenic mouse model. *Hepatology* 2000; **32**: 1248-1254

41 **Zhang BB,** Cai WM, Weng HL, Hu ZR, Lu J, Zheng M, Liu RH. Diagnostic value of platelet derived growth factor-BB, transforming growth factor-beta$_1$, matrix metalloproteinase-1, and tissue inhibitor of matrix metalloproteinase-1 in serum and peripheral blood mononuclear cells for hepatic fibrosis. *World J Gastroenterol* 2003; **9**: 2490-2496

42 **Tangkijvanich P,** Melton AC, Chitapanarux T, Han J, Yee HF. Platelet-derived growth factor-BB and lysophosphatidic acid distinctly regulate hepatic myofibroblast migration through focal adhesion kinase. *Exp Cell Res* 2002; **281**: 140-147

43 **Di Sario A,** Bendia E, Svegliati-Baroni G, Marzioni M, Ridolfi F, Trozzi L, Ugili L, Saccomanno S, Jezequel AM, Benedetti A. Rearrangement of the cytoskeletal network induced by platelet-derived growth factor in rat hepatic stellate cells: role of different intracellular signalling pathways. *J Hepatol* 2002; **36**: 179-190

44 **Kinnman N,** Goria O, Wendum D, Gendron MC, Rey C, Poupon R, Housset C. Hepatic stellate cell proliferation is an early platelet-derived growth factor-mediated cellular event in rat cholestatic liver injury. *Lab Invest* 2001; **81**: 1709-1716

45 **Kinnman N,** Hultcrantz R, Barbu V, Rey C, Wendum D, Poupon R, Housset C. PDGF-mediated chemoattraction of hepatic stellate cells by bile duct segments in cholestatic liver injury. *Lab Invest* 2000; **80**: 697-707

46 **Ikeda K,** Wakahara T, Wang YQ, Kadoya H, Kawada N, Kaneda K. *In vitro* migratory potential of rat quiescent hepatic stellate cells and its augmentation by cell activation. *Hepatology* 1999; **29**: 1760–1767

47 **Marra F,** Gentilini A, Pinzani M, Choudhury GG, Parola M, Herbst H, Dianzani MU, Laffi G, Abboud HE, Gentilini P. Phosphatidylinositol 3-kinase is required for platelet-derived growth factor's actions on hepatic stellate cells. *Gastroenterology* 1997; **112**: 1297–1306

48 **Marra F,** Romanelli RG, Giannini C, Failli P, Pastacaldi S, Arrighi MC, Pinzani M, Laffi G, Montalto P, Gentilini P. Monocyte chemotactic protein-1 as a chemoattractant for human hepatic stellate cells. *Hepatology* 1999; **29**: 140–148

49 **Carloni V,** Romanelli RG, Pinzani M, Laffi G, Gentilini P. Focal adhesion kinase and phospholipase C gamma involvement in adhesion and migration of human hepatic stellate cells. *Gastroenterology* 1997; **112**: 522–531

50 **Pinzani M.** PDGF and signal transduction in hepatic stellate cells. *Front Biosci* 2002; **7**: d1720-1726

51 **Nelson DR,** Lauwers GY, Lau JY, Davis GL. Interleukin 10 treatment reduces fibrosis in patients with chronic hepatitis C: a pilot trial of interferon nonresponders. *Gastroenterology* 2000; **118**: 655-660

52 **Reitamo S,** Remitz A, Tamai K, Uitto J. Interleukin-10 modulates type I collagen and matrix metalloprotease gene expression in cultured human skin fibroblasts. *J Clin Invest* 1994; **94**: 2489-2492

53 **Kovalovich K,** DeAngelis RA, Li W, Furth EE, Ciliberto G, Taub R. Increased toxin-induced liver injury and fibrosis in interleukin-6-deficient mice. *Hepatology* 2000; **31**: 149-159

54 **Louis H,** Van Laethem JL, Wu W, Quertinmont E, Degraef C, Van den Berg K, Demols A, Goldman M, Le Moine O, Geerts A, Deviere J. Interleukin-10 controls neutrophilic infiltration, hepatocyte proliferation, and liver fibrosis induced by carbon tetrachloride in mice. *Hepatology* 1998; **28**: 1607-1615

55 **Chen YX,** Wang XZ, Weng SG, Chen ZX, Huang YH, Zhang LJ. Effects of IL-10 and PDGF on expression of TGF-β_1 at hepatic stellate cells. *Zhongxiyi Jiehe Ganbin Zazhi* 2002; **12**: 343-345

Edited by Chen WW **Proofread by** Zhu LH and Xu FM

PO Box 2345, Beijing 100023, China
Fax: +86-10-85381893
E-mail: wjg@wjgnet.com www.wjgnet.com

World J Gastroenterol 2004;10(17):2580-2584
World Journal of Gastroenterology
Copyright © 2004 by The WJG Press ISSN 1007-9327

• BRIEF REPORTS •

Ischemic preconditioning protects liver from hepatectomy under hepatic inflow occlusion for hepatocellular carcinoma patients with cirrhosis

Shao-Qiang Li, Li-Jian Liang, Jie-Fu Huang, Zhi Li

Shao-Qiang Li, Li-Lian Liang, Jie-Fu Huang, Department of Hepatobiliary Surgery, the First Affiliated Hospital, Sun Yat-sen University, Guangzhou 510080, Guangdong Province, China
Zhi Li, Department of Pahtology, Sun Yat-sen University, Guangzhou 510080, Guangdong Province, China
Correspondence to: Professor Li-Jian Liang, MD, PhD. Department of Hepatobiliary Surgery, the First Affiliated Hospital, Sun Yat-sen University, Guangzhou 510080, Guangdong Province, China. lianglijian@163.net
Telephone: +86-20-87755766 Ext. 8096
Fax: +86-20-87755766 Ext. 8663
Received: 2003-11-27 **Accepted:** 2003-12-22

Abstract

AIM: To investigate the protective effect of ischemic preconditioning (IPC) on hepatocellular carcinoma (HCC) patients with cirrhosis undergoing hepatic resection under hepatic inflow occlusion (HIO) and its possible mechanism.

METHODS: Twenty-nine consecutive patients with resectable 0HCC were randomized into two groups: IPC group: before HIO, IPC with 5 min of ischemia and 5 min of reperfusion was given; control group: no IPC was given. Liver functions, hepatic Caspase-3 activity, and apoptotic cells were compared between these two groups.

RESULTS: On postoperative days (POD) 1, 3 and 7, the aspartate transaminase (AST) and alanine transaminase (ALT) levels in the IPC group were significantly lower than those in the control group (P<0.05). On POD 3 and 7, the total bilirubin level in the IPC group was significantly lower than that in the control group (P<0.05). On POD 1, the albumin level in the IPC group was higher than that in the control group (P = 0.053). After 1 h of reperfusion, both hepatic Caspase-3 activity and apoptotic sinusoidal endothelial cells in the IPC group were significantly lower than those in the control group (P<0.05).

CONCLUSION: IPC has a potential protective effect on HCC patients with cirrhosis. Its protective mechanism underlying the suppression of sinusoidal endothelial cell apoptosis is achieved by inhibiting Caspase-3 activity.

Li SQ, Liang LJ, Huang JF, Li Z. Ischemic preconditioning protects liver from hepatectomy under hepatic inflow occlusion for hepatocellular carcinoma patients with cirrhosis. *World J Gastroenterol* 2004; 10(17): 2580-2584
http://www.wjgnet.com/1007-9327/10/2580.asp

INTRODUCTION

Hepatic inflow occlusion (HIO), also called Pringle's maneuver[1], is an effective and simple technique to control blood loss from the raw surface during hepatic parechymal transaction, and has been widely used during hepatectomy. However, HIO could also result in hepatic ischemic- reperfusion (I/R) injury, especially in case of cirrhosis. It is generally accepted that cirrhotic liver is particular sensitive to ischemia. Although warm ischemia for cirrhotic liver should not exceed 30 min[2], prolonged HIO might cause dysfunction of the remnant liver, which was a major risk factor associated with postoperative morbidity and mortality[3]. Therefore, therapeutic modalities to ameliorate this injury are critically important in liver surgery.

Ischemic preconditioning (IPC), defined as giving a short period of ischemia and reperfusion and subsequently sustaining a prolonged ischemic insult, was first described by Murry *et al*.[4] in 1986, and then this protective phenomenon was found in various visceral organs including the liver[5-9].

However, up to now, the data of IPC available were most focused on animal models. Recently, Clavien *et al*.[10]. reported the first clinical trial, suggesting a beneficial effect of IPC during major hepatectomy on patients who were subjected to 30 min of ischemia. But there was no cirrhotic case in Clavien's series. In China and other Asia areas, more than 80% of hepatocellular carcinoma (HCC) patients had underlying cirrhosis or hepatitis due to hepatitis B virus infection[11]. Whether IPC has the similar protective effect on I/R injury encountered in hepatectomy for cirrhotic liver is unclear. Hence, we conducted this prospective randomized clinical trial on cirrhotic HCC patients to test whether IPC could protect cirrhotic liver against I/R injury during tumor resection under HIO, and to explore its possible protective mechanism.

MATERIALS AND METHODS

Patients

Fifty-six consecutive patients with HCC were treated at the Department of Hepatobiliary Surgery, the First Affiliated Hospital of Sun Yat-Sen University between January 1, 2001 and April 30, 2001. Among them, 29 patients whose tumors were considered to be resectable after preoperative investigations, including liver function tests, liver function reserve (oral glucose tolerance test, OGTT)[12], abdominal ultrasound, CT assessment and laporotomy, were recruited in this study. The resectable criteria we used were as followings. (1) The general condition of the patients was good and they could tolerate hepatectomy. (2) The tumor did not extend beyond half of the liver and had no distant metastasis. (3) Liver function belonged to Child A or B and liver function reserve was type P_1 or P_2 according to OGTT, which is a test widely used to evaluate liver function reserve[12]. Briefly, patients were fasted overnight, and the fast blood glucose (FBS) was measured next morning, then 75 *g* of glucose diluted in pure water was given to the patients orally. One and 2 h after glucose solution was drunk, blood glucose concentration (BGC) was measured respectively. If BGC after 2 h was still higher than that after 1 h, it was the linear type (L type). If BGC after 2 h was between the FBS and that after 1 h, it was the parabolic type 2 (P_2 type). If BGC after 2 h was lower than 7.3 μmol/L, it was parabolic type 1 (P_1 type). P_1 type indicated the best liver function reserve, and patients could tolerate right

or left hepatectomy. P_2 type was moderate, and patients could tolerate segmentectomy or irregular hepatectomy. L type indicated the poor liver function reserve, and patients could only tolerate local tumor resection. The other 27 unresectable cases were excluded.

Then 29 resectable cases were randomized into IPC group (n = 14) and control group groups (n = 15) by permuted block without stratification. Our previous study indicated that IPC with 5 min of ischemia and 5 min of reperfusion produced the best protection on cirrhotic rat liver I/R model[13]. Therefore, IPC with these time intervals was applied in these patients. Prior to liver parenchymal transection under HIO, IPC with 5 min of ischemia and 5 min of reperfusion was conducted in the IPC group. No IPC was given prior to liver parenchymal transection performed under HIO in the control group.

This protocol was performed under the consent of patients approved by the Ethical Committee of Sun Yat-sen University.

Procedures and biopsy

General anesthesia was performed. Bilateral subcoastal incision was made. A further abdominal exploration was conducted to exclude intra-abdominal metastasis. After mobilization of the liver prior to parenchymal transection, HIO was achieved by clamping the portal pedicles using a tourniquet. Blood inflow was initiated when hemostasis was achieved after removal of the tumor. The procedures available in these patients included irregular hepatectomy, segmentectomy and right/left hepatectomy according to the tumor's location and liver function tests. Liver parenchyma was transected by diathermy and crushing hepatic tissue with an artery forceps. Tubular structures on the raw surface were divided and ligated. All hepatectomies were finished within one time of HIO in our series, and the time of HIO not including the ischemic phase of IPC in the IPC group were recorded. Intraoperative blood loss was accurately calculated from the suction bottles and surgical pads. No cell saver was used in our series. Before HIO and 1 h after reperfusion, a small piece of liver tissue was harvested by wedge resection in remnant liver. The procedures were performed by the same surgical team.

Liver function test

Peripheral blood was sampled before operation and on postoperative days (POD) 1, 3, 7. Aspartate transaminase (AST), alanine transaminase (ALT), total bilirubin (TBIL), albumin (ALB) were measured using an auto biochemical analyzer (HITACHI 7 170A, Japan).

Hepatic Caspase-3 activity assay

Caspase-3 activity was quantified by proteolytic cleavage of the fluorogenic substrate 7-amino-4-trifluoro-methylcoumarin-conjugated Asp-Glu-Val-Asp tetrapeptide (AMC-DEVD)[14]. Briefly, fresh liver tissue (20 mg) was homogenized in a lysis buffer at 4 °C. After 4 times of freezing and thawing, lysates were centrifuged at 15 000 *g* for 10 min, supernatants were collected. Then Caspase-3 activity was measured using a fluorescence spectrophotometer (HITACHI F-3 010, Japan) and a Caspase-3 fluorescenic kit (Sigma Co. USA) according to the manufacturer's instructions. Capase-3 activity was expressed as nmol AMC release per hour per mg liver tissue.

TUNEL assay

Apoptosis was detected by terminal deoxynucleotieyl mediated nick end labeling (TUNEL) assay[15]. Paraffin-embedded liver tissue was cut into 5-μm thick sections. After deparaffinized in series of alcohol solutions, a TUNEL kit (Boehinger Mannheim Co. Germany) was used according to the manufacturer's protocols. Five high power fields (×400) were selected randomly in each specimen, for which apoptotic cells were calculated by a pathologist.

Statistical analysis

Data are expressed as mean±SD. Means were compared between these two groups by t test (continuous data) or chi-square test (categorical data). P value less than 0.05 was considered statistically significant.

RESULTS

Clinical characteristics of these two groups

The clinical characteristics (Table 1) including age, gender, Child's classification, tumor size, operation procedure, operation time, liver ischemic time and blood loss were compared between these two groups, and there was no statistical significance, indicating that the characteristics of the two groups were homogeneous and comparable.

Table 1 clinical characteristics of these two groups

Data	IPC group	control group	P value
Age (yr)	50.4±10.7	49.5±10.3	0.605
Gende1r			0.684
Male	12	12	
Female	2	3	
Child's classification			0.684
Grade A	12	12	
Grade B	2	3	
Grade C	0	0	
OGTT			0.867
P_1 type	3	4	
P_2 type	8	9	
L type	4	3	
Cirrhosis[1]			0.316
(+)	13	12	
(-)	1	3	
Tumor size (cm)	7.1±3.6	7.9±2.9	0.544
Procedures			0.971
Right/left hepatectomy	2	2	
Segmentectomy	4	4	
Irregular hepatectmoy	8	9	
Operation times (min)	191.3±74.9	208.2±45.3	0.485
Ischemic times (min)	18.0±3.6	17.4±2.3	0.602
(Range)	(15-25)	13-22)	
Blood loss (mL)	469.2±292.6	602.0±310.6	0.257

[1]Cirrhosis: (+) referrs to macroscopic cirrhosis, which was diagnosed during surgery, (-) referrs to that we could not diagnose cirrhosis during surgery by naked eyes, however, it was diagnosed mild cirrhosis and hepatitis by microscopic pathology. The etiology of cirrhosis was hepatitis B virus infection in our series.

IPC protected cirrhotic liver from I/R injury

Serum AST and ALT levels were sensitive parameters to assess the severity of liver injury. As shown in Table 2, on postoperative d 1, 3, 7, the AST and ALT levels in the IPC group were significantly lower than those in the control group (P<0.05). On postoperative d 3, 7, the TBIL levels in the IPC group were also lower than those in the control group (P<0.05). On postoperative d 1, the ALB level in the IPC group was higher than that in the control group, but it did not reach statistical significance. These data suggest that IPC could effectively protect cirrhotic liver from I/R injury. I/R injury could inhibit albumin synthesis, however IPC could ameliorate this albumin-synthesis inhibition.

Table 2 Comparison of liver functions between two groups before and after operation

Date	AST (U/L)		ALT (U/L)		TBIL (μmol/L)		ALB (g/L)	
	Control	IPC	Control	IPC	Control	IPC	Control	IPC
Preop	64.7±39.2	60.1±55.4	56.7±53.9	54.8±45.0	22.6±13.1	18.9±7.4	41.2±5.6	40.6±3.7
POD1	1856.4±310.9	433.8±143.8[b]	802.9±280.1	430.9±179.4[b]	33.1±23.9	26.7±10.3	32.9±4.6	36.2±3.9
POD 3	409.6±197.4	156.7±52.5[b]	417.3±162.6	200.9±88.6[b]	49.1±35.4	25.9±9.2[a]		
POD 7	85.3±45.5	56.5±18.9[a]	130.1±49.0	89.9±42.8[a]	39.7±29.3	22.8±8.0[a]		

Note: preop = preoperation. [a]$P<0.05$, *vs* control (independent *t* test): [b]$P<0.01$, *vs* control (independent *t* test).

Postoperative mortality, morbidity and hospitalized days

There was no operative and hospital mortality in both groups. The common postoperative morbidity was pleural effusion and liver failure. Pleural effusion was confirmed by chest *X*-ray. Postoperative liver failure was defined as the total bilirubin was higher than 2 times of its normal level, and massive ascites occurred. Pleural effusion occurred in 2 cases (14.3%) of the IPC group, and in 5 cases (33.3%) of the control group ($P = 0.390$), who needed repeated pleural tapping. No in the IPC group was complicated with liver failure after surgery. However, liver failure occurred in 3 cases of the control group after operation. These 3 patients recovered after conservative treatment. Other postoperative complications including subphrenic collection were found in 2 cases of the control group, who were treated by fine needle aspiration guided by ultrasound. Bile leakage from the transection surface was found in 1 case of the IPC group, who was cured by local drainage. No wound infection occurred in both groups. The mean hospitalized time of the IPC group was 12.8 d, which was significantly shorter than that of the control group (12.8±3.1 d *vs* 18.6±9.1 d, $P = 0.034$).

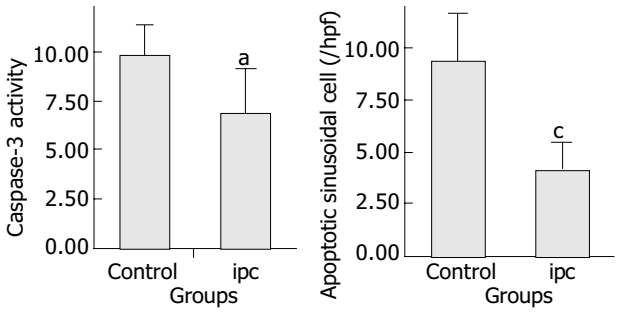

Figure 1 Comparison of Caspase-3 activity and SEC apoptosis between control group and IPC group [a]$P = 0.047$, *vs* control, [c]$P = 0.002$, *vs* control, (*t* test) (casapse-3 activity unit: nmol AMC· h^{-1}· mg^{-1} (tissue)) hpf: high power field.

Effect of IPC on Caspase-3 activity and apoptosis

To investigate the effect of IPC on Caspase-3 activity and apoptosis, 5 cases in each group were selected prospectively, whose hepatic Caspase-3 activity and apoptotic cells were detected respectively. One hour after reperfusion, the hepatic Caspase-3 activity in the IPC group was significantly lower than that in the control group ($P<0.05$), and subsequently, the apoptotic sinusoidal endothelial cells (SECs) in the IPC group were also less than those in the control group ($P<0.05$) (Figures 1, 2). Only few hepatocytes underwent apoptosis in the control group in this checking time point (Figure 2). These data indicated that IPC inhibited Caspase-3 activity and subsequently SEC apoptosis in the remnant liver.

DISCUSSION

Hemmorrhage is the major lethal factor during hepatic resection. Hemostasis can be achieved by HIO or total vascular occlusion. The latter nevertheless was the safe choice for patients whose tumor involved major hepatic veins and inferior vena cava[16]. But clinically, the vast majority of liver resections do not need this method for its detrimental effect of systemic circulation disturbance. HIO or Pringle's maneuver, which has the least hemodynamic effect, has been widely used in liver surgery[17]. However, HIO could also result in liver I/R injury, which is one of the major factors leading to postoperative liver dysfunction. Cirrhotic liver is very vulnerable to ischemic injury. Though warm ischemia for cirrhotic liver should not exceed 30 min, and the majority of liver resections could be finished within this limit interval by using diathermy and crushing hepatic tissue with an artery forceps, the deleterious effect of ischemia could not be neglected. In order to minimize liver I/R injury, intermittent hepatic inflow occlusion (iHIO) has been used in HCC resection[18.19]. However, massive bleeding might result from iHIO during reperfusion interval, which might increase blood transfusion and the possibility of postoperative morbidity and tumor recurrence[20].

Our results demonstrated that HIO could cause massive

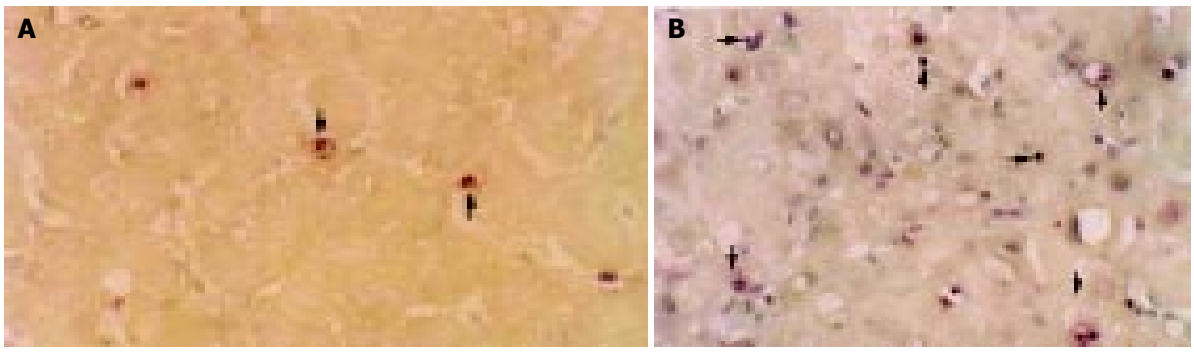

Figure 2 Typical features of apoptosis after 1 h of reperfusion (TUNEL assay, ×200). Bold arrows show the SEC apoptosis and the black arrows indicate scanty of hepatocyte apoptosis. A: IPC group, B: control group.

liver injury and inhibit albumin synthesis in cirrhotic patients. However, IPC could significantly protect cirrhotic liver from I/R injury during hepatic resection under hepatic inflow occlusion in cirrhotic HCC patients. These were represented by a dramatically decrease in postoperative AST, ALT and TBIL levels; a relatively higher serum albumin level; an uneventful postoperative course and a relatively short hospital stay in the IPC group.

IPC is a simple procedure, which can produce dramatic protective effect on I/R injury. However, its clinical application is rare.

The protective mechanism of IPC has not been fully understood. Intrinsic nitric oxide (NO) synthesis, adenosine release[18] and decreasing leukocyte/endothelial cell interactions[21] have been reported to be the protective mechanisms underlying I/R injury.

Apoptosis, or programmed cell death, which is a distinct form of cell death from necrosis, has been documented to be a pivotal mechanism responsible for I/R injury encountered in liver surgery and liver graft preservation[22-25]. However, this cell pathology was challenged by other authors, who documented that cell necrosis was the major cell death in rat liver I/R model subjected to 60 or 120 min of ischemia[26]. Jaeschke *et al*.[27]. believed that both apoptosis and necrosis occurred in liver I/R. Actually, in our previous cirrhotic rat liver I/R model, we used H&E staining, TUNEL assay and electron microscope to investigate the cellular pathology, and found that there was no obvious necrosis but massive hepatocyte apoptosis mediated by Fas apoptotic pathway subjected to 30 min of liver ischemia and 6 h of reperfusion[28]. This discrepancy might be due to the different time of ischemia and reperfusion used in each experiment.

In this clinical trial, we found that the major cell type undergoing apoptosis in the control group was SECs subjected to 1 h of reperfusion, only a few apoptotic hepatocytes were found at this checking time point. However, in our previous animal model[28], after 6 h of reperfusion, massive apoptotic hepatocytes were seen, indicating that the cell type undegoing apoptosis might be time dependent. In the rat liver cell apoptosis model induced by intraperitoneal injection of Fas antibody[29] and liver graft cold I/R model[25], 1 h after antibody administration or reperfusion, SEC apoptosis was predominant. However, 2 to 6 h after antibody administration or rerperfusion, hepatocytes were the major cell type underging apoptosis. Though we did not check apoptosis after 6 h of reperfusion in this clinical trail, we believed that during this period of time, hepatocytes might undergo apoptosis predominantly, thus subsequently resulting in liver injury and clinical manifestations.

As to the cellular mechanism of IPC related to apoptosis, Yadav *et al*.[30]. reported that the protective mechanism of IPC underlying hepatocyte and SEC apoptosis was achieved by inhibiting Caspase-3. It has been found that caspase-3 is a cysteine specific protease, an "executor" leading to DNA fragmentation in apoptotic signal cascades[31]. We demonstrated that IPC could protect cirrhotic liver from I/R injury by inhibiting hepatocyte and SEC apoptosis through down-regulation of Fas expression and suppression of Caspase-3 activity in cirrhotic rat liver I/R model[13]. In this study, we demonstrated again that the protective mechanism of IPC against liver I/R injury in cirrhotic patients was achieved by inhibiting Caspase-3 activity and subsequently apoptosis.

Why IPC down-regulates Caspase-3 activity is still under investigation. IPC could result in inhibition of intrinsic NO synthesis. *In vitro* and *in vivo* studies indicated that NO could inhibit Capase-3 by S-nitrosation in Cys-163 residue of Caspase-3[32].

In conclusion, IPC can protect potentially cirrhotic liver against I/R injury when hepatic resection is performed under hepatic inflow occlusion in HCC patients with cirrhosis. Its protective mechanism underlying SEC apoptosis is achieved by inhibiting caspase-3 activity. IPC is a simple procedure with a potential protective effect, and it is recommended for clinical application.

REFERENCES

1 **Pringle JH**. Notes on the arrest of hepatic hemorrhage due to trauma. *Ann Surg* 1908; **48**: 541-549
2 **Nagasue N,** Uchida M, Kubota H, Hayashi T, Kohno H, Nakamura T. Cirrhotic livers can tolerate 30 minutes ischaemia at normal environmental temperature. *Eur J Surg* 1995; **161**: 181-186
3 **Belghiti J,** Noun R, Zante E, Ballet T, Sauvanet A. Portal triad clamping or hepatic vascular exclusion for major liver resection. A controlled study. *Ann Surg* 1996; **224**: 155-161
4 **Murry CE,** Jennings RB, Reimer KA. Preconditioning with ischemia: a delay of lethal cell injury in ischemic myocardium. *Circulation* 1986; **74**: 1124-1136
5 **Karck M,** Tanaka S, Bolling SF, Simon A, Su TP, Oeltgen PR, Haverich A. Myocardial protection by ischemic preconditioning and delta-opioid receptor activation in the isolated working rat heart. *J Thorac Cardiovasc Surg* 2001; **122**: 986-992
6 **Sola A,** De Oca J, Gonzalez R, Prats N, Rosello-Catafau J, Gelpi E, Jaurrieta E, Hotter G. Protective effect of ischemic preconditioning on cold preservation and reperfusion injury associated with rat intestinal transplantation. *Ann Surg* 2001; **234**: 98-106
7 **Ogawa T,** Mimura Y, Hiki N, Kanauchi H, Kaminishi M. Ischaemic preconditioning ameliorates functional disturbance and impaired renal perfusion in rat ischaemia-reperfused kidneys. *Clin Exp Pharmacol Physiol* 2000; **27**: 997-1001
8 **Peralta C,** Prats N, Xaus C, Gelpi E, Rosello-Catafau J. Protective effect of liver ischemic preconditioning on liver and lung injury induced by hepatic ischemia-reperfusion in the rat. *Hepatology* 1999; **30**: 1481-1489
9 **Yoshizumi T,** Yanaga K, Soejima Y, Maeda T, Uchiyama H, Sugimachi K. Amelioration of liver injury by ischaemic preconditioning. *Br J Surg* 1998; **85**: 1636-1640
10 **Clavien PA,** Yadav S, Sindram D, Bentley RC. Protective effects of ischemic preconditioning for liver resection performed under inflow occlusion in humans. *Ann Surg* 2000; **232**: 155-162
11 **Tang ZY,** Yu YQ, Zhou XD, Ma ZC, Yang R, Lu JZ, Lin ZY, Yang BH. Surgery of small hepatocellular carcinoma. Analysis of 144 cases. *Cancer* 1989; **64**: 536-541
12 **Lü MD,** Huang JF, Liang LJ, Peng BG. Oral glucose tolerance test and glucagons loading test as useful parameters for evaluating liver functional reserve. *Zhonghua Waike Zazhi* 1993; **31**: 532-534
13 **Li SQ,** Liang LJ, Huang JF. Effects of ischemic preconditioning on hepatocyte apoptosis induced by hepatic ischemia-reperfusion in cirrhotic rats. *Zhongguo Bingli Shengli Zazhi* 2002; **18**: 55-58
14 **Enari M,** Talanian RV, Wong WW, Nagata S. Sequential activation of ICE-like and CPP32-like proteases during Fas-mediated apoptosis. *Nature* 1996; **380**: 723-726
15 **Gavrieli Y,** Sherman Y, Ben-Sasson SA. Identification of programmed cell death in situ via specific labeling of nuclear DNA fragmentation. *J Cell Biol* 1992; **119**: 493-501
16 **Huguet C,** Gavelli A, Chieco PA, Bona S, Harb J, Joseph JM, Jobard J, Gramaglia M, Lasserre M. Liver ischemia for hepatic resection: where is the limit? *Surgery* 1992; **111**: 251-259
17 **Man K,** Fan ST, Ng IO, Lo CM, Liu CL, Wong J. Prospective evaluation of Pringle maneuver in hepatectomy for liver tumors by a randomized study. *Ann Surg* 1997; **226**: 704-713
18 **Selzner N,** Rudiger H, Graf R, Clavien PA. Protective strategies against ischemic injury of the liver. *Gastroenterology* 2003; **125**: 917-936
19 **Belghiti J,** Noun R, Malafosse R, Jagot P, Sauvanet A, Pierangeli F, Marty J, Farges O. Continuous versus intermittent portal triad clamping for liver resection: a controlled study. *Ann Surg* 1999; **229**: 369-375
20 **Asahara T**, Katayama K, Itamoto T, Yano M, Hino H, Okamoto Y, Nakahara H, Dohi K, Moriwaki K, Yuge O. Perioperative blood transfusion as a prognostic indicator in patients with

hepatocellular carcinoma. *World J Surg* 1999; **23**: 676-680

21 **Cheng XD**, Jiang XC, Liu YB, Peng CH, Xu B, Peng SY. Effect of ischemic preconditioning on P-selectin expression in hepatocytes of rats with cirrhotic ischemia-reperfusion injury. *World J Gastroenterol* 2003; **9**: 2289-2292

22 **Kohli V,** Selzner M, Madden JF, Bentley RC, Clavien PA. Endothelial cell and hepatocyte deaths occur by apoptosis after ischemia-reperfusion injury in the rat liver. *Transplantation* 1999; **67**: 1099-1105

23 **Gao W,** Bentley RC, Madden JF, Clavien PA. Apoptosis of sinusoidal endothelial cells is a critical mechanism of preservation injury in rat liver transplantation. *Hepatology* 1998; **27**: 1652-1660

24 **Sasaki H,** Matsuno T, Tanaka N, Orita K. Activation of apoptosis during the reperfusion phase after rat liver ischemia. *Transplant Proc* 1996; **28**: 1908-1909

25 **Natori S,** Selzner M, Valentino KL, Fritz LC, Srinivasan A, Clavien PA, Gores GJ. Apoptosis of sinusoidal endothelial cells occurs during liver preservation injury by a caspase-dependent mechanism. *Transplantation* 1999; **68**: 89-96

26 **Gujral JS**, Bucci TJ, Farhood A, Jaeschke H. Mechanism of cell death during warm hepatic ischemia-reperfusion in rats: apoptosis or necrosis? *Hepatology* 2001; **33**: 397-405

27 **Jaeschke H**, Lemasters JJ. Apoptosis versus oncotic necrosis in hepatic ischemia / reperfusion injury. *Gastroenterology* 2003; **125**: 1246-1257

28 **Li SQ**, Liang LJ, Huang JF, Li Z. Hepatocyte apoptosis induced by hepatic ischemia-reperfusion injury in cirrhotic rats. *Hepatobiliary Pancreat Dis Int* 2003; **2**: 102-105

29 **Wanner GA,** Mica L, Wanner-Schmid E, Kolb SA, Hentze H, Trentz O, Ertel W. Inhibition of caspase activity prevents CD95-mediated hepatic microvascular perfusion failure and restores Kupffer cell clearance capacity. *FASEB J* 1999; **13**: 1239-1248

30 **Yadav SS**, Sindram D, Perry DK, Clavien PA. Ischemic preconditioning protects the mouse liver by inhibition of apoptosis through a caspase-dependent pathway. *Hepatology* 1999; **30**: 1223-1231

31 **Schulz JB**, Weller M, Moskowitz MA. Caspases as treatment targets in stroke and neurodegenerative diseases. *Ann Neurol* 1999; **45**: 421-429

32 **Rossig L,** Fichtlscherer B, Breitschopf K, Haendeler J, Zeiher AM, Mulsch A, Dimmeler S. Nitric oxide inhibits caspase-3 by S-nitrosation *in vivo*. *J Biol Chem* 1999; **274**: 6823-6826

Edited by Wang XL and Xu FM

PO Box 2345, Beijing 100023, China
Fax: +86-10-85381893
E-mail: wjg@wjgnet.com www.wjgnet.com

World J Gastroenterol 2004;10(17):2585-2587
World Journal of Gastroenterology
Copyright © 2004 by The WJG Press ISSN 1007-9327

• BRIEF REPORTS •

Clinical analysis of primary small intestinal disease: A report of 309 cases

Jun Zhan, Zhong-Sheng Xia, Ying-Qiang Zhong, Shi-Neng Zhang, Lin-Yun Wang, Hong Shu, Zhao-Hua Zhu

Jun Zhan, Zhong-Sheng Xia, Ying-Qiang Zhong, Shi-Neng Zhang, Lin-Yun Wang, Hong Shu, Zhao-Hua Zhu, Gastrointestinal Division of Internal Medicine, Second Hospital, Sun Yat-Sen University, Guangzhou 510120, Guangdong Province, China
Correspondence to: Dr. Jun Zhan, Gastrointestinal Division of Internal Medicine, Second Hospital, Sun Yat-Sen University, Guangzhou 510120, Guangdong Province, China
Telephone: +86-20-81332598
Received: 2004-01-10 **Accepted:** 2004-03-06

Abstract

AIM: To evaluate the major clinical symptom, etiology, and diagnostic method in patients with primary small intestinal disease in order to improve the diagnosis.

METHODS: A total of 309 cases with primary small intestinal disease were reviewed, and the major clinical symptoms, etiology, and diagnostic methods were analyzed.

RESULTS: The major clinical symptoms included abdominal pain (71%), abdominal mass (14%), vomiting (10%), melaena (10%), and fever (9%). The most common disease were malignant tumor (40%). diverticulum (32%) and benign tumor (10%). Duodenal disease was involved in 36% of the patients with primary small intestinal diseases. The diagnostic rate for primary small intestinal diseases by double-contrast enteroclysis was 85.6%.

CONCLUSION: Abdominal pain is the most common clinical symptom in patients with primary small intestinal disease. Malignant tumors are the most common diseases. Duodenum was the most common part involved in small intestine. Double-contrast enteroclysis was still the simplest and the most available examination method in diagnosis of primary small intestinal disease. However, more practical diagnostic method should be explored to improve the diagnostic accuracy.

Zhan J, Xia ZS, Zhong YQ, Zhang SN, Wang LY, Shu H, Zhu ZH. Clinical analysis of primary small intestinal disease: A report of 309 cases. *World J Gastroenterol* 2004; 10(17): 2585-2587
http://www.wjgnet.com/1007-9327/10/2585.asp

INTRODUCTION

Clinically, primary small intestinal disease is relatively rare. Accounting for only 1-4% of digestive diseases[1]. In spite of the development of techniques in endoscopy and the innovation of equipments, such as capsule endoscopy[2,3] and double-balloon push enteroscopy[4,5], diagnosis of primary small intestinal disease is still difficult. For example, uncontrollability in the movement of endoscopic capsule, the influence of fluid inside gastrointestinal tract, poor discrimination in images and unavailability of biopsy decrease the practicability of capsule endoscopy in clinical practice[6]. Theoretically, there is no blind region in total small intestine for double-balloon push enteroscopy, as the new instrument has been put into practice recently. However, it is almost impossible for double-balloon push enteroscopy to search all small intestines through either mouth or anus. Furthermore, double-balloon push enteroscopy has other limitations, such as long time of examination and patients' prolonged endurance[7]. Therefore, the diagnosis of primary small intestinal disease is still difficult. In this study, by clinical analysis of 309 cases of patients with primary small intestinal disease, we aimed to investigate clinical symptoms, etiology, and diagnostic methods in primary small intestinal disease in order to increase the knowledge in primary small intestinal disease and improve the diagnosis.

MATERIALS AND METHODS

Criteria for selected patients

All selected patients had clinical symptoms or signs of the digestive system. The diagnosis of small intestinal disease was confirmed by means of laparotomy, pathology and other examinations. Primary small intestinal disease included duodenal disease, jejunal disease and ileal disease. However, duodenal bulb ulcer was not included. Secondary small intestinal diseases were also excluded.

Method of analysis

A total of 309 cases with primary small intestinal disease were reviewed, and the major clinical symptoms, etiology, and diagnostic methods were analyzed.

RESULTS

From January 1976 to July 2003, 309 cases with primary small intestinal disease were collected. Among them, there were 167 males, 142 females, with age ranging from 2 to 87 years old, and an average age of 51.2 years.

Among the 309 cases, 216 cases were confirmed by surgical operations, 53 by double-contrast enteroclysis, 24 by gastric endoscopy or enteroscopy and biopsy and 16 by a combination of clinical and other examinations. Among the 216 cases with surgical operations, diagnosis could not be definitely made in 142 cases until laparotomy was performed. Lesions were found in 89 of 104 cases examined by double-contrast enteroclysis, giving a positive rate of 85.6%. The major clinical symptoms were abdominal pain, abdominal mass, vomiting, melaena, fever, hematochezia and diarrhea. Some cases had two or more symptoms (Table 1). The most common diseases were malignant tumor (40%), diverticulum (32%) and benign tumor (10%). Duodenal disease was involved in 36% of the patients with primary small intestinal diseases. The distribution of the major diseases of 309 cases is listed in Table 2.

Table 1 Major clinical symptoms of 309 cases with primary small intestinal disease

Symptom	*n* (%)	Symptom	*n* (%)
Abdominal pain	218 (71)	Hematochezia	19 (6)
Abdominal mass	44 (14)	Diarrhea	14 (5)
Vomiting	32 (10)	Jaundice	13 (4)
Melaena	30 (10)	Haematemesis	3 (1)
Fever	27 (9)	Others	8 (3)

Table 2 Distribution of major diseases in 309 cases with primary small intestinal disease

Disease	*n* (%)
Small intestinal diverticulum	100 (32)
Small intestinal adenocarcinoma	35 (11)
Small intestinal leiomyosarcoma	34 (11)
Small intestinal lymphoma	29 (9)
Crohn's disease	15 (5)
Small intestinal leiomyomas	13 (4)
Hemorrhagic necrotizing enteritis	13 (4)
Ampullar carcinoma	11 (4)
Small intestinal malignant mesenchymoma	11 (4)
Small intestinal polyp	10 (3)
Small intestinal twist	8 (3)
Small intestine multiple perforation	4 (1)
Terminal ileal ulcer	3 (1)
Small intestinal cavernous hemangioma	2 (1)
Small intestinal malabsorption syndrome	2 (1)
Small intestinal internal hernia	2 (1)
Small intestinal fistula	2(1)
Others[1]	15(5)

[1]Including jejunal malignant melanoma, jejunal malignant angioendothelioma, ileal liposarcoma, small intestinal malignant reticulosis, small intestinal fibrosarcoma, jejunal lipoma, jejunal fibroma, jejunal neurofibroma, ileal neurilemmoma, small intestinal benign mesenchymaloma, small intestinal teratoma, small intestinal inflammatory pseudotumor, terminal ilealitis, eosinophilic enteritis and idiopathic small intestinal obstruction which had 1 case respectively.

DISCUSSION

Distribution of major diseases in patients with primary small intestinal disease

In this study, 216 (70%) of 309 cases were diagnosed as having primary small intestinal disease by a combination of surgical operations and pathology. In addition, 24 of 309 cases were diagnosed by a combination of gastric endoscopy or enteroscopy and biopsy. Therefore, a total of 240 (78%) cases were diagnosed by pathology. Based on the analysis of the characteristics of the diseases, we found that malignant tumor was the most common disease in primary small intestinal disease. Overall, 125 patients had malignant tumors, 35 (11%) with adenocarcinoma, 34 (11%) with leiomyosarcoma, 29 (9%) with small intestinal lymphoma, and 11 (4) with ampullar carcinoma. These patients accounted for 40% of the cases with primary small intestinal disease. There were only 32 (10%) cases with small intestinal benign tumor, mainly including 13 (4%) cases of small intestinal leiomyomas, and 10 (3%) with small intestinal polyps. The ratio of small intestinal benign over malignant tumors was almost 1:4 (32: 125), which indicates that most of small intestinal neoplasms are malignant, and thus small intestinal malignant tumors contribute significantly to small intestinal disease. This finding is consistent with previous domestic reports by Liu *et al*.[8] and Shi *et al*.[9], but different from the oversea reports that small intestinal benign tumor is more common than small intestinal malignant tumor[10]. Our observations suggest that malignant tumors should be considered if small intestinal disease is under consideration, and further examinations should be taken as soon as possible to assure or exclude small intestinal malignant tumor. In this way, patients with small intestinal malignant tumor would receive optimum management through the early diagnosis and early treatment strategy, and thus prognosis would be significantly improved.

Among the 309 cases, 100 had small intestinal diverticulum, which contributed to 32% of cases and was the second common diagnosis in small intestinal disease. Among patients with small intestinal diverticulum, 72 (72%) had duodenal diverticulum, and 28 (28%) had jejunal or/and ileal diverticulum, which indicates that duodenal diverticulum is much more common than jejunal or/and ileal diverticulum. The data suggest that more attention should be paid to duodenal diverticulum, especially diverticulum of descending part of duodenum because diverticulum in this site is not only common but also detectable easily by gastric endoscopy or barium meal examination.

In addition, 84 cases had other small intestinal benign disease, which contributed to 27% of patients with small intestinal diseases, mainly including 32 (10%) with small intestinal benign tumor, 15 (5%) with Crohn's disease, 13 (4%) with hemorrhagic necrotizing enteritis and 8 (3%) with small intestinal twist. These data indicate that small intestinal benign tumor is the most common disease among small intestinal non-diverticular benign disease. It is also noticed that 111 cases with duodenal diseases contributed to 36% of the 309 patients with primary small intestinal disease. There were 72 cases with diverticulum accounting for 65% of patients with duodenal disease, 37 with malignant tumor accounting for 33% of patients with duodenal disease, and 2 with duodenal polyps. Since the human small intestine is 5 to 6 meters long, and duodenum is only 0.25 meter long, which is not longer than 1/20 of full length of small intestine. However, more than one third of small intestinal diseases were duodenal diseases. Therefore, duodenum is the most common part involved in small intestinal disease, and special attentions should be paid to duodenal disease, especially between descending part and ascending part of duodenum when small intestinal disease is under consideration, because duodenum is not only commonly involved but also shallow enough to be easily detected by gastric endoscopy or a barium meal examination without need for other complex examinations.

Major clinical symptoms in patients with primary small intestinal disease

Clinical symptoms of primary small intestinal disease in this study included abdominal pain, abdominal mass, vomiting, melaena, fever, hematochezia, diarrhea, jaundice, haematemesis, marasmus, abdominal distension, and constipation. Among these symptoms, abdominal pain was the most common clinical symptom as 218 cases had abdominal pain, which contributed to 71% of cases with primary small intestinal disease. The site of abdominal pain was mainly located around the navel. The second common symptom was abdominal mass. Altogether 44 cases had abdominal mass, which contributed to 14% of cases with primary small intestinal disease. The other common symptoms were vomiting, melaena and fever. Fever was caused mostly by small intestinal lymphoma and hemorrhagic necrotizing enteritis. However, hematochezia, diarrhea, jaundice, haematemesis were less common. Hematochezia was often characterized by dark-red stool and negative findings by enteroscopy. Haematemesis was a rare symptom, but if it occurred, then the volume of bleeding would be enormous. Therefore, the symptoms of patients with primary small intestinal disease are lacking of specificity as these symptoms may occur in patients with upper digestive disease and colon disease. So small intestinal disease could not be diagnosed only by symptoms, which is also one of the reasons for the difficulty in the diagnosis of primary small intestinal disease. However, when patients had above mentioned symptoms, especially melaena, hematochezia, haematemesis and enteremphraxis, but no positive findings were found by gastric endoscopy and enteroscopy at the same time, further examinations should be

given to patients to verify or exclude small intestinal disease. These examinations include double-contrast enteroclysis, selective arteriography, small intestinal endoscopy, capsule endoscopy, and double-balloon push enteroscopy.

Examinations methods for the diagnosis of primary small intestinal disease

In spite of so many examination methods, how to select appropriate examinations is a question to be often asked in clinical work. We found that some patients were finally definitely diagnosed as having primary small intestinal disease through almost all the examinations, which not only put heavy economical burden on patients, but also increased suffering of patients, and especially delayed the diagnosis of disease. However, if an examination was correctly selected, the diagnosis could be easily achieved. Capsule endoscopy is nontraumatic method for the examination of small intestinal disease, however, uncontrollability in movement of capsule endoscopy, poor discrimination in images and unavailability of biopsy, expensive price, and time-consuming decrease the practicability of this method in clinical practice. The traditional enteroscopy can only observe the digestive tract 1 meter above jejunum to Treitz ligament due to itself limitation, which means that most of small intestinal could not be diagnosed by the traditional enteroscopy. Radiography includes selective arteriography and double-contrast enteroclysis. Selective arteriography is a useful examination for patients with main clinical symptoms of melaena, hematochezia or haematemesis. The diagnosis rate of selective arteriography is increased especially when a patient is bleeding[11]. Otherwise, double-contrast enteroclysis is a very valuable examination for patients with main clinical symptoms of abdominal pain, abdominal mass, vomiting, or diarrhea. In this study, among the 309 cases with primary small intestinal disease, 104 cases were examined by double-contrast enteroclysis, and 89 cases were found lesion in small intestine, with a positive rate of 85.6%, which was similar to report by Wang *et al* [12]. This positive rate is significantly higher than that (70%) reported by Zhan *et al*, based on the hospitalized patients in our hospital before 1997[13]. The improvement of diagnosis accuracy may be related to the better choice made by doctors for examinations, the improved experience of examiners and more attention paid to small intestinal disease over the past 6 years. Unfortunately, only one third of cases with primary small intestinal disease were examined by double-contrast enteroclysis in this study. The reasons for this included unawareness of double-contrast enteroclysis by physicians, emergency that did not allow patient for double-contrast enteroclysis but for laparotomy and situations that patients had a complete or incomplete intestinal obstruction. In fact, patients with incomplete intestinal obstruction can be examined by double-contrast enteroclysis with meglucamine diatrizoate instead of barium by placing a tube into duodenum during gastric endoscopy, which could not only increase the diagnosis rate, but also be more available and safer for patients[14]. Because some endoscopic capsules can not move out of body in some patients until laparotomy was performed, it is suggested that double-contrast enteroclysis should be performed before capsule endoscopy. By this way, doctors not only obtain primary knowledge if there is a matter with patient, but also obtain the information of the intestinal movement, which would help determine whether capsule endoscopy is suitable for the patient and thus avoid the situation which endoscopic capsule can not naturally move out of the body[15]. Double-balloon push enteroscopy has been applied recently to provide a powerful tool for diagnosis of small intestinal disease. Therefore, we would draw a conclusion from what mentioned above that as a traditional nontraumatic or microtraumatic examination, double-contrast enteroclysis has advantages in simplicity and availability, little torment, high diagnosis accuracy and low price. Therefore, at present, double-contrast enteroclysis still plays an important role in diagnosis of small intestinal disease. We are hoping that double-balloon push enteroscopy and other newer and more practical examinations could aid in diagnosis of small intestinal disease with the development of technology in endoscopy and general use of endoscopic equipment.

REFERENCES

1 **Li YN**. Striving for improvement in diagnosis of small intestinal disease. *Zhonghua Xiaohua Zazhi* 1992; **12**: 249
2 **Yu M**. M2A capsule endoscopy. A breakthrough diagnostic tool for small intestine imaging. *Gastroenterol Nurs* 2002; **25**: 24-27
3 **Ell C**, Remke S, May A, Helou L, Henrich R, Mayer G. The first prospective controlled trial comparing wireless capsule endoscopy with push enteroscopy in chronic gastrointestinal bleeding. *Endoscopy* 2002; **34**: 685-689
4 **Yamamoto H**, Sekine Y, Sato Y, Higashizawa T, Miyata T, Iino S, Ido K, Sugano K. Total enteroscopy with a nonsurgical steerable double-balloon method. *Gastrointest Endosc* 2001; **53**: 216-220
5 **Yamamoto H**, Sugano K. A new method of enteroscopy- the double-balloon method. *Can J Gastroenterol* 2003; **17**: 273-274
6 **Lewis BS**, Swain P. Capsule endoscopy in the evaluation of patients with suspected small intestinal bleeding: Results of a pilot study. *Gastrointest Endosc* 2002; **56**: 349-353
7 **Zhong J**, Zhang CL, Zhang J, Wu YL, Jiang SH. Application of double-balloon push enteroscopy in diagnosis of small bowel diseases. *Zhonghua Xiaohua Zazhi* 2003; **23**: 591-594
8 **Liu DD**, Wang JY, Sheng XZ. Clinical analysis of small intestinal tumor in 93 cases. *Fudan Xuebao Yixue Kexueban* 2001; **28**: 145-147
9 **Shi HQ**, Huang JY, Cheng J, Shao Z, Xu JW. Clinical analysis of 142 cases of primary small intestinal tumor. *Zhejiang Linchuan Yixue* 2002; **4**: 642-643
10 **Lewis BS**, Kornbluth A, Waye JD. Small bowel tumors: yield of enteroscopy. *Gut* 1991; **32**: 763-765
11 **Ding JZ**, Li QY, Kuang J, Jin XT, Li HW. The significance of auxiliary examinations in diagnosis of haemorrahgic small intestinal disease. *Shijie Huaren Xiaohua Zazhi* 2002; **10**: 603-604
12 **Wang AY**, Lin SR, Liu X. Clinical diagnostic value of double-contrast enteroclysis. *Zhonghua Xiaohua Zazhi* 1992; **12**: 27
13 **Zhan J**, Gan XL, Wu XL, Li JG, Zeng ZY. Clinical analysis of 224 cases of small intestinal disease. *Zhonghua Neike Zazhi* 2000; **39**: 592-593
14 **Chen MX**. Clinical diagnostic value of double-contrast enteroclysis by placing tube under endoscopy. *Zhonghua Xiaohua Zazhi* 2002; **22**: 444
15 **Costamagna G**, Shah SK, Riccioni ME, Foschia F, Mutignani M, Perri V, Vecchioli A, Brizi MG, Picciocchi A, Marano P. A prospective trial comparing small bowel radiographs and video capsule endoscopy for suspected small bowel disease. *Gastroenterology* 2002; **123**: 999-1005

Edited by Xia HHX **Proofread by** Chen WW and Xu FM

PO Box 2345, Beijing 100023, China
Fax: +86-10-85381893
E-mail: wjg@wjgnet.com www.wjgnet.com

World J Gastroenterol 2004;10(17):2588-2591
World Journal of Gastroenterology
Copyright © 2004 by The WJG Press ISSN 1007-9327

• BRIEF REPORTS •

Chylous ascites: Treated with total parenteral nutrition and somatostatin

Qi Huang, Zhi-Wei Jiang, Jun Jiang, Ning Li, Jie-Shou Li

Qi Huang, Zhi-Wei Jiang, Jun Jiang, Ning Li, Jie-Shou Li, Department of General Surgery, Jinling Hospital, School of Medicine, Nanjing University, Nanjing 210002, Jiangsu Province, China
Correspondence to: Dr. Zhi-Wei Jiang, Institute of General Surgery, Jinling Hospital, 305 Zhongshan East Road, Nanjing 210002, Jiangsu Province, China. doctorhq007@sina.com
Telephone: +86-25-4806187
Received: 2003-10-31 **Accepted:** 2003-12-16

Abstract

AIM: To determine the effects of total parenteral nutrition and somatostatin on patients with chylous ascites.

METHODS: Five patients were diagnosed with chylous ascites on the basis of laboratory findings of ascites sample from Nov 1999 to May 2003. Total parenteral nutrition and somatostatin or its analogue was administered to 4 patients, while the other one only received total parenteral nutrition. All the patients had persistent peritoneal drainage, with the quantity and quality of drainage fluid observed daily. Necessary supportive treatments were given to the patients individually during the therapy.

RESULTS: Two of 4 patients who received somatostatin therapy obtained complete recovery within 10 d without any recurrence while on a normal diet. In these 2 patients, the peritoneal drainage reduced to zero in one and the other's decreased from 2 000 mL to 80 mL with a clear appearance and negative qualitative analysis of chyle. Recurrent chylous ascites, though relieved effectively by the same method every time, developed in one patient with advanced pancreatic cancer. The other patient's lymphatic fistula was blocked with the fibrin glue after conservative treatment. The patient who only received total parenteral nutrition was cured 24 d after therapy.

CONCLUSION: Total parenteral nutrition along with somatostatin can relieve the symptoms and close the fistula in patients with chylous ascites rapidly. It appears to be an effective therapy available for the treatment of chylous ascites caused by various disorders.

Huang Q, Jiang ZW, Jiang J, Li N, Li JS. Chylous ascites: Treated with total parenteral nutrition and somatostatin. *World J Gastroenterol* 2004; 10(17): 2588-2591
http://www.wjgnet.com/1007-9327/10/2588.asp

INTRODUCTION

Chylous ascites, an uncommon disease usually caused by obstruction or rupture of the peritoneal or retroperitoneal lymphatic glands, is defined as the accumulation of chyle in the peritoneal cavity[1]. It is a difficult disorder due to the serious mechanical, nutritional and immunological consequences of the constant loss of protein and lymphocytes[2]. Morton's dramatic and detailed account in 1694 of a 2-year-old boy with tuberculosis who died of chylous ascites was the first clear report of chyloperitoneum.

Many pathological conditions can result in this disease, including congenital defects of the lymphatic system, nonspecific bacterial, parasitic and tuberculous peritoneal infection, liver cirrhosis, malignant neoplasm, blunt abdominal trauma and surgical injury[1]. Over all, the most common cause in adults is believed to be abdominal malignancy, while congenital lymphatic abnormalities in pediatric population. Press *et al*. reported an incidence of 1 per 20 464 admissions at the Massachusetts General Hospital during a 20-year period[3]. They found, however, a 1 per 11 589 incidence in the last years of their study. Most investigators believe that the incidence of chylous ascites is increasing because of more aggressive thoracic and retroperitoneal surgery and with the prolonged survival of patients with cancer[4-8]. Some new techniques, such as laparoscopic surgery and transplantation, also lead to postoperative chylous ascites[9-11]. Kaas *et al*. found that 12 (7.4%) of 163 patients with complex surgical procedures developed chylous ascites[12].

Though the incidence of chylous ascites has increased in recent years, the treatment remains unsatisfactory in some cases because of prolonged duration of disease. Conservative treatment of chylous ascites, recommended in most patients, involves paracentesis, a medium chain triglyceride (MCT) based diet, total parenteral nutrition (TPN), recently used somatostatin and so on. Surgery is only recommended when conservative treatment fails[2]. In a review of 156 patients with chylous ascites resolved after intervention, 51 patients were successfully treated surgically; 105 patients were treated conservatively[13]. Usually the MCT based diet is the first choice, TPN is recommended after dietary manipulation has failed, and somatostatin therapy is attempted only if chylous ascites has been refractory to all conservative measures. It will take several weeks to 2 mo to close the lymphatic fistula adequately with routine conservative regimens[13].

Here we report on our successful use of persistent peritoneal drainage, TPN as well as somatostatin in treatment of 5 cases of chylous ascites.

MATERIALS AND METHODS

Five adult patients with chylous ascites were admitted to our hospital from November 1999 to May 2003. On admission, computerized tomography (CT) examination was performed to reveal the etiology, and the diagnosis was confirmed by analyzing the cloudy ascites fluid obtained through paracentesis or peritoneal drainage. Table 1 shows the clinical features, CT findings and laboratory findings of ascites samples from 5 patients.

As soon as the diagnosis was confirmed, every patient was put in fasting state and received fluid replenishment until disturbance of water, electrolytes and acid-base was corrected. A single lumen central venous catheter was inserted into the peritoneal cavity for continuous drainage in 3 patients, while peritoneal cavity drainage tubes inserted during the operation were reserved in patient 4 and 5. The quality and quantity of drainage fluid were monitored daily. Then TPN (non-protein calorie 25 kcal/(kg·d), nitrogen 0.2-0.25 g/(kg·d), glucose: fat ratio 6:4) via central vein was administered to patients at gradually increasing dose. Somatostatin (Stilamin, Laboratoires Serono S. A.) was administered to patient 2 and 4 through continuous intravenous infusion at a dose of 3 mg per 12 h.

Patient 3 and 5 received subcutaneous administration of the somatostatin analogue, octreotide (Sandostatin, Novartis Pharma AG), at a dose from 100 μg to 200 μg 3 times daily. Necessary supportive treatments, such as albumin, diuretics and antibiotics, were given to the patients individually during the therapy. In addition, patient 5 received abdominal cavity and peripheral venous chemotherapy at the same time.

RESULTS

Figure 1 shows the change of drainage volume, the duration of TPN and somatostatin therapy of 5 patients. Once the peritoneal drainage was zero (in patient 1 and 4) or was proved non-chylous ascites (in patient 2 and 3), TPN and somatostatin dose would diminish gradually along with the recovery of oral low fat diet. Patient 3 and 4, who received somatostatin therapy, obtained complete recovery within 10 d, while patient 1 who only received TPN was cured 24 d after therapy. The drainage of patient 3 decreased from 2 000 mL to 80 mL within 10 d with a clear appearance and negative qualitative analysis of chyle, and the volume remained unchanged when she received normal diet. Then patient 3 was referred to department of gastroenterology for further treatment of the established liver cirrhosis, which caused the remaining ascites. All these 3 patients' drainage

Table 1 Clinical features, CT and laboratory findings for 5 patients with chylous ascites

Patient	Age in yr/Sex	Medical/ Surgical condition	CT findings	Laboratory findings of ascites			
				Qualitative analysis of chyle	Leukocyte count (/mm^3)/ Lymphocyte (%)	Total protein/ Albumin (g/L)	Cholesterol/ Triglyceride (mmol/L)
1	48/M	Two wk after radical distal subtotal gastrectomy for gastric cancer	Large volume of ascites	+	1 600/95	49.4/30.9	1.92/7.14
2	50/M	Five mo after pancreaticoduodenectomy for pancreatic cancer	Large volume of ascites, multiple metastases involving liver and lymph nodes	+	120/95	15.0/10.1	1.59/2.41
3	65/F	Half a year after cure of the tuberculous peritoneal infection	Large volume of ascites, liver cirrhosis	+	560/50	23.2/14.2	2.11/5.68
4	50/F	One wk after finding of 400 mL milky fluid in pelvic cavity during laparoscopy cholecystectomy	Small volume of ascites in pelvic cavity	+	190/88	52.8/32.0	0.67/3.01
5	44/F	10 d after radical pelvic lymphadenectomy for ovarian cancer	Small volume of fluid in pelvic cavity	+	890/92	47.7/31.9	1.47/7.11

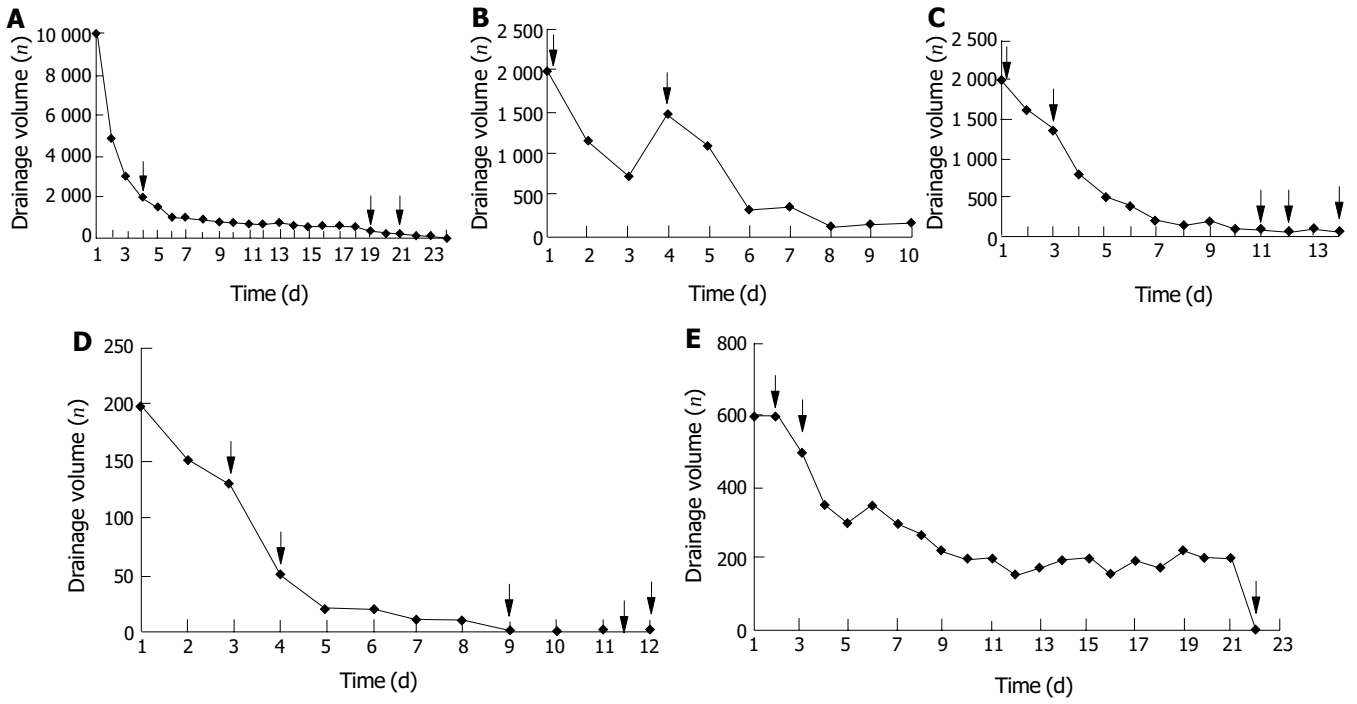

Figure 1 **C**hange of drainage volume and the duration of TPN and somatostatin therapy in 5 patients.↓The beginning and the end of TPN, ↓the beginning and the end of somatostatin therapy, ↓ the beginning of food intake, ↓blockage of the fistula. A: Patient 1 who only received TPN recovered fully after 24 d of therapy; B: Patient 2 suffered from repeated recurrence though the drainage volume decreased from 2 000 mL to 100 mL within 11 d; C: Chylous ascites never recurred in patient 3 after the drainage volume decreased to 80 mL within 10 d with negative qualitative analysis of chyle; D: Patient 4 recovered fully within 9 d; E: Chylous fistula of patient 5 showed refractory to therapy and was sealed with fibrin glue.

catheters were removed after they had normal diet for 3 d. The drainage volume of patient 5, though dropped from 600 mL to 200 mL within 10 d, remained unchanged for 11 d with positive qualitative analysis of chyle. Then we successfully used fibrin glue to block up the lymphatic fistula that was proved mature with X-ray fistulography. CT follow-up examinations did not reveal the presence of ascitic fluid. The nutritional status of them was well maintained during therapy. Follow-up study found no recurrence in these 4 patients while on normal diet after 6 mo. Though the drainage decreased from 2 000 mL to 100 mL within 11 d and was proved non-chylous ascites, repeated recurrences developed in patient 2 who died of advanced pancreatic cancer 3 mo later.

DISCUSSION

Our results showed that TPN along with somatostatin appears to be an effective therapy available for the treatment of chylous ascites caused by various disorders.

There are multiple causes of chylous ascites. The most common ones in Western countries are abdominal malignancy and cirrhosis, which account for over two thirds of all cases. In contrast, infectious etiologies, such as tuberculosis and filariasis, account for the majority of cases of chylous ascites in Eastern and developing countries[14]. Previous studies showed the effect of some regimen in the treatment of chylous ascites caused by one kind of pathological condition. In the present series, various etiological factors including surgical injury (patient 1 and 5), pancreatic cancer (patient 2), liver cirrhosis (patient 3) and idiopathic cause (patient 4) demonstrate the wide indications of our treatment. It also indicates the change of etiology spectrum in China, operation and cancer have become the common causes now.

Treatment of the underlying cause of chylous ascites is of pivotal importance in managing patients with chylous ascites, especially those having an infectious, inflammatory, or hemodynamic cause. But conservative treatment is usually vital for most patients to relieve the symptoms and restore nutritional deficits. Paracentesis is not only a diagnostic but also therapeutic method in the management of chylous ascites. Despite several definite drawbacks and complications, repeated paracentesis is commonly included in the nonoperative treatment regimens to relieve abdominal distention[13]. In three patients of this series, repeated paracentesis was replaced by persistent peritoneal drainage with a single lumen central venous catheter, which permitted us to monitor the quality and quantity of drainage daily. In patient 4 and 5, peritoneal drainage tube inserted during the operation was reserved until recovery. No tube blockage, catheter-related sepsis or any other complications developed in all patients. So persistent peritoneal drainage may be a much better and accepted choice than repeated paracentesis.

Fasting, together with TPN, can decrease the lymph flow in thoracic duct dramatically from 220 mL/(kg·h) to 1 mL/(kg·h)[13]. Furthermore, TPN restores nutritional deficits and balances metabolic impairments imposed by long-standing chylous ascites and repeat sessions of paracentesis. So fasting and TPN are essential in nonoperative management of chylous ascites. In the past, however, TPN was usually recommended as the second line treatment when enteral dietary manipulation failed[13]. Routine conservative treatment, using TPN only or combined with an MCT diet, needed 2 to 6 wk to cure 60% to 100% of cases[14,15]. In our study, patient 1 who only received fasting and TPN recovered completely after 24 d.

Initial experience with continuous intravenous high dose somatostatin for the closure of postoperative lymphorrhagia was reported in 1990 by Ulibarri *et al*. The exact mechanisms of somatostatin on drying lymphatic fistulas are not completely understood. It has been previously shown to decrease the intestinal absorption of fats, lower triglyceride concentration in the thoracic duct and attenuate lymph flow in the major lymphatic channels[16]. In addition, it also decreases gastric, pancreatic and intestinal secretions, inhibits motor activity of the intestine, slows the process of intestinal absorption and decreases splanchnic blood flow, which may further contribute to decreased lymph production. It has also been speculated that somatostatin improves chylous ascites by inhibition of lymph fluid excretion through specific receptors found in the normal lymphatic vessels of intestinal wall[17,18]. Shapiro *et al*. reported rapid resolution of chylous ascites after liver transplantation within 2 d after administration of the octreotide combined with total parenteral nutrition[17]. Satisfactory results were also achieved by others[16,19-23]. To our knowledge, however, most of these articles included just one case. Somatostatin therapy also remains an indefinite or second-line method in treatment of chylous ascites. The recommended algorithm for the management of chylous ascites in a review in 2000, only regarded somatostatin in combination with TPN as an unproved alternative method[13]. Another algorithm in 2002 recommended somatostatin therapy only after a period of combined dietary intervention and TPN had failed [14]. Our results showed that 2 of 4 patients treated with somatostatin or its analogue recovered completely within 10 d with well maintained nutritional status and no significant side effect, while the symptoms of patient 2 relieved despite of relapse. As to patient 5, the conservative treatment decreased the fistula drainage greatly and paved the way for the subsequent management. In this case we are inclined to surmise that chemotherapy may affect the closure of lymphatic fistula. These results suggest that somatostatin along with TPN can close the lymphatic leakage or relieve the symptom effectively and rapidly, in comparison with conventional regimens.

The outcome of chylous ascites mostly depends on the underlying pathological condition causing lymphatic leakage. The mortality of chylous ascites, especially those caused by surgery, has decreased much than before[15], but that caused by malignancy remains high. In our study, TPN and somatostatin could not control the chylous ascites completely in patient 2, so necessary adjustment of this regimen or more aggressive therapy should be applied to stop the lymphatic leakage in these patients. Peritoneovenous shunt has been proved to be a valuable method especially for those cancer patients who are refractory to conservative treatment[24-26].

We conclude that TPN with somatostatin should be the first-line therapy for chylous ascites caused by various disorders, and started as soon as possible. Some other methods should also be attempted to close the fistula that is refractory to conservative treatment. Further studies of multicenter clinical trials involving more patients to compare the efficacy and cost between this regimen and the others are suggested.

REFERENCES

1 **Browse NL,** Wilson NM, Russo F, al-Hassan H, Allen DR. Aetiology and treatment of chylous ascites. *Br J Surg* 1992; **79**: 1145-1150
2 **Leibovitch I.** Postoperative chylous ascites-the urologist's view. *Drugs Today* 2002; **38**: 687-697
3 **Press OW**, Press NO, Kaufman SD. Evaluation and management of chylous ascites. *Ann Intern Med* 1982; **96**: 358-364
4 **Halkic N,** Abdelmoumene A, Suardet L, Mosimann F. Postoperative chylous ascites after radical gastrectomy. A case report. *Minerva Chir* 2000; **58**: 389-391
5 **Warner RR,** Croen EC, Zaveri K, Ratner L. A carcinoid tumor associated with chylous ascites and elevated tumor markers. *Int J Colorectal Dis* 2002; **17**: 156-160
6 **Amin R.** Chylous ascites from prostatic adenocarcinoma. *Urology* 2002; **59**: 773
7 **Tokiwa K,** Fumino S, Ono S, Iwai N. Results of retroperitoneal lymphadenectomy in the treatment of abdominal neuroblastoma.

Arch Surg 2003; **138**: 711-715

8 **Sexton WJ,** Wood CG, Kim R, Pisters LL. Repeat retroperitoneal lymph node dissection for metastatic testis cancer. *J Urol* 2003; **169**: 1353-1356

9 **Senyuz OF,** Senturk H, Tasci H, Kaya G, Ozbay G, Sariyar M. Chylous ascites after liver transplantation with mesentero-portal jump graft. *J Hepatobiliary Pancreat Surg* 2001; **8**: 571-572

10 **Shafizadeh SF,** Daily PP, Baliga P, Rogers J, Baillie GM, Rajagopolan PR, Chavin KD. Chylous ascites secondary to laparoscopic donor nephrectomy. *Urology* 2002; **60**: 345

11 **Bacelar TS,** de Albuquerque AC, de Arruda PC, Ferraz AA, Ferraz EM. Postoperative chylous ascites: a rare complication of laparoscopic Nissen fundoplication. *JSLS* 2003; **7**: 269-271

12 **Kaas R**, Rustman LD, Zoetmulder FA. Chylous ascites after oncological abdominal surgery: incidence and treatment. *Eur J Surg Oncol* 2001; **27**: 187-189

13 **Aalami OO**, Allen DB, Organ CH Jr. Chylous ascites: A collective review. *Surgery* 2000; **128**: 761-778

14 **Leibovitch I**, Mor Y, Golomb J, Ramon J. The diagnosis and management of postoperative chylous ascites. *J Urol* 2002; **167**(2pt 1): 449-457

15 **Lee YY,** Soong WJ, Lee YS, Hwang B. Total parenteral nutrition as a primary therapeutic modality for congenital chylous ascites: report of one case. *Acta Paediatr Taiwan* 2002; **43**: 214-216

16 **Collard JM**, Laterre PF, Boemer F, Reynaert M, Ponlot R. Conservative treatment of postsurgical lymphatic leaks with somatostatin-14. *Chest* 2000; **117**: 902-905

17 **Shapiro AM,** Bain VG, Sigalet DL, Kneteman NM. Rapid resolution of chylous ascites after liver transplantation using somatostatin analog and total parenteral nutrition. *Transplantation* 1996; **61**: 1410-1411

18 **Reubi JC,** Horisberger U, Waser B, Gebbers JO, Laissue J. Preferential location of somatostatin receptors in germinal centers of human gut lymphoid tissue. *Gastroenterology* 1992; **103**: 1207-1214

19 **Rimensberger PC,** Muller-Schenker B, Kalangos A, Beghetti M. Treatment of a persistent postoperative chylothorax with somatostatin. *Ann Thorac Surg* 1998; **66**: 253-254

20 **Laterre PF**, Dugernier T, Reynaert MS. Chylous ascites: diagnosis, causes and treatment. *Acta Gastroenterol Belg* 2000; **63**: 260-263

21 **Al-Sebeih K**, Sadeghi N, Al-Dhahri S. Bilateral chylothorax following neck dissection: a new method of treatment. *Ann Otol Rhinol Laryngol* 2001; **110**: 381-384

22 **Leibovitch I,** Mor Y, Golomb J, Ramon J. Chylous ascites after radical nephrectomy and inferior vena cava thrombectomy. Successful conservative management with somatostatin analogue. *Eur Urol* 2002; **41**: 220-222

23 **Leong RW,** House AK, Jeffrey GP. Chylous ascites caused by portal vein thrombosis treated with octreotide. *J Gastroenterol Hepatol* 2003; **18**: 1211-1213

24 **Wagayama H,** Tanaka T, Shimomura M, Ogura K, Shiraki K. Pancreatic cancer with chylous ascites demonstrated by lymphoscintigraphy: successful treatment with peritoneovenous shunting. *Dig Dis Sci* 2002; **47**: 1836-1838

25 **Manolitsas TP,** Abdessalam S, Fowler JM. Chylous ascites following treatment for gynecologic malignancies. *Gynecol Oncol* 2002; **86**: 370-374

26 **Camoglio FS,** Dipaola G, Cervellione RM, Chironi C, Giacomello L, Zanatta C, Ottolenghi A. Treatment of neonatal chylous ascites using a modified Denver peritoneovenous shunt: a case report. *Pediatr Med Chir* 2003; **25**: 145-147

Edited by Zhu LH **Proofread by** Chen WW and Xu FM

PO Box 2345, Beijing 100023, China
Fax: +86-10-85381893
E-mail: wjg@wjgnet.com www.wjgnet.com

World J Gastroenterol 2004;10(17):2592-2594
World Journal of Gastroenterology
Copyright © 2004 by The WJG Press ISSN 1007-9327

• BRIEF REPORTS •

Glutamine supplemented parenteral nutrition prevents intestinal ischemia- reperfusion injury in rats

Guo-Hao Wu, Hao Wang, Yan-Wei Zhang, Zhao-Han Wu, Zhao-Guang Wu

Guo-Hao Wu, Hao Wang, Yan-Wei Zhang, Zhao-Han Wu, Zhao-Guang Wu, Department of General Surgery, Zhongshan Hospital, Fudan University, Shanghai 200032, China
Correspondence to: Guo-Hao Wu, Department of General Surgery, Zhongshan Hospital, Fudan University, Shanghai 200032, China. wugh@zshospital.net
Telephone:+86-21-64041990 Ext. 2365 **Fax:** +86-21-64038472
Received: 2004-02-02 **Accepted:** 2004-02-24

Abstract

AIM: To examine whether glutamine prevents the injury to the intestinal mucosa after intestinal ischemia-reperfusion (I/R) in rats.

METHODS: Thirty male Sprague-Dawley rats were randomly divided into 3 groups: a standard parenteral nutrition (PN) group (n = 10); an I/R-PN group (n = 10); an I/R-glutamine enriched PN (I/R-Gln) group (n = 10). The superior mesenteric artery (SMA) was clamped. After 60 min of ischemia, reperfusion was initiated and infusion was started. All rats received isocaloric and isonitrogenous nutritional support for 48 h. Spleen, liver, mesenteric lymph nodes (MLN), and intestinal segments were removed for morphological and biochemical analyses, and blood samples were collected for bacterial culture and measurement of endotoxin levels. The permeability of intestinnal mucosa was assayed by measurement of D-(-)-lactate levels in plasma.

RESULTS: In I/R-PN group, extensive epithelial atrophy was observed, mucosal thickness, villous height, crypt depth and villous surface area were decreased significantly compared with PN group, whereas these findings did not occur in the I/R-Gln group. The incidence of intestinal bacterial translocation to spleen, liver, MLN, and blood was significantly higher in I/R-PN group than that in other groups. Plasma endotoxin levels significantly increased in the I/R-PN group compared with the I/R-Gln group. Remarkably higher values of D-(-)-lactate were also detected in PN group compared with that in I/R-Gln group.

CONCLUSION: Glutamine protects the morphology and function of intestinal mucosa from injury after I/R in rats.

Wu GH, Wang H, Zhang YW, Wu ZH, Wu ZG. Glutamine supplemented parenteral nutrition prevents intestinal ischemia-reperfusion injury in rats. *World J Gastroenterol* 2004; 10 (17): 2592-2594

http://www.wjgnet.com/1007-9327/10/2592.asp

INTRODUCTION

Ischemia-reperfusion (I/R) of the gut is a common event in a variety of clinical conditions, such as trauma, burn, septic shock, heart or aortic surgery, and liver or small bowel transplantation[1,2]. Intestinal I/R results in many adverse events to the small intestine such as edema and disruption of the structural and functional mucosa. This injury includes mucosal and vascular permeability, change bacterial translocation, and a high death rate[3,4]. It has been proposed that most of the mucosal injury resulted from I/R are mediated by reactive oxygen derived free radicals produced and released when hypoxic tissues are reoxygenated during reperfusion. Clinical and experimental studies suggest that I/R-induced intestinal injury play a role in the pathogenesis of systemic inflammation, respiratory failure, and multiple-organ failure (MOF)[5].

Glutamine (GLN) is the primary metabolic fuel of small intestinal enterocytes, and has been shown to be an essential metabolic component of the proliferative response of enterocytes. Studies have shown that glutamine reduced atrophy of intestinal mucosa in rats on total parenteral nutrition (TPN), prevented intestinal mucosal injury accompanying small bowel transplantation, chemotherapy, and radiation. It was also reported that glutamine supplemented TPN prevented intestinal I/R injury, and improved survival after intestinal I/R in animal models[6,7]. Thus, GLN treatment seems to be a preventive and therapeutic method for gut I/R-induced organ injury. However, despite the positive result from previous studies, glutamine has not been used extensively to treat preexisting intestinal I/R injury. The purpose of this study was to examine whether glutamine prevented damage to the intestinal mucosa after intestinal I/R in rats.

MATERIALS AND METHODS

Experimental protocol/procedures

Thirty male Sprague-Dawley rats weighing 350 to 450 g were employed after a period of acclimatization. After an overnight fast, the rats were anesthetized with sodium pentobarbital 25 mg/kg intraperitoneally. Through a midline laparotomy, the superior mesenteric artery (SMA) was carefully isolated and clamped at its origin from the abdominal aorta. After 60 min of ischemia, the clamp was removed from the SMA and reperfusion was initiated. The abdominal incision was closed and infusion was started immediately. A silastic catheter was inserted through the right jugular vein, tunneled subcutaneously, and brought out through the skin of midscapular region. The rats were randomly divided into 3 groups: a standard parenteral nutrition (PN) group (n = 10); an I/R-PN group (n = 10); an I/R-glutamine enriched PN (I/R-Gln) (n = 10). The SMA of sham rats in PN group was isolated but not clamped. All rats were maintained in individual metabolic cages, and received parenteral nutritional support for 48 h. The composition of the TPN solution is shown in Table 1. Both solutions were isocaloric (174.3 kcal/kg·d) and isonitrogenous (1.0 g/kg·d). After 48 h' nutritional support, a 20-cm long intestinal segment was obtained from a point 10 cm distal to the ligament of Treiz for morphological and biochemical analysis. Spleen, liver, MLN, and blood samples were collected for bacterial culture and measurement of endotoxin levels.

Histologic evaluation and biochemical analysis

Intestinal samples corresponding to the first 5 cm of the resected intestinal segment were fixed in 40 g/L formaldehyde. All samples were embedded in paraffin and stained with hematoxylin and eosin. Three paraffin sections were prepared from each fixed tissue sample, and each slide was analyzed. A blinded

observer performed the histologic analyses using the histologic scoring system. Mucosal wall thickness, villous height, crypt depth and villous surface area were measured under light microscope. All measurements were made in triplicate, and mean values were obtained. The 15 cm of the intestinal segment left was sampled, and the mucosal sample was immediately scraped from the underlying muscular layer with a glass slide. The mucosa was weighed and stored at -70 °C until analysis. DNA and RNA content was measured by the fluorometric method. Protein content was determined by the bicichoninic acid method.

Intestinal permeability

The permeability of intestinal mucosa was assayed by measurement of D-lactate levels in plasma. The procedure used a glycine-hydrazine buffer at pH 9.5 and 25 °C. The assay was based on the enzymatic oxidation of D-lactate with a specific D-lactic dehydrogense coupled to reduction of NAD^+ with the spectrophotometric measurement of NADH at 340 nm. Plasma was separated from the blood sample by centrifugation and stored at -70 °C until analysis. Quantification of D-lactate was performed by fluorescence spectrometry as described by Shimojo *et al*.[8]. The measurements were made with a Beckman DU fluorescence spectrophotometer at 340 nm. D-lactate standard stock solution was 0.47 mg/mL Li lactate (0.44 mg/mL D-lactic acid) and was diluted for standard curves. D-lactic dehydrogenase was from Sigma Biochemicals and was diluted with water to about 600 U/mL. Sigma assay kit 826-UV was used for D-lactate analysis.

Bacterial translocation measurements

Rats were killed, and their mesenteric lymph nodes, spleens and livers were removed. The tissues were transferred to grinding tubes containing sterile BHI to detect aerobic bacteria or sterile 10 A broth to detect lactobacilli. The tissues were homogenized, and BHI tubes were incubated aerobically, whereas the 10 A broth tubes were incubated in 100 mL/L carbon dioxide at 37 °C. After incubation, 0.2 mL of the tissues homogenates was spread on blood agar plates to detect aerobic bacteria, *E. coli* or lactobacilli. The tissues homogenates were Gram- stained to confirm that bacteria present in the homogenates grew on the agar plates.

Statistical analysis

Data were analyzed using standard statistical software (SPSS 10.0). For normally distributed data, a paired Student's *t* test was used for statistical analysis. A probability value less than or equal to 0.05 was considered statistically significant. All data were expressed as mean±SE.

RESULTS

The mortality rate was 0% (0/10), 28.6% (4/14), and 16.7% (2/12) in the PN, I/R-PN, and I/R-Gln groups, respectively. It was significantly higher in I/R-PN group compared with that in the PN group and I/R-Gln group (P<0.05).

In the I/R-PN group, extensive mucosal damage characterized by extensive edema, leukocytic infiltration, epithelial sloughing, mucosal ulceration of villous tips, and mucosal atrophy was observed. This did not occur in the PN group and I/R- Gln group, and no histologic difference was noted between the PN group and I/R- Gln group. Mucosal wall thickness, villous height, crypt depth and villous surface area decreased significantly in the I/R-PN group compared with those in the PN group and I/R-Gln group (P<0.05; Table 2). Mucosal wet weight, protein, DNA content and RNA content decreased significantly in the I/R-PN group compared with those in the PN group and I/R- Gln group (P <0.05; Table 3).

Plasma D-lactate levels significantly increased in the I/R-PN group (0.15±0.04 mmol/L) compared with those in the PN group (0.08±0.02 mmol/L; P<0.05) and I/R- Gln group (0.10±0.02 mmol/L; P<0.05). No significant difference was observed between PN group and I/R- Gln group.

The incidence of intestinal bacterial translocation to MLN, spleen, liver, and blood was significantly higher in I/R-PN group compared with that in PN group and I/R- Gln group. There was no significant difference between PN group and I/R- Gln group (P<0.05; Table 4). The plasma endotoxin levels increased in I/R-PN group (14.5±0.12 pg/mL) compared with PN group (9.2±0.8 pg/mL; P<0.05) and I/R- Gln group (10.5±0.9 pg/mL; P<0.05).

Table 1 Composition of parenteral nutrition solutions (per 100 mL)

	PN	I/R- Gln
Glucose (g)	17.9	17.9
Fat emulsion (g)	5.6	5.6
Amino acid (g)	5.8	2.2
Ala-Glu (g)	0.0	3.6
Nitrogen (g)	0.93	0.93
NPC (kcal)	122.0	122.0
NPC/N	131.2	131.2

Table 2 Morphologic parameters

	PN (n = 10)	I/R-PN (n = 10)	I/R- Gln (n = 10)
Mucosal wall thickness (μm)	566.5±37.4[a]	418.2±39.6	564.4±59.3[a]
Villous height (μm)	404.2±39.1[a]	290.8±48.8	396.4±60.5[a]
Crypt depth (μm)	214.5±29.4[a]	136.6±20.2	204.9±38.6[a]
Villous surface area (mm^2)	0.118±0.010[a]	0.065±0.006	0.112±0.012[a]

[a]P<0.05 *vs* I/R-PN; PN: parenteral nutrition; I/R: ischemia-reperfusion Gln: glutamine.

Table 3 Mucosal wet weight and biochemistry

	PN (n = 10)	I/R-PN (n = 10)	I/R- Gln (n = 10)
Mucosal wet weight (mg/cm)	74.6±16.3[a]	55.2±12.0	82.8±18.2[a]
Protein content (mg/cm)	3.25±0.92[a]	1.73±0.60	3.16±0.47[a]
DNA content (mg/cm)	1.42±0.20[a]	0.64±0.12	1.33±0.17[a]
RNA content (mg/cm)	4.53±0.58[a]	3.26±0.78	4.45±0.84[a]

[a]P<0.05 *vs* I/R-PN; PN: parenteral nutrition; I/R: ischemia-reperfusion Gln: glutamine.

Table 4 Bacterial translocation measurements

	PN (n = 10)	I/R-PN (n = 10)	I/R- Gln (n = 10)
Rate of BT	10% (1/10)	100% (10/10)	20% (2/10)
MLN	1	9	2
Blood	1	7	1
Liver	0	5	0
Spleen	0	4	1

BT: bacterial translocation, MLN: mesenteric lymph mode.

DISCUSSION

Ischemia of the gut is a common event after trauma and a significant predisposing factor of MOF. Intestinal I/R injury results in

many adverse events to the small intestine such as interstitial edema and disruption of the structural and functional mucosa. These increase the permeability of the intestinal mucosa and promote bacterial translocation. Clinical and experimental studies suggest that I/R-induced intestinal injury plays a role in the pathogenesis of systemic inflammation, respiratory failure, and MOF[9,10]. Glutamine is the primary metabolic fuel of small amino acid pool in the body, and has been shown to be an essential metabolic component of the proliferative response of enterocytes. Studies showed that glutamine supplementation of TPN improved survival after gut I/R injury[6,11], reduced atrophy of intestinal mucosa in rats on total parenteral nutrition[12], prevented intestinal mucosal injury accompanying short bowel, small bowel transplantation, chemotherapy, and radiation[13-17]. In the present study, the mortality rate was 28.6% in the I/R-PN group and apparent mucosal damage, such as epithelial sloughing and mucosal ulceration was observed histologically. A 100% survival was achieved in the PN group, 16.7% in I/R-Gln group, and only minor histologic changes of the small intestine were observed in PN and I/R-Gln groups. The I/R-Glin rats had a greater villous height, more mucosal protein, DNA and RNA content, and a lower degree of intestinal permeability compared with the I/R-TPN rats. This suggests that Gln supplemented TPN plays an important role in the maintenance of intestinal structure and barrier function in I/R-injured rats.

The intestinal mucosa, especially in the region of villi, is especially susceptible to hypoxia because of the microvascular architecture and its high energy demand. Intestinal ischemia perpetuates the bacteremic condition by promoting translocation of bacteria into the circulation. Several experimental and clinical studies have shown that intestinal ischemia decreases barrier function of the gut and enhances translocation of bacteria and toxin[18,19]. In our I/R model, the SMA of rats was clamped for 60 min, and the rats were killed 48 h after intestinal I/R. Mesenteric lymph nodes, spleens, livers and blood were then cultured quantitatively. Almost all MLN had positive cultures and grew significantly great numbers of enteric bacteria, spread to the blood, liver and spleen in I/R-PN group. The most common bacterium discovered from solid viscera was *E. coli*, other species included *enterococcus, pseudomonas, proteus, and staphylococcus*. While, only 20% MLN cultures were positive, less than 10% spread to blood and spleen in I/R-Gln group. Additionally, plasma D-lactate and endotoxin levels increased significantly in I/R-PN group compared with that in I/R-Gln group. These findings indicated that the increase of intestinal permeability and the incidence of bacterial translocation in the intestinal I/R rats were prevented by glutamine supplementation.

In conclusion, the present study demonstrates that glutamine supplemented TPN protects rat intestine from morphologic and functional mucosal injury after intestinal I/R. These results suggest that glutamine would be clinically useful in the treatment of intestinal I/R injury.

REFERENCES

1 **Nowicki PT,** Nankervis CA. The role of the circulation in the pathogenesis of necrotizing enterocolitis. *Clin Perinatol* 1994; **21**: 219-234

2 **Grant D,** Wall W, Mimeault R, Zhong R, Ghent C, Garcia B, Stiller C, Duff J. Successful small-bowel/liver transplantation. *Lancet* 1990; **335**: 181-184

3 **Deitch EA**, Morrison J, Berg R, Specian RD. Effect of hemorrhagic shock on bacterial translocation, intestinal morphology, and intestinal permeability in conventional and antibiotic-decontaminated rats. *Crit Care Med* 1990; **18**: 529-536

4 **Deitch EA**, Bridges W, Berg R, Specian RD, Granger DN. Hemorrhagic shock-induced bacterial translocation: the role of neutrophils and hydroxyl radicals. *J Trauma* 1990; **30**: 942-951

5 **Deitch EA.** Multiple organ failure. Pathophysiology and potential future therapy. *Ann Surg* 1992; **216**: 117-134

6 **Ikeda S**, Zarzaur BL, Johnson CD, Fukatsu K, Kudsk KA. Total parenteral nutrition supplementation with glutamine improves survival after gut ischemia/reperfusion. *J Parenter Enteral Nutr* 2002; **26**: 169-173

7 **Tazuke Y**, Wasa M, Shimizu Y, Wang HS, Okada A. Alanyl-glutamine- supplemented parenteral nutrition prevents intestinal ischemia-reperfusion injury in rats. *J Parenter Enteral Nutr* 2003; **27**: 110-115

8 **Shimojo N,** Naka K, Nakajima C, Yoshikawa C, Okuda K, Okada K. Test-strip method for measuring lactate in whole blood. *Clin Chem* 1989; **35**: 1992-1994

9 **Swank GM**, Deitch EA. Role of the gut in multiple organ failure: bacterial translocation and permeability changes. *World J Surg* 1996; **20**: 411-417

10 **Diebel LN,** Dulchavsky SA, Brown WJ. Splanchnic ischemia and bacterial translocation in the abdominal compartment syndrome. *J Trauma* 1997; **43**: 852-855

11 **Fukatsu K,** Ueno C, Hashiguchi Y, Hara E, Kinoshita M, Mochizuki H, Hiraide H. Glutamine infusion during ischemia is detrimental in a murine gut ischemia/reperfusion model. *J Parenter Enteral Nutr* 2003; **27**: 187-192

12 **Buchman AL.** Glutamine: commercially essential or conditionally essential? A critical appraisal of the human data. *Am J Clin Nutr* 2001; **74**: 25-32

13 **Gu Y**, Wu ZH. The anabolic effects of recombinant human growth hormone and glutamine on parenterally fed, short bowel rats. *World J Gastroenterol* 2002; **8**: 752-757

14 **Platell CFE**, Coster J, McCauley RD, Hall JC. The management of patients with the short bowel syndrome. *World J Gastroenterol* 2002; **8**: 13-20

15 **Frankel WL**, Zhang W, Afonso J, Klurfeld DM, Don SH, Laitin E, Deaton D, Furth EE, Pietra GG, Naji A. Glutamine enhancement of structure and function in transplanted small intestine in the rat. *J Parenter Enteral Nutr* 1993; **17**: 47-55

16 **Huang EY,** Leung SW, Wang CJ, Chen HC, Sun LM, Fang FM, Yeh SA, Hsu HC, Hsiung CY. Oral glutamine to alleviate radiation-induced oral mucositis: a pilot randomized trial. *Int J Radiat Oncol Biol Phys* 2000; **46:** 535–539

17 **Decker-Baumann C,** Buhl K, Frohmuller S, von Herbay A, Dueck M, Schlag PM. Reduction of chemotherapy-induced side-effects by parenteral glutamine supplementation in patients with metastatic colorectal cancer. *Eur J Cancer* 1999; **35:** 202-207

18 **Wischmeyer PE**, Lynch J, Liedel J, Wolfson R, Riehm J, Gottlieb L, Kahana M. Glutamine administration reduces Gram-negative bacteremia in severely burned patients: a prospective, randomized, double-blind trial versus isonitrogenous control. *Crit Care Med* 2001; **29**: 2075-2080

19 **Pscheidl E**, Schywalsky M, Tschaikowsky K, Boke-Prols T. Fish oil-supplemented parenteral diets normalize splanchnic blood flow and improve killing of translocated bacteria in a low-dose endotoxin rat model. *Crit Care Med* 2000; **28**: 1489-1496

Edited by Zhang JZ **Proofread by** Zhu LH and Xu FM

PO Box 2345, Beijing 100023, China
Fax: +86-10-85381893
E-mail: wjg@wjgnet.com www.wjgnet.com

World J Gastroenterol 2004;10(17):2595-2597
World Journal of Gastroenterology
Copyright © 2004 by The WJG Press ISSN 1007-9327

• BRIEF REPORTS •

Effects of dendritic cells transfected with full-length wild-type *p53* and stimulated by gastric cancer lysates on immune response

Hua-Wen Sun, Qi-Bing Tang, Yong-Jun Cheng, Sheng-Qian Zou

Hua-Wen Sun, Department of General Surgery, Renmin Hospital, Wuhan University, Wuhan 430060, Hubei Province, China
Qi-Bing Tang, Yong-Jun Cheng, Sheng-Qian Zou, Department of General Surgery, Tongji Hospital, Tongji Medical College, Huazhong University of Science and Technology, Wuhan 430030, Hubei Province, China
Correspondence to: Dr. Hua-Wen Sun, Department of General Surgery, Renmin Hospital, Wuhan University, Wuhan 430060, Hubei Province, China. sxshwyq@sina.com
Telephone: +86-27-88317091
Received: 2003-10-20 **Accepted:** 2003-12-16

Abstract

AIM: To investigate the effects of dendritic cells (DCs) transfected with full-length wild-type p53 and stimulated by gastric cancer lysates on immune response.

METHODS: The wild-type *p53* was transduced to DCs with adenovirus, and the DCs were stimulated by gastric cancer lysates. The surface molecules (B7-1, B7-2, MHC-I, MHC-II) of all DCs were detected by FACS, and the ability of the DCs to induce efficient and specific immunological response in anti-^{51}Cr-labeled target cells was studied. BALB/c mice injected with DCs and Mk28 were established, and CTL response in mice immunized with Lywt-p53DC was evaluated. Tumor-bearing mice were treated with Lywt-p53DC.

RESULTS: The surface molecules of Lywt-p53DC had a high expression of B7-1 (86.70±0.07%), B7-2 (18.77±0.08%), MHC-I (87.20±0.05%) and MHC-II (56.70±0.07%); T lymphocytes had a specific CTL lysis ability induced by Lywt-p53DC; the CTL lysis rate was as high as 81%. The immune protection of Lywtp-53DC was obvious, the tumor diameter in Lywtp-53DC group was 3.10±0.31 mm, 2.73±0.23 mm, 3.70±0.07 mm on d 13, 16 and 19, respectively, which were smaller than control, DC, wtp53DC and LyDC group (P<0.05). Tumor growth rate in Lywtp53DC group was slower than that in other groups (P<0.05).

CONCLUSION: DCs transfected with wild-type p53 and stimulated by gastric cancer lysates have specific CTL killing activity.

Sun HW, Tang QB, Cheng YJ, Zou SQ. Effects of dendritic cells transfected with full-length wild-type *p53* and stimulated by gastric cancer lysates on immune response. *World J Gastroenterol* 2004; 10(17): 2595-2597
http://www.wjgnet.com/1007-9327/10/2595.asp

INTRODUCTION

Dendritic cells (DCs) are the most potent antigen-presenting cells and are actively used in cancer immunotherapy. The wild-type p53 can be recognized as an antigen and can induce specific CTLs in the host body. It is an effective method to immunize body with p53 in p53-overexpressing tumor cells. p53-based immunization is an attractive approach to cancer immunotherapy due to the accumulation of p53 protein in gastric cancer. We detected the effects of DCs transfected with full-length wild-type p53 and modified by gastric cancer lysates on immune response and tried to make DC induce efficient and specific anti-tumor immunological response.

MATERIALS AND METHODS

Animals and cell lines

Eight-week-old female BALB/c mice were purchased from Hubei Animal Center and housed in pathogen-free units of Tongji Hospital experiment center.

Gastric cancer cells (Mk28) were obtained from Hubei cell culture center and cultured in complete culture medium (CCM) containing RPMI 1640 supplemented with 25 mL HEPES, 100 mL/LFCS, and antibiotics (100 U/mL penicillin, 100 μg/mL streptomycin, 0.25 μg/mL amphotericin B). It is a relatively immunogenic tumor that carries a mutant endogenous *p53* gene. P815 mastocytoma cells were obtained from ATC Company and cultured in CCM. The cell cultures were maintained at 37 in 50 mL/L CO_2 humidified atmosphere.

Reagents

Ad-mp53 was constructed by cloning the 1.5-kb murine p53 cDNA (obtained from Sigma, Wuhan, China) into pAd1/CMV that contains CMV promoter and bovine growth hormone polyA signal sequence. This plasmid was co-transfected with pBHG10 into 293 cells. Recombinant adenovirus was selected based on PCR analysis of individual plaques. Control adenovirus (Ad-c) was prepared by deletion of E1 region from adenovirus serotype.

FITC-labeled mouse anti-mouse p53 antibody and isotype mouse IgG2a were purchased from Serotec Company (New York, USA). FITC-labeled anti-mouse CD11c antibody and isotype mouse IgG2a, k, PE-labeled anti-mouse I-Ad, anti-mouse B7-1, B7-2, MHC-I, MHC-II antibody and isotype mouse IgG2a, k, as well as hamster anti-mouse CD40 (HM40-3) monoclonal antibody and anti-hamster IgM were purchased from Sigma Company.

Generation of DCs

DCs were generated from bone marrow of naive syngeneic mice in CCM supplemented with 20 ng/mL murine GM-CSF, 10 ng/mL IL-4, and 50 μmol/L 2-mercaptoethanol. The cells were maintained at 37 in a 50 mL/L CO_2 humidified atmosphere. Half of the medium was replaced on d 3. After 5-6 d in culture, cells were collected and enriched by centrifugation over a 135 g/L metrizamide gradient. The purity of DCs fraction was higher than 80% as determined by FACS analysis of surface molecules expression (B7-1, B7-2, MHC-I, MHC-II).

Infection of cells with adenovirus

DCs were infected with Ad-c or Ad-p53 (10 000 viral particles per cell) for 90 min in 0.5 mL serum-free RPMI 1 640 medium supplemented with 20 ng/mL GM-CSF and 10 ng/mL IL-4 in 24-well plates followed by culturing in CCM with the same cytokines for 48 h. This dose was selected after some preliminary

experiments, and did not affect cell viability (95% viable after trypan blue staining).

Preparation of lysates and DCs loaded with tumor cell lysates

DCs were washed twice in PBS and incubated with 14 μg/mL hamster anti-mouse CD40 monoclonal antibody for 25 min on ice, then washed in RPMI 1 640 twice and cultured in 1 mL CCM supplemented with 3.5 μg/mL anti-hamster IgM, 20 ng/mL GM-CSF and 10 ng/mL IL-4 overnight. Four kinds of DCs such as DC, wtp53DC, LyDC, and Lywtp53 were collected and loaded with tumor cell lysates.

FACS analysis of four kinds of DCs surface molecules expression

DCs were estimated by intracellular staining followed by flow cytometry. Cells were washed in PBS twice, fixed by 2.5 g/L paraformaldehyde solution for 30 min on ice, washed in PBS, permeabilized by 2 g/L Tween 20 for 15 min at 37 , washed in PBS, incubated with FITC-labeled mouse anti-mouse p53 antibody or isotype mouse IgG2a for 25 min on ice, washed twice in PBS and analyzed by FACScalibur low cytometer.

To study the expression of surface molecules, DCs were washed twice in PBS, incubated with 1 μg/10^6 cells FITC-labeled anti-mouse CD11c antibody and PE-labeled anti-mouse I-Ad or anti-mouse B7-1, B7-2, MHC-I, MHC-II antibody for 25 min on ice, washed twice in PBS and analyzed by flow cytometry. Non-specific binding was estimated using FITC-labeled isotype mouse IgG2a, k and PE-labeled isotype mouse IgG2b, k.

Immune protection effect of Lywtp53 and treatment in mice

DCs were generated from bone marrow of BALB/c mice and infected with adenovirus as described above. Forty-eight hours later cells were washed 3 times in PBS and injected to BALB/c mice (2×10^5 /mouse) 3 to 4 times with a 10-14 d interval. Seven days after the last immunization Mk28 tumor cells (3.5×10^5/mouse) were inoculated s.c. and the size of the tumor was observed.

The same tumor model was used to evaluate the effectiveness of treatment. Five hundred thousand Mk28 cells were inoculated s.c. shaved backs of BALB/c mice. The treatment was started when tumors reached 4-6 mm in diameter (d 7). Mice were treated with DCs prepared as described above. The treatment was repeated 4 times with 5- to 6-d intervals. Tumor sizes were measured every 3-5 d for 4 wk.

CTL assay

Splenocytes (effector cells) freshly isolated or restimulated for 7 d with 4 kinds of DCs were mixed with different ^{51}Cr-labeled target cells: Mk28 cells pre-incubated for 48 h with 5 ng/mL murine IFN-γ or p815 cells infected with Ad-p53 or Ad-c. After 6-h incubation and harvesting of supernatants, the radioactivity was measured by gamma-counter. To estimate the maximum ^{51}Cr-release, 10 g/L triton X-100 was used. The percentage of cell lysis was calculated as follows: (experimental release-spontaneous release)/(maximum release-spontaneous release) ×100%.

RESULTS

DCs surface molecules expression

Surface molecules of lywt-p53DC highly expressed were detected by FACS: B7-1 (86.70±0.07%), B7-2 (18.77±0.08%), MCH-I (87.20±0.05%), MCH-II (56.70±0.07%).

Induction of CTL response in mice immunized with DCs

To induce an immune response against wild-type p53, we started with three immunizations of BALB/c mice with DCs generated from bone marrow progenitors of syngeneic mice and transduced with Ad-p53 loaded with lysates as described in MATERIALS AND METHODS. We found statistically significant differences in tumor formation between mice immunized with Lywtp53 DCs and control groups (9 mice per group), and no differences between wtp53DC and LyDC.

The presence of Mk28-specific CTLs was evaluated in mice immunized with activated Ad-p53-transduced DCs. Six-hour standard CTL assay was performed 1 mo and 1 wk after the last immunization (1 mo after inoculation of Mk28 cells into immunized mice). Freshly isolated splenocytes were mixed with ^{51}Cr-labeled Mk28 cells at different ratios. Splenocytes from mice injected with Ad-c-infected DCs demonstrated no ability to lyse target cells, whereas splenocytes from mice immunized with Ad-p53-transduced DCs demonstrated low, but clearly significant cytotoxicity against Mk28 cells (Figure 1).

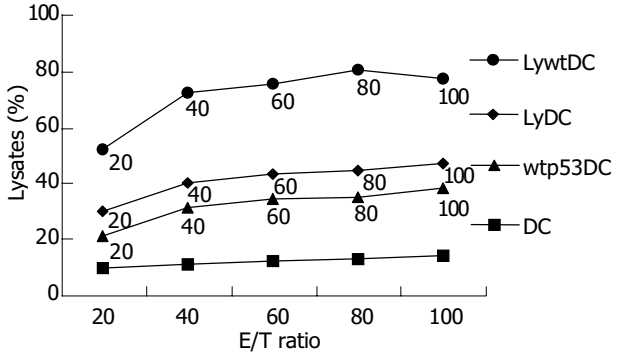

Figure 1 Lysis ability of DCs.

Table 1 Surface molecules expression of 4 kinds of DCs stimulated with lysates (n = 10, mean±SD, %)

Surface molecules	DC	Wtp53DC	LyDC	Lywtp53
B7-1	36.70±0.07	61.77±0.08	67.20±0.05	86.70±0.07[a]
B7-2	5.27±0.01	9.90±0.04	9.13±0.03	18.77±0.08[a]
MHC-I	44.03±0.04	69.13±0.05	68.10±0.03	87.20±0.05[a]
MHC-II	17.13±0.12	31.10±0.31	32.73±0.23	56.70±0.07[a]

[a]P<0.05 *vs* any group of DC, wtp53DC and LyDC.

Table 2 Immune protection of DCs (mean±SD, n = 10)

Group	Tumor diameter after inoculation (mm)			
	d 10	d 13	d 16	d 19
Control	3.72±0.01	6.70±0.02	7.10±0.09	9.90±0.02
DC	3.70±0.01	5.70±0.08	6.10±0.04	9.70±0.08
Wtp53DC	3.07±0.01	6.90±0.04	7.13±0.03	8.22±0.08
LyDC	4.03±0.04	6.13±0.05	7.10±0.03	8.77±0.05
Lywtp53	3.13±0.02	3.10±0.31[a]	2.73±0.23[a]	3.70±0.07[a]

[a]P<0.05 *vs* control, DC, wtp53DC and LyDC group.

Table 3 Immune treatment of DCs (mean±SD, n = 10)

Group	Tumor diameter after inoculation (mm)			
	d 7	d 12	d 15	d 18
Control	5.72±0.02	7.88±0.09	9.20±0.11	11.90±0.09
DC	4.70±0.03	7.71±0.08	9.02±0.04	10.70±0.68
Wtp53DC	5.03±0.09	6.90±0.09	7.13±0.11	8.29±0.05
LyDC	5.06±0.01	6.13±0.08	7.10±0.05	8.77±0.03
Lywtp53	5.19±0.09	5.10±0.39	6.73±0.66[a]	6.79±0.77[a]

[a]P<0.05 *vs* control, DC, wtp53DC and LyDC group.

The immune protection of Lywtp53DC group was obvious, the tumor size of Lywtp53DC group was smaller than control, DC, wtp53DC and LyDC group on d 13, 16 and 19 (Table 2).

Treatment of tumor-bearing mice with Ad-p53-transduced DCs and CTL response are shown in Table 3. On d 15 and 18, the growth rate of tumor in Lywtp53DC group was slower than any of the other group (Table 3).

DISCUSSION

p53 protein is an attractive target for immunotherapy of cancer. Normal cells have very low levels of p53, whereas accumulation of this protein because of mutations or functional inactivation is observed in 50% of human malignancies. This provides, in theory, potential targets for CTLs that recognize class I MHC-bound epitopes[1-3].

In this study we have demonstrated that activated DCs transduced with full-length wild-type p53 loaded with lysates are able to break tolerance to this self-protein and induce potent antitumor response with no detectable autoimmune abnormalities. Wild-type, p53-derived, self-MHC-self-peptide complexes expressed by bone marrow-derived cells in the thymus cause negative selection of immature thymic T cells with a high avidity for such complexes[4,5]. These results in deletion of T cells with sufficient avidity to recognize natural wild-type p53 epitopes presented by MHC class I molecules on tumor cells and thus prevent immune response. Only low avidity CTLs survive during the induction of self-tolerance[6-8].

We suggest here another method of immunotherapy based on the use of full-length wild-type p53. This approach may be devoid of many limitations of peptide-based immunization and would provide a valuable option for clinical trials. Overexpression of wild-type p53 in antigen-presenting cells would allow presentation of several different epitopes. The feasibility of such an approach was shown previously in model experiments in which each of the different minimal epitopes combined to a single fusion protein can be presented separately on the cell surface and be recognized by specific CTLs[9,10].

The study demonstrated that the wild type p53 was transduced to DCs with adenovirus, and the DCs were stimulated by gastric cancer lysates. The T lymphocytes had specific CTL lysis ability induced by Lywt-p53DC loaded with lysates, the CTL lysis rate was as high as 81%. The surface molecules of Lywt-p53DC showed a high expression of B7-1 (86.70±0.07%), B7-2 (18.77±0.08%), MHC-I (87.20±0.05%), MHC-II (56.70±0.07%); There were significant differences in tumor sizes between Lywtp53DC group and any other group. In Lywtp53DC group, the growth rate of tumor was slower than any one of the other group (P<0.05). These studies showed that Lywtp53 DC had immune protection effect on mice, especially loaded with lysates[11-14].

Because of a polyclonal nature of T cells generated after two rounds of stimulations with p53 DCs, it is possible that some level of cytotoxicity against tumor cells could be mediated by alloreactivity. When the DCs were loaded with lysates of tumor, the lysates will be presented to APC, and the process can increase immunogenicity in the body. DCs were recognized; the specificity of CTLs was enhanced[15,16].

In conclusion, these data indicate that DCs transduced with full-length wild-type p53 loaded with lysates are able to generate a CTL response specifically for tumors with p53 overexpression. These findings demonstrate that this approach may overcome tolerance to self-protein and may serve as a valuable option in cancer immunotherapy.

REFERENCES

1 **Nikitina EY**, Clark JI, Van Beynen J, Chada S, Virmani AK, Carbone DP, Gabrilovich DI. Dendritic cells transduced with full-length wild-type p53 generate antitumor cytotoxic T lymphocytes from peripheral blood of cancer patients. *Clin Cancer Res* 2001; **7**: 127-135

2 **Nagayama H**, Sato K, Morishita M, Uchimaru K, Oyaizu N, Inazawa T, Yamasaki T, Enomoto M, Nakaoka T, Nakamura T, Maekawa T, Yamamoto A, Shimada S, Saida T, Kawakami Y, Asano S, Tani K, Takahashi TA, Yamashita N. Results of a phase I clinical study using autologous tumour lysate-pulsed monocyte-derived mature dendritic cell vaccinations for stage IV malignant melanoma patients combined with low dose interleukin-2. *Melanoma Res* 2003; **13**: 521-530

3 **Adams M**, Navabi H, Jasani B, Man S, Fiander A, Evans AS, Donninger C, Mason M. Dendritic cell (DC) based therapy for cervical cancer: use of DC pulsed with tumour lysate and matured with a novel synthetic clinically non-toxic double stranded RNA analogue poly [I]: poly [C (12) U] (Ampligen R). *Vaccine* 2003; **21**: 787-790

4 **Shimizu K**, Thomas EK, Giedlin M, Mule JJ. Enhancement of tumor lysate- and peptide-pulsed dendritic cell-based vaccines by the addition of foreign helper protein. *Cancer Res* 2001; **61**: 2618-2624

5 **Eura M,** Chikamatsu K, Katsura F, Obata A, Sobao Y, Takiguchi M, Song Y, Appella E, Whiteside TL, DeLeo AB. A wild-type sequence p53 peptide presented by HLA-A24 induces cytotoxic T lymphocytes that recognize squamous cell carcinomas of the head and neck. *Clin Cancer Res* 2000; **6**: 979-986

6 **Huang HL**, Wu BY, You WD, Shen MS, Wang WJ. Influence of dendritic cell infiltration on prognosis and biologic characteristics of progressing gastric cancer. *Zhonghua Zhongliu Zazhi* 2003; **25**: 468-471

7 **Ishigami S,** Natsugoe S, Tokuda K, Nakajo A, Xiangming C, Iwashige H, Aridome K, Hokita S, Aikou T. Clinical impact of intratumoral natural killer cell and dendritic cell infiltration in gastric cancer. *Cancer Lett* 2000; **159**: 103-108

8 **Weisbart RH**, Miller CW, Chan G, Wakelin R, Ferreri K, Koeffler HP. Nuclear delivery of p53 C-terminal peptides into cancer cells using scFv fragments of a monoclonal antibody that penetrates living cells. *Cancer Lett* 2003; **195**: 211-219

9 **Asai T**, Storkus WJ, Mueller-Berghaus J, Knapp W, DeLeo AB, Chikamatsu K, Whiteside TL. *In vitro* generated cytolytic T lymphocytes reactive against head and neck cancer recognize multiple epitopes presented by HLA-A2, including peptides derived from the p53 and MDM-2 proteins. *Cancer Immun* 2002; **2**: 3

10 **Portefaix JM**, Rio MD, Granier C, Roquet F, Pau B, Navarro-Teulon I. Peptides derived from the two regulatory domains of p53 are recognized by two p53-activating antibodies. *Peptides* 2003; **24**: 339-345

11 **Takenobu T**, Tomizawa K, Matsushita M, Li ST, Moriwaki A, Lu YF, Matsui H. Development of p53 protein transduction therapy using membrane-permeable peptides and the application to oral cancer cells. *Mol Cancer Ther* 2002; **1**: 1043-1049

12 **Hoffmann TK,** Loftus DJ, Nakano K, Maeurer MJ, Chikamatsu K, Appella E, Whiteside TL, DeLeo AB. The ability of variant peptides to reverse the nonresponsiveness of T lymphocytes to the wild-type sequence p53 (264-272) epitope. *J Immunol* 2002; **168**: 1338-1347

13 **Portefaix JM**, Fanutti C, Granier C, Crapez E, Perham R, Grenier J, Pau B, Del Rio M. Detection of anti-p53 antibodies by ELISA using p53 synthetic or phage-displayed peptides. *J Immunol Methods* 2002; **259**: 65-75

14 **Kanovsky M**, Raffo A, Drew L, Rosal R, Do T, Friedman FK, Rubinstein P, Visser J, Robinson R, Brandt-Rauf PW, Michl J, Fine RL, Pincus MR. Peptides from the amino terminal mdm-2-binding domain of p53, designed from conformational analysis, are selectively cytotoxic to transformed cells. *Proc Natl Acad Sci U S A* 2001; **98**: 12438-12443

15 **Ferries E**, Connan F, Pages F, Gaston J, Hagnere AM, Vieillefond A, Thiounn N, Guillet J, Choppin J. Identification of p53 peptides recognized by CD8 (+) T lymphocytes from patients with bladder cancer. *Hum Immunol* 2001; **62**: 791-798

16 **Petersen TR,** Buus S, Brunak S, Nissen MH, Sherman LA, Claesson MH. Identification and design of p53-derived HLA-A2-binding peptides with increased CTL immunogenicity. *Scand J Immunol* 2001; **53**: 357-364

Edited by Zhu LH and Chen WW **Proofread by** Xu FM

PO Box 2345, Beijing 100023, China
Fax: +86-10-85381893
E-mail: wjg@wjgnet.com www.wjgnet.com

World J Gastroenterol 2004;10(17):2598-2601
World Journal of Gastroenterology
Copyright © 2004 by The WJG Press ISSN 1007-9327

• BRIEF REPORTS •

Combined hepatic resection with fenestration for highly symptomatic polycystic liver disease: A report on seven patients

Guang-Shun Yang, Qi-Gen Li, Jun-Hua Lu, Ning Yang, Hai-Bin Zhang, Xue-Ping Zhou

Guang-Shun Yang, Qi-Gen Li, Jun-Hua Lu, Ning Yang, Hai-Bin Zhang, Xue-Ping Zhou, Eastern Hepatobiliary Hospital, Second Military Medical University, Shanghai 200438, China
Correspondence to: Dr. Guang-Shun Yang, Eastern Hepatobiliary Hospital, Second Military Medical University, Shanghai 200438, China. guangshun@smmu.edu.cn
Telephone: +86-21-25070803
Received: 2003-03-02 **Accepted:** 2003-05-21

Abstract

AIM: To evaluate the immediate and long-term results in a series of patients with highly symptomatic polycystic liver disease (PLD) treated by combined hepatic resection with cystic fenestration.

METHODS: We reviewed our recent experience with a combined hepatic resection-fenestration procedure in seven highly symptomatic patients with PLD. Clinical data, liver manifestation of computed tomography (CT), and morbidity were recorded pre- and post-operation. Follow-up was made by clinical and CT examinations in all patients.

RESULTS: Symptomatic relief and reduction in abdominal girth were obtained in all patients during an average follow-up period of 20.4 mo. CT scans confirmed post-resection hypertrophy of the spared liver and lack of significant cyst progression. All patients had mild to severe ascites. Two patients were complicated with pleural effusion.

CONCLUSION: Some highly symptomatic patients with massive PLD may benefit from combined hepatic resection and fenestration at acceptable risk. To stitch the dissected hepatic ligaments could prevent the instable remnant liver from kinking and collapsing.

Yang GS, Li QG, Lu JH, Yang N, Zhang HB, Zhou XP. Combined hepatic resection with fenestration for highly symptomatic polycystic liver disease: A report on seven patients. *World J Gastroenterol* 2004; 10(17): 2598-2601
http://www.wjgnet.com/1007-9327/10/2598.asp

INTRODUCTION

Polycystic liver disease (PLD) is a rare, benign inherited condition, frequently associated with polycystic disease of the kidney[1]. Unusually as liver failure appears, some patients may be highly symptomamtic due to the compression of liver enlargement or liver complications, therefore requiring treatment.

Highly symptomatic patients with PLD almost exhaust all conservative therapeutic options, and surgery is considered as the best possible procedure[2]. The purpose of this study was to evaluate the immediate surgical results and the short- and long-term outcome in patients treated with hepatic resection combined with cyst fenestration on the basis of our preliminary understanding and experience.

MATERIALS AND METHODS

From October 1995 to September 2002, we examined and operated on 6 women and 1 man with highly symptomatic PLD at our hospital. All operations were performed by a single surgeon (G.S.Yang). In this retrospective study, the medical records were reviewed. The mean interval from diagnosis of PLD to surgical treatment was 4.3 years, ranging from 2 to 11 years. Patient age ranged from 36-54 years, averaging 44.1 years. Specific symptoms included pain, massive abdominal distention, early satiety, regurgitation and supine dyspnea. Six patients were complicated with polycystic kidney disease but had no clinical evidence of abnormal renal function. Four patients had undergone percutaneous cyst aspiration with alcohol sclerotherapy before operation.

Preoperative workup included hematologic, hepatic and renal laboratory tests, and determinations of both respiratory and cardiovascular performance. CT scan was performed to delineate cyst distribution to assess portal vein patency and to serve as a baseline for follow-up comparison in each patient. No patient underwent angiography. The clinical features of these patients are summarized in Table 1.

Preoperative preparations of each patient were an overnight lavage bowel preparation and venous catheterization. The abdomen was explored through a bilateral subcostal incision. The hepatoduodenal ligament was exposed to provide access to a vascular clamping and identification of major vascular and biliary structures. The liver was mobilized by the division of hepatic peritoneal attachments, which was facilitated by sequential fenestration of accessible cysts according to the Lin technique[3]. Liver segments spared of cystic involvement were identified to define limits to resection. Non-anatomic segmental or lobar resection was executed due to cystic distortion of normal anatomy. Significant islands of functional liver parenchyma were preserved as many as possible. After resection of major cystic segments, extensive fenestration of residual cysts was performed by excision of the cyst walls. Finally, cyst cavities exposed to the peritoneum were fulgurated by argon beam coagulation (Bard Electromedical Systems, USA) in an attempt to ablate secretory epithelium and reduce postoperative peritoneal fluid losses. Cholecystectomy in conjunction with hepatectomy was performed in three patients. The hepatic resection bed was drained by two large closed suction drains. After operation, patients were sent to the surgical intensive care unit for close monitoring.

All patients were followed up through telephone calls or at clinic. Special data included hepatic and renal function, symptomatic relief, the patients' working capacity and CT scans.

RESULTS

The surgical outcome of our patients is presented in Table 2. The histologic examination showed von Meyenburg's complexes in all cases. There was no hospital death. All patients had ascites, the majority of them were successfully managed with diuretics and drainage within one week. The average duration of drainage was 11 d, with a range of 5-26 d. Drainage

Table 1 Clinical findings of patients with PLD

Patient no.	Age (yr)	Gender	Family history	Symptoms	Other involved organs	Previous treatment
1	48	Female	No siblings	Abdominal distention, regurgitation	None	None
2	41	Female	Father, two sisters, brother	Abdominal pain and distention	Kidney	PCA+AS (5 times)
3	54	Female	Sister	Early satiety, regurgitation	Kidney	PCA+AS (2 times)
4	45	Male	Sister	Abdominal pain and distention	Kidney	PCA+AS (2 times)
5	43	Female	Sister, brother, grandmother	Abdominal pain and distention, early satiety, dyspnea	Kidney	PCA+AS (2 times)
6	36	Female	Mother, sister	Abdominal pain and distention, early satiety, supine dyspnea	Kidney	None
7	42	Female	Father	Abdominal distention, regurgitation	Kidney	None

PCA+AS, Percutaneous cyst aspiration with alcohol sclerotherapy.

Table 2 Operative data, surgical outcome, and follow-up of patients with PLD

Patient no.	Hepatic resection	Blood loss (mL)	Cystic fluid aspirated (mL)	Days of hospital stay (after operation)	Postoperative complications	Symptomatic relief	Reduction in size of liver
1	III, IVb, V	400	1 500	21 (12)	Acites	Marked	Marked
2	II, III, V	800	3 000	25 (14)	Acites	Marked	Marked
3	Right semi hepatectomy, cholecystectomy	200	1 200	16 (8)	Mild acites	Marked	Marked
4	Right smi hepatectomy, cholecystectomy	300	1 800	24 (16)	Moderate acites	Marked	Marked
5	II, III, IVb	1 500	6 500	83 (29)	Severe acites, left pleural effusion	Moderate	Moderate
6	II, III, VI, VII	3 400	4 000	42 (16)	Severe acites, right pleural effusion	Marked	Marked
7	II, III, VI	300	2 500	27 (11)	Acites	Marked	Marked

Table 3 Review of the literature: mortality, morbidity and outcome of patients with PLD treated by combined hepatic resection an cystic fenestration

Authors	No. of patients	Mortality (no.)	Morbidity (no.)	Follow-up (mos)	No. of symptom-free patients
Armitage *et al*.[12] (1984)	1	0	0	12	1
Iwatsuki *et al*.[13] (1988)	6	0	0	-	-
Newman *et al*.[2] (1990)	9	1	6	17	7
Sanchez *et al*.[8] (1991)	2	0	0	48	2
Vauthey *et al*.[1] (1992)	5	0	4	14	5
Henne-Bruns *et al*.[14] (1993)	8	0	3	15	6
Soravia *et al*.[15] (1995)	10	1	2	68	6
Que *et al*.[16] (1995)	31	1	18	29	28
Vons *et al*.[17] (1998)	12	1	10	34	10
Johnson *et al*.[18] (1999)	1	0	0	18	1
Our series	7	0	7	0	6
Total	92	4 (4.3%)	50 (54.3%)		72 (78.3%)

was continued by needle aspiration in Patients 5 and 6 immediately after a two-week closed suction drainage. The change was an attempt to prevent ascites from infection. Furthermore Patient 5 required thoracentesis due to left pleural effusion.

All patients experienced relief of abdominal symptoms and had normal hepatic and renal laboratory tests. Abdominal girth was reduced markedly in six patients and moderately in one. Repeated abdominal CT scans in these patients failed to show significant development of cysts in the previously spared liver segments during a mean follow-up period of 20.4 mo, with a range from 2 to 86 mo. Indeed, as shown in Figure 1, CT scans confirmed post-resection hypertrophy of the spared liver and lack of clinically significant cyst progression.

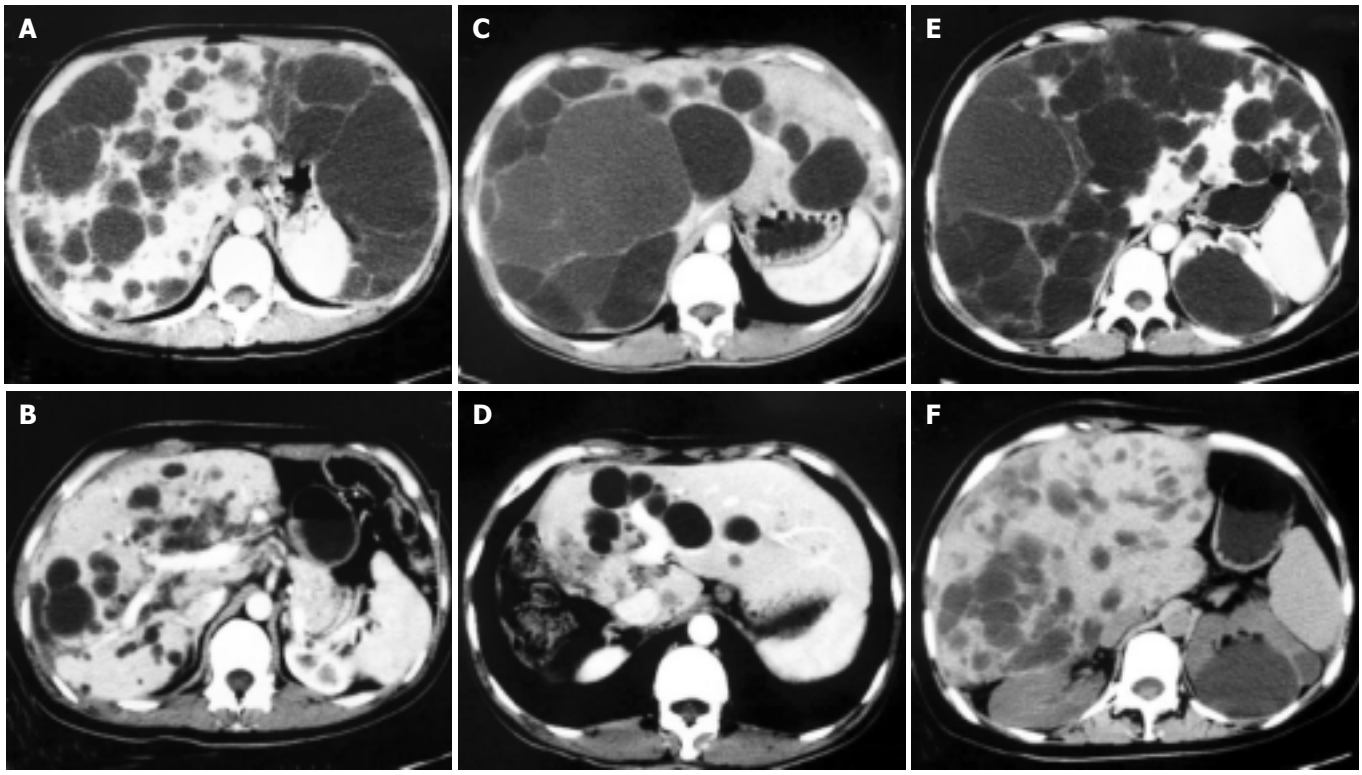

Figure 1 CT scans of livers in PLD patients before (left panels) and 3 mo (right panels) after operation, show that hypertrophy of spared liver and lack of clinically significant cyst progression, and that operative methods totally depend on cystic distribution in different patients, e.g., lateral segment removal from A to B, right semi-hepatectomy resection from C to D, whereas extensive fenestration of posterior and interior cysts from E to F.

DISCUSSION

PLD is a rare disorder usually associated with autosomal dominant polycystic kidney disease, with an increasing prevalence associated with age and female sex[4]. Symptoms arise from liver enlargement and compression of adjacent structures. Most symptomatic patients complained of increasing abdominal girth and a chronic dull abdominal pain. Liver enlargement may cause early satiety, weight loss, respiratory compromise, and physical disability. Complications such as ascites, esophageal varices, jaundice and hepatic failure, are rare[5-7].

A variety of treatment have been advocated for the few patients with incapacitating symptoms. Percutaneous aspiration with alcohol sclerotherapy seems valuable for solitary cysts but does not provide relief for patients with PLD because cyst collapse may not be sufficient[8]. Cyst fenestration with internal drainage into the peritoneal cavity, described by Lin in 1968, may fail to achieve long-term favorable outcome[9]. In practice, the efficacy of the Lin decompression for PLD is limited by extent of cysts, access to central cysts, postoperative walling off of cysts, and the rigid architecture of the fenestrated liver, which does not completely collapse[2]. Liver transplantation might be considered for patients with a "syndrome of lethal exhaustion" from PLD[7,10,11].

Armitage and Blumgart[12] described in 1984 a patient with PLD who underwent partial hepatic resection and cyst fenestration. This procedure allowed the excision of most prominent cysts with minimal resection of liver tissue; liver parenchyma was preserved despite the polycystic disease. Other reports have shown the feasibility of such an approach (Table 3)[1,2,8,12-18]. We reported a similar favorable outcome. During a mean follow-up of 20.4 mo, six of seven patients were symptom free. Herein, we emphasize that the result might be achieved by a careful selection of patients and by an experienced surgeon. The head surgeon of our surgical team has abundant experiences of more than 1400 hepatectomies for liver tumors during the same study period.

The postoperative morbidity rate in reviewed reports was 54.3%. The majority of immediately postoperative complications in our series were ascites and transient pleural effusion. Ascites was easily treated by diuretics and effective drainage or followed by needle aspiration. None of our patients had kidney failure requiring dialysis before or after operation. Ascites occurred in the patients with renal dysfunction may be refractory and even increased the chance to be infected or bring forth malnutrition[17]. The elucidation for the mechanism of hepatic cystic epithelium secretion may be a key to solve this problem[19].

The literature review showed an overall mortality rate of 4.3%. There is only one report that the cause of death was related to this procedure for patients with PLD[15]. Acute Budd-Chiari syndrome developed shortly after fenestration of posterior cyst, which provoked a liver collapse. In practice, to stitch on the dissected triangular, falciform and round ligaments easily kept the stability of the remnant liver, which was weakened by extensive fenestration of posterior and interior cysts. Patient 6 is a good example in our series. In patients 3 and 4, we found that the left lobes twisted towards right due to gravity after right semi-hepatectomy in operation. Connecting the falciform and round ligaments easily enabled the remnants fixed, avoiding occurrence of kinking. It may be unnecessary to avoid fenestration of posterior cysts and propose a frontal hepatectomy. Two patients in literature died from postoperative intracerebral bleeding, suggesting that evaluation of selected patients' cerebral vasculature to detect aneurismal disease is essential[2,16].

Our follow-up duration is limited and our preliminary study includes just seven selected patients. Therefore, the long-term benefit of combined hepatic resection and fenestration should be further evaluated. On the basis of our experience and review of the available literature, however, this approach

could be feasible, with an acceptable risk as well as a favorable long-term outcome at follow-up. To stitch the dissected hepatic ligaments could prevent the instable remnant liver from kinking and collapsing.

REFERENCES

1 **Vauthey JN,** Maddern GJ, Blumgart LH. Adult polycystic disease of the liver. *Br J Surg* 1991; **78:** 524-527
2 **Newman KD,** Torres VE, Takela J, Nagorney DM. Treatment of highly symptomatic polycystic liver disease: preliminary experience with a combined hepatic resection-fenestration procedure. *Ann Surg* 1990; **212:** 30-37
3 **Lin TY,** Chen CC, Wang SM. Treatment of non-parasitic cystic disease of the liver: a new approach to therapy with polycystic liver. *Ann Surg* 1968; **168:** 921-927
4 **Grunfeld JP,** Albouze G, Jungers P, Landais P, Dana A, Droz D, Moynot A, Lafforgue B, Boursztyn E, Franco D. Liver changes and complications in adult polycystic kidney disease. *Adv Nephrolo Necker Hosp* 1985; **14:** 1-20
5 **Ratcliffe PJ,** Teeders S, Theaker JM. Bleeding oesophageal varices and hepatic dysfunction in adult polycystic liver disease. *Br Med J* 1984; **288:** 1330-1331
6 **Wittig JH,** Burns R, Lonmire WP. Jaundice associated with polycystic liver disease. *Am J Surg* 1978; **138:** 383-386
7 **Washburn WK,** Johnson LB, Lewis WD, Jenkins RL. Liver transplantation for adult polycystic liver disease. *Liver Transpl Surg* 1996; **2:** 17-22
8 **Sanchez H,** Gagner M, Rossi RL, Lewis WD, Muson JL, Braasch JW. Surgical management of nonparasitic cystic liver disease. *Am J Surg* 1991; **161:** 113-119
9 **Tan YM,** Oli LL, Mack PO. Current status in the surgical management of adult polycystic liver disease. *Ann Acad Med Singapore* 2002; **31:** 216-222
10 **Swenson K,** Seu P, Kinkhabwala M, Marggard M, Martin P, Goss J, Brasuttil R. Liver transplantation for adult polycystic liver disease. *Hepatology* 1998; **28:** 412-415
11 **Starzl TE,** Reyes J, Tsakis A, Mieles L, Todo S, Gordon R. Liver transplantation for polycystic liver disease. *Arch Surg* 1990; **125:** 575-577
12 **Armitage NC,** Blumgart LH. Partial resection and fenestration in the treatment of polycystic liver disease. *Br J Surg* 1984; **71:** 242-244
13 **Iwatsuki S,** Starzl TE. Personal experience with 411 hepatic resections. *Ann Surg* 1988; **208:** 421-434
14 **Henne-Bruns K,** Klomp HJ, Kremer B. Non-parasitic liver cysts and polycystic liver disease: results of surgical treatment. *Hepatogastroenterology* 1993; **40:** 1-5
15 **Soravia C,** Mentha G, Giostra E, Morel P, Rohner A. Surgery for adult polycystic liver disease. *Surgery* 1995; **117:** 272-275
16 **Que F,** Nagorney DM, Gross JB Jr, Torres VE. Liver resection and cyst fenestration in the treatment of severe polycystic liver disease. *Gastroenterology* 1995; **108:** 487-494
17 **Vons C,** Chauveau D**,** Martinod E, Smadja C, Capron F, Grunfeld JP, Franco D. Liver resection in patients with polycystic liver disease. *Gastroenterol Clin Biol* 1998; **22:** 50-54
18 **Johnson LB,** Kuo PC, Plotkin JS. Transverse hepatectomy for symptomatic polycystic liver disease. *Liver* 1999; **19:** 526-528
19 **Everson GT,** Emmett M, Brown WR, Redmond P, Thickman D. Functional similarities of hepatic cystic and biliary epithelium: studies of fluid constituents and *in vivo* secretion in response to secretin. *Hepatology* 1990; **11:** 557-565

Edited by Ma JY **Proofread by** Xu FM

PO Box 2345, Beijing 100023, China
Fax: +86-10-85381893
E-mail: wjg@wjgnet.com www.wjgnet.com

World J Gastroenterol 2004;10(17):2602-2604
World Journal of Gastroenterology
Copyright © 2004 by The WJG Press ISSN 1007-9327

• CASE REPORT •

Detection of *BCL2-IGH* rearrangement on paraffin-embedded tissue sections obtained from a small submucosal tumor of the rectum in a patient with recurrent follicular lymphoma

Naohisa Yoshida, Kenichi Nomura, Yosuke Matsumoto, Kazuhiro Nishida, Naoki Wakabayashi, Hideyuki Konishi, Shoji Mitsufuji, Keisho Kataoka, Takeshi Okanoue, Masafumi Taniwaki

Naohisa Yoshida, Naoki Wakabayashi, Hideyuki Konishi, Shoji Mitsufuji, Keisho Kataoka, Takeshi Okanoue, Molecular Gastroenterology and Hepatology, Kyoto Prefectural University of Medicine Graduate School of Medical Science, Kyoto 602-8566, Japan
Kenichi Nomura, Yosuke Matsumoto, Kazuhiro Nishida, Molecular Hematology and Oncology, Kyoto Prefectural University of Medicine Graduate School of Medical Science, Kyoto 602-8566, Japan
Masafumi Taniwaki, Clinical Molecular Genetics and Laboratory Medicine, Kyoto Prefectural University of Medicine Graduate School of Medical Science, Kyoto 602-8566, Japan
Correspondence to: Kenichi Nomura, M.D., Ph.D., Molecular Hematology and Oncology, Kyoto Prefectural University of Medicine Graduate School of Medical Science, Kawaramachi-Hirokoji, Kamigyo-ku, Kyoto 602-8566, Japan. nomuken@sun.kpu-m.ac.jp
Telephone: +81-75-251-5521 **Fax:** +81-75-251-0710
Received: 2004-01-15 **Accepted:** 2004-02-24

Abstract

A 59-year-old woman was admitted to our hospital because of recurrent follicular lymphoma (FL). Colonoscopic examination revealed a rectal submucosal tumor (SMT) without any erosions and ulcers. In this patient, it was difficult to distinguish non-Hodgkin's lymphoma (NHL) invasion from other disorders of the colon including carcinoid tumor merely based on endoscopic findings. Histopathologic and immunohistochemical studies on biopsy specimens showed an infiltration of atypical lymphocytes that were positive for CD20 and BCL2 but negative for UCHL-1. Fluorescence *in situ* hybridization on paraffin-embedded tissue sections (T-FISH) identified a translocation of *BCL2* with *IGH* gene. Based on these findings, the tumor was defined as an invasion of FL. T-FISH method is useful for the detection of a monoclonality of atypical lymphocytes in an SMT of the gastrointestinal tract, and particularly for the detection of chromosomal translocations specific to lymphoma subtypes.

Yoshida N, Nomura K, Matsumoto Y, Nishida K, Wakabayashi N, Konishi H, Mitsufuji S, Kataoka K, Okanoue T, Taniwaki M. Detection of *BCL2-IGH* rearrangement on paraffin-embedded tissue sections obtained from a small submucosal tumor of the rectum in a patient with recurrent follicular lymphoma. *World J Gastroenterol* 2004; 10 (17): 2602-2604
http://www.wjgnet.com/1007-9327/10/2602.asp

INTRODUCTION

Primary gastrointestinal (GI) lymphomas are uncommon tumors, constituting less than 2% of all GI malignancies[1]. The stomach, however, is the most frequent site of extranodal NHL. Of all GI NHLs, the incidence of gastric lymphomas ranged from 51% to 86%[2,3], while that of colonic lymphomas ranged from 1.6% to 16.2%[4,5]. Diagnosis of GI lymphomas may be complicated due to difficulties in pathological diagnosis and in staging with endoscopic biopsies. In fact, it is occasionally difficult not only to distinguish NHL from other tumors but also to define subtypes of NHL on the basis of endoscopic and histological findings of biopsy specimens[6,7]. Although flowcytometric analysis is efficient for differential diagnosis of lymphomas, obtaining a diagnostic biopsy may sometimes be difficult because GI lymphomas spread submucosally and have normal surface qualities; therefore, a number of specimens are required for an accurate diagnosis.

On the other hand, chromosomal translocations are closely associated with distinctive subtypes of malignant lymphoma[8]. Both chromosomal banding and fluorescence *in situ* hybridization (FISH) are used for the detection of specific translocation. In addition, we have developed a procedure using FISH directly on paraffin embedded tissue sections (T-FISH), enabling us to perform cytogenetic analyses on both archival and small biopsy specimens[9,10].

In the current study, using T-FISH we detected rearrangement of the *BCL2* with immunoglobulin heavy chain (*IGH*) gene on biopsy specimens obtained from a small rectal submucosal tumor (SMT), thereby differentiating follicular lymphoma (FL) from other neoplastic tumors of colon as well as other types of lymphoma.

CASE REPORT

A 59-year-old woman was admitted to our hospital because of the swelling of multiple cervical lymph nodes. The patient had suffered from stage IV disease of FL since 1997. Although multiple chemotherapies including high dose regimen supported by autologous hematopoietic stem cell transplantation were administered, complete remission has not been achieved. At the current hospitalization, the patient showed elevated soluble interleukin-2 receptor (1 024 U/L), while no abnormal cells were detected in both the peripheral blood and bone marrow. Gallium-scintigraphy showed abnormal accumulation at cervical and supra-clavicular lesions. Gastroscopic examination revealed no remarkable abnormalities, whereas colonoscopic examination detected a small elevated lesion (7 mm×8 mm in size) on the rectum.

The surface of tumor was slightly reddish, but no erosions and ulcers were noted (Figure 1). No definitive deformity of colonic wall was detected with double-contrast barium enema (Figure 2). The tumor invasion was confined to the second layer of colonic wall based on the endoscopic ultrasonographic findings (Figure 3). Flowcytometric analyses were not able to be performed because of small specimens obtained from diagnostic biopsies. Histopathologic and immunohistochemical studies on biopsy specimens showed the aggregation of atypical medium-sized lymphocytes having irregularly enlarged nuclei that were positive for CD20, CD10 and BCL2, but negative for UCHL-1 and CD5 (Figures 4A-C).

Using DHAP regimen (cisplatin 70 mg/m^2, Ara-C 1.4 g/m^2 ×2, dexamethasone 40 mg×4), the patient achieved a partial response, followed by the administration of rituximab. The rectal lesion disappeared on d 120.

In order to confirm a diagnosis of lymphoma and define specific chromosomal abnormalities, we performed T-FISH analyses on the sample obtained from a rectal SMT according to the protocol already described elsewhere[9,10]. Briefly, sections from paraffin-embedded tissues were placed on slides, and then deparaffinized in xylene. Each slide was dehydrated in ethanol and treated with 0.2 mol/L HCl and 0.05 mg/mL proteinase K in TEN (0.05 mol/L tris-HCl, pH 7.8, 0.01 mol/L EDTA, and 0.01 mol/L NaCl buffer) for 10 min at 37 °C. FISH probes and samples were denatured simultaneously for 10 min at 90 °C, and were hybridized overnight at 42 °C. LSI IGH/BCL2, IGH/BCL1 and MALT1 probes (Vysis, CA, USA) were used for the detection of t (14; 18), t (11; 14), and 18q21 translocations, respectively. Images of signal were captured by a CCD camera. T-FISH detected fusion signals of *BCL2* and *IGH* genes on 75 of 100 nuclei (Figure 5), defining the invasion of FL with t (14; 18) (q32; q21). On the other hand, 95 of 100 nuclei showed negative results for both t (11; 14) and 18q21 translocations.

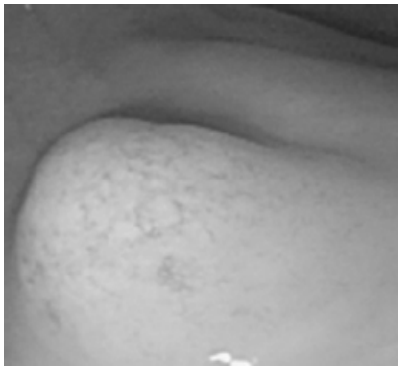

Figure 1 Endoscopic examination revealed a small submucosal tumor on rectum.

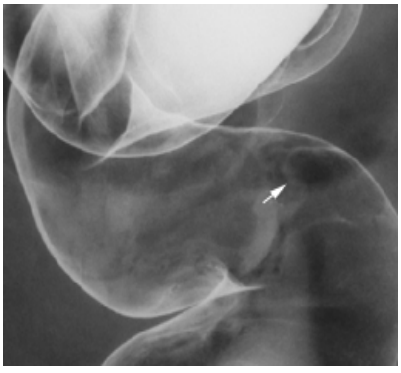

Figure 2 Double-contrast barium enema revealed no definite deformity of the GI wall at the lesion.

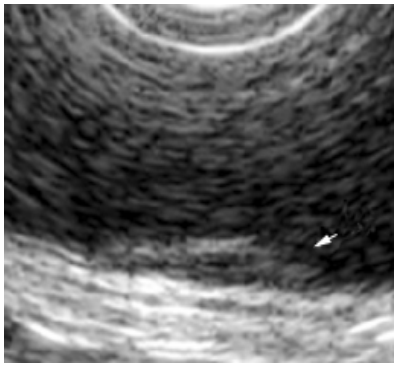

Figure 3 Endoscopic ultrasonography showed that the tumor was confined at the second layer of the colonic wall.

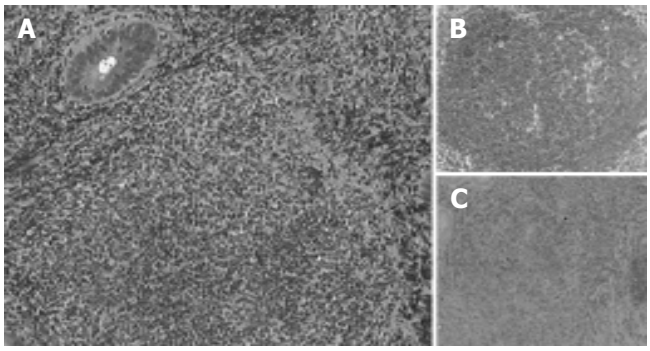

Figure 4 Histopathological studies showed aggregated atypical lymphocytes (A). Immunohistochemical analysis revealed that these lymphocytes were positive for CD20 and BCL2 (B and C).

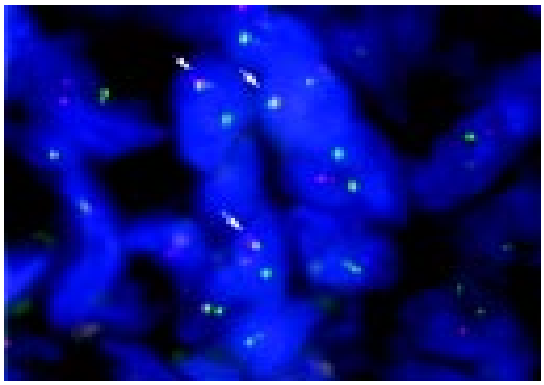

Figure 5 T-FISH detected fusion signals of IGH and BCL2 genes in nuclei as indicated by arrows.

DISCUSSION

We demonstrated rearrangement of *BCL2* with *IGH* gene on a small rectal SMT in a patient with recurrent lymphoma using T-FISH, thereby defining colonic involvement of FL. It is difficult to discriminate NHL from other disorders of the GI tract only based on endoscopic and histological findings[11]. Although endoscopic procedures are important not only in the detection of other disorders involving GI tract, but also in providing a means for pathologic diagnosis through biopsy, it should be noted, however, that obtaining a diagnostic biopsy may be difficult because GI lymphomas spread submucosally and have normal surface qualities. Since most GI lymphomas and other malignancies including adenocarcinoma and carcinoid tumor frequently display a polypoid growth pattern involving the mucosa, submucosa and muscularis[12], it is sometimes difficult to make differential diagnosis based on the histological findings.

In the current patient, immunohistochemical studies defined a diagnosis of lymphoid lesion of a rectal SMT, although flowcytometric analysis was not successful because of small specimens obtained from diagnostic biopsy. There are many kinds of SMTs originating in the colon, for example, lipoma, malignant lymphoma, carcinoid tumor, *etc*[13]. Flowcytometric and immunocytochemical studies are useful for demonstration of a monoclonal population of lymphocytes of a lesion of interest, since most GI lymphomas are virtually always of the B-cell type. However, it should be noted that there are certain subtypes preferentially involving GI tract including mantle cell lymphoma, and mucosa-associated lymphoid tissue (MALT) lymphoma[14]. In this respect, cytogenetic study is necessary for the determination of these subtypes, since chromosomal translocations are closely associated with distinctive subtypes of NHL[14]. More than 90% of mantle cell lymphoma was related to the translocation of *IGH* with *BCL1* gene[15]. MALT lymphoma

was related to the translocation of *API2* with *MALT1* at frequencies of 18.8%[9]. Approximately 60% of FL showed the translocation of *BCL2* with *IGH* (Matsumoto *et al*. in press). Hence, T-FISH is a useful method not only to make definitive diagnosis of NHL but also to define its subtypes. In addition, a few biopsy samples are enough for T-FISH analysis when compared with flowcytometric analysis and polymerase chain reaction (PCR). Furthermore, the tissues embedded for a period of 15 years were available for T-FISH analysis[9,10].

At present there is considerable controversy concerning the treatment of primary and secondary GI lymphomas. Rituximab has recently included in treatment option[16]. In our patient with recurrent FL, salvage therapy including high-dose Ara-C with rituximab was performed. Because *API2-MALT1*-positive lymphoma has demonstrated a more aggressive subgroup[17], T-FISH will provide novel information for the selection of treatment for GI lymphomas.

In conclusion, our results indicate that T-FISH is a promising procedure for the routine detection of genetic alterations in GI lymphomas, it enables us to not only make definitive diagnosis of NHL but also to define its subtypes.

REFERENCES

1 **Frazee RC,** Roberts J. Gastric lymphoma treatment. Medical versus surgical. *Surg Clin North Am* 1992; **72:** 423-431

2 **Radaszkiewicz T,** Dragosics B, Bauer P. Gastrointestinal malignant lymphomas of the mucosa-associated lymphoid tissue: factors relevant to prognosis. *Gastroenterology* 1992; **102:** 1628-1638

3 **Hansen PB,** Vogt KC, Skov RL, Pedersen-Bjergaard U, Jacobsen M, Ralfkiaer E. Primary gastrointestinal non-Hodgkin's lymphoma in adults: a population-based clinical and histopathologic study. *J intern Med* 1998; **244:** 71-78

4 **Otter R,** Bieger R, Klutin PM, Hermans J, Willemze R. Primary gastrointestinal non-Hodgkin's lymphoma in a population-based registry. *Br J Cancer* 1989; **60:** 745-750

5 **Crump M,** Gospodarowicz M, Shephers FA. Lymphoma of the gastrointestinal tract. *Semin Oncol* 1999; **26:** 324-337

6 **Takenaga T,** Yamamoto N, Yamanaka A, Yamada M, Takasimizu K, Sasabe M, Tamura Y, Kurosawa K, Fujimoto H, Ookusa T, Nakamura E, Hisayama Y. Gastrointestinal involvement of malignant lymphoma. *Gastroenterol Endosc* 1988; **30:** 2218-2224

7 **Damaj G,** Verkarre V, Delmer A, Solal-Celigny P, Yakoub-Agha I, Cellier C, Maurschhauser F, Bouabdallah R, Leblond V, Lefrere F, Bouscary D, Audouin J, Coiffier B, Varet B, Molina T, Brousse N, Hermine O. Primary follicular of the gastrointestinal tract: a study of 25 cases and a literature review. *Ann Oncol* 2003; **14:** 623-629

8 **Ong ST,** Le Beau MM. Chromosomal abnormalities and molecular genetics of non-Hodgkin's lymphoma. *Semin Oncol* 1998; **25:** 447

9 **Nomura K,** Yoshino T, Nakamura S, Akano Y, Tagawa H, Nishida K, Seto M, Nakamura S, Ueda R, Yamaguti H, Taniwaki M. Detection of t (11;18) (q21;q21) in marginal zone lymphoma of mucosa-associated lymphocytic tissue type on paraffin-embedded tissue sections by using fluorescence *in situ* hybridization. *Cancer Genet Cytogenet* 2003; **140:** 49-54

10 **Nomura K,** Sekoguchi S, Ueda K, Nakao M, Akano Y, Fujita Y, Yamashita Y, Horiike S, Nishida K, Nakamura S, Taniwaki M. Differentiation of follicular from mucosa-associated lymphoid tissue lymphoma by detection of t (14;18) on single-cell preparations and paraffin-embedded sections. *Genes Chromosomes Cancer* 2002; **33:** 213-216

11 **Shepherd NA,** Hall PA, Coates PJ, Levison DA. Primary malignant lymphoma of the colon and rectum. A histopathological and immunohistochemical analysis of 45 cases with clinicopathological correlations. *Histopathology* 1988; **12:** 235-252

12 **Coulson WF.** The Stomach. In: Coulson WF, ed. Surgical Pathology, Philadelphia:J.B. *Lippincott Company* 1988: 123-125

13 **Kawamoto K**, Yamada Y, Furukawa N, Utsunomiya T, Haraguchi Y, Mizuguchi M, Oiwa T, Takano H, Masuda K. Endoscopic submucosal tumorectomy for gastrointestinal submucosal tumors restricted to the submucosa. *Gastrointest Endosc* 1997; **46:** 311-317

14 **Jaffe ES,** Harris NL, Stein H, Vardiman JW, eds.Tumours of Haematopoietic and Lymphoid Tissues, 3rd ed. *Lyon France*: *IARC* 2001

15 **Hui P,** Howe JG, Crouch J, Nimmakayalu M, Qumsiyeh MB, Tallini G, Flynn SD, Smith BR. Real-time quantitative RT-PCR of cyclin D1 mRNA in mantle cell lymphoma: comparison with FISH and immunohistochemistry. *Leuk Lymphoma* 2003; **44:** 1385-1394

16 **Press OW**, Unger JM, Braziel RM, Maloney DG, Miller TP, LeBlanc M, Gaynor ER, Rivkin SE, Fisher RI. A phase 2 trial of CHOP chemotherapy followed by tositumomab/iodine I 131 tositumomab for previously untreated follicular non-Hodgkin lymphoma: Southwest Oncology Group Protocol S9911. *Blood* 2003; **102:** 1606-1612

17 **Sakugawa ST,** Yoshino T, Nakamura S, Inagaki H, Sadahira Y, Nakamine H, Okabe M, Ichimura K, Tanimoto M, Akagi T. API2-MALT1 fusion gene in colorectal lymphoma. *Mod Pathol* 2003; 1232-1241

Edited by Zhu LH **Proofread by** Xu FM

PO Box 2345, Beijing 100023, China
Fax: +86-10-85381893
E-mail: wjg@wjgnet.com www.wjgnet.com

World J Gastroenterol 2004;10(17):2605-2606
World Journal of Gastroenterology
Copyright © 2004 by The WJG Press ISSN 1007-9327

• CASE REPORT •

Mesenteric Ischemia: An unusual presentation of fistula between superior mesenteric artery and common hepatic artery

Ertugrul Kayacetin, Serdar Karaköse, Aydin Karabacakoglu, Dilek Emlik

Ertugrul Kayacetin, Department of Gastroenterology, Meram Medical Faculty, Selcuk University, Konya-Turkey
Serdar Karaköse, **Aydin Karabacakoglu, Dilek Emlik,** Department of Radiology, Meram Medical Faculty, Selcuk University, Konya-Turkey
Correspondence to: Dr. Ertugrul Kayacetin, Selcuk Universitesi Meram Tip Fakultesi, Ic Hastalikleri AD, Gastroenterology BD, Konya-Turkey. ekayacetin@mynet.com
Telephone: +90-332-3218694
Received: 2004-03-05 **Accepted:** 2004-04-14

Abstract

Chronic mesenteric ischemia is an uncommon condition associated with a high morbidity and mortality. We reported a 36-year old women with postprandial abdominal pain due to chronic mesenteric ischemia caused by a fistula between superior mesenteric and common hepatic artery.

Kayacetin E, Karaköse S, Karabacakoglu A, Emlik D. Mesenteric Ischemia: An unusual presentation of fistula between superior mesenteric artery and common hepatic artery. *World J Gastroenterol* 2004; 10(17): 2605-2606
http://www.wjgnet.com/1007-9327/10/2605.asp

INTRODUCTION

Chronic mesenteric ischemia (CMI) is an uncommon condition associated with a high morbidity and mortality and the symptoms may be nonspecific until late in the course of disease[1,2].

The most common cause of CMI is atherosclerosis. Involvement of the celiac, superior mesenteric, and inferior mesenteric arteries at their origins is typical[3]. We reported an abnormal communication between the superior mesenteric artery (SMI) and common hepatic artery (CHA) which caused splanchnic hypoperfusion. To our knowledge, this entity has not been reported previously in the literature.

CASE REPORT

The patient was a 36-year old woman who had complained of severe postprandial abdominal pain and abdominal distention for 9 mo. The pain was described as a severe, poorly localized one radiating to the back. No fever, nause or vomiting, hematochezia, or weight change was reported. She had no history of previous trauma, abdominal surgery, hepatic or pancreatic disease. Hematological and biochemical test results on admission were as follows: white blood cell count, 7 000/mm^3 (normal, 4.0-10.0); hemoglobin, 13.4 g/dL (normal, 12.1-17.2); platelets, 177 10^3/uL (normal, 150-400); total bilirubin, 0.36 mg/dL (normal, 0.1-1.3); albumin, 4.6 g/dL (normal, 3.5-5.2); aspartate aminotransferase, 29 u/L (normal, 10-31); alanine aminotransferase, 30 u/L (normal, 10-31); amylase, 74 u/L (normal, 0-90); lactate dehydrogenase, 335 u/L (normal, 220-450).

On physical examination, pulse rate was 84/min and arterial blood pressure was 110/70 mm Hg. Rectal examination revealed no mass and the stool was hemoccult negative. Computerized tomography of the abdomen, plain abdominal radiography and upper endoscopy were normal. Abdominal ultrasonography showed a slightly enlarged liver with normal echo pattern and communication between the common hepatic artery and superior mesenteric artery (Figure 1). On Doppler ultrasound, arterial flow was observed within this fistula (Figure 2). We suspected CMI and consequently performed anjiography. Celiac arteriogram revealed an abnormal fistula from the SMA to the CHA and not any other arterial communications (Figure 3).

Figure 1 Sonogram showing a fistula (thin arrow) between superior mesenteric artery (arrowhead) and common hepatic artery (thick arrow).

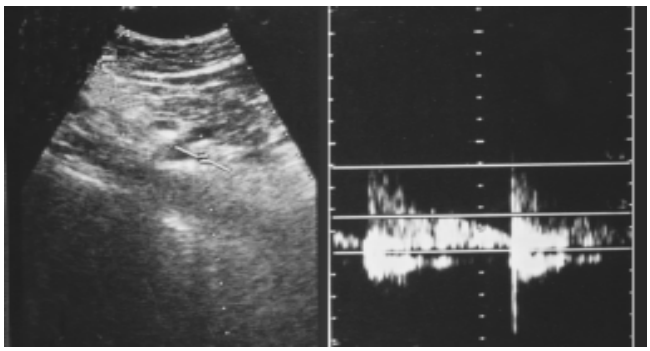

Figure 2 Color doppler sonogram of fistula revealing arterial flow.

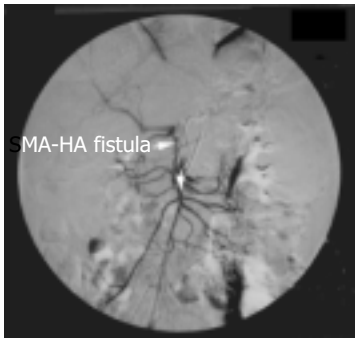

Figure 3 Selective superior mesenteric artery angiography showing a fistula between superior mesenteric artery and common hepatic artery.

A small quantity diet with low fat content was adviced to the patient who responded well to this measure and after one month she was free of abdominal pain, and also of abdominal distension, hence we did not plan to perform surgery or interventional radiology.

DISCUSSION

The major vascular supply of the bowel depends on the celiac, superior mesenteric and inferior mesenteric arteries. The superior mesenteric artery is the largest of all the aortic branches and carries over 10% of the cardiac output. Splanchnic circulation was about 30% of the circulating blood volume[4,5].

CMI is a disputatious diagnostic problem. Most patients do not develop ischemic symptoms because of the abundant collateral circulation of these intestines. Usually at least two of the three mesenteric arteries must be significantly stenotic before symptoms developed[6,7].

Clasically, postprandial abdominal pain, known as "intestinal angina", was almost invariably the principal symptom. Other less consistent symptoms included bloating, flatulance, nause, and variable changes in bowel habit[2,8,9]. Superior mesenteric artery blood flow increased after ingestion of meals with a high fat content[5]. Our patient reported significant crampy abdominal pain after heavy meal, meanwhile consuming small and low fat meal did not cause pain. The pathophysiological mechanism in this case was an arterial abnormality which was an abnormal communication between SMI and CHA. Under such a condition blood perfusion became impaired. A higher blood pressure in SMA could force flow towards CHA. Blood flow might be sufficient to sustain resting metabolic needs, but after a heavy meal, however, splanchnic blood flow did not increase because of this steal phenomenon.

A diagnosis of vasculogenic mesenteric ischemia was made on the basis of the clinical history and dupplex ultrasonography findings. Other causes of abdominal pain were excluded. Large majority of cases of colonic ischemia were due to non-occlusive diseases[10]. Other less common causes of CMI were vasculitis, SLE, sick cell disease, hypercoagulable states, medications (estrojen, danazol, vazopressin, gold, psychotropic drugs), and cocaine abuse[1,11].

Clinical presentations of the patient might depend on the size and amount of blood flow through the fistula, ranging from asymptomatic cases to overt intestinal ischemia.

We suggested nutritional measures aiming at avoiding large meals and reduction of long-chain fat content.

In a patient with an unexplaniable chronic abdominal pain, after exclusion of common reasons, vascular abnormalities must be suspected. Like in our case, there might be other abnormal vascular communications, thus even in a young patient vascular examinations might be necessary.

REFERENCES

1 **Rogers DM**, Thompson JE, Garrett WV, Talkington CM, Patman RD. Mesenteric vascular problems. A 26-year experience. *Ann Surg* 1982; **195:** 554-565
2 **Croft RJ**, Menon GP, Marston A. Does 'intestinal angina' exist? A critical study of obstructed visceral arteries. *Br J Surg* 1981; **68:** 316-318
3 **Kazmers A**. Operative management of chronic mesenteric ischemia. *Ann Vasc Surg* 1998; **12:** 299-308
4 **Muller AF**. Role of duplex Doppler ultrasound in the assessment of patients with postprandial abdominal pain. *Gut* 1992; **33:** 460-465
5 **Sidery MB**, Macdonald IA, Blackshaw PE. Superior mesenteric artery blood flow and gastric emptying in humans and the differential effects of high fat and high carbohydrate meals. *Gut* 1994; **35:** 186-190
6 **Thomas JH**, Blake K, Pierce GE, Hermreck AS, Seigel E. The clinical course of asymptomatic mesenteric arterial stenosis. *J Vasc Surg* 1998; **27:** 840-844
7 **Kolkman JJ**, Groeneveld AB. Occlusive and non-occlusive gastrointestinal ischaemia: a clinical review with special emphasis on the diagnostic value of tonometry. *Scand J Gastroenterol Suppl* 1998; **225:** 3-12
8 **Bower TC**. Ischemic colitis. *Surg Clin North Am* 1993; **73:** 1037-1053
9 **Zelenock GB**, Graham LM, Whitehouse WM Jr, Erlandson EE, Kraft RO, Lindenauer SM, Stanley JC. Splanchnic arteriosclerotic disease and intestinal angina. *Arch Surg* 1980; **115:** 497-501
10 **Marston A**, Clarke JM, Garcia Garcia J, Miller AL. Intestinal function and intestinal blood supply: a 20 year surgical study. *Gut* 1985; **26:** 656-666
11 **Patel A**, Kaleya RN, Sammartano RJ. Pathophysiology of mesenteric ischemia. *Surg Clin North Am* 1992; **72:** 31-41

Edited by Wang XL and Chen WW **Proofread by** Xu FM

PO Box 2345, Beijing 100023, China
Fax: +86-10-85381893
E-mail: wjg@wjgnet.com www.wjgnet.com

World J Gastroenterol 2004;10(17):2607-2608
World Journal of Gastroenterology
Copyright © 2004 by The WJG Press ISSN 1007-9327

• CASE REPORT •

Severe hypercholesterolemia associated with primary biliary cirrhosis in a 44-year-old Japanese woman

Tatsuo Kanda, Osamu Yokosuka, Hiroshige Kojima, Fumio Imazeki, Keiich Nagao, Ichiro Tatsuno, Yasushi Saito, Hiromitsu Saisho

Tatsuo Kanda, Osamu Yokosuka, Hiroshige Kojima, Fumio Imazeki, Hiromitsu Saisho, First Department of Medicine, Chiba University School of Medicine, Chiba 260-8670, Japan
Tatsuo Kanda, Keiich Nagao, Health Sciences Center, Chiba University, Chiba 260-8670, Japan
Ichiro Tatsuno, Yasushi Saito, Second Department of Medicine, Chiba University School of Medicine, Chiba 260-8670, Japan
Correspondence to: Osamu Yokosuka, M.D., First Department of Medicine, Chiba University School of Medicine, 1-8-1 Inohana, Chuo-ku, Chiba-City, Chiba 260-8670, Japan. kandat-cib@umin.ac.jp
Telephone: +81-43-226-2086 **Fax:** +81-43-226-2088
Received: 2004-02-02 **Accepted:** 2004-02-24

Abstract

A 44-year-old woman developed jaundice and was diagnosed as stage II of primary biliary cirrhosis (PBC). She showed a severely high total cholesterol level. This article focuses on atypical presentations of PBC and the need to test the total cholesterol level of PBC patients.

Kanda T, Yokosuka O, Kojima H, Imazeki F, Nagao K, Tatsuno I, Saito Y, Saisho H. Severe hypercholesterolemia associated with primary biliary cirrhosis in a 44-year-old Japanese woman. *World J Gastroenterol* 2004; 10(17): 2607-2608
http://www.wjgnet.com/1007-9327/10/2607.asp

CASE REPORT

A 44-year-old gentlewoman was admitted in August 1996 due to a feeling of itching and jaundice. She had no special past history, such as operation, blood transfusion, tattooing or illicit drug use. She did not drink or smoke. There were no particular familial histories such as liver disease or hyperlipidemia. The patient had been on medication for hyperlipidemia, with a daily intake of 10 mg of pravastatin sodium, 12 g of cholestyramine, and 600 mg of ursodeoxycholic acid since one month earlier.

On admission, her height, body mass and body mass index (BMI) were 154.5 cm, 46.0 kg and 19.3 kg/m^2, respectively. Her physical examination revealed mild anemia and jaundice. Xanthoma was noticed around her eyes, but thickened Achilles tendon was not seen on X-ray examination. Her liver and spleen were not enlarged. There was no pretibial edema in her feet.

Blood test results were compatible with the picture of primary biliary cirrhosis (PBC). The serum bilirubin level was 57 mg/L (normal 2-12 mg/L), direct bilirubin was 42 mg/L (normal <3 mg/L), alkaline phosphatase was 2 362 IU/L (normal 115-359 IU/L), and alanine aminotransferase was 105 IU/L (normal 8-42 IU/L). Prothrombin time was within normal limits at 11.8 seconds. Platelet count was 277×10^9/L. Renal function was normal. Ultrasound scan showed normal liver size and biliary trees were normal. There were no gallstones or ascites. Intimal medial thickness (IMT) of the right common carotid artery did not show any increase on high-resolution B mode ultrasonography.

Serology tests for hepatitis B and C viruses were negative. Anti-mitochondrial antibody (AMA) and anti-mitochondrial M2 antibody were positive (×320) and 41.5 (normal <7). Anti-nuclear antibody (ANA) and anti-smooth muscle antibody were both negative. IgG and IgM were 27.42 g/L (normal 8.7-17 g /L) and 11.89 g/L (normal 0.35-2.20 g/L), respectively. Thyroid gland functions were within normal limits at this time.

Her serum total cholesterol level was 13.90 g/L (normal 1.25-2.20 g/L), triglyceride 1.12 g/L (normal 0.35-1.50 g/L), high-density lipoprotein (HDL) cholesterol 1.03 g/L (normal >0.40 g/L), and blood glucose 1.03 g/L. She was positive for lipoprotein X. LCAT was not detectable, compatible with Frederickson type V hypercholesterolemia [apolipoprotein A-I 0.48 g/L (normal 1.26-1.65 g/L), A-II 0.24 g/L (normal 0.246-0.333 g/L), B 1.44 g/L (normal 0.66-1.01 g/L), C-II 333 mg/L (normal 15-38 mg/L), C-III 3.42 g/L (normal 26-46 mg/L) and E 450 mg/L (normal 29-53 mg/L)].

Liver biopsy showed no cirrhosis but revealed compatibility with PBC stage II (according to Ludwig). She was re-started on ursodeoxycholic acid at 900 mg/d and probucol at 500 mg/d. She was diagnosed as subclinical hypothyroidism [TSH 11.5 μIU/mL (normal 0.35-4.94 μIU/mL), free T3 1.45 pg/mL (normal 1.71-3.71 pg/mL) and free T4 8.2 ng/L (normal 7.0-14.8 ng/L)] in April 1999 and 0.05 mg/d of levothyroxine sodium was begun. However, her total cholesterol level remained quite similar to that before treatment as in October 2000 it was still high (10.11g/L).

DISCUSSION

In PBC patients, a hyperlipidemic state is often observed; however, this case illustrated an unusual presentation of severe hypercholesterolemia. According to Talwalkar and Lindor[1], up to 85% of patients presented with hypercholesterolemia at diagnosis. However, such a degree of hypercholesterolemia was not observed in many cases. In fact, our survey of more than 100 cases of PBC who visited our clinic revealed only this one case with a level of hypercholesterolemia higher than 10 g/L.

Earlier cross sectional studies reported higher levels of total cholesterol and lower levels of HDL cholesterol in patients with advanced disease compared with those in the earlier stages[2,3]. On the other hand, Nikkila *et al*.[4] reported that reduced hepatic synthesis and internal absorption in the terminal stage of PBC might lead to decreased total cholesterol levels. Although high levels of lipoprotein X, comprised of nonesterified cholesterol and phospholipids, were present in the serum of patients with PBC[5], our patient was at stage II of early PBC, even if her serum bilirubin level was 57 mg/L. Hypothyroidism and subclinical hyperthyroidism often caused hyperlipidemia[6,7]. In our patient, hypercholesterolemia did not improve after thyroid hormone therapy.

In PBC, marked hypercholesterolemia was not associated with an excess risk of cardiovascular disease, whereas less advanced patients with moderate hypercholesterolemia were exposed to an increased cardiovascular risk[8]. There is no doubt that a reduction in serum cholesterol levels in PBC patients could be achieved with medical therapy[9,10], so our patient continued to be observed with medical therapy.

In conclusion, we report a case of severe hypercholesterolemia, not familial, but associated with early-stage PBC. Further studies of severe hypercholesterolemia are warranted.

REFERENCES

1 **Talwalkar JA**, Lindor KD. Primary biliary cirrhosis. *Lancet* 2003;

362: 53-61

2 **Jahn CE**, Schaefer EJ, Taam LA, Hoofnagle JH, Lindgren FT, Albers JJ, Jones EA, Brewer HB Jr. Lipoprotein abnormalities in primary biliary cirrhosis. Association with hepatic lipase inhibition as well as altered cholesterol esterification. *Gastroenterology* 1985; **89:** 1266-1278

3 **Crippin JS**, Lindor KD, Jorgensen R, Kottke BA, Harrison JM, Murtaugh PA, Dickson ER. Hypercholesterolemia and atherosclerosis in primary biliary cirrhosis: what is the risk? *Hepatology* 1992; **15:** 858-862

4 **Nikkila K**, Hockerstedt K, Miettinen TA. High cholestanol and low campesterol-to-sitosterol ratio in serum of patients with primary biliary cirrhosis before liver transplantation. *Hepatology* 1991; **13:** 663-669

5 **Seidel D**, Alaupovic P, Furman RH, McConathy WJ. A lipoprotein characterizing obstructive jaundice. II. Isolation and partial characterization of the protein moieties of low density lipoproteins. *J Clin Invest* 1970; **49:** 2396-2407

6 **Ganotakis ES**, Mandalaki K, Tampakaki M, Malliaraki N, Mandalakis E, Vrentzos G, Melissas J, Castanas E. Subclinical hypothyroidism and lipid abnormalities in older women attending a vascular disease prevention clinic: effect of thyroid replacement therapy. *Angiology* 2003; **54:** 569-576

7 **Kong WM**, Sheikh MH, Lumb PJ, Naoumova RP, Freedman DB, Crook M, Dore CJ, Finer N, Naoumova P. A 6-month randomized trial of thyroxine treatment in women with mild subclinical hypothyroidism. *Am J Med* 2002; **112:** 348-354

8 **Longo M**, Crosignani A, Battezzati PM, Squarcia Giussani C, Invernizzi P, Zuin M, Podda M. Hyperlipidaemic state and cardiovascular risk in primary biliary cirrhosis. *Gut* 2002; **51:** 265-269

9 **Chauhan SS**, Zucker SD. Hypercholesterolemia in primary biliary cirrhosis: getting to the heart of the matter? *Gastroenterology* 2003; **124:** 854-856

10 **Kanda T**, Yokosuka O, Imazeki F, Saisho H. Bezafibrate treatment: a new medical approach for PBC patients? *J Gastroenterol* 2003; **38:** 573-578

Edited by Zhu LH and Xu FM

PO Box 2345, Beijing 100023, China
Fax: +86-10-85381893
E-mail: wjg@wjgnet.com www.wjgnet.com

World J Gastroenterol 2004;10(17):2609-2612
World Journal of Gastroenterology
Copyright © 2004 by The WJG Press ISSN 1007-9327

• CASE REPORT •

EUS mini probes in diagnosis of cystic dystrophy of duodenal wall in heterotopic pancreas: A case report

Ivan Jovanovic, Srbislav Knezevic, Marjan Micev, Miodrag Krstic

Ivan Jovanovic, Miodrag Krstic, Clinic of Gastroenterology and Hepatology, Institute of Digestive Diseases, Belgrade, Serbia and Montenegro
Srbislav Knezevic, First Surgical Clinic, Belgrade, Serbia and Montenegro
Marjan Micev, Clinical Center of Serbia, Belgrade, Institute for Medical Research, Belgrade, Serbia and Montenegro
Correspondence to: Ivan Jovanovic, MD, PhD, Clinic of Gastroenterology and Hepatology, Clinical Center of Serbia, Belgrade, 6 Koste Todorovic, 11000 Belgrade, Serbia and Montenegro. ivangastro@beotel.yu
Telephone: +381-63-357080 **Fax:** +381-11-3614744
Received: 2004-01-16 **Accepted:** 2004-03-04

Abstract

Cystic dystrophy of the duodenal wall is a rare condition characterized by the development of cysts in heterotopic pancreatic tissue localized in the duodenal wall. A 38-year-old man was admitted to the hospital for abdominal pain and vomiting after food intake. The diagnosis of acute pancreatitis was initially suspected. Abdominal ultrasound examination revealed thickening of the second portion of duodenal wall within which, small cysts (diameter, less than 1 cm) were present in the vicinity of pancreatic head. The head of pancreas appeared enlarged (63 mm×42 mm) and hypoechoic. Upper endoscopy and barium X-ray series were performed revealing a severe circumferential deformation, as well as 4 cm long stenosis of the second portion of the duodenum. CT examination revealed multiple cysts located in an enlarged, thickened duodenal wall with moderate to strong post-contrast enhancement. We suspected that patient had cystic dystrophy of duodenal wall developed in the heterotopic pancreas and diagnosis was confirmed by endoscopic ultrasound (EUS). Endoscopic ultrasound (EUS) revealed circular stenosis from the duodenal bulb onwards. A twenty megaHertz mini-probe examination further showed diffuse (intramural) infiltration of duodenal wall limited to the submucosa and muscularis propria of the second portion of duodenum with multiple microcysts within the thickened mucosa and submucosa. Patient was successfully surgically treated and pancreatoduodenectomy was performed. The pathological examination confirmed a diagnosis of cystic dystrophy of a heterotopic pancreas. Endoscopic ultrasonography features allow preoperative diagnosis of cystic dystrophy of a heterotopic pancreas in duodenal wall, with intraluminal 20 MHz mini probe sonography being more efficient in cases of luminal stenosis.

Jovanovic I, Knezevic S, Micev M, Krstic M. EUS mini probes in diagnosis of cystic dystrophy of duodenal wall in heterotopic pancreas: A case report. *World J Gastroenterol* 2004; 10 (17): 2609-2612
http://www.wjgnet.com/1007-9327/10/2609.asp

INTRODUCTION

The most common type of heterotopic tissue in the gastrointestinal tract is pancreas. Pancreatic heterotopia is defined as the presence of abnormally located (aberrant) pancreatic tissue with no contact (vascular, neural, and anatomical) with the normal pancreas, and possesses its own duct system and vascular supply[1,2]. Heterotopic pancreatic tissue has been found in several abdominal and intrathoracic locations, most frequently in the stomach (25-60%) or duodenum (25-35%)[3].

Cystic dystrophy of the duodenal wall in heterotopic pancreas is a relatively rare clinical disorder affecting young men in particular[4]. Diagnosis is usually suspected during initial investigation of non-specific clinical symptoms such as abdominal pain, duodenal obstruction and weight loss and finally confirmed by imaging techniques, mainly endoscopic ultrasound which localizes precisely cysts in duodenal wall.

The purpose of this report was to present a case with this anomaly and provide up-to-date literature review on this topic.

CASE REPORT

A 38-year-old man who was admitted for clarification of several months of upper abdominal pain, vomiting after food intake accompanied by a weight loss. The patient had no history of alcohol abuse, and smoked 20 cigarettes per day. Physical examination revealed tachypnea and tachycardia, and a blood pressure 100/70 mmHg. There was abdominal tenderness in upper abdomen. Hematological and blood bio-chemical tests were performed (Tables 1, 2) showing a sevenfold increased level of serum amylase (625 U/L, range 20-90 U/L) accompanied by an elevated alkaline phosphatase, and markers of acute hepatocyte injury such as alanine (AST) and aspartate aminotransferase (ALT) and gama GT. Bilirubin levels remained normal. The urine had a pH 6.5 and a specific gravity of 1.010. The sediment contained 3-5 red cells and 0-2 white cells per high-power field. A diagnosis of acute pancreatitis was initially suspected.

Ultrasonographic examination revealed an enlarged steatotic liver, no stones in gall bladder, and a common bile duct diameter of 8 mm with no signs of stone obstruction. Second portion duodenal wall appeared thicker within which, small cysts (diameter, less than 1 cm) were present in the vicinity of pancreatic head. The head of pancreas appeared enlarged (63 mm×42 mm) and hypoechoic.

An upper GI endoscopy also revealed a severe semispherical deformation of second portion of duodenum without mucosal lesions. Due to the stenosis the endoscope could not be passed distal to upper duodenal flexure. Biopsy of the duodenal mucosa detected moderate inflammatory changes (Figure 1).

A barium meal revealed a severe circumferential deformation, as well as 4 cm long stenosis of the second portion of the duodenum (Figure 2).

We suspected that the patient had cystic dystrophy of duodenal wall developed in the heterotopic pancreas which was highly indicated by computed tomography and endoscopic ultrasound (EUS).

CT examinations revealed multiple cysts located in an enlarged, thickened duodenal wall with moderate to strong post-contrast enhancement.

Endoscopic ultrasound (EUS) revealed circular stenosis from the duodenal bulb onwards. Twenty megaHertz mini-probe

examinations further showed diffuse (intramural) infiltration of duodenal wall limited to the submucosa and muscularis propria of the second portion of duodenum with multiple, very small anechoic spots, like microcysts (Figure 3A, B). EUS did not reveal any tumors of the pancreas.

MRI examinations showed a suspicious 6 cm×4 cm solid and partly cystic tumor of processus uncinatus of pancreas.

The patient was successfully surgically treated and pancreatoduodenectomy was performed (Figure 4). Pathological examinations confirmed a diagnosis of cystic dystrophy of a heterotopic pancreas (Figure 5).

Table 1 Hematologic tests

Variable	Value	Initial tests	Repeated stests
Hematocrit (%)	35-54	43	49.7
White cell count ($\times10^9$)	4.0-10.0	12.0	17.7
Differential count ($\times10^9$)			
Neutrophils	1.4-6.5	4.3	2.8
Lymphocytes	1.2-3.4	5.6	2.8
Monocytes	0.1-0.6	2.1	1.1
Prothrombin time (% quick)	75-120	114	115

Table 2 Blood bio-chemical tests

Variable	Initial test	Repeated test
Sodium (mmol/L)	132	148
Potassium (mmol/L)	2.5	4.6
Chloride (mmol/L)	75	107
Urea nitrogen (mmol/L)	9.4	2.8
Creatinine (μmol/L)	80	57
Glucose (mmol/L)	8.5	4.3
Bilirubin (μmol/L)	13	13
AST (U/L)	50	153
LT (U/L)	93	217
Alkaline phosphatase (U/L)	361	980
Alpha amylase (U/L)	627	354

Figure 1 Endoscopic image of the stenotic postbulbar duodenum.

Figure 2 Severe circumferential deformation, as well as 4 cm long stenosis of the second portion of the duodenum on X-ray series.

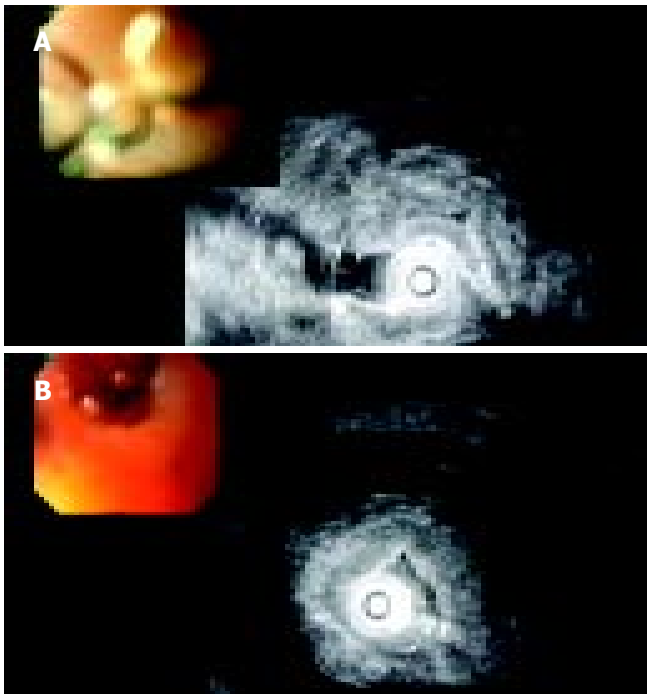

Figure 3 A: EUS image of diffusely thickened duodenal wall. B: EUS image of multiple microcysts in diffusely thickened duodenal wall.

Figure 4 Surgical specimen of resected duodenal wall: Macrocysts in the thickened wall.

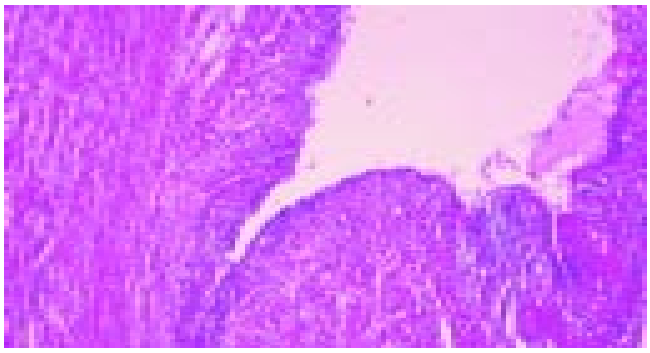

Figure 5 Irregular pseudocystic change in myofibroblastic stromal proliferation is considered as common histological findings in this lesion (HE, 112×).

DISCUSSION

The pancreas develops from two primitive diverticula, dorsal and ventral, that arise from the duodenum and the base of the liver, respectively, in the fifth week of gestation. During the seventh week, the two primordia fuse. The ventral portion gives rise to part of the head of the pancreas and the uncinate process,

and the dorsal portion becomes the body. In more than half the cases of pancreatic heterotopia, pancreatic tissue has been located in the duodenum or the pylorus but other sites have also been involved[2].

Pancreatic heterotopia can develop due to either metaplasia of multipotent endodermal cells in situ or transplantation of embryonic pancreatic cells to adjacent structures[2]. Heterotopic pancreatic tissues may be found in the mucosa or the muscularis or may be attached to the serosa of the gastrointestinal tract. Heterotopic pancreatic tissues that lack both acinar and endocrine cells have been called myoepithelial hamartoma, adenomyosis, or adenomyoma. Despite its congenital origin, pancreatic heterotopia was usually discovered in adults due to its complications[5]. Most frequently it was found incidentally during autopsies, operations or during endoscopic examinations of the upper GI tract[6]. The occurrence rate of heterotopic pancreas in autopsy series was estimated to be about 0.55% to 13.7%[4,7].

Despite many advances of new diagnostic tools and methods, the diagnosis of heterotopic pancreas prior to surgery is still difficult. Heterotopic pancreas is usually asymptomatic and does not require treatment (i.e. surgical excision). However, sometimes, there were evident clinical symptoms[8]. The most common symptoms attributed to heterotopic pancreas were: abdominal pain, nausea, vomiting, anemia, weight loss and melena[9]. Rare manifestations and complications of heterotopic pancreas included acute and chronic pancreatitis[10], biliary obstruction, intestinal obstruction, cystic dystrophy and malignant degeneration[5,11,12].

The differential diagnosis of a cystic dystrophy of heterotopic pancreas includes disorders in three broad categories: inflammatory lesions, neoplasms, and congenital anomalies.

Complications of pancreatic heterotopia usually include inflammation with a formation of an inflammatory mass, ulceration, bleeding and obstruction with clinical manifestations of acute and chronic pancreatitis. Chronic pancreatitis with mucinous metaplasia of the ductal epithelium can further be complicated by prominent exudation of mucin into the stroma, mimicking mucinous carcinoma[13].

The most challenging differential diagnosis of cystic dystrophy of heterotopic pancreas is cystic (mucinous) neoplasms. It has been demonstrated that pancreatic carcinomas or endocrine tumors can also develop in heterotopic pancreatic tissue[14,15]. In this case, CT findings are non-specific. Endoscopic and upper GI barium X-ray series can reveal duodenal stenosis and submucosal masses if there are no mucosal lesions and biopsies from the lesions cannot always provide a representative tissue specimen. The introduction of endoscopic ultrasonography (EUS) makes the diagnosis of cystic dystrophy of the duodenal wall in heterotopic pancreas easier[16]. Furthermore, endoscopic ultrasonography is a reliable method providing precise localization, extent and characteristics of the submucosal mass, making possible to differentiate it from all other causes of stenosis such as tumor and pancreas annulare[17].

However, although there is good correlation between EUS[16], computer tomography (CT) and nuclear magnetic resonance (NMR) findings with histological changes[17,18], the definite diagnosis is often made only from surgical excision.

The treatment of this disease is controversial. There are reports of successful treatment with long-acting somatostatin synthetic stable analog[19]. In some 40% of patients reduction in cyst size could be accomplished after three months of treatment[16]. But, on the other hand, octreotide/analog treatment was of a limited value regarding already formed stenosis of the duodenum (in regards to persistent duodenal stenosis)[20,21]. Furthermore, the necessary duration of treatment has not been established yet.

Ponchon *et al*. offered an alternative to surgical treatment for endoscopic fenestration of cysts, but that approach was feasible only for cases where cysts were fewer, not dispersed and relatively larger in size[22].

Despite the encouraging attempts to treat cystic dystrophy of duodenal wall in heterotopic pancreas with conservative approaches, the treatment is still primarily surgical[20,21,23,24].

Moreover, there is a difficult therapeutic dilemma: if such a lesion should be treated by duodenopancreatectomy or limited local excision?

Regarding the surgical procedures, there were data that conservative surgical procedures including segmental duodenal resection could be an alternative approach to the Whipple procedure[25], but in other cases of pancreatic surgery, they were associated with a considerable morbidity and mortality[26-28], and should be reserved for specialized centers[29].

In conclusion, we demonstrated a rare case of cystic dystrophy of heterotopic pancreas in duodenal wall. Cystic dystrophy of aberrant pancreatic tissue can be either isolated or as in our case associated with acute pancreatitis and duodenal stenosis. Although the condition is benign, clinical symptoms vary and patients are usually referred for suspected pancreatic neoplasms or acute pancreatitis. Endoscopic ultrasonographic features allow preoperative diagnosis of cystic dystrophy of a heterotopic pancreas in duodenal wall, with intraluminal 20 MHz mini-probe sonography being more efficient in cases of luminal stenosis.

REFERENCES

1 **Dolan RV,** ReMine WH, Dockerthy MB. The fate of heterotopic pancreatic tissue. A study of 212 cases. *Arch Surg* 1974; **109:** 762-765

2 **Skandalakis JE,** Grey SW. Embriology for surgeons: the embryological basis for treatment of congenital anomalies. 2nd ed. Baltimore: *Williams Wilkins* 1994: 366-387

3 **Moen J,** Mack E. Small bowel obstruction caused by heterotopic pancreas in an adult. *Am Surg* 1989; **55:** 503-504

4 **Scarpelli DG**. The Pancreas In: Rubin E, Faber JL (Eds). Pathology. *Philadelphia: Lippincott* 1988: 811

5 **Burke GW**, Binder SC, Barron AM, Dratch PL, Umlas J. Heterotopic pancreas: gastric outlet obstruction secondary to pancreatitis and pancreatic pseudocyst. *Am J Gastroenterol* 1989; **84:** 52-55

6 **Jaffe R.** The pancreas. In: Wigglesworth JS, Singer DB, Eds. Textbook of Fetal and Perinatal Pathology. Vol 2. Boston, Mass: *Blackwell Scientific* 1991: 1021-1055

7 **Armstrong CP,** King PM, Dixon KM. The clinical significance of heterotopic pancreas in the gastrointestinal tract. *Br J Surg* 1981; **68:** 384-387

8 **Pang LC**. Pancreatic heterotopia: a reappraisal and clinicopathologic analysis of 32 cases. *South Med J* 1988; **81:** 1264-1275

9 **Hsia CY,** Wu CW, Lui WY. Heterotopic pancreas: a difficult diagnosis. *J Clin Gastroenterol* 1999; **28:** 144-147

10 **Chung JP,** Lee I, Kim KW. Duodenal ectopic pancreas complicated by chronic pancreatitis and pseudocyst formation: a case report. *J Korean Med Sci* 1994; **9:** 351-356

11 **Flejou JF,** Potet F, Molas G, Bernades P, Amouzal P, Fekete F. Cystic dystrophy of the gastric and duodenal wall developing in heterotopic pancreas: an unrecognized entity. *Gut* 1993; **34:** 343-347

12 **Jeng K,** Yang KC, Kuo H. Malignant degeneration of heterotopic pancreas. *Gastrointest Endosc* 1991; **37:** 196-198

13 **Nopajaroonsri C.** Mucus retention in heterotopic pancreas of the gastric antrum: a lesion mimicking mucinous carcinoma. *Am J Surg Pathol* 1994; **18:** 953-957

14 **Kaneda M,** Yano T, Yamamoto T, Suzuki T, Fujimori K, Itoh H, Mizumoto R. Ectopic pancreas in the stomach presenting as an inflammatory abdominal mass. *Am J Gastroenterol* 1989; **84:** 663-666

15 **Al-Jitawi SA,** Hiarat AM, Al-Majali SH. Diffuse myoepithe-

lial hamartoma of the duodenum associated with adenocarcinoma. *Clin Oncol* 1984; **10:** 289-293

16 **Palazzo L,** Borotta E, Napoleon B. Is endoscopic ultrasonography accurate for the localization of pancreatic and duodenal tumors in patients with multiple endocrine neoplasia type I. *Gastroenterology* 1994; **106:** A313

17 **Vullierme MP,** Vilgrain V, Flejou JF, Zins M, O'Toole D, Ruszniewski P, Belghiti J, Menu Y. Cystic dystrophy of the duodenal wall in the heterotopic pancreas: radiopathological correlations. *J Comput Assist Tomogr* 2000; **24:** 635-643

18 **Procacci C,** Graziani R, Zamboni G, Cavallini G, Pederzoli P, Guarise A, Bogina G, Biasiutti C, carbognin G, Bergamo-Andreis IA, Pistolesi GF. Cystic dystrophy of the duodenal wall: radiologic findings. *Radiology* 1997; **205:** 741-747

19 **Basili E,** Allemand I, Ville E, Laugier R. Lanreotide acetate may cure cystic dystrophy in heterotopic pancreas of the duodenal wall. *Gastroenterol Clin Biol* 2001; **25:** 1108-1111

20 **Rubay R,** Bonnet D, Gohy P, Laka A, Deltour D. Cystic dystrophy in heterotopic pancreas of the duodenal wall: medical and surgical treatment. *Acta Chir Belg* 1999; **99:** 87-91

21 **Bittar I,** Cohen Solal JL, Cabanis P, Hagege H. Cystic dystrophy of an aberrant pancreas. Surgery after failure of medical therapy. *Presse Med* 2000; **29:** 1118-1120

22 **Ponchon T,** Napoleon B, Hedelius F, Bory R. Traitement endoscopique de la dystrophie kistique de la paroi duodenale. *Gastroenterol Clin Biol* 1997; **21:** A63

23 **Glaser M,** Roskar Z, Skalincky M, Krajnc I. Cystic dystrophy of the duodenal wall in a heterotopic pancreas. *Wien Klin Wochenschr* 2002; **114:** 1013-1016

24 **Wind P,** Pardies P, Roullet MH, Rouzier R, Zinzindohoue F, Cugnenc PH. Cystic dystrophy of the duodenal wall in aberrant pancreas. *Ann Chir* 1999; **53:** 164-167

25 **Marmorale A,** Tercier S, Peroux JL, Monticelli I, Mc Namara M, Huguet C. Cystic dystrophy in heterotopic pancreas of the second part of the duodenum. One case of conservative surgical procedure. *Ann Chir* 2003; **128:** 180-184

26 **Lansing PB,** Blalock JB, Oschner JL. Pancreaticoduodenetctomy: a retrospective review, 1949-1969. *Am Surg* 1972; **38:** 79-84

27 **Connolly MM,** Dawson PJ, Michelassi F, Moossa AR, Lowenstein F. Survival in 1001 patients with carcinoma of the pancreas. *Ann Surg* 1987; **206:** 366-372

28 **Herter FP,** Cooperman AM, Ahlborn TN, Antinori C. Saurgical experience with pancreatic and periampullary cancer. *Ann Surg* 1982; **195:** 274-280

29 **Hanyu F,** Suzuki M, Imaizumi T. Whipple operation for pancreatic carcinoma: Japanese experiment. In: Berger HG, Buchler MW, Malfertheiner P, eds. Standards in Pancreatic SurgeryBerlin Heidelberg: *Springer Verlag* 1993: 646

Edited by Zhu LH **Proofread by** Xu FM

PO Box 2345, Beijing 100023, China
Fax: +86-10-85381893
E-mail: wjg@wjgnet.com www.wjgnet.com

World J Gastroenterol 2004;10(17):2613-2615
World Journal of Gastroenterology
Copyright © 2004 by The WJG Press ISSN 1007-9327

• CASE REPORT •

Imaging findings of splenic hamartoma

Ri-Sheng Yu, Shi-Zheng Zhang, Jian-Ming Hua

Ri-Sheng Yu, Jian-Ming Hua, Department of Radiology, Second Affiliated Hospital, School of Medicine, Zhejiang University, Hangzhou 310009, Zhejiang Province, China
Shi-Zheng Zhang, Department of Radiology, Sir Run Run Shaw Hospital, School of Medicine, Zhejiang University, Hangzhou 310009, Zhejiang Province, China
Correspondence to: Dr. Ri-Sheng Yu, Department of Radiology, the Second Affiliated Hospital, School of Medicine, Zhejiang University, Hangzhou 310009, Zhejiang Province, China. yurisheng2003@yahoo.com.cn
Telephone: +86-571-87783860 **Fax:** +86-571-87783804
Received: 2003-10-08 **Accepted:** 2003-11-13

Abstract

AIM: To assess CT and MR manifestations and their diagnostic value in splenic hamartoma with review of literatures.

METHODS: We described a woman who was accidentally found to have a splenic tumor by ultrasound of the abdomen. CT and MR findings of this splenic hamartoma were proved by pathology retrospectively.

RESULTS: The CT and MR findings in this case included a ball-like mass with homogeneous mild-hypodensity lesions on non-enhanced CT scans or isointensity on T_1-weighted images and mild hypointensity on T_2-weighted images, progressive homogeneous enhancement on multiple-phase spiral CT and MR enhanced scans, and isodense enhancement on delayed post-contrast CT scans and obvious hyperintensity relative to the spleen on delayed MR images.

CONCLUSION: Splenic hamartoma has some specific radiological features. However, the diagnosis of this disease must be based on clinical features and confirmed by pathology.

Yu RS, Zhang SZ, Hua JM. Imaging findings of splenic hamartoma. *World J Gastroenterol* 2004; 10(17): 2613-2615
http://www.wjgnet.com/1007-9327/10/2613.asp

INTRODUCTION

Splenic hamartoma is a rare benign vascular tumor[1]. Up to now, less than 50 cases in Chinese literature or about 160 cases in the world have been reported after the first description by Rokitansky in 1861.

Imaging features of splenic hamartoma have been described by several researchers at computed tomography (CT), magnetic resonance imaging (MRI) and sonography[2-8] and the imaging appearance of these lesions is considered as nonspecific and a histopathological confirmation is often required[9-11].

This paper described the CT and MRI features of splenic hamartoma in a 40-year-old patient with review of the literature.

CASE REPORT

A 40-year-old woman was accidentally diagnosed having a splenic tumor by ultrasound of the abdomen. She did not complained about fever, fatigue, abdominal pain, or weight loss was complained. She denied any history of hepatitis or tuberculosis. Physical examination was entirely normal. There was no evidence of jaundice, peripheral lymphadenopathy or hepatosplenomegaly. Her hemoglobin was 125 g/L, the number of white blood cells was 7.3×10^9/L and the number of platelets was 176×10^9/L. Both stool and urinate routine tests and hepatic and renal function tests were normal. Chest x-ray was also normal.

Spiral CT of the abdomen before contrast medium administration revealed a 3.8-cm diameter, homogeneous mild-hypodensity lesion within the spleen (Figure 1A). During hepatic artery phase following bolus injection of intravenous contrast, the lesion showed a slightly homogeneous enhancement (Figure 1B). During the portal venous phase and hepatic parechymal phase, the lesion showed a progressively homogeneous enhancement. On delayed images up to 5 min after-contrast injection, the tumor was isodense with the spleen (Figure 1C). CT diagnosis was a splenic hemangioma.

MRI of the abdomen showed a 3.6 cm×3.8 cm×4.2 cm ball-like mass with isointensity on T_1-weighted images (Figure 2A) and mild hypointensity on T_2-weighted images (Figure 2B). The lesion demonstrated a diffuse heterogeneous enhancement on images obtained early after contrast medium administration (Figure 2C) and became more uniformly enhanced on the portal venous phase and hepatic parechymal phase. It was hyperintense compared to the spleen on the delayed images (Figure 3). The MR examination yielded a diagnosis of splenic hemangioma. A 4.0-cm diameter tumor was found in the spleen during operation. The pathologic diagnosis was a splenic hamartoma (Figure 4).

Figure 1 CT scans of splenic hamartoma. A: Homogeneous mild hypodensity lesion within the spleen found by unenhanced CT scan, B: Mild-homogeneous enhancement of the mass found by enhanced CT scan on hepatic artery phase, C: Isodense tumor with normal spleen **o**n delayed enhanced CT images.

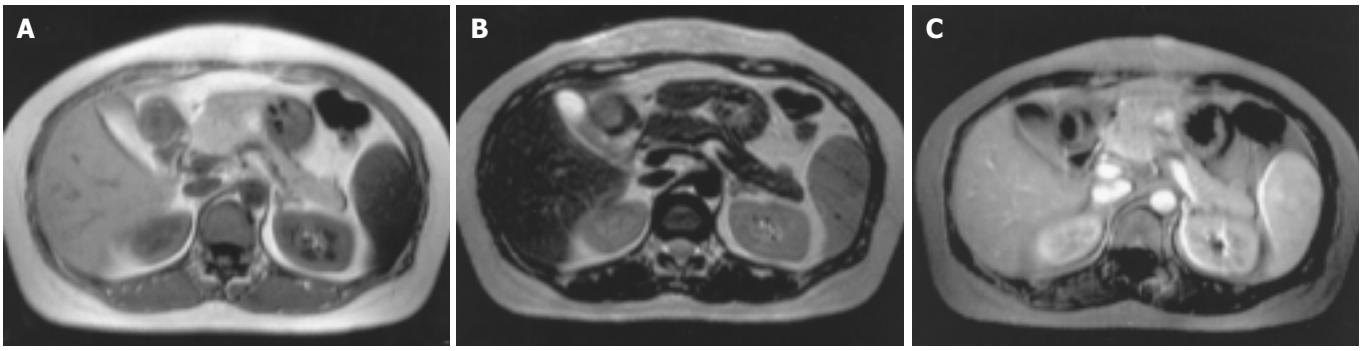

Figure 2 MR images of splenic hamartoma. A: Round-like mass with isointensity relative to the spleen on MR T_1-weighted images, B: Mild-hypointense mass on MR T_2-weighted images, C: Diffuse heterogeneous enhancement of mass by enhanced MR scan on early portal venous phase.

Figure 3 Obviously hyperintense tumor with normal spleen **o**n delayed enhanced MR images.

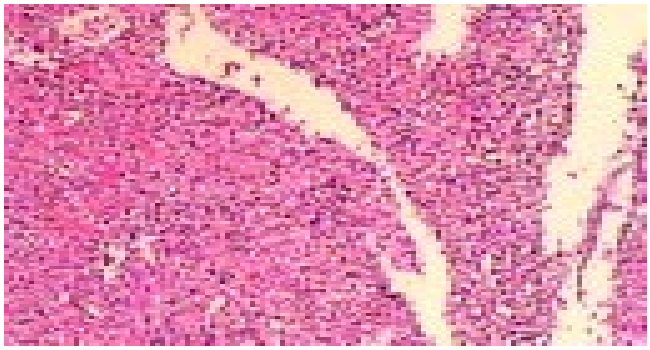

Figure 4 Red marrow tissue and some blood sinusoid structures with lymphocytes and macrophages in hamartoma. Fibrosis was remarkable. (HE, original magnification×100).

DUSCUSSION

Hamartoma of the spleen is a rare benign lesion and the diagnosis is difficult to make preoperatively. Histologically it is composed of an aberrant mixture of the normal tissue components of the spleen, so hamartoma of the spleen is often called splenoma, splenadenoma or nodular hyperplasia[2,3].

Splenic hamartoma occurs most commonly in adults. About 14.3% of the reported cases of splenic hamartoma occurred in pediatric patients[12]. Most patients were asymptomatic, they were incidentally found during imaging studies, laparotomy or autopsy[2,3]. Our case was accidentally discovered by ultrasound examination of the abdomen. Symptomatic splenic hamartoma was rare but nearly half of splenic hamartoma pediatric patients had symptoms[12]. A minority of these lesions had hematologic symptoms such as pancytopenia, anemia, and thrombocytopenia[12-16]. Spontaneously ruptured splenic hamartoma has been reported[17,18]. Symptomatic splenic hamartoma with renal, cutaneous abnormalities or portal hypertension and heterotopic ovarian splenoma were described accidentally[19-21].

A few radiological findings in splenic hamartoma have been described[2-8]. Sonography was a more sensitive modality than CT in demonstrating the lesion, which showed hyperechoic masses with cystic components ocasionally[2]. But hypoechoic splenic mass was found and color Doppler sonography showed blood-flow signals inside the mass in a recent report[4]. CT could reveal splenomegaly and homogeneous or heterogeneous low-density or isodense masses with calcification[2,5,6] or fatty components, which are characteristic CT findings. Dense spreading enhancement on dynamic CT and prolonged enhancement on delayed post-contrast scans were noted in singular mass[5]. But low-density masses relative to the spleen were seen in multiple splenic hamartomas after contrast medium administration[2]. The CT findings in this case were similar to those in Ohtomo's report[5], which included a homogeneous mild-hypodensity lesion on non-enhanced scans, a progressive homogeneous enhancement on multiple-phase spiral CT enhanced scans and an isodense enhancement on delayed post-contrast scans.

There were two types of MRI findings in splenic hamartomas, fibrous and non-fibrous splenic hamartomas. Histopathologically, fibrous splenic hamartomas had a dominant fibrous tissue and MRI showed isointensity or hyperintensity on T_1-weighted images, hypointensity on T_2-weighted images[3,7]. We consider hypointensity on T_2-weighted images is one of the common MRI findings in splenic hamartomas. Non-fibrous splenic hamartomas are more common and MRI showed isointensity on T_1-weighted images, hyperintensity on T_2-weighted images[6,8]. Both of the tumors demonstrated diffuse heterogeneous enhancement on the hepatic artery phase or early dynamic contrast-enhanced scans, which became more uniformly enhanced on delayed images[3,5,8]. This case belonged to fibrous type and the MRI findings were similar to those in Fernandez-Canton's report besides obvious hyperintensity relative to the spleen on delayed images[3]. We agree with that diffuse progressive enhancement and prolonged enhancement were the characteristic radiological findings[5].

In short, the following clinical features and radiographic findings may suggest the diagnosis of splenic hamartomas: (1) asymptomatic and incidental findings in adults; (2) possible association with hematologic symptoms such as pancytopenia, anemia, and thrombocytopenia or spontaneous rupture of splenic mass; (3) plenic mass with calcification or fatty components on plain CT, and isointensity on T_1-weighted images, heterogeneous hyperintensity or hypointensity on T_2-weighted images; (4) dense spreading enhancement and obviously prolonged enhancement on postcontrast CT and MRI. Though splenic hamartomas have some clinical and CT features, the final and exact diagnosis depends on histopathologic examination.

Splenic haemangioma should be differentiated from splenic hamartomas[8]. They have similar clinical and radiological findings. But the latter is manifested by splenic mass with calcification or fatty component on plain CT. The lesions appear isointense on T_1-weighted images, heterogeneous hyperintense or hypointense on T_2-weighted images. CT and MRI can demonstrate diffuse enhanced lesions on the hepatic artery phase or early dynamic contrast-enhanced scans. The typical CT and MRI features of the former include early peripheral nodular enhancement, hypointensity on T_1-weighted images and homogeneous hyperintensity on T_2-weighted images. Rare calcification and no fatty component of splenic haemangioma are seen on plain CT. In addition, splenic lymphoma and metastases were also considered to be different from splenic hamartomas[5,8]. Most of splenic lymphomas are multiple, secondary lesions and often have extra-splenic lymphoma. Splenic metastases usually have a history of primary extra-splenic malignant neoplasms and hepatic metastases. Both splenic lymphoma and metastases seldom have dense spreading enhancement or prolonged enhancement on post-contrast CT and MRI.

REFERENCES

1 **Arber DA,** Strickler JG, Chen YY, Weiss LM. Splenic vascular tumors: a histologic, immunophenotypic, and virologic study. *Am J Surg Pathol* 1997; **21**: 827-835

2 **Zissin R,** Lishner M, Rathaus V. Case report: unusual presentation of splenic hamartoma; computed tomography and ultrasonic findings. *Clin Radiol* 1992; **45**: 410-411

3 **Fernandez-Canton G,** Capelastegui A, Merino A, Astigarraga E, Larena JA, Diaz-Otazu R. Atypical MRI presentation of a small splenic hamartoma. *Eur Radiol* 1999; **9**: 883-885

4 **Tang S,** Shimizu T, Kikuchi Y, Shinya S, Kishimoto R, Fujioka Y, Miyasaka K. Color Doppler sonographic findings in splenic hamartoma. *J Clin Ultrasound* 2000; **28**: 249-253

5 **Ohtomo K,** Fukuda H, Mori K, Minami M, Itai Y, Inoue Y. CT and MR appearances of splenic hamartoma. *J Comput Assist Tomogr* 1992; **16**: 425-428

6 **Thompson SE,** Walsh EA, Cramer BC, Pushpanathan CC, Hollett P, Ingram L, Price D. Radiological features of a symptomatic splenic hamartoma. *Pediatr Radiol* 1996; **26**: 657-660

7 **Chevallier P,** Guzman E, Fabiani P, Dib M, Oddo F, Padovani B. Fibrous splenic hamartoma: imaging features. *J Radiol* 1999; **80**: 1668-1671

8 **Ramani M,** Reinhold C, Semelka RC, Siegelman ES, Liang L, Ascher SM, Brown JJ, Eisen RN, Bret PM. Splenic hemangiomas and hamartomas: MR imaging characteristics of 28 lesions. *Radiology* 1997; **202**: 166-172

9 **Kumar PV.** Splenic hamartoma. A diagnostic problem on fine needle aspiration cytology. *Acta Cytol* 1995; **39**: 391-395

10 **Lee SH.** Fine-needle aspiration cytology of splenic hamartoma. *Diagn Cytopathol* 2003; **28**: 82-85

11 **Keogan MT,** Freed KS, Paulson EK, Nelson RC, Dodd LG. Imaging-guided percutaneous biopsy of focal splenic lesions: update on safety and effectiveness. *Am J Roentgenol* 1999; **172**: 933-937

12 **Hayes TC,** Britton HA, Mewborne EB, Troyer DA, Saldivar VA, Ratner IA. Symptomatic splenic hamartoma: case report and literature review. *Pediatrics* 1998; **101**: E10

13 **Fujii T,** Obara T, Shudo R, Tanno S, Maguchi H, Saitoh Y, Ura H, Kohgo Y. Splenic hamartoma associated with thrombocytopenia. *J Gastroenterol* 1997; **32**: 114-118

14 **Beham A,** Hermann W, Vennigerholz F, Schmid C. Hamartoma of the spleen with haematological symptoms. *Virchows Arch A Pathol Anat Histopathol* 1989; **414**: 535-539

15 **Wirbel RJ,** Uhlig U, Futterer KM. Case report: splenic hamartoma with hematologic disorders. *Am J Med Sci* 1996; **311**: 243-246

16 **Compton CN,** McHenry CR, Aijazi M, Chung-Park M. Thrombocytopenia caused by splenic hamartoma: resolution after splenectomy. *South Med J* 2001; **94**: 542-544

17 **Ferguson ER,** Sardi A, Beckman EN. Spontaneous rupture of splenic hamartoma. *J La State Med Soc* 1993; **145**: 48-52

18 **Yoshizawa J,** Mizuno R, Yoshida T, Kanai M, Kurobe M, Yamazaki Y. Spontaneous rupture of splenic hamartoma: a case report. *J Pediatr Surg* 1999; **34**: 498-499

19 **Kassarjian A,** Patenaude YG, Bernard C, Bell L. Symptomatic splenic hamartoma with renal, cutaneous, and hematological abnormalities. *Pediatr Radiol* 2001; **31**: 111-114

20 **Singh K,** Subbramaiah A, Choudhary SR, Bhasin DK, Wig JD, Radotra B, Nagi B. Splenic hamartoma with portal hypertension: a case report. *Trop Gastroenterol* 1992; **13**: 155-159

21 **Cualing H,** Wang G, Noffsinger A, Fenoglio-Preiser C. Heterotopic ovarian splenoma: report of a first case. *Arch Pathol Lab Med* 2001; **125**: 1483-1485

Edited by Zhang JZ and Wang XL **Proofread by** Xu FM

PO Box 2345, Beijing 100023, China
Fax: +86-10-85381893
E-mail: wjg@wjgnet.com www.wjgnet.com

World J Gastroenterol 2004;10(17):2616-2617
World Journal of Gastroenterology
Copyright © 2004 by The WJG Press ISSN 1007-9327

• CASE REPORT •

Brunner's gland adenoma of duodenum: A case report and literature review

Yu-Ping Gao, Jian-Shan Zhu, Wen-Jun Zheng

Yu-Ping Gao, Jian-Shan Zhu, Wen-Jun Zheng, Department of Pathology, Affiliated Renji Hospital, Shanghai Second Medical University, Shanghai 200001, China
Correspondence to: Dr Yu-Ping Gao, Department of Pathology, Affiliated Renji Hospital, Shanghai Second Medical University, 145 Shandong (c) Road, Shanghai 200001, China. jzmgyp@online.sh.cn
Telephone: +86-21-58752345 Ext. 3349
Fax: +86-21-58752345 Ext. 3349
Received: 2003-11-21 **Accepted:** 2004-01-15

Abstract

AIM: To analyze the clinicopathological features of Brunner's gland adenoma of the duodenum.

METHODS: A rare case of Brunner's gland adenoma of the duodenum was described and related literature was reviewed.

RESULTS: Brunner's gland adenoma of the duodenum appeared to be nodular hyperplasia of the normal Brunner's gland with an unusual admixture of normal tissues, including ducts, adipose tissue and lymphoid tissue. We suggested that it might be designated as a duodenal hamartoma rather than a true neoplasm.

CONCLUSION: The most common location of the lesion is the posterior wall of the duodenum near the junction of its first and second portions. It can result in gastrointestinal hemorrhage and duodenal obstruction. Endoscopic polypectomy is a worthy treatment for benign Brunner's gland adenomas, as malignant changes in these tumors have never been proven.

Gao YP, Zhu JS, Zheng WJ. Brunner's gland adenoma of duodenum: A case report and literature review. *World J Gastroenterol* 2004; 10(17): 2616-2617
http://www.wjgnet.com/1007-9327/10/2616.asp

INTRODUCTION

Brunner's gland adenoma, also known as Brunneroma or polypoid hamartoma, is a rare, benign, proliferative lesion arising from the Brunner's glands of the duodenum, accounting for 10.6% of benign tumors of the duodenum. The time patients are usually asymptomatic and lesions are discovered incidentally. These lesions manifest occasionally as a rare cause of duodenal obstruction or upper gastrointestinal hemorrhage, and require surgical excision[1]. This article reports a case of Brunner's gland adenoma, and reviews briefly its clinical presentations, pathological features and therapy.

CASE REPORT

A 32-year-old Chinese man complained of two episodes of melenas and a two-month history of vague epigastric discomfort. The patient had in October 2001 his first tarry stool episode without nausea, vomiting and epigastralgia. Endoscopic examination revealed a mild ulcer in the duodenal bulb. The symptoms were relieved by antacids and H_2 blockers. He reported however another tarry stool in September 2002 and complained about epigastric pain without nausea and vomiting during the preceding 2 mo. Antacids were taken and the pain was relieved. Vital signs were normal and no anemia was reported when he was admitted. The physical examination had no unremarkable finding. The abdomen was soft without palpating pain and jumping pain.

However, X-rays barium radiological examination of the upper gastrointestinal in October 2002 revealed a nodular, polypoid-filling defect mass measuring 3 cm×2.5 cm with a smooth surface and no ulceration in the duodenal bulb. A tumor was suspected. Follow-up endoscopy disclosed a lobulated, red-color tumor, occupying the anterior wall of the bulb. The surface of the tumor was smooth with mild depression at the top. The mucosa had no erosions and ulcers. Multiple biopsy specimens were taken and interpreted as "mucosal mild-medium atypia." CT scan was negative. A preoperative diagnosis of malignant tumor was made and the patient prepared for operation. On October 25, 2002, at the time of operation, a pedunculated polyp on a short broad-based stalk, 3.5 cm×3 cm×2 cm in size, was found in the anterior wall of the duodenal bulb. The common bile duct was normal. The lesion was amputated at the base of the stalk.

The resected specimen showed a lobulated, polypoid mass measuring 3.3 cm×2.5 cm×2.5 cm projecting into the duodenum. The stalk was measured 1.8 cm in diameter and 0.5 cm in length. The tumor was completely enveloped by the intact thin duodenal mucosa. The surface of the tumor was smooth without erosions and ulcers. The cut surface of tumor had a gray-red or gray-yellow color, revealing lobules. The consistency was moderate. On microscopic examination, the tumor was composed of hyperplasia of Brunner's glands. The hyperplasia formed lobules that were separated by intervening bands of fibrous tissue, adipose tissue, ducts and well developed aggregated lymphoid. No sign of malignancy was found in the hyperplasia, Brunner's glands as well as the surrounded duodenal mucosa. The frozen sections and the final pathologic diagnosis were assessed as Brunner's gland adenoma. The patient had an uneventful postoperative course and was discharged on the tenth postoperative day. He has remained symptom free ever since and no episode of recurrent melenas has been reported.

DISCUSSION

Besides the duodenal gland, the duodenum has Brunner's glands under the mucin. Its structure and function are similar to glands of the pylorus. Brunner's glands secrete an alkaline fluid composed of viscous mucin, whose function appears to protect the duodenal epithelium from acid chyme of the stomach. Brunner's glands consist of submucosal mucin-secreting glands located exclusively in the duodenum. They extend from the pylorus distally for a variable distance, usually stopping at the first and second portions of the duodenum, and less often stopping at the third and fourth portions.

In 1688 Brunner gave a precise anatomic description of the duodenal submucosal glands and coined the term "pancreas secundarium." In 1846 Middeldorpf correctly identified these glands as a separate entity, which he proposed be named Brunner's

glands. Salvioli reported the first adenoma of Brunner's gland in 1876. Since then, 150 cases or so have been reported in literature of English language[2].

The etiology of Brunner's gland adenoma remains obscure. It tends to present predominantly in the fifth and sixth decades of man's life with no sex predominance. It has been found although the size of adenoma might extend from 1-12 cm, it is generally 1-2 cm in diameter[3]. The most common location for the lesion is the posterior wall of the duodenum near the junction of its first and second portions. Brunner's gland adenoma was rarely found extending to the proximal jejunum[4].

Brunner's gland adenoma has fallen into two categories: symptomatic tumors and asymptomatic ones that are only found incidentally. Symptomatic tumors can further be divided into hemorrhagic and obstructive tumors. The clinical manifestations of the former are gastrointestinal hemorrhage, due to ulceration or erosion of the tumor. Obstructive tumors occur when hyperplasia diffuses or a single adenoma grows too large, causing epigastric bloating, discomfort, vomiting or weight loss. Duodenal intussusception has been reported only in two patients[2], probably because of the fixation of duodenum to the posterior abdominal wall. There are also reports about patients who complained of diarrhea owing to duodenal motor disturbances[5].

Preoperative histological diagnosis at present is not always easy. In X-rays barium examination, the findings are often nonspecific because there is usually a sessile or pedunculated polypoid-filling defect in the duodenal bulb. Some doctors hold that hypotonic duodenography should play a vital role in establishing the diagnosis and should be treated as the best method to check the surface of the lesion. Endoscopy has an additional function in diagnosing and treating Brunner's gland adenoma, since it can verify the histological diagnosis and remove the tumor simultaneously. Endoscopic pinching biopsy however usually gave a negative result because the tumor was almost covered entirely with thick intact duodenal mucosa in the biopsy sites and the biopsy was often not deep enough to reach the submucosal tumor tissue[6]. In our case, the endoscopic biopsy was negative, and the condition was diagnosed as chronic gastritis, although the final pathologic diagnosis indicated that the patient suffered from Brunner's gland adenoma. CT examination appeared to be unrevealing.

Pathomorphological features of Brunner's gland are characterized by the presence of nondysplastic, lobulated Brunner's glands. Its hyperplasia is divided into diffuse hyperplasia, nodular hyperplasia and adenomatous hyperplasia with or without erosion or ulcer. In our opinion, the unusually admixture of normal tissues, including Brunner's glands, ducts, adipose tissue, and lymphoid tissue, supports the designation of these lesions as a hamartoma or nodular hyperplasia rather than a true neoplasm. It is a tumor without malignant predisposition. The malignant type is rare. Fujimaki *et al*. reported recently one patient with a focus atypical gland[7].

It is still controversial whether asymptomatic Brunner's gland adenoma found incidentally needs surgical removal. Some people think that it needs no treatment, whereas others hold that it should undergo endoscopic excision in order to prevent complications. There have been several reports[2,4] that Brunner's gland adenoma could give rise to acute profuse bleeding, which results in shock of patients. Symptomatic Brunner's gland adenoma, in our point of view, usually needs surgical treatment. When the tumor is small or pedunculated, endoscopic polypectomy is the first choice. Open surgical excision is reserved for cases where snaring has failed or when tumor is too large. The outcome of operation is usually excellent and there is no recurrent ever reported.

REFERENCES

1 **Matsumoto T**, Iida M, Matsui T, Yao T, Fujishima M. A large Brunner's gland adenoma removed by endoscopic polypectomy. *Endoscopy* 1990; **22:** 192-193

2 **Peetz ME**, Moseley HS. Brunner's gland hyperplasia. *Am Surg* 1989; **55:** 474-477

3 **Nakanishi T**, Takeuchi T, Hara K, Sugimoto A. A great Brunner's gland adenoma of the duodenal bulb. *Dig Dis Sci* 1984; **29:** 81-85

4 **Levine JA**, Burgart LJ, Batts KP, Wang KK. Brunner's gland hamartomas: clinical presentation and pathological features of 27 cases. *Am J Gastroenterol* 1995; **90**: 290-294

5 **Spellberg MA**, Vucelic B. A case of Brunner's glands hyperplasia with diarrhea responsive to cimetidine. *Am J Gastroenterol* 1980; **73**: 519-522

6 **Gourtsoyiannis NC**, Zarifi M, Gallis P, Mouchtouris A, Livaditou A. Radiologic appearances of Brunner's gland adenoma: a case report. *Eur J Radiol* 1990; **11**: 188-190

7 **Fujimaki E**, Nakamura S, Sugai T, Takeda Y. Brunner's gland adenoma with a focus of p53-positive atypical glands. *J Gastroenterol* 2000; **35:** 155-158

Edited by Qiu WS and Wang XL **Proofread by** Xu FM